UNIVERSITY OF NEWCASTLE UPON TYNE

DEPARTMENT OF MINING ENGINEERING

THE STUDY OF HIGH PRESSURE WATER JET ASSISTED CUTTING OF COAL SAMPLES IN THE LABORATORY

JOHN MARTIN

Thesis submitted for the degree of

Doctor of Philosophy of the

University of Newcastle upon Tyne

NEWCASTLE UNIVERSITY LIBRARY

091 51192 2

Thesis L 3901

September 1991

ACKNOWLEDGEMENTS

The author should like to express his gratitude to the people below without whose help, guidance, benevolence and encouragement, this research work would not have been achieved:

Professor J.F.Tunnicliffe, Head of the Department of Mining Engineering, University of Newcastle upon Tyne, for providing the opportunity and resources to carry out this research.

Dr. R.J.Fowell, Reader, for his advice, constant interest and encouragement in supervising the project.

Dr. K.Hurt, HQTD, British Coal, project engineer, for his assistance and interest.

Mr. N.Tomlin, acting Head of the Dapartment of Mining Engineering, for securing and providing facilities, and other academic staff of the Mining Department for their enduring willingness to help.

Mr. M.McKenna, Chief Technician of the Department of Mining Engineering, and his technical staff, Mr. V.Willey, Mr. R.Jensen, Mr. R.Liddell and Mr. J.Williams, for their hard work, ideas and technical skills and dexterity.

Mrs. B.Leggatt, Departmental Secretary, for her typing assistance and friendly disposition.

Dr. I.Anderson, Dr. J.Cheung, Mr. T.Gillani, Dr. J.Chen, Mr J.Searle, Dr. A.Langman, Mr. R.Al-Affidh, Dr. A.Waggott, the late Mr. A.Cammack, Dr. H.Hoang, Dr. A.Laderian, Dr. Choi, Dr. M.Farrelly, Dr. G.Richardson, Dr. A.Berry, Mr A.Young and Mr. M.Horton, and other research colleagues for their technical advice, cooperation, friendship, and ceaseless though somewhat Bohemian humour.

British Coal and the Science and Engineering Research Council, for their financial and technical assistance.

Contents

Abstract i
List of Figures ii
List of Tables and Plates xii
Nomenclature xiv

CHAPTER ONE

1 INTRODUCTION 1

CHAPTER TWO

2 LITERATURE REVIEW 4
2.1 High Pressure Water Jet Assisted Coal Excavation 4
2.1.1 Drum Shearers 4
2.1.2 Coal Ploughs 11
2.1.3 Continuous Miners 12
2.2 Coal Cutting Theory 13
2.3 High Pressure Water Jet Technology 14
2.3.1 Fluids Mechanics of Water Jets 14
2.3.2 Water Jet Cutting Theories 16
2.3.2.1 Crow's Theory 16
2.3.2.2 Rehbinder's Theory 16
2.3.2.3 Hashish - Du Plessis' Theory 17
2.3.2.4 Empirical Approach 18
2.3.3 Water Jet Cutting 19
2.3.3.1 Jet Characteristics 20
2.3.3.2 Operational Parameters 24
2.4 Hybrid Cutting 34
2.4.1 Jet Pressure 34
2.4.2 Lead-on and Side-off (Offset) Distance 39
2.4.3 Jet Position 39
2.4.4 Cutting Speed 41
2.4.5 The Theory of the Water Jet Assisted Cutting Mechanism 46

CHAPTER THREE

3 OBJECTIVES OF RESEARCH PROGRAMME AND EXPERIMENTAL DESIGN 50
3.1 Introduction 50
3.2 Objectives 50
3.3 Research Programme 51
3.3.1 General Test Procedure 52
3.3.2 Experimental Design 55
3.3.3 Replication and Randomization 57
3.3.4 Jet Penetration Tests 57

3.3.5 Statistical Analysis 58

CHAPTER FOUR

4 THE NEWCASTLE WATER JET RESEARCH FACILITY, INSTRUMENTATION, DATA ACQUISITION
AND ANALYSIS 59
4.1 Introduction 59
4.2 Linear Cutting Rig 59
4.2.1 Frame Structure 59
4.2.2 Specimen Table 61
4.2.3 Slide Assembly 62
4.2.4 Vertical Stiffeners (Clamps) 62
4.2.5 Clamping Hydraulic System 64
4.2.6 Main Hydraulic System 64
4.3 High Pressure Water System 69
4.4 Rig Relocation 70
4.5 Repairs and Modifications 72
4.5.1 Hydraulic Accumulators 72
4.5.2 Hydraulic Network 72
4.5.3 Electrical Factors 73
4.6 Preparation and Mounting of Coal Samples 75
4.7 Nozzle Design 75
4.8 Cutting Tool 80
4.9 Jet Mounting 80
4.10 Debris Collection 80
4.11 Coal Size Determination 82
4.11.1 Sieves, Sample Divider and Sieve Vibrator 82
4.11.2 Sieve Analysis 83
4.12 Force Measurement 85
4.12.1 Steel Dynamometer, Signal Conditioning and Calibration 85
4.12.2 Dynamometer, Signal Conditioning and Calibration 88
4.12.3 Data Analysis 92
4.13 Water Jet Pressure Measurement 96
4.13.1 Instrumentation 96
4.13.2 Calibration 96
4.14 Nozzle Diameter 97
4.15 Ram Speed Determination 100

CHAPTER FIVE

5 JET PENETRATION TESTS 101
5.1 Introduction 101
5.2 Analysis of Bituminous Coal and Anthracite Coal 101
5.2.1 Analysis of Traverse Speed and Jet Pressure 102
5.2.2 Analysis of Traverse Speed and Coal Type 104
5.2.3 Analysis of Jet Pressure and Coal Type 105
5.2.4 Complete Analysis of Variance 106
5.3 Analysis of Cleat Orientation in the Anthracite Coal 109
5.3.1 Complete Analysis of Variance 110
5.4 Graphical Representation of Jet Penetration Results 111
5.4.1 Equation Fitting 117
5.4.2 Hydraulic Specific Energies 124
5.5 Conclusions 132

CHAPTER SIX

6 ERIN AND ANTHRACITE COAL RESULTS 135
6.1 Introduction 135
6.2 Coal Description 135
6.2.1 Erin Coal 135
6.2.2 Anthracite Coal 136
6.3 Coal Cutting Results 138
6.3.1 Erin and Anthracite Trials 139
6.3.1.1 Conclusions 169
6.3.2 Cleat Orientation Trials 170
6.3.2.1 Conclusions 190
6.3.3 Breakout 191
6.3.3.1 Erin Coal - Cleat Parallel 192
6.3.3.2 Anthracite Coal - Cleat Parallel 197
6.3.3.3 Anthracite Coal - Cleat Horizontal 201
6.3.3.4 Conclusions 209
6.3.4 Specific Energy 210
6.3.4.1 Specific Energy of Shearer Loaders 218
6.3.4.2 Conclusions 224
6.4 Particle Size Analysis 225
6.4.1 Erin Coal - Cleat Parallel 225
6.4.2 Anthracite Coal - Cleat Parallel 229
6.4.3 Discussion on the Erin and Anthracite Results 234
6.4.4 Anthracite Coal - Cleat Horizontal 236
6.4.5 Discussion on Cleat Orientation 240
6.4.6 Conclusions 242
6.5 Summary 243

CHAPTER SEVEN

7 TEST SERIES ONE AND TWO RESULTS 245
7.1 Introduction 245
7.2 Objectives and Research Programme 245
7.2.1 Objectives 245
7.2.2 Test Programme 246
7.2.2.1 Test Series One 246
7.2.2.2 Test Series Two 248
7.3 Research Apparatus 249
7.4 Test Series One 251
7.4.1 Coal Cutting Results 251
7.4.1.1 Conclusions 269
7.4.2 Pre-cut Slot Tests 270
7.4.2.1 Conclusions 282
7.4.3 Specific Energy 283
7.4.4 Sieve Analysis Results 286
7.4.4.1 Jet Assisted Tests 286
7.4.4.2 Pre-Cut Slot Results 289
7.4.4.3 Discussion 292
7.4.4.4 Conclusions 292
7.5 Test Series Two 293
7.5.1 Lead and Offset Distance Analysis 293
7.5.1.1 Discussion 313
7.5.1.2 Conclusions 316
7.5.2 Sieve Analysis Results 317
7.6 Summary 323

CHAPTER EIGHT

8 DISCUSSION, CONCLUSIONS AND RECOMMENDATIONS 325
8.1 Discussion 325
8.2 Conclusions 332
8.2.1 Jet Penetration 333
8.2.2 Cutting Performance 333
8.2.3 Breakout 335
8.2.4 Specific Energy 335
8.2.5 Size Distribution 336
8.3 Recommendations 337
REFERENCES
BIBLIOGRAPHY
APPENDICES

ABSTRACT

A series of experiments were conducted to investigate high pressure water jet assisted coal cutting. The research was sponsored by British Coal and carried out in the Department of Mining Engineering at the University of Newcastle upon Tyne.

Two coals were tested: a black, coherent, anthracite; and a heavily cleated, friable, dull coloured bituminous coal. The tests modelled as closely as possible a vane pick on a two start shearer drum.

The experiment was performed on a modified 50 tonne linear cutting rig at a speed of 1.1m/s, using jet pressures of 35MPa, 70MPa, and 105MPa at different flow rates. A 75kW double acting intensifier type pump supplied the high pressure water for the jet. A relieved cutting mode was adopted with a line spacing of 70mm and a 30mm nominal depth of cut. An actual production cutting tool (heavy duty 75mm radial with a HW tip) cut the coal in both the sharp and blunt states. Additional tests were also performed by pre-slotting the coal with a water jet before cutting it and by examining the effect of varying the lead and offset distances on the parameters measured below.

Parameters measured were the cutting forces in three orthogonal directions; the breakout patterns; and the coal size distribution. The coal yields and specific energies were calculated from the experimental data.

Both coals achieved benefit from jet assistance but at different pressures depending upon the coal type and tool wear. The breakout pattern differed between the two coals but generally fracture occurred along the major cleat planes. Both coals were easier to cut when the major cleat was orientated in the horizontal plane rather than in the vertical plane. Specific energy increased linearly with jet power. In most cases the quantity of fine coal (-0.5mm) produced decreased with jet assistance.

LIST OF FIGURES

Figure 2.1	Bit temperature as a function of bit speed and water jet pressure (After Taylor et al, 1989).
Figure 2.2	Relationship between power consumption and cutting performance for a coal plough (After Henkel and Kraemer, 1982).
Figure 2.3	Diagrammatic representation of jet structure (After Yanaida and Ohashi, 1980).
Figure 2.4	Illustration of Hashish - Du Plessis' jet cutting theory (After Hashish, 1981).
Figure 2.5	Effect of nozzle shape on performance (After Leach and Walker, 1966).
Figure 2.6	Typical nozzle geometry (After Summers, 1980).
Figure 2.6a	Influence of the convergence angle on the coefficient of discharge (After Summers, 1980).
Figure 2.7	Influence of nozzle diameter on depth of cut in coal (After Evener and Tooley, 1985).
Figure 2.8	Influence of nozzle pressure on depth of cut in coal (After Evener and Tooley, 1985).
Figure 2.9	Depth of jet penetration vs. jet pressure in coal (After Fowell and Johnson, 1984).
Figure 2.10	Penetration vs. nozzle pressure for Berea sandstone with traverse speed as parameter, 0.008in. nozzle (After Harris and Mellor, 1974).
Figure 2.11	Operational parameters.
Figure 2.12	Relationship between stand-off distance and depth of cut in sub-bituminous coal (After Du Plessis and Hashish, 1980).
Figure 2.13	Two kinds of impingement angle in slot cutting (After Matsuki et al, 1988).
Figure 2.14	Normalised depth of cut as a function of jet inclination or impingement angle (After Matsuki et al, 1988).
Figure 2.15	Effect of the transverse (sideway) inclination on the depth of slot (After Matsuki et al, 1988).
Figure 2.16	The change of slot contour with the impingement angle (After Matsuki et al, 1988).
Figure 2.17	Comparison of single and multipass penetrations in Berea sandstone at 45 000psi with a 0.008in. nozzle (After Harris and Mellor, 1974).
Figure 2.18	Comparison of first then second pass in anthracite at 69MPa and 0.6mm nozzle (After Saunders and Blackwell, 1981).
Figure 2.19	Penetration vs. traverse speed for Berea sandstone with nozzle pressure as parameter, 0.008in. nozzle (After Harris and Mellor, 1974).
Figure 2.20	Penetration vs. traverse speed for Indiana limestone with nozzle pressure as parameter, 0.008in. nozzle (After Harris and Mellor, 1974).
Figure 2.21	Penetration vs. traverse speed for Berea sandstone and Indiana limestone at 62MPa and increased stand-off (After Kovscek et al, 1989).

Figure 2.22 Average depth of slot vs. traverse velocity for a sub-bituminous coal (After Evener and Tooley, 1985).

Figure 2.23 Variation in the coal penetration vs. traverse speed (After Kuzmich, 1972).

Figure 2.24 Mean normal force reductions vs. jet pressure for five rock types (After Ip, 1986).

Figure 2.25 Mean force reductions vs. jet pressure at different nozzle diameters (After Ip, 1986).

Figure 2.26 Mean cutting and normal force vs. jet pressure for two bituminous coals (After Fowell and Johnson, 1984).

Figure 2.27 Pick wear rate in Hard York sandstone as a function of jet pressure at varying levels of cutting speed (After Barham and Buchanan, 1987).

Figure 2.28 Jet-before and jet-after tool configurations (After Ip, 1986).

Figure 2.29 Variation of mean cutting force with depth of cut for duckbill pick (After O'Dogherty and Burney, 1963).

Figure 2.30 Pick wear rate in Hard York sandstone as a function of jet pressure, at varying levels of cutting speed (After MacAndrew et al, 1987).

Figure 2.31 Reduction of bit forces (given as percentage of forces when cutting dry) as function of jet energy per unit length cut. Shaded areas are 90% confidence bands for these results (After Hood et al, 1990).

Figure 3.1 Operational configuration.

Figure 3.2 Relieved cutting pattern.

Figure 3.3 Orientation of test coal to direction of cut.

Figure 4.1 Diagram of test facility

Figure 4.2 Cutter slider.

Figure 4.3 Calibration arrangement.

Figure 4.4 High pressure hydraulic circuit.

Figure 4.5 Hydraulic cylinder and network.

Figure 4.6 Formwork for casting coal samples in pitch.

Figure 4.7 M.R.D.E./N.C.B. Nozzle design.

Figure 4.8 Artificial wearflat specifications.

Figure 4.9 Calibration arrangement (steel dynamometer).

Figure 4.10-12 Steel dynamometer normal, cutting and sideway forces calibration curves respectively, showing the interaction.

Figure 4.13-15 Four-pillar dynamometer normal, cutting and sideway forces calibration curves respectively, showing the interaction.

Figure 4.16 Diagram of force measurement zones.

Figure 5.1 Jet penetration vs. jet pressure for the Erin coal.

Figure 5.2 Jet penetration vs. jet pressure for the anthracite (cleat parallel).

Figure 5.3 Jet penetration vs. jet pressure for the anthracite (cleat horizontal).

Figure 5.4 Average jet penetration vs. jet pressure for the anthracite (over both cleat orientations).
Figure 5.5 Jet penetration vs. jet power for the Erin coal.
Figure 5.6 Jet penetration vs. jet power for the anthracite (cleat parallel).
Figure 5.7 Jet penetration vs. jet power for the anthracite (cleat horizontal).
Figure 5.8 Average jet penetration vs. jet power for the anthracite (over both cleat orientations).
Figure 5.9 Jet penetration vs. traverse speed for the Erin coal.
Figure 5.10 Jet penetration vs. traverse speed for the anthracite (cleat parallel).
Figure 5.11 Jet penetration vs. traverse speed for the anthracite (cleat horizontal).
Figure 5.12 Average jet penetration vs. traverse speed for the anthracite (over both cleat orientations).
Figure 5.13 Hydraulic specific energy vs. jet pressure for the Erin coal.
Figure 5.14 Hydraulic specific energy vs. jet pressure for the anthracite (cleat parallel).
Figure 5.15 Hydraulic specific energy vs. jet pressure for the anthracite (cleat horizontal).
Figure 5.16 Average hydraulic specific energy vs. jet pressure for the anthracite (over both cleat orientations).
Figure 5.17 Hydraulic specific energy vs. jet power for the Erin coal.
Figure 5.18 Hydraulic specific energy vs. jet power for the anthracite (cleat parallel).
Figure 5.19 Hydraulic specific energy vs. jet power for the anthracite (cleat horizontal).
Figure 5.20 Average hydraulic specific energy vs. jet power for the anthracite (over both cleat orientations).
Figure 5.21 Hydraulic specific energy vs. traverse speed for the Erin coal.
Figure 5.22 Hydraulic specific energy vs. traverse speed for the anthracite (cleat parallel).
Figure 5.23 Hydraulic specific energy vs. traverse speed for the anthracite (cleat horizontal).
Figure 5.24 Average hydraulic specific energy vs. traverse speed for the anthracite (over both cleat orientations).
Figure 6.1 Force vs. jet pressure for the Erin coal and for a sharp pick.
Figure 6.2 Force vs. jet pressure for the Erin coal and for a blunt pick.
Figure 6.3 Force vs. jet pressure for the anthracite (cleat parallel) and for a sharp pick.
Figure 6.4 Force vs. jet pressure for the anthracite (cleat parallel) and for a blunt pick.
Figure 6.5 Force vs. jet power for the Erin coal and for a sharp pick.
Figure 6.6 Force vs. jet power for the Erin coal and for a blunt pick.
Figure 6.7 Force vs. jet power for the anthracite (cleat parallel) and for a sharp pick.
Figure 6.8 Force vs. jet power for the anthracite (cleat parallel) and for a blunt pick.

Figure 6.9 % force decrease vs. jet pressure for the Erin coal and for a sharp pick.
Figure 6.10 % force decrease vs. jet pressure for the Erin coal and for a blunt pick.
Figure 6.11 % force decrease vs. jet power for the Erin coal and for a sharp pick.
Figure 6.12 % force decrease vs. jet power for the Erin coal and for a blunt pick.
Figure 6.13 % force decrease vs. jet pressure for the anthracite (cleat parallel) and for a sharp pick.
Figure 6.14 % force decrease vs. jet pressure for the anthracite (cleat parallel) and for a blunt pick.
Figure 6.15 % force decrease vs. jet power for the anthracite (cleat parallel) and for a sharp pick.
Figure 6.16 % force decrease vs. jet power for the anthracite (cleat parallel) and for a blunt pick.
Figure 6.17 Mean peak force vs. jet pressure for the Erin coal and for a sharp pick.
Figure 6.18 Mean peak force vs. jet pressure for the Erin coal and for a blunt pick.
Figure 6.19 Mean peak force vs. jet pressure for the anthracite (cleat parallel) and for a sharp pick.
Figure 6.20 Mean peak force vs. jet pressure for the anthracite (cleat parallel) and for a blunt pick.
Figure 6.21 Mean peak force vs. jet power for the Erin coal and for a sharp pick.
Figure 6.22 Mean peak force vs. jet power for the Erin coal and for a blunt pick.
Figure 6.23 Mean peak force vs. jet power for the anthracite (cleat parallel) and for a sharp pick.
Figure 6.24 Mean peak force vs. jet power for the anthracite (cleat parallel) and for a blunt pick.
Figure 6.25 % mean peak force decrease vs. jet pressure for the Erin coal and for a sharp pick.
Figure 6.26 % mean peak force decrease vs. jet pressure for the Erin coal and for a blunt pick.
Figure 6.27 % mean peak force decrease vs. jet pressure for the anthracite (cleat parallel) and for a sharp pick.
Figure 6.28 % mean peak force decrease vs. jet pressure for the anthracite (cleat parallel) and for a blunt pick.
Figure 6.29 % mean peak force decrease vs. jet power for the Erin coal and for a sharp pick.
Figure 6.30 % mean peak force decrease vs. jet power for the Erin coal and for a blunt pick.
Figure 6.31 % mean peak force decrease vs. jet power for the anthracite (cleat parallel) and for a sharp pick.
Figure 6.32 % mean peak force decrease vs. jet power for the anthracite (cleat parallel) and for a blunt pick.
Figure 6.33 Force vs. jet pressure for the anthracite (cleat horizontal) and for a sharp pick.

Figure 6.34 Force vs. jet pressure for the anthracite (cleat horizontal) and for a blunt pick.

Figure 6.35 Force vs. jet power for the anthracite (cleat horizontal) and for a sharp pick.

Figure 6.36 Force vs. jet power for the anthracite (cleat horizontal) and for a blunt pick.

Figure 6.37 % force decrease vs. jet pressure for the anthracite (cleat horizontal) and for a sharp pick.

Figure 6.38 % force decrease vs. jet pressure for the anthracite (cleat horizontal) and for a blunt pick.

Figure 6.39 % force decrease vs. jet power for the anthracite (cleat horizontal) and for a sharp pick.

Figure 6.40 % force decrease vs. jet power for the anthracite (cleat horizontal) and for a blunt pick.

Figure 6.41 Mean peak force decrease vs. jet pressure for the anthracite (cleat horizontal) and for a sharp pick.

Figure 6.42 Mean peak force decrease vs. jet pressure for the anthracite (cleat horizontal) and for a blunt pick.

Figure 6.43 Mean peak force decrease vs. jet power for the anthracite (cleat horizontal) and for a sharp pick.

Figure 6.44 Mean peak force decrease vs. jet power for the anthracite (cleat horizontal) and for a blunt pick.

Figure 6.45 % mean peak force decrease vs. jet pressure for the anthracite (cleat horizontal) and for a sharp pick.

Figure 6.46 % mean peak force decrease vs. jet pressure for the anthracite (cleat horizontal) and for a blunt pick.

Figure 6.47 % mean peak force decrease vs. jet power for the anthracite (cleat horizontal) and for a sharp pick.

Figure 6.48 % mean peak force decrease vs. jet power for the anthracite (cleat horizontal) and for a blunt pick.

Figure 6.49 Effect of depth of cut on breakout.

Figure 6.50 Idealized breakout for heavily cleated friable coal.

Figure 6.51 Erin coal yield vs. jet pressure.

Figure 6.52 Erin coal yield vs. jet power.

Figure 6.53 Breakout for cleat parallel to direction of cut.

Figure 6.54 Anthracite (cleat parallel) coal yield vs. jet pressure.

Figure 6.55 Anthracite (cleat parallel) coal yield vs. jet power.

Figure 6.56 Breakout for cleat horizontally orientated.

Figure 6.57 Anthracite (cleat horizontal) coal yield vs. jet pressure.

Figure 6.58 Anthracite (cleat horizontal) coal yield vs. jet power.

Figure 6.59 Specific energy vs. jet pressure for the Erin coal.

Figure 6.60 Specific energy vs. jet power for the Erin coal.
Figure 6.61 Specific energy vs. jet pressure for the anthracite (cleat parallel) coal.
Figure 6.62 Specific energy vs. jet power for the anthracite (cleat parallel) coal.
Figure 6.63 Specific energy vs. jet pressure for the anthracite (cleat horizontal) coal.
Figure 6.64 Specific energy vs. jet power for the anthracite (cleat horizontal) coal.
Figure 6.65 Sieve analysis: Fraction % by mass vs. nominal aperture size with jet pressure as parameter; Erin coal; sharp pick.
Figure 6.66 Sieve analysis: Fraction % by mass vs. nominal aperture size with jet pressure as parameter; Erin coal; blunt pick.
Figure 6.67 % fraction difference (compared to the dry cut results) vs. sieve nominal aperture size: Jet pressure as parameter; Erin coal; sharp pick.
Figure 6.68 % fraction difference (compared to the dry cut results) vs. sieve nominal aperture size: Jet pressure as parameter; Erin coal; blunt pick.
Figure 6.69 Median particle size vs. jet pressure for the Erin coal.
Figure 6.70 Median particle size vs. jet power for the Erin coal.
Figure 6.71 Sieve analysis: Fraction % by mass vs. nominal aperture size with jet pressure as parameter; anthracite (cleat parallel) coal; sharp pick.
Figure 6.72 Sieve analysis: Fraction % by mass vs. nominal aperture size with jet pressure as parameter; anthracite (cleat parallel) coal; blunt pick.
Figure 6.73 % fraction difference (compared to the dry cut results) vs. sieve nominal aperture size: Jet pressure as parameter; anthracite (cleat parallel) coal; sharp pick.
Figure 6.74 % fraction difference (compared to the dry cut results) vs. sieve nominal aperture size: Jet pressure as parameter; anthracite (cleat parallel) coal; blunt pick.
Figure 6.75 Median particle size vs. jet pressure for the anthracite (cleat parallel) coal.
Figure 6.76 Median particle size vs. jet power for the anthracite (cleat parallel) coal.
Figure 6.77 Sieve analysis: Fraction % by mass vs. nominal aperture size with jet pressure as parameter; anthracite (cleat horizontal) coal; sharp pick.
Figure 6.78 Sieve analysis: Fraction % by mass vs. nominal aperture size with jet pressure as parameter; anthracite (cleat horizontal) coal; blunt pick.
Figure 6.79 % fraction difference (compared to the dry cut results) vs. sieve nominal aperture size: Jet pressure as parameter; anthracite (cleat horizontal) coal; sharp pick.
Figure 6.80 % fraction difference (compared to the dry cut results) vs. sieve nominal aperture size: Jet pressure as parameter; anthracite (cleat horizontal) coal; blunt pick.
Figure 6.81 Median particle size vs. jet pressure for the anthracite (cleat horizontal) coal.
Figure 6.82 Median particle size vs. jet power for the anthracite (cleat horizontal) coal.
Figure 6.83 Suggested breakout for cleat horizontally orientated and with high pressure water jet assistance.

Figure 7.1 Plan view of coal blocks used in Test Series One and Two.
Figure 7.2 Test Series One: Force vs. jet pressure: Erin coal; cleat parallel; sharp pick.
Figure 7.3 Test Series One: Force vs. jet pressure: Erin coal; cleat parallel; blunt pick.
Figure 7.4 Test Series One: Force vs. jet pressure: Erin coal; cleat horizontal; sharp pick.
Figure 7.5 Test Series One: Force vs. jet pressure: Erin coal; cleat horizontal; blunt pick.
Figure 7.6 Test Series One: Force vs. jet power: Erin coal; cleat parallel; sharp pick.
Figure 7.7 Test Series One: Force vs. jet power: Erin coal; cleat parallel; blunt pick.
Figure 7.8 Test Series One: % force decrease vs. jet pressure: Erin coal; cleat parallel; sharp pick.
Figure 7.9 Test Series One: % force increase vs. jet pressure: Erin coal; cleat parallel; blunt pick.
Figure 7.10 Test Series One: % force decrease vs. jet pressure: Erin coal; cleat horizontal; sharp pick.
Figure 7.11 Test Series One: % force increase vs. jet pressure: Erin coal; cleat horizontal; blunt pick.
Figure 7.12 Test Series One: Mean peak force vs. jet pressure: Erin coal; cleat parallel; sharp pick.
Figure 7.13 Test Series One: Mean peak force vs. jet pressure: Erin coal; cleat parallel; blunt pick.
Figure 7.14 Test Series One: Mean peak force vs. jet pressure: Erin coal; cleat horizontal; sharp pick.
Figure 7.15 Test Series One: Mean peak force vs. jet pressure: Erin coal; cleat horizontal; blunt pick.
Figure 7.16 Test Series One: % mean peak force decrease vs. jet pressure: Erin coal; cleat parallel; sharp pick.
Figure 7.17 Test Series One: % mean peak force increase vs. jet pressure: Erin coal; cleat parallel; blunt pick.
Figure 7.18 Test Series One: % mean peak force decrease vs. jet pressure: Erin coal; cleat horizontal; sharp pick.
Figure 7.19 Test Series One: % mean peak force increase vs. jet pressure: Erin coal; cleat horizontal; blunt pick.
Figure 7.20 Test Series One: Force vs. jet pressure: Erin coal; cleat parallel; sharp pick; with pre-cut slot.
Figure 7.21 Test Series One: Force vs. jet pressure: Erin coal; cleat horizontal; sharp pick; with pre-cut slot.
Figure 7.22 Test Series One: % force decrease vs. jet pressure: Erin coal; cleat parallel; sharp pick; with pre-cut slot.
Figure 7.23 Test Series One: % force decrease vs. jet pressure: Erin coal; cleat horizontal; sharp pick; with pre-cut slot.

Figure 7.24 Test Series One: Mean peak force vs. jet pressure: Erin coal; cleat parallel; sharp pick; with pre-cut slot.

Figure 7.25 Test Series One: Mean peak force vs. jet pressure: Erin coal; cleat horizontal; sharp pick; with pre-cut slot.

Figure 7.26 Test Series One: % mean peak force decrease vs. jet pressure: Erin coal; cleat parallel; sharp pick; with pre-cut slot.

Figure 7.27 Test Series One: % mean peak force decrease vs. jet pressure: Erin coal; cleat horizontal; sharp pick; with pre-cut slot.

Figure 7.28 Test Series One: Specific energy vs. jet pressure.

Figure 7.29 Test Series One: Specific energy vs. jet power.

Figure 7.30 Test Series One: Specific energy vs. jet pressure: Pre-cut slot tests.

Figure 7.31 Test Series One: Specific energy vs. jet power: Pre-cut slot tests.

Figure 7.32 Test Series One: Fraction % by mass vs. nominal aperture size with jet pressure as parameter; sharp pick.

Figure 7.33 Test Series One: Fraction % by mass vs. nominal aperture size with jet pressure as parameter; blunt pick.

Figure 7.34 Test Series One: % fraction difference (compared to the dry cut results) vs. sieve nominal aperture size: Jet pressure as parameter; sharp pick.

Figure 7.35 Test Series One: % fraction difference (compared to the dry cut results) vs. sieve nominal aperture size: Jet pressure as parameter; blunt pick.

Figure 7.36 Test Series One: Median particle size vs. jet pressure.

Figure 7.37 Test Series One: Median particle size vs. jet pressure. With pre-cut slot.

Figure 7.38 Test Series One: Fraction % by mass vs. nominal aperture size with jet pressure as parameter; sharp pick; with pre-cut slot.

Figure 7.40 Test Series Two: Force vs. offset distance: cleat parallel; sharp pick; 70MPa pressure; 2mm lead distance.

Figure 7.41 Test Series Two: Force vs. offset distance: cleat horizontal; sharp pick; 70MPa pressure; 2mm lead distance.

Figure 7.42 Test Series Two: Force vs. offset distance: cleat parallel; sharp pick; 70MPa pressure; 10mm lead distance.

Figure 7.43 Test Series Two: Force vs. offset distance: cleat horizontal; sharp pick; 70MPa pressure; 10mm lead distance.

Figure 7.44 Test Series Two: Force vs. offset distance: cleat parallel; sharp pick; 70MPa pressure; 50mm lead distance.

Figure 7.45 Test Series Two: Force vs. offset distance: cleat horizontal; sharp pick; 70MPa pressure; 50mm lead distance.

Figure 7.46 Test Series Two: Force vs. offset distance: cleat parallel; sharp pick; 70MPa pressure; 100mm lead distance.

Figure 7.47 Test Series Two: Force vs. offset distance: cleat horizontal; sharp pick; 70MPa pressure; 100mm lead distance.

Figure 7.48 Test Series Two: Force vs. lead distance: cleat parallel; sharp pick; 70MPa pressure; 0mm offset distance.

Figure 7.49 Test Series Two: Force vs. lead distance: cleat horizontal; sharp pick; 70MPa pressure; 0mm offset distance.

Figure 7.50 Test Series Two: Force vs. lead distance: cleat parallel; sharp pick; 70MPa pressure; 35mm offset distance.

Figure 7.51 Test Series Two: Force vs. lead distance: cleat horizontal; sharp pick; 70MPa pressure; 35mm offset distance.

Figure 7.52 Test Series Two: Force vs. lead distance: cleat parallel; sharp pick; 70MPa pressure; 50mm offset distance.

Figure 7.53 Test Series Two: Force vs. lead distance: cleat horizontal; sharp pick; 70MPa pressure; 50mm offset distance.

Figure 7.54 Test Series Two: Mean peak force vs. offset distance: cleat parallel; sharp pick; 70MPa pressure; 2mm lead distance.

Figure 7.55 Test Series Two: Mean peak force vs. offset distance: cleat horizontal; sharp pick; 70MPa pressure; 2mm lead distance.

Figure 7.56 Test Series Two: Mean peak force vs. offset distance: cleat parallel; sharp pick; 70MPa pressure; 10mm lead distance.

Figure 7.57 Test Series Two: Mean peak force vs. offset distance: cleat horizontal; sharp pick; 70MPa pressure; 10mm lead distance.

Figure 7.58 Test Series Two: Mean peak force vs. offset distance: cleat parallel; sharp pick; 70MPa pressure; 50mm lead distance.

Figure 7.59 Test Series Two: Mean peak force vs. offset distance: cleat horizontal; sharp pick; 70MPa pressure; 50mm lead distance.

Figure 7.60 Test Series Two: Mean peak force vs. offset distance: cleat parallel; sharp pick; 70MPa pressure; 100mm lead distance.

Figure 7.61 Test Series Two: Mean peak force vs. offset distance: cleat horizontal; sharp pick; 70MPa pressure; 100mm lead distance.

Figure 7.62 Test Series Two: Mean peak force vs. lead distance: cleat parallel; sharp pick; 70MPa pressure; 0mm offset distance.

Figure 7.63 Test Series Two: Mean peak force vs. lead distance: cleat horizontal; sharp pick; 70MPa pressure; 0mm offset distance.

Figure 7.64 Test Series Two: Mean peak force vs. lead distance: cleat parallel; sharp pick; 70MPa pressure; 35mm offset distance.

Figure 7.65 Test Series Two: Mean peak force vs. lead distance: cleat horizontal; sharp pick; 70MPa pressure; 35mm offset distance.

Figure 7.66 Test Series Two: Mean peak force vs. lead distance: cleat parallel; sharp pick; 70MPa pressure; 50mm offset distance.

Figure 7.67 Test Series Two: Mean peak force vs. lead distance: cleat horizontal; sharp pick; 70MPa pressure; 50mm offset distance.

Figure 7.68 Operational parameters in Test Series Two.

Figure 7.69 Test Series Two: Fraction % by mass vs. nominal aperture size with offset distance as parameter; sharp pick; 2mm lead distance.

Figure 7.70 Test Series Two: Fraction % by mass vs. nominal aperture size with offset distance as parameter; sharp pick; 10mm lead distance.

Figure 7.71 Test Series Two: Fraction % by mass vs. nominal aperture size with offset distance as parameter; sharp pick; 50mm lead distance.

Figure 7.72 Test Series Two: Fraction % by mass vs. nominal aperture size with offset distance as parameter; sharp pick; 100mm lead distance.

Figure 7.73 Test Series Two: Fraction % by mass vs. nominal aperture size with lead distance as parameter; sharp pick; 0mm offset distance.

Figure 7.74 Test Series Two: Fraction % by mass vs. nominal aperture size with lead distance as parameter; sharp pick; 35mm offset distance.

Figure 7.75 Test Series Two: Fraction % by mass vs. nominal aperture size with lead distance as parameter; sharp pick; 50mm offset distance.

Figure 7.76 Test Series Two: Median particle size vs. offset distance with lead distance as parameter; sharp pick.

Figure 7.77 Test Series Two: Median particle size vs. lead distance with offset distance as parameter; sharp pick.

Figure 8.1 Idealised mechanism of coal fracture with a radial pick.

Figure 8.2 Idealised mechanism of coal fracture showing path of jet.

List of Tables

Table 1.1	Coal size distributions produced by various coal winning machines and methods (After Summers and Summers, 1980).
Table 3.1	Factors that effect jet assisted cutting with levels for the experiment.
Table 3.2	Parameters to investigate the effect of coal strength.
Table 3.3	Parameters to investigate the effect of cleat orientation.
Table 3.4	Parameters and levels for jet penetration tests.
Table 4.1	The maximum volume of charge that may be put on a sieve.
Table 5.1	Results of jet penetration tests with the cleat parallel for Erin and anthracite coals.
Table 5.2	Two way table for the jet pressure and traverse speed.
Table 5.3	ANOVA table for the jet pressure and traverse speed.
Table 5.4	Two way table for the traverse speed and coal type.
Table 5.5	ANOVA table for the traverse speed and coal type.
Table 5.6	Two way table for the jet pressure and coal type.
Table 5.7	ANOVA table for the jet pressure and coal type.
Table 5.8	Complete ANOVA table for the Erin and anthracite coal tests.
Table 5.9	Results of jet penetration tests with the cleat parallel and horizontal for the anthracite coal.
Table 5.10	Complete ANOVA table for the anthracite coal tests.
Table 5.11	Equation fitting results summary from jet penetration tests.
Table 5.12	Equation fitting results from jet penetration tests in the Erin coal.
Table 5.13	Equation fitting results from jet penetration tests in the anthracite (cleat parallel).
Table 5.14	Equation fitting results from jet penetration tests in the anthracite (cleat horizontal).
Table 6.1	Basic factorial design for experiment with the Erin and anthracite coals.
Table 6.2-4	Mean normal, cutting and sideway force ANOVA tables for the Erin and anthracite tests.
Table 6.5-7	Mean peak normal, cutting and sideway force ANOVA tables for the Erin and anthracite tests.
Table 6.8	Basic factorial design for the cleat orientation experiment in the anthracite coal.
Table 6.9-11	Mean normal, cutting and sideway force ANOVA tables for the cleat orientation tests in the anthracite.
Table 6.12-14	Mean peak normal, cutting and sideway force ANOVA tables for the cleat orientation tests in the anthracite.
Table 7.1	Main parameters and levels of Test Series One.
Table 7.2	Main parameters and levels of Test Series Two.

Table 7.3	Basic factorial design for Test Series One.
Table 7.4-6	Mean normal, cutting and sideway force ANOVA tables for Test Series One.
Table 7.7-9	Mean peak normal, cutting and sideway force ANOVA tables for Test Series One.
Table 7.10	Basic factorial design for the pre-cut slot tests in Test Series One.
Table 7.11-13	Mean normal, cutting and sideway force ANOVA tables for the pre-cut slot tests in Test Series One.
Table 7.14-16	Mean peak normal, cutting and sideway force ANOVA tables for the pre-cut slot tests in Test Series One.
Table 7.17	Basic factorial design for Test Series Two.
Table 7.18-20	Mean normal, cutting and sideway force ANOVA tables for Test Series Two.
Table 7.21	Mean peak normal force ANOVA table for Test Series Two.

List of Plates

Plate 4.1	Main structure of linear cutting rig partially assembled.
Plate 4.2	Presswell 'hydraflo' 75kW high pressure intensifier type water pump.
Plate 4.3	Preparation and mounting of an anthracite coal specimen.
Plate 4.4	Coal sample cast in pitch and mounted on the rig ready for testing.
Plate 4.5	450mm diameter round hole sieves.
Plate 4.6	Sample divider.
Plate 4.7	Sieve vibrator for 200mm diameter sieves.
Plate 6.1-4	Breakout patterns for the sharp and blunt pick, 35MPa and 105MPa pressure treatments respectively, in the Erin coal.
Plate 6.5-8	Breakout patterns for the sharp and blunt pick dry cuts, and the sharp pick 70MPa treatment and the blunt pick 35MPa and 70MPa treatments respectively.
Plate 6.9-12	Breakout patterns for the sharp and blunt pick, dry and 35MPa pressure treatments respectively, in the anthracite (cleat horizontal).

NOMENCLATURE

The nomenclature used throughout the text is given below. Note that some terms have more than one definition but the appropriate meaning shall be apparant from the context.

A	Force acting on positive rake angle part of a cutting tool.
B	Force acting on the negative rake angle part of a cutting tool.
C	Force acting on the wear flat.
C_d	Nozzle coefficient of discharge.
d	Nozzle diameter; tool nominal depth of cut; shearer drum diameter; or the nominal sieve aperture size.
$d_{50\%}$	Median particle size.
D	Slot width or tool nominal depth of cut.
F	Friction force on the positive rake angle part of a cutting tool.
G	Friction force acting on the wear flat.
h	Slot depth (jet penetration).
I	Moment of inertia of a shearer drum.
F_{cj}, F_c	Resultant mean cutting force with, without jet assistance acting on a shearer drum.
F_{ck}	Average clearance kerf tool cutting force.
F_{cv}	Average vane tool cutting force.
F_{hj}, F_h	Shearer haulage force with, without jet assistance.
F_{nj}, F_n	Resultant mean normal force with, without jet assistance acting on a shearer drum.
F_{nk}	Average clearance kerf tool normal force.
F_{nv}	Average vane tool normal force.
g	Acceleration due to gravity.
M	Mass of shearer.
MCF	Mean cutting force.
MNF	Mean normal force.
MSF	Mean sideway force.
MPCF	Mean peak cutting force.
MPNF	Mean peak normal force.
MPSF	Mean peak sideway force.
n	Number of jets supplied with high pressure water.
N	Force acting on the zero rake angle part of a cutting tool.
p	Number of vane picks.
P	Jet stagnation pressure or the cumulative percentage undersize.
P_a	Atmospheric pressure.
P_e	Pressure loss between pump exit and nozzle exit.

P_{hsv}	Hollow shaft venturi pump power.
P_o	Jet stagnation pressure at the bottom of a slot.
P_w	Jet power.
q	Number of clearance kerf picks.
Q	Jet flow rate.
r	Ratio of the average clearance kerf tool cutting force to the vane tool cutting force.
R	Ratio of mean cutting force reduction due to jet assistance to the unassisted mean cutting force for a linear single pick test.
R_c	Ratio of the resultant drum cutting force reduction due to jet assistance to the unassisted drum cutting force.
R_h	Ratio of the shearer haulage force reduction due to jet assistance to the unassisted haulage force.
R_n	Ratio of the resultant drum normal force reduction due to jet assistance to the unassisted drum normal force.
R_t	Ratio of drum torque reduction due to jet assistance to the unassisted drum torque.
s	Ratio of the average clearance kerf tool normal force to the vane tool normal force.
S	Line spacing.
S_j, S	Shearer haulage speed with, without jet assistance.
SE_j, SE	Specific energy with, without jet assistance.
T_j, T	Drum torque with, without jet assistance.
V	Jet velocity.
v_t	Cutting speed.
V_t	Jet traverse speed.
w	Cutting tool width or drum angular rotational speed.
w_b	Web width.
Y_j, Y	Coal yield with, without jet assistance.
α	Angular acceleration of a shearer drum.
μ	Coefficient of friction.
ϕ	Jet inclination to the vertical in the plane at 90° to the traverse direction.
ρ	Density.
σ	Compressive stress.
σ_c	Unconfined compressive strength.
σ_o^2	Experimental error variance.
τ	Shear stress.
θ	Jet inclination to the vertical in the direction of travel.

CHAPTER ONE

1 INTRODUCTION

High pressure water jet assisted cutting has captured great interest in the mining industry since the mid 1970's. Its original application as such was to rock cutting with a view to improving the cutting performance and extending the operating range of boom type road-heading machines. A prototype machine was manufactured and trials carried out. On the basis of the results commercial roadheaders are now available.

The benefits derived by these machines have been documented throughout the literature: lower cutting forces; reduced vibration; longer pick life; reduced dust make amongst the important findings.

It is not too surprising then that investigations were begun into whether the technique could be applied to coal cutting and if similar benefits could be derived.

A preliminary investigation in to jet assisted coal cutting was conducted at the University of Newcastle upon Tyne, (Fowell and Johnson, 1984), and indicated that the cutting forces could be reduced, in the two coals tested, by jet assistance. Concurrently, a prototype coal cutting machine was being developed by British Coal for underground trials which subsequently took place at Golborne Colliery, in the then Western Area of British Coal. The trials below ground suggested that definite and quantitative benefit could be obtained from water jet assistance.

Tests were also being undertaken by the U.S. Bureau of Mines, using a prototype machine to cut simulated coal or 'coalcrete'. Underground trials were arranged and performed at Auguste Victoria Mine in the F.R.G. These tests revealed advantages from the hybrid cutting and that further trials were required.

From the British point of view, special interest lay in the influence jet assistance would have on the fines production. Summers and Summers (1980), produced Table 1.1 below which illustrates the coal size distributions produced by various coal winning machines and methods.

Size Hole (cm2)	Handfilled Coal (%)	Trepanner (%)	Conveyor Mounted Trepanner (%)	Shearer Loader (%)	Hydrominer (%)
+10	18.5	18.2	11.3	4.2	28.8
10.0 - 5.0	19.3	14.1	14.0	5.8	21.1
5.0 - 2.5	15.0	12.7	11.2	9.7	31.1
2.5 - 1.25	17.9	15.5	16.7	20.1	10.0
1.25 - 0	29.3	39.5	46.7	60.2	9.0
Total	100.0	100.0	100.0	100.0	100.0

Table 1.1

The size fractions indicate that a shearer loader produces a large proportion of small and fine coal. The fines in particular are a problem since they cost twice as much to wash and recover from the run-of-mine which obviously increases the cost of production.

It is in this environment that the present study was commissioned by British Coal, under the direction of the Rock Mechanics Branch, H.Q.T.D., Bretby.

The programme was carried out in the Department of Mining Engineering at the University of Newcastle upon Tyne. A 50 tonne linear planing rig, previously utilized for jet assisted hard rock cutting, was transported to the Department of Mining Engineering, erected in the laboratory and suitably modified.

Jet assisted cutting was performed up to pressures of 105MPa with varying flow rates and at a cutting speed of 1.1m/s, the fastest available to the linear rig. Two coals were tested, a coherent, shiny black anthracite and a heavily cleated, friable bituminous coal. A detailed description of the experimental design and procedure is given in the text.

A parallel series of coal cutting tests, carried out at British Coal's Swadlincote Test Site, were analysed in the Department and these comprise Test Series One and Two. The effect of different jet powers was examined and the influence of lead and offset distances at a jet pressure of 70MPa.

All the tests modelled as closely as possible a vane pick on a two start shearer drum. The parameters measured were the cutting forces in three orthogonal directions, the breakout patterns, specific energy and the coal size distributions. Cutting with a sharp and blunt tool and changing the cleat orientation of the coal allowed further comparisons to be made.

CHAPTER TWO

2 LITERATURE REVIEW

2.1 High Pressure Water Jet Assisted Coal Excavation

A review of the application of high pressure water jet assisted cutting to the conventional coal winning machines employed throughout the world is given below. The technology has also been utilized on tunnelling machines but that area shall not be considered here.

2.1.1 Drum Shearers

Shearer loaders are the predominant longwall mining machine. Although rarely achieved these machines are capable of excavating in excess of 20 000 tonnes per day and therefore have a tremendous potential to be exploited. The performance of these machines is largely governed by the design of the shearer drum and the type of cutting picks used (Pomeroy, 1968). Computer aided design has without doubt greatly increased the cutting and loading efficiencies of shearer drums (Morris, 1980), but the factor that has not changed dramatically is the cutting tool itself. The traditional tungsten carbide tipped pick has the following disadvantages (Kenny and Johnson, 1976; Kogelmann and Thimons, 1986):

- High cutting and thrust forces generated, particularly in the case of hard minerals;
- High total forces and torques exerted on the machine, requiring ever larger and heavier machines to be developed;
- High dynamic forces, shock loads, machine vibration - hence use of heavier components;
- Dust make during cutting;
- Friction at mineral/tool interface creating high temperatures and possibly sparking, thereby increasing the risk of a frictional ignition;
- High tool wear rate, particularly in the case of abrasive and hard minerals;

- High tool costs, especially in situations of a high wear rate;

- High proportion of fine material may be produced.

It has been shown that the above disadvantages can be reduced and in some cases almost entirely eliminated by applying high pressure water jets to roadheading machines (Clark, 1984; Morris and Tomlin, 1984; Pugh, 1986). If this can be observed in roadheading machines then why not shearer loaders?

In 1984, the U.S. Bureau of Mines equipped a longwall double ended ranging drum Joy 1-LS1 shearer, with a water jet assisted mechanical cutting system to investigate the effect this would have on machine performance, airborne dust make, and the size distribution of the coal produced (Kovscek et al, 1985).

These tests were not performed below ground but on the surface on a simulated coal block (coalcrete) composed of coal, flyash and concrete. The shearer cutting efficiency was determined by comparing the motor energy required to cut one ton of coalcrete when cutting 'dry', i.e. with normal dust suppression sprays at 1.3MPa pressure, and with high pressure water jet assistance.

No significant change in the shearer motor energy was observed as the water pressure was increased up to 41.4MPa. Airborne dust levels were reduced: Increasing the water pressure from 1.3MPa to 6.9MPa did not significantly reduce the dust make (only by 4.2%). However, a further increase from 6.9MPa to 20.7MPa rapidly reduced the levels (by 79.2% at 20.7MPa). A subsequent increase from 20.7MPa to 41.4MPa gave only slight additional decrease of dust make (from 79.2% to 80.4%). The median size of the coalcrete particles produced tended to increase with increasing water jet pressure.

In 1984, the Excavation and Tunnelling Equipment Corporation of State College, Pennsylvania, a subsidiary of Gebr. Eickhoff, was awarded a contract from the U.S. Bureau of Mines to develop and install below ground a shearer assisted with 70MPa pressure water jets (Nienhaus et al, 1986).

Underground trials took place at Auguste Victoria Mine, Marl, FRG. An Eickhoff EW-200/170-L was fitted with a purpose built drum. The drum incorporated a phasing system that delivered high pressure water only to the picks in the cut. The drum was divided into ten sectors but only five of these were supplied with high pressure water at a time, via manifolds and hoses. No information is given in the literature regarding the reliability of the phasing system.

Trial results indicate that only a minimal influence on the shearer motor energy was achieved by using water jet assistance, even though at 41.4MPa pressure, almost 33% of the total energy supplied during cutting was provided by the water jets.

Underground airborne dust levels were reduced 70% to 80% on raising the water pressure from 2.3MPa to 12.4MPa. A subsequent increase to 49.6MPa yielded no further significant benefit.

Similar effects on particle size to the surface trials in coalcrete were reported for the underground tests. The percentage of -6.3mm particles was reduced from 37% to 28%. An explanation for this phenomenon is that the jet flushes away the cut coal from the pick preventing further crushing, and since there is no cushion of broken coal infront of the pick, it can apply a direct force onto the unbroken coal surface which tends to produce less fines.

A concurrent study on the effects of temperature on a cutting tool indicated that the water jets improved the life of the picks. At a pick speed of 1.88m/s (370ft/min), the pick tip temperature was reduced from 350°C while cutting without jet assistance, to 120°C when

using jets at 44.8MPa pressure. This is illustrated in Fig.2.1. A qualitative assessment of this cooling effect was given: The mineworkers commented that the picks lasted twice as long before a change was necessary.

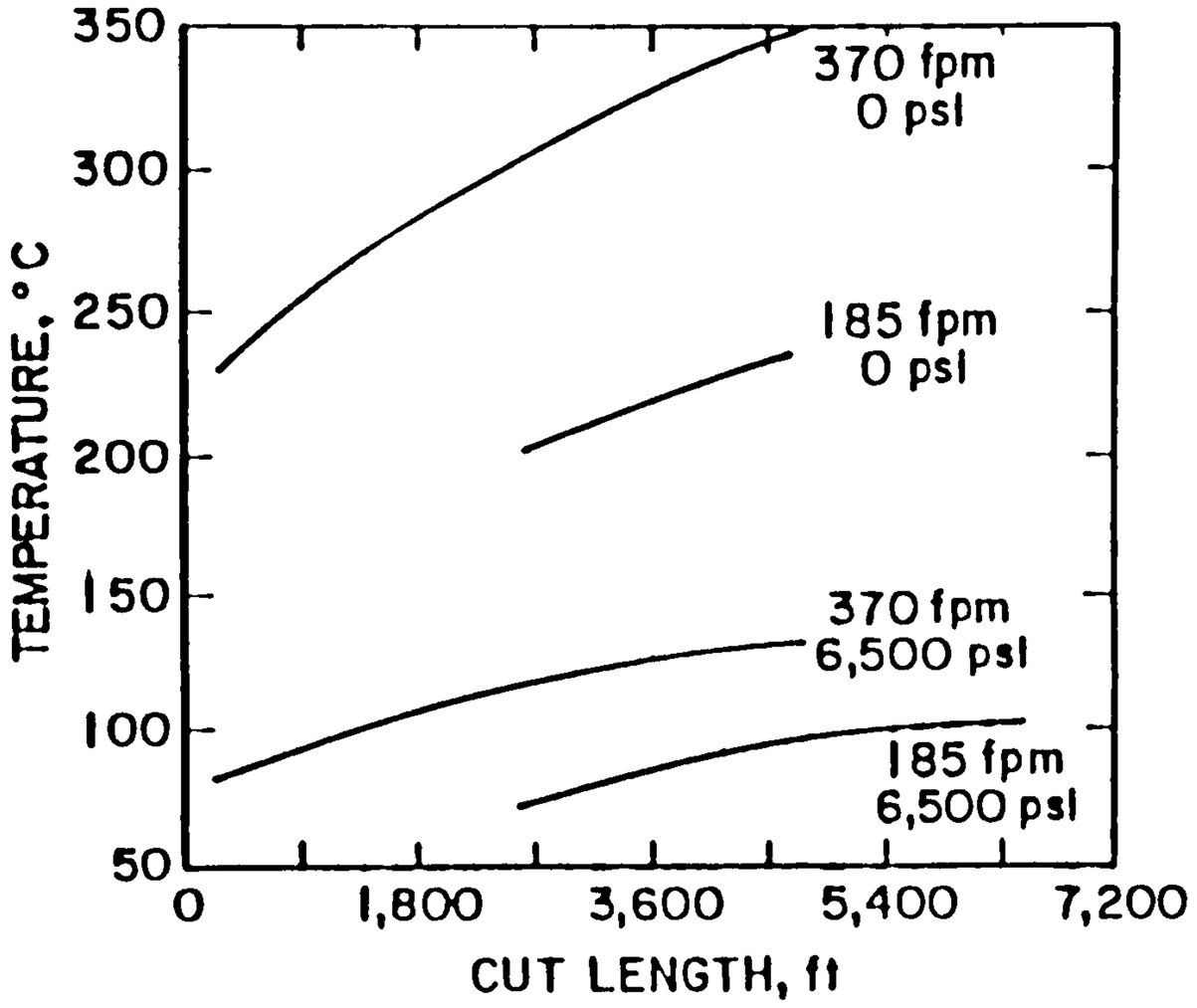


Fig.2.1 Bit temperature as a function of bit speed and water jet pressure.

From a safety viewpoint, the shearer driver had to wear protective glasses, a transparent shield was fitted between him and the drum and other personnel had to maintain a distance of 3.5m ahead of the cutting drum to avoid projectiles. The phased water supply helped in minimizing the danger from projectiles and the most vulnerable position was in working ahead of the drum (Taylor et al, 1989).

A qualifying statement must be made at this point about the underground trials. Two different designs of drum were used in the tests; one employing radial picks and one equipped with conical or pencil point picks. Other factors such as drum rotational speed and the number of picks varied also. Only the drum with conical picks was supplied with high pressure water

jets but comparisons were made between the two. The authors state that in the case of improved product size the benefit could be attributed to the greater depth of cut taken by the jet assisted drum as well as the jet assistance. In this respect then, the results are not entirely conclusive.

In the United Kingdom, similar research has been carried out by the British Coal Corporation. The primary objectives of this research were to:

- Improve the product size i.e. larger coal and less fines;
- Improve pick life;
- Reduce make of airborne dust; and
- Reduce power consumption and/or haulage force, leading to greater cutting rates and hence enhanced productivity.

Underground trials have been carried out at Golborne Colliery, with a 200kW Anderson Strathclyde AB16 SERDS. High pressure water jets up to a maximum of 69MPa were applied to the fifteen clearance ring tools of the drum.

The major aim was to reduce the percentage of fine coal produced. However, little improvement was observed when cutting with fifteen picks in the clearance ring. On reducing the number to nine, but still employing fifteen jets, fines production was decreased by 20% at 65.5MPa water pressure or 1% of the total product. Other results reported were (Mort, 1988):

- Up to 25% reduction in haulage force (depending on water jet pressure), thereby enabling the machine to cut faster. The haulage speed increased from 0.055m/s to 0.076m/s without stalling the machine;

- The total power consumption increased greatly with water pressure. However, a phased water system would alleviate this somewhat;

- The power consumption of the drum was reduced. This could extend gearhead life;

- Reduction in dust generation with an increase in water pressure, despite using 33% less water at 65.5MPa than with normal dust suppression sprays;

- Machine vibration was observed to be lower when using high pressure water;

- Due to the smoother and faster cutting machine, roof conditions were improved when moving through unstable ground.

Suggested aspects that need to be investigated include optimizing the shearer drum with respect to the greater haulage rates possible; the determination of the optimum number of high pressure water jet assisted picks on the clearance ring; and the manufacture of a complete high pressure water jet equipped machine rather than retrofitted apparatus.

Pugh (1986) reported the intention of the then Western Area of British Coal, to install several longwall shearers equipped with high pressure water jets. One reason for this is the reduced risk of frictional ignition it is thought these machines would offer. The friction at the pick/mineral interface creates high temperatures which in certain conditions may cause an ignition of methane or an explosion (Kenny and Johnson, 1977; Truemann, 1985). This hazard may be totally eliminated provided a water jet is directed immediately behind the cutter pick and has sufficient power to reach the critical hot zone which causes the danger. This application has particular relevance to seams designated with a high ignition temperature potential (Pugh, 1986; Singhal et al, 1987).

Research into applying high pressure water jets to shearers in the U.S.S.R. has been carried out and reports claim that the jets reduce the dust content in the air and the proportion of fines produced (+25mm size fraction increased by 70%) (Kouzmich and Tolchenkin, 1985).

In summary a water jet assisted shearer potentially offers the following advantages:

- Coarser coal and less fines which should reduce coal preparation costs and provide a more valuable commodity;
- Dust reductions of as much as 80%, especially in the -5 micron respirable quartz dust;
- Lower bit costs and greater machine availability through reduced tool wear (fewer bit changes);
- Reduced frictional ignition hazard, particularly if the jet is impinged immediately behind the bit tip;
- No increase in water consumption over the conventional dust suppression sprays especially if a phasing system is utilized;
- Less cutting vibration which should reduce maintenance costs and extend the shearer's lifetime;
- Increased rock cutting capability for mining through faults and rock bands.

However, the major disadvantage that could outweigh the above factors is the great amount of energy required to provide water jet assistance, which considering the already high cost of a typical heavy duty longwall installation (approximately £8m upwards), is very significant.

2.1.2 Coal Ploughs

Much of the early work with water jet assisted coal cutting was carried out on the coal plough. It was hoped that a jet assisted plough would be able to cut a wider web during each pass. Research in Poland, resulted in trials at Rymer Colliery in 1965 where excavation rates of 250 t/hr were achieved with a jet assisted plough (Souder and Evans, 1983).

In Germany, two experimental jet systems were investigated at the surface testing site of Bergbau-Forschung GmbH. Essen (Henkel, 1980). One was based on the Gleithobel plough design. The plough was assisted by a number of jets (up to 16) at 70MPa pressure. The resultant machine called the Hydrohobel, has undergone both surface and underground trials. The surface trials, in a simulated coal face, indicated that a 10% reduction in normal cutting forces was possible. Underground tests were conducted at Lohberg Colliery. Fig.2.2, shows that an improved cutting performance was achieved with the Hydrohobel

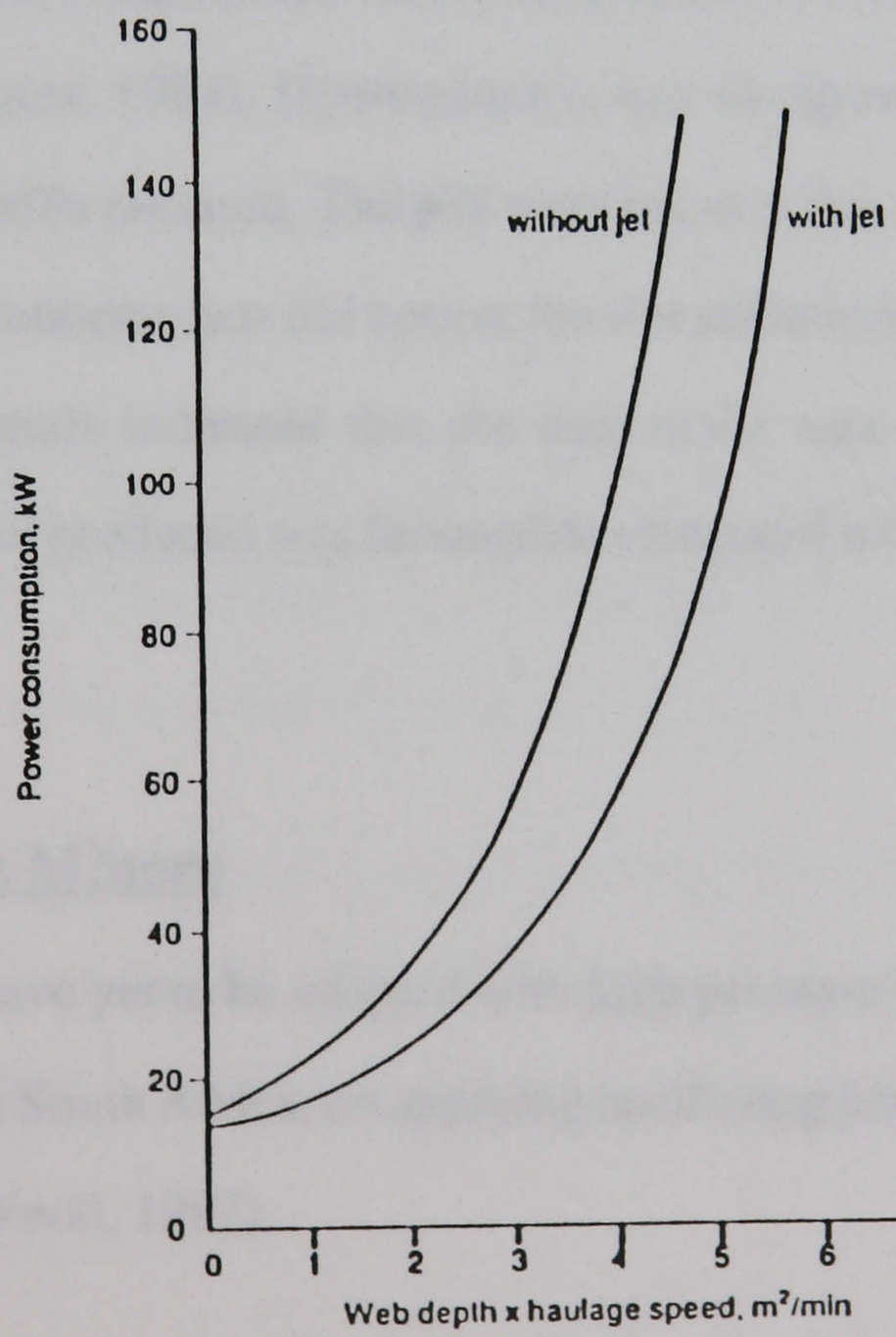


Fig. 2.2 Relationship between power consumption and cutting performance (Henkel and Kraemer, 1982)

over the conventional Gleithobel. However, the energy requirements of the high pressure water system are not included in the graph and thus the results were not entirely encouraging (Henkel and Kraemer, 1981). Two significant observations made were that the Hydrohobel produced considerably less dust and a larger particle size.

The second system employed fewer jets but these were oscillated in the vertical plane. Oscillating jets at 70MPa would cut a slot in the coal for the plough to advance in to and prise the coal off the face. This machine, called the Jet-miner, can take a web depth of 0.3m. Trial results showed that dust production was reduced and the coal size was larger than that produced by an ordinary plough (Henkel and Kraemer, 1981; Henkel, 1984). Problems with the machine were guidance difficulties; the unsatisfactory cutting of stone bands; the jet oscillating mechanism; and problems cutting through faults. Research into the Jet-miner is continuing (Wood, 1987).

Research in the U.S.A. concentrated on the development of the Hydrominer (Summers and Barker, 1978; Summers, 1984). Hydrominer I, was designed to operate in a seam 1.37m high using jets at 70MPa pressure. The jets were to cut a slot and slice off the coal from the face. However, the stationary jets did not cut the slot sufficiently and so oscillating jets were employed. Surface trials indicated that the dust make was greatly reduced and the size distribution of the coal produced was favourable compared to that of other mining machines - see Table 1.1.

2.1.3 Continuous Miners

Continuous miners have yet to be adapted with high pressure water jets. However, research is being conducted in South Africa, on applying oscillating jets at between 100 and 200MPa to these machines (Wood, 1987).

2.2 Coal Cutting Theory

The most widely accepted and documented coal cutting theory is that proposed by Evans, concerning his experiments on driving wedges into buttocks of coal (Evans, 1962). Fracture is caused by the pick creating a tensile force in the coal large enough to propagate cracks over a curved failure plane. Hence the breakage is tensile and the force required to cut the coal is proportional to its tensile strength.

The theory has been expanded by Evans over the years to cover blunt wedges (Evans, 1965) and the tensile failure mechanism has been applied to rock cutting with point attack tools (Hurt and Evans, 1981). Roxborough, has also successfully applied and extended the theory to rock cutting (Roxborough, 1973).

Nishimatsu (1972), detailed a theory on rock cutting whereby the tool creates a 'built-up edge' of finely crushed rock on its face. This crushed material generates the stresses that lead to crack propagation and rock failure along a failure plane. The stresses acting on the failure plane at the point of fracture are determined from Mohr's envelopes for the rock. Hence, the force required to cut the rock is proportional to its shear strength and indeed the rock fails under a shear force.

The two theories differ then in the manner of failure but Nishimatsu, gives a very comprehensive description of the cycle of rock cutting that accounts both for the chips produced and for the sizeable amount of crushed material produced.

Other important factors relating to coal cutting and cutting efficiency are extensively covered elsewhere (Pomeroy and Brown, 1968; Pomeroy, 1963). These factors include pick type, geometry and size, depth of cut, line spacing, and cutting speed.

2.3 High Pressure Water Jet Technology

2.3.1 Fluid Mechanics of Water Jets

The fluid mechanics of a water jet is governed by Bernoulli's equation relating pressure to jet velocity:

$$P = P_a + \frac{\rho V^2}{2} + P_e \qquad (2.1)$$

Where

P = Nozzle stagnation pressure

P_a = Atmospheric pressure

P_e = Pressure loss between pump exit and nozzle exit

ρ = Density of fluid

V = Jet velocity

At high pressures the pressure loss can be considered negligible and therefore the above equation reduces to:

$$P = \frac{\rho V^2}{2} \quad \Rightarrow \quad V = \left(\frac{2P}{\rho} \right)^{0.5} \qquad (2.2)$$

Assuming the fluid remains virtually incompressible, the jet flow rate may be determined by:

$$Q = C_d \frac{\pi d^2}{4} V \qquad (2.3)$$

Where Q = Jet flow rate

d = Nozzle diameter

V = Jet velocity

C_d = Nozzle coefficient of discharge

Also,

$$\text{Jet Power} = PQ = C_d \frac{\pi d^2}{4} P^{1.5} d^2 = C_d \frac{\pi \rho}{8} d^2 V^3 \qquad (2.4)$$

Fig.2.3, shows the structure of a high pressure water jet in air (Yanaida and Ohashi, 1980). One can see that the jet is initially coherent in the vicinity of the nozzle, becomes unstable as the distance from the nozzle increases and eventually breaks up into droplets.

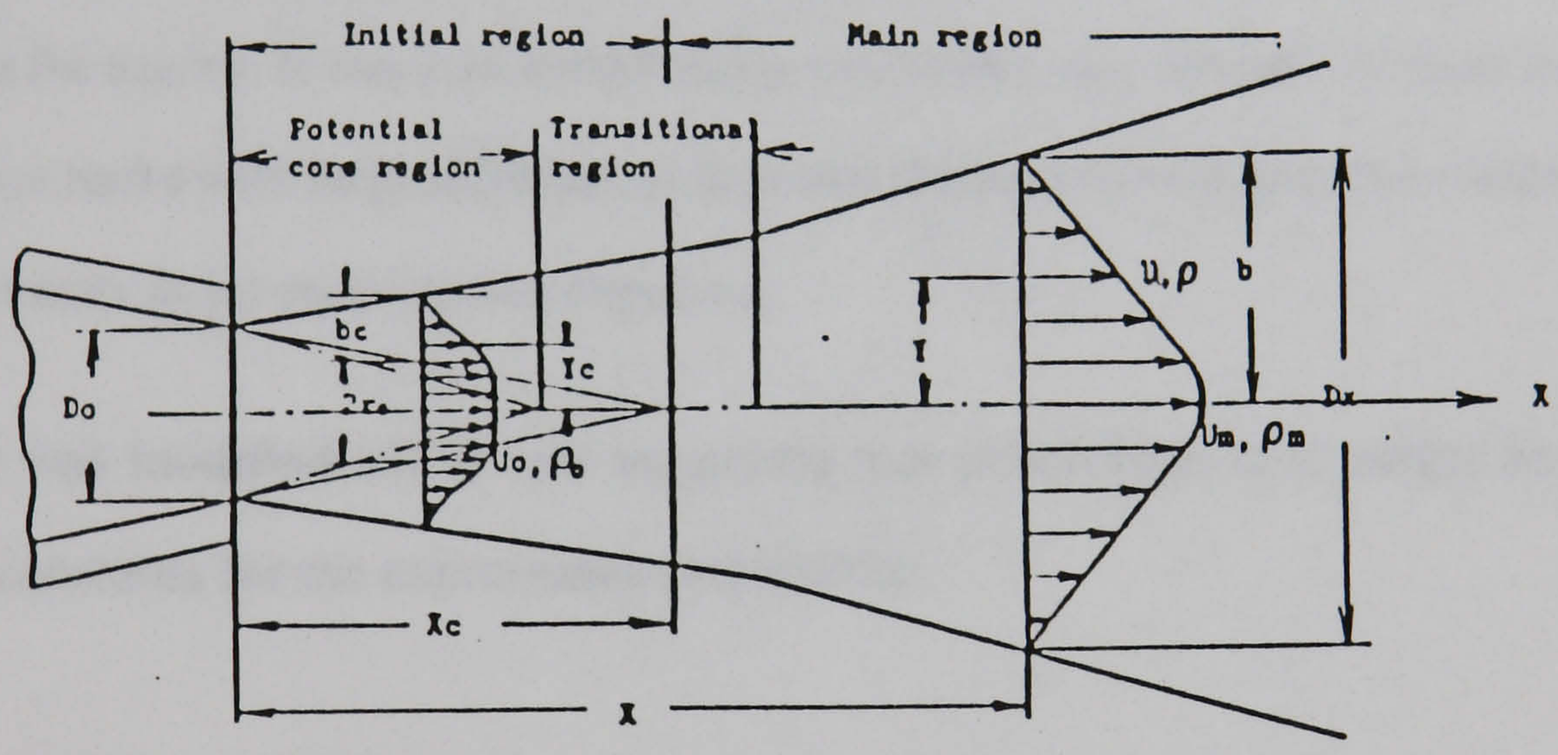


Fig.2.3 Jet Structure

Infact the structure of the jet is divided into three zones: the initial region characterised by having a constant axial dynamic pressure; the main region which has a constant axial velocity; and the final region where the jet diffuses. From this we can see that the pressure of a jet decreases as the distance from the nozzle increases, hence the stand-off distance has an effect on the penetrating ability of a jet.

2.3.2 Water Jet Cutting Theories

2.3.2.1 Crow's Theory

Crow (1973), developed a theory to explain the cutting action of a continuous water jet. Basically, the jet hits the rock at an angle and curves against the granular rock surface. Cavitation bubbles would cover the rock surface but the curvature of the jet stream causes sufficient water pressure to close the bubbles and expose the grains of the rock to direct impact from the water. The water pressure exerts a force acting normally on the rock grains which would keep the grains in their sockets if it were not for the fact that water, under pressure, could permeate beneath the surface of the rock and balance the forces. This allows frictional forces acting on the grains to remove them.

Crow, developed an expression to predict the kerf depth and performed experiments on four rocks to test the theory. It was concluded that permeability was not as important as originally thought since rocks with large differences in permeabilities did not give the correspondingly large differences in jet penetrations expected.

The theory was modified and it was suggested that penetration tests might be needed to determine constants for the expressions empirically.

2.3.2.2 Rehbinder's Theory

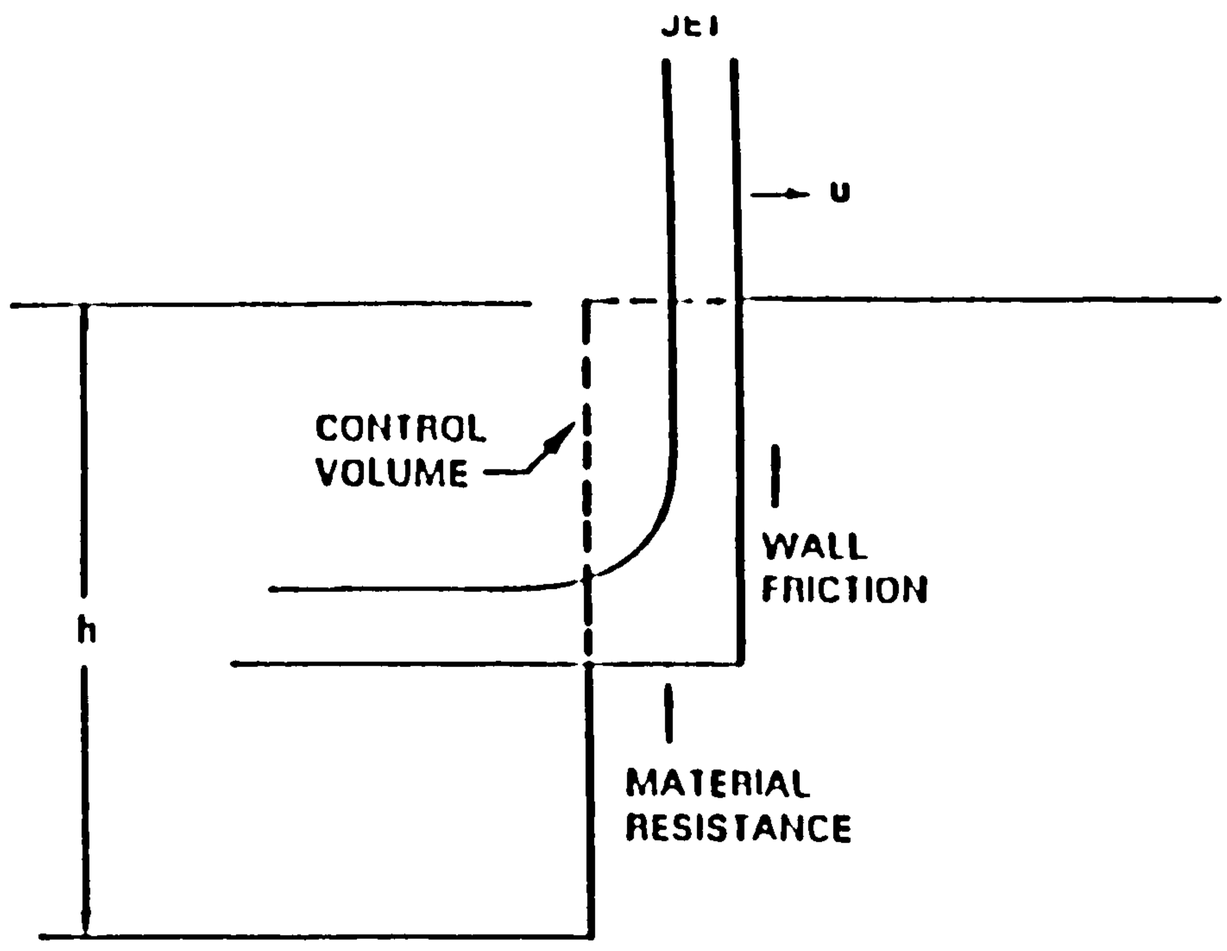
Rehbinder (1977), developed a theory utilizing Darcy's law of a fluid flowing through a porous medium. The cutting process is by erosion rather than hydraulic fracturing and factors such as rock compressive strength, tensile strength, etc., do not enter the theory explicitly but, Rehbinder states, would be represented implicitly through the jet threshold pressure required to penetrate the rock.

To use the prediction formula one has to carry out an experiment, on the particular rock, to determine its threshold pressure, permeability, grain size and a constant of proportionality.

The fact that viscosity is included in the derived expressions means the theory may be applied to cutting fluids in addition to water.

2.3.2.3 Hashish - Du Plessis' Theory

Hashish and Du Plessis (1978), derived what is commonly called the 'General Cutting Equation'. The equation is based on an analysis of an idealised control volume as shown in Fig.2.5.



Control Volume of Jet Penetration

Fig.2.4 Illustration of Hashish - du Plessis' Jet Cutting Theory (after Hashish 1981).

The forces acting on the control surfaces are F_{mech}, the resistance of the material to fracture, and F_{sh}, the friction force acting along the wall of the kerf. The depth of cut in a time interval t, was found by equating the momentum equation for the fluid passing through the control volume to their expression for the rock resistance to failure.

The theory predicts the depth and width of cut, volume removed and the hydraulic specific energy. A reference experiment has to be carried out to find certain constants for each material.

2.3.2.4 Empirical Approach

Due to the difficulty of incorporating all of the jet parameters, operational parameters, the relevant rock properties into a theoretical model, and the need to carry out rock characterising experiments anyway, empirical equations have been developed.

The 'Dimensionless Cutting Equation' was proposed by Nikonov (1971), and Nikonov and Golden (1972). This is based on the Russian data for coal cutting by continuous, fine, high pressure water jets. The equation is:

$$\frac{h}{d} = 0.5\left(\frac{P}{\sigma_c} - 0.2\right)\left(\frac{V_t}{V}\right)^{-0.5} \tag{2.5}$$

Where

h = Slot depth

d = Nozzle diameter

P = Jet pressure

σ_c = Unconfined compressive strength

V_t = Traverse velocity

V = Jet speed

Cooley (1980), used data from various researchers and suggested a modified dimensionless cutting equation as follows:

$$\frac{h}{d} = B\left(\frac{P}{\sigma_c} - 0.2\right)\left(\frac{V_t}{V}\right)^{-m} \tag{2.6}$$

Where B = Constant for each material

m = Constant, equal to 0.5 for coal and generally between 0.5 and 1.0 for other materials

The equation is valid for stand-off distances less than 100 nozzle diameters.

Kuzmich (1972) and Kuzmich et al (1982), also modified the equation for water jet rock cutting as below:

$$\frac{h}{d} = 0.11\left(\frac{P}{\sigma_c}\right)^{0.75}\left(\frac{V_t}{V}\right)^{0.5} \tag{2.7}$$

Ip (1986) has postulated a modified Kuzmich equation as shown below:

$$\frac{h}{d} = B\left(\frac{P}{\sigma_c}\right)^{m}\left(\frac{V_t}{V}\right)^{n} \tag{2.8}$$

Where B, m and n are constants for each material.

2.3.3 Water Jet Cutting

The cutting action of a water jet on a material is influenced by the characteristics of the jet, how it is applied, and the properties of the material being cut.

2.3.3.1 Jet Characteristics

The parameters that affect the cutting characteristics of a water jet are listed below:

i) Type of Jet

a. Continuous - this type of jet should produce an unbroken jet stream of constant pressure, hitting the target material. In reality due to the kinds of pumps producing the jet, the pressure is not constant and exerts a fluctuating force on the target. This type of jet is utilized on roadheading machines and shearers.

b. Interrupted - these jets consist of a series of discrete slugs of water. As one slug hits the target it should have dissipated out the way of the succeeding slug, thereby avoiding the cushioning effect experienced in stationary continuous jets, and repeatedly subjecting the target to water hammer.

c. Cavitating jets - cavitation bubbles are generated in the jet stream as it passes through the nozzle. The bubbles collapse as they hit the target transmitting high forces. Cavitation jets have been employed in the laboratory to cut coal (Conn and Rudy, 1978). It was concluded that the 'Cavijet', could cut a slot to a similar depth as a non-cavitating one but requiring one fifth the pressure.

d. Abrasive entrained jets - small particles of abrasive material are introduced into the jet usually downstream of the nozzle (thereby minimizing the wear on the nozzle). The abrasive elements assist the cutting action by hitting and wearing away the target material.

Many abrasives have been tested (Baumann et al, 1986). The choice depends to a large extent on the hardness of the material to be cut, e.g. silica sand may not furnish the required depth

of cut in rock and therefore one might opt for garnet or aluminium oxide (Nakaya et al, 1984). A five-fold increase in the penetration over continuous jets has been reported (Reichman, 1984).

e. Pulsed jets - jets of short duration are produced at very high pressures (up to 690MPa) and velocities, which shatter the target by water hammer (Vallve et al, 1980).

ii) Nozzle Material

Nozzles are manufactured from various materials including: stainless steel; tungsten carbide; synthetic sapphire; or ruby (corundum). The material chosen depends to a large degree on the pressure of the jet. For example, at very high pressures a hard nozzle material e.g. Corundum, is required otherwise the nozzle will wear quickly and its efficiency seriously impaired. Hence, stainless steel is used for low and medium pressure applications whilst tungsten carbide for medium to high. However, at very high pressures, tungsten carbide nozzles wear rapidly due to its soft cobalt matrix.

Corundum may be used at very high pressures since it is an extremely hard, abrasion resistant material. It can also suffer most chemical reagents. It has a fine surface finish, which affects the efficiency of a nozzle (Summers, 1983), and a precise nozzle diameter can be made. Consequently, ruby and sapphire are good materials to use when making small diameter nozzles.

Tungsten carbide nozzles will last about 200 hours at 70MPa pressure whereas sapphire ones survive 1000 hours (Kogelmann, 1986).

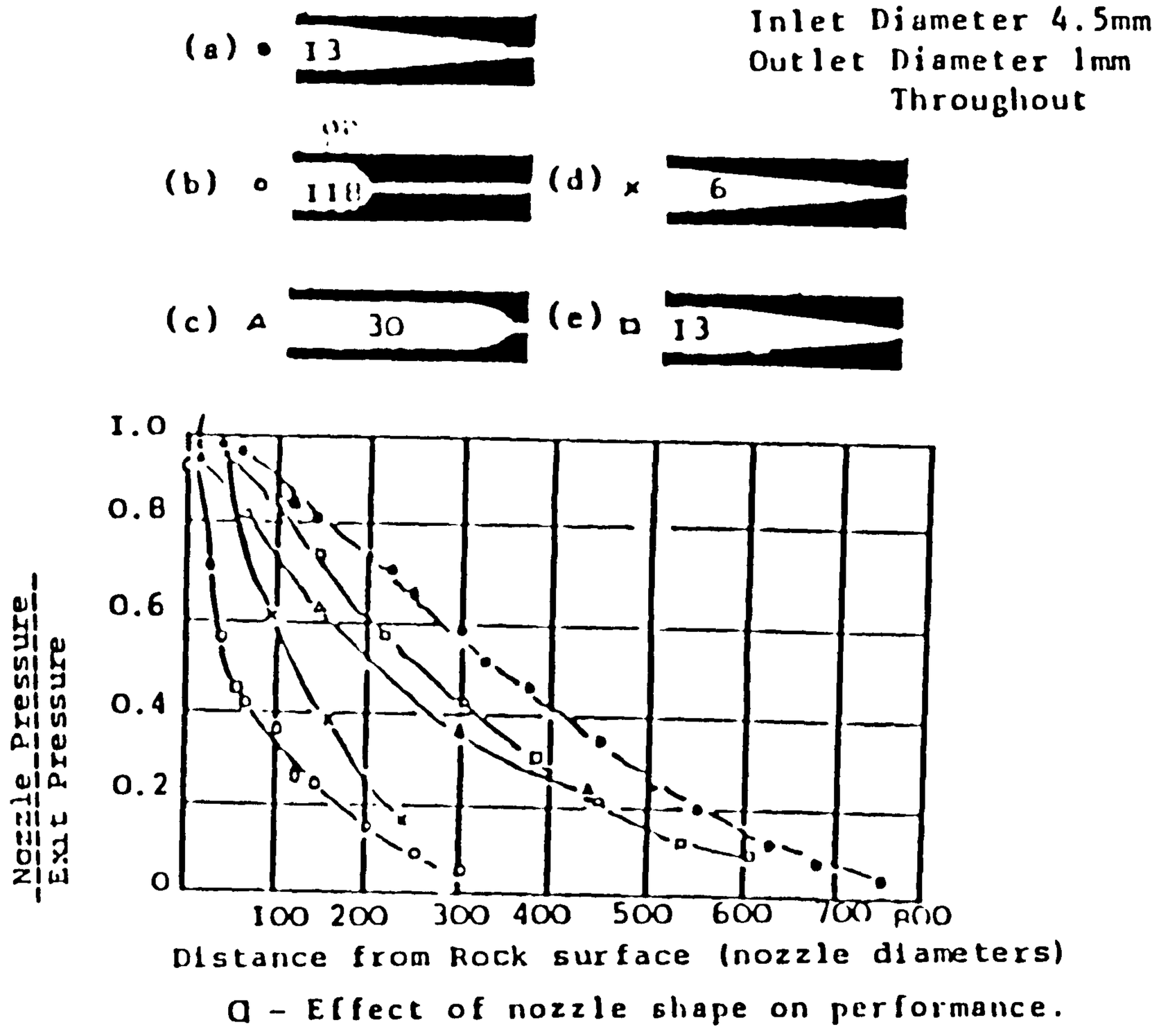
iii) Nozzle Design

The effect of nozzle design is illustrated in Fig.2.5. Five different nozzle shapes are shown with their corresponding performance characteristics (Leach and Walker, 1966). Nozzle (a) is the most efficient design which corroborates research carried out elsewhere (Shavlovsky, 1972). The best design appears to be that shown in Fig.2.6, with a convergence angle of 13° followed by a straight section of 2-4 times the nozzle diameter. Fig.2.6a, indicates the influence the convergence angle has on the discharge coefficient of a nozzle (Summers, 1984); again a small convergence angle is intimated.

Another factor affecting jet efficiency is the straightness of the flow entering the nozzle. Reports claim (Summers, 1984) that by endeavouring to ensure the piping immediately behind the nozzle is straight and aligned with the nozzle axis for at least 100 pipe diameters, the nozzle efficiency can be significantly increased.

iv) Jet Additive

Substances such as glycerin, sodium carboxymethyl cellulose, detergent, and long chain water soluble polymers e.g. polyethylene (Polyox), have been used as additives in water jets and their effect examined. Generally they have had a beneficial effect, making the jet more coherent and more powerful. For example, by adding high molecular weight polymers the penetration depth may be increased by 70% (Baumann and Henneke, 1980).



Q - Effect of nozzle shape on performance.

(after Leach and Walker)

Fig.2.5

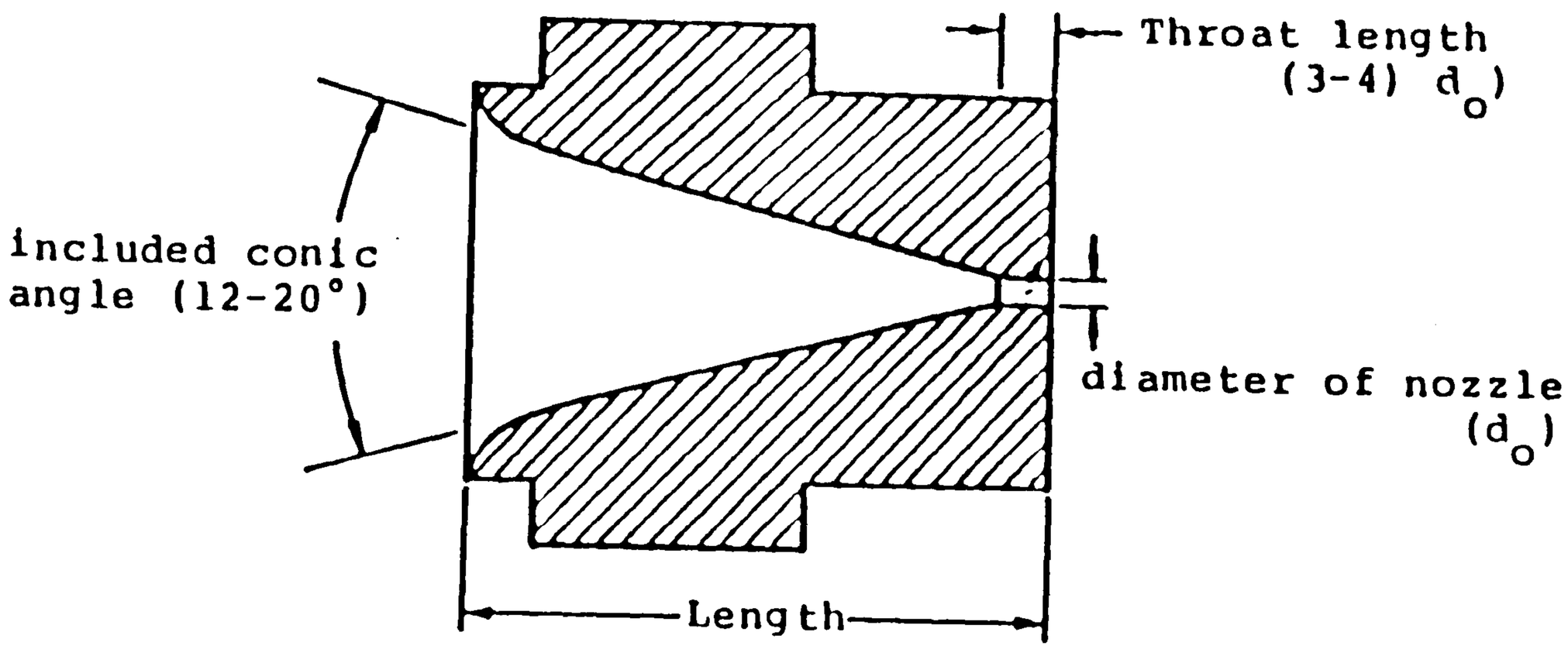


Fig.2.6 Typical nozzle geometry.

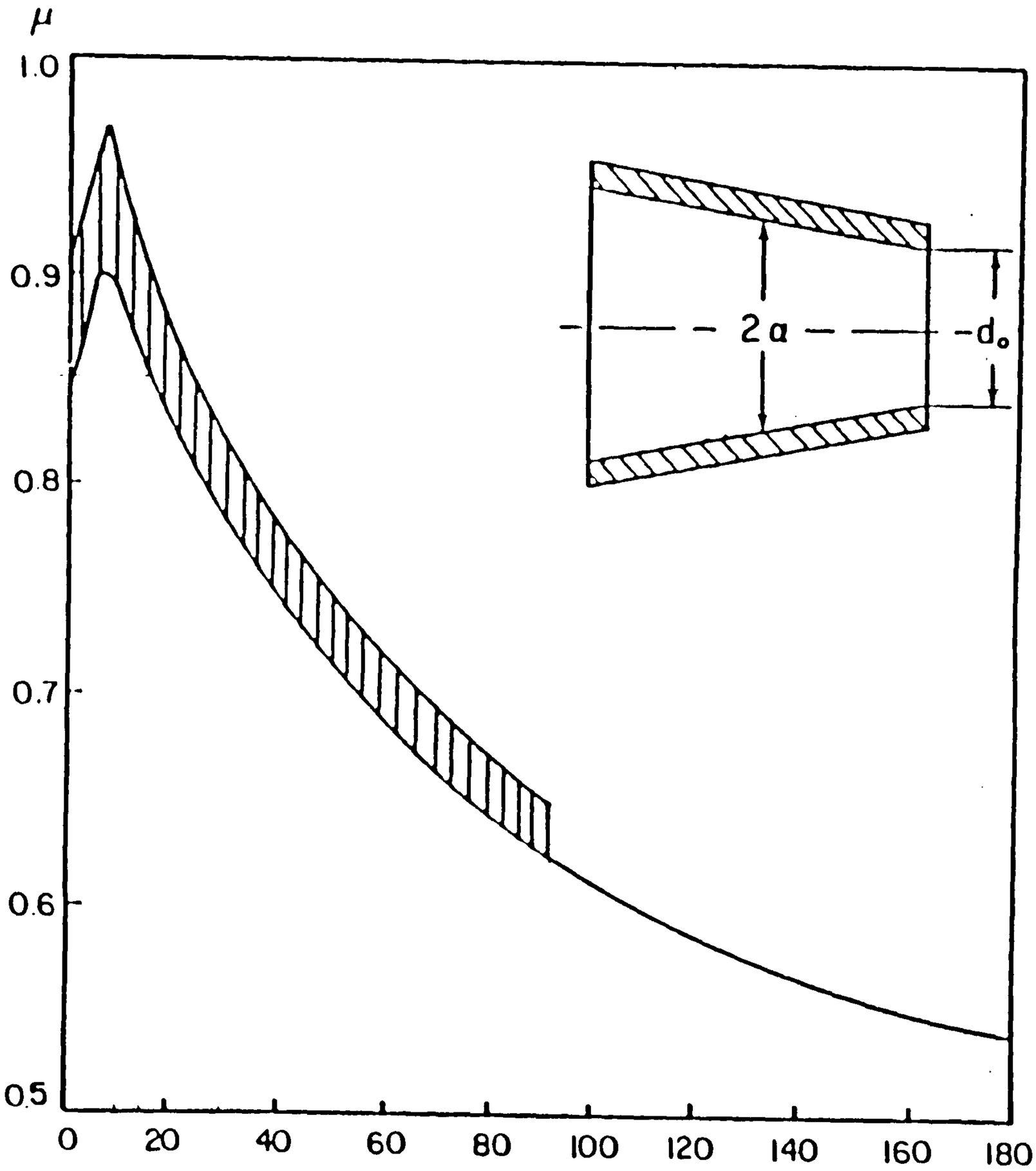


Fig.2.6a The effect of included angle on the coefficient of discharge, after Yufin.

v) Nozzle Flow Rate (Diameter) and Pressure

Expressions for jet pressure and flow rate are given below:

$$P = \frac{V^2}{2\rho} \qquad \text{and} \qquad Q = C_d \frac{\pi d^2}{4} V \tag{2.9}$$

Where, P = Pressure V = Exit velocity

Q = Flow rate C_d = Coefficient of discharge

ρ = Fluid density

Note that the formulae have a common factor in the jet velocity. Hence, it is difficult to consider these parameters separately since they are not independent of each other.

The influence of nozzle diameter and pressure on the mean depth of penetration in a sub-bituminous coal are given in Fig.2.7-8, (Evener and Tooley, 1985). The results are for a slow traverse speed of 0.1m/s and low jet pressures. Fig.2.9, illustrates penetration results for two bituminous coals at higher jet pressures and with a sandstone for comparison (Fowell and Johnson, 1984). A definite threshold pressure is only suggested for the sandstone and other workers have found the form of the relationship between penetration and jet pressure as in Fig.2.10 (Harris and Mellor, 1974).

2.3.3.2 Operational Parameters

Fig.2.11 illustrates the main operational parameters involved with high pressure water jet assisted cutting.

i) Stand-off Distance

Fig.2.12 indicates the relationship between stand-off distance and the depth of slot cut by jets of 0.3mm diameter but at different pressures in a sub-bituminous coal (Du Plessis and

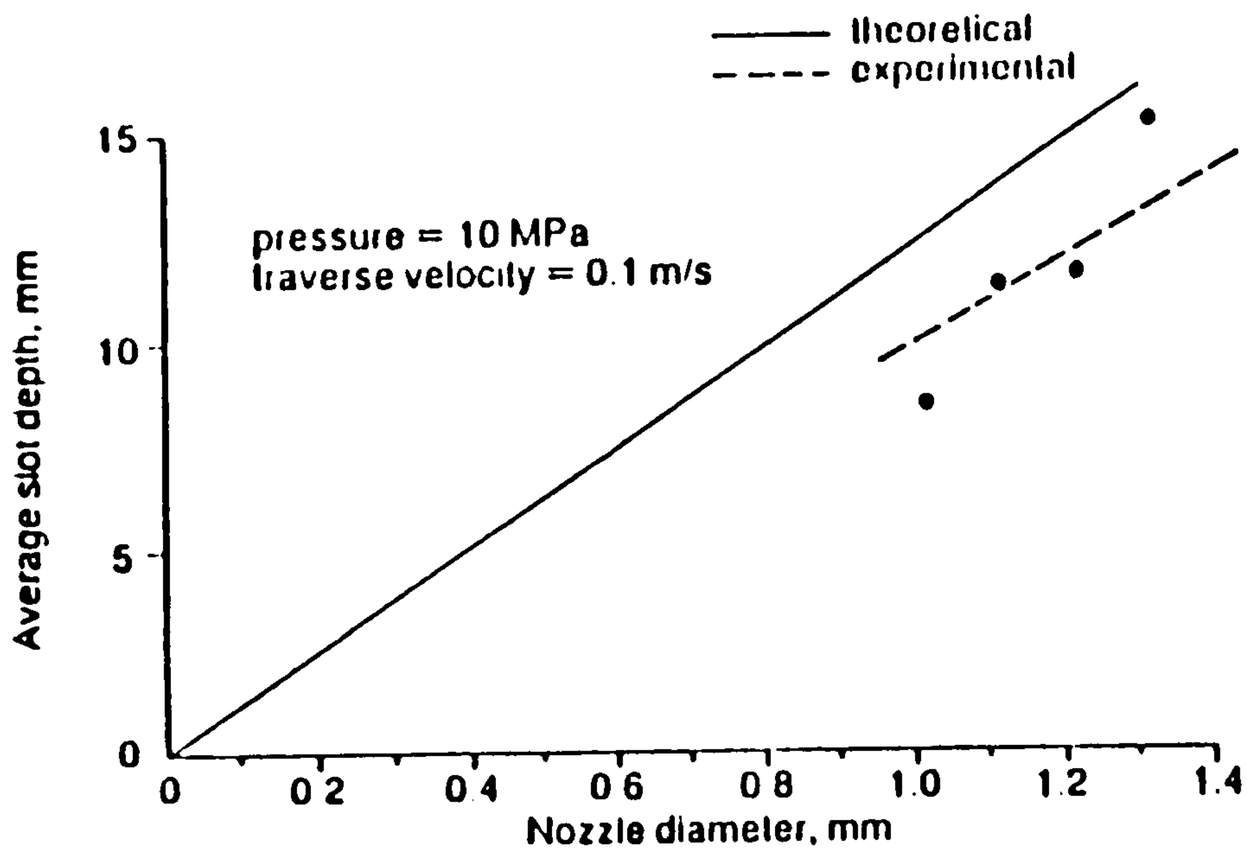


Fig.2.7 **Influence of nozzle diameter on depth of cut in coal (Enever and Tooley, 1985)**

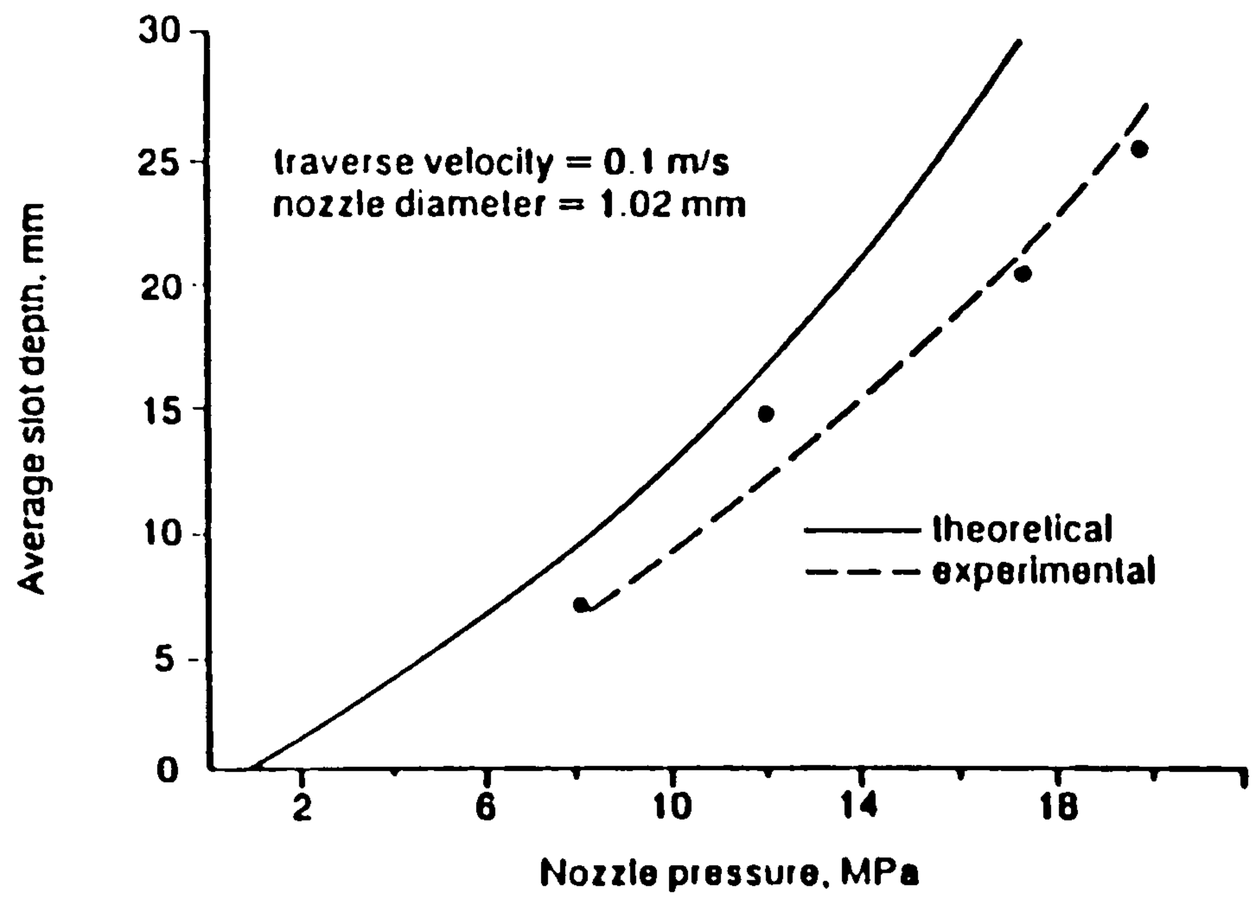
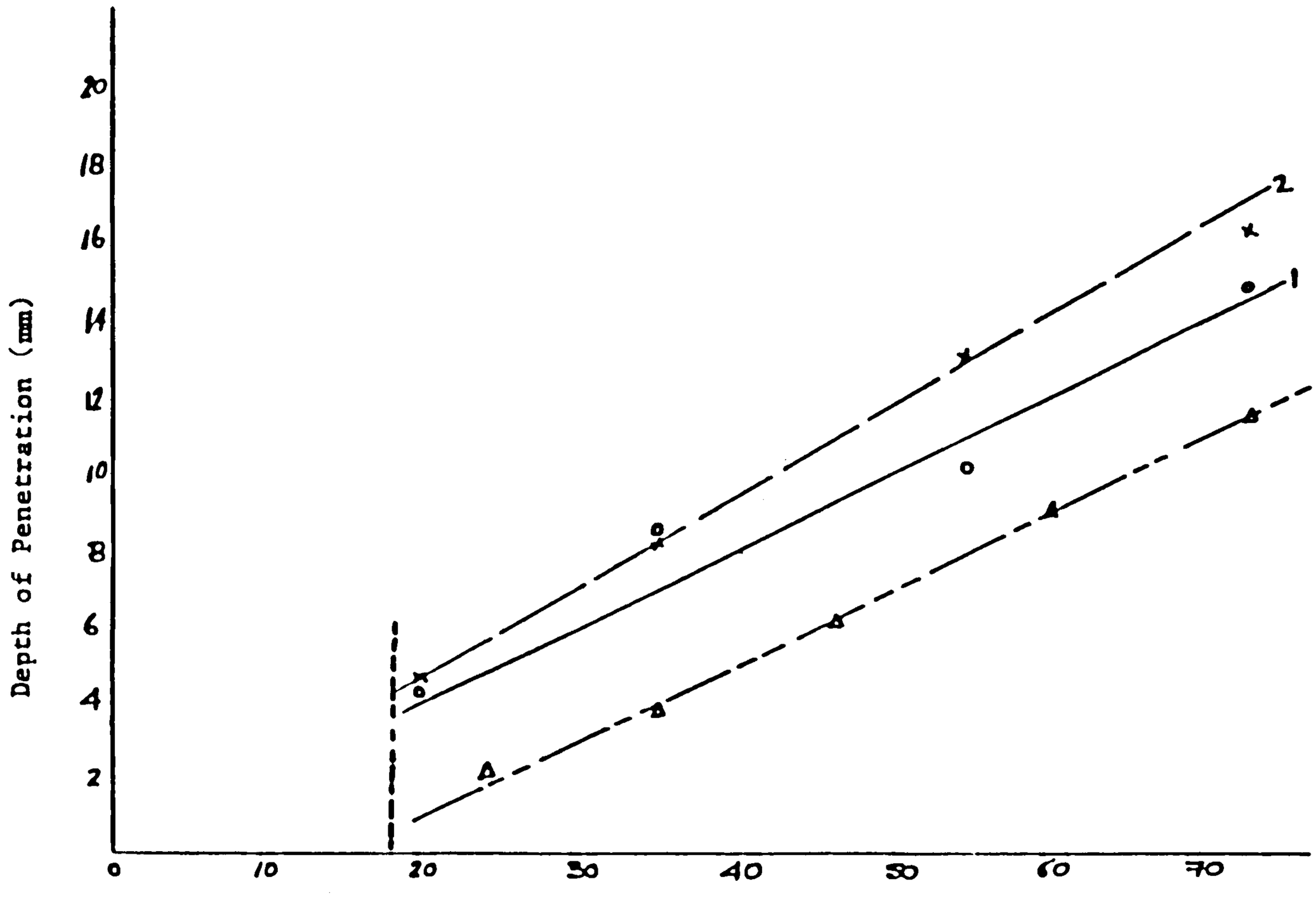


Fig.2.8 **Influence of nozzle pressure on depth of cut in coal (Enever and Tooley, 1985)**

Key: O = Block 1)
X = Block 2) Coal
Δ = Dumfries Sandstone.



Jet Pressure (MPa)

Fig.2.9 Depth of Jet Penetration vs. Jet Pressure

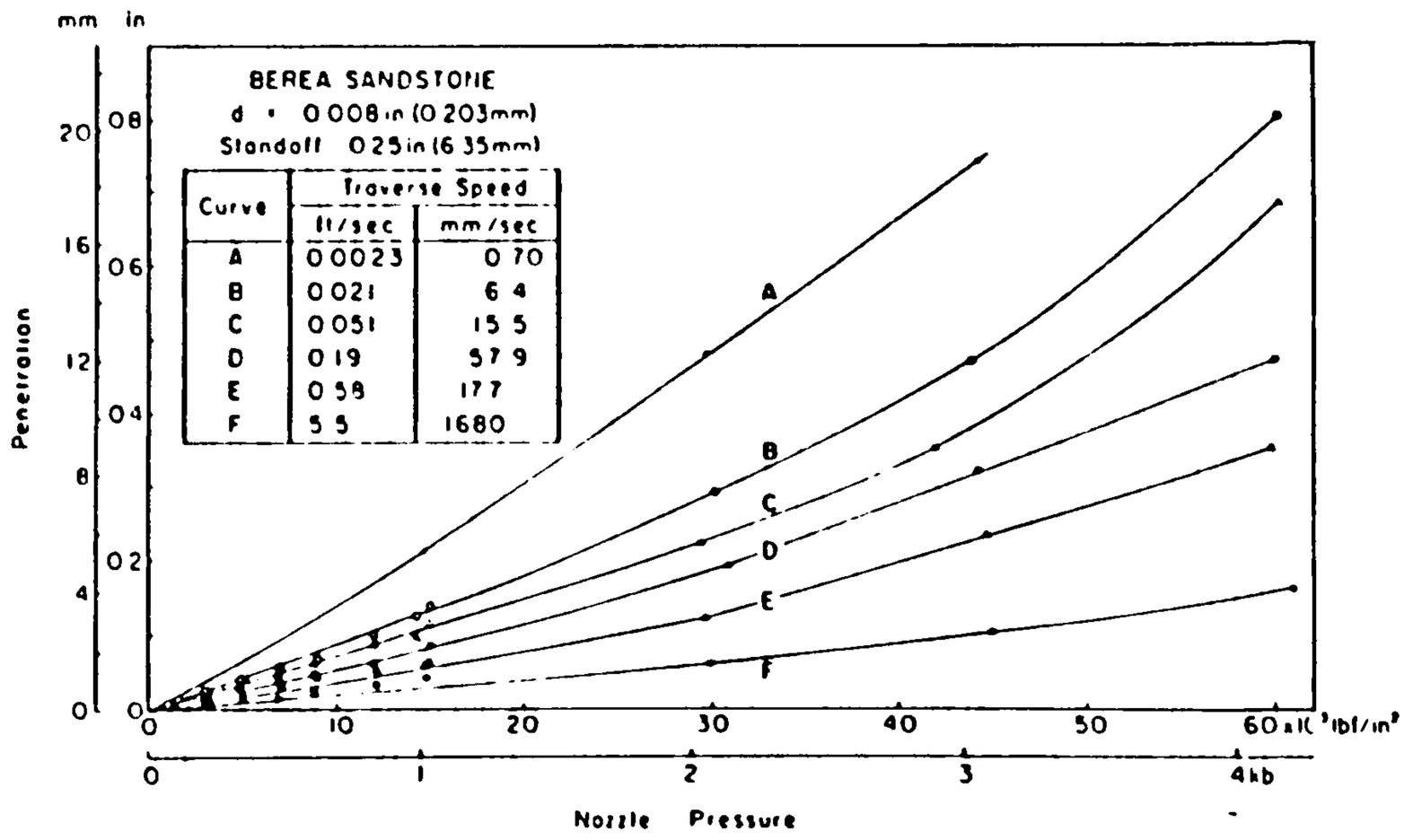


Fig.2.10 Penetration vs, nozzle pressure for Berea sandstone with traverse speed as parameter, 0.008in. nozzle.

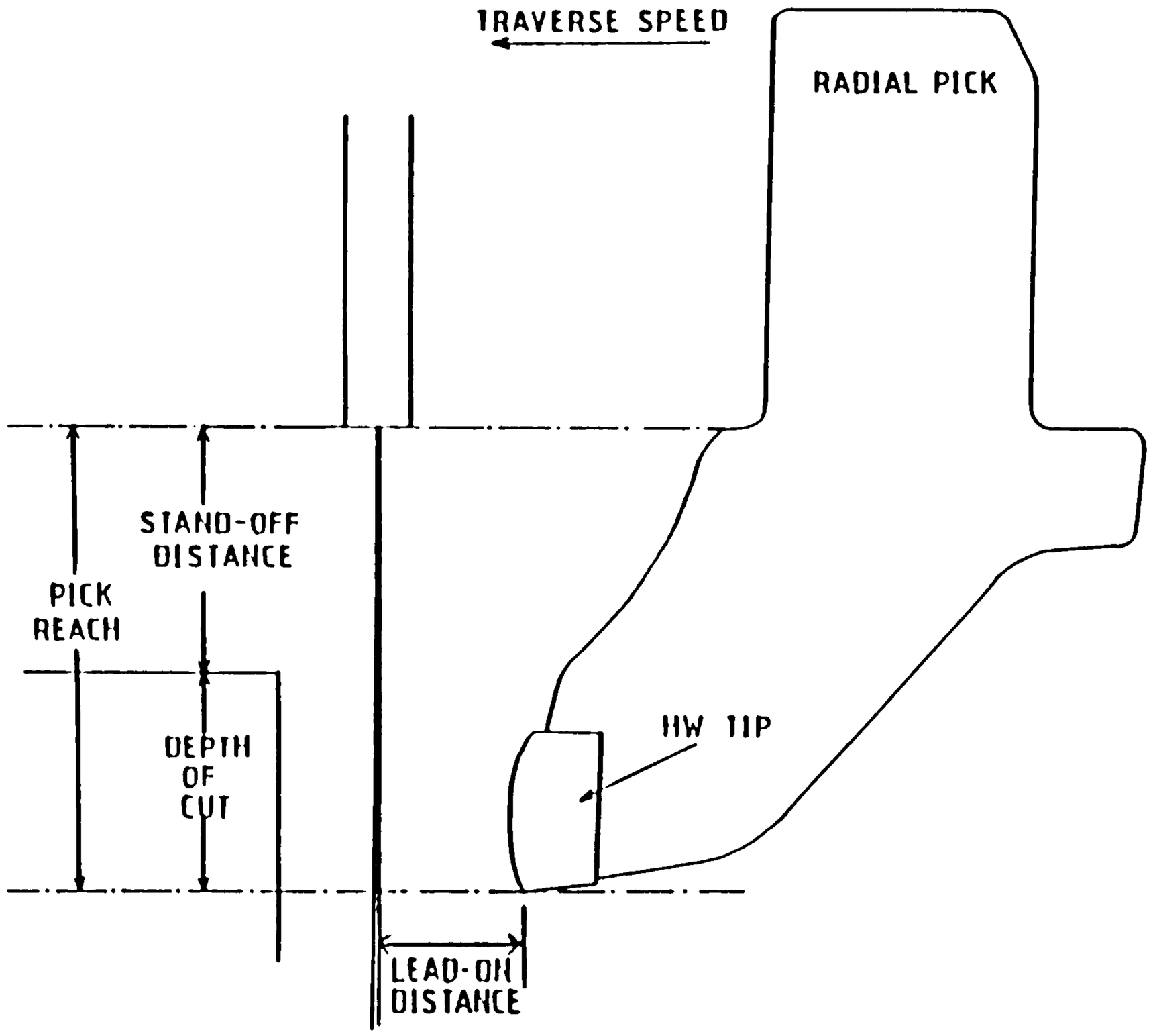


Fig.2.11

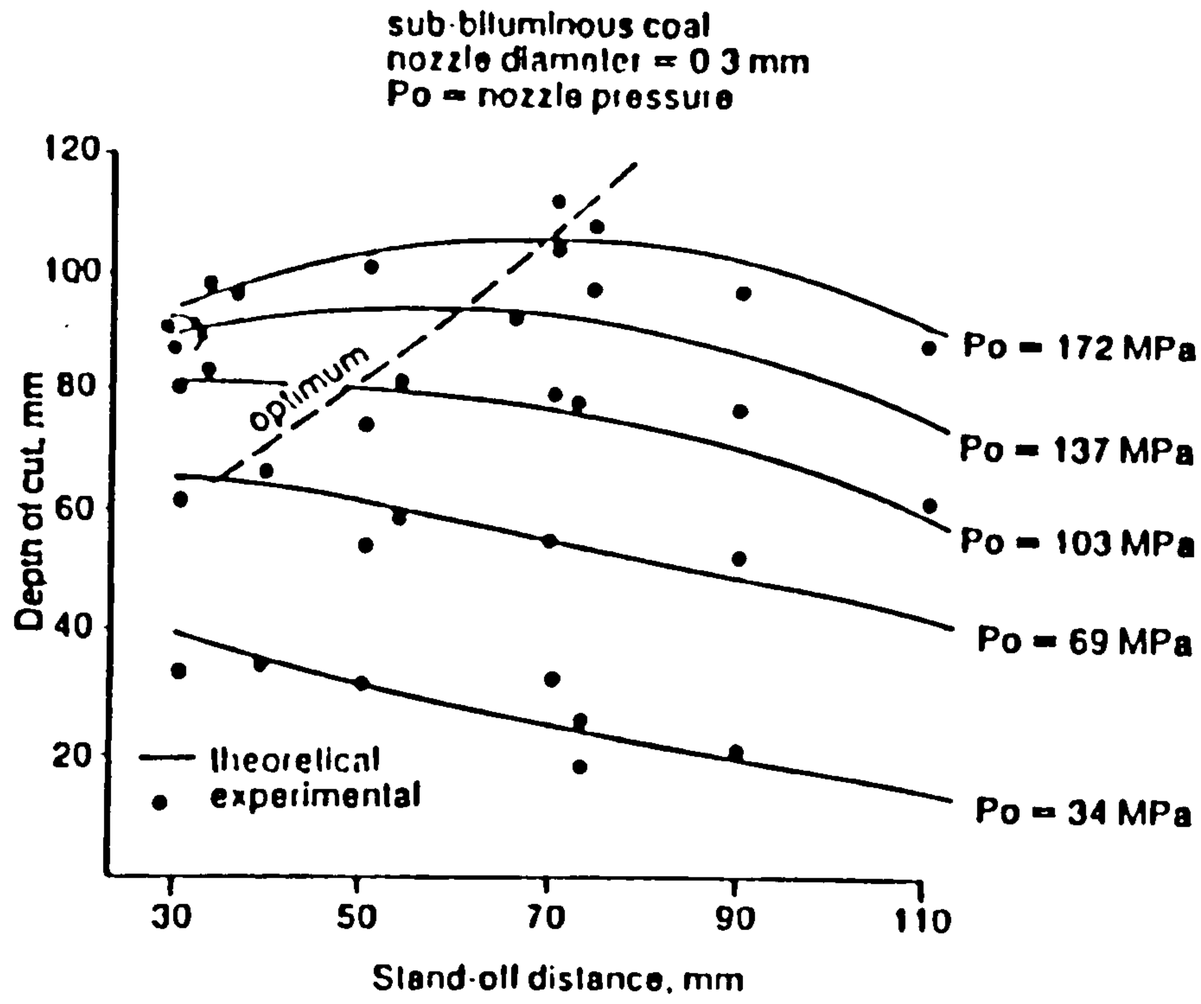


Fig.2.12 **Relationship between stand-off distance and depth of cut in sub-bituminous coal (Du Plessis and Hashish, 1980)**

Hashish, 1980). Fig.2.13 suggests that at low pressures the depth of cut decreases with increasing stand-off distance as one would expect. However, at higher pressures the depth of cut increases to a maximum and then decreases as the stand-off distance is increased. This implies that at high pressures i.e. above 70MPa, an optimum stand-off distance for maximum jet penetration exists for a particular pressure.

The jet disperses and gradually dissipates its energy as it travels further from the nozzle due to the viscosity of water in air. This is why the jet structure can be segregated into three regions as previously described; and explains why stand-off distance has an effect on its penetrating ability. Since pressure losses occur with stand-off distance, it is recommended that the stand-off distance should be no more than 100 nozzle diameters. At this distance the pressure of the jet is about 90% of the exit pressure.

ii) Jet Impingement Angle

Two impingement angles shall be considered, as shown in Fig.2.13. The angle ϕ, is measured in the plane perpendicular to the traverse direction. Fig.2.14, shows the effect of ϕ as it varies between $\pm 45^\circ$ on the jet penetration in a Japanese welded tuff (a porous volcanic rock) for the stand-off distance shown.

θ, is measured in the same plane to the traverse direction from the vertical. Fig.2.15, indicates how the penetration changes by moving θ between $\pm 45^\circ$. The results have been normalized to the slot depth when $\theta = 0^\circ$. Plots for the jet passing through both air and water before slotting the rock are shown.

All the jets flowing through air gain a 20% increase in penetration when the jet is inclined 10° towards the traverse direction. The slot cross-section formed by varying θ is given in Fig.2.16, (Matsuki et al, 1988).

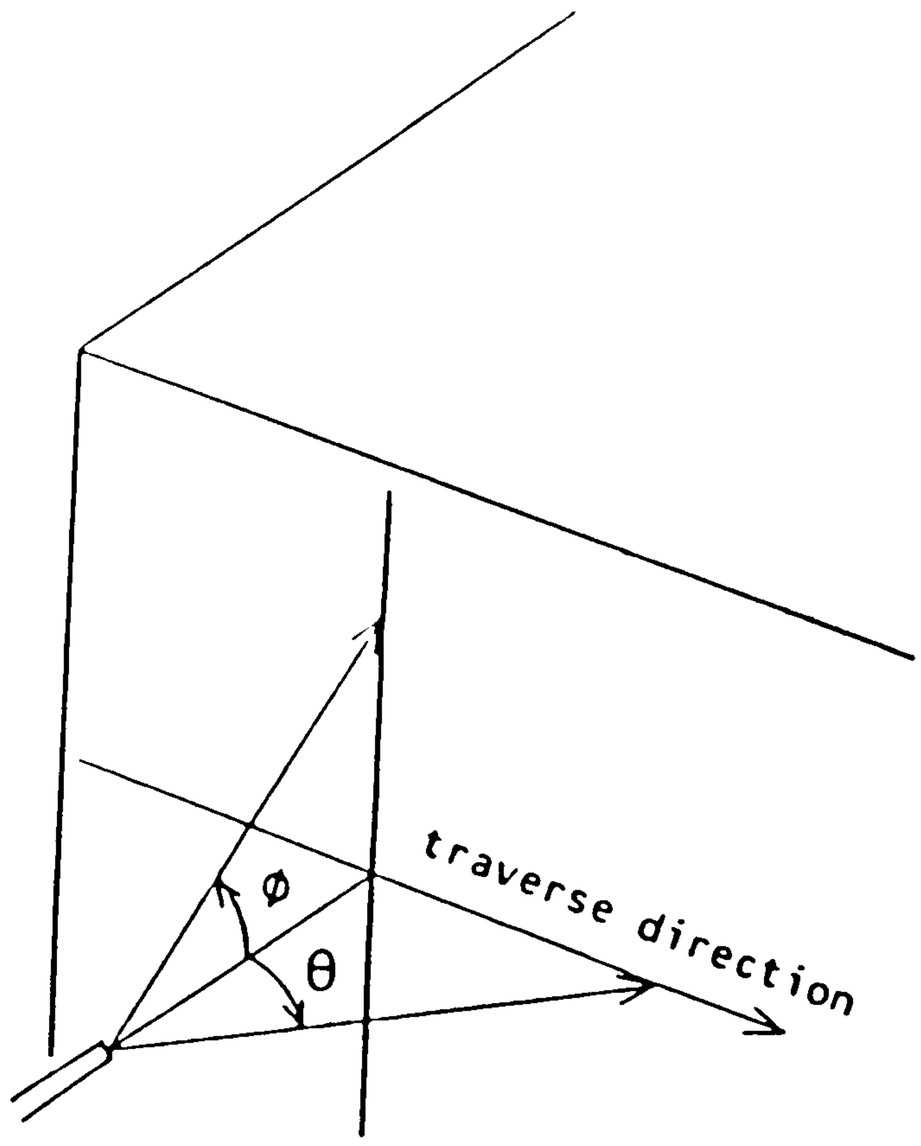


Fig.2.13 Two kinds of impinging angle in slot cutting

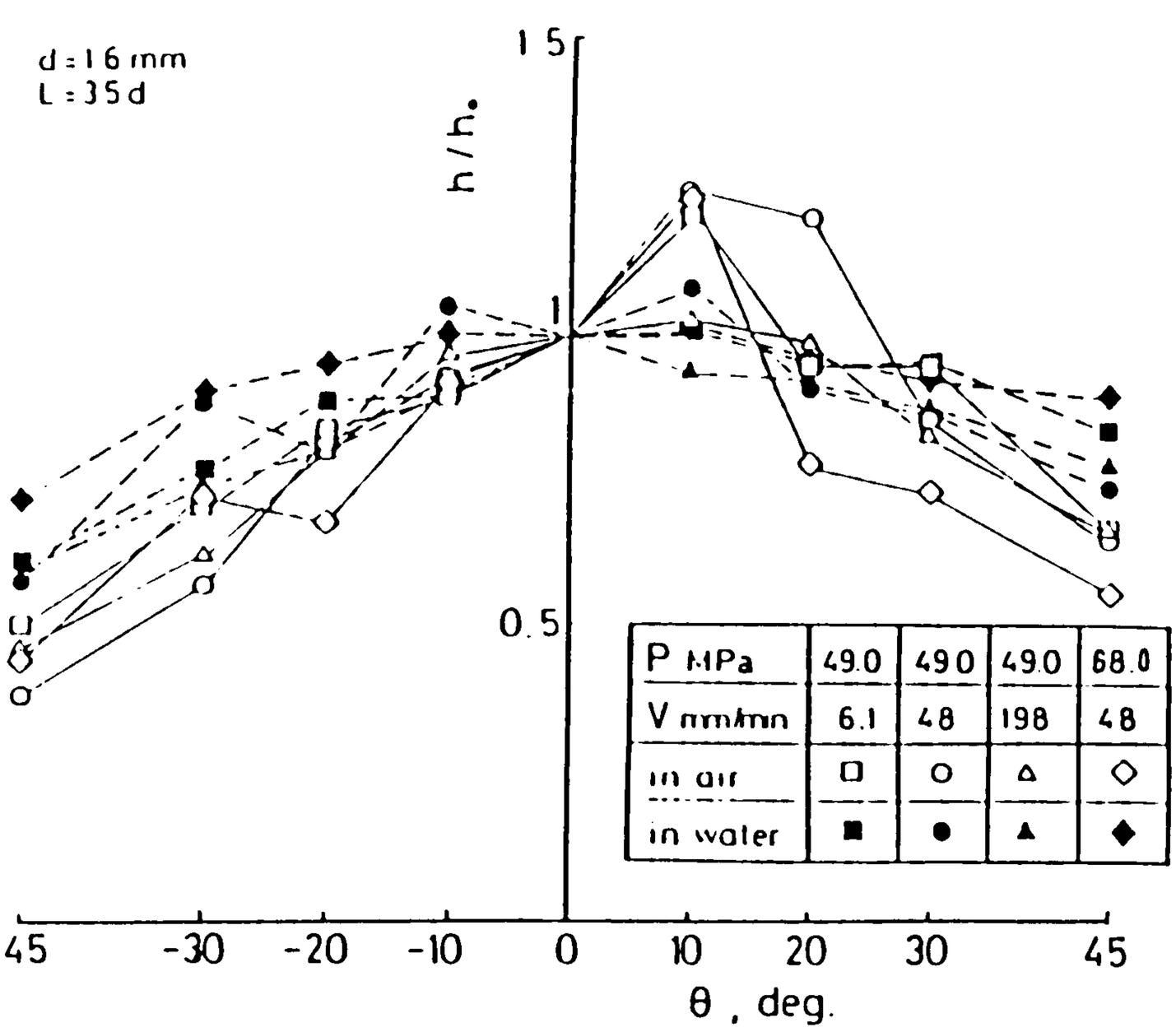


Fig.2.14 Normalized depth of cut (h/h_o) as a function of the angle θ

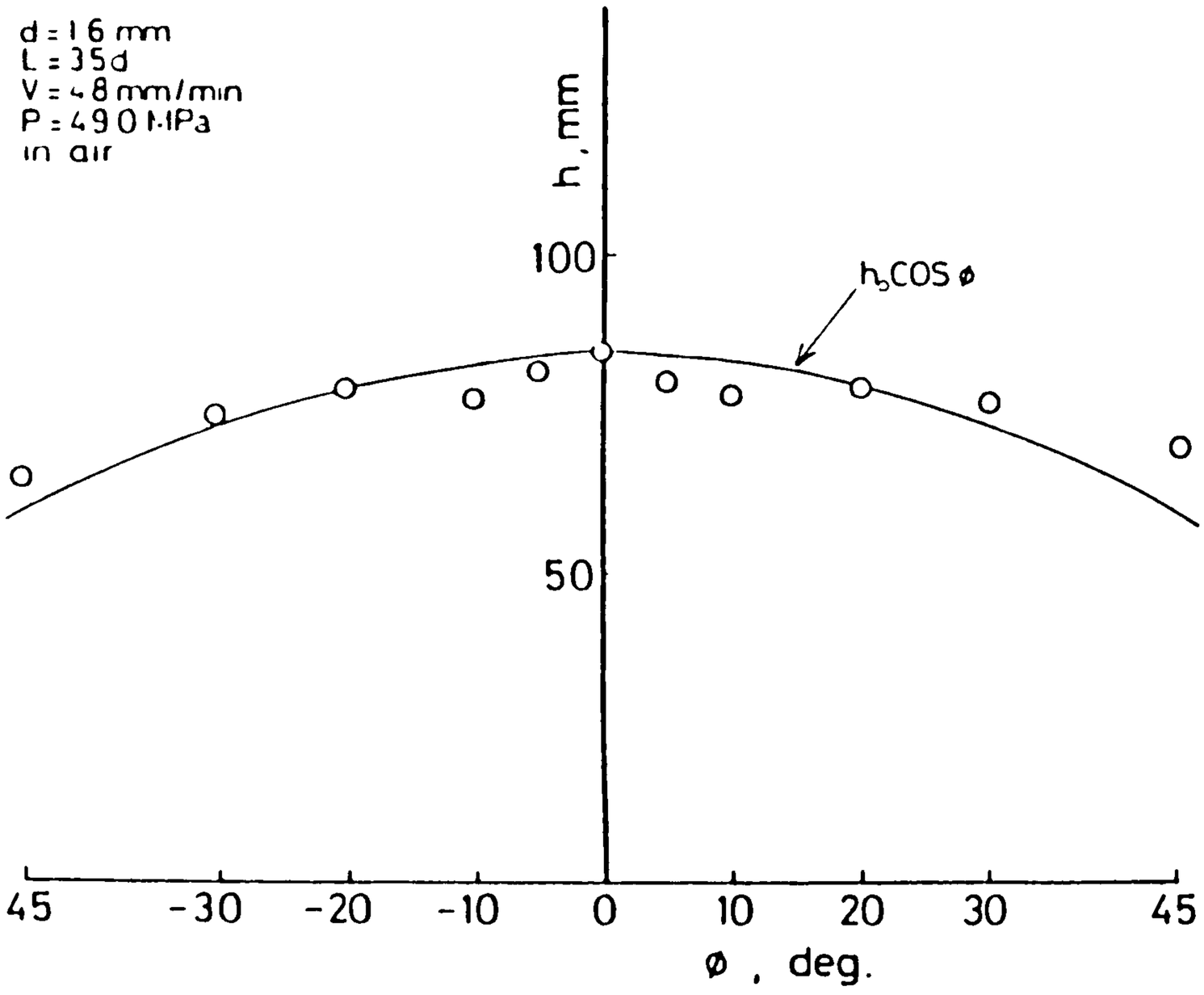


Fig.2.15 Effect of the angle ø on the depth of cut h in air

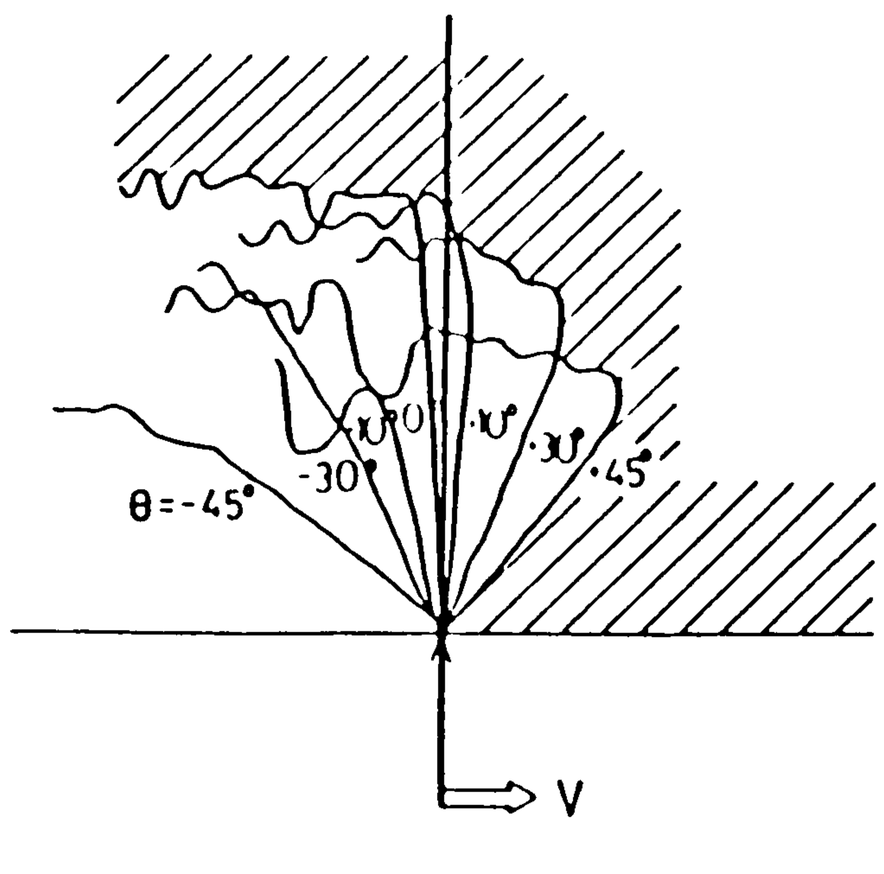


Fig.2.16 The change of slot contour with the impinging angle θ

iii) Number of Passes

Fig.2.17, illustrates the advantage to multiple passes of the jet. The first pass gives a penetration of about 8.5mm, corresponding to energy level C. After three passes of the same jet at the same power, the depth has increased to 16.5mm. Another jet of the same total cumulative power as that expended in all three passes procures a penetration of only 10mm - line A on the graph (Harris and Mellor, 1974).

Fig.2.18, shows the effect in coal after one then a second pass of the jet. The increase in penetration on the second pass is less than on the first. Two factors can account for this: the stand-off distance has increased reducing the pressure of the jet at the bottom of the slot; and the jet stream flows against the kerf wall (that has been previously cut) which subjects it to additional frictional resistance, thereby also reducing its pressure.

The law of diminishing returns applies such that if more passes were made the slot depth would increase but at a decreasing rate. Thus the suggested maximum number of jet passes is five (Tecen, 1982).

iv) Traverse Speed

This is another extremely important factor influencing jet penetration. For stationary jets in rock, most penetration takes place within 10msecs (Brook and Page, 1972). After this period the water and eroded debris at the bottom of the slot, in trying to escape, actually impedes further penetration and damping of the incoming jet stream occurs (the cushioning effect).

Figs.2.19-20 illustrate the effect of increasing traverse speed on penetration depth for Berea sandstone and Indiana limestone respectively (Harris and Mellor, 1974). Results by other researchers on the same rock but at a lower pressure and greater stand-off distance are shown in Fig.2.21 (Kovscek et al, 1989).

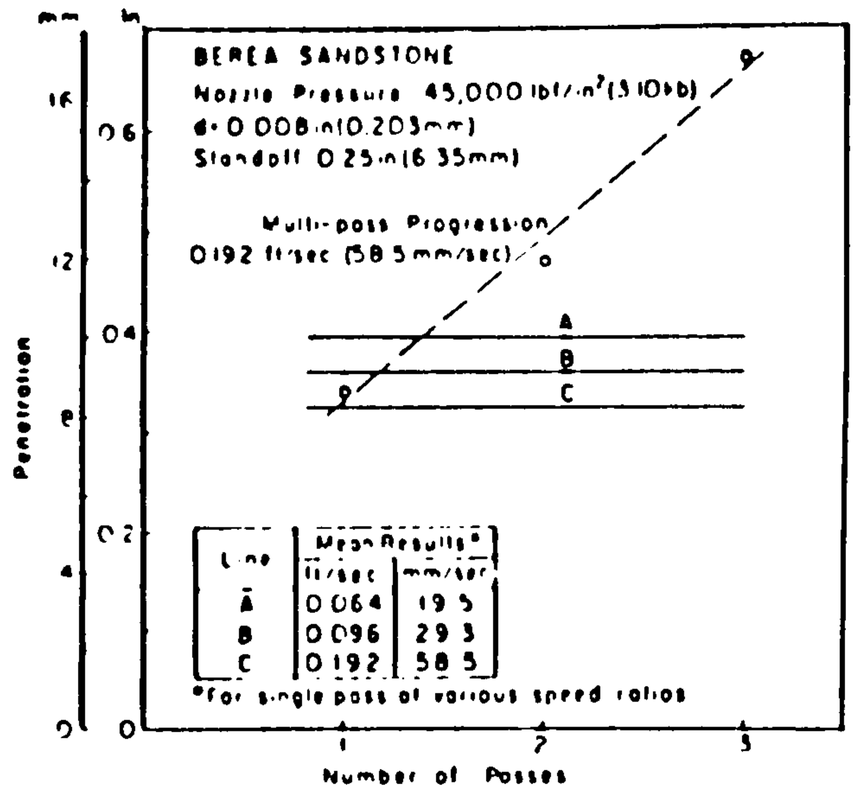


Fig.2.17 Comparison of single and multipass penetrations in Berea sandstone at 45 000psi with an 0.008in. nozzle.

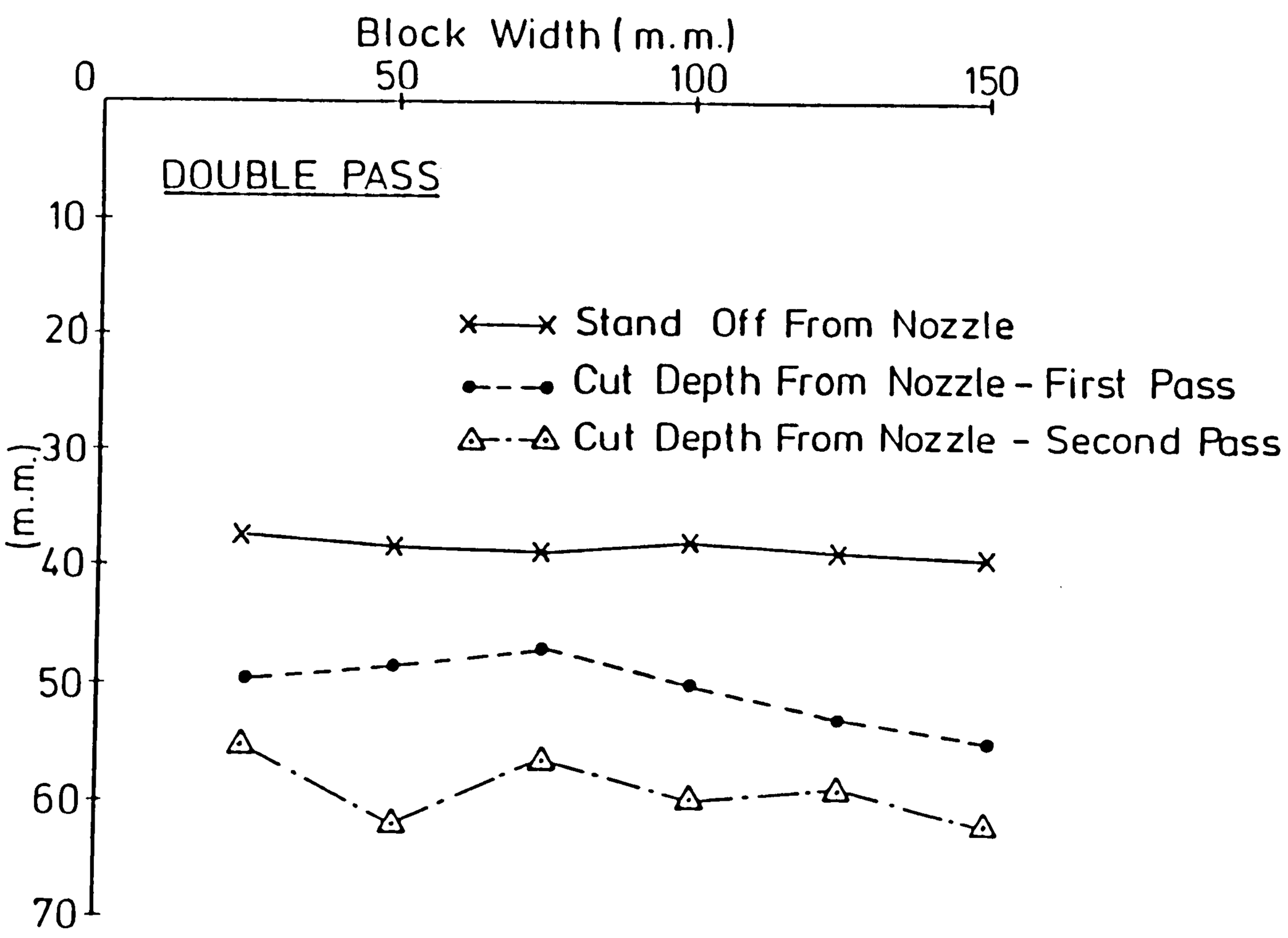


Fig.2.18 Comparison of first then second pass in anthracite coal at 69MPa and 0.6mm nozzle.

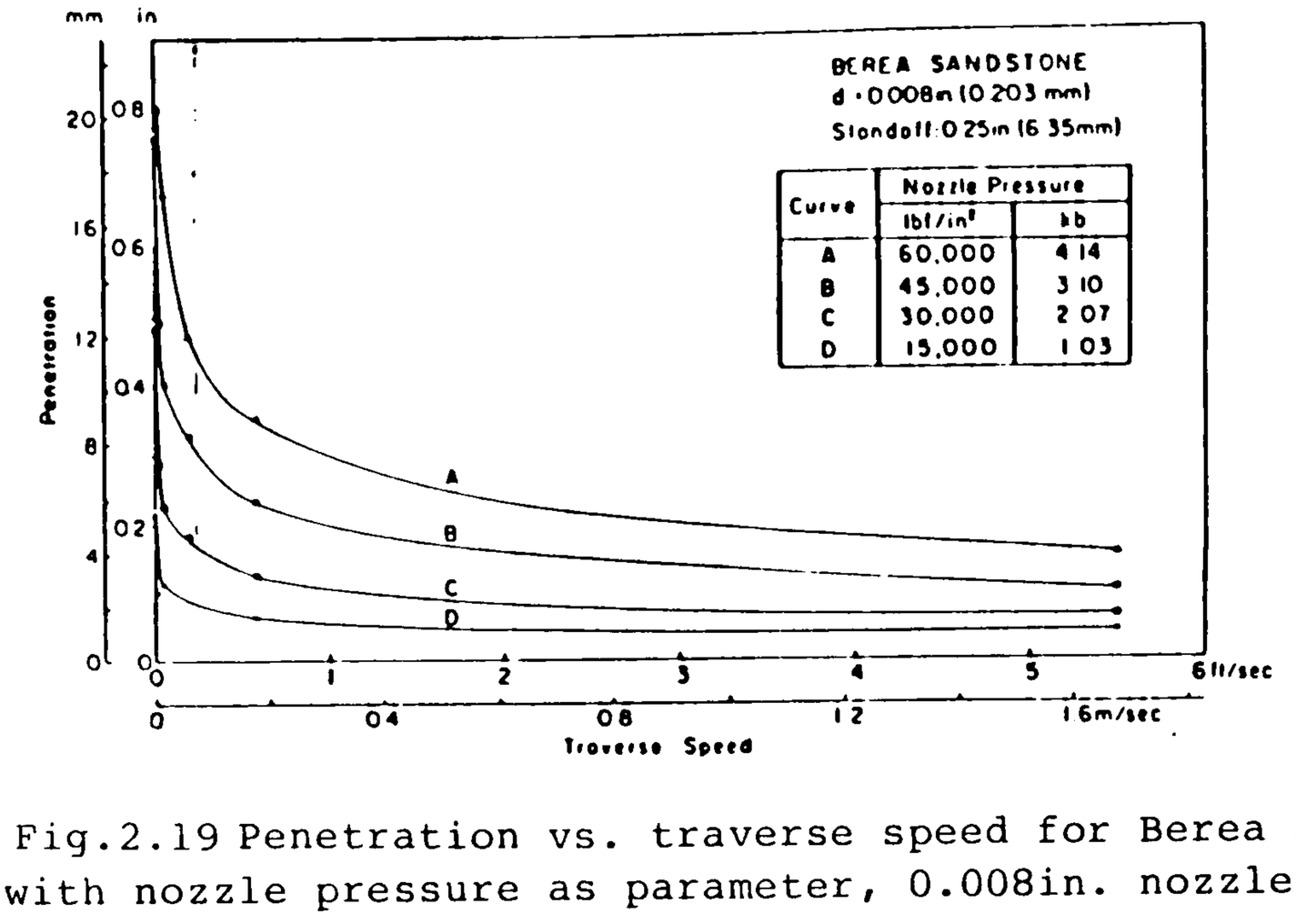


Fig.2.19 Penetration vs. traverse speed for Berea sandstone with nozzle pressure as parameter, 0.008in. nozzle.

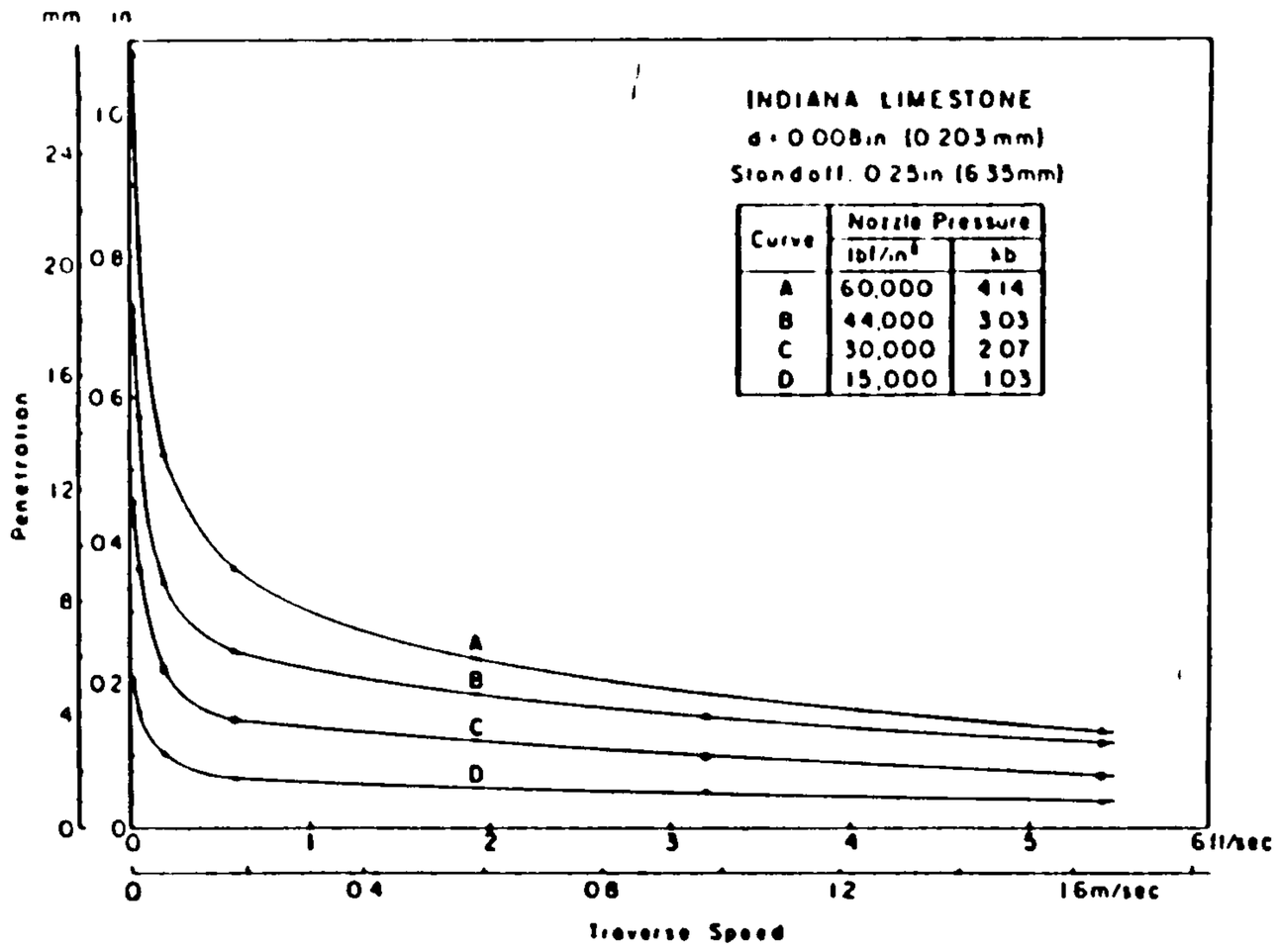


Fig.2.20 Penetration vs. traverse speed for Indiana limestone with nozzle pressure as parameter, 0.008in. nozzle.

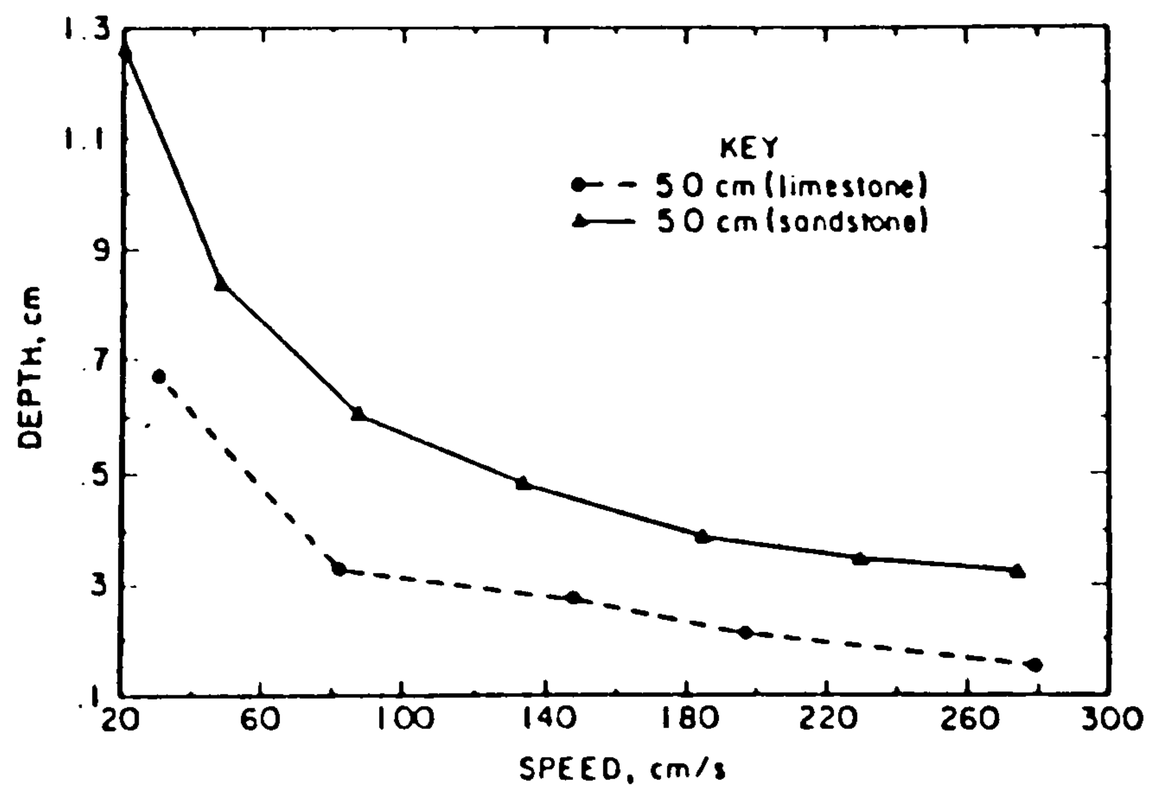


Fig.2.21 Penetration vs. traverse speed for Berea sandstone and Indiana limestone at 62MPa and increased stand-off.

In both cases, a rapid decrease in penetration with traverse speed is evident, followed by a region of more gradual decrease. One can see that the different operating conditions affect the form of the graphs but nevertheless, a zone of rapid decrease exists.

A similar trend is observed in coal, Figs.2.22-23. The exponential decay is not so pronounced but still there. Also, as the traverse speed approaches the cutting speeds of coal winning machines, the slot depth is considerably reduced. Hence the need to use high pressures and power to achieve what one considers a desirable penetration: and good reason to carry out tests in the laboratory at the same speed as one expects in the field.

2.4 Hybrid Cutting

This section reviews what the current terminology describes as 'jet assisted cutting': the mechanical action of a cutting tool being assisted by an auxiliary water jet (Hood et al, 1990). This is the method employed by the jet assisted tunnelling and coal cutting machines in British coal mines.

2.4.1 Jet Pressure

Research has been conducted to investigate the effect of jet pressure on pick forces and wear rate (Ip and Fowell, 1987; MacAndrew et al, 1987). Fig.2.24, indicates to what extent the mean normal force of a radial type pick may be reduced with jet assistance for several rocks. Fig.2.25, suggests that tool force reductions do not continuously increase as the pressure is increased but reaches a maximum for a certain set of operating parameters. For the graphs shown, the maximum tool force reductions obtained are approximately 50% and 30% for the mean normal and cutting forces respectively.

The jet pressure and other factors that obtain the maximum force reductions, correspond to the set of jet parameters that would give a penetration of 20%-30% of the nominal depth of

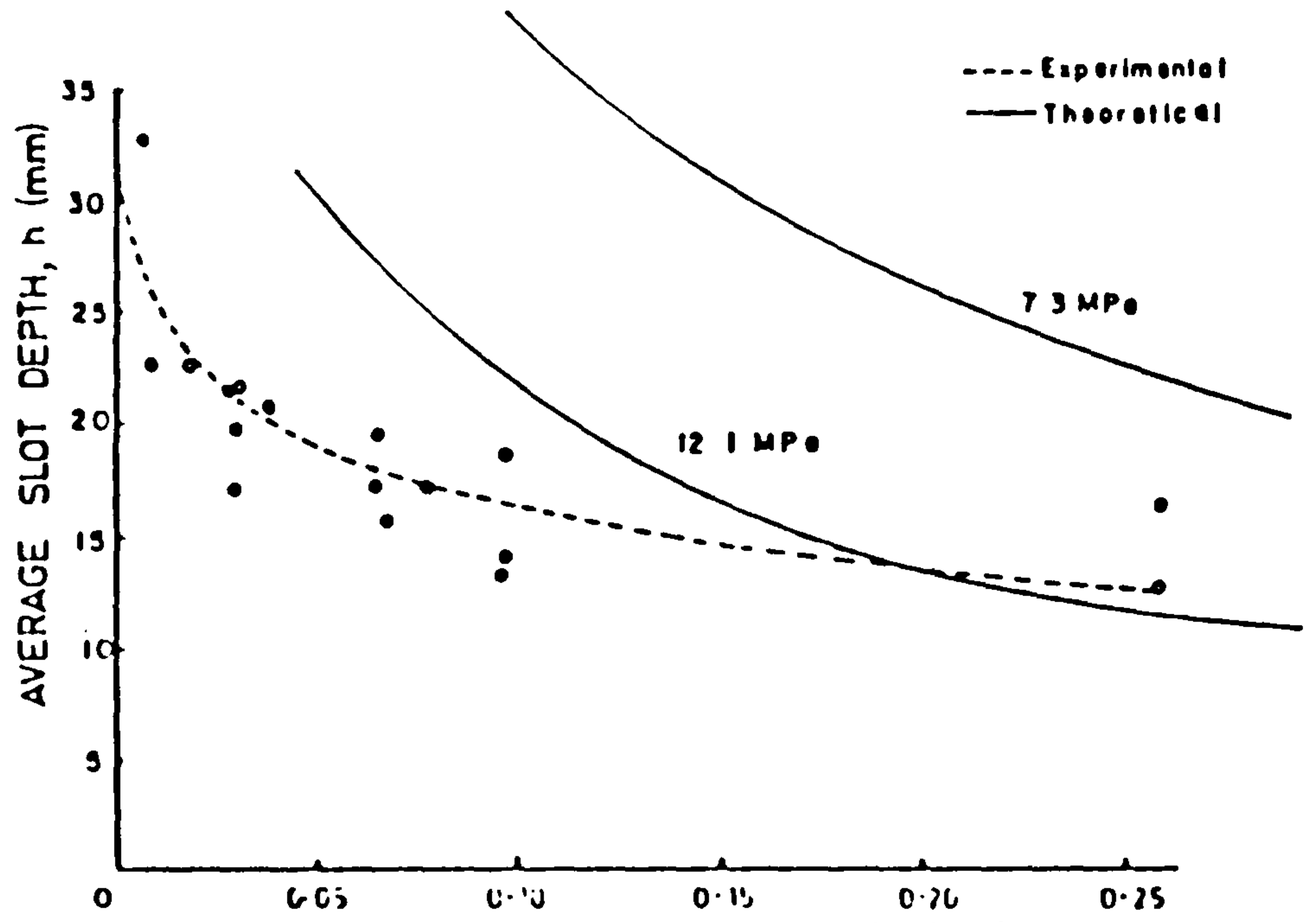


Fig.2.22—Average depth of slot (h) versus traverse velocity (V_t) for traversing tests:

$d_n = 1.02$ mm
$P_n = 15.0$ MPa

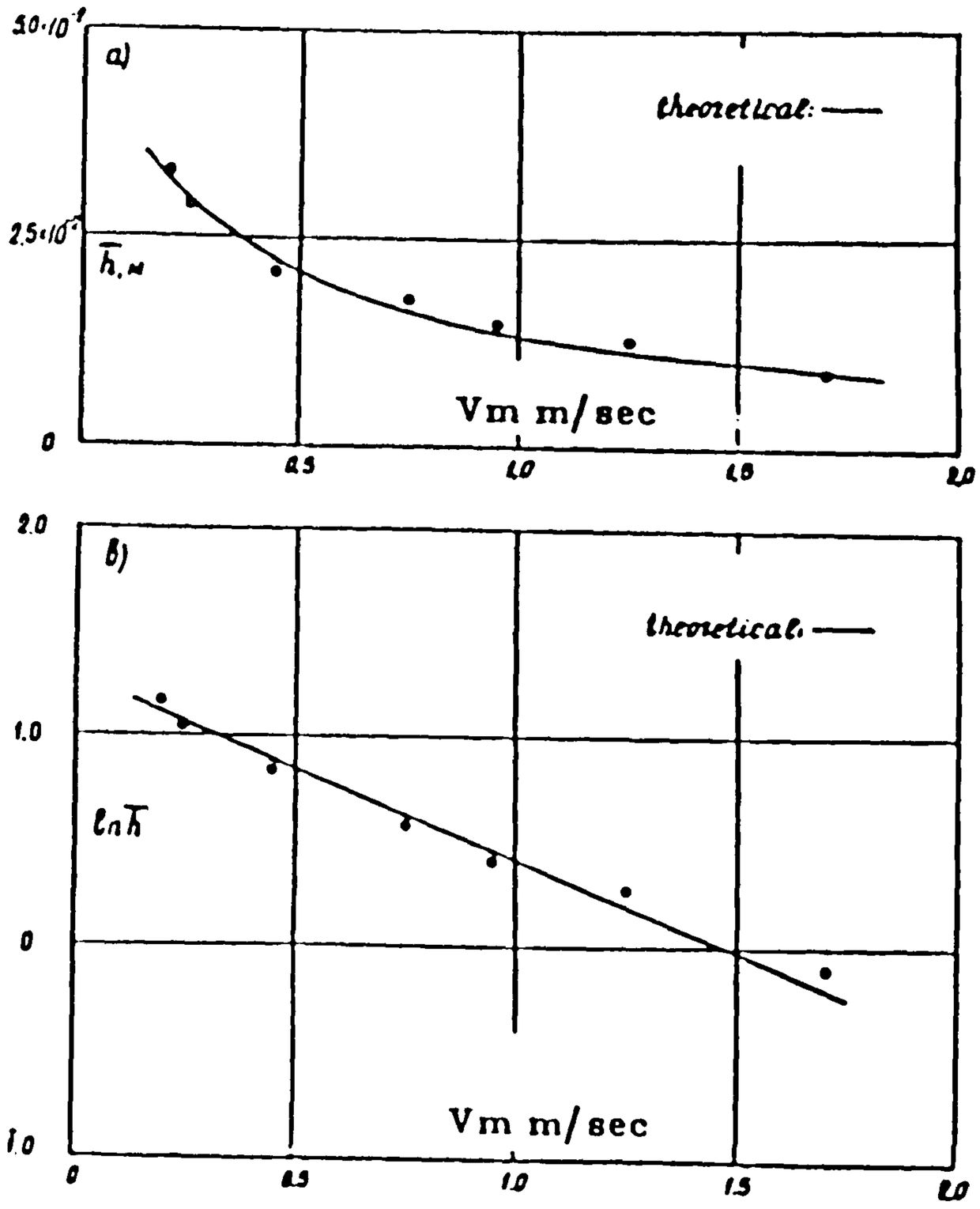


Fig.2.23 Variation in the coal penetration vs. jet traverse speed.

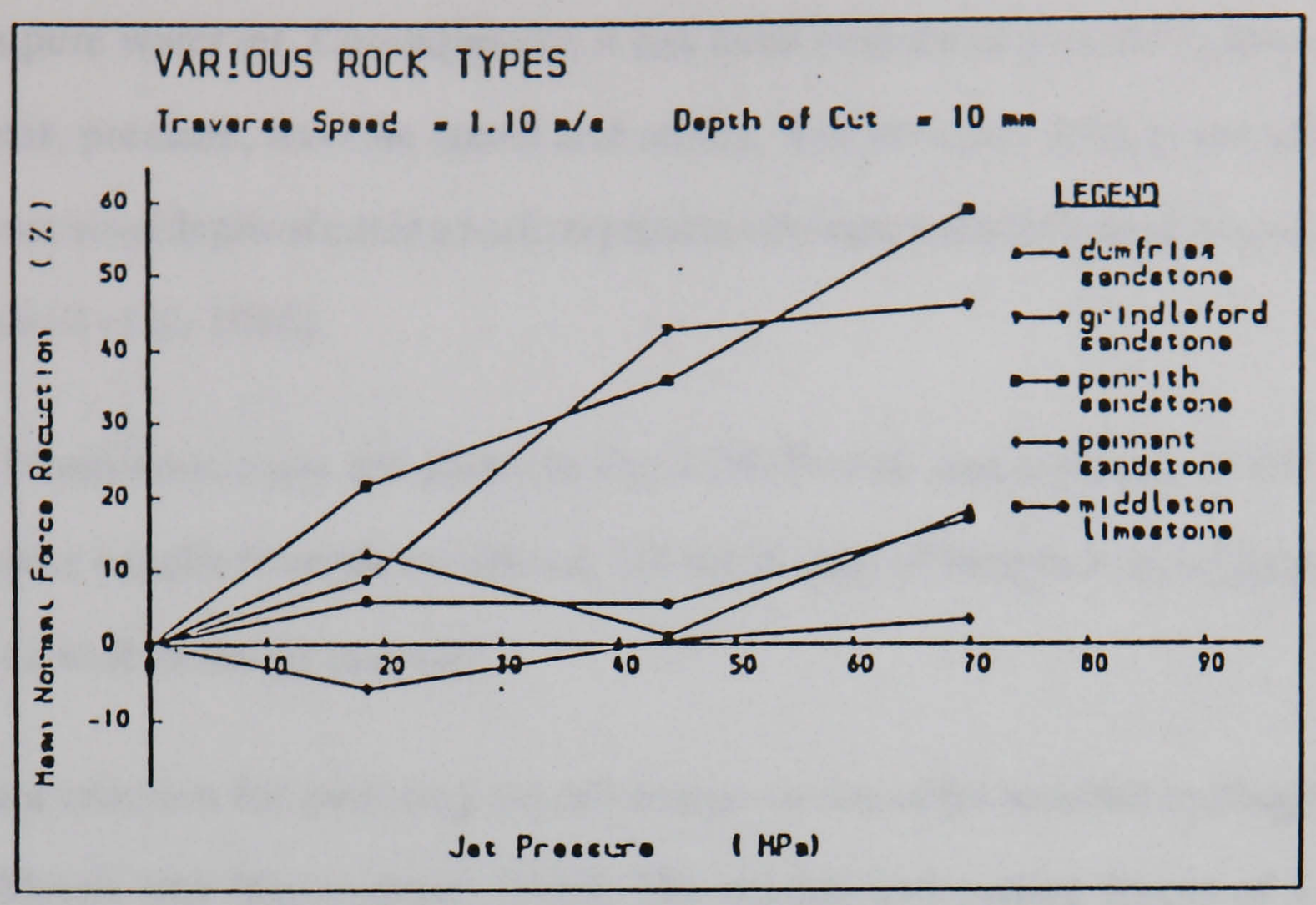


Fig.2.24 Mean Normal Force Reductions vs. Jet Pressure for Five Rock Types.

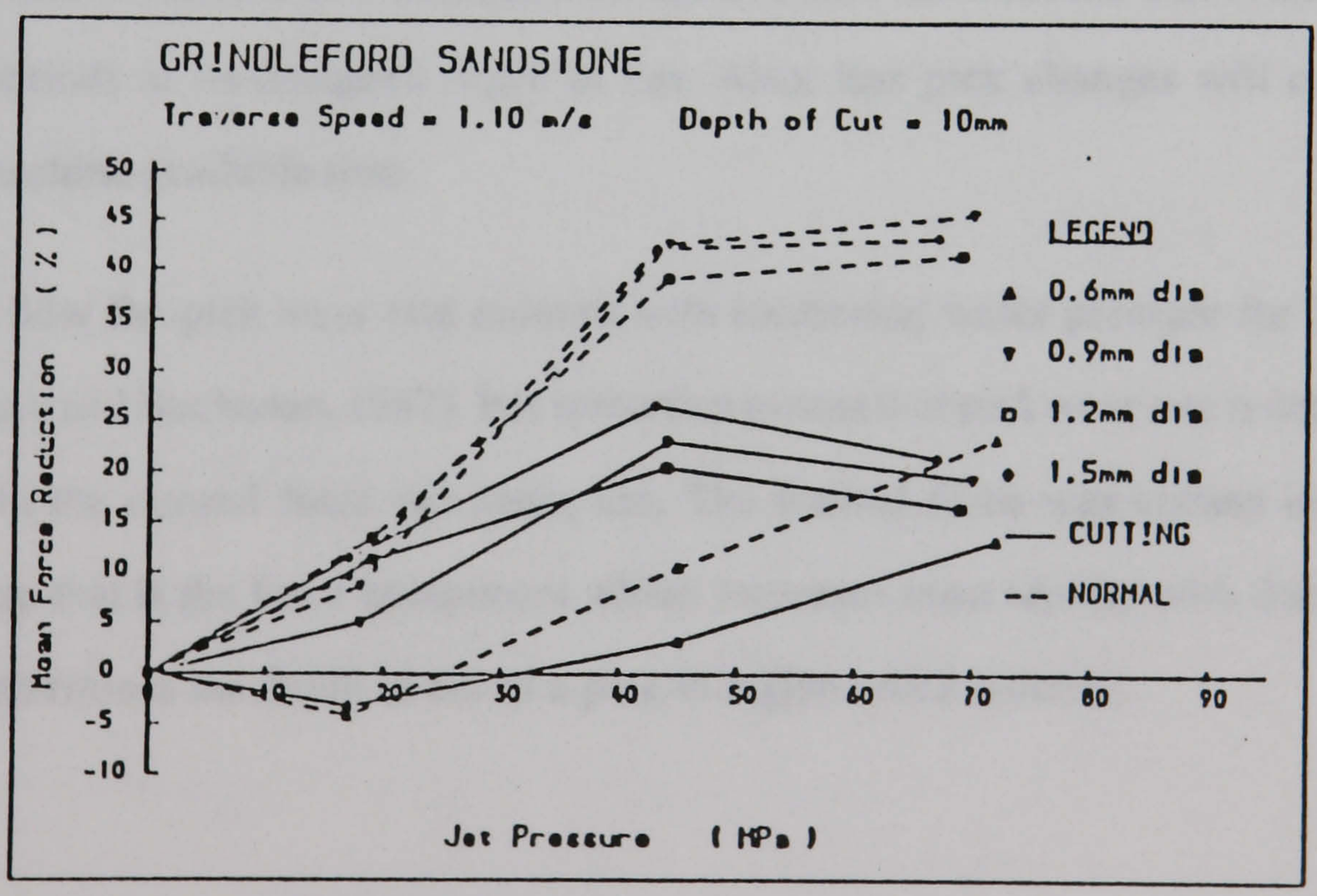


Fig.2.25 Mean Force Reductions vs. Jet Pressure at different Nozzle Diameters.

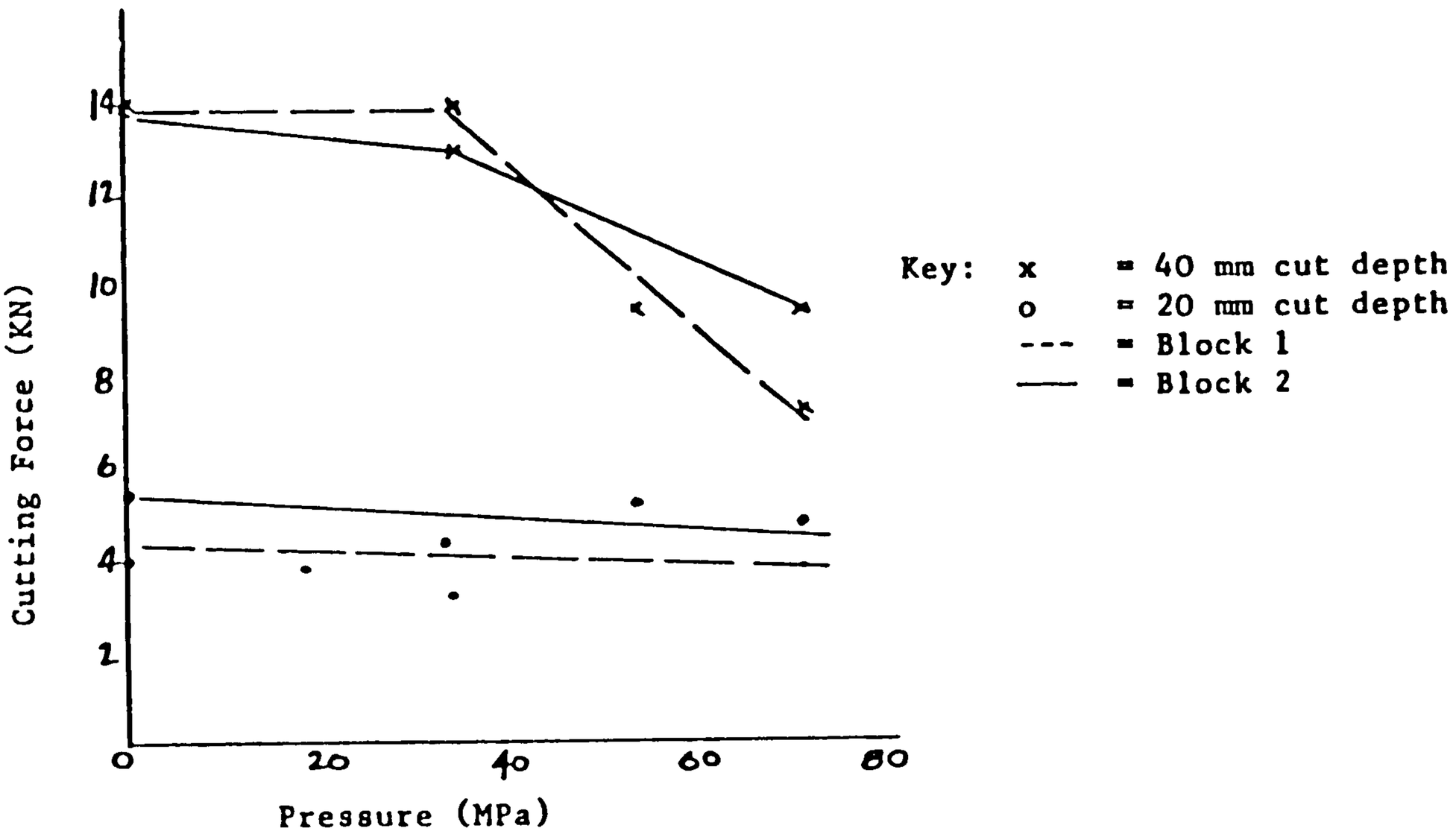
cut if acting as a pure water jet. Consequently, it has been postulated that the combination of nozzle diameter, pressure, traverse speed and others, that procures a jet penetration of 20%-30% of the nominal depth of cut in a rock, represents the optimum jet assisted conditions for that rock (Fowell et al, 1986).

Results for two bituminous coals are given in Fig.2.26 (Fowell and Johnson, 1984). The results suggest some benefit from jet assistance, but the degree of benefit may be related to the depth of cut as well as the jet pressure.

Another important criterion for assessing the advantage or not of jet assisted cutting is the tool wear rate (Morris and MacAndrew, 1986). The normal and cutting forces of a pick increase rapidly as the tool wears such that a wear flat of only a few millimetres can result in tool forces many times their initial value (Kenny and Johnson, 1976). There is a limit to the extent tool forces may reach before affecting a shearer's haulage speed: this mainly depends on the installed power. If the tool forces become too great, then the depth of cut taken by a cutting machine will decrease to compensate, hence the slower haulage speed. Therefore, if the rate at which a tool wears can be reduced then the machine will be able to cut for longer periods at its designed depth of cut. Also, less pick changes will occur, increasing the machine available time.

Fig.2.27, shows how the pick wear rate reduces with increasing water pressure for York sandstone (Barham and Buchanan, 1987). It is important to note that pick wear rate is defined as the increase in the normal force per metre cut. The normal force was chosen in this definition because that is the force component which increases most rapidly with distance cut and which determines the depth of cut of a pick in a given rock material.

Force vs. Jet Pressure for 20mm and 40mm Nominal Depths of Cut



Note: All results obtained at a Traverse Speed of 1.04m/s.

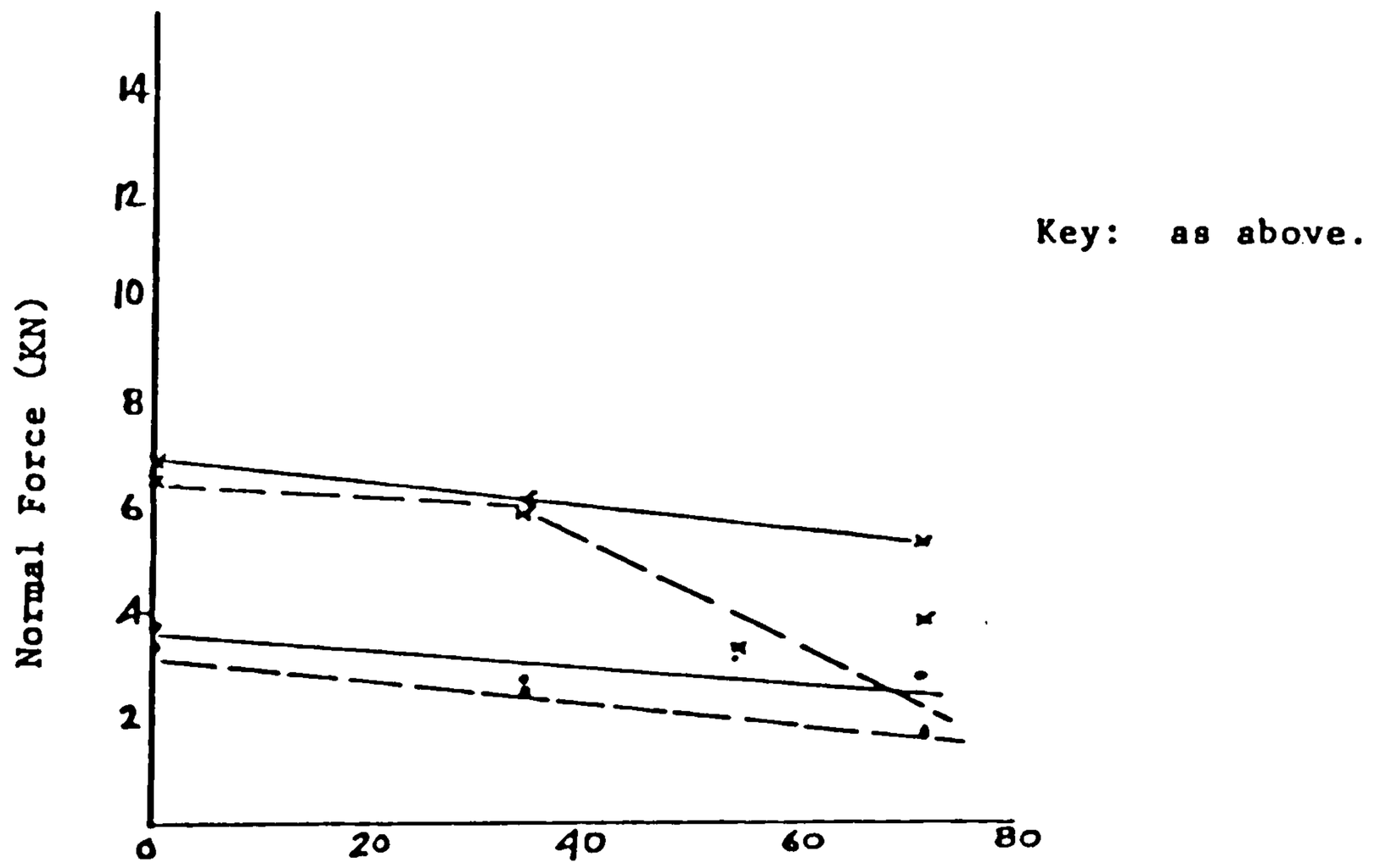


Fig.2.26 Mean Cutting and Normal Force Reductions vs. Jet Pressure for two Bituminous Coals.

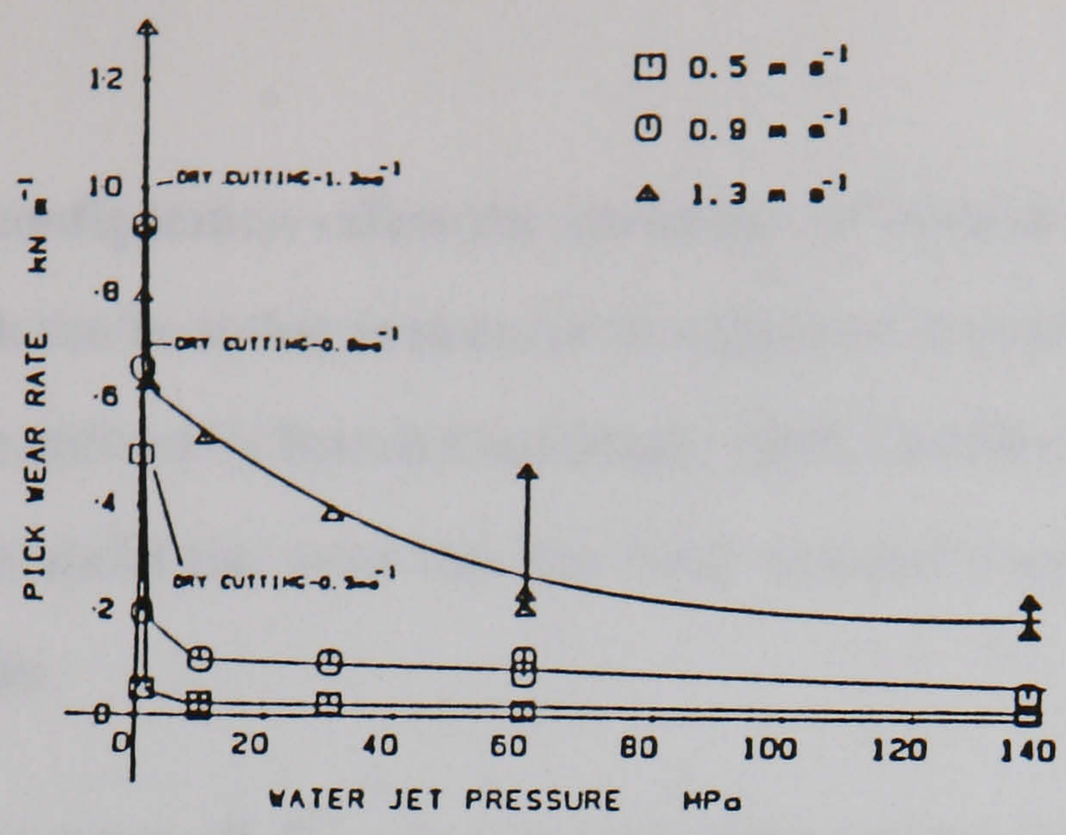


Fig.2.27 Pick Wear Rate in Hard York Sandstone as a Function of Jet Pressure at Varying Levels of Cutting Speed

2.4.2 Lead-on and Side-off (Offset) Distance

Tool forces increase as the lead-on distance increases. It has been recommended by Fowell et al (1985) and Hood (1976), that the lead-on distance be kept within 1-2mm.

The same effect is observed with side-off distance: as this is increased the tool forces increase and in general this parameter is maintained zero. However, these results are for hard rock and the present study shall deal with this factor also.

2.4.3 Jet Position

Three jet positions have been adopted: the jet infront of the pick; the jet passing through (through pick flushing); and the jet impinging behind the pick.

Through pick flushing intuitively appeals most since the stand-off distance is reduced to a minimum, the jet is precisely positioned where it is considered needed and maximum cooling of the tip is achieved. However, the jet orifice weakens the carbide tip; the jet may be easily blocked; and the tools are more expensive to manufacture. For these reasons through pick flushing is not widely used: although considering the weak, brittle nature of coal, there is a good argument to apply this technique to coal cutting machines.

The jet-behind-tool configuration offers the advantage of immediately cooling the rock behind the pick which can be so hot as to cause an explosion in methane rich atmospheres. This method has been utilized by British Coal (Pugh, 1986). Additionally, the jets cools the pick tip and in some rocks the wear rate has been reduced much more than with the jet-before-tool position.

Disadvantages are, the stand-off distance is usually large and the jet impinges at the same angle as the clearance angle of the pick. This means that when a wear flat is generated, the jet erodes a slot in the rock beneath the pick tip and hence does not completely relieve the pick from crushing events (Ip, 1986). Fig.2.28, illustrates the phenomenon diagrammatically. In this situation the jet does not clear the debris away as efficiently either.

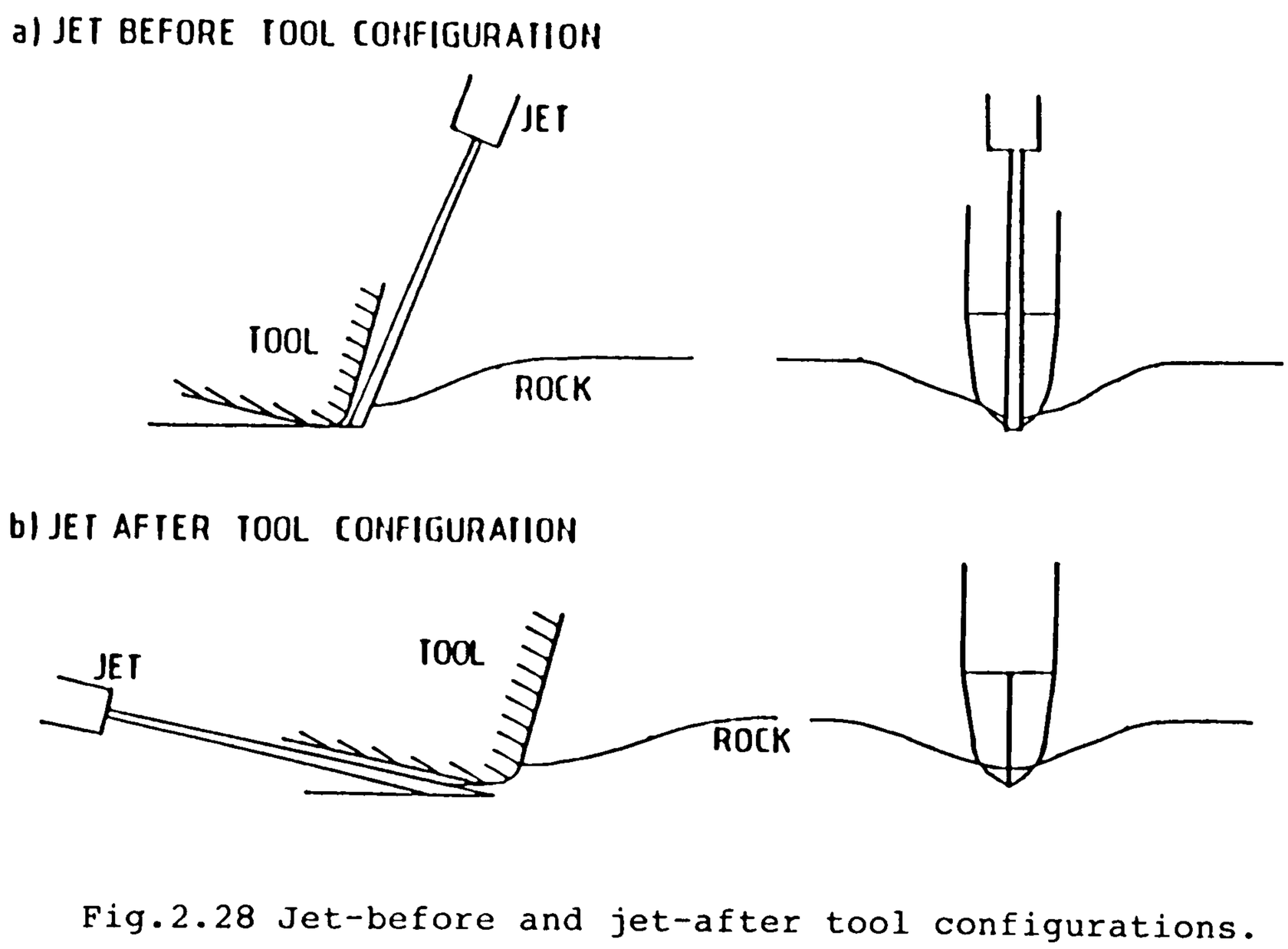


Fig.2.28 Jet-before and jet-after tool configurations.

The jet-before-tool arrangement is the one most commonly employed. Hood (1976), recommends that the jet stream should flow parallel to and within 2mm of the tool front face. Since most commercial tools have rather complex and differing geometries, this proves impractical and the jet is made to impinge 1-2mm infront of the tool tip. Thus, in practice, the jet has to penetrate the rock somewhat before it can offer any assistance to the cutting process. The cut debris is flushed away by the jet, sometimes causing projectiles potentially harmful to personnel.

In the jet-before-tool mode, the nozzle is vulnerable to damage by the ejected debris. For this reason the nozzle cannot be placed too close to the rock surface without being protected.

2.4.4 Cutting Speed

Work to investigate the effect of cutting speed on the magnitude of the cutting forces has been conducted at various research centres.

O'Dogherty and Burney (1963), carried out tests in two coals: Dunsil and Garw, both bituminous. The tests were purely speed trials without water jet assistance. However, the results are useful and confirm other researchers results in rock. At cutting speeds of 1.02, 2.03 and 3.05m/s at depths of cut 2.5, 5.0, 11.6 and 14.0mm, no significant variation in the mean cutting force was evident in either coal. They concluded that the cutting force was practically proportional to the depth of cut taken, not to the cutting speed over the range examined, Fig.2.29.

A tentative explanation for this was given and was related to the speed of tensile crack propagation in coal. For Barnsley Hards, this speed had been estimated in excess of 500m/s when crushing cubes of the coal. The authors suggest therefore, that a cutting tool travelling at 3m/s cannot be expected to significantly modify the fracture process and hence the cutting

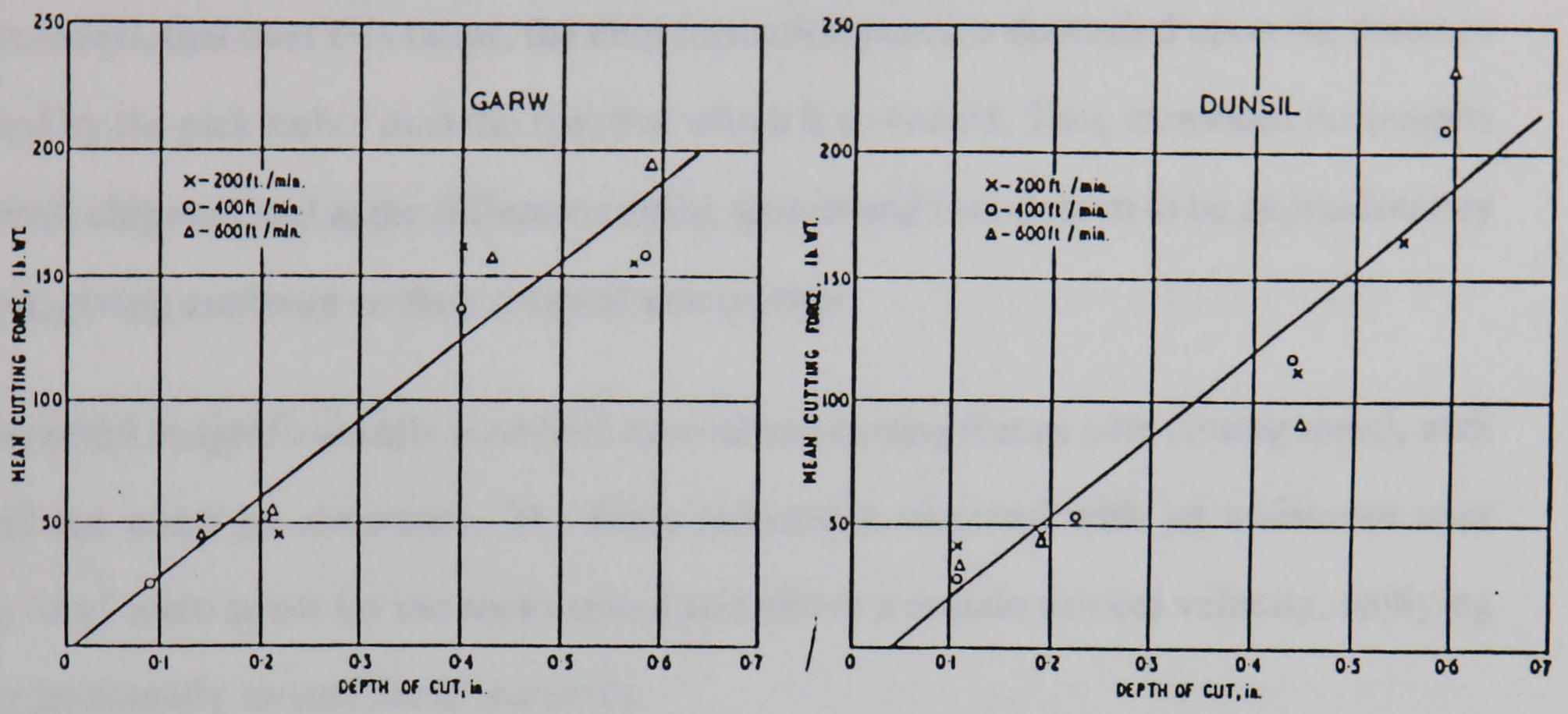


Fig.2.29 Variation of mean cutting force with depth of cut for duckbill pick.

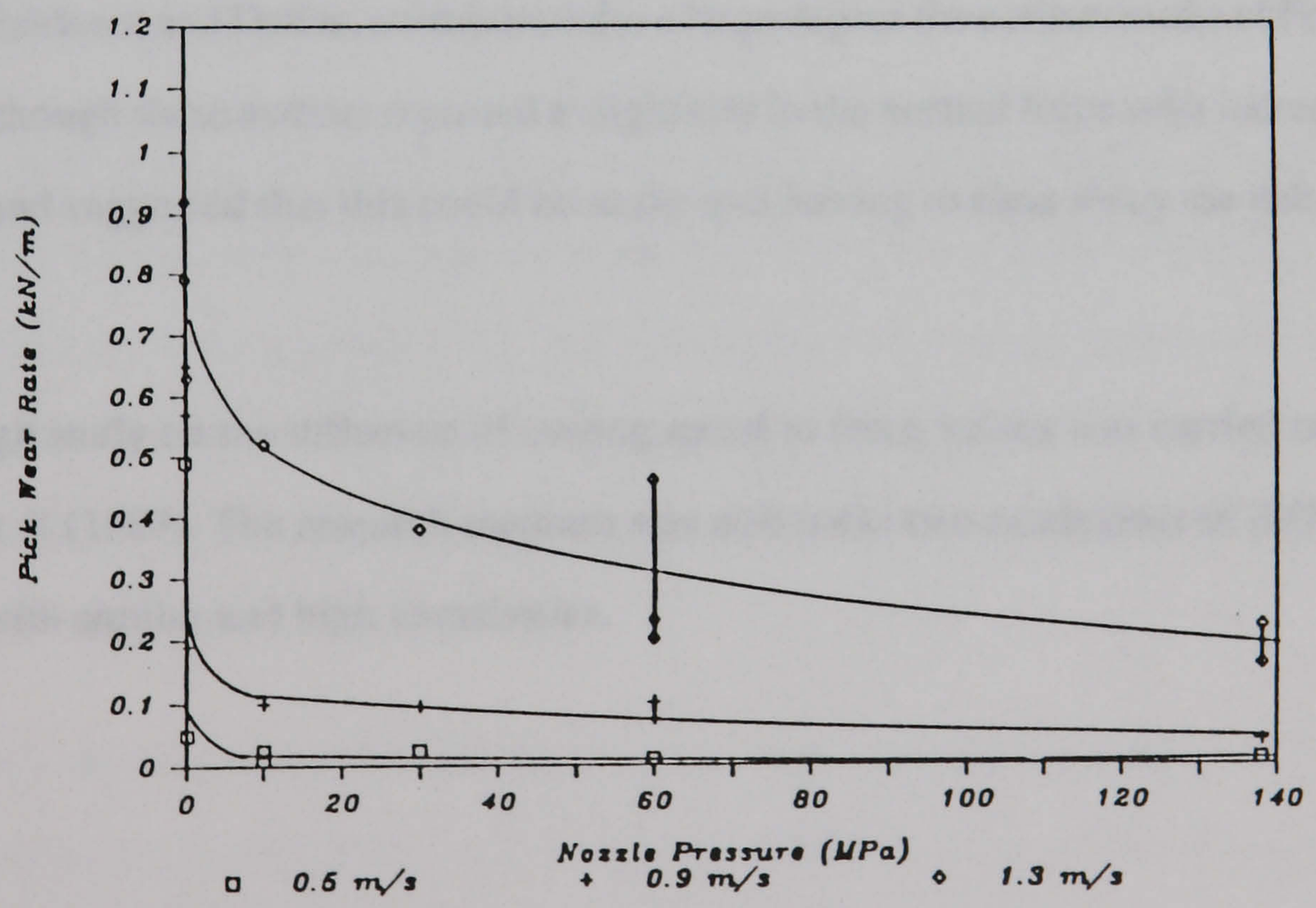


Fig.2.30 Pick wear rate in hard York sandstone as a function of jet pressure, at varying levels of cutting speed.

force. No results for the normal force were published.

Fairhurst and Deliac (1986), investigated cutting speed in rock over the range 0.63 to 3.0m/s. They assumed, that over this range, the chip formation process depended upon the distance traversed by the pick rather than the speed at which it traversed. They measured the lengths of the rock chips created at the different cutting speeds and found them to be approximately constant, giving credence to their original assumption.

They reported insignificant effect on both normal and cutting forces with cutting speed, with and without water jet assistance. The force reductions obtained with jet assistance over cutting 'dry' were small for the rocks tested and above a certain critical velocity, applying a water jet actually caused force increases.

It could be that for brittle materials like rock and coal, the speed of fracture propagation is so great compared to the cutting speeds used in mining practice, that the effect of cutting speed on the failure mechanism can be considered negligible.

The results of Fairhurst and Deliac, corroborated to a large degree the earlier results of Fowell et al (1985): although these authors reported a slight rise in the normal force with increasing cutting speed and suggested that this could be to the tool having to clear away the debris at a faster rate.

A very thorough study on the influence of cutting speed to force values was carried out by MacAndrew et al (1987). The research medium was also rock: two sandstones of different strengths but with similar and high abrasivities.

The authors took a different approach and as part of their study investigated how the pick wear rate was affected by cutting speed. The trials were done with and without water jet assistance. As stated previously, the pick wear rate is defined as the increase in normal force per metre cut.

Fig.2.30, illustrates the results for Hard York sandstone. One can see that a water jet at 10MPa can have a great effect on the wear rate. Also, it is quite clear from these results that the cutting speed has a greater influence on the wear rate than water jet pressure. The authors concluded that the increased wear rate caused by increasing the cutting speed, cannot practically be counteracted by increasing the water jet pressure.

One criticism could be that the authors maintained the water flow rate constant at 4l/min, and if they had increased this perhaps the cutting speed would not have been so dominant. However, they stress the need to consider what is realistic in they mining environment. Large quantities of water may so adversely affect the geological conditions that mining becomes quite impractical, no matter what force, wear rate, or other reductions are obtained for the cutting machine.

It appears then, that varying the cutting speed over the range used on mining machinery, does not significantly influence the force value necessary to cut a mineral. However, the effect of increasing the cutting speed is to generate more heat in the tool and increase the rate at which a wear flat forms. These effects may be reduced somewhat by the addition of a water jet immediately infront of the cutting tool: the effect being to cool the tip down and thereby reduce the wear rate.

Another approach taken by Hood (Hood et al, 1990), is to determine the amount of water jet energy per unit length cut that gives a certain reduction in tool forces, compared to cutting dry at a particular cutting speed. Then, if one wants to maintain these force reductions at a

faster cutting speed, one should increase the jet pressure or flow rate until the same energy per unit length cut is provided. Fig.2.31, illustrates Hood's evidence to support this, with the proviso that tests at greater cutting speeds should be conducted to confirm the initial findings.

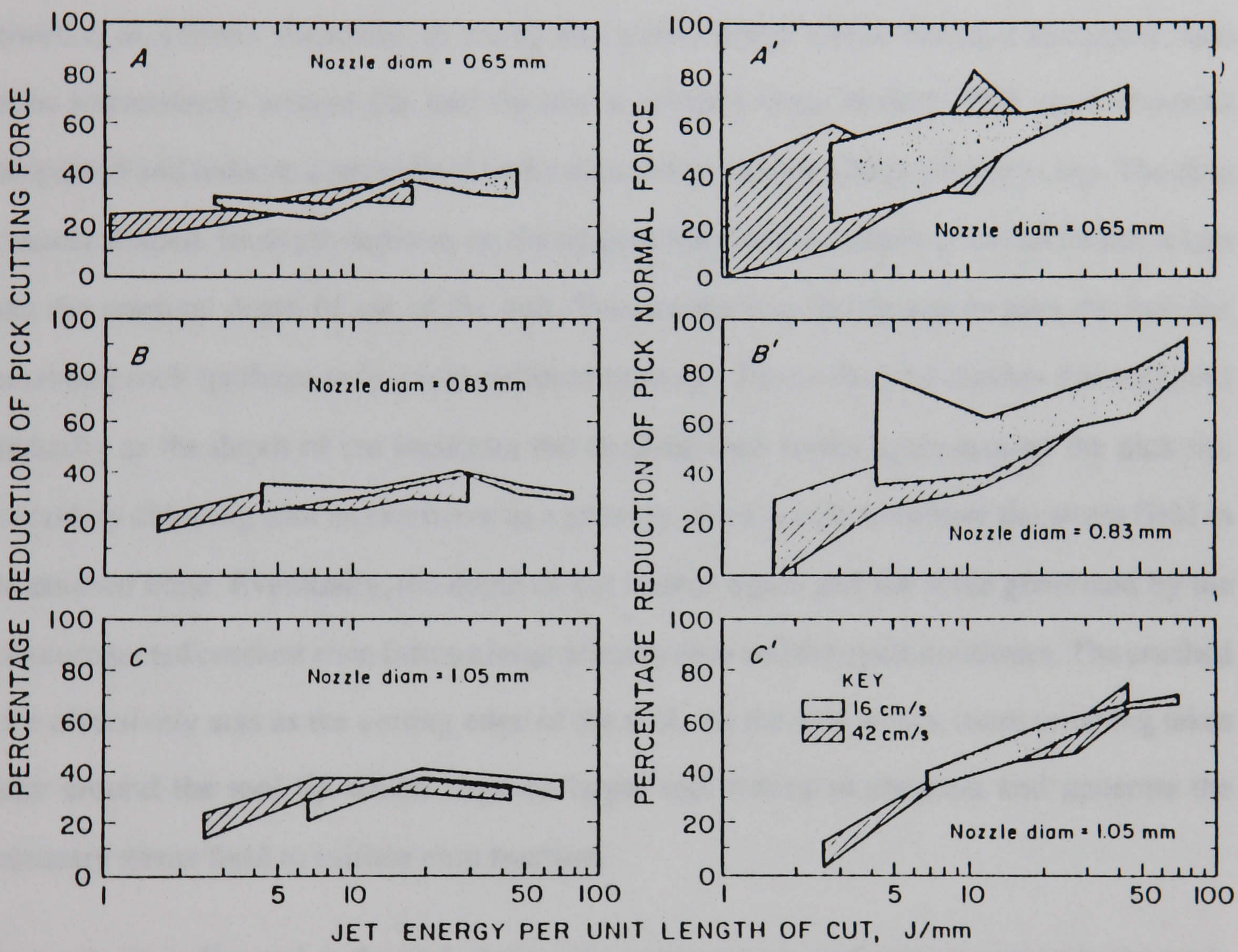


Fig.2.31 Reduction of bit forces (given as percentage of forces measured when cutting dry) as function of jet energy per unit length cut. Shaded ares are 90% confidence bands for these results.

2.4.5 The Theory of the Water Jet Assisted Cutting Mechanism

Several theories on the way a water jet assists the cutting action of a drag bit have been presented. All are empirically derived, being explanations of observed experimental phenomena. Since most research on hybrid cutting has been conducted in rock, the theories are concerned with rock cutting.

A very thorough and systematic account of the mechanism of hybrid cutting is given by Fowell et al, (1986). Basically, as a drag tool cuts through a rock material a crushed zone forms immediately around the tool tip and is roughly cone shaped. This zone becomes compacted and induces a stress field in the rock which causes a large primary chip. The chip is saucer shaped. Its depth depends on the tip geometry and the depth of cut taken but is less than the nominal depth of cut of the tool. This means that the tip has to pass through the remaining rock (perhaps only a few millimetres deep). Hence the tool crushes this rock and gradually as the depth of cut increases the crushed zone forms again around the pick tip. Secondary chipping (not as extensive as a primary chip) occurs to relieve the stress field in the crushed zone. Eventually, the depth of cut is deep again and the force generated by the now compacted crushed zone forms a large primary chip and the cycle continues. The crushed zone effectively acts as the cutting edge of the tool. As the tool wears, more crushing takes place around the tool tip which requires larger tool forces to compact and generate the necessary stress field to initiate chip fracture.

If a weak jet is directed at the pick during the cutting cycle and cannot penetrate the rock, then effectively the above mechanism is unaltered. As the jet power is increased, the jet penetrates the rock and offers some relief to the tool tip during the crushing phase and less force is needed for this operation. If the jet penetration continues and disturbs the crushed

zone around the tip, then chipping events are affected (since the crushed zone acts as the cutting edge) and the tool merely crushes the rock with small chipping apparent: the tool is essentially making a groove through which to pass rather than creating large chips.

The authors conclude that optimum jet penetration would be that which did not affect the crushed zone but nevertheless reduced crushing. In this way efficient chipping would occur and unnecessary, energy consuming crushing and profiling would be minimised. This holds true for both sharp and blunt picks since the authors found optimal jet assistance in both cases. Other factors are proposed by which the cutting process is helped: cooling of the tool; reduced friction between the tool and the rock; and in debris clearance.

Fairhurst and Deliac (1986), propose that the cutting process consists of cyclic crushing of small chips, followed by increasing pick penetration and ultimate failure of 'large' chips. The jet helps in debris removal, reduces the tool wear and cools the tool down. A critical velocity is postulated above which the jet may increase the tool forces. This could be due to the jet not having the required power to penetrate the rock at this speed and actually holding the chips down. The critical velocity decreases with increasing rock strength and increases with greater jet power.

Wang and Wolgamott (1978), state that mechanically created cracks form under the pick which are filled and opened by high pressure water. In this way the jets assist the mechanical fracture process initiated by the pick: Hence less force needs to be applied on the rock by the tool to complete the process. The point is made that the pressure required to open the cracks is much less than that for kerfing. Thus, low pressures, around half the compressive strength of the rock, should be used.

Dubugnon, postulates that the action of the jet is to remove the crushed material underneath the cutting zone enter and weaken the dilated material ahead of the tool and extend the fractures made by the tool.

Hood et al (1990) suggest that with the jet aimed parallel to the front face of the pick i.e. at the rake angle, and as close as possible to it (within 2mm), and having sufficient power to penetrate and remove the crushed compacted material around the pick, significant benefit should be obtained. Cracks propagated by the tool are entered by high pressure water and assist in the fracture.

The crushed rock around the tool is postulated to act as a cushion between the tool and rock. Hence to generate the force necessary to induce fracture, energy is wasted in compressing the fine, crushed material. By removing this, the tool can apply a direct, undamped force to the rock and cause failure at a lower force level in the pick.

To support this idea Hood, quotes the concept of the 'coefficient of cutting friction', defined as the ratio of the cutting to the normal force. He states that this ratio is seen to increase when force reductions due to jet assistance are procured, and suggests that the friction between the tool and rock is therefore actually increased by jet assistance.

MacAndrew et al (1987), report that a jet assists the cutting process in two ways. The first is in harmony with Fowell et al (1985), for sharp tools at slow cutting speeds. The second is to hard rocks where any benefit is derived from the cooling of the pick.

Emphasis is placed on the roll of the cutting speed and the degree to which the jet can cool the pick tip. As a pick cuts through a rock, the cobalt in the tungsten carbide matrix leaches down to form a hard layer that resists abrasive wear of the tool. As the heat generated in the

tool increases, particularly at fast cutting speeds, the carbide softens and the hard layer is abraded away. This continues and the wear flat gradually enlarges causing both the cutting and normal force components to increase considerably. Eventually the tool has to be replaced.

A water jet with enough power to constantly cool the carbide tip and thereby maintain the hard cobalt layer, reduces the rate at which the wear flat forms and hence the rate the forces increase. The tools last longer, which is the benefit most sought after from the viewpoint of the authors.

If the cutting speed is such that the water jet cannot penetrate the rock and adequately cool the carbide insert, then jet assistance is of no practical use: indeed, the tool may be subjected to alternate cooling and heating which leads to its ultimate catastrophic failure due to thermal stresses being induced in the insert. Therefore the authors also suggest the concept of a critical cutting velocity for a particular rock, above which no practical benefit may be obtained from jet assistance.

Mazurkiewwicz and Summers (1986), present a theory on coal. A cutting tool is said to crush the coal and form a zone of fine material which 'acts as a plastic shield' to the surface the tool is cutting in to. High forces are then needed to cut the coal and a large proportion of fines is produced.

The existence of bedding and cleat planes is extended to a microscopic level and with jet assistance, the water penetrates into the material along cracks and any crushed and free coal is immediately flushed away from the impact zone. Cracks, bedding and cleat planes are extended by the high pressure water until they meet and form free particles from the coal mass.

3 OBJECTIVES OF RESEARCH PROGRAMME AND EXPERIMENTAL DESIGN

3.1 Introduction

Research into high pressure water jet assisted cutting has been quite extensive, but not entirely conclusive, over the past decade. The majority of the work has been directed to rock cutting and its application to tunnelling machines, and the benefits claimed are well documented in the literature.

Fundamental research into assisted coal cutting though has lagged behind and this research project is an attempt to bridge the gap. The programme below details the experiment conducted in the Mining Department of the University of Newcastle upon Tyne. In addition to this programme the analysis of the results of a parallel study in jet assisted coal cutting were performed in the Department and are included in this volume but covered in a separate section.

3.2 Objectives

The objectives of the project are stated below:

- To ascertain whether high pressure water jet assisted coal cutting reduces the proportion of fine coal produced, and to what extent, as compared to unassisted trials;
- To examine the effect of sharp and blunt picks on cutting performance with jet assistance;
- To assess the influence of cleat direction on cutting performance, product size and breakout pattern with jet assistance;
- To investigate the effect of coal strength on the effectiveness of high pressure water jet assisted cutting.

3.3 Research Programme

The table below lists the variables or factors that affect jet assisted cutting. The level at which each factor was tested in this experiment are also indicated, together with their values.

Factor	Level	Value
A) Jet		
1. Jet pressure	4	0, 35, 70, 105MPa
2. Nozzle Diameter	4	0, 0.62, 0.75, 0.82mm
3. Nozzle Design	1	M.R.D.E.
4. Nozzle Material	2	Tungsten Carbide/Brass
5. Additive	1	No Additive
6. Jet Type	1	Continuous
7. Jet Fluid	1	Water
B) Operational		
8. Stand-off Distance	1	75mm
9. Lead Distance	1	1-2mm
10. Jet Position	1	Infront of pick
11. Side-off Distance	1	Zero
12. Number of Passes	1	One
13. Cutting Mode	1	Relieved
14. Depth of Cut	1	30mm
15. Line Spacing	1	70mm
16. Traverse Speed	1	1.1m/s
17. Tool Type	1	75mm radial with HW tip
18. Tool Wear	2	Sharp/Blunt
19. Offset Angle (Skew)	1	Zero
20. Cutting w.r.t Cleat	2	Parallel/Perpendicular
C) Coal		
21. Coal Type	2	Bituminous/Anthracite

Table 3.1

The number of possible variable combinations is quite staggering and consequently a very selective programme was chosen. Obviously jet pressure and water flow rate are fundamental parameters in assessing the effectiveness of water jet assisted cutting and these two factors were varied. They were varied such that the power quadrupled as the pressure and flow rate doubled. Hence a wide range of jet powers are represented by these two parameters. The jet position and lead distance were fixed at what is considered as the optimum position for jet assistance. The depth of cut and line spacing are typical values of those used in the field. The state of bluntness of a cutting tool influences the forces it requires to cut a mineral and so this was of interest too.

More pertinent to coal mining than to rock cutting is the influence on the product size of jet assistance and therefore the debris was collected after each treatment and a size analysis carried out. The cost of reclaiming fine coal via froth flotation is twice as much as washing the larger fractions from the run of mine. Thus the size analysis was a major part of the experiment since this would indicate if jet assistance significantly reduced the fine coal fraction.

3.3.1 General Test Procedure

All the coal blocks were mounted such that the cutting pick cut through the bedding planes. This was maintained even when the cleat orientation was changed.

The nozzle was positioned infront of the pick so that the jet could impinge 1-2mm ahead of the tip. Due to the geometry of the tip the jet had to be inclined from the vertical about 12.5° to achieve this specification. The Wimet 75mm radial pick was used which is commonly employed on coal shearers although larger extra heavy duty 100mm reach picks are now being introduced.

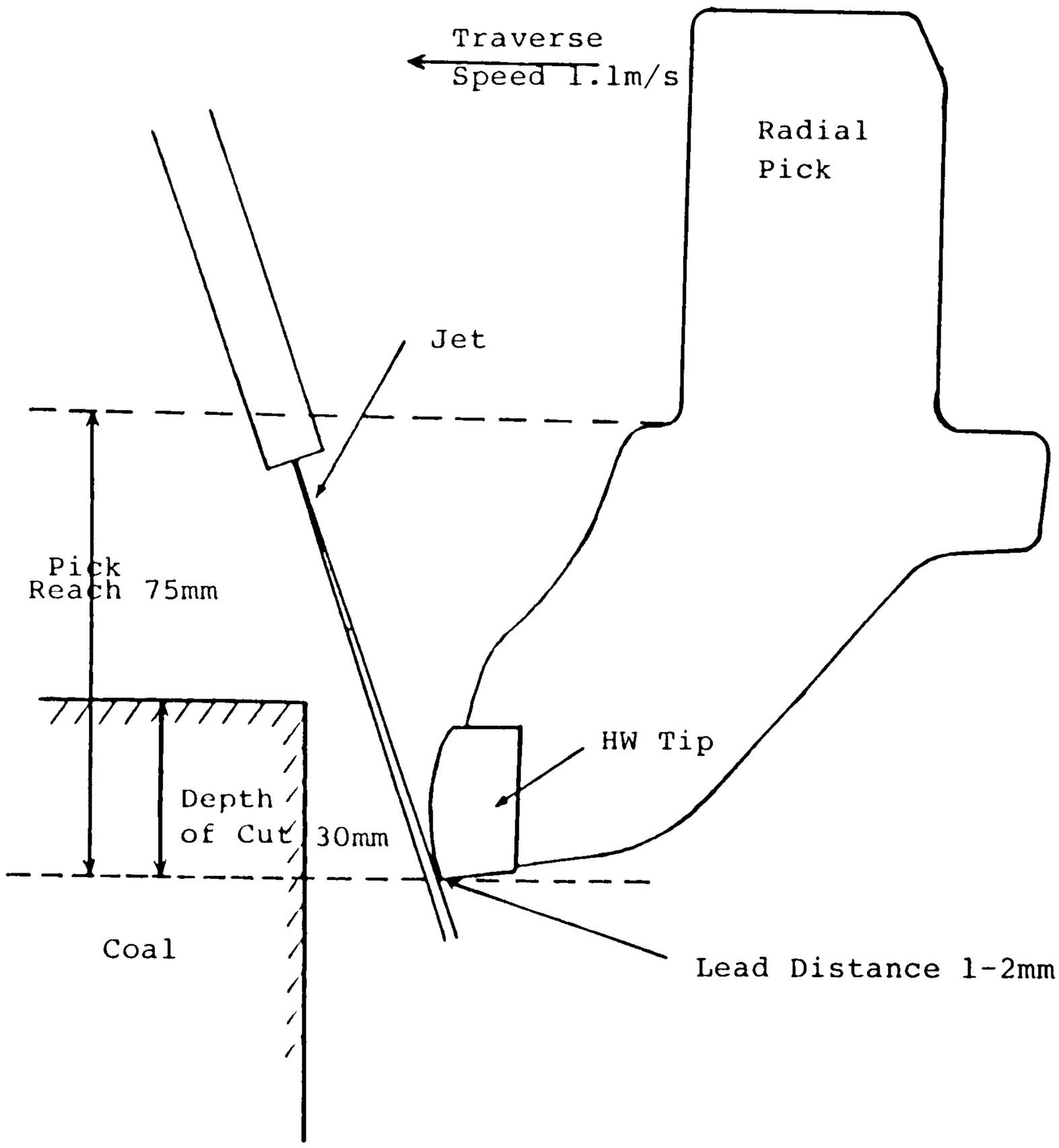
A cutting speed of 1.1m/s, the fastest presently available on the linear rig, was adopted throughout the tests. This was to approach as near as possible the actual cutting speeds of coal winning machines which are in the region of 3-4m/s.

All the tests were conducted with a relieved cutting pattern to model the actual mining situation where this is the case. The depth of cut was 30mm and the line spacing was 70mm, giving a line spacing to depth of cut ratio of 2.33. Fig 3.1 illustrates the general operational configuration of the experiment together with a diagram of the relieved cutting pattern.

One can see from the diagram that the depth of cut is a nominal figure. Line three would form the actual cuts taken in the experiment since in practice a pick would rarely cut into a level surface: the surface would depend upon the breakout characteristics of the particular mineral. Hence the coal surface had to be conditioned before a set of tests were conducted. For example, the coal was cut with a sharp tool and a 35MPa pressure water jet. The loose coal was cleared away and then on the freshly prepared surface the actual recorded tests were performed with a sharp tool assisted with the 35MPa pressure water jet. This was done to ensure that the breakout profile from the previous treatment did not affect the results of the following one. The breakout angle in the diagram is chosen purely for illustrative purposes.

As the jet pressure was increased so was the flow rate. The following combinations were used: 35, 70, 105MPa at 4, 8, 12l/min respectively.

Operational Configuration



Relieved Cutting Pattern

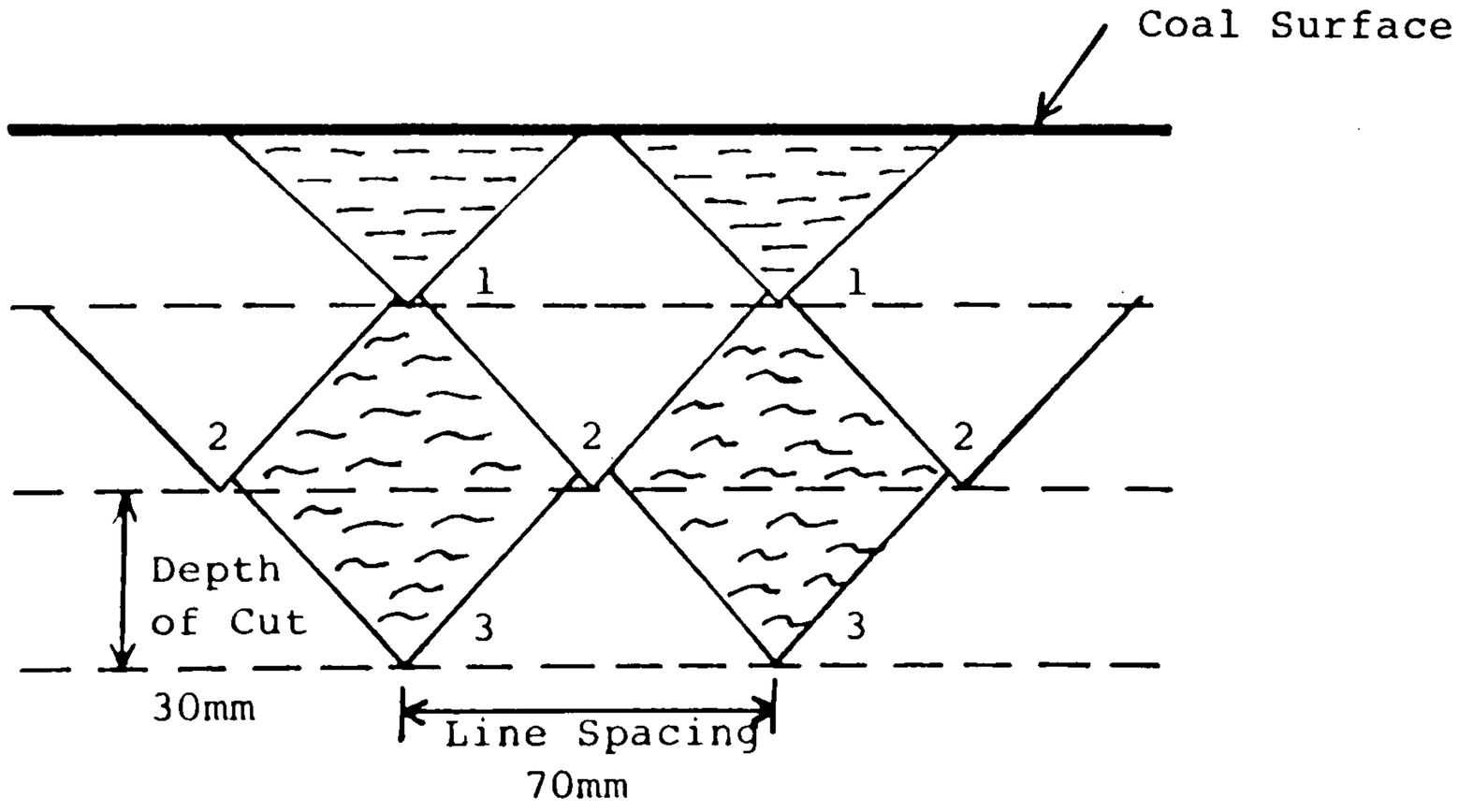


Fig.3.1

3.3.2 Experimental Design

The parameters to assess the effect of coal strength are given in the table below.

Factor	Level	Value
1. Jet pressure	4	0, 35, 70, 105MPa
2. Nozzle Diameter	4	0, 0.62, 0.75, 0.82mm
3. Tool Type	1	75mm radial
4. Tool Wear	2	Sharp/Blunt
5. Cutting w.r.t Cleat	1	Parallel to main cleat
6. Coal Type	2	Bituminous/Anthracite

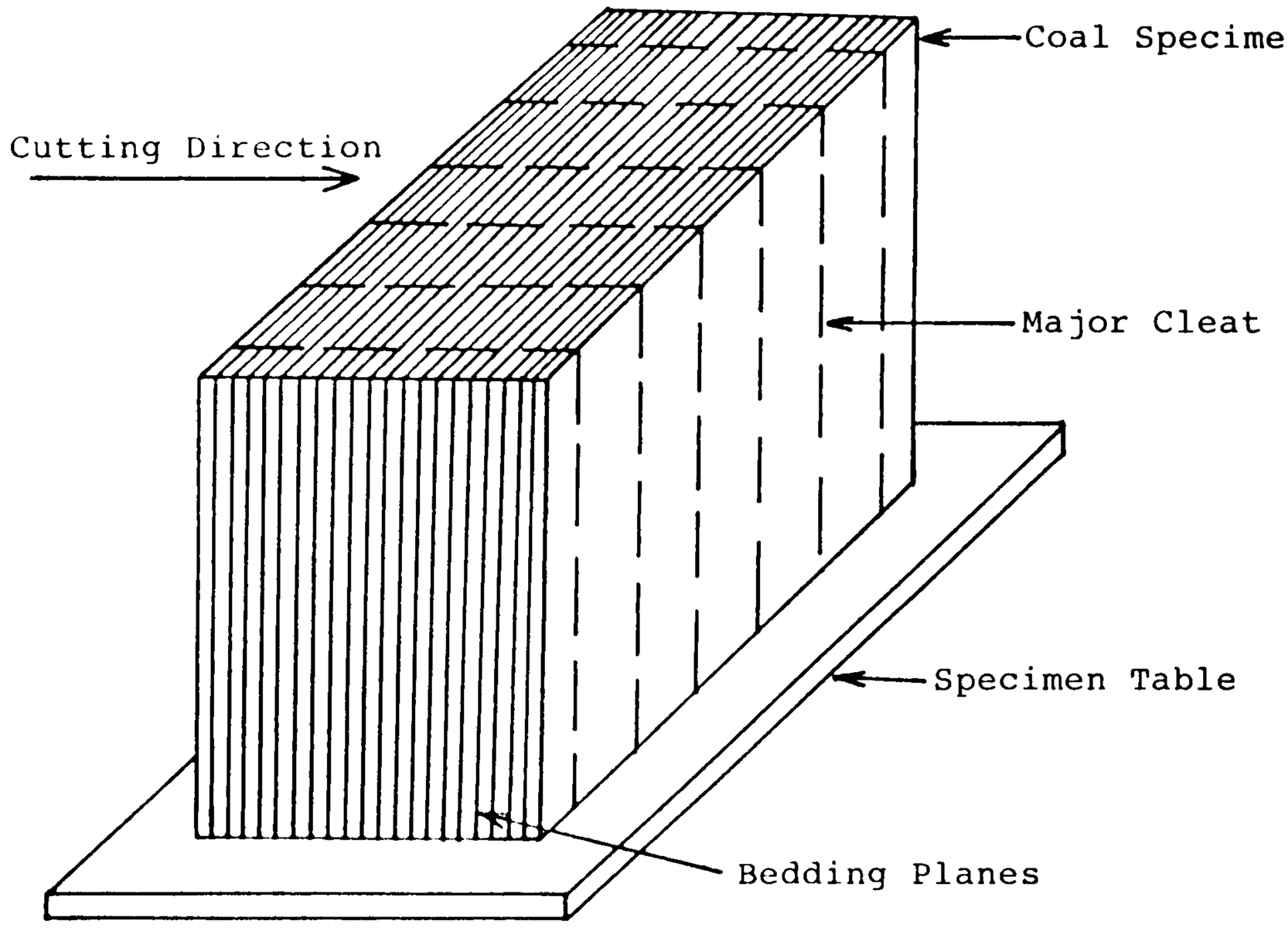
Table 3.2

The table describes a 4 x 2 x 2 full factorial experiment, the nozzle diameters change with the jet pressure and are thus not considered as an independent factor. During this experiment the pick forces, product size and breakout pattern were recorded.

The influence of cleat orientation was investigated in the stronger anthracite coal. The extreme situations were examined with the tool cutting along the main cleat i.e. 0° or parallel to it, and then with the coal block rotated through 90° so that the tool was cutting at 90° or perpendicular to it. However, in both cases the pick still cut through the bedding planes. Fig 3.3 clarifies how the bedding planes and major cleat are related to the cutting direction.

Table 3.3 below formally describes the experiment. The table represents a 4 x 2 x 2 full factorial design. As before the jet pressures and flow rates are considered as one factor. The pick forces, product size and breakout pattern were the measured parameters.

Major Cleat Parallel to Direction of Cut



Major Cleat Horizontal to Direction of Cut

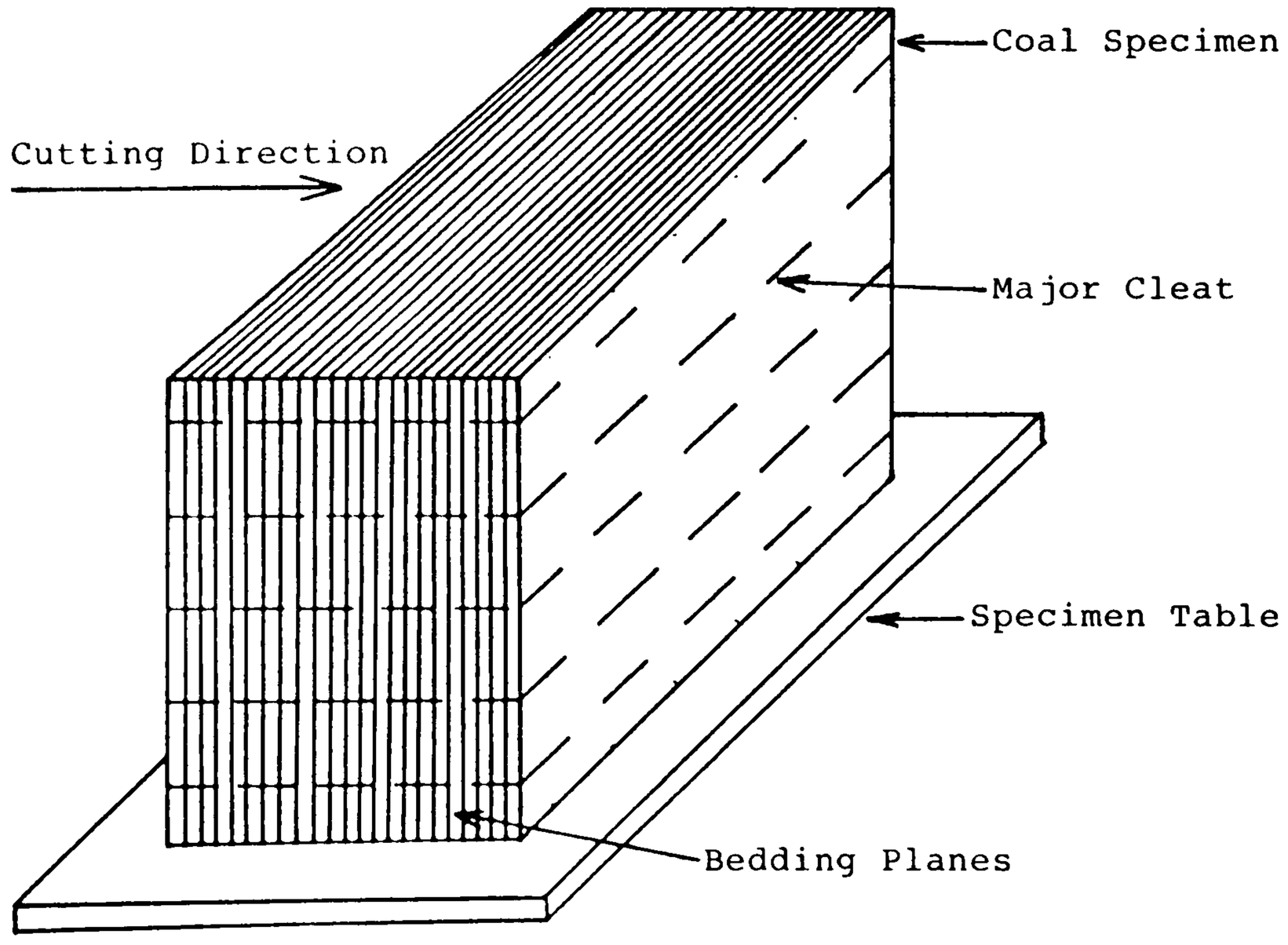


Fig.3.3

Factor	Level	Value
1. Jet pressure	4	0, 35, 70, 105MPa
2. Nozzle Diameter	4	0, 0.62, 0.75, 0.82mm
3. Tool Type	1	75mm radial
4. Tool Wear	2	Sharp/Blunt
5. Cutting w.r.t Cleat	2	0°/90° to main cleat
6. Coal Type	1	Anthracite

Table 3.3

3.3.3 Replication and Randomization

Due to the heterogeniety and anisotropy of the coal, the treatments were repeated as many times as the amount of test material would allow. This would minimize the experimental and standard errors of the results. The minimum number of replications for a treatment was five and the maximum was eleven. The average for the whole experiment was seven replications per treatment.

The treatments were carried out in a limited random order which was determined by the use of nine figure random number tables. The order was limited in the sense that all the replications for each treatment were carried out successively. Also, cuts with the sharp and blunt tools at the same water pressure followed one another.

3.3.4 Jet Penetration Tests

Trials were undertaken to assess the penetrating abilities of the respective jets in the different coals. The table below describes the levels of the factors in the experiment.

Factor	Level	Value
1. Jet pressure	4	35, 52.5, 70, 105MPa
2. Nozzle Diameter	3	0.62, 0.75, 0.82mm
3. Cutting w.r.t Cleat	2	0°/90° to main cleat
4. Coal Type	2	Bituminous/Anthracite
5. Traverse Speed	4	0.24, 0.64, 0.9, 1.1m/s

Table 3.4

The coal surface was first levelled by closely spaced shallow cuts in each coal block. The tool was set at a depth of cut of 30mm and then taken out of its holder, this meant that the jet was operating under the same conditions as the cutting tests apart from the levelled surface. The jet pressure and diameter were varied in the same combination as the cutting tests and so are considered as one factor viz. jet power. The 0.62mm diameter nozzle was combined with pressures at 35MPa and 52.5MPa, which was an addition to the coal cutting situation.

3.3.5 Statistical Analysis

The statistical analysis is described as the results are presented. The factorial design is quite common and thus software was available on the University Mainframe computer to double check the analysis outlined in the text. Since the number of replications for each treatment varied, according to the amount of coal available, the analysis was complicated slightly and computer verification proved invaluable. Programmes utilized for the analysis were 'Glim 3' and 'SPSSx'.

CHAPTER FOUR

4 THE NEWCASTLE WATER JET RESEARCH FACILITY, INSTRUMENTATION, DATA ACQUISITION AND ANALYSIS

4.1 Introduction

The experimental apparatus is a 50 tonne rock planing machine designed by the Design Unit, University of Newcastle upon Tyne. The basic equipment has been modified over successive research projects to meet particular specifications required from time to time. It can accommodate both disc cutters or drag picks, with or without water jet assistance.

Two Presswell 'Hydraflo' high pressure water pumps are available to the rig affording a wide range of pressures and flow rates. The jets may be positioned infront of or behind the drag tool. Lead-on and offset distances may also be varied.

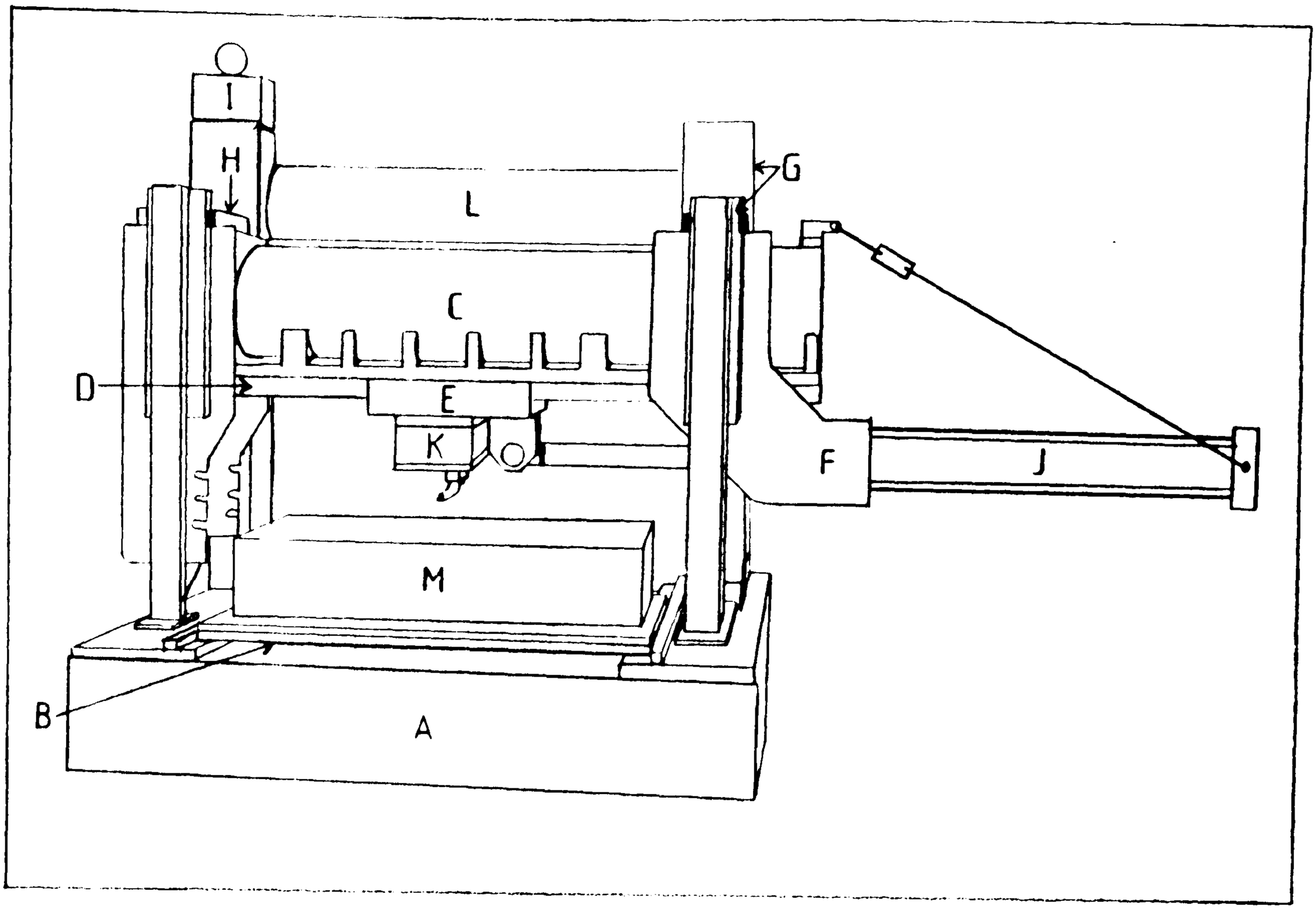
The main structure is shown diagrammatically in Fig.4.1.

4.2 Linear Cutting Rig

The linear cutting rig comprises the following components.

4.2.1 Frame Structure

The base of the structure is rectangular and consists of four substantial rectangular pieces attached by 36, 32mm diameter bolts. The base provides tracks for a specimen table to traverse along. Two large columns are welded to the base and support the guides for the cutter guide assembly to follow whilst ascending or descending. Two smaller vertical columns, also having guides for the cutter slide assembly, have been bolted onto the base opposite the main columns. These have been added to ensure the cutter slider assembly travels in the vertical plane and to make the whole structure more rigid. A large cylindrical beam is bolted inbetween the two main vertical columns at the top, to provide longitudinal



Key:

A. Structure base.

B. Specimen table.

C. Cylindrical strengthening beam of slide assembly.

D. Slide bed.

E. Cutter slider.

F. Support frame for the hydraulic ram.

G. Guides for the whole slide assembly.

H. Vertical stiffeners (clamps).

I. Clamp hydraulic power pack.

J. Hydraulic cylinder (pipework not shown).

K. Dynamometer, toolholder and cutting tool.

L. Cylindrical strengthening beam for the main structure.

M. Coal specimen.

Fig.4.1

rigidity to the system.

The whole apparatus rests on a concrete floor. It is levelled to prevent it deforming under its own weight and the vibrations attendant to cutting. A level machine also means that a plane, level surface may readily be obtained on a rock specimen if required and the depth of cut is maintained constant in any one test.

The rig stands approximately 2.6m high and weighs in the region of twelve tonnes.

4.2.2 Specimen Table

The specimen table traverses at 340mm/min on tracks provided by the base of the main frame structure. It is a reinforced 50mm x 1630mm x 1070mm steel plate. A sample is mounted on a 25mm thick steel base plate the same size and bolted onto it around its circumference by 24, 18mm diameter bolts. This secures the sample rigidly to the specimen table.

Spacing the cuts is achieved by traversing the table via two motor-driven screw jacks. The distance moved is measured from an arbitrarily set datum (e.g. the centre of the specimen table) by a rack and pinion operated multi-turn potentiometer to an accuracy of ±1mm. A d.v.m. displays the reading on the control panel. The table is stopped at either end of its travel by limit switches fitted 900mm apart.

A hydraulic cylinder is incorporated in the specimen table. This may be connected to the main hydraulic circuit. When activated the cylinder presses against the base of the rig and holds the specimen table rigid during a cutting trial. This is particularly useful where large forces are expected.

The largest size of specimen that may be accommodated is 1400mm x 900mm x 900mm.

4.2.3 Slide Assembly

The slide assembly consists of: a large diameter cylindrical beam; a slide bed; a cutter slider; a support frame for the cutting ram; and the guides to facilitate vertical movement (see Fig.4.1).

Four motor-driven screw jacks move the assembly up and down at a rate of 30mm/min. A rack and pinion activated potentiometer and digital display, indicate the height of the cutting tool to ±0.1mm accuracy. Again, the reference point for measuring the height is fixed arbitrarily by the rig operator. The screw jacks and d.v.m. height indicator are used to set the depth of cut.

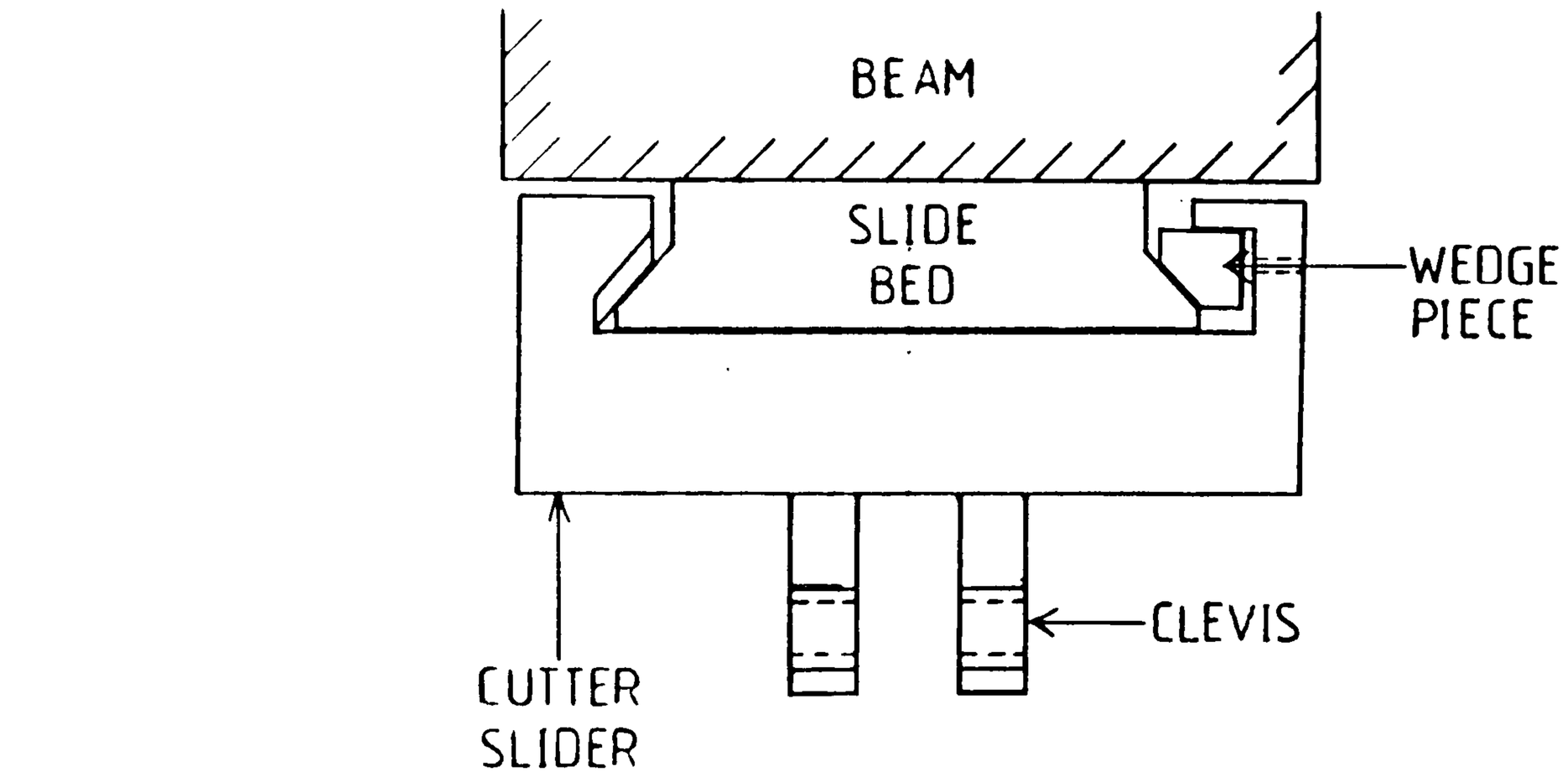
Fig.4.2 shows the slider. Any play in the slider due to wear can be taken-up by adjusting the wedge piece. A hydraulic cylinder is connected to the slider via a clevis. The ram causes the slider to traverse. A dynamometer is bolted onto the slider with the drag pick and water jet arrangement.

The length of cut is determined by the position of two limit switches attached at either end of the slide bed. Slider velocity may be varied up to a maximum of 1.1m/s.

4.2.4 Vertical Stiffeners (Clamps)

During previous cutting trials in hard rock, it was observed that the slide assembly flexed slightly under the high normal forces encountered. In order to reduce this vertical deflection, hydraulically actuated clamps have been mounted on the slide assembly which grip the adjacent guide columns and thereby restrict vertical displacement during a test (Fauvel, 1981).

Whilst engaged in a calibration, a check was made to ascertain if the vertical displacement could appreciably affect the depth of cut required in the coal study.


BEAM
SLIDE
BED
WEDGE
PIECE
CLEVIS
CUTTER
SLIDER

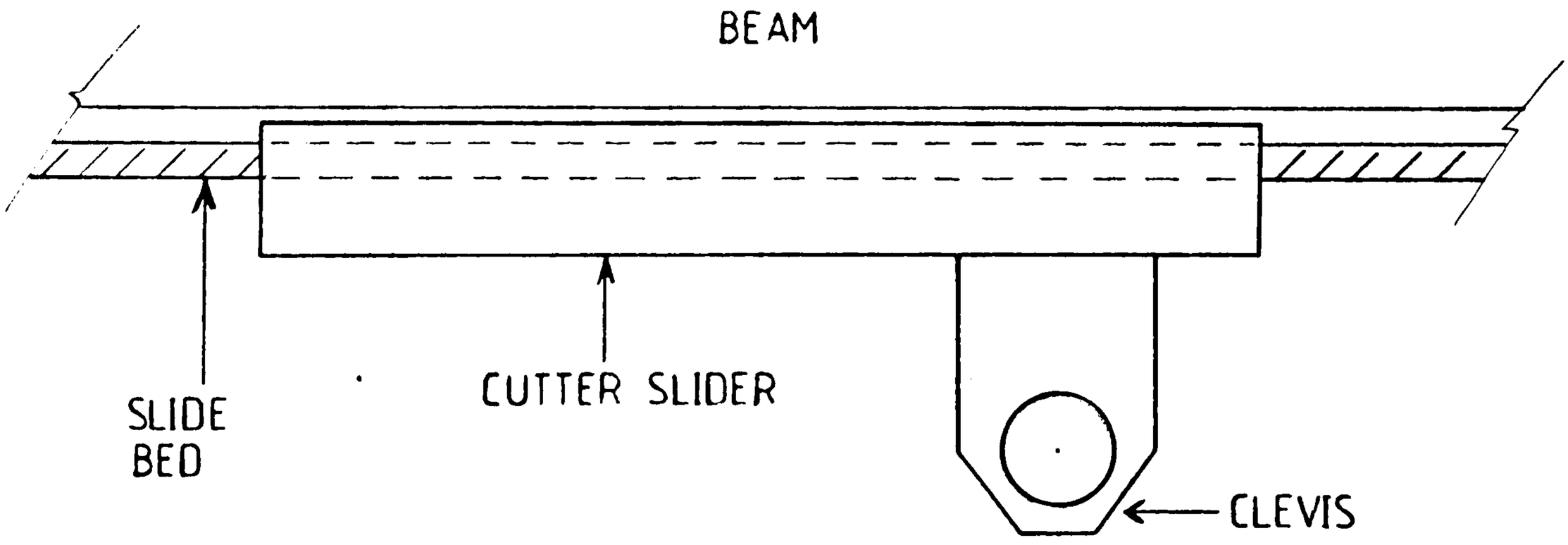

BEAM
SLIDE
BED
CUTTER SLIDER
CLEVIS

Fig.4.2

Initially, the relative movement between the cutter slider and the slide bed was examined. A dial gauge anchored on the slide bed with its pointer positioned on the slider was set up, Fig.4.3. The wedge piece in the slider was loosened so the maximum displacement would be obtained. A vertically acting load was applied to the slider.

At a load of 5.4kN the slider raised 0.28mm. Thereafter, up to 40kN, no further displacement was observed.

A similar test was then made with the dial gauge base on the calibration plate and the pointer resting on the bottom edge of the toolholder, Fig.4.3

The load was increased to 40kN several times with the clamps both on and off. The maximum displacements recorded in both conditions were 0.60mm and 0.75mm respectively.

Since the normal forces experienced in the coal cutting trials were typically below 3kN and the depth of cut was 30mm, it was concluded that at such force levels the degree of flexure would not affect the results.

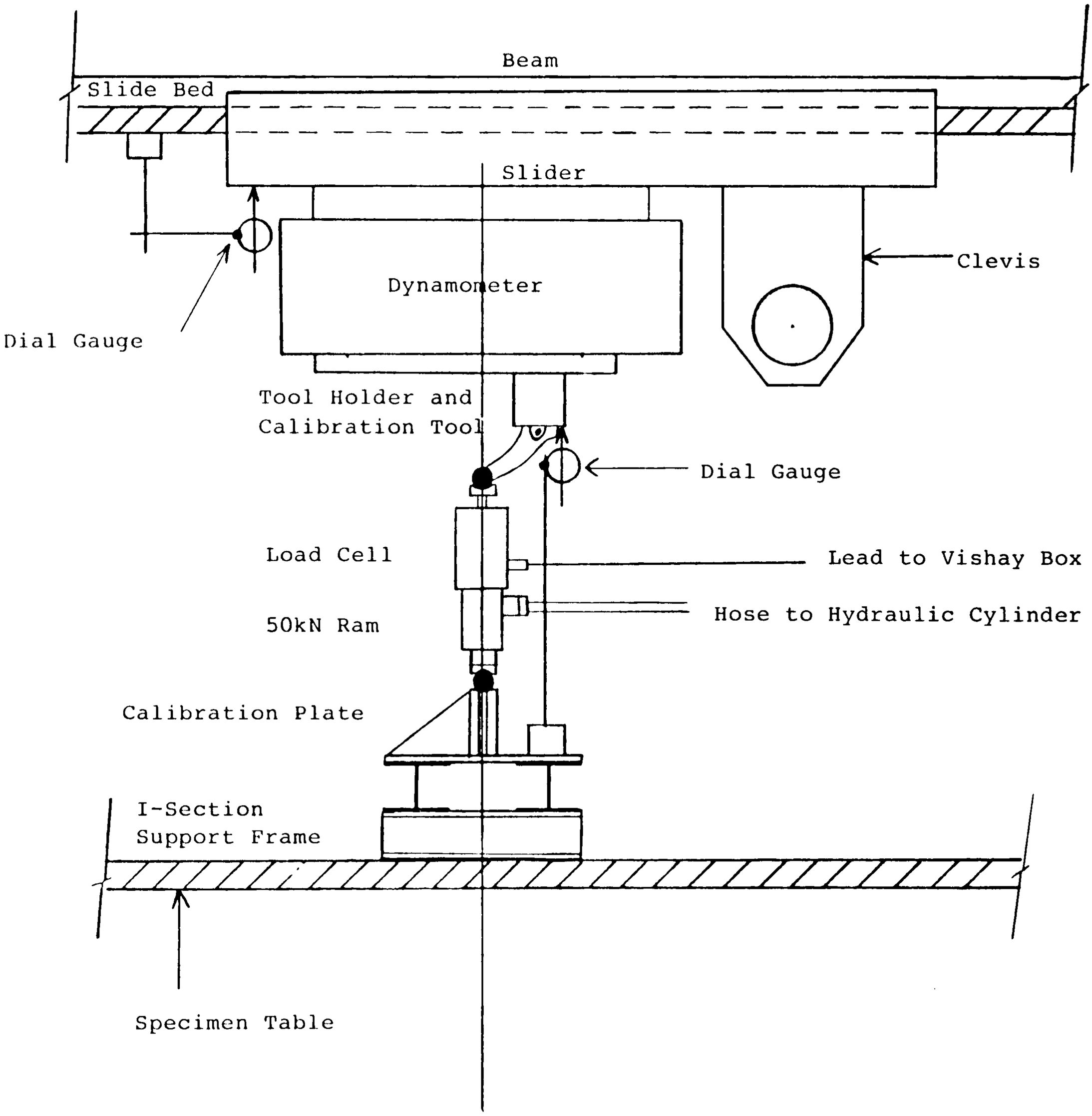
4.2.5 Clamping Hydraulic System

This system is independent of the main hydraulic circuit and provides the fluid power to operate the vertical stiffeners at 15.1MPa oil pressure. The electrical design of the rig does not allow the slide assembly to be raised or lowered whilst this hydraulic system is activated. The clamp power is initiated from the control panel.

4.2.6 Main Hydraulic System

The main hydraulic circuit is shown in Fig.4.4. It is designed to enable the ram to extend at a constant speed; the maximum being 1.1m/s.

Calibration Arrangement



Not to Scale

Fig.4.3

High Pressure Hydraulic Circuit

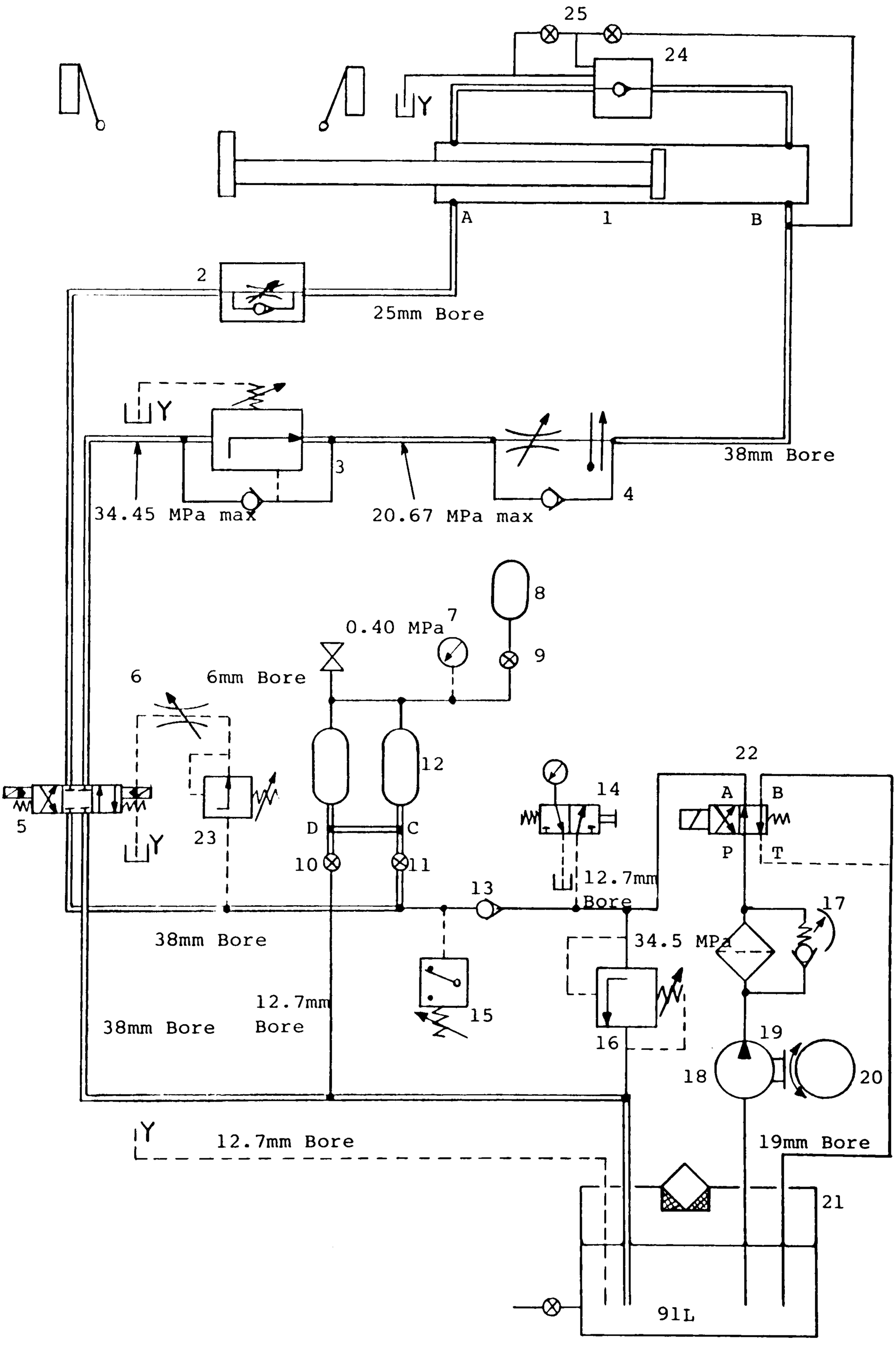


Fig.4.4

Key:

1. Double acting hydraulic cylinder. 102mm Bore x 2083mm Stroke, 20.67MPa maximum pressure.
2. Throttle check valve. 34.45/20.67MPa, max. reverse flow 113.75l/min.
3. Pressure reducing valve, 34.45MPa, with check valve 227.5 l/min.
4. Flow Control Valve, 20.67MPa. Temperature and pressure compensated with reverse flow check valve.
5. Directional control valve, solenoid pilot operated, 34.45MPa, 227.5l/min.
6. Fine throttle valve, 1/4in. B.S.P.
7. Pressure gauge, 0-40MPa.
8. Gas back-up bottle, 91l, 34.45MPa.
9. Gas shut-off valve, 3/4in. B.S.P., 34.45MPa.
10. Accumulator vent valve, 1/2in. B.S.P., 34.45MPa.
11. Accumulator shut-off valve, 1 1/2in. B.S.P., 34.45MPa.
12. Hydraulic accumulator, draw-off 54l. Pressure:max. 34.45MPa; min 20.67MPa.
13. Check valve, 1/4in. B.S.P.
14. Pressure gauge with isolating valve, 34.45MPa service pressure, 41.34MPa indicated.
15. Pressure switch, 34.45MPa max, low pressure differential.
16. Relief valve, 1/4in. B.S.P., line mounting 34.45MPa max. 8.19l/min.
17. 15 micron pressure filter, 34.45MPa, 8.19l/min.
18. High pressure pump, 34.45MPa, 8.19l/min.
19. Bell-mounting housing and flexible coupling.
20. 7.5kW T.E.F.C. foot and flange mounted motor.
21. 91l hydraulic tank with sight glass, filler breather, drain-plug assembly and cover.
22. Solenoid operated by-pass valve, 34.45MPa.
23. Pressure reducing valve, 34.45MPa.
24. Pilot operated check valve.
25. Manually operated flow control valves.

Basically, a high pressure/low volume pump (18) charges two 54 litre nominal capacity hydro-pneumatic bladder accumulators with hydraulic oil (12). To allow a greater draw-off from the accumulators, a 91 litre auxiliary gas back-up bottle is connected in circuit (8). By this means enough oil may be stored in the accumulators to ensure that the ram travels its full stroke at a constant speed when they are discharged.

A flow control valve (4) determines the ram velocity. When the directional control valve (5) is operated, the pneumatic energy stored in the accumulators and gas back-up bottle is released forcing hydraulic fluid into the ram (1) and thus extending it. The ram is double acting and is similarly retrieved.

To obtain the oil flow rate required to reach a 1.1m/s velocity, the fluid from the annulus of the ram is circulated via a pilot operated check valve (24) to the other side of the cylinder i.e. from side A to side B.

The speed of the ram is depends upon the oil flow rate which is a function of the oil pressure. Therefore, provided enough fluid is available, the ram speed depends upon the oil pressure for any particular setting of the flow control valve. Hence, to obtain a constant velocity the oil pressure must be maintained constant. This is achieved by the pressure reducing valve (3).

Fluid downstream of the pressure reducing valve is maintained at 20.67MPa by dumping excess oil to tank. To continue at this constant pressure, the accumulators must be discharging oil at a pressure greater than this value.

Valves (16) and (23) safeguard against the system pressure increasing above 34.45MPa, the designed maximum. Pressure switch (15) automatically cuts out the high pressure pump at the maximum system pressure.

The accumulators have to be recharged for each successive cut; this takes about ten minutes.

A low pressure/high volume gear pump (not shown in Fig.4.4) is also part of the design. This pump by-passes the accumulators and directly delivers fluid to the ram. It is utilized to prepare specimens for a cutting regime e.g. trimming rock surfaces.

Further details concerning the hydraulic cylinder and accumulators are given in the appendices.

4.3 High Pressure Water System

A 75kW Presswell Engineering Ltd. Hydraflo intensifier type pump supplies high pressure water up to 70MPa at a maximum flow rate of 45 litres/min. The water passes through stainless steel tubing and braided flexible hose to the nozzle.

The double acting intensifier on this pump may be replaced with another unit to deliver water up to 207MPa at 15 litres/min if required.

During the course of the experiment an additional Presswell Hydraflo pump was acquired enabling tests to be performed up to 248MPa when desired.

A 228 litre capacity header tank was the source of water to the pump. The outlet to the tank must be at least 2m above the inlet to the intensifier. Both pumps can also be adapted to accept mains water supply.

Since the pumps are not used continuously, a small amount of soluble oil is added to the water reservoir to lubricate the intensifier piston and inhibit internal corrosion.

4.4 Rig Relocation

On commencing the project, the experimental apparatus was assembled in the Department of Geotechnical Engineering, university of Newcastle upon Tyne. Hence it had to be dismantled, transported and erected in the Department of Mining Engineering before actual testing could begin. The relocation was carried out by the technical staff of the Mining Department.

Plate 4.1, shows the basic main frame structure partially assembled. The screw jacks, for raising and lowering the slide assembly, are clearly visible. The hydraulic cylinder is not connected but the cutter slider is shown in the centre of the picture. The ram attaches to the clevis.

One can see how the base is bolted together and how substantial the structure is. The specimen table (not shown) would carry the coal sample and be situated below the cutter slider. Other items were added later and included: the vertical stiffeners (immediately above the screw jacks); two more guide columns; the ram; the specimen table screw jacks; and the power pack for the clamps.

One of the high pressure pumps is shown in Plate 4.2. The 75kW motor is to the bottom right. To the left of this is the oil tank which masks the main swashplate oil pump behind it. Left again, one can see a small round stainless steel cylinder adjacent the chain hook; turning this alters the water pressure. On top is the intensifier unit which may be changed for a higher rated one. The high pressure tubing is not shown connected.

Electrical contractors were employed to re-wire the rig.

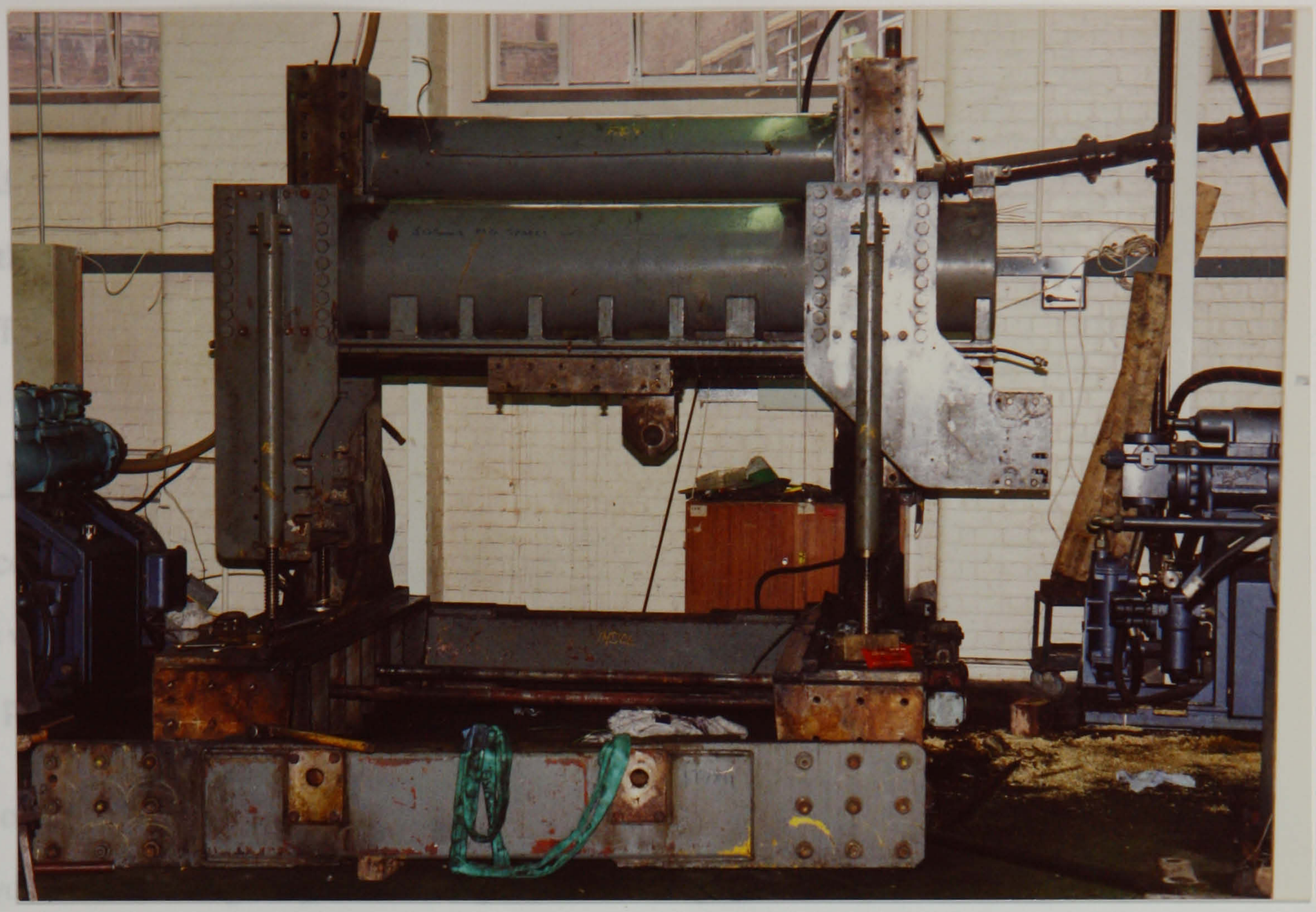


Plate 4.1 Rig main frame structure.

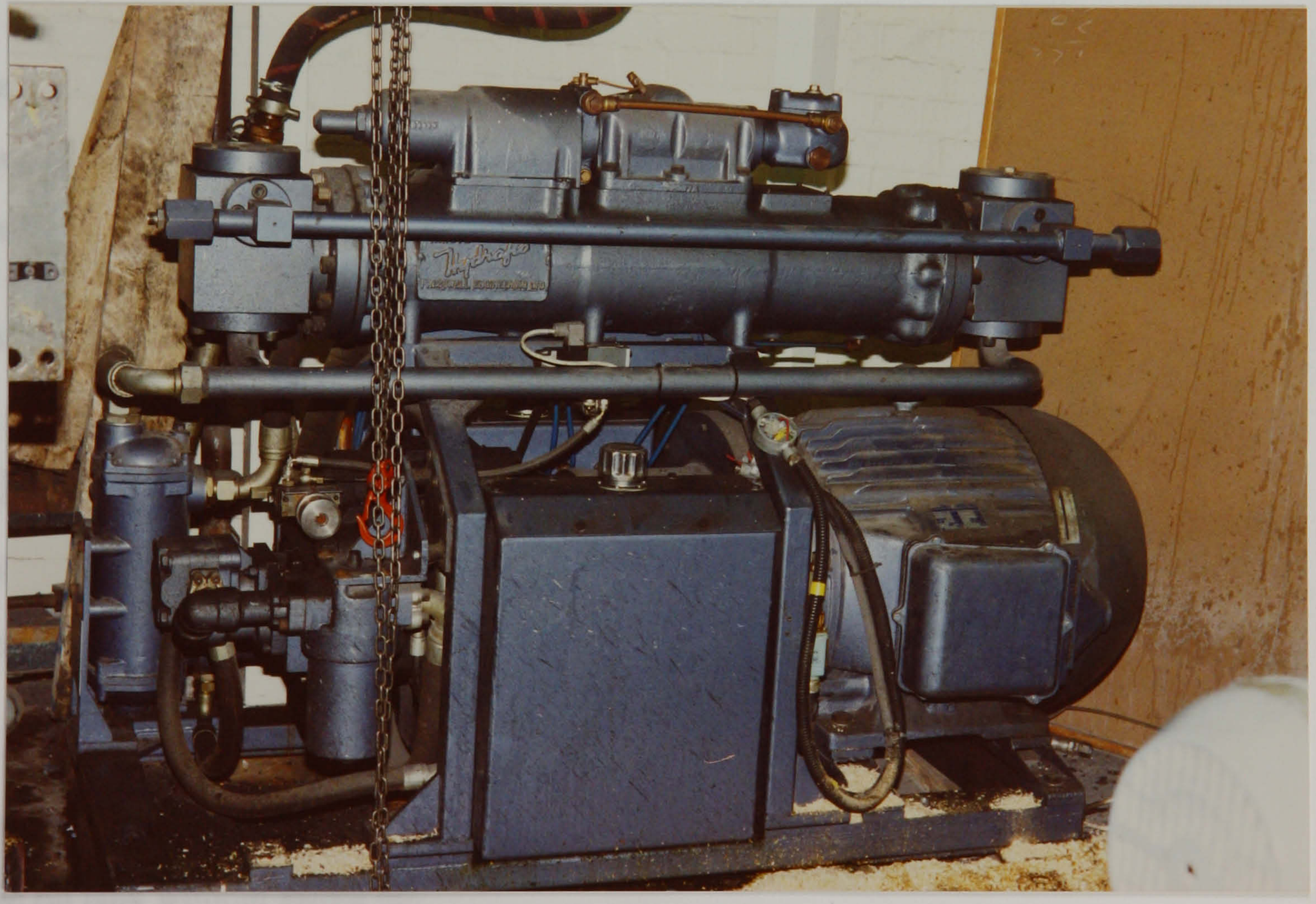


Plate 4.2 High pressure pump.

4.5 Repairs and Modifications

After the rig had been assembled, difficulties were experienced in rendering it operational and effort was directed to this end.

4.5.1 Hydraulic Accumulators

The accumulators were charged with dry, oxygen free nitrogen. Four 175bar nitrogen cylinders were discharged into the accumulators and gas back-up bottle. A severe leak occurred in the pneumatic pipework requiring new seals to be fitted throughout.

Upon operating the hydraulic cylinder it became apparent that gas was being introduced into the hydraulic circuit giving erratic, unpredictable response. Both accumulators were dismantled. The bladders were checked for leaks by inflating them to one and a half times their original size and immersing in water. One bladder exhibited pin-prick holes near the gas valve stem and was replaced.

Another problem occurred when a leak was observed from the fluid port assembly of one accumulator. It was found that the anti-extrusion ring had split. A replacement was obtained and fitted.

Details and diagrams of the accumulators are given in the appendices.

4.5.2 Hydraulic Network

The solenoid operated by-pass valve (22 in Fig.4.4) was malfunctioning: the solenoid was changed.

A hair-line fracture was discovered in the outlet pipe to the low pressure pump. This was repaired. A valve has been fitted on the suction side of the pump so that it can be separated from the oil tank without losing oil.

A problem was experienced with the pilot operated check valve. As stated previously, this valve allows fluid from the annulus of the ram to circulate to the cylinder and thereby complement the oil flow from the accumulators as the ram extends. One observed that after extending the ram it was necessary to wait a few minutes before it could be retrieved. Advice was sought on this matter and it was suggested that the pressure acting on the pilot piston inside the check valve was not dissipating as quickly as desired. A modification to the hydraulic network proved this to be the case and resolved the situation.

Fig.4.5, illustrates the change made to the circuit. Ignoring valve V2 for the moment, to extend the ram valve V1 must be open. Pressure from the inlet to the ram is diverted via V1 to X. This operates a pilot piston that opens the check valve thereby allowing fluid to pass from B to A. When the ram has travelled its stroke say, the pressure in the pilot line should dissipate through Y to tank. This was not occurring fast enough to allow the ram to be immediately retrieved, even when V1 was closed. Therefore, valve V2 was added which could be opened at the end of the ram's stroke and instantly reduce the pressure acting on the pilot piston. This resolved the problem.

To help purge the system additional bleed points were made on the pipework to the hydraulic cylinder.

4.5.3 Electrical Factors

Before it was relocated the controls for the rig and the high pressure pump were on separate electrical control panels. Therefore these were all transferred on the same panel to make operation easier. An emergency stop button was added to isolate all power to the apparatus when needful.

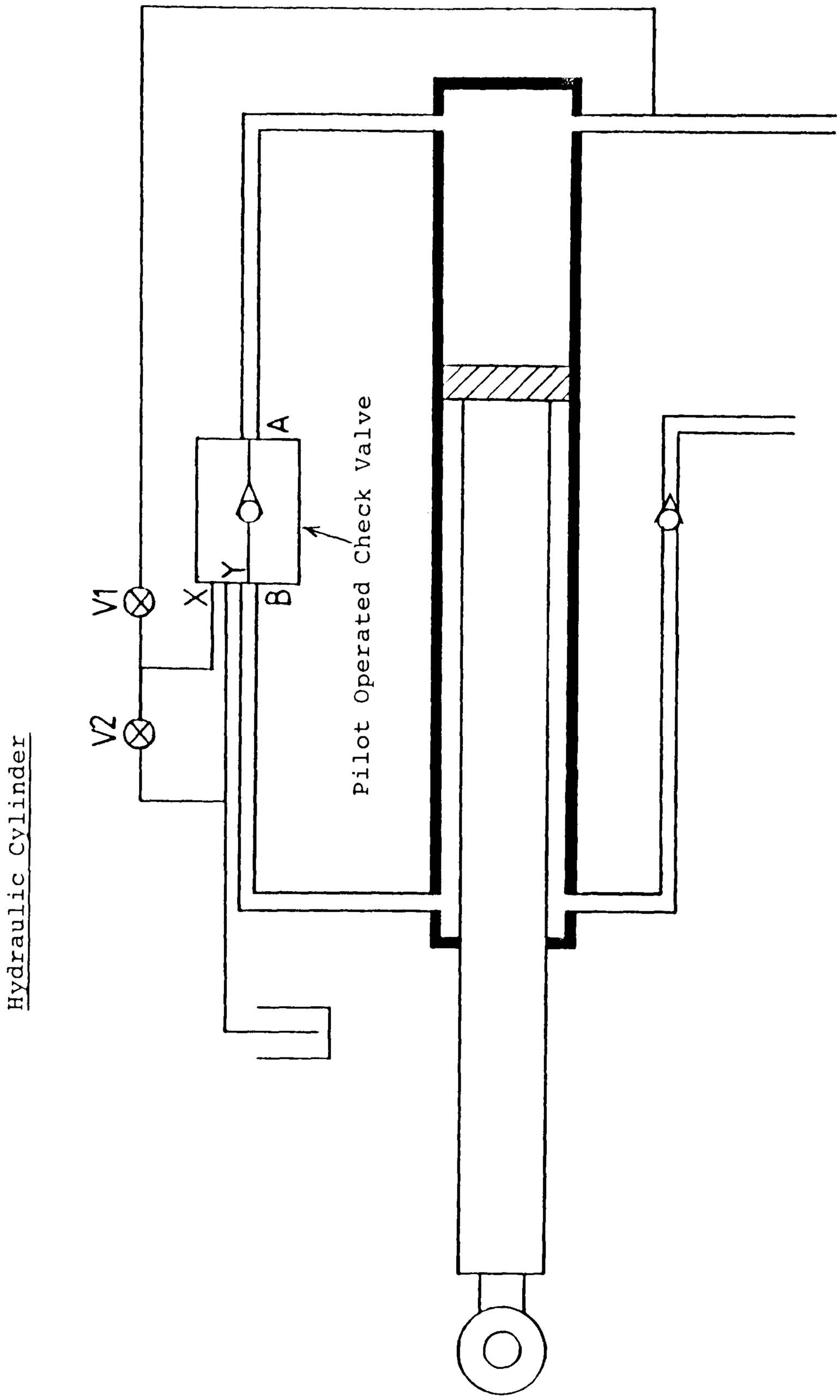


Fig.4.5

A few electrical faults were rectified: The pressure switch on one of the high pressure pumps had been connected incorrectly; the servo unloader valve was not being supplied at 240V ac but at 110V; and the Department electrical engineer installed a neutral line to the three phase power supply.

4.6 Preparation and Mounting of Coal Samples

Previous coal cutting tests conducted in the Mining Department at Newcastle have shown that it is essential to cast the coal specimen in a supporting medium before cutting it, otherwise the coal is liable to break up and split along the bedding or cleat planes. This is particularly pertinent to high pressure water jet assisted cutting. Therefore all the coal samples were cast in pitch before the cutting trials began.

One bituminous and two anthracite coal samples were trimmed to the correct size and mounted on a 1630mm x 1070mm x 25mm steel base plate, Plate 4.3. Each block was raised 25mm above the plate's surface to allow molten pitch to flow underneath it during casting and firmly secure it to the plate. Fig.4.6, illustrates the wooden formwork used in casting the coal; the sides were coated with aluminium foil to prevent the pitch adhering to the plywood.

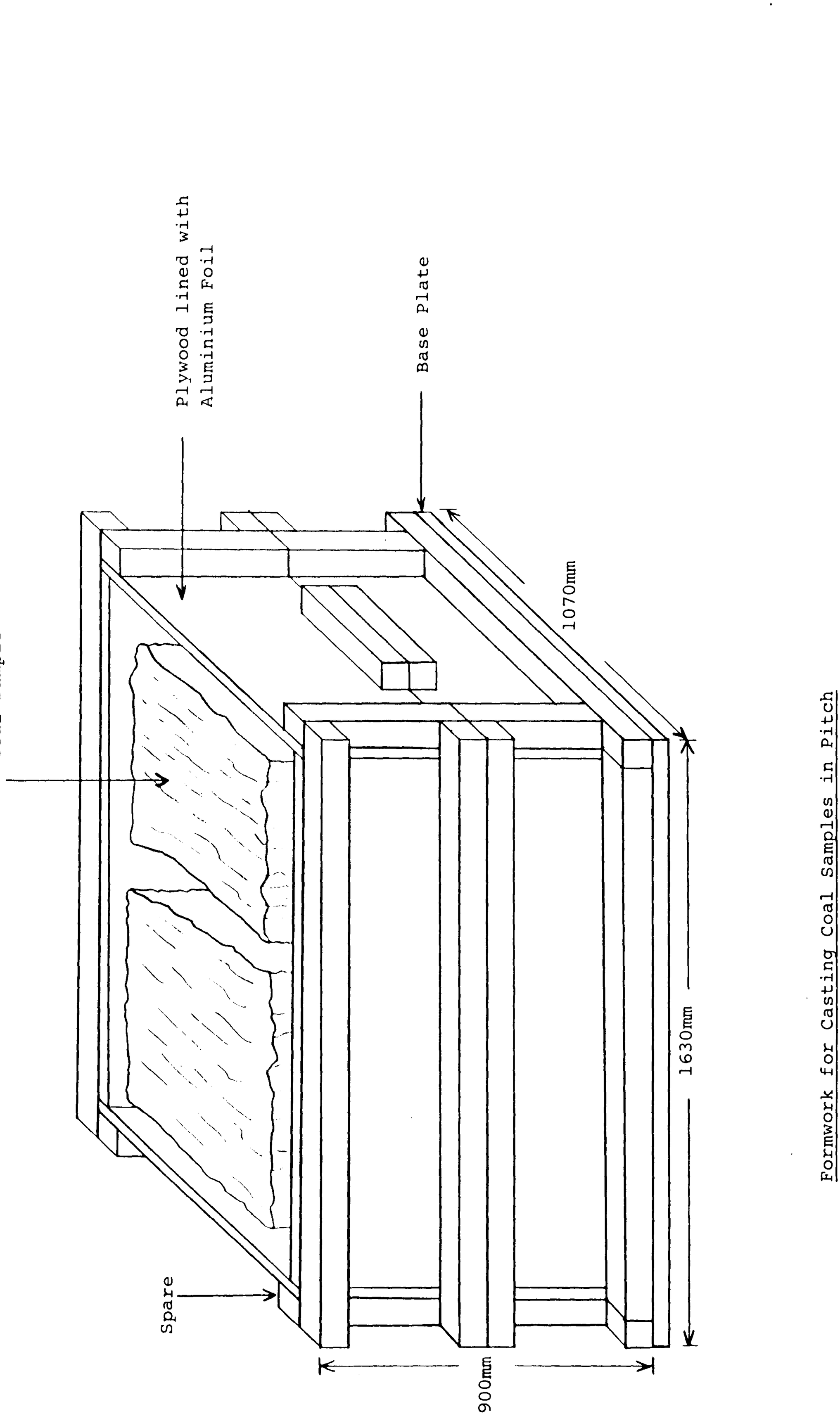
A 68 litre propane gas heated tar boiler was hired and the casting performed by the Department Technicians and the author. Plate 4.4, shows the final product bolted onto the specimen table. The channel section clamp inhibited large slabs of pitch breaking off at the end of a cut.

4.7 Nozzle Design

The nozzles used were to M.R.D.E./N.C.B. design, Fig.4.7. One set of nozzles were made in tungsten carbide and another in brass.



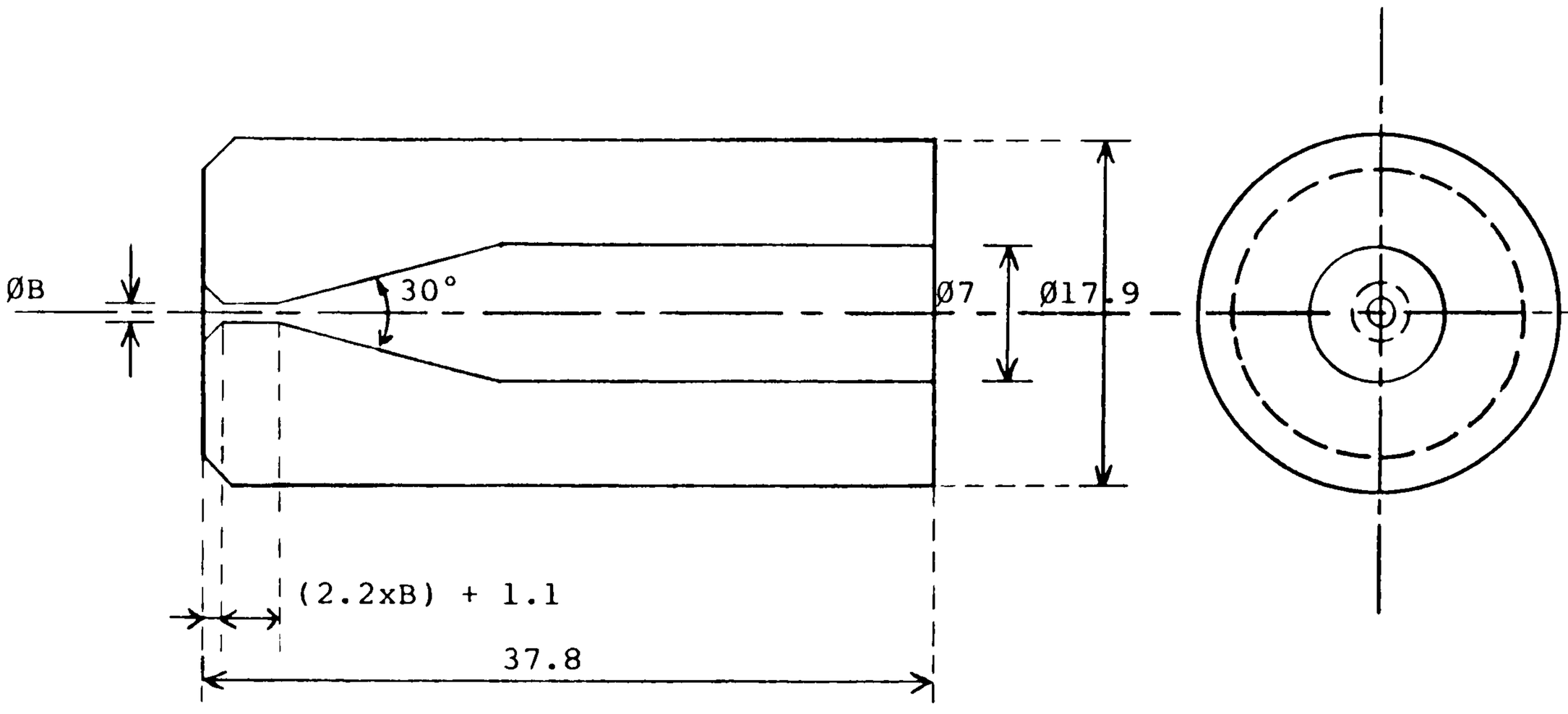
Plate 4.3 Mounting of coal samples.



Formwork for Casting Coal Samples in Pitch

Fig.4.6

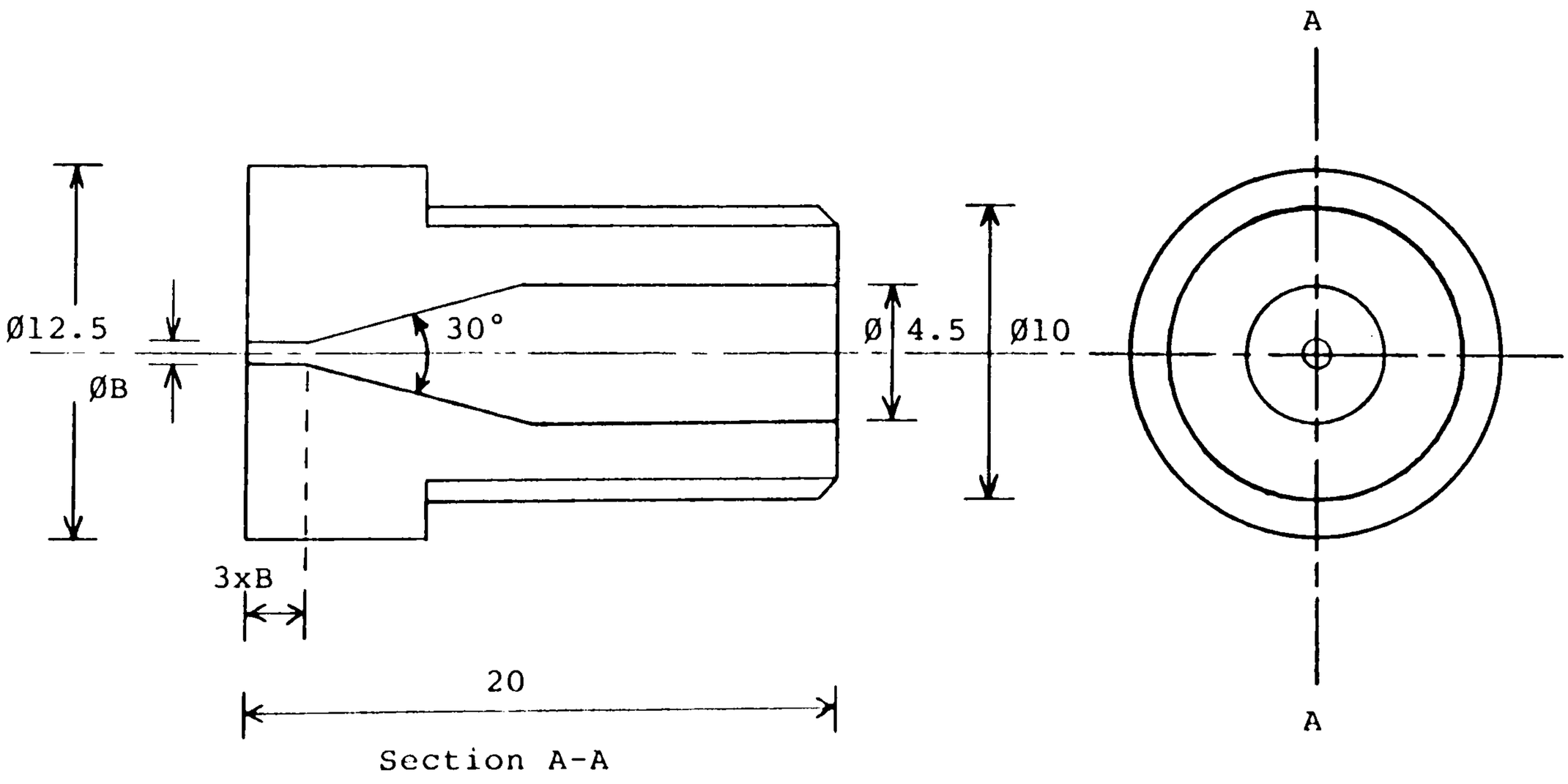
M.R.D.E./N.C.B. Nozzle Design



Section A-A

Material: Tungsten Carbide

Size in mm



Section A-A

Material: Brass

Fig.4.7



Plate 4.4 Prepared coal sample on the rig.

The brass nozzles were manufactured in the Department workshop. A problem was in achieving the 30° convergence angle. A 45° angle could be obtained by grinding down the tip of a standard drill bit of the correct diameter. However, if the tip is ground further, one also grinds off the cutting edge rendering the bit useless. Therefore, the Department Technicians machined a special cutting tool which produced the required 30° angle.

4.8 Cutting Tool

Wimet 75mm radial cutting tools with HP tips were used throughout the experiment: typical of the kind that equip underground coal cutting machines.

Fig.4.8, shows the specification of the artificial wear flat generated to make the blunt tool. The tool was prepared in a grinding machine.

Any protruding solder around the tungsten carbide insert was filed down so each tool presented the same cross-sectional area to the coal and would not be a factor influencing the force readings when a tool change was undertaken.

4.9 Jet Mounting

The jet was mounted infront of the cutting tool at a 2mm lead distance. The lead distance was set by running the water pump at a low pressure e.g. 7-10MPa, such that the jet stream did not curve under gravity due to its inclination and fixing the nozzle in the correct position.

4.10 Debris Collection

The dynamometers and jet mountings were shrouded to prevent the coal debris scattering off the coal block and being lost. Wooden guards were erected at the back and sides of the rig to ensure all the coal was available for collection after a series of cuts.

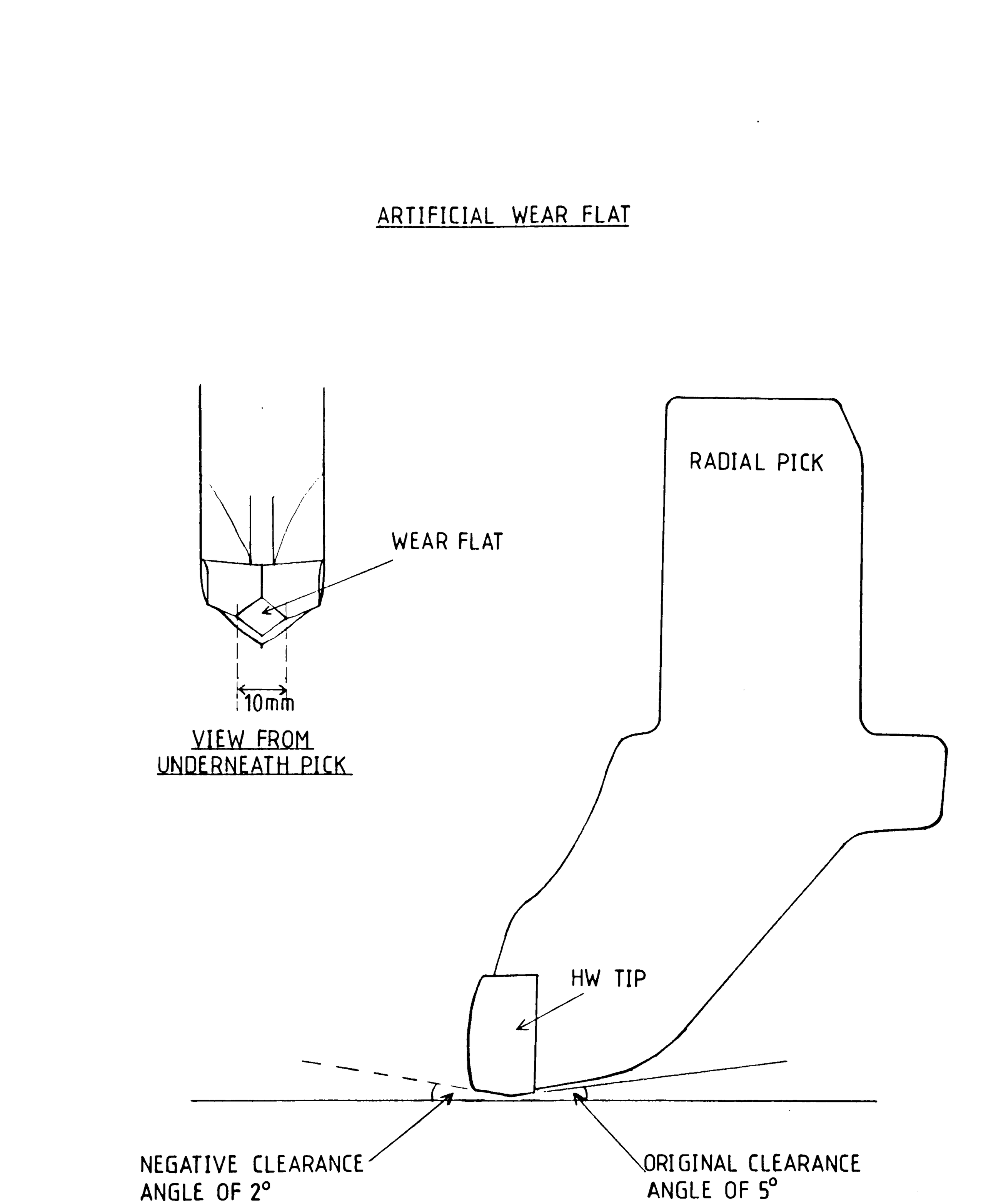

ARTIFICIAL WEAR FLAT
WEAR FLAT
10mm
VIEW FROM
UNDERNEATH PICK
RADIAL PICK
HW TIP
NEGATIVE CLEARANCE
ANGLE OF 2°
ORIGINAL CLEARANCE
ANGLE OF 5°

Fig.4.8

Before the coal debris was removed from the surface of the coal block it was allowed to dry. The large size could be cleared off by dustpan and brush. The smaller particles were vacuumed into an industrial wet and dry vacuum cleaner. The immediate floor space and underneath the specimen table were checked for coal particles that may have escaped the shrouding or fallen off the coal block.

The samples were emptied into plastic sacks. These were labelled and sealed so no extraneous material could be unwittingly added.

4.11 Coal Size Determination

A major part of the experiment was to determine the size distribution of the cut product.

4.11 1 Sieves, Sample Divider and Sieve Vibrator

Five 450mm diameter round hole laboratory test sieves, a collection pan and lid were purchased from Christison Scientific Equipment Limited. The nominal aperture sizes were 50mm, 28mm, 12.5mm, 6.3mm and 3.15mm.

All the sieves were manufactured to conform with B.S. 410 'Test Sieves', and were delivered with a test certificate. They were made from perforated tinned steel plate except the 3.15mm hole sized one which was produced from brass.

The -3.15mm coal was sieved into two further fractions: 3.15 - 0.5mm and -0.5mm. The -0.5mm coal is classed as fine coal. 200mm diameter wire mesh sieves were used to carry out this stage of the analysis. They also complied with B.S. 410.

4.11.2 Sieve Analysis

The coal was sieved using the 450mm diameter round hole sieves into the following size fractions:

+50

50 - 28

28 - 12.5

12.5 - 6.3

6.3 - 3.15

-3.15

The amount of charge was limited to guarantee efficient sieving. A small plastic container proved useful for measuring the charge. Its dimensions were 190mm x 160mm x 160mm, giving a volume of 4864cm^3.

The maximum volume of material that could be placed on any sieve was taken as the cross-sectional area of the sieve multiplied by twice the sieve aperture size. The table below illustrates the maximum charge volume for each of the 450mm diameter sieves.

Nominal Aperture Size (mm)	Volume of Charge (cm^3)
50	15 904
28	8 906
12.5	3 976
6.3	2 004
3.15	1 002

Table 4.1

The container ensured the charge satisfied the above conditions.

The coal particles were individually presented to the orifices in the 50mm, 28mm and 12.5mm hole sieves. Charge remaining on the 6.3mm and 3.15mm sieves was hand sieved for four minutes, shaking the sieves to and fro horizontally at a rate of about 120 times per minute and amplitude 70mm. Every twenty seconds the sieves were given a circular movement to enhance sieving efficiency. When the 6.3mm sieve was emptied the 3.15mm one was further sieved for one minute to ensure a good end point. A start/stop clock timed the operation. The charge and each fraction was weighed on a Mettler PE11 electronic balance to the nearest 0.1g.

An electric sieve shaker was adapted to accept the 450mm diameter sieves but its motion was considered too violent for the coal, especially the bituminous coal, and it was feared it would cause degradation of the coal and influence the results; hence it was not utilized.

Since a 0.5mm nominal aperture size sieve could not be obtained in the 450mm diameter size, the -3.15mm size coal was sieved on 200mm diameter test sieves. These sieves take a smaller charge and so a representative sample from the -3.15mm fraction was procured via a Pascall Engineering Co. Ltd. rotary divider.

The charge was weighed to the nearest 0.01g on an Oertling R20 balance and was maintained approximately 50g - 55g, for each analysis. It was machine sieved for 20 minutes on a Fritsch 'Analysette' sieve shaker, followed by a final one minute hand sieve before the respective over- and undersize were weighed on the Oertling balance; again to the nearest 0.01g. The quantity of the -3.15mm fraction sieved as the representative sample depended upon the total amount in the fraction, but typically between 500g - 1200g were sieved to estimate the 3.15 - 0.5 and -0.5mm fractions. A certain amount of loss occurred during the sieving and this was recorded with the results.

Plates 4.5, 4.6 and 4.7 show the large sieves, the sample divider and the small sieve on the vibrator, respectively.

4.12 Force Measurement

Force determination was achieved by a four post strain-gauged dynamometer. Two designs of dynamometer were actually utilized during the course of the experiment.

The dynamometer automatically resolves the force required to cut the coal into three orthogonal components: normal (vertical); cutting (horizontal); and sideway (lateral). Each component is measured by a full Wheatstone bridge. The strain gauges for each bridge are strategically placed so as to strain only when the force acts in a certain direction. Thus, if a pure vertical force is applied to the dynamometer only the normal force bridge would unbalance and indicate the force magnitude. Interaction between bridges may take place however depending upon the design of the dynamometer.

4.12.1 Steel Dynamometer, Signal Conditioning and Calibration

This dynamometer was originally used. Its design is described in Allington's Thesis (1969) and has been successfully applied in a number of research projects. It is equipped with 24 strain gauges, eight in each bridge, distributed about four pillars. The pillars support a central plate to which the cutting tool is attached through a toolholder. The surrounding body bolts on to a backplate and to the cutter slider.

The dynamometer had to be protected by a thin sheet-metal casing since the coal particles proved very sharp and at one point cut through the original metallic tape that was protecting the strain gauges, disconnecting a wire from the sideway component bridge. This was repaired and no problems were thereafter encountered.



Plate 4.5 450mm diameter round hole sieves.



Plate 4.6 Sample divider.



Plate 4.7 200mm diameter siev on sieve vibrator.

Thorn EMI SE 4300 Carrier Amplifiers energised the bridges and the signals were stored on a tape recorder before analysis.

The general arrangement for calibrating the normal force is shown in Fig.4.9. The load was increased up to a maximum of 20kN for the normal and cutting components and 6kN for the sideway component. Voltage readings from the dynamometer were recorded at predetermined force values; these being indicated by a calibrated load cell and P-3500 Vishay strain indicator. The tape recorder was played back through an A/D converter on to an IBM PC XT computer. Data was transferred from the PC on to Newcastle University's Mainframe computer and the calibration curves plotted as in Figs.4.10, 4.11, and 4.12. As one can see, there is significant interaction between the normal and cutting force bridges.

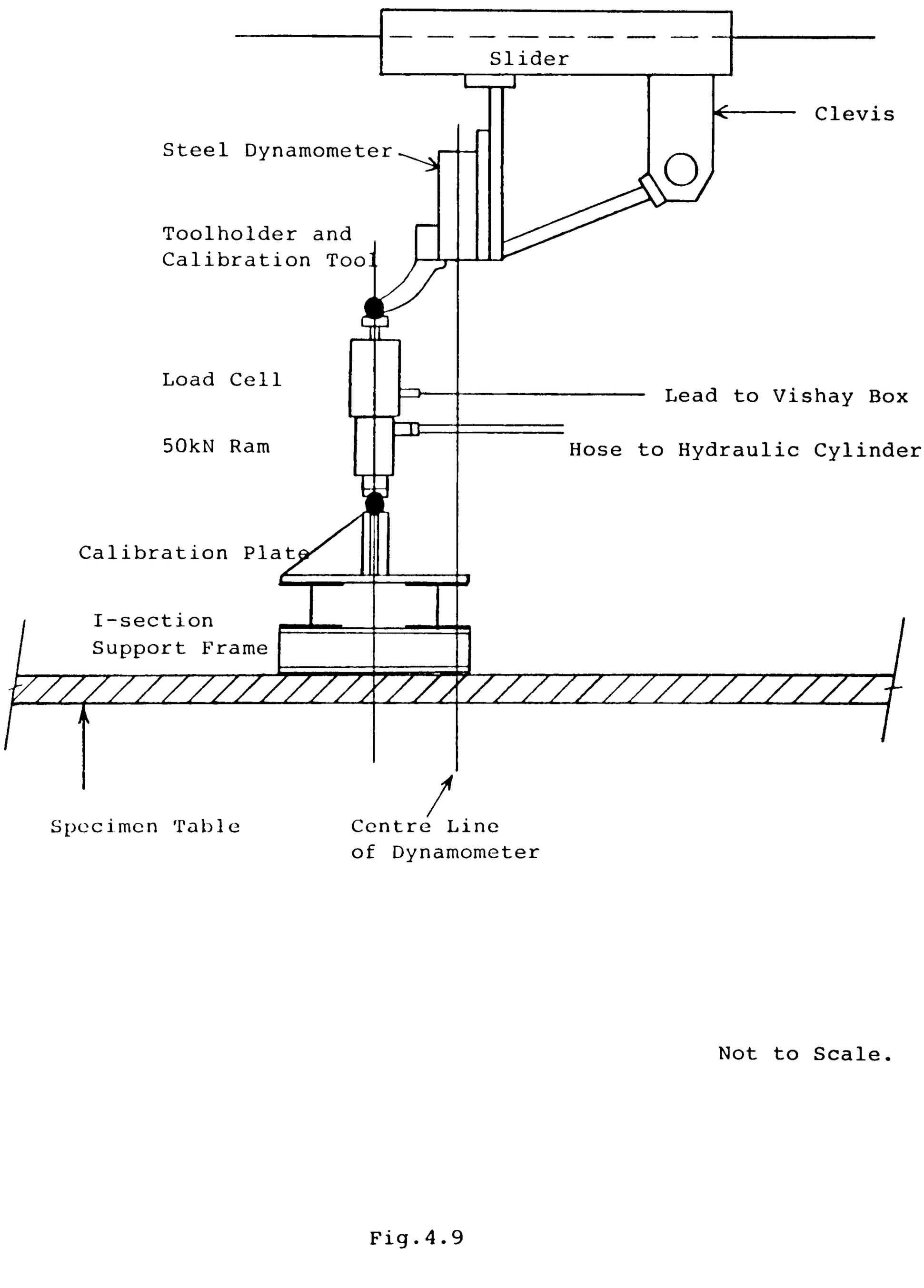
Fig.4.9 helps to explain the reason for the interaction: Since the tool tip is quite forward of the dynamometer's centre line, a moment as well as the normal force is acting which if too large causes the interaction. This was anticipated and 12mm of the tool shank was removed to bring the tool nearer the centre line and reduce the moment, but due to the pick design the interaction was still evident.

The equations of the curves were calculated and the effect of the interaction was subtracted from the raw data mathematically in order to correct the force readings. An alternate dynamometer became available and this was subsequently used.

4.12.2 Dynamometer, Signal Conditioning and Calibration

A diagram of the calibration arrangement with the alternative four post dynamometer is given previously in Fig.4.3. A base attaches the dynamometer to the slider. Four rectangular pillars, connected to the base, support another plate to which the toolholder is bolted. It

Calibration Arrangement



Not to Scale.

Fig.4.9

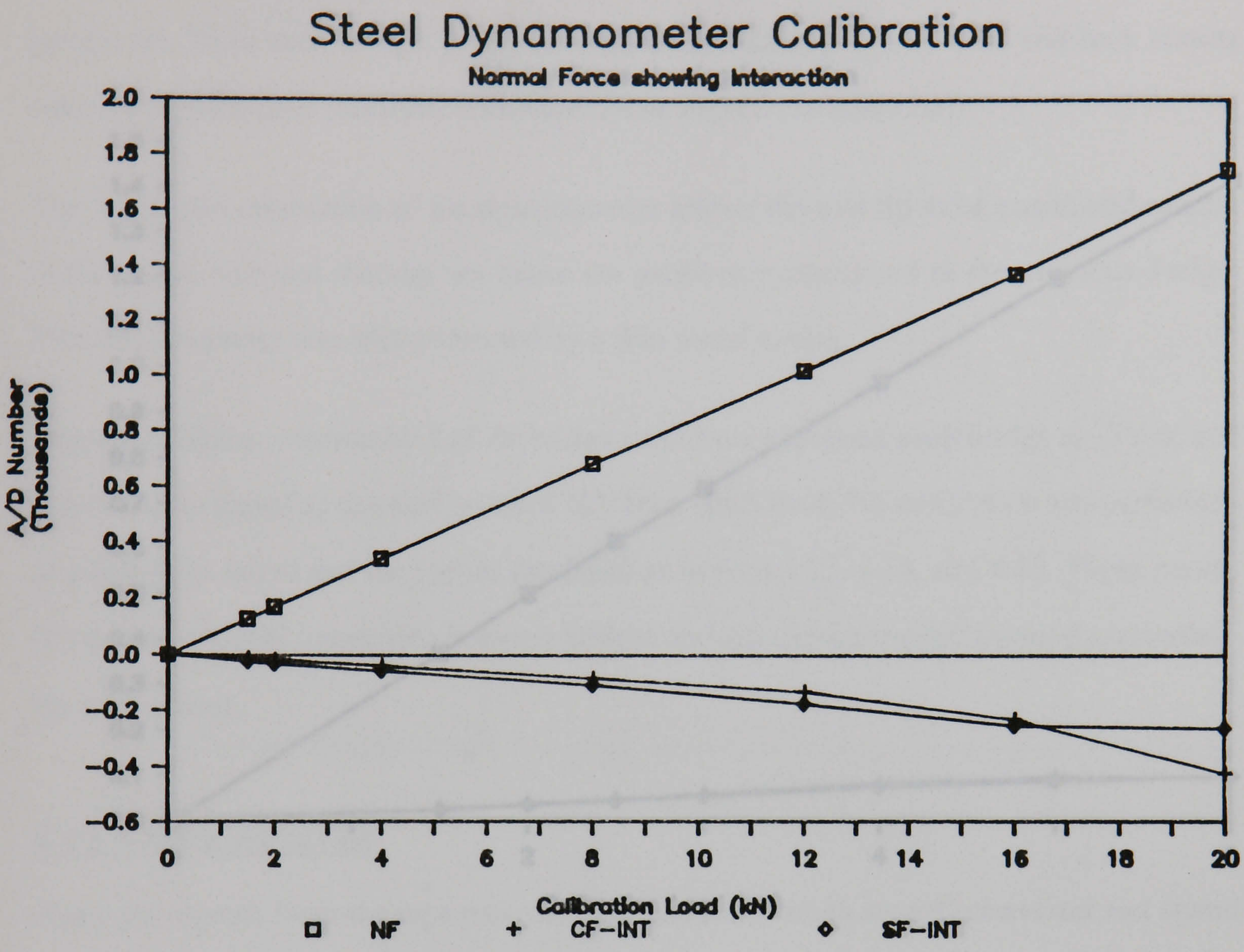


Fig.4.10

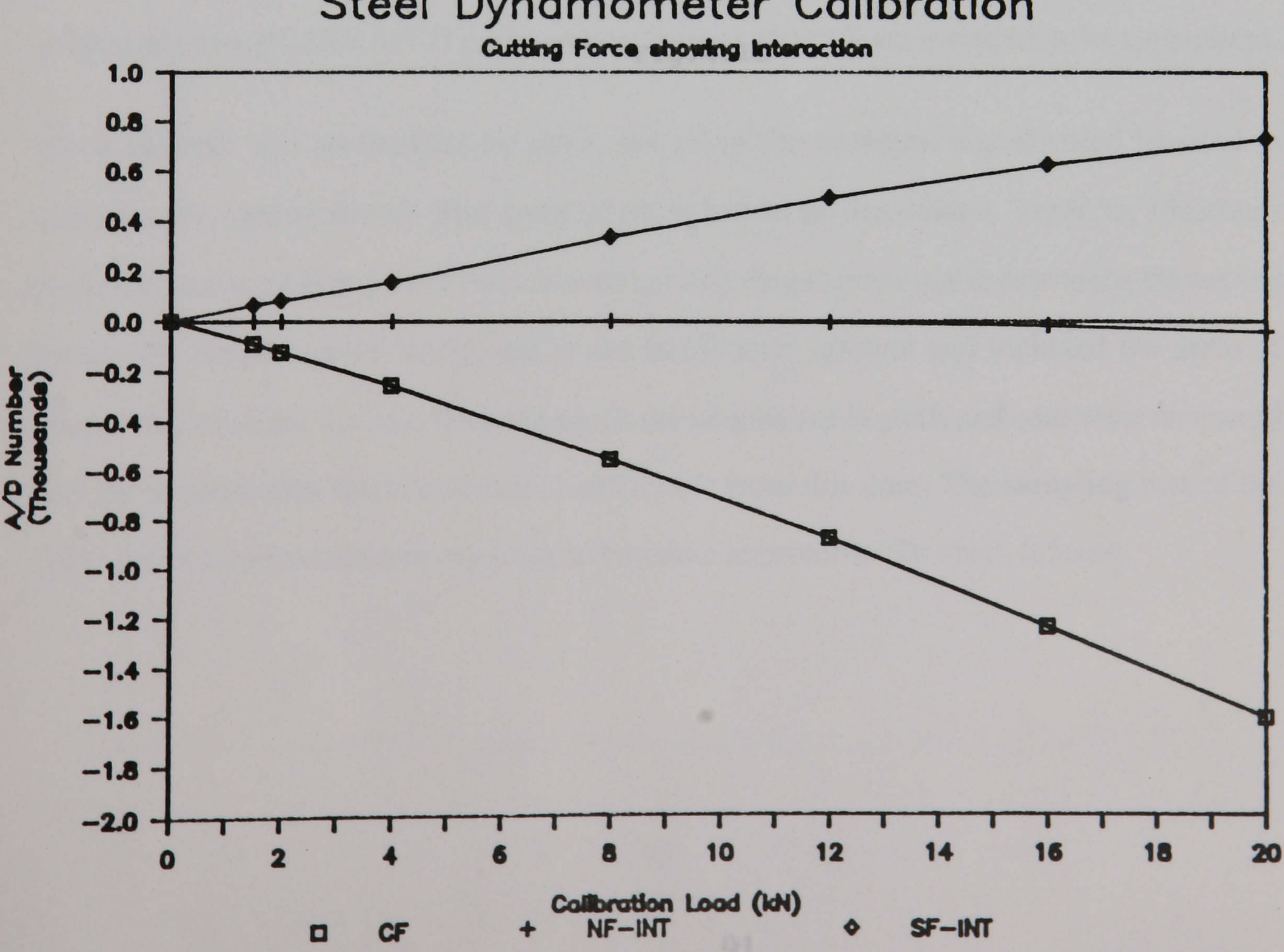


Fig.4.11

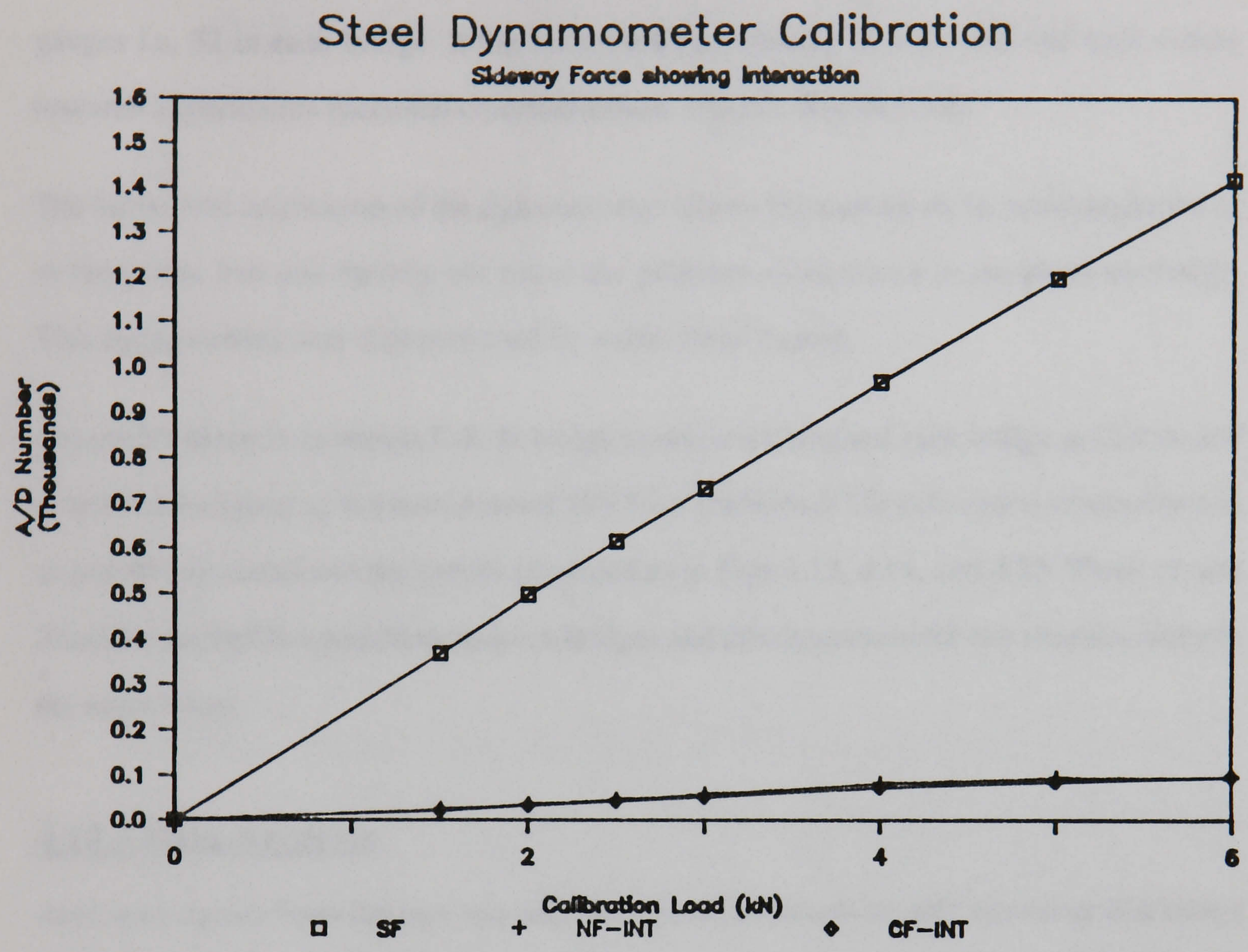

Steel Dynamometer Calibration
Sideway Force showing Interaction
A/D Number (Thousands)
1.6
1.5
1.4
1.3
1.2
1.1
1.0
0.9
0.8
0.7
0.6
0.5
0.4
0.3
0.2
0.1
0.0
0
2
4
6
Calibration Load (kN)
SF
NF-INT
CF-INT

Fig.4.12

measures force in three mutually perpendicular planes, as before, and is fitted with 96 strain gauges i.e. 32 in each bridge. It has been used successfully in both coal and rock cutting research experiments (personal communication, HQTD, British Coal).

The horizontal orientation of the dynamometer allows the tool tip to be positioned exactly in the centre line and thereby not cause the problem encountered in the previous design. This dynamometer was also protected by a thin metal casing.

Bryans Southern Instruments Ltd. dc bridge amplifiers energised each bridge at 15V dc and amplified the signal up to a maximum of 10V for a 20kN load. The calibration was performed as previously stated and the curves produced as in Figs.4.13, 4.14, and 4.15. These curves illustrate negligible interaction between bridges and this dynamometer was used to complete the experiment.

4.12.3 Data Analysis

Analogue signals from the tape recorder were passed through an A/D converter and stored on floppy disk by an IBM PC. The data was transferred to the Mainframe computer and analysed by two FORTRAN 77 programmes; listings of which are included in the appendices.

Since the coal was surrounded by pitch, not all of the analogue signal could be used to calculate the cutting forces. The areas of pitch had to be discounted. Fig.4.16, illustrates regions termed cut(1) and cut(2) which were used by the programmes to determine the cutting forces; the lengths called tar(1), tar(2) and tar(3) were ignored and included the areas of pitch. After clearing the coal from the block the lengths cut in pitch and coal were measured and the programmes calculated cut(1) and cut(2) from this data. The sampling rate of the A/D converter allowed force readings to be taken approximately every 0.5mm.

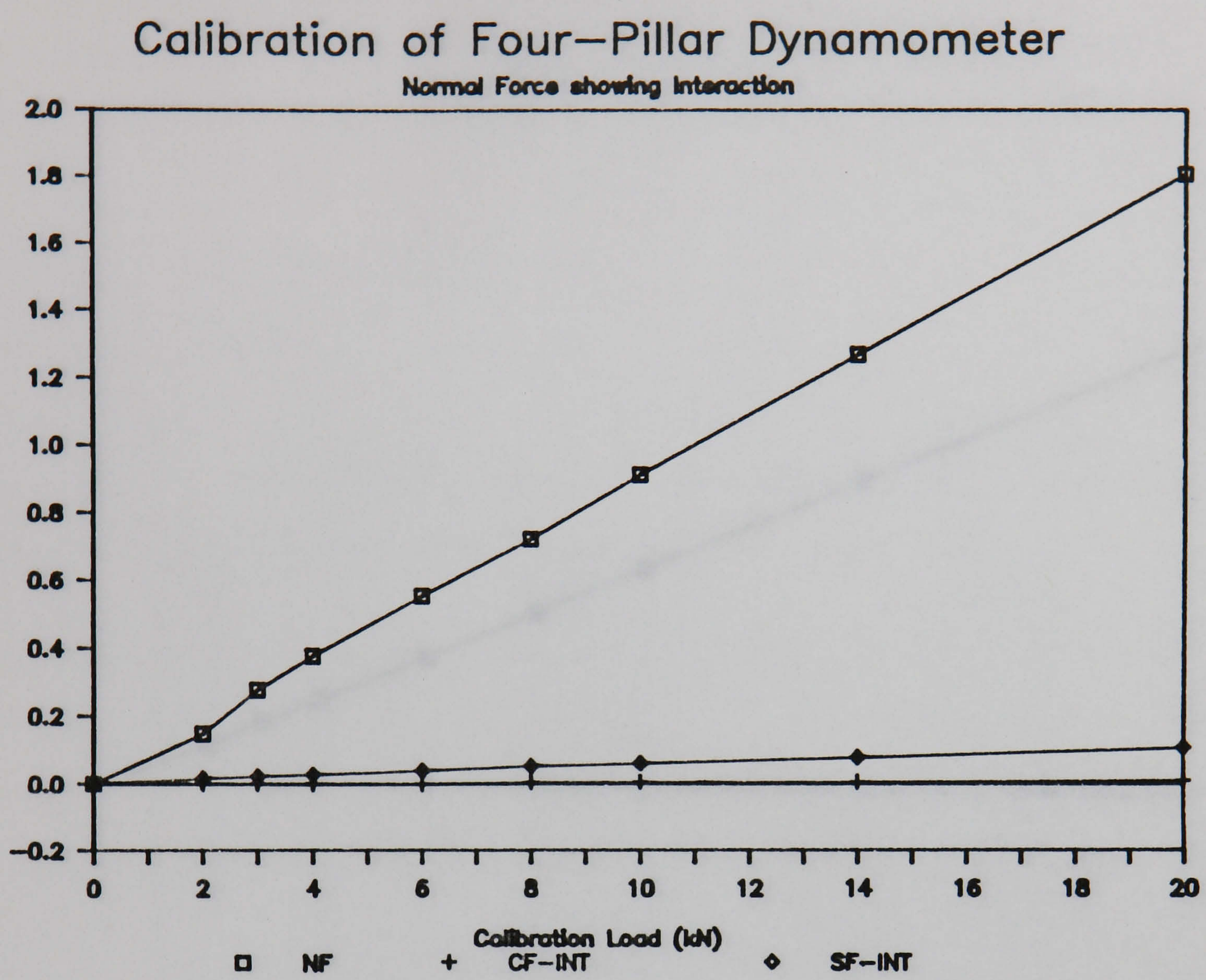


Fig.4.13

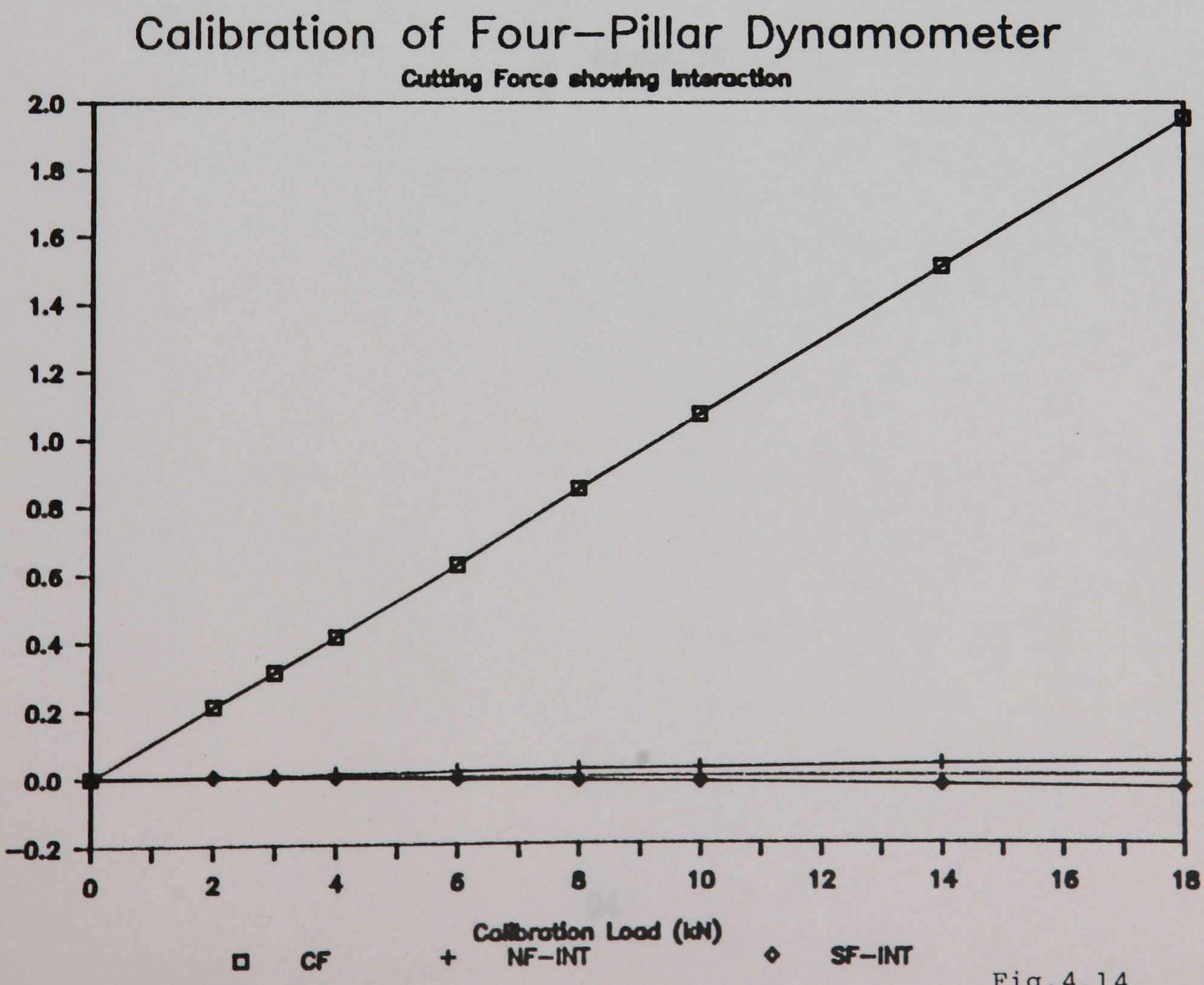


Fig.4.14

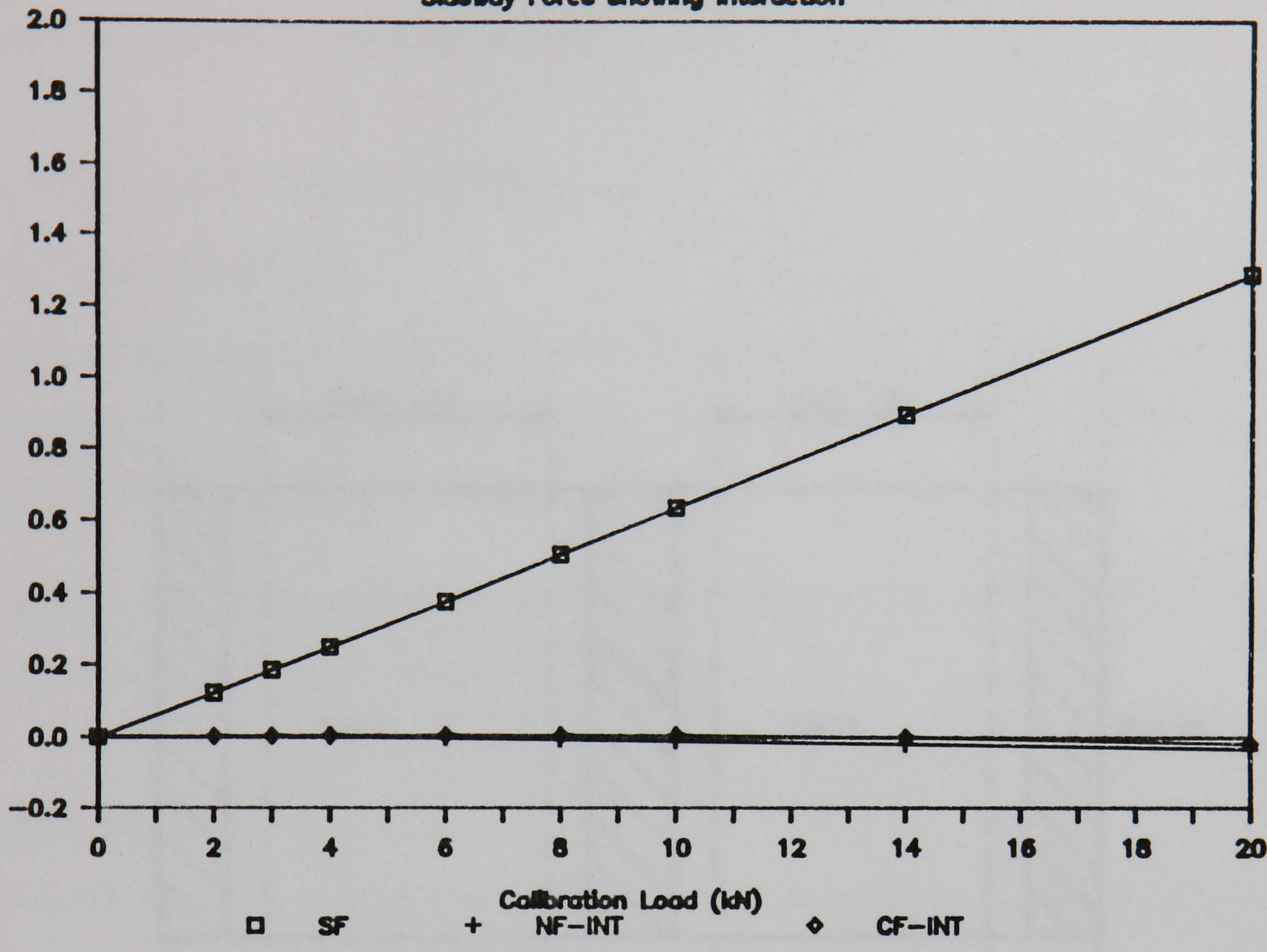

Calibration of Four–Pillar Dynamometer
Sideway Force showing Interaction
A/D Number (Thousands)
2.0
1.8
1.6
1.4
1.2
1.0
0.8
0.6
0.4
0.2
0.0
–0.2
0
2
4
6
8
10
12
14
16
18
20
Calibration Load (kN)
SF
NF–INT
CF–INT

Fig.4.15

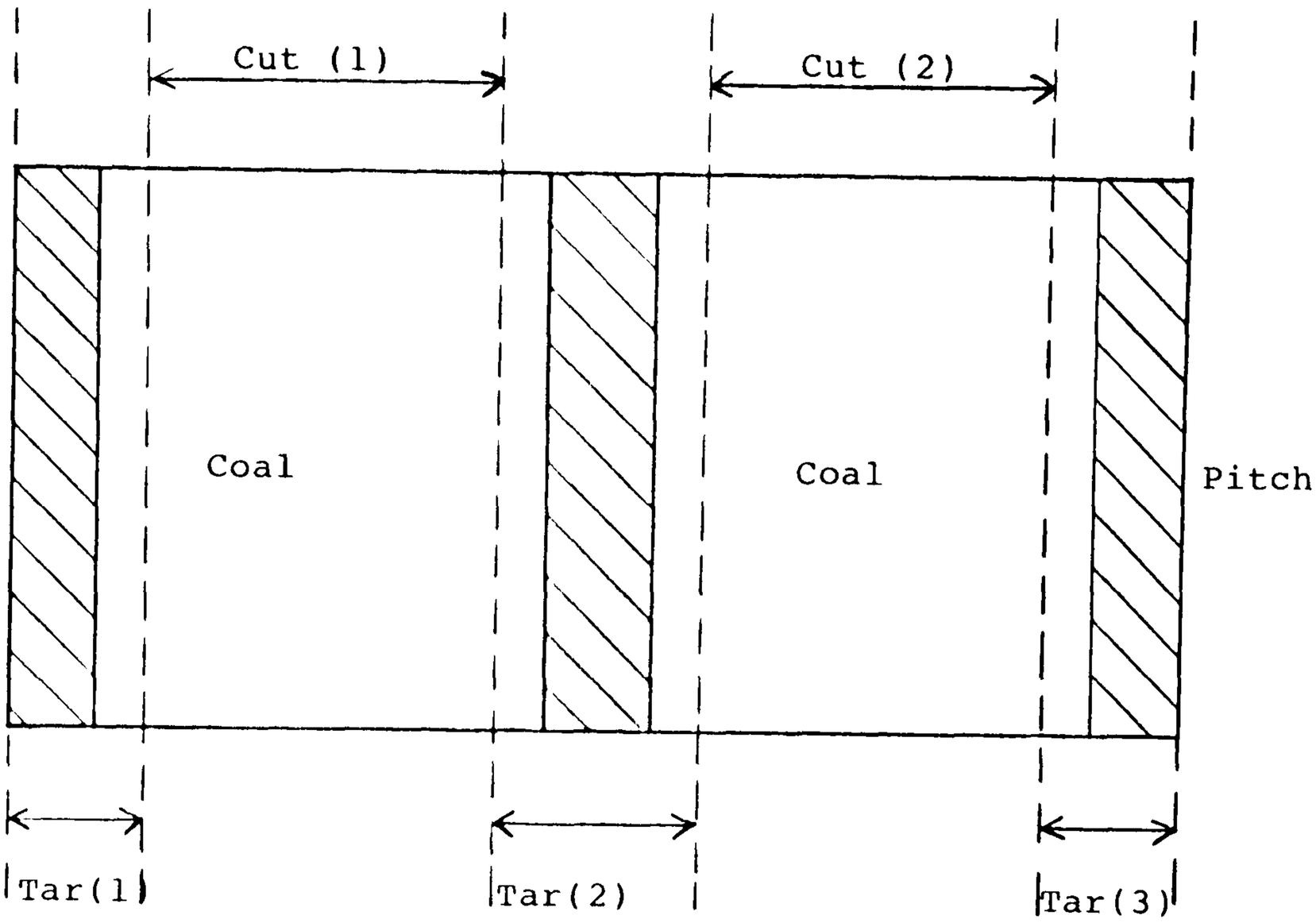


Fig.4.16

The mean forces are taken as the average over both cut(1) and cut(2). The mean peak are the 95 percentiles over both blocks. The mean and mean peak forces in each individual region cut(1) and cut(2) were also calculated.

4.13 Water Jet Pressure Measurement

4.13.1 Instrumentation

Water jet pressure was monitored by an Intersonde Ltd. diaphragm type pressure transducer, with a range up to 200MPa. The transducer power supply and signal conditioning units were Intersonde K2020 and K3020 modules respectively.

The pressure was measured about 2m from the nozzle exit at a t-piece in the stainless steel piping so that the transducer would not be damaged.

4.13.2 Calibration

A calibration certificate was supplied from the manufacturers and allowed quick calibration without recourse to a dead weight pressure tester.

A switch on the power supply module connects an internal calibration resistor across one arm of the transducer bridge. From the calibration certificate, this produces an imbalance of 75.94% of the full scale voltage output. In this state, the bridge voltage may be adjusted such that at a pressure of 200MPa a voltage output of 2000mV is obtained. Therefore, a d.v.m. can be used to directly indicate the water pressure.

The water pressure from the intensifier was observed to vary due to its reciprocating motion, hence an average pressure was set for the tests by the aid of a programmable digital voltmeter.

4.14 Nozzle Diameter

Tests were undertaken to determine the nozzle diameters for the project. An approximate value of the coefficient of discharge of the M.R.D.E. design of nozzle was required. Two nozzles were available with 0.92mm and 1.21mm diameters, and the flow rates for these nozzles were measured over a range of pressures.

The jet was allowed to discharge in to a large bucket for 0.5 to 4 minutes depending on the pressure. A steel pipe with a bend in, was screwed in to the nozzle casing to dissipate the jet energy and allow the water to be collected without excessive splashing. From this the flow rates could be calculated.

The coefficient of discharge is defined as the actual flow rate divided by the theoretical flow rate. Values between 0.833 to 0.866 were obtained for the discharge coefficients of the jets. An examination of the flow rates and pressures indicated that the nozzles needed would all be less than 0.92mm in diameter.

Other researchers values were consulted as a comparison. Ip (1986) reports values ranging from 0.817 to 0.841 for jet diameters 0.60mm and 0.90mm. These were for nozzles with a 45° convergence angle. Tecen (1982) gives figures of 0.80 to 0.82 for nozzles of 0.6mm and 1.1mm diameter and convergence angle 13°.

The relationship between nozzle diameter d, flow rate Q, pressure P, density ρ, and coefficient of discharge C_d, is,

$$d = \left\{ \frac{2^{1.5} \rho^{0.5} Q}{\pi C_d P^{0.5}} \right\}^{0.5} \tag{4.1}$$

If the flow rate Q, is in litres/min, the pressure P, in MPa, the water density constant at $10^3 kg/m^3$ at these pressures, then the nozzle diameter is determined from the equation:

$$d = \left\{ \frac{0.4745Q}{C_d P^{0.5}} \right\}^{0.5} \qquad (4.2)$$

1. Taking Q = 4 l/min, P = 35MPa.

   a. For C_d = 0.800 d = 0.63mm

   b. For C_d = 0.817 d = 0.63mm

   c. For C_d = 0.833 d = 0.62mm

   d. For C_d = 0.866 d = 0.61mm

2. Taking Q = 8 l/min, P = 70MPa.

   a. For C_d = 0.800 d = 0.75mm

   b. For C_d = 0.817 d = 0.75mm

   c. For C_d = 0.833 d = 0.74mm

   d. For C_d = 0.866 d = 0.72mm

3. Taking Q = 12 l/min, P = 105MPa.

   a. For C_d = 0.800 d = 0.83mm

   b. For C_d = 0.817 d = 0.82mm

   c. For C_d = 0.833 d = 0.82mm

   d. For C_d = 0.866 d = 0.80mm

Therefore nozzle diameters of the order shown above were sought. The actual diameters were determined by the drill sizes which were available to produce the orifice. Actual diameters were 0.62mm, 0.75mm and 0.82mm for the respective flow rates and pressures.

An examination of the possible errors associated with the nozzle diameter and coefficient of discharge was undertaken. Rearranging the previous equation:

$$Q = \frac{C_d d^2 P^{0.5}}{0.4745} \tag{4.3}$$

If a change δQ is brought about by changes $\delta C_d, \delta d$ and δP then,

$$\delta Q = \frac{\partial Q}{\partial C_d}\delta C_d + \frac{\partial Q}{\partial d}\delta d + \frac{\partial Q}{\partial P}\delta P \tag{4.4}$$

Hence,

$$\frac{\delta Q}{Q} = \frac{\delta C_d}{C_d} + 2\frac{\delta d}{d} + \frac{1}{2}\frac{\delta P}{P} \tag{4.5}$$

Taking an error range in C_d as ±0.03 from an average of 0.850, and in d as ±0.02mm then,

1. For Q = 4 l/min, P = 35MPa and d = 0.62mm,

$$\frac{\delta Q}{Q} = \pm\frac{0.03}{0.85} \pm 2 \times \frac{0.02}{0.62} = \pm 0.10$$

$$\delta Q = \pm 0.10 \times 4 = \pm 0.40 \text{ l/min}$$

2. For Q = 8 l/min, P = 70MPa and d = 0.75mm,

$$\frac{\delta Q}{Q} = \pm\frac{0.03}{0.85} \pm 2 \times \frac{0.02}{0.75} = \pm 0.09$$

$$\delta Q = \pm 0.09 \times 8 = \pm 0.72 \text{ l/min}$$

3. For Q = 12 l/min, P = 105MPa and d = 0.82mm,

$$\frac{\delta Q}{Q} = \pm\frac{0.03}{0.85} \pm 2 \times \frac{0.02}{0.82} = \pm 0.08$$

$$\delta Q = \pm 0.08 \times 12 = \pm 0.96 \text{ l/min}$$

The pressure error is ignored since the jet pressure could easily be set to within 0.5MPa of the required value and thus the error would be small. Therefore, these are the maximum combined errors in the flow rate (8% to 10%) expected due to the nozzle diameter and coefficient of discharge not being exact.

4.15 Ram Speed Determination

It was important that the ram speed be fixed at 1.1m/s. Therefore trials were conducted to set the cutting speed and ensure that it was constant over the entire length of cut.

Limit switches were attached to the cutter slider assembly such that they would be activated by the cutter slider as it traversed. They were connected to the start and stop terminals of a timer counter and placed 1.5m apart. An average speed of 1.1m/s was obtained when the flow control valve was turned to its extreme position.

CHAPTER FIVE

5 JET PENETRATION TESTS

5.1 Introduction

The following tests were performed to characterise the coals with respect to jet penetration. Jet assisted rock cutting research has shown that an optimum penetration exists for the jet which gives maximum enhancement to the cutting process, therefore, this aspect had to be investigated in the coal also. In the present study though one is more interested in fines reduction and if the penetration depth can be shown to influence this.

As shown in the literature review, jet penetration is quite sensitive to traverse velocity. The maximum cutting speed of the linear rig is currently 1.1m/s, but on actual coal cutting machines the cutting speed is between 3-4m/s, thus an idea of how the jet penetration is influenced by traverse speed in the coals is required and if this can be offset by increasing the jet power and to what degree.

Tests were carried out in each coal block. For the purposes of comparison the Erin coal results will be compared to those of the anthracite block in which the cleat was orientated parallel to the cutting direction. Then the effect of cleat on jet penetration within the anthracite coal shall be examined.

5.2 Analysis of Bituminous Coal and Anthracite Coal

Table 5.1 below gives the results for the jet penetration tests in the anthracite and bituminous coals. It represents a 4 x 4 x 2 factorial experiment. The slot was vacuumed clear of water and debris and its depth measured with a depth gauge to ±0.25mm. An average of 17 measurements were taken over the length of the slot (about 1.2m) to determine its mean depth.

Speed (m/s)	Anthracite Coal				Erin (bituminous) Coal			
	35 (MPa)	52.5 (MPa)	70 (MPa)	105 (MPa)	35 (MPa)	52.5 (MPa)	70 (MPa)	105 (MPa)
0.24	11.1	18.0	37.6	51.4	15.9	23.4	42.5	76.0
0.64	9.2	14.3	26.6	40.0	11.9	16.3	33.9	51.1
0.90	8.4	11.1	23.0	26.7	11.2	15.5	28.0	38.1
1.10	6.5	10.5	21.3	22.1	10.7	10.7	28.2	26.4

Table 5.1

The statistical analysis employed to ascertain the effects on penetration of jet pressure (or power), traverse speed and coal type is given below. It is conducted in stages so that if interactions exist between the main variables they may be estimated.

5.2.1 Analysis of Traverse Speed and Jet Pressure

Table 5.2 comprises the summed results of Table 5.1 for the two different coals. This is required so that the effect of jet pressure and traverse speed can be examined independently of the coal type.

	Jet Pressure				
Speed (m/s)	35 (MPa)	52.5 (MPa)	70 (MPa)	105 (MPa)	Sums (mm)
0.24	27.0	41.4	80.1	127.4	275.9
0.64	21.1	30.6	60.5	91.1	203.3
0.90	19.6	26.6	51.0	64.8	162.0
1.10	17.2	21.2	49.5	48.5	136.4
Sums (mm)	84.9	119.8	241.1	331.8	777.6

Table 5.2

An inspection of the sums columns appears to show that the effect on penetration of jet pressure (or power) is much greater than the traverse speed over the range tested.

The calculations below are a shorthand method of determining the sums of squares for the analysis of variance table for the pressure and traverse speed. By constructing Table 5.3, an estimate of the mean square or variance due to the interaction between jet pressure and traverse speed as well as the main effects can be obtained.

Correction due to mean = $777.6^2/32 = 18\ 895.7$

Total sums of squares:

$(27^2 + \ldots\ldots + 48.5^2)/2 - 18\ 895.7 = 25\ 935.2 - 18\ 895.7 = 7\ 039.5$

Sums of squares due to traverse speed:

$(275.9^2 + 203.3^2 + 162.0^2 + 136.4^2)/8 - 18\ 895.7 = 1\ 391.9$

Sums of squares due to jet pressure:

$(84.9^2 + 119.8^2 + 241.1^2 + 331.8^2)/8 - 18\ 895.7 = 4\ 826.9$

Source of Variation	Sums of Squares	Degrees of Freedom	Mean Square
Between Pressures	4 826.9	3	1 609.0
Between Speeds	1 391.9	3	464.0
Interaction between Pressures and Speeds	820.7	9	91.2
Sub Total	7 039.5	15	

Table 5.3

5.2.2 Analysis of Traverse Speed and Coal Type

Each value in Table 5.4, is an average over the four pressures used in the tests. Hence now the effect of jet pressure has been eliminated and the effects of coal type and any interaction between coal type and traverse velocity may be determined.

	Coal Type		
Speed (m/s)	Anthracite	Bituminous	Sums (mm)
0.24	118.1	157.8	275.9
0.64	90.1	113.2	203.3
0.90	69.2	92.8	162.0
1.10	60.4	76.0	136.4
Sums (mm)	337.8	439.8	777.6

Table 5.4

The analysis of variance table for the two effects is constructed as before.

Total sums of squares:

$(118.1^2 + \ldots\ldots + 76^2)/16 - 18\,895.7 = 1\,755.6$

Sums of squares due to traverse speed:

$(275.9^2 + 203.3^2 + 162.0^2 + 136.4^2)/8 - 18\,895.7 = 1\,391.9$

Sums of squares due to coal type:

$(337.8^2 + 439.8^2)/16 - 18\,895.7 = 325.1$

Source of Variation	Sums of Squares	Degrees of Freedom	Mean Square
Between Coals	325.1	1	325.1
Between Speeds	1 391.9	3	464.0
Interaction between Coals and Speeds	38.6	3	12.9
Sub Total	1 755.6	7	

Table 5.5

5.2.3 Analysis of Jet Pressure and Coal Type

The final two-way table to complete the analysis is that between jet pressure and coal type as shown in Table 5.6. The same procedure is followed as above. In this case the influence of traverse velocity has been isolated since each value in the table is the sum over the four traverse speeds. The analysis of variance table is given in Table 5.7.

	Coal Type		
Pressure (MPa)	Anthracite	Bituminous	Sums (mm)
35.0	35.2	49.7	84.9
52.5	53.9	65.9	119.8
70.0	108.5	132.6	241.1
105.0	140.2	191.6	331.8
Sums (mm)	337.8	439.8	777.6

Table 5.6

Total sums of squares:

$(35.2^2 + \ldots\ldots + 191.6^2)/4 - 18\ 895.7 = 5\ 274.0$

Sums of squares due to jet pressure:

$(84.9^2 + 119.8^2 + 241.1^2 + 331.8^2)/8 - 18\ 895.7 = 4\ 826.9$

Sums of squares due to coal type:

$(337.8^2 + 439.8^2)/16 - 18\ 895.7 = 325.1$

Source of Variation	Sums of Squares	Degrees of Freedom	Mean Square
Between Coals	325.1	1	325.1
Between Pressures	4 826.9	3	1 609.0
Interaction between Coals and Pressures	122.0	3	40.7
Sub Total	5 274.0	7	

Table 5.7

5.2.4 Complete Analysis of Variance

One now has calculated the variance or mean squares for the three main effects; pressure, traverse velocity and coal type, on the jet penetration in the two coals. Also, all the two-way interactions have been quantified in terms of variance. From these results the final analysis of variance table for the whole experiment may be constructed.

The total sums of squares for the whole experiment is calculated as follows from the results in Table 5.1:

$(11.1^2 + \ldots\ldots + 26.4^2)/32 - 18\ 895.7 = 7\ 607.0$

By subtracting all the other sums of squares terms from this grand total, the final three-way interaction between coals, pressures and speeds may be found. Table 5.8 below shows the complete breakdown of the results.

Source of Variation	Sums of Squares	Degrees of Freedom	Mean Square	F-ratio
Between Coals	325.1	1	325.1	35.8
Between Pressures	4 826.9	3	1 609.0	177.0
Between Speeds	1 391.9	3	464.0	51.0
Interaction between Coals and Pressures	122.0	3	40.7	4.5
Interaction between Coals and Speeds	38.6	3	12.9	1.4
Interaction between Pressures and Speeds	820.7	9	91.2	10.0
Interaction between Coals, Pressures and Speeds	81.8	9	9.1	
Total	7 607.0	31		

Table 5.8

Since the experiment was not replicated there is no experimental error term in the table. Thus, since its variance is small compared to the main effects and it has nine degrees of freedom, one must assume that the three-way interaction is most unlikely to be a significant factor on jet penetration and use this as an estimate of the experimental error variance (Davies, 1961).

The statistical significance of each term is determined by the F-ratio. This is the ratio of the particular treatment variance to that of the experimental error or residual variance. If the value of the F-ratio is greater than that given in F-tables, then the treatment is statistically significant i.e. the probability that the effect of the treatment is due to the experimental error is very small.

From Table 5.8, it was found that the jet penetration was significantly affected by jet pressure, traverse speed and coal type at the 1% level. From the F-ratios one might say the jet pressure generally has a greater effect than traverse speed and coal type. However, one must take into account the range over which each factor is varied before making general conclusions. For example if the traverse speed had covered extremely slow speeds, the situation may have reversed, and the traverse speed seemed more influential on penetration. Nevertheless, in the range tested jet pressure or power appears the most dominant factor.

Another highly significant factor (1% level) was the interaction between jet pressure and traverse speed. The interaction may be interpreted as follows: The difference between the penetrations of the jet at two different pressures say, is not identical at a slow and faster traverse speed. Thus if a jet is traversing at 0.64m/s say and giving penetrations of h_{35} and h_{70} at pressures of 35MPa and 70MPa respectively and a similar jet traversing at 1.1m/s gives corresponding penetrations of h'_{35} and h'_{70}, then if $h_{0.64} = h_{70} - h_{35}$ and $h_{1.1} = h'_{70} - h'_{35}$ then the interaction term means $h_{0.64} \neq h_{1.1}$.

Another significant term, though at the 5% level, is the interaction between jet pressure and coal type. This effect may be understood in a similar fashion as above. Consider two jets at 35MPa and 70MPa giving penetrations h_{35} and h_{70} in the anthracite say. The difference in penetration depth is $h_{An} = h_{70} - h_{35}$. A similar experiment in the bituminous (Erin) coal would give a difference $h_{Bit} = h_{70} - h_{35}$. But $h_{An} \neq h_{Bit}$, hence the significant interaction term. This bears out by examining the data in Table 5.6.

The interaction term between coal types and traverse speed is not significant and very close to unity. The converse conclusion from that detailed above would be that the differences in penetrations between the two coals seems very unlikely to vary as the traverse speed changes.

As the interaction between pressure, coal type and traverse speed is taken as an estimate of the experimental error variance, then the experimental error = $\sqrt{9.1}$ = 3.0mm. Therefore, the 95% confidence limits (with nine degrees of freedom) for testing for significant differences between each measurement are ±2.26 x 3.0 × 1.41 = ±9.6mm.

Thus significant differences in jet penetrations are observed as the jet pressure increases, as the traverse speed decreases and between the two coals.

5.3 Analysis of Cleat Orientation in the Anthracite Coal

Table 5.9 below includes the results for the tests undertaken with the cleat arranged in a horizontal orientation to the traverse direction.

Speed (m/s)	Cleat Parallel				Cleat Perpendicular			
	35 (MPa)	52.5 (MPa)	70 (MPa)	105 (MPa)	35 (MPa)	52.5 (MPa)	70 (MPa)	105 (MPa)
0.24	11.1	18.0	37.6	51.4	8.9	13.5	31.8	55.6
0.64	9.2	14.3	26.6	40.0	9.6	10.0	23.7	33.2
0.90	8.4	11.1	23.0	26.7	5.8	9.0	16.4	34.8
1.10	6.5	10.5	21.3	22.1	6.2	7.7	15.8	27.5

Table 5.9

The analysis was performed as previously described and so will not be repeated. The final analysis of variance table is given in Table 5.10.

5.3.1 Complete Analysis of Variance

Source of Variation	Sums of Squares	Degrees of Freedom	Mean Square	F-ratio
Between Cleat	25.0	1	25.0	3.5
Between Pressures	3 971.5	3	1 323.8	186.5
Between Speeds	881.6	3	293.9	41.4
Interaction between Cleat and Pressures	70.1	3	23.4	3.3
Interaction between Cleat and Speeds	9.3	3	3.1	0.4
Interaction between Pressures and Speeds	432.8	9	48.1	6.8
Interaction between Cleat, Pressures and Speeds	64.3	9	7.1	
Total	5 454.6	31		

Table 5.10

Similarly, the F-ratios indicate that the jet pressure and traverse speed are highly significant factors on jet penetration. The effect of cleat orientation is not significant except at the 10% level and is very small compared to the F-ratios of the other two main effects.

The interaction between jet pressure and traverse speed is highly significant but nevertheless small compared to the main effects of pressure and speed. Interaction between cleat orientation and jet pressure is only significant at the 10% level and thus can virtually be discounted as an influence on the penetration. The other two-way interaction, that of cleat orientation and traverse speed is not significant and has no bearing on the results in this coal.

As before the highest order interaction term is chosen as an estimate of the experimental error variance. The interaction term between cleat and traverse speed could be added to increase the degrees of freeedom of the experimental error estimate, but it would not substantially alter the conclusions. Thus the experimental error = $\sqrt{7.1}$ = 2.7mm, and the 95% confidence limits for testing for significant differencs between each measurement are ±2.26 x 2.7 × 1.41 = ±8.6mm.

Again the trend is for the differences in the results to be significant as the jet pressure increases and as the traverse speed decreases. There is practically no effect between the two extreme cleat orientations.

5.4 Graphical Representation of Jet Penetration results

The results are presented graphically in Fig.5.1-4. Since the cleat made little difference to the penetration in the anthracite coal, Fig.5.4 shows the averaged results for this coal. This has smoothed out the randomity due to the experimental error and illustrates the trend which is similar to that of the Erin coal.

A straight line equation, $y = mx + c$, fits the curves quite well with correlation coefficients around 0.960 and above, except for the fastest traverse speeds in Fig.5.1 and Fig.5.2, where they are 0.806 and 0.896 respectively. However, when the curves are extrapolated to the abscissa, the threshold pressure does not decrease as the traverse speed decreases but usually increases, especially in the Erin coal. A visual inspection of the gradients of the curves makes the point clearer; at a slower traverse speed the gradient is steeper. This suggests the curves tend towards the origin rather than directly to the abscissa, and a better fit is obtained to a power relationship rather than a linear one.

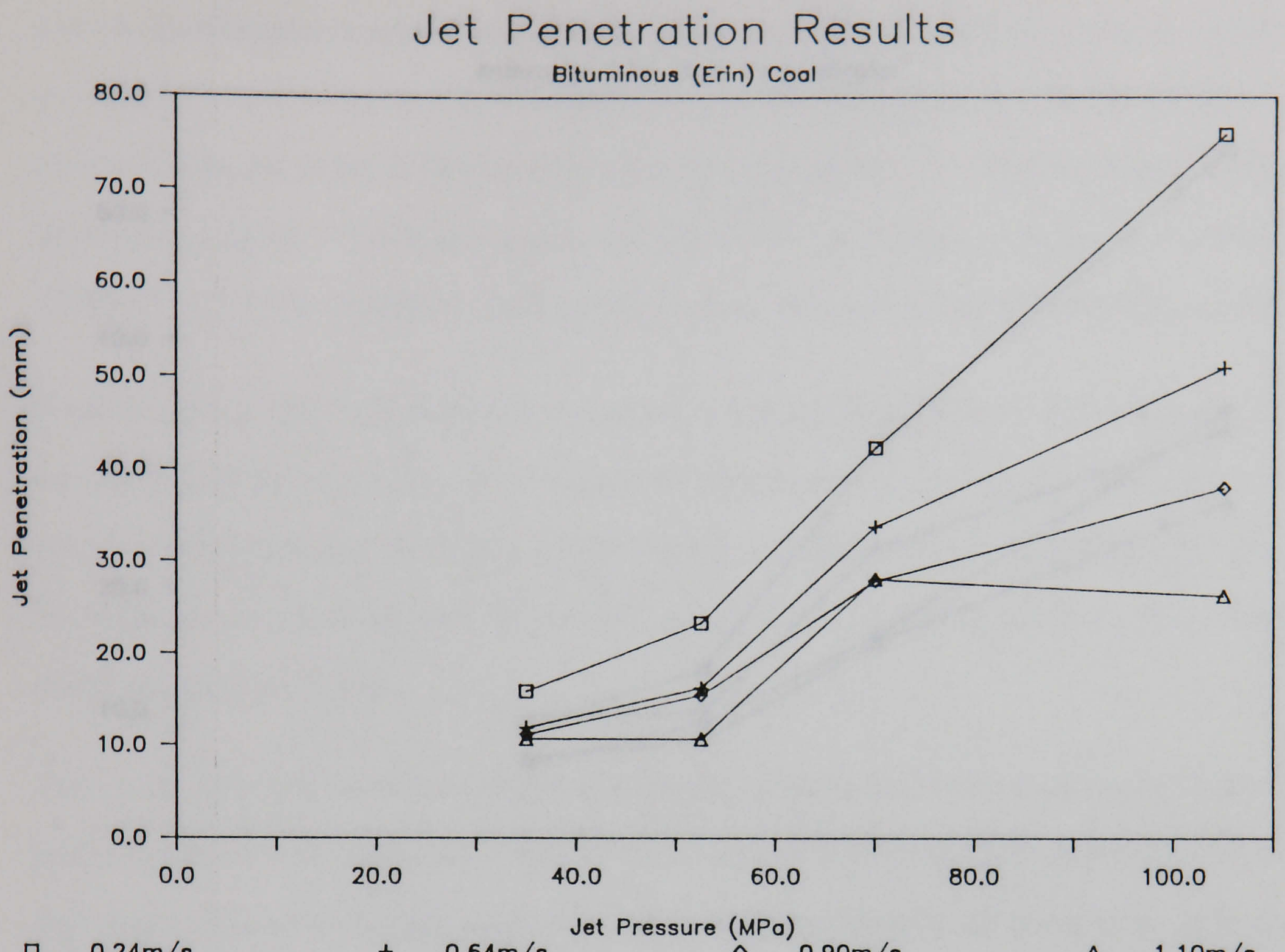

Jet Penetration Results
Bituminous (Erin) Coal
80.0
70.0
60.0
50.0
40.0
30.0
20.0
10.0
0.0
Jet Penetration (mm)
0.0
20.0
40.0
60.0
80.0
100.0
Jet Pressure (MPa)
0.24m/s
0.64m/s
0.90m/s
1.10m/s

Fig.5.1

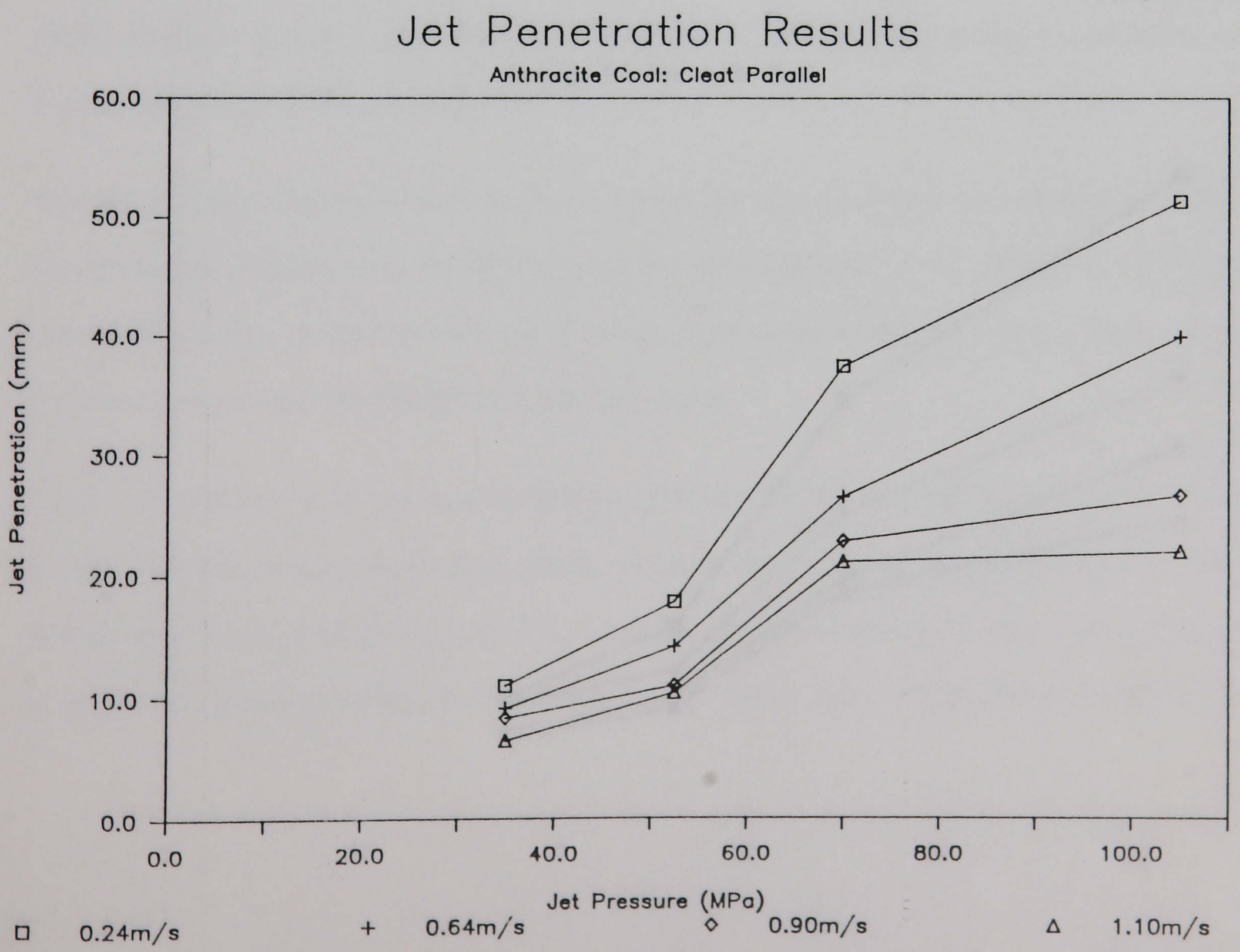

Jet Penetration Results
Anthracite Coal: Cleat Parallel
60.0
50.0
40.0
30.0
20.0
10.0
0.0
Jet Penetration (mm)
0.0
20.0
40.0
60.0
80.0
100.0
Jet Pressure (MPa)
0.24m/s
0.64m/s
0.90m/s
1.10m/s

Fig.5.2

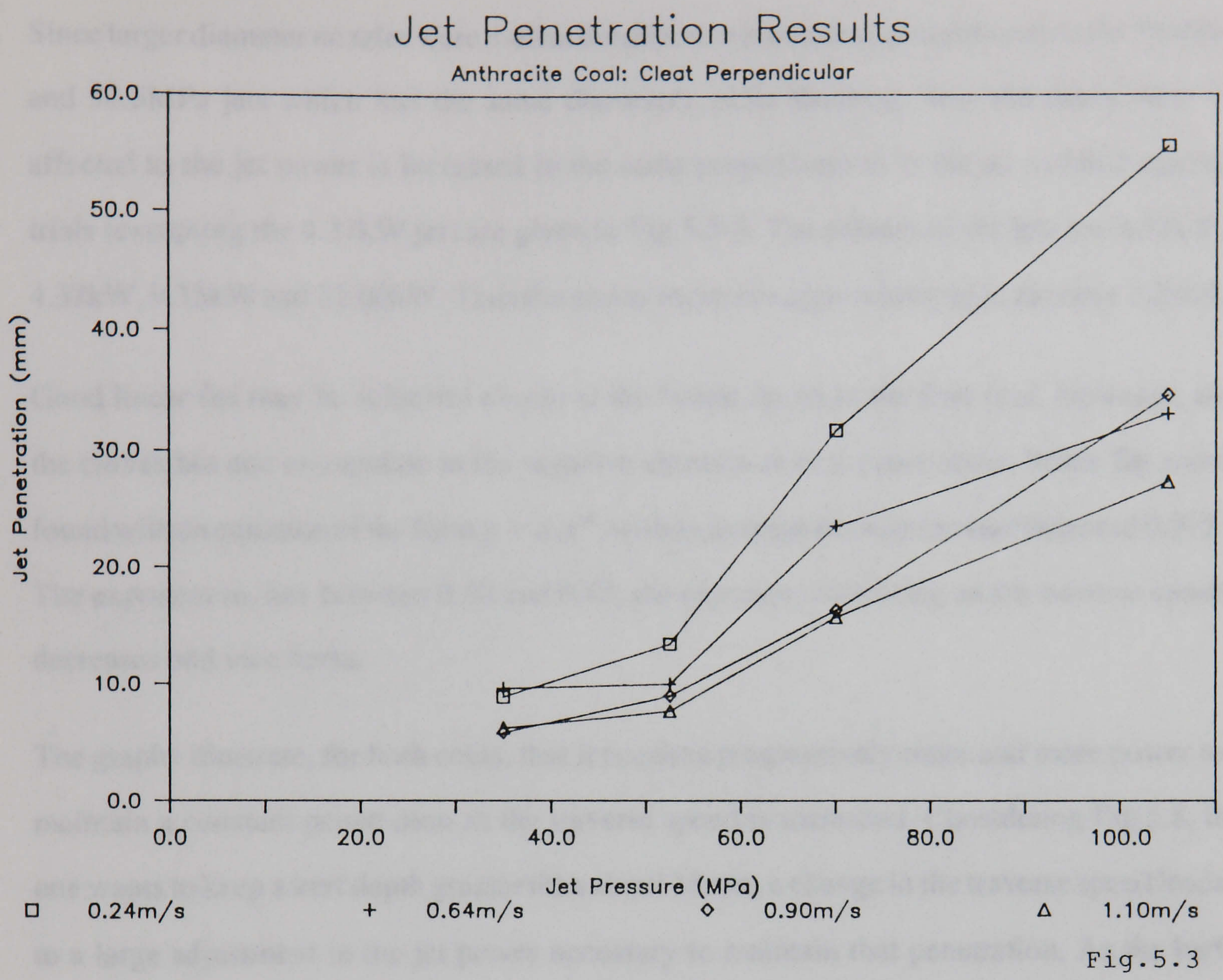

Jet Penetration Results
Anthracite Coal: Cleat Perpendicular
60.0
50.0
40.0
30.0
20.0
10.0
0.0
Jet Penetration (mm)
0.0
20.0
40.0
60.0
80.0
100.0
Jet Pressure (MPa)
0.24m/s
0.64m/s
0.90m/s
1.10m/s

Fig.5.3

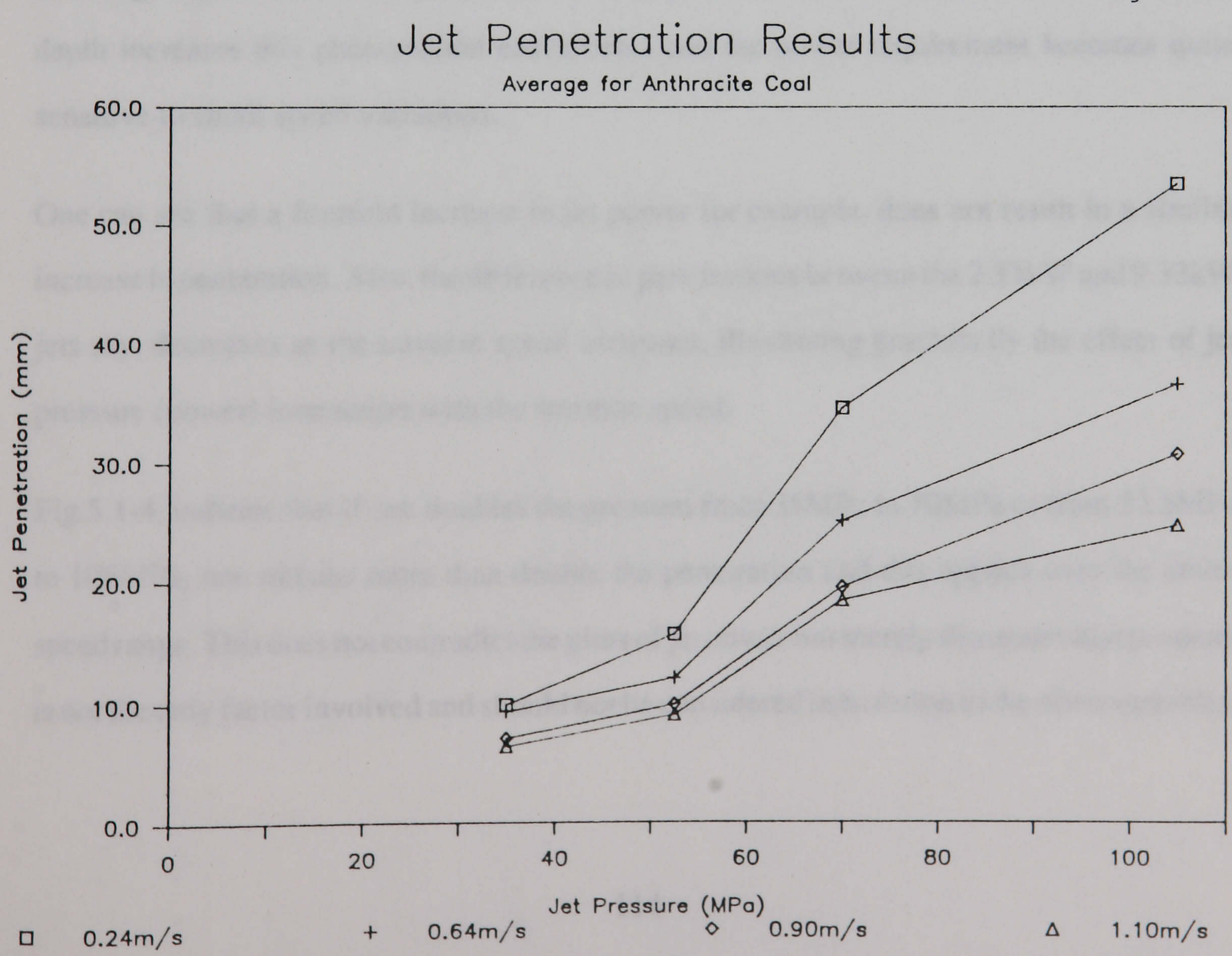

Jet Penetration Results
Average for Anthracite Coal
60.0
50.0
40.0
30.0
20.0
10.0
0.0
Jet Penetration (mm)
0
20
40
60
80
100
Jet Pressure (MPa)
0.24m/s
0.64m/s
0.90m/s
1.10m/s

Fig.5.4

Since larger diameter nozzles were used at the different pressures (except between the 35MPa and 52.5MPa jets which had the same diameter), plots showing how the penetration is affected as the jet power is increased in the same proportions as in the jet assisted cutting trials (excepting the 4.37kW jet) are given in Fig.5.5-8. The powers of the jets are 2.33kW, 4.37kW, 9.33kW and 21.00kW. Thus the power increases approximately in the ratio 1:2:4:9.

Good linear fits may be achieved except at the fastest speed in the Erin coal. However, all the curves but one extrapolate to the negative abscissa at zero penetration. Better fits were found with an equation of the form $y = a\,x^m$, with an average correlation coefficient of 0.975. The exponent m, lies between 0.50 and 0.87, the exponent increasing as the traverse speed decreases and vice versa.

The graphs illustrate, for both coals, that it requires progressively more and more power to maintain a constant penetration as the traverse speed is increased. Considering Fig.5.8, if one wants to keep a kerf depth greater than about 18mm, a change in the traverse speed leads to a large adjustment in the jet power necessary to maintain that penetration. As the kerf depth increases this phenomenon exacerbates and the power requirement becomes quite sensitive to small speed variations.

One can see that a fourfold increase in jet power for example, does not result in a similar increase in penetration. Also, the difference in penetrations between the 2.33kW and 9.33kW jets say, decreases as the traverse speed increases, illustrating graphically the effect of jet pressure (power) interaction with the traverse speed.

Fig.5.1-4, indicate that if one doubles the pressure from 35MPa to 70MPa or from 52.5MPa to 105MPa, one obtains more than double the penetration and this applies over the entire speed range. This does not contradict the plots of jet power but merely illustrates that pressure is not the only factor involved and should not be considered in isolation to the other variables.

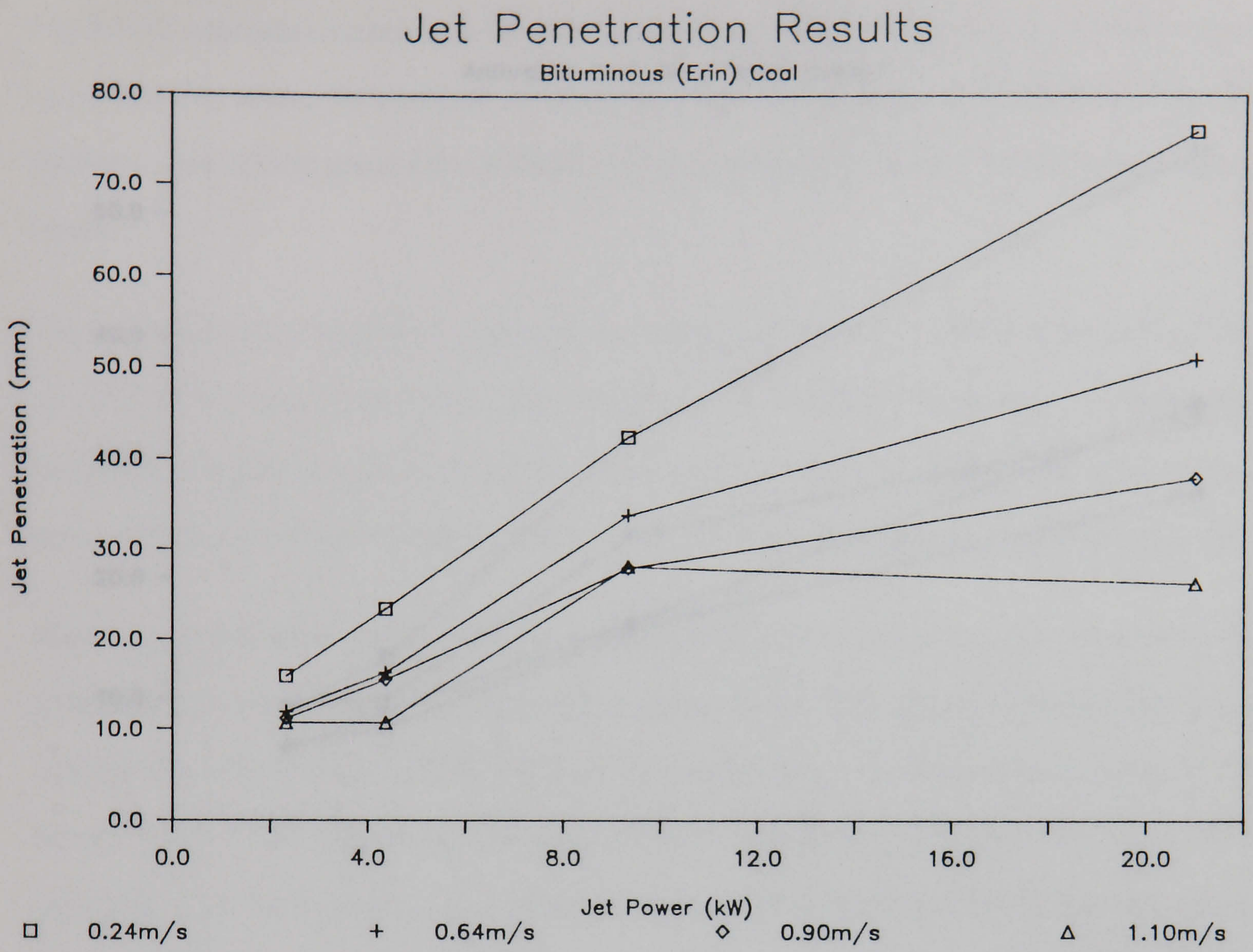

Jet Penetration Results
Bituminous (Erin) Coal
Jet Penetration (mm)
80.0
70.0
60.0
50.0
40.0
30.0
20.0
10.0
0.0
0.0
4.0
8.0
12.0
16.0
20.0
Jet Power (kW)
□ 0.24m/s
+ 0.64m/s
◇ 0.90m/s
△ 1.10m/s

Fig.5.5

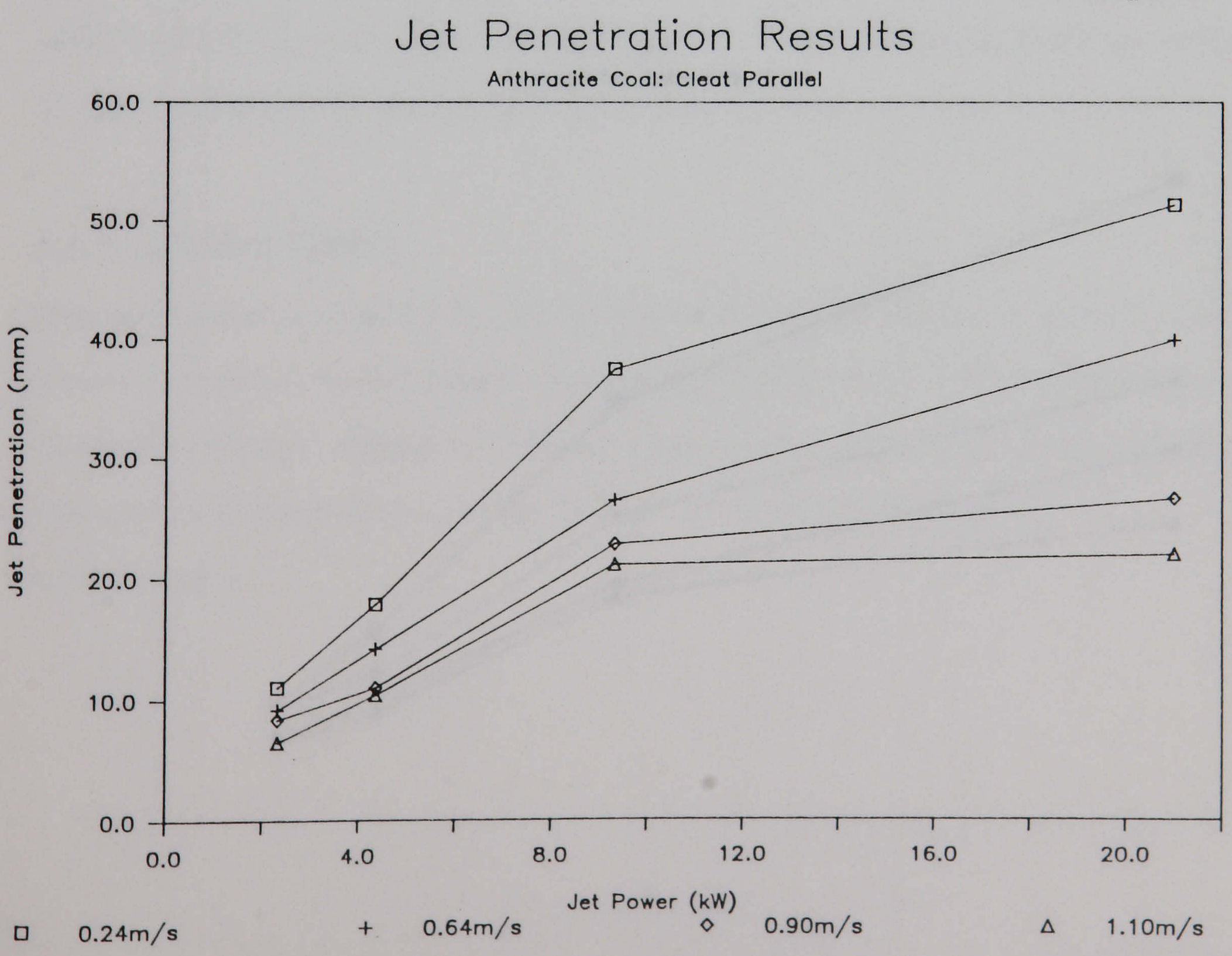

Jet Penetration Results
Anthracite Coal: Cleat Parallel
Jet Penetration (mm)
60.0
50.0
40.0
30.0
20.0
10.0
0.0
0.0
4.0
8.0
12.0
16.0
20.0
Jet Power (kW)
□ 0.24m/s
+ 0.64m/s
◇ 0.90m/s
△ 1.10m/s

Fig.5.6

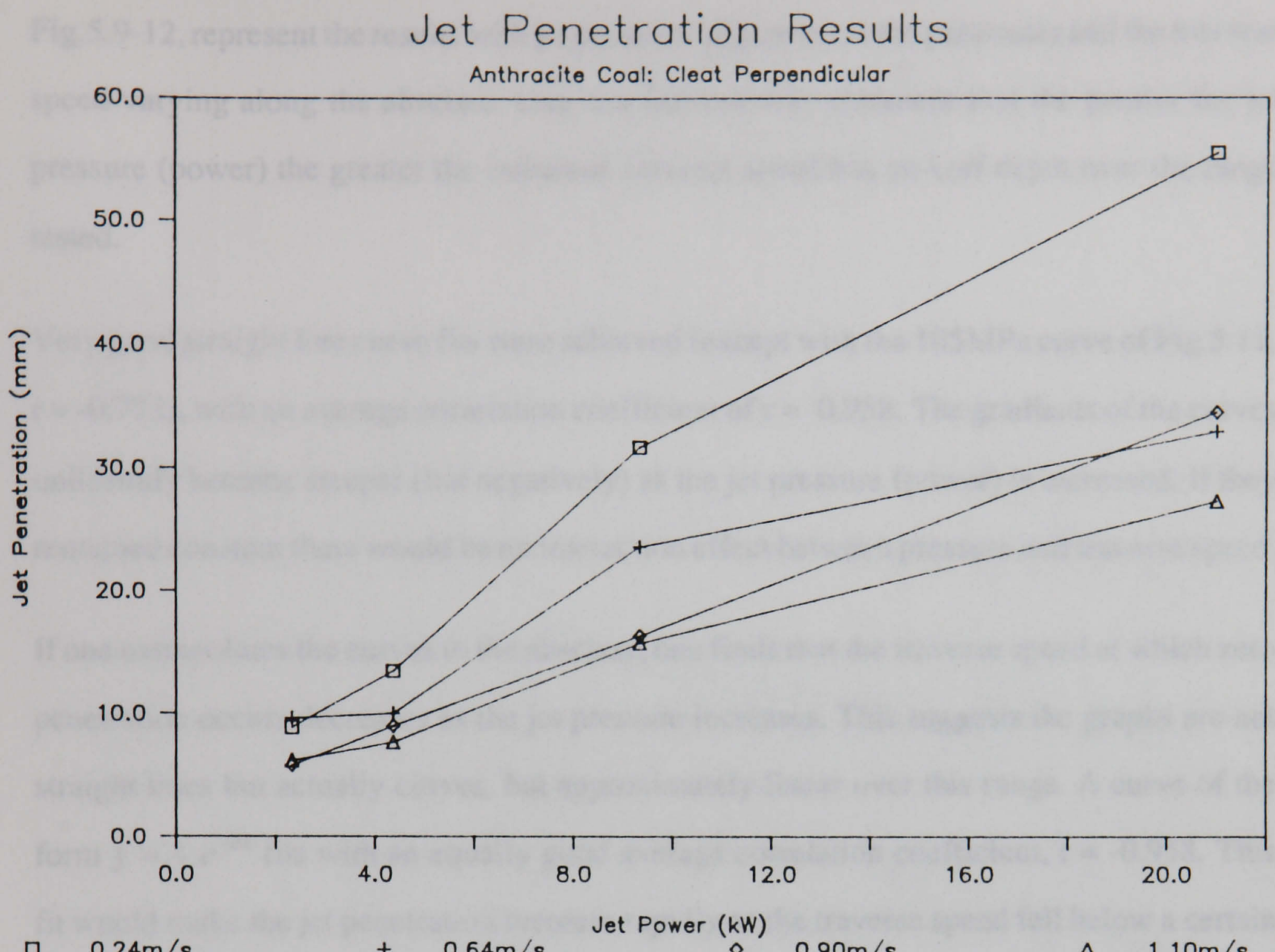

Jet Penetration Results
Anthracite Coal: Cleat Perpendicular
Jet Penetration (mm)
60.0
50.0
40.0
30.0
20.0
10.0
0.0
0.0
4.0
8.0
12.0
16.0
20.0
Jet Power (kW)
□ 0.24m/s
+ 0.64m/s
◇ 0.90m/s
△ 1.10m/s

Fig.5.7

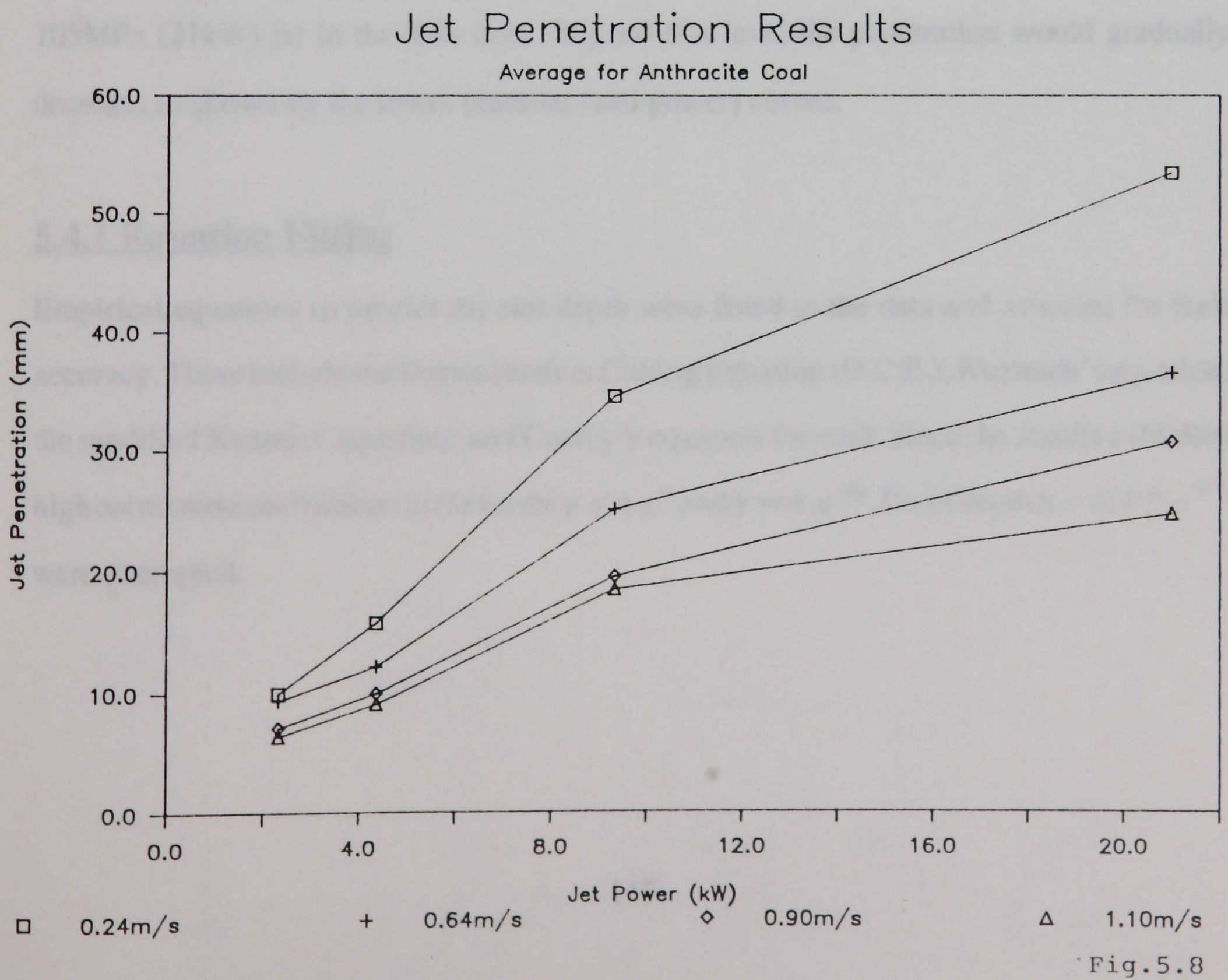

Jet Penetration Results
Average for Anthracite Coal
Jet Penetration (mm)
60.0
50.0
40.0
30.0
20.0
10.0
0.0
0.0
4.0
8.0
12.0
16.0
20.0
Jet Power (kW)
□ 0.24m/s
+ 0.64m/s
◇ 0.90m/s
△ 1.10m/s

Fig.5.8

Fig.5.9-12, represent the results with jet pressure (or power) as the parameter and the traverse speed varying along the abscissa. One can immediately comment that the greater the jet pressure (power) the greater the influence traverse speed has on kerf depth over the range tested.

Very good straight line curve fits were achieved (except with the 105MPa curve of Fig.5.11, r = -0.773), with an average correlation coefficient of r = -0.958. The gradients of the curves uniformily become steeper (but negatively) as the jet pressure (power) is increased. If they remained constant there would be no interaction effect between pressure and traverse speed.

If one extrapolates the curves to the abscissa, one finds that the traverse speed at which zero penetration occurs decreases as the jet pressure increases. This suggests the graphs are not straight lines but actually curves, but approximately linear over this range. A curve of the form $y = A.e^{-Bx}$ fits with an equally good average correlation coefficient, r = -0.958. This fit would make the jet penetration increase rapidly as the traverse speed fell below a certain level for a particular jet power. From Fig.5.9, this level seems to have been reached for the 105MPa (21kW) jet in the Erin coal. Beyond this level the penetration would gradually decrease as shown by the lower pressure (and power) curves.

5.4.1 Equation Fitting

Empirical equations to predict the slot depth were fitted to the data and assessed for their accuracy. These include the Dimensionless Cutting Equation (D.C.E.); Kuzmich's equation; the modified Kuzmich equation; and Cooley's equation for coal. Since the results exhibited high correlation coefficients to the forms $y = a\,x^m$ and $y = A.e^{-Bx}$, fits of depth $h = B.P_w^m.e^{-n.V_t}$ were attempted.

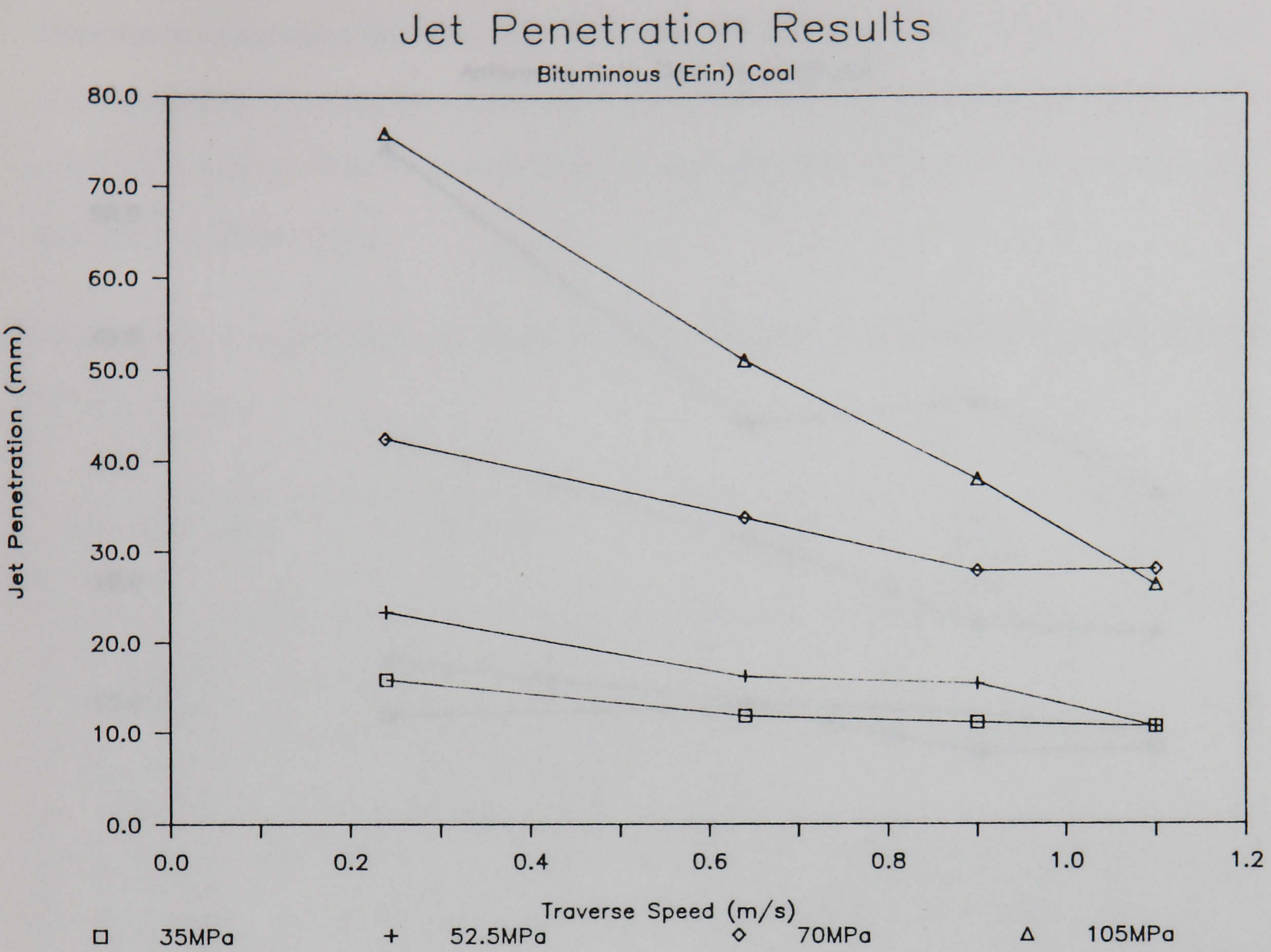


Fig.5.9

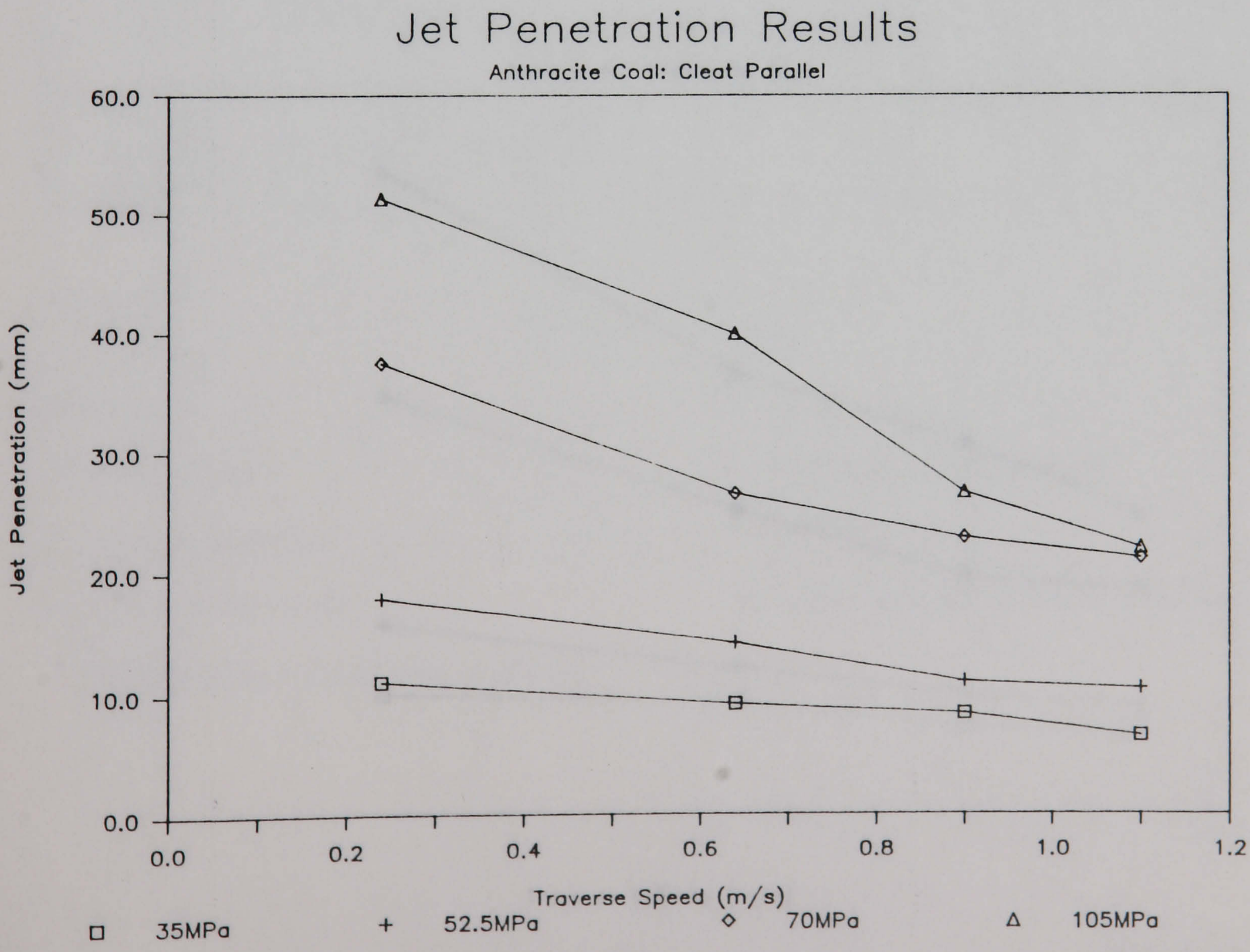


Fig.5.10

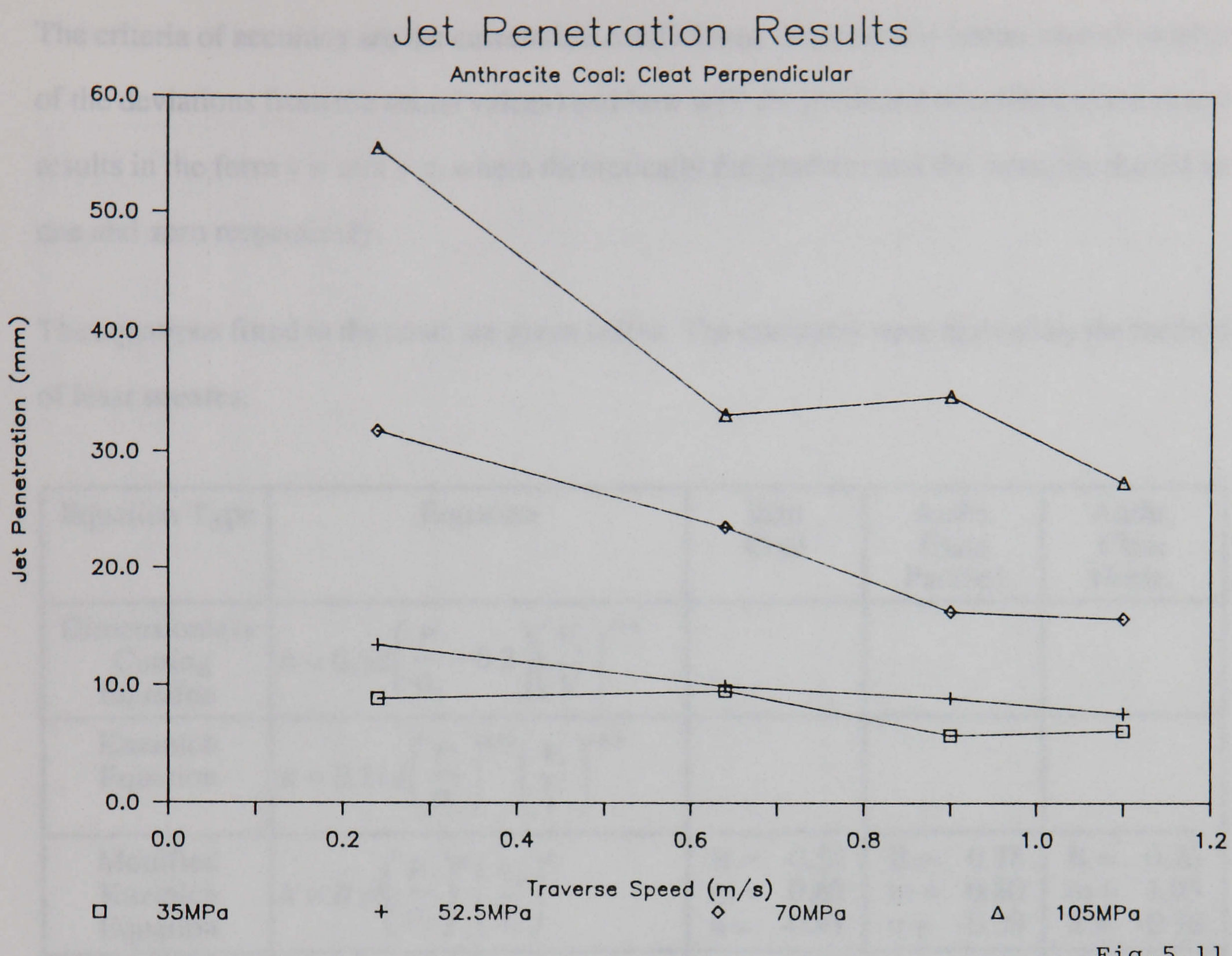


Fig.5.11

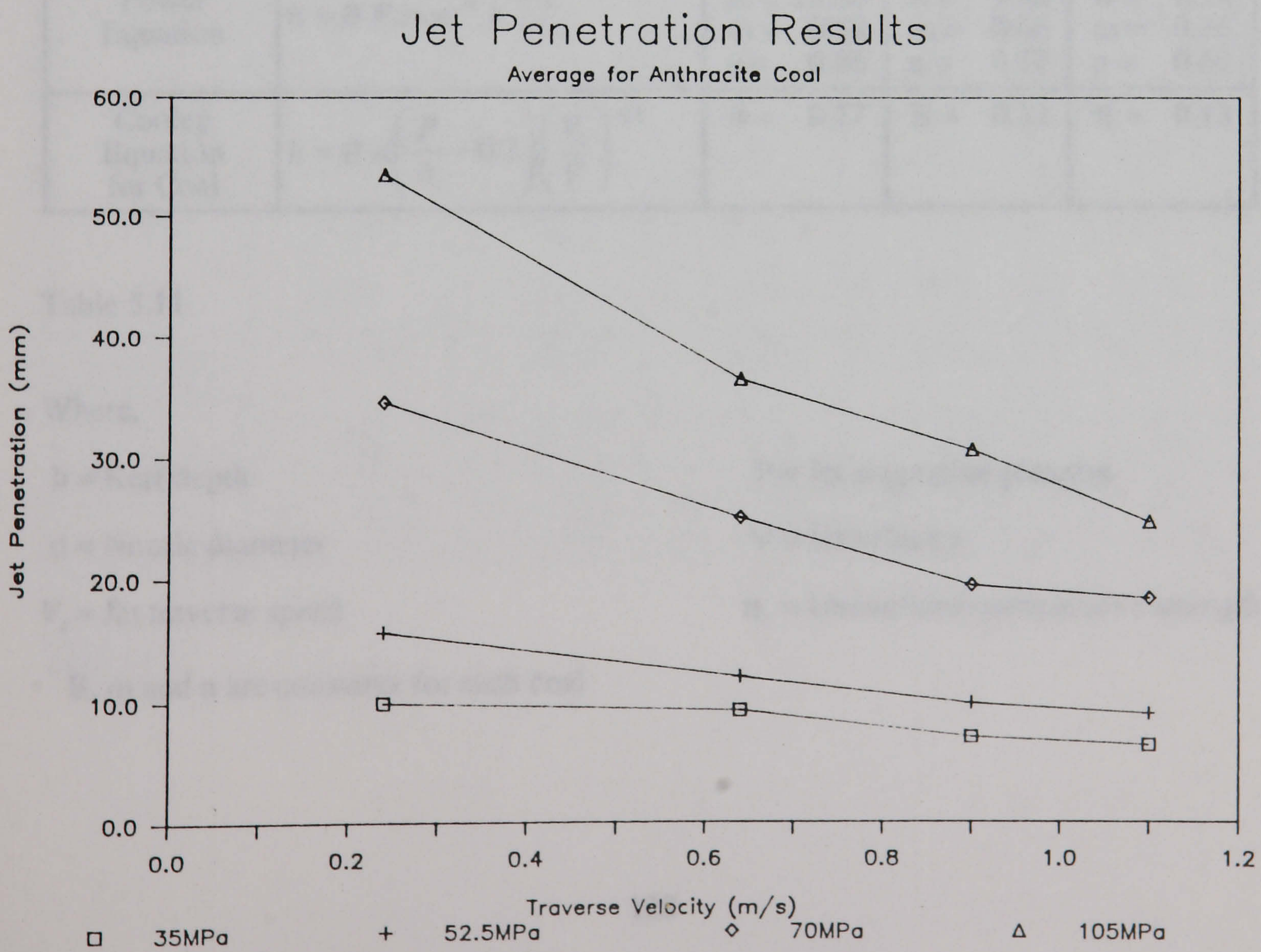


Fig.5.12

The criteria of accuracy are the correlation coefficients, the residuals (mean sum of squares of the deviations from the actual values) and how well the predicted data fitted to the actual results in the form $y = m.x + c$, where theoretically the gradient and the intercept should be one and zero respectively.

The equations fitted to the coals are given below. The constants were derived by the method of least squares.

Equation Type	Equation	Erin Coal	Anthr. Cleat Parallel	Anthr. Cleat Horiz.
Dimensionless Cutting Equation	$h = 0.5d\left(\frac{P}{\sigma_c} - 0.2\right)\left(\frac{V_t}{V}\right)^{-0.5}$			
Kuzmich Equation	$h = 0.11d\left(\frac{P}{\sigma_c}\right)^{0.75}\left(\frac{V_t}{V}\right)^{-0.5}$			
Modified Kuzmich Equation	$h = B.d\left(\frac{P}{\sigma_c}\right)^{m}\left(\frac{V_t}{V}\right)^{n}$	B = 0.54 m = 0.69 n = -0.47	B = 0.78 m = 0.80 n = -0.39	B = 0.26 m = 1.05 n = -0.38
Power Equation	$h = B.Power^{m}.e^{-n.V_t}$	B = 12.90 m = 0.59 n = 0.86	B = 9.02 m = 0.66 n = 0.77	B = 6.14 m = 0.76 n = 0.69
Cooley Equation for Coal	$h = B.d\left(\frac{P}{\sigma_c} - 0.2\right)\left(\frac{V_t}{V}\right)^{-0.5}$	B = 0.27	B = 0.32	B = 0.13

Table 5.11

Where,

h = Kerf depth

d = Nozzle diameter

V_t = Jet traverse speed

P = Jet stagnation pressure

V = Jet velocity

σ_c = Unconfined compressive strength

B, m and n are constants for each coal

Erin Coal

Actual Kerf Depth (mm)	D.C.E (mm)	Kuzmich (mm)	Modified Kuzmich (mm)	Power (mm)	Cooley (mm)
15.9	26.6	4.9	18.6	17.2	14.4
23.4	45.2	7.3	27.1	24.9	24.5
42.5	79.3	11.8	42.8	38.9	43.0
76.0	145.7	19.3	68.1	62.5	79.0
11.9	16.3	3.0	11.7	12.2	8.8
16.3	27.7	4.5	17.0	17.7	15.0
33.9	48.5	7.2	26.9	27.6	26.3
51.1	89.2	11.8	42.9	44.4	48.3
11.2	13.7	2.5	10.0	9.8	7.4
15.5	23.3	2.6	14.5	14.2	12.6
28.0	40.9	6.1	22.9	22.1	22.2
38.1	75.2	10.0	36.5	35.5	40.8
10.7	12.4	2.3	9.1	8.2	6.7
10.7	21.1	3.4	13.2	11.9	11.4
28.2	37.0	5.5	20.8	18.6	20.1
26.4	68.0	9.0	33.2	29.9	36.9
Correlation Coefficient	0.973	0.970	0.972	0.978	0.973
Residuals	759.1	591.7	21.3	27.7	21.6
y = m.x + c	m = 1.95 c = -5.50	m = 0.25 c = 0.08	m = 0.86 c = 2.40	m = 0.81 c = 2.42	m = 1.06 c = -3.00

Table 5.12

Anthracite (Cleat Parallel)

Actual Kerf Depth (mm)	D.C.E (mm)	Kuzmich (mm)	Modified Kuzmich (mm)	Power (mm)	Cooley (mm)
11.1	16.5	3.5	12.2	13.1	10.5
18.0	28.5	5.3	18.3	19.8	18.2
37.6	50.5	8.5	29.5	32.5	32.1
51.4	93.4	14.0	48.3	55.4	59.4
9.2	10.1	2.2	8.3	9.6	6.4
14.3	17.5	3.2	12.4	14.5	11.1
26.6	30.9	5.2	20.0	23.9	19.7
40.0	57.2	8.6	32.9	40.7	36.4
8.4	8.5	1.8	7.2	7.9	5.4
11.1	14.7	2.7	10.9	11.9	9.4
23.0	26.1	4.4	17.5	19.6	16.6
26.7	48.2	7.2	28.8	33.3	30.7
6.5	7.7	1.6	6.7	6.7	4.9
10.5	13.3	2.5	10.0	10.2	8.5
21.3	23.6	4.0	16.2	16.8	15.0
22.1	43.6	6.5	26.6	28.6	27.7
Correlation Coefficient	0.959	0.963	0.963	0.967	0.985
Residuals	209.8	347.0	16.1	11.4	20.0
y = m.x + c	m = 1.71 c = -5.50	m = 0.24 c = 0.04	m = 0.86 c = 1.06	m = 1.01 c = 0.10	m = 1.09 c = -3.50

Table 5.13

Anthracite (Cleat Horizontal)

Actual Kerf Depth (mm)	D.C.E (mm)	Kuzmich (mm)	Modified Kuzmich (mm)	Power (mm)	Cooley (mm)
8.9	40.4	6.6	10.0	9.9	10.7
13.5	68.1	9.8	16.5	15.9	18.0
31.8	118.9	15.8	28.6	28.2	31.4
55.6	217.7	26.0	51.7	52.1	57.5
9.6	24.7	4.0	6.9	7.5	6.5
10.0	41.7	6.0	11.4	12.1	11.0
23.7	72.8	9.7	19.8	21.4	19.2
33.2	133.3	15.9	25.8	39.6	35.2
5.8	20.8	3.4	6.1	6.3	5.5
9.0	35.2	5.1	10.1	10.1	9.3
16.4	61.4	8.2	17.4	17.9	16.2
34.8	112.4	13.4	31.5	33.2	29.7
6.2	18.9	3.1	5.6	5.5	5.0
7.7	31.8	4.6	9.3	8.8	8.4
15.8	55.6	7.4	16.1	15.6	14.7
27.5	101.7	22.7	29.2	28.9	26.8
Correlation Coefficient	0.985	0.918	0.987	0.984	0.985
Residuals	4268.1	147.0	5.4	6.1	5.7
y = m.x + c	m = 3.76 c = -0.40	m = 0.45 c = 1.30	m = 0.92 c = 1.42	m = 0.95 c = 1.30	m = 0.99 c = -0.05

Table 5.14

All the predictions proved to be highly correlated with the actual kerf depths. However the Dimensionless Cutting Equation and Kuzmich's Equation gave results that were consistently too high and too low respectively as reflected in the large residual values. The two equations are generalised forms and the constants in Kuzmich's equation have been derived from rock cutting experiments and so the results are not too surprising.

When modified versions of the two equations are fitted viz. Cooley's equation and the modified Kuzmich equation (Ip, 1986), then excellent predictions are obtained; the Cooley equation being particularly good.

The 'Power' equation is an attempt to incorporate the relationships suggested in Section 1.4, and an equally accurate prediction to the other equations is obtained. The form of the equation allows one to predict the kerf depth at any traverse speed including that of a stationary jet, but with the reservation that one is extrapolating outside of the range the variables were tested.

5.4.2 Hydraulic Specific Energies

The hydraulic specific energies were calculated from the equation below:

$$\text{Hydraulic Specific Energy} = \frac{\text{Jet Power}}{2.5d.h.V_t} \qquad (5.1)$$

Where

d = nozzle diameter

h = slot depth

V_t = traverse speed

The average width of the slot was assumed to be two and a half times the nozzle diameter.

Fig.5.13-16, illustrate the relationship between specific energy and the jet pressure. The graphs show a trend for the specific energy to increase with jet pressure. Specific energies are extremely high and indicate that fine water jets by themselves are not a feasable method of coal excavation. Generally the values were higher in the anthracite coal, particularly at the 0.24m/s traverse speed.

A marked increase (at least double) in specific energy is evident at the slowest traverse speed in both coals. At the other traverse speeds the graphs are close together irrespective of jet pressure.

Fig.5.17-20, show the same results against jet power. Again the curves indicate the inefficiency of traversing a jet at a slow speed. The 2.33kW jet seems to be the most efficient in terms of specific energy.

Fig.5.21-24, highlight the influence of the traverse speed. Although the traverse speeds are not equally spaced, the difference in the energy requirements between the 0.24m/s and 0.64m/s to the 0.64m/s and 1.1m/s traverse speeds is quite disproportionate and is manifest in both coals. Above 0.64m/s the specific energy decreases monotonically.

The Erin coal seems to exhibit a minimum for two of the curves. This could be explained by the penetrations achieved by these two particular jets as shown in Fig.5.5 and Fig.5.9. The least efficient jet is that at 105MPa (21kW) and the most efficient at 35MPa (2.33kW). The 70MPa (9.33kW) jet is more efficient throughout the speed range than the 52.5MPa (4.37kW) one, the larger diameter of the 70MPa jet may account for this.

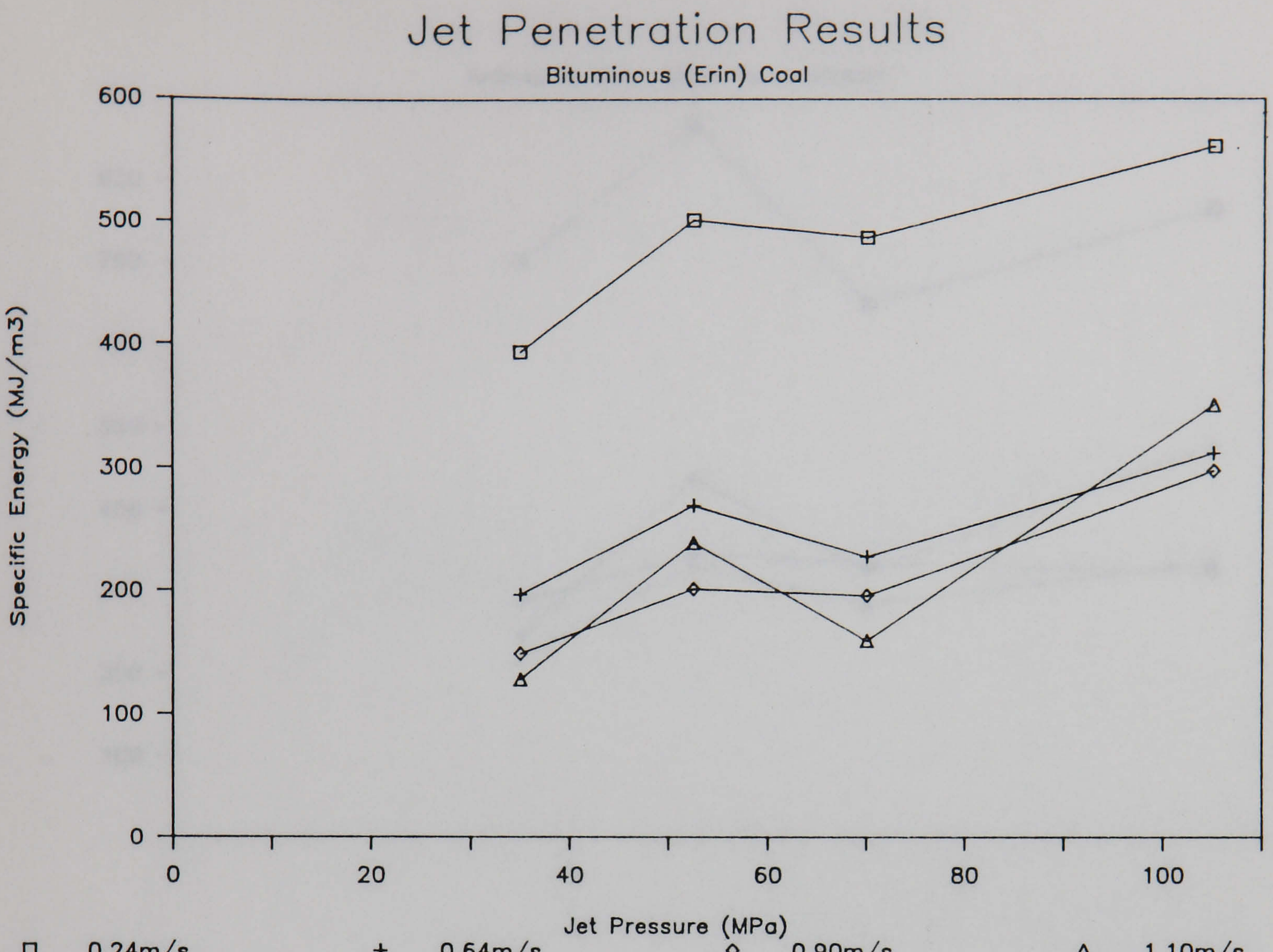


Fig.5.13

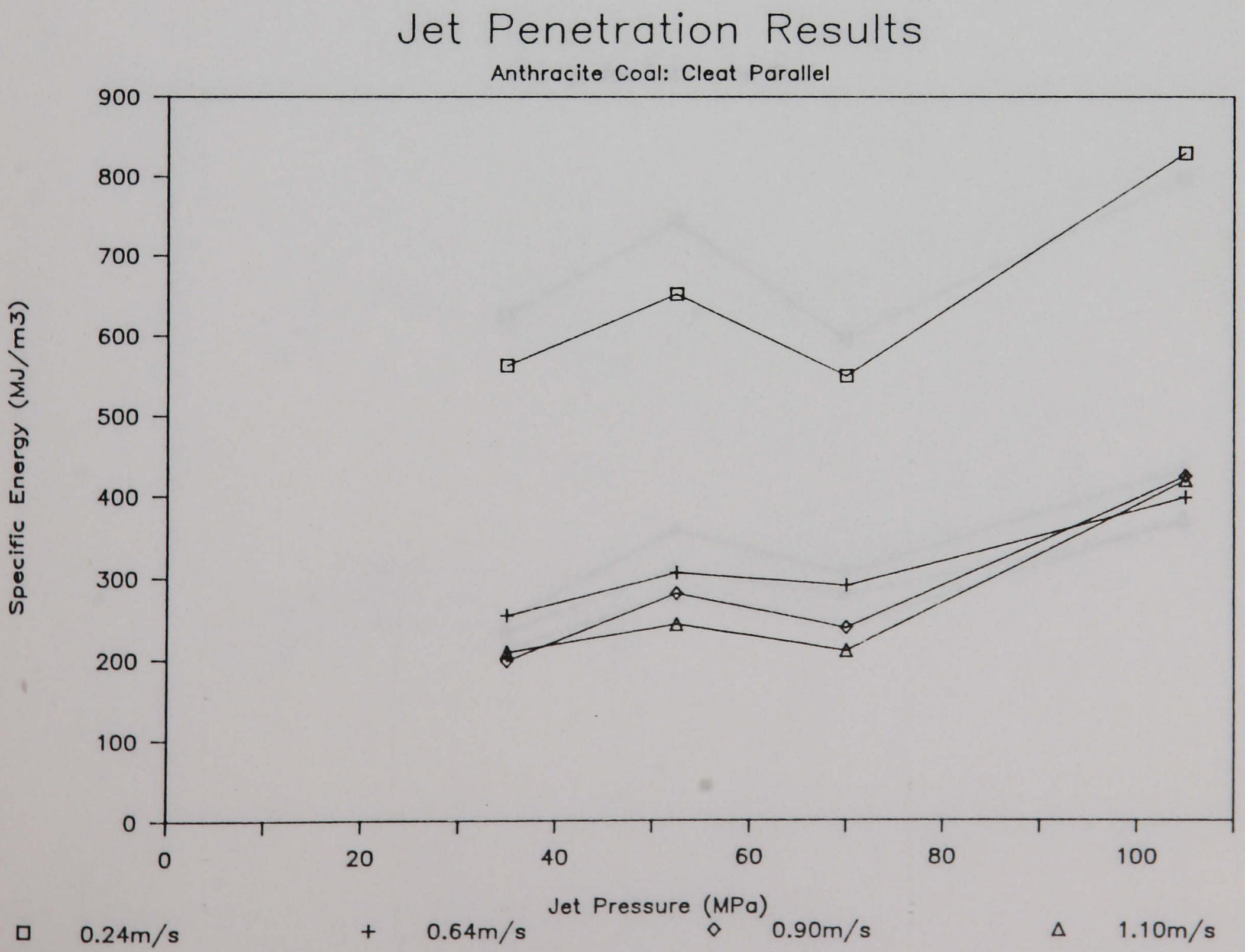


Fig.5.14

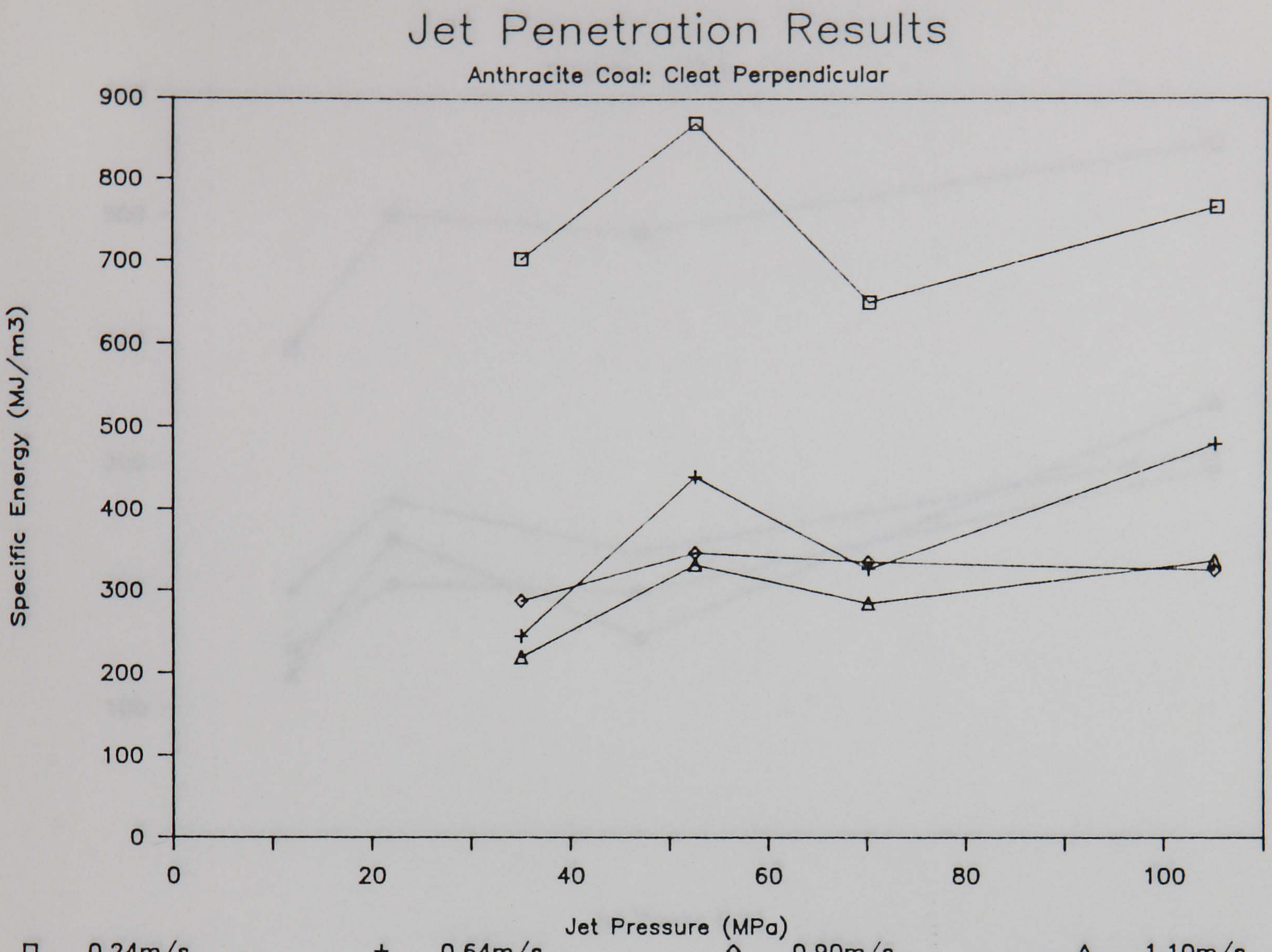


Fig.5.15

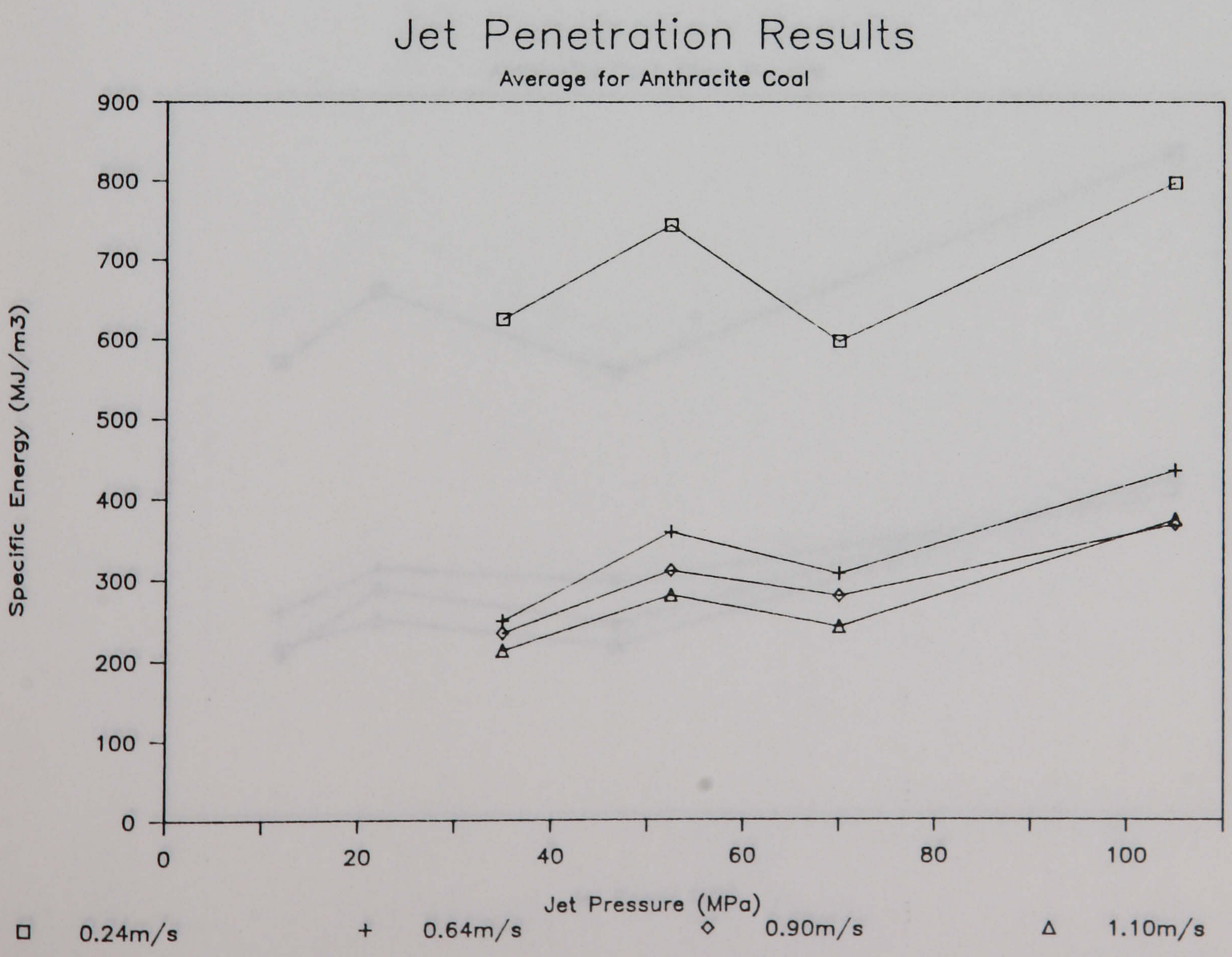


Fig.5.16

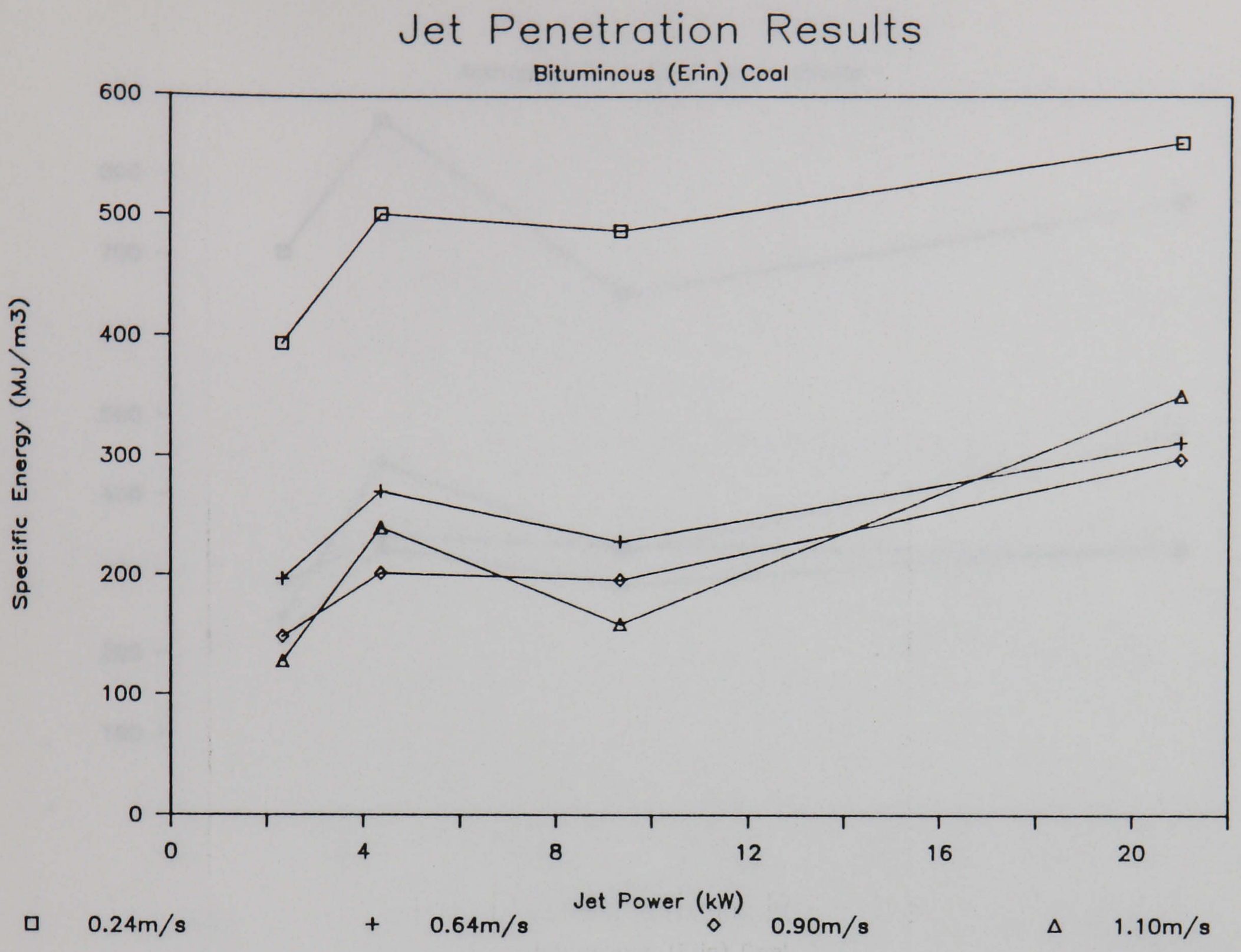


Fig.5.17

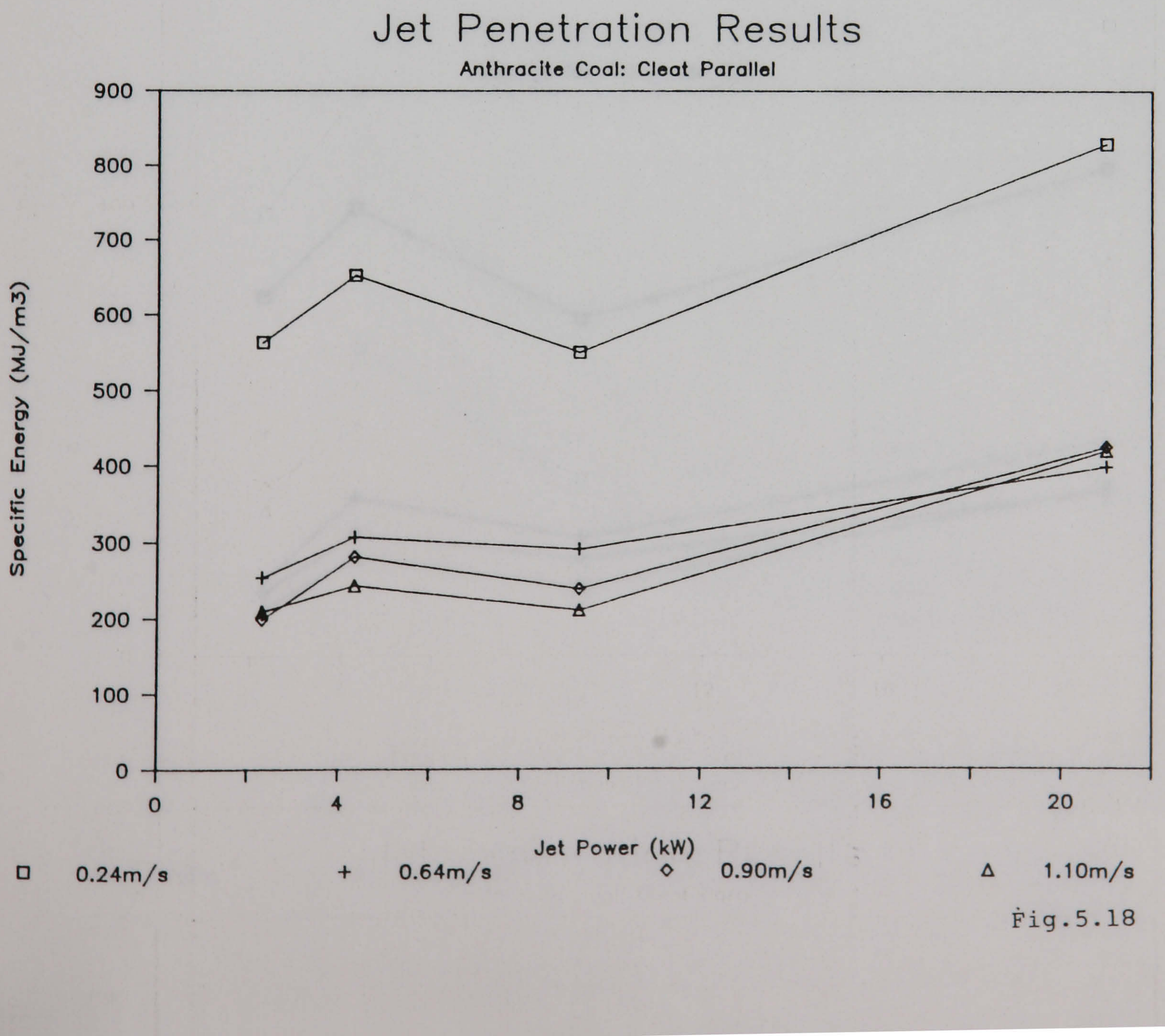


Fig.5.18

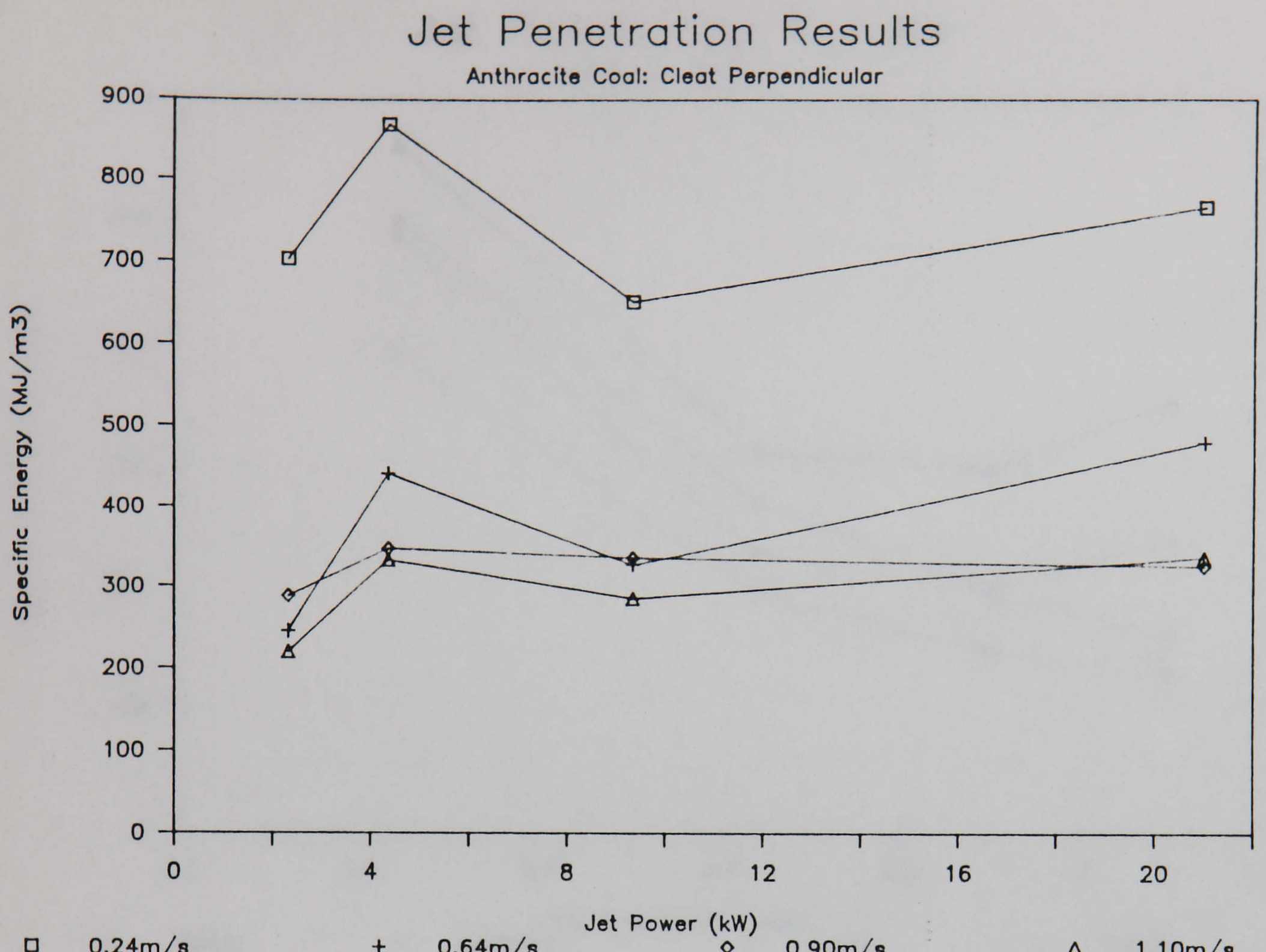


Fig.5.19

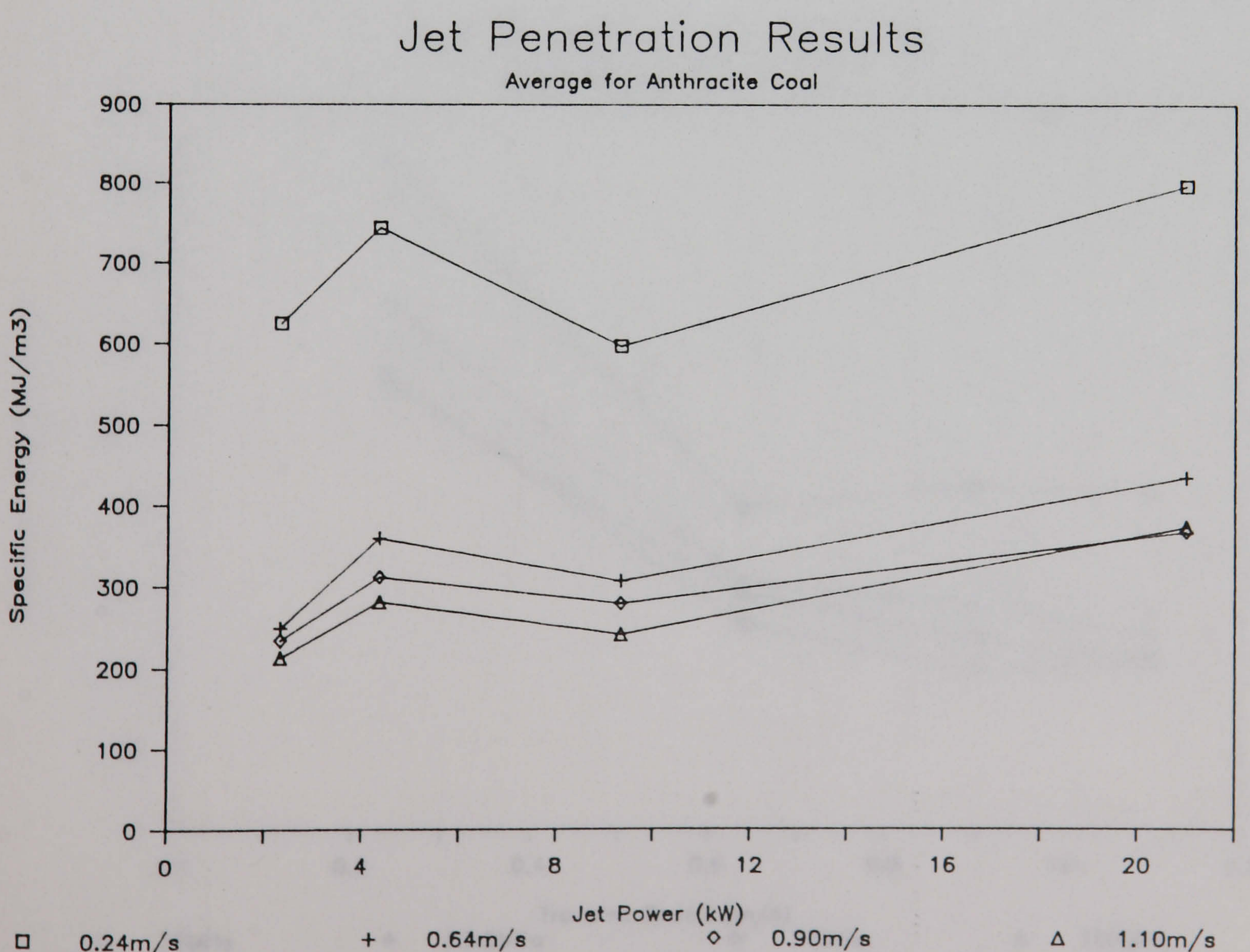


Fig.5.20

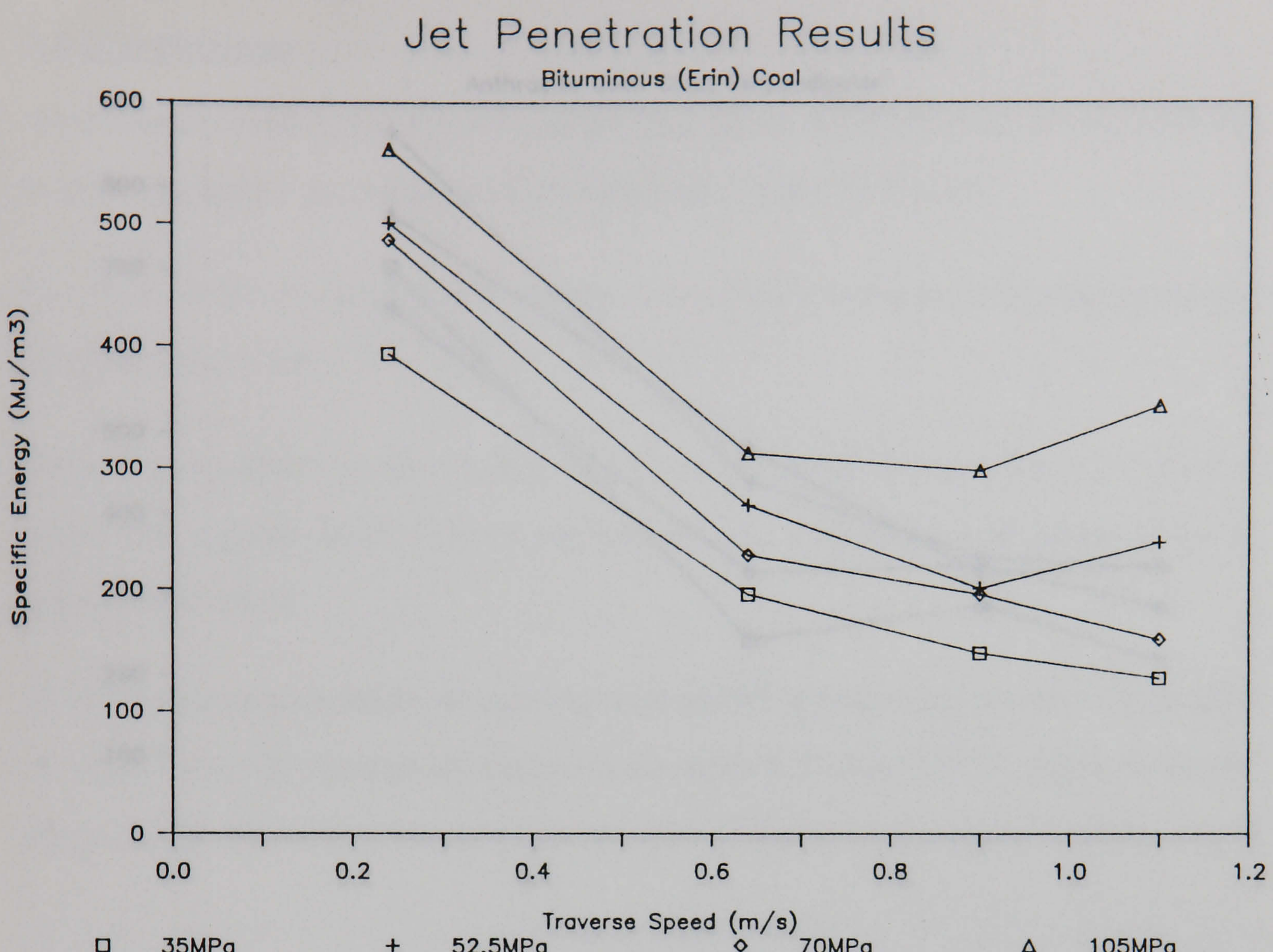


Fig.5.21

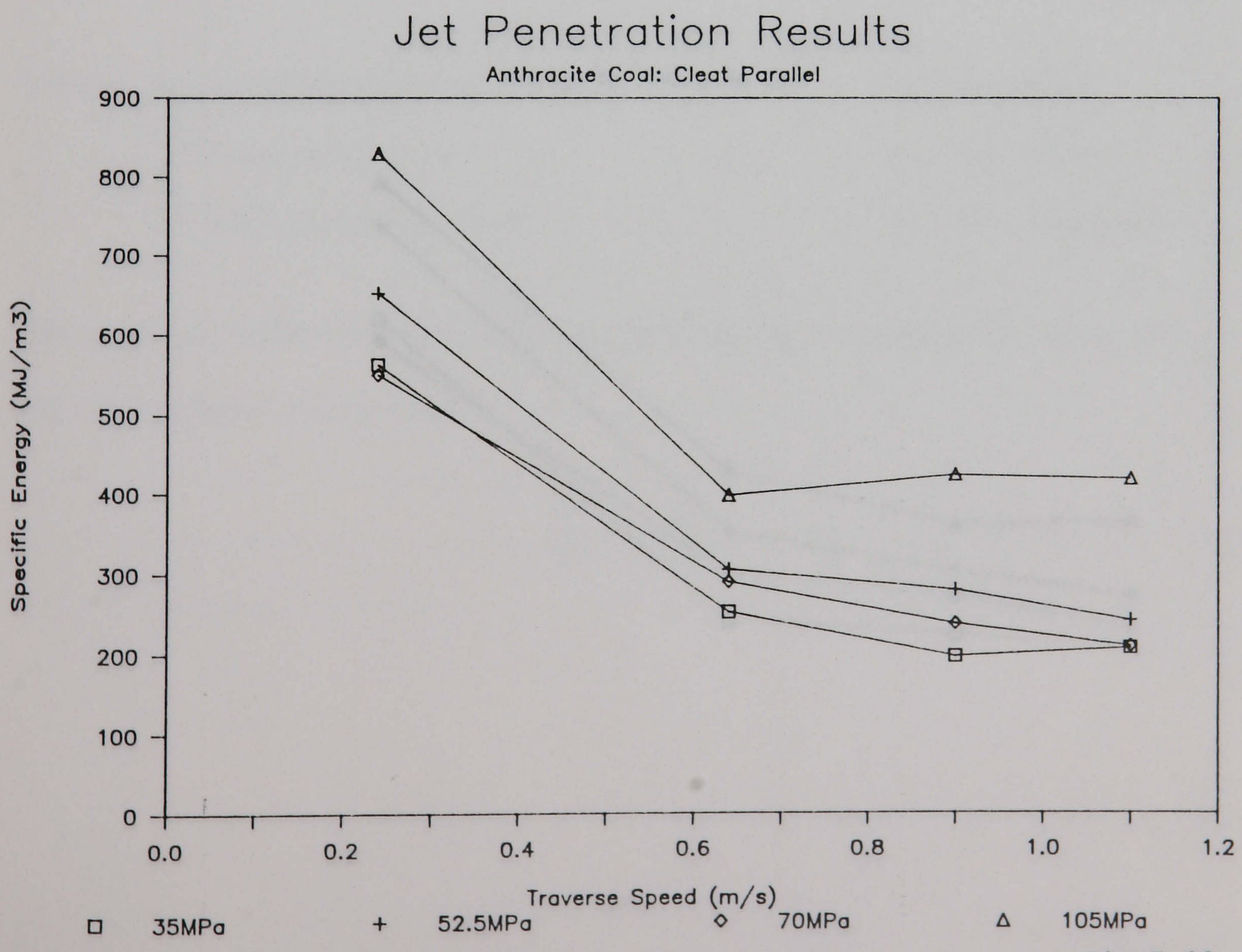


Fig.5.22

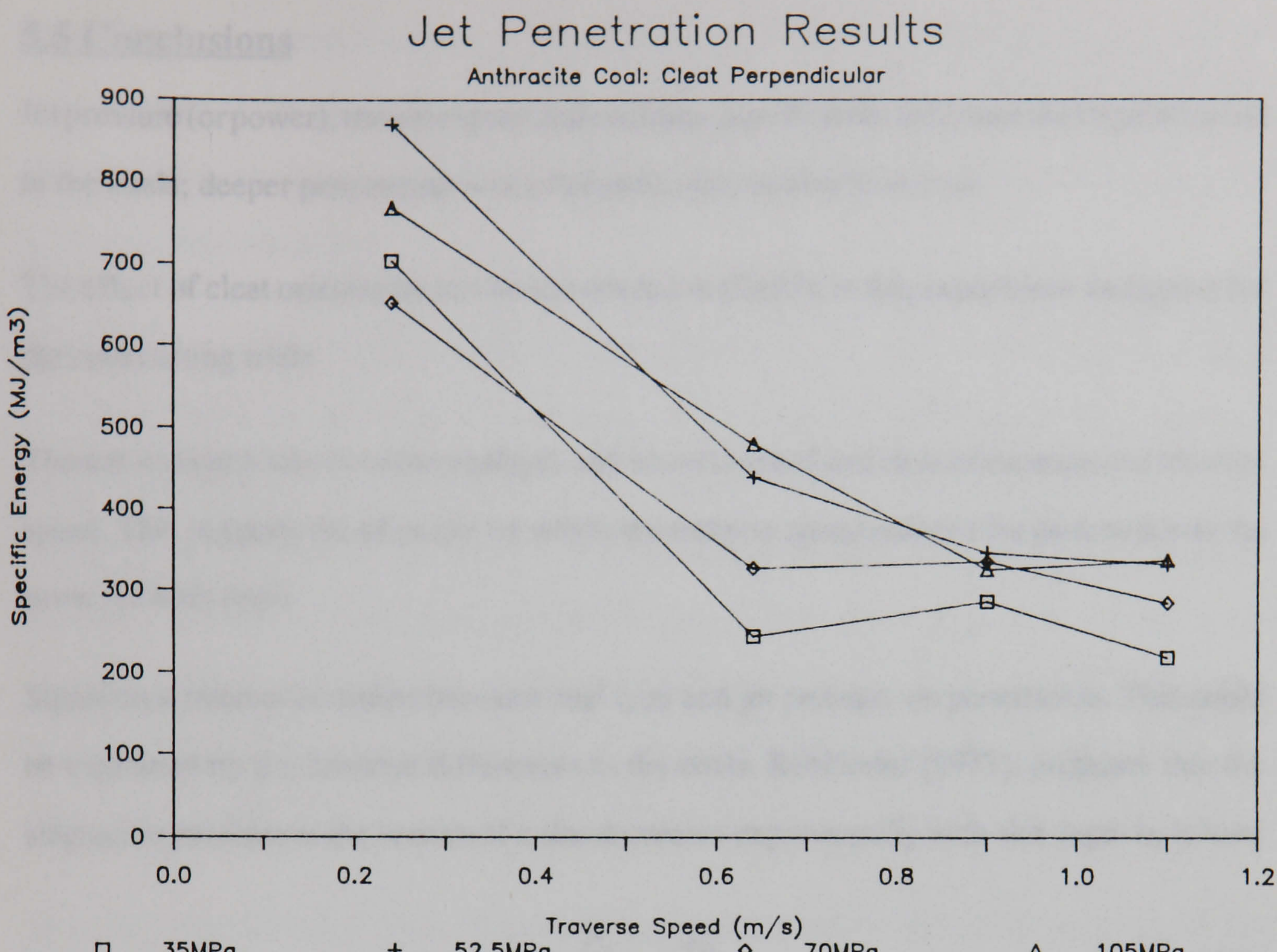


Fig.5.23

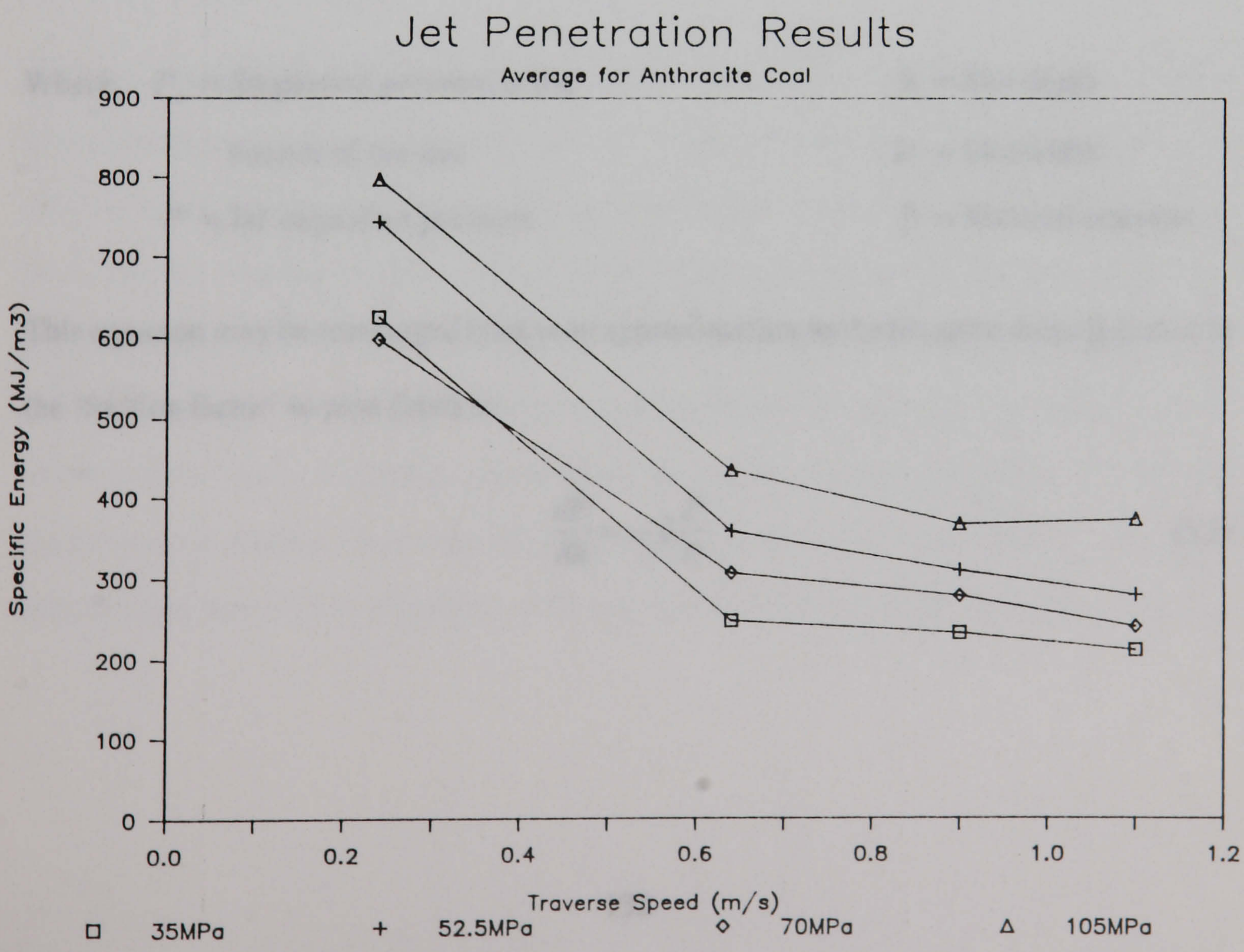


Fig.5.24

5.5 Conclusions

Jet pressure (or power), traverse speed and coal type significantly influence the jet penetration in the coals; deeper penetration was achieved in the weaker Erin coal.

The effect of cleat orientation can be considered negligible in this experiment and hence for the coal cutting trials.

There is no interaction between coal type and traverse speed and cleat orientation and traverse speed. This suggests the principle by which the traverse speed reduces the penetration is the same for both coals.

Significant interaction exists between coal type and jet pressure on penetration. This could be explained by the inherent differences in the coals. Rehbinder (1977), proposes that the stagnation pressure at the bottom of a slot decreases exponentially with slot depth as below:

$$\frac{P_o}{P} = e^{-\beta\frac{h}{D}} \tag{5.2}$$

Where, P_o = Stagnation pressure at the bottom of the slot

P = Jet stagnation pressure

h = Slot depth

D = Slot width

β = Material constant

This equation may be rearranged (this is an approximation to the pressure drop; β is akin to the 'friction factor' in pipe flow) to:

$$\frac{dP}{dh} = -\beta\frac{P}{D} \tag{5.3}$$

Thus the pressure drop depends upon the material the jet is cutting through, the jet pressure and inversely to the slot width. Presumably β would differ for the two coals resulting in different pressure drops even when the pressure and slot width were identical. Hence the reason for this interaction.

Interaction is highly significant between jet pressure and traverse speed. This means that the effect of jet pressure on penetration is influenced by the traverse speed: the two factors are not independent. An explanation to this could be that the effect of the pressure drop is amplified by the traverse speed (since this interaction is larger). Also, the effect was significant within the anthracite when considering cleat. In this circumstance, β would be constant, but the pressure drop would still vary as the nozzle pressure and diameter were changed. By this means the interaction effect could be maintained even within the same coal, which is the case.

Jet penetration becomes more sensitive to traverse speed as the jet power is increased and this is evident in both coals.

The data suggests the relationship between kerf depth and jet power is not quite linear but has a curvature component, although the graphs become more linear as the traverse speed decreases. An explanation to this may be obtained from a consideration of the pressure drop in the kerf in a similar manner as above. If the acceleration of the eroded coal particles by the jet is considered negligible and by considering the effects of frictional resistance at the kerf wall, the approximate equation above can be derived, to account for the pressure drop down the slot. From the equation, the pressure drop would change when the jet pressure and diameter were altered. Thus each jet in this experiment would have separate values for pressure loss down the slot, leading to the non-linear difference in penetrations achieved.

Empirical equations fitted to the data predicted accurate and highly correlated kerf depths. The exceptions were the generalised forms viz. the Dimensionless Cutting Equation and Kuzmich's Equation. Cooley's equation (a simple modification to the D.C.E.) was particularly good.

With respect to specific energy, slowly traversing jets are inefficient. The low power/fast traverse rate jet gave the best result in both coals.

CHAPTER SIX

6 ERIN AND ANTHRACITE COAL RESULTS

6.1 Introduction

This chapter presents the results of the research programme. The cutting tool experienced relief in the tests and models as far as possible a typical vane tool on a shearer drum: the major differences being tool speed and the linear path travelled.

The influence of jet assistance on the cutting forces, breakout and particle size is given with reference to the two coals and cleat orientations. Some attention is given to specific energy since this is important with respect to the unit costs of coal mining.

6.2 Coal Description

6.2.1 Erin Coal

This coal was supplied by British Coal from the Erin Remainder opencast site near Chesterfield, Nottinghamshire. The seams mined at the site are the Swinton Pottery, Clowne, Upper Foxearth, Lower Foxearth, Sough and Furnace. It is a bituminous coal, generally a dull grey colour indicating the durain content, but also with quite frequent shiny black vitreous bands. The bedding planes were easily visible and the coal was heavily cleated. The cleat was arranged to be vertical and parallel to the cutting direction, and can be seen in photographs that appear later in the text. The coal was friable, dusty to handle, contained a few areas of very dull, almost powdery coal, and had a band of iron pyrites in one block.

Coal cubes were prepared to assess its compressive strength. The cubes were nominally 78mm × 78mm × 78mm in dimensions. Two surfaces of each cube were ground parallel and smooth such that the compression load would act perpendicularly to the bedding planes. Six cubes were tested in an Avery-Denison 3000kN capacity compression machine at a loading rate of 12.5kN/min, within the range suggested by the I.S.R.M. The average com-

pressive strength was 12.6MPa ±3.9MPa. The density was estimated from the coal cubes at 1212kg/m^3. This value is judged to be on the low side since the cubes had lost moisture and their sides were rough and pitted despite being cut by a diamond saw. Cylinders could not be prepared from this coal since it kept shearing in the core barrel along the bedding planes.

6.2.2 Anthracite Coal

The anthracite was acquired again from British Coal, from the Ffos Las opencast site near Kidwelly, Pontypridd, South Wales. The seams mined are the Drap, Mole Rider, Mole, Graigog Rider, Graigog, Green, Kings, Big, Yard Rider, Yard, and Two Feet. Four large blocks were available and so the cleat was investigated in this coal.

The coal was black and shiny. The photographs later in the text show how the flash of the camera was reflected by the clean vitreous surfaces. Bedding planes could be seen which were arranged such that the tool cut through them. The coal consisted mainly of clarain and vitrain, fusain was noticeable on some fracture planes whilst collecting the debris after cutting and during the size analysis.

The coal was not very friable or dusty but coherent and quite clean on the hands. The cleat was not as dense as in the Erin coal. One block contained a very dense band of fused coal and iron pyrites about 40mm wide. The pyrites occurred as small spheres about 1mm in diameter.

Cubes were prepared as with the Erin sample for compressive testing. With the load applied perpendicularly to the bedding planes, the average compressive strength was 19.4MPa ±6.0MPa from twelve cubes. Some cubes contained pyrites and consequently were stronger and contributed to the standard deviation.

Since more coal was available, cubes with the load applied in a parallel direction to the bedding planes were also tested and gave a compressive strength of 8.5MPa ±3.7MPa, indicating the degree of anisotropy. The density, estimated from the cubes, was 1496kg/m^3.

Since the anthracite was not very friable, Brazilian Discs could be obtained. Each disc was 38mm in diameter and 21mm long. They were compressed in a 250kN capacity Avery testing machine at a loading rate of 1.25kN/min.

Fifteen disc were crushed until failure with the load acting perpendicularly to the bedding. Ten discs contained between 20%-30% pyrites (visual approximation) and gave an average tensile strength of 1.89MPa ±0.25MPa. The other five discs contained no pyrites and their mean strength was 0.54MPa ±0.15MPa.

Five more discs were loaded to failure with the bedding planes parallel to the loading direction. Two samples with 20%-50% pyrites had an average strength of 1.44MPa ±0.37MPa. The last three samples had no pyrites and their tensile strength was 0.43MPa ±0.07MPa.

The strength of the anthracite is greater when the load is applied perpendicularly to the bedding than in a parallel direction. In this experiment the tool cuts perpendicularly or through the bedding planes for both coals and cleat orientations.

The strengths of the coals are given for comparative purposes. Coal strength depends greatly on the size and orientation of the specimen tested and should strictly be treated on a statistical basis (Pomeroy and Brown, 1968). The smaller the sample the more likely one is to be testing the strengths of the constituent lithotypes and lose the macro influences of cleat and bedding. In this sense coal is much more complicated than other rocks.

Despite the bands of pyrites in both coals neither sharp nor blunt cutting tool exhibited any signs of abrasive wear. And this after each tool had cut at least 250m in the coals throughout the course of the experiment.

6.3 Coal Cutting Results

Due to the variability within and between the coals, as indicated above, a statistical approach to the evaluation of treatment effects is taken. A graphical representation and discussion is given but the statistical significance of the differences indicated on the graphs should be kept in mind.

The force values were calculated for relieved cutting. Hence the first cut of each treatment had to be ignored during the analysis since this cut would be taken in solid coal, unrelieved from a preceding cut. The first cut taken in each treatment did have an effect on the average if included but not in all cases. Another reason to discount the first cut was because of the unequal number of replications per treatment that were taken, so if included the first cut effect would not be averaged out evenly among the treatments.

The statistical analysis was performed on Newcastle University's Mainframe computer using the statistics software GLIM 3.12.

6.3.1 Erin and Anthracite Trials

The purpose of these tests was to investigate the effect of high pressure water jet assistance on cutting performance in the different coal types.

The factorial experiment is described in Table 6.1. Each cell contains the number of replications taken for that treatment. The mean and mean peak normal, cutting and sideway forces were recorded for each treatment. All the coal debris was collected and sieved but the size analysis will be detailed in a separate section.

	Erin Coal		Anthracite Coal	
	Sharp Pick	Blunt Pick	Sharp Pick	Blunt Pick
0MPa	10X	9X	6X	4X
35MPa	8X	8X	4X	6X
70MPa	8X	8X	4X	4X
105MPa	8X	7X	7X	6X

Table 6.1

Mean Normal Force ANOVA

Source of Variation	Sums of Squares	Degrees of Freedom	Mean Square	F-ratio & (Significance Level)
Between Pressures	3.900	3	1.300	27.7 (4.0)
Between Pick Wear	4.600	1	4.600	97.9 (6.9)
Between Coals	2.850	1	2.850	60.6 (6.9)
Interaction between Pressures & Pick Wear	1.350	3	0.450	9.6 (4.0)
Interaction between Pressures & Coals	1.480	3	0.493	10.5 (4.0)
Interaction between Coals & Pick Wear	5.381	1	5.381	114.5 (6.9)
Interaction between Pressures, Coals & Pick Wear	1.524	3	0.508	10.8 (4.0)
Experimental Error	4.155	89	0.047	
Total	25.250	104		

Table 6.2

Experimental Error Variance, $\sigma_0^2 = \pm 0.047$kN. Using an average number of replications of 105/16 = 6.6, then the standard error between any two means is $\sigma_0\sqrt{\frac{2}{6.6}} = 0.12kN$. From this the 95% confidence limits for tests of significance may be calculated. With eleven degrees of freedom the test statistic, t = 2.20, hence the 95% confidence limits = ±2.20 x 0.12 = ±0.26kN. This is a two tailed test which allows one to judge if there has been a significant increase or decrease in force value.

From the F-ratios in Table 6.2, it appears all the effects and interactions are highly significant (the degree of significance is shown for that at the 1% level). However, the interaction effects are much smaller than the main effects and may largely be ignored. The exception is for the coals and pick wear interaction which has the greatest influence on the mean normal force.

This interaction coupled with the large pick wear effect indicates that the mean normal force is influenced more by changes in pick wear (bluntness) and between coals rather than by changes in the water jet pressure.

One normally expects the normal force to be sensitive to the size of the pick wear flat and this is corroborated in the statistical analysis.

The results are plotted in Fig.6.1-4. For the sharp pick in the Erin coal there is little difference in mean normal force with jet pressure. From the t-test, there is only a significant difference between the dry cuts and those taken at 105MPa, and this in absolute terms represents 0.27kN and is borderline. The blunt pick in Fig.6.2, shows a greater difference between treatments. In this case all the jet assisted cuts have been significantly reduced compared to the dry cuts.

Within the jet assisted blunt tool cuts there is significant difference between the 70MPa and 105MPa cuts but this difference is only just significant (by 0.03kN). The rise in force value from the 35MPa to the 70MPa value is not statistically significant, Fig.6.2.

The increase in force between the dry sharp pick cuts and the dry blunt pick ones is just significant, Fig.6.1-2. There are no significant differences between corresponding jet assisted cuts within the Erin coal and thus the forces have been reduced to about the same level in both cases of sharp and blunt picks.

Larger differences are experienced in the anthracite coal. The normal force sharp pick, dry cut result, Fig.6.3, is significantly higher than all the related jet assisted ones. There are no significant differences between the jet assisted cuts themselves and indeed the force values are remarkably close, almost constant over the jet pressure range.

The blunt pick results, Fig.6.4, exhibit a relatively large increase in normal force in this coal. All the forces, except those at the 105MPa mark, have increased between 2.9 to 5.6 times

their sharp pick value and represent a significant increase. Significant benefit from jet assistance is only gained at 105MPa pressure with the blunt pick, the 35MPa and 70MPa pressure jets making little impression.

The differences in force values between the two coals are only significant when comparing the blunt pick results. Corresponding sharp pick normal forces between the coals are not significantly different from a statistical viewpoint. This would account for the large interaction term in Table 6.4.

Fig.6.5-8, illustrate the same results plotted against jet power. In terms of jet power and for the Erin coal, most benefit has been attained with the 2.33kW jet for both pick wear states.

The anthracite gives a similar response with the sharp pick, Fig.6.7, but as the pick wears, as it were, more jet power is required to furnish a force decrease, Fig.6.8. A slight increase in mean normal force is indicated in Fig.6.8 by the 2.33kW jet but this is not statistically significant. If one follows the trend of the normal force curve then significant force reduction will be achieved between the power range of 9.33kW to 21kW.

The percentage force reductions against jet pressure and power are given in Fig.6.9-16. For the Erin coal, most advantage has been achieved with the 35MPa, 2.33kW water jet. The 70MPa jet yields a consistently lower value for the sharp and blunt pick but according to the force values this is not statistically significant. The 105MPa, 21kW water jet gives most percentage reduction but at the expense of a nine-fold increase in jet power over the 2.33kW jet. Also, most gain from jet assistance to the mean normal force in the Erin coal is realised when the tool wears, Fig.6.11-12.

Fig.6.13-16, show the anthracite results. The sharp pick graphs have a similar form to the Erin coal - most benefit being obtained by a 2.33kW jet. The blunt pick curves are quite different. Comparable force reduction does not occur until after the 70MPa or 9.33kW points

on the abscissa. Tool wear has a considerable effect on the reduction in mean normal force that may be obtained from jet assistance in the anthracite; the 35MPa and 70MPa water jets prove ineffective. Only the 105MPa pressure jet renders substantial advantage and this is more than with the sharp tool which is consistent with the Erin coal results.

Mean Cutting Force ANOVA

Source of Variation	Sums of Squares	Degrees of Freedom	Mean Square	F-ratio & (Significance Level)
Between Pressures	18.320	3	6.107	47.3 (4.0)
Between Pick Wear	0.040	1	0.040	0.3 (6.9)
Between Coals	8.250	1	9.120	64.0 (6.9)
Interaction between Pressures & Pick Wear	0.790	3	0.263	2.0 (4.0)
Interaction between Pressures & Coals	0.960	3	0.320	2.5 (4.0)
Interaction between Coals & Pick Wear	1.610	1	1.610	12.5 (6.9)
Interaction between Pressures, Coals & Pick Wear	0.570	3	0.190	1.5 (4.0)
Experimental Error	11.460	89	0.129	
Total	42.000	104		

Table 6.3

Experimental Error Variance, $\sigma_0^2 = \pm 0.129$kN. The standard error between mean values = $\sigma_0\sqrt{\frac{2}{6.6}} = 0.20kN$. Therefore, the 95% confidence limits for a two tailed significance test = $\pm 2.20 \times 0.20 = \pm 0.43$kN.

In the case of the mean cutting force, jet assistance has a large influence on the force value. Also, the coal type, as one would expect, has a great effect. Contrary to the normal force,

the pick wear does not have a significant effect on the mean cutting force, however, this is modified by the interaction term between coals and pick wear. The data suggest that within the same coal, pick wear has negligible influence on cutting force. But, when comparing the force levels between the two coals then the tool sharpness is a significant factor.

Fig.6.1-16, give the results for the mean cutting force also. The trends are similar to the mean normal force but clearer. The significant differences in the Erin coal, Fig.6.1-2, are those between dry cutting and the group of jet assisted cuts. There are no significant force differences between the 35MPa, 70MPa and 105MPa pressure assisted cuts with the sharp pick, Fig.6.1. In the blunt pick, Fig.6.2, the 70MPa pressure jet value is significantly higher than that of the 105MPa tests but not the 35MPa cuts. When comparing the force levels between the sharp and blunt tools, the t-tests also indicate that tool bluntness has not made a significant change in mean cutting force in the Erin coal.

The sharp pick in the anthracite shows the same trend as in the Erin coal, Fig.6.3. There is the slight rise in mean cutting force with the 70MPa jet, but statistically it is not significant. As the tool wears the response to jet assistance in the anthracite changes: greater jet pressure is required to procure a force reduction of significance. Fig.6.7-8, suggest that the main influence of the blunt tool is to make the 2.33kW jet ineffective, the other points on the graph have risen but follow the same trend as with the sharp pick. From the t-test, although the mean cutting forces have generally increased with the blunt tool compared to the sharp tool, the only statistically significant increase is that of the 35MPa jet. It seems the 9.33kW and 21kW jets still have enough power to produce a large force decrease. The mean cutting force curve in Fig.6.8, has become linear over the power range with a correlation coefficient of -0.989.

Table 6.3, indicates a significant difference in mean cutting force between the coals. The graphs show that the mean cutting forces for the sharp pick in the Erin coal are significantly greater than the respective anthracite ones, with and without jet assistance. This also generally applies to the blunt pick tests but the force margins are narrower. The author expected larger forces in the anthracite.

An explanation to this phenomenon is given with regard to the lithotypes that comprise the two coals. The anthracite contains a greater proportion of vitrain and clarain than the bituminous coal and conversely the Erin coal consists of more durain than the anthracite.

On a microscopic level vitrain is composed of vitrinite and clarain mainly comprises vitrinite but also a smaller percentage of exinite and inertinite. Durain consists mainly of inertinite with lesser components of vitrinite and exinite.

A characteristic of vitrinite is its brittleness (Leonard, 1979), hence although of a higher rank and harder, the anthracite is more brittle compared to the bituminous Erin coal and tends to fracture and splinter more easily. The bituminous coal is tougher and requires a larger cutting force to induce fracture.

From Fig.6.8-16, one can see that the percentage force decreases are not greatly influenced by tool wear for the mean cutting force in the Erin coal. This contrasts with the mean normal force where the benefit from jet assistance doubles as the pick wears (excepting the 70MPa pressure jet). Thus most gain from jet assistance in the Erin coal is obtained with the normal force as the tool wears.

Considering the force reductions in the anthracite, Fig.6.12-16, illustrate the point that the effectiveness of the 35MPa water jet is severely impaired when the tool wears. The force reductions of the other two jets are not as drastically affected - at least for the cutting force, the mean normal force is reduced even more.

The cutting force curve in Fig.6.16, displays linearity and fits to a straight line with a correlation coefficient of 0.947.

Mean Sideway Force ANOVA

Source of Variation	Sums of Squares	Degrees of Freedom	Mean Square	F-ratio & (Significance Level)
Between Pressures	0.869	3	0.290	14.5 (4.0)
Between Pick Wear	0.057	1	0.290	14.5 (6.9)
Between Coals	0.517	1	0.057	2.9 (6.9)
Interaction between Pressures & Pick Wear	0.383	3	0.517	25.9 (4.0)
Interaction between Pressures & Coals	0.040	3	0.128	0.7 (4.0)
Interaction between Coals & Pick Wear	0.085	1	0.085	4.2 (6.9)
Interaction between Pressures, Coals & Pick Wear	0.197	3	0.066	3.3 (4.0)
Experimental Error	1.740	89	0.020	
Total	3.888	104		

Table 6.4

Experimental Error Variance, $\sigma_0^2 = \pm 0.020$kN. The standard error between mean values = $\sigma_0\sqrt{\frac{2}{6.6}} = 0.08kN$. Therefore, the 95% confidence limits for a two tailed significance test = $\pm 2.20 \times 0.08 = \pm 0.17$kN.

One would expect the mean sideway force to tend close to zero over the length of a cut. However, since the present study was undertaken in the relieved cutting mode, a small

residual sideway force was measured acting towards the relieved side of the cut. This force has been significantly affected by jet assistance and by differences between the pick wear states.

The interaction between jet pressure and pick wear indicates an effect on sideway force due to pick wear as the jet pressure is changed. The other interaction effects have no bearing on the results.

The t-tests elaborate on the significant factors indicated in Table 6.4. Apparently, the sharp pick cuts in both coals yield no significant force differences, although the mean sideway forces in the Erin coal are generally higher than in the anthracite, Fig.6.1-3. Thus the significant pressure term is derived from the effects with the blunt tools and the results show that in both coals, the dry unassisted cuts are significantly higher than all the related jet assisted tests. As with the other force components, with the blunt tools, the significance lies between the unassisted and all the jet assisted cuts. There are no significant effects between the jet assisted cuts themselves.

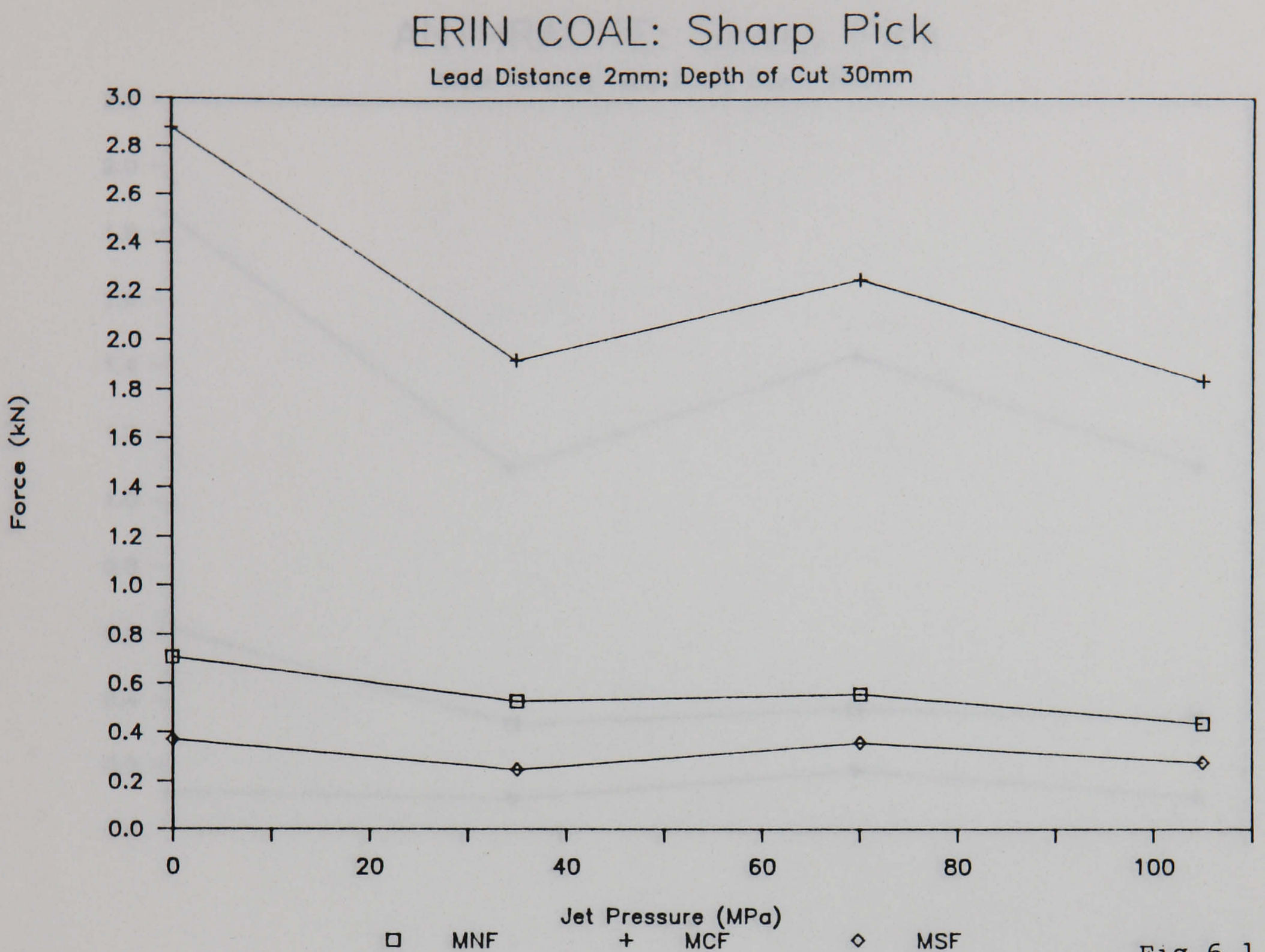

ERIN COAL: Sharp Pick
Lead Distance 2mm; Depth of Cut 30mm
Force (kN)
3.0
2.8
2.6
2.4
2.2
2.0
1.8
1.6
1.4
1.2
1.0
0.8
0.6
0.4
0.2
0.0
0
20
40
60
80
100
Jet Pressure (MPa)
MNF
MCF
MSF

Fig.6.1

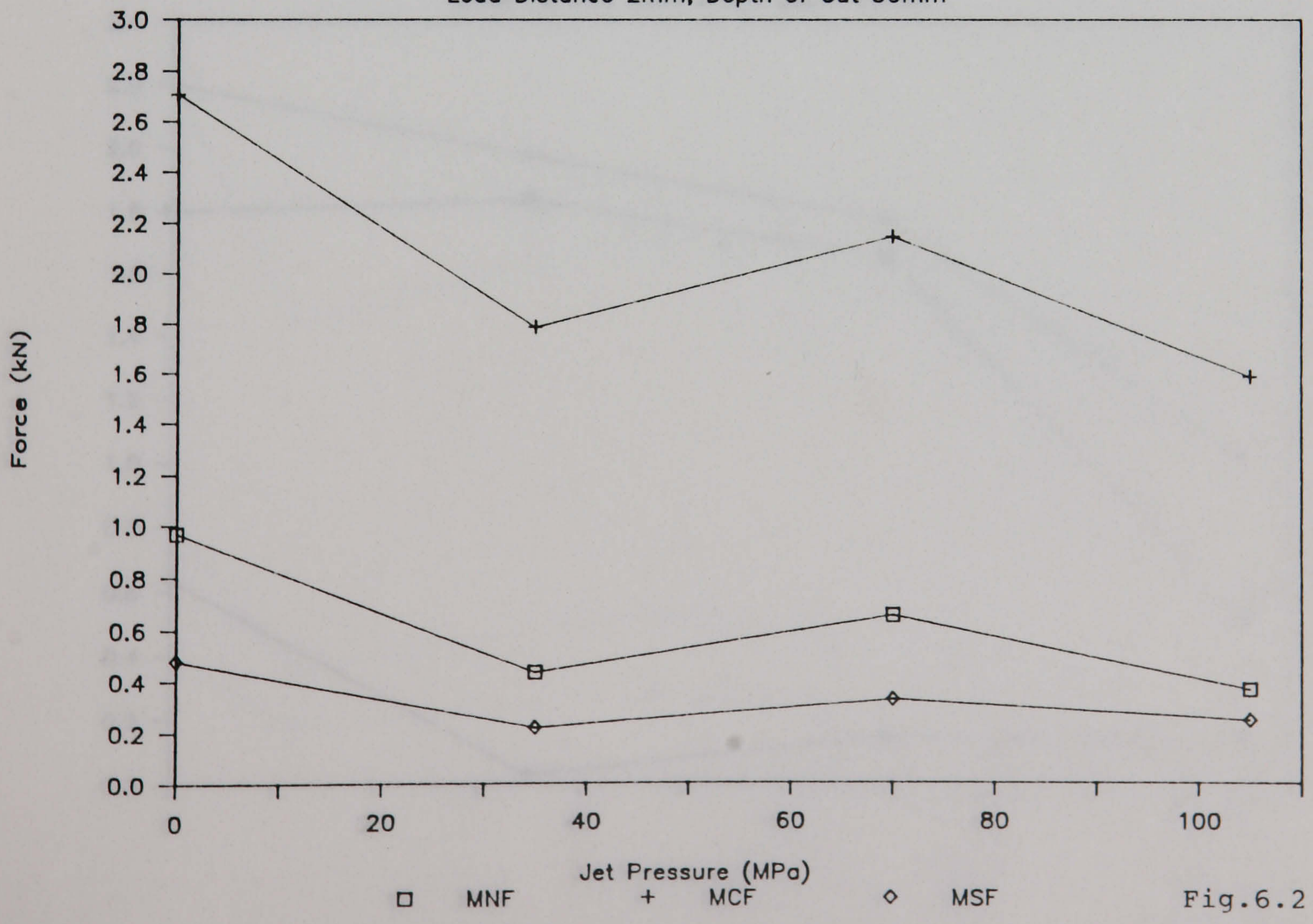

ERIN COAL: Blunt Pick
Lead Distance 2mm; Depth of Cut 30mm
Force (kN)
3.0
2.8
2.6
2.4
2.2
2.0
1.8
1.6
1.4
1.2
1.0
0.8
0.6
0.4
0.2
0.0
0
20
40
60
80
100
Jet Pressure (MPa)
MNF
MCF
MSF

Fig.6.2

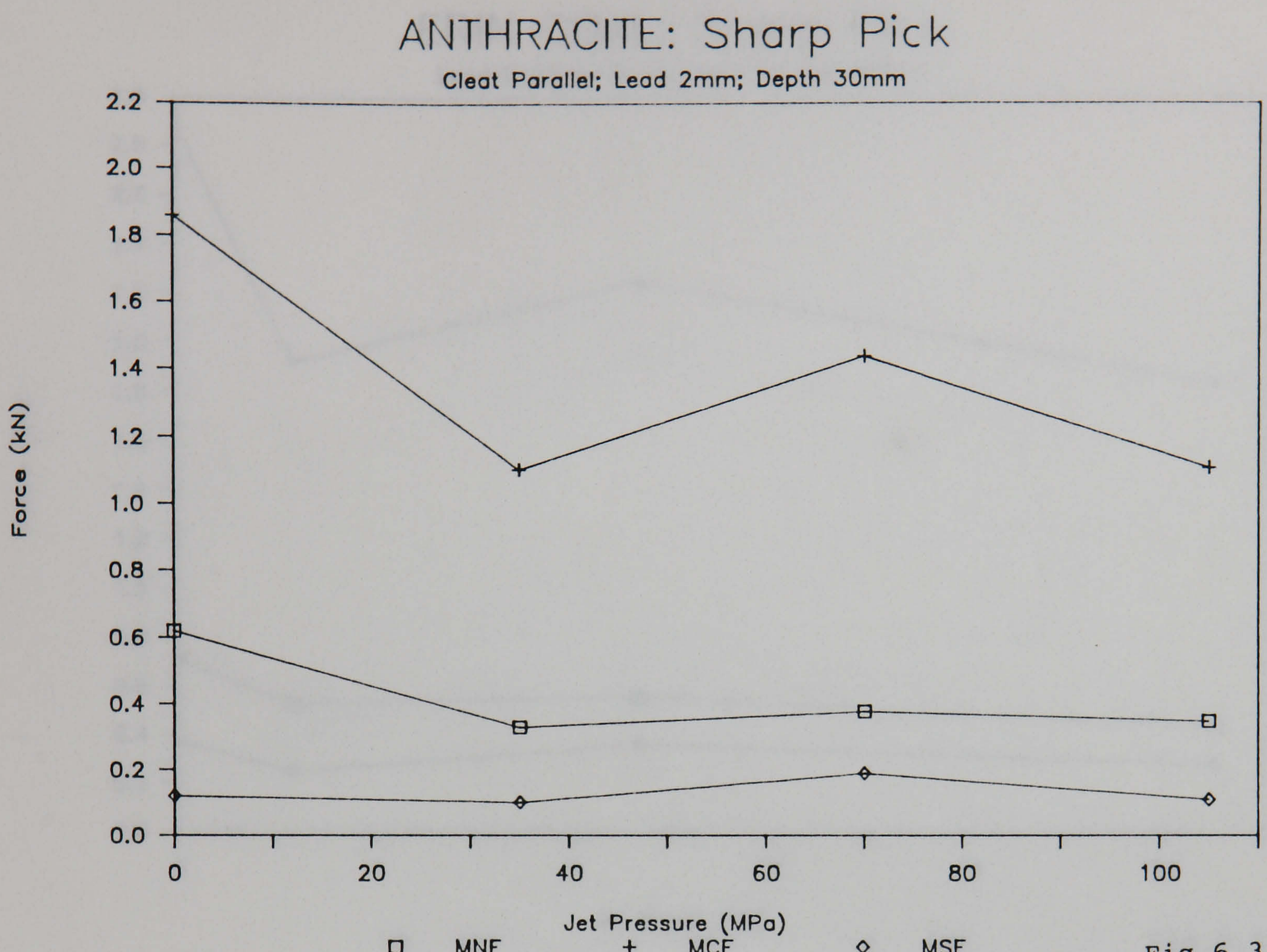

ANTHRACITE: Sharp Pick
Cleat Parallel; Lead 2mm; Depth 30mm
Force (kN)
2.2
2.0
1.8
1.6
1.4
1.2
1.0
0.8
0.6
0.4
0.2
0.0
0
20
40
60
80
100
Jet Pressure (MPa)
MNF
MCF
MSF

Fig.6.3

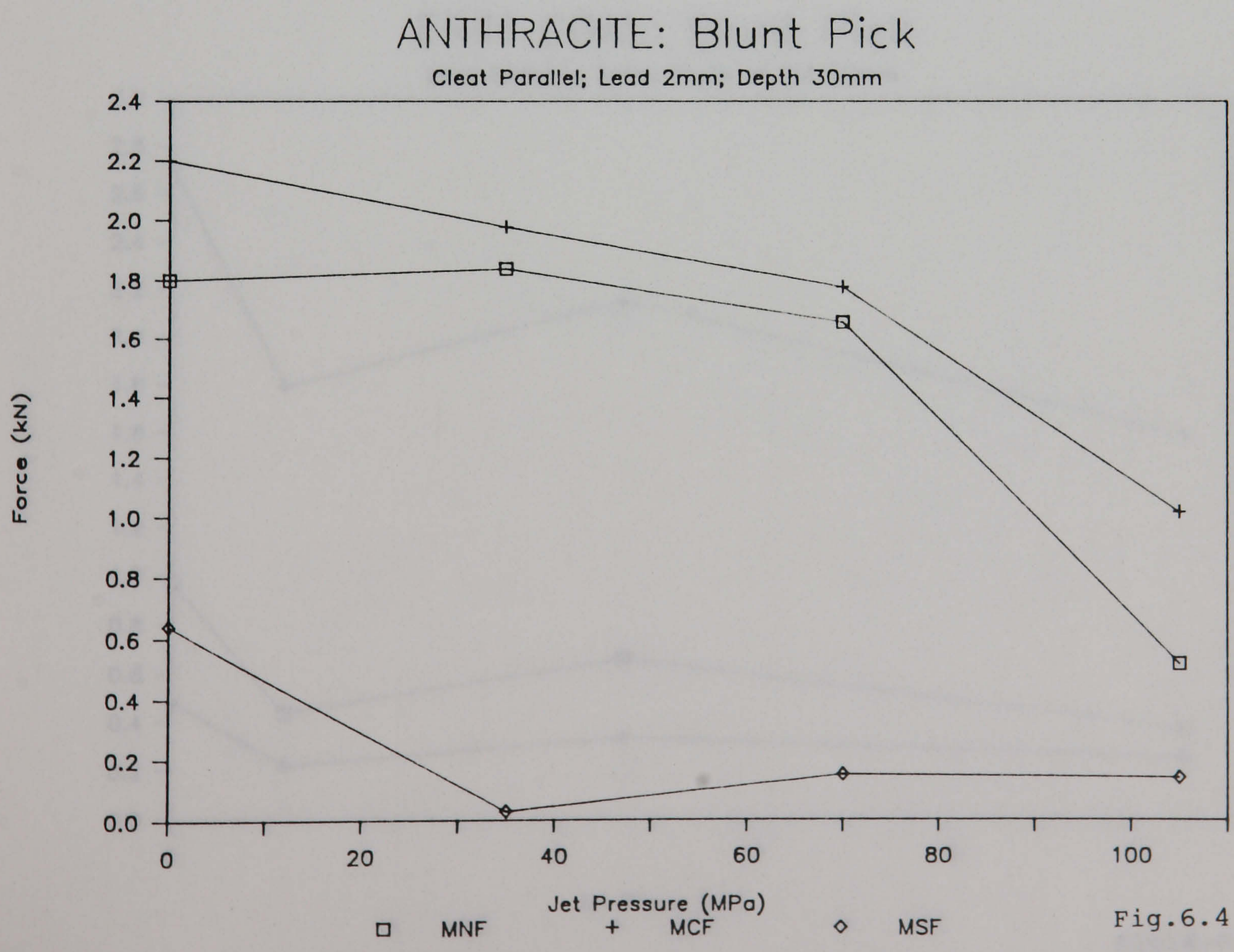

ANTHRACITE: Blunt Pick
Cleat Parallel; Lead 2mm; Depth 30mm
Force (kN)
2.4
2.2
2.0
1.8
1.6
1.4
1.2
1.0
0.8
0.6
0.4
0.2
0.0
0
20
40
60
80
100
Jet Pressure (MPa)
MNF
MCF
MSF

Fig.6.4

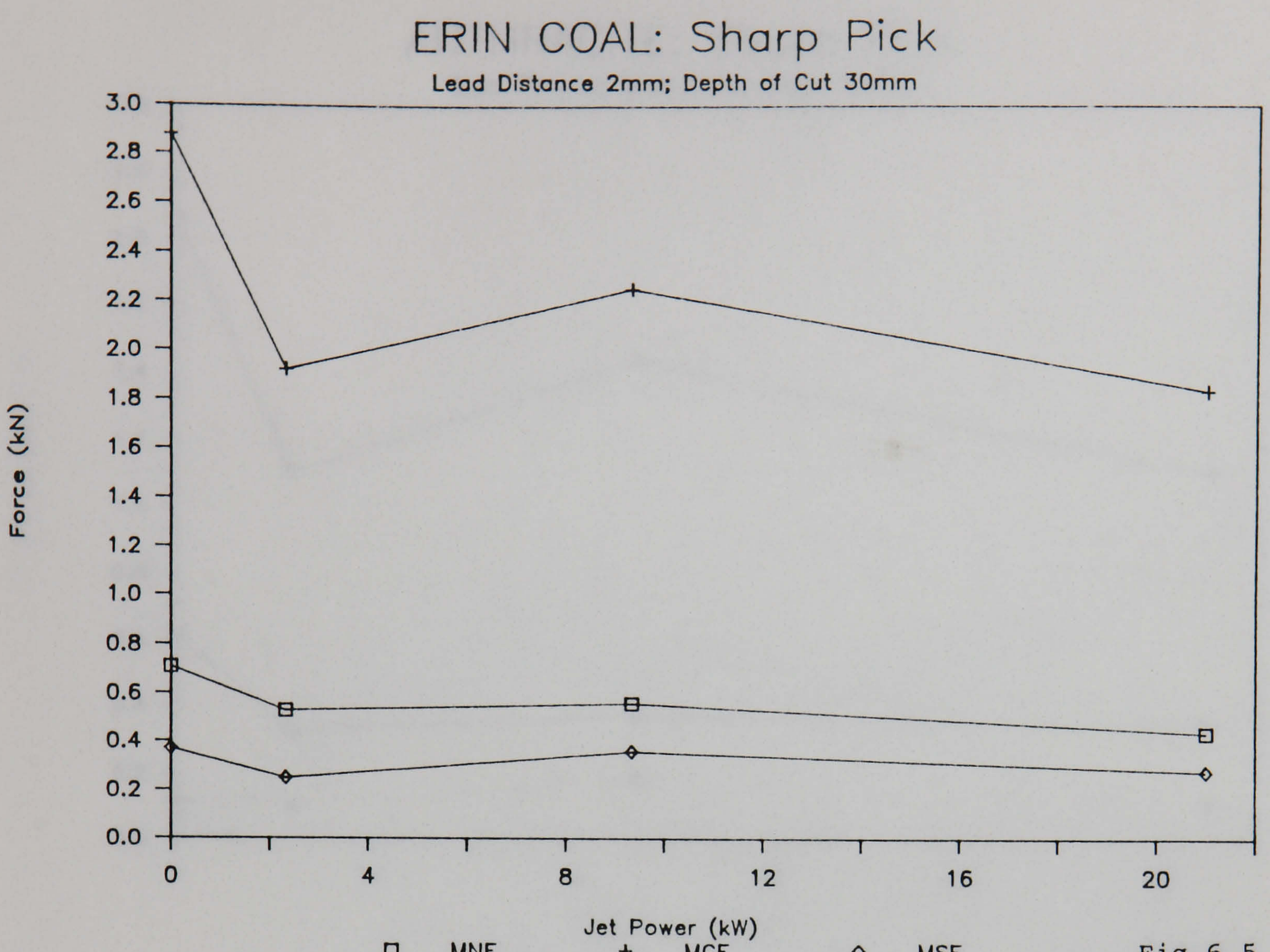

ERIN COAL: Sharp Pick
Lead Distance 2mm; Depth of Cut 30mm
Force (kN)
3.0
2.8
2.6
2.4
2.2
2.0
1.8
1.6
1.4
1.2
1.0
0.8
0.6
0.4
0.2
0.0
0
4
8
12
16
20
Jet Power (kW)
MNF
MCF
MSF

Fig.6.5

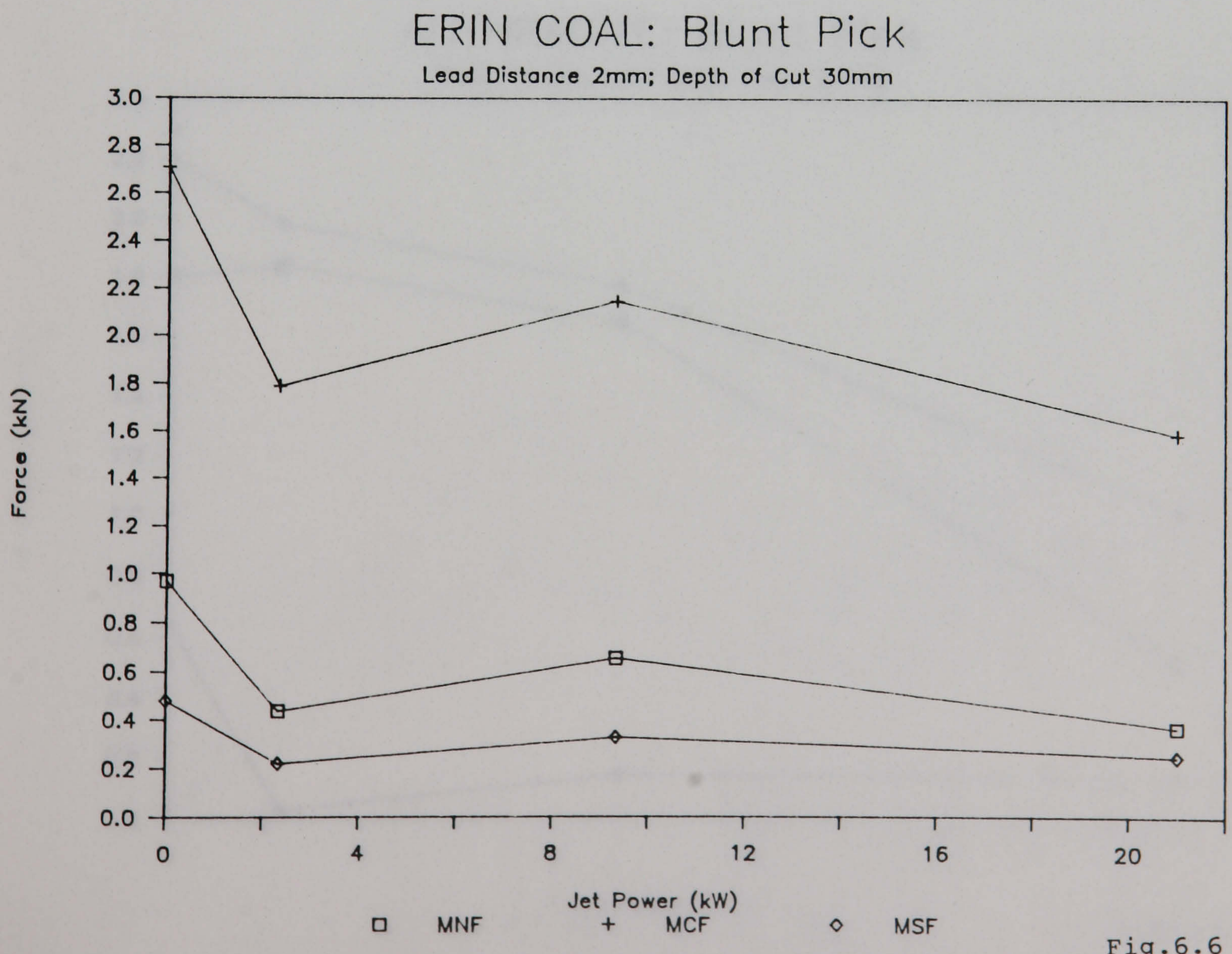

ERIN COAL: Blunt Pick
Lead Distance 2mm; Depth of Cut 30mm
Force (kN)
3.0
2.8
2.6
2.4
2.2
2.0
1.8
1.6
1.4
1.2
1.0
0.8
0.6
0.4
0.2
0.0
0
4
8
12
16
20
Jet Power (kW)
MNF
MCF
MSF

Fig.6.6

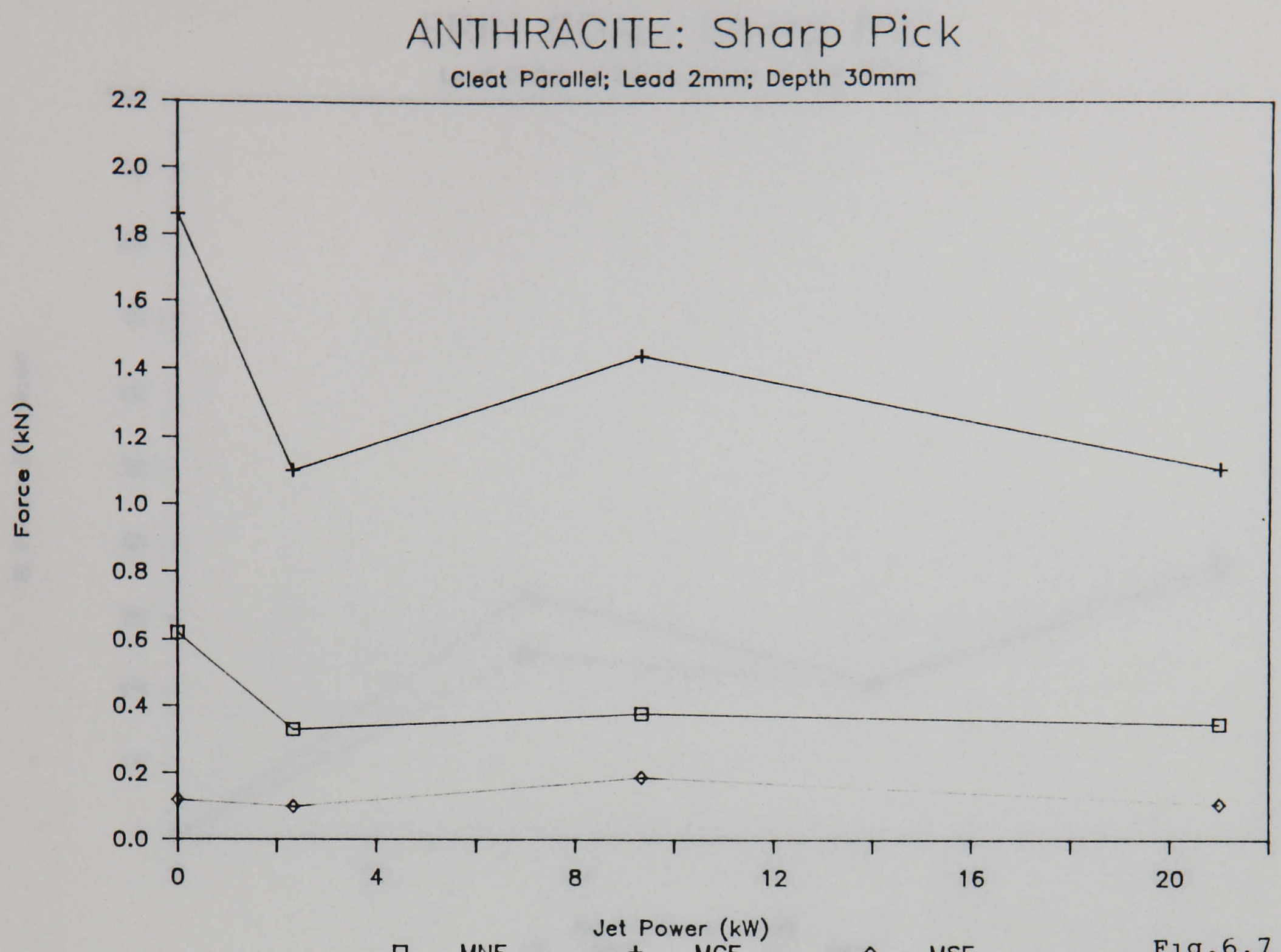

ANTHRACITE: Sharp Pick
Cleat Parallel; Lead 2mm; Depth 30mm
Force (kN)
2.2
2.0
1.8
1.6
1.4
1.2
1.0
0.8
0.6
0.4
0.2
0.0
0
4
8
12
16
20
Jet Power (kW)
MNF
MCF
MSF

Fig.6.7

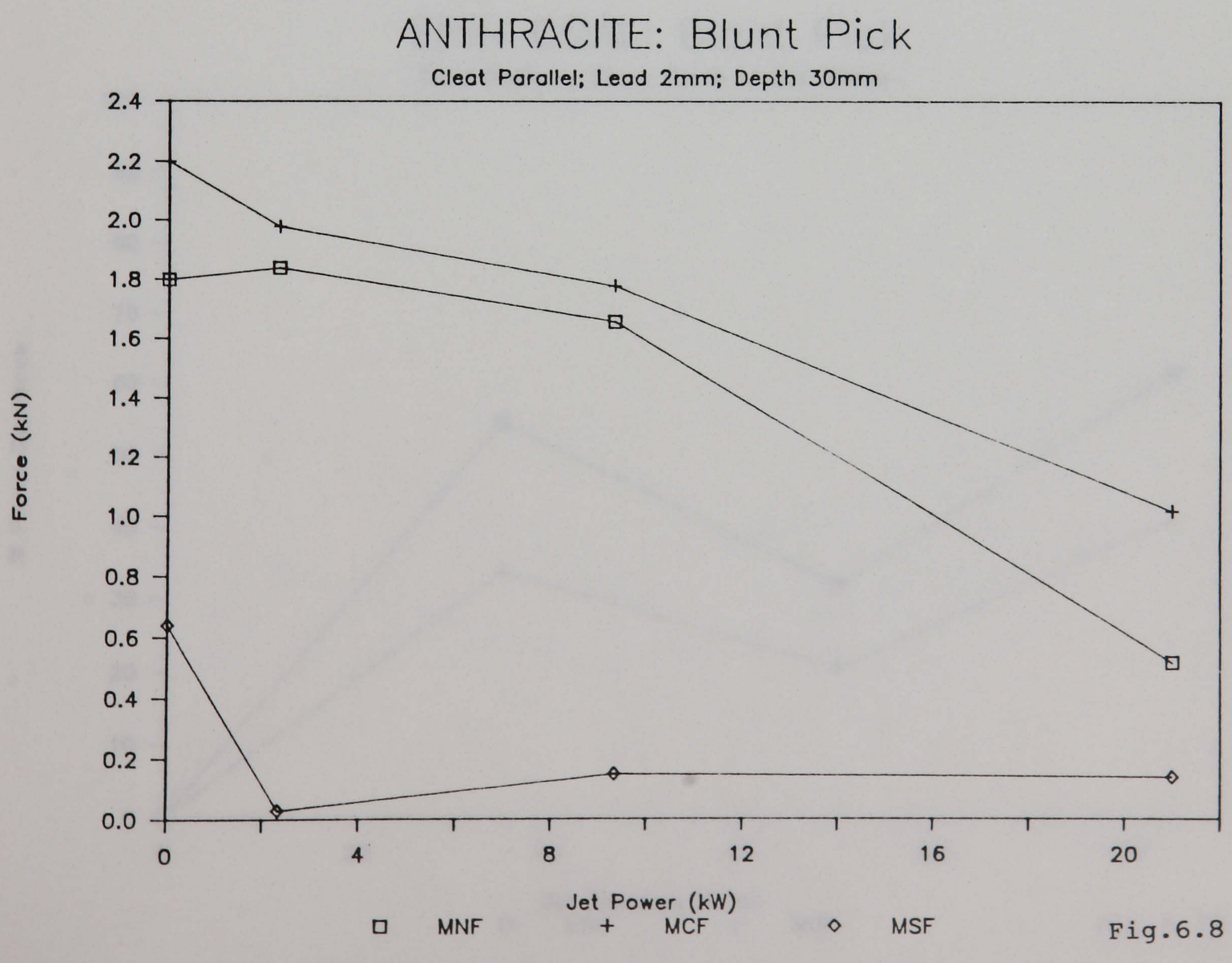

ANTHRACITE: Blunt Pick
Cleat Parallel; Lead 2mm; Depth 30mm
Force (kN)
2.4
2.2
2.0
1.8
1.6
1.4
1.2
1.0
0.8
0.6
0.4
0.2
0.0
0
4
8
12
16
20
Jet Power (kW)
MNF
MCF
MSF

Fig.6.8

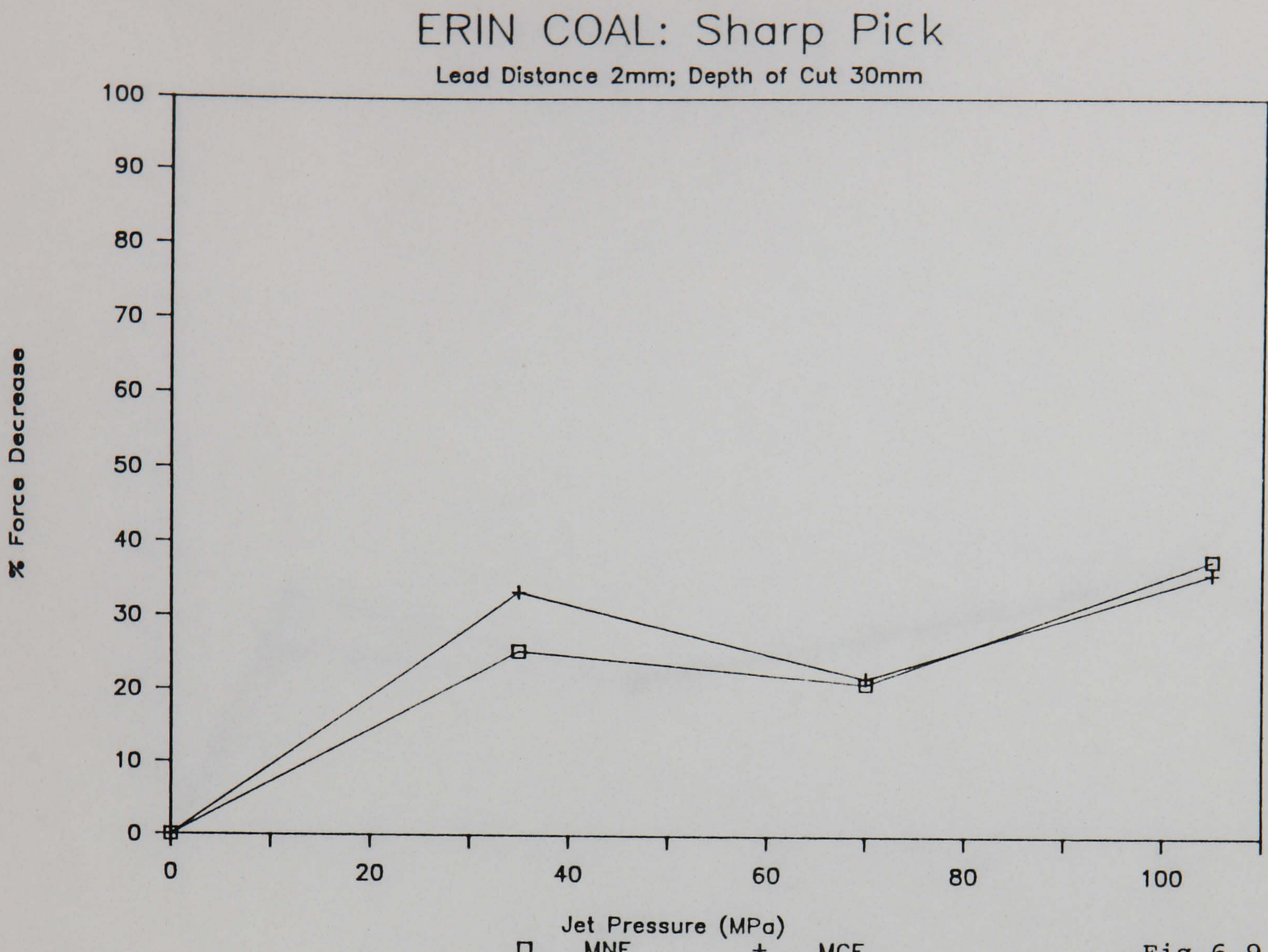


Fig.6.9

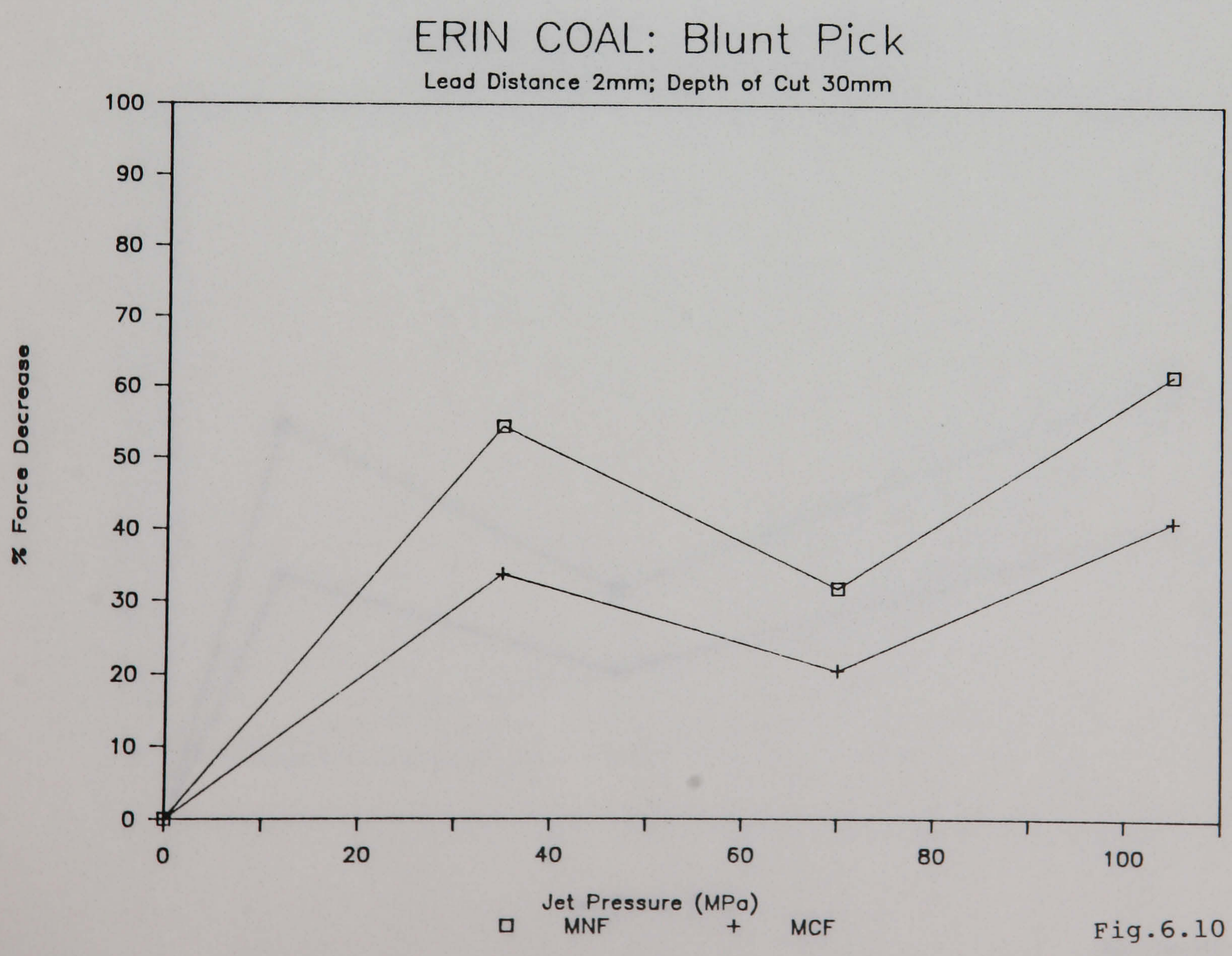


Fig.6.10

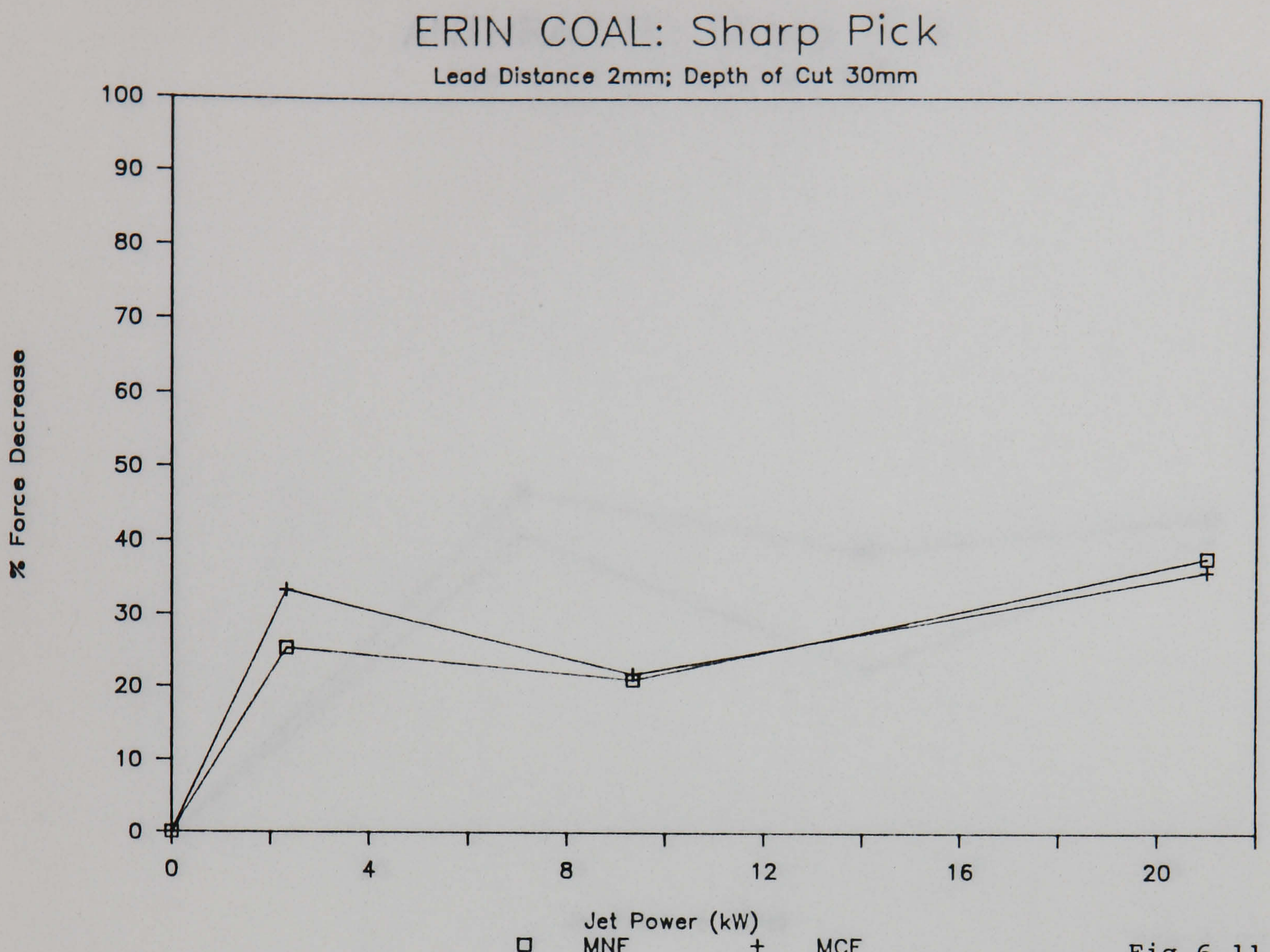


Fig.6.11

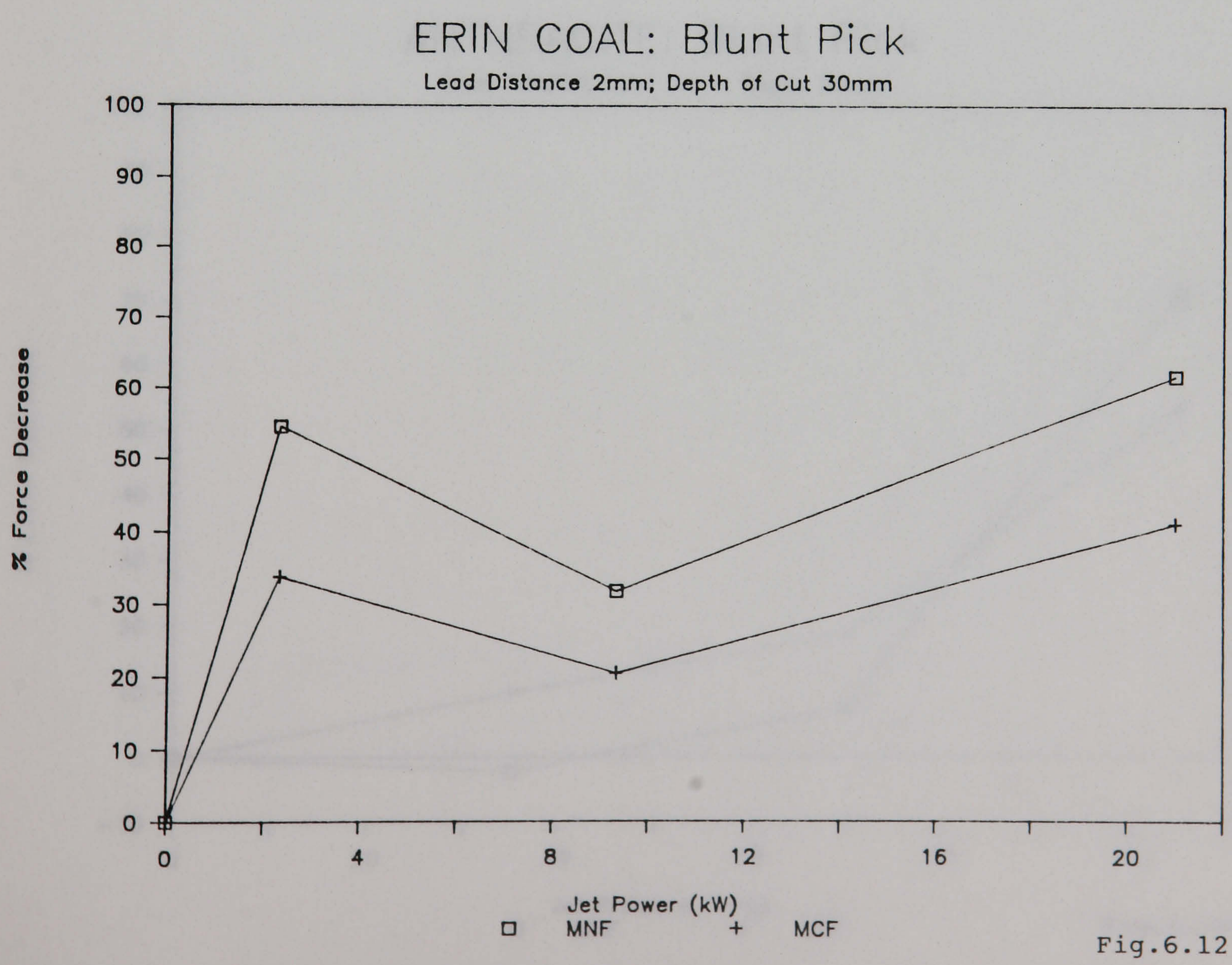


Fig.6.12

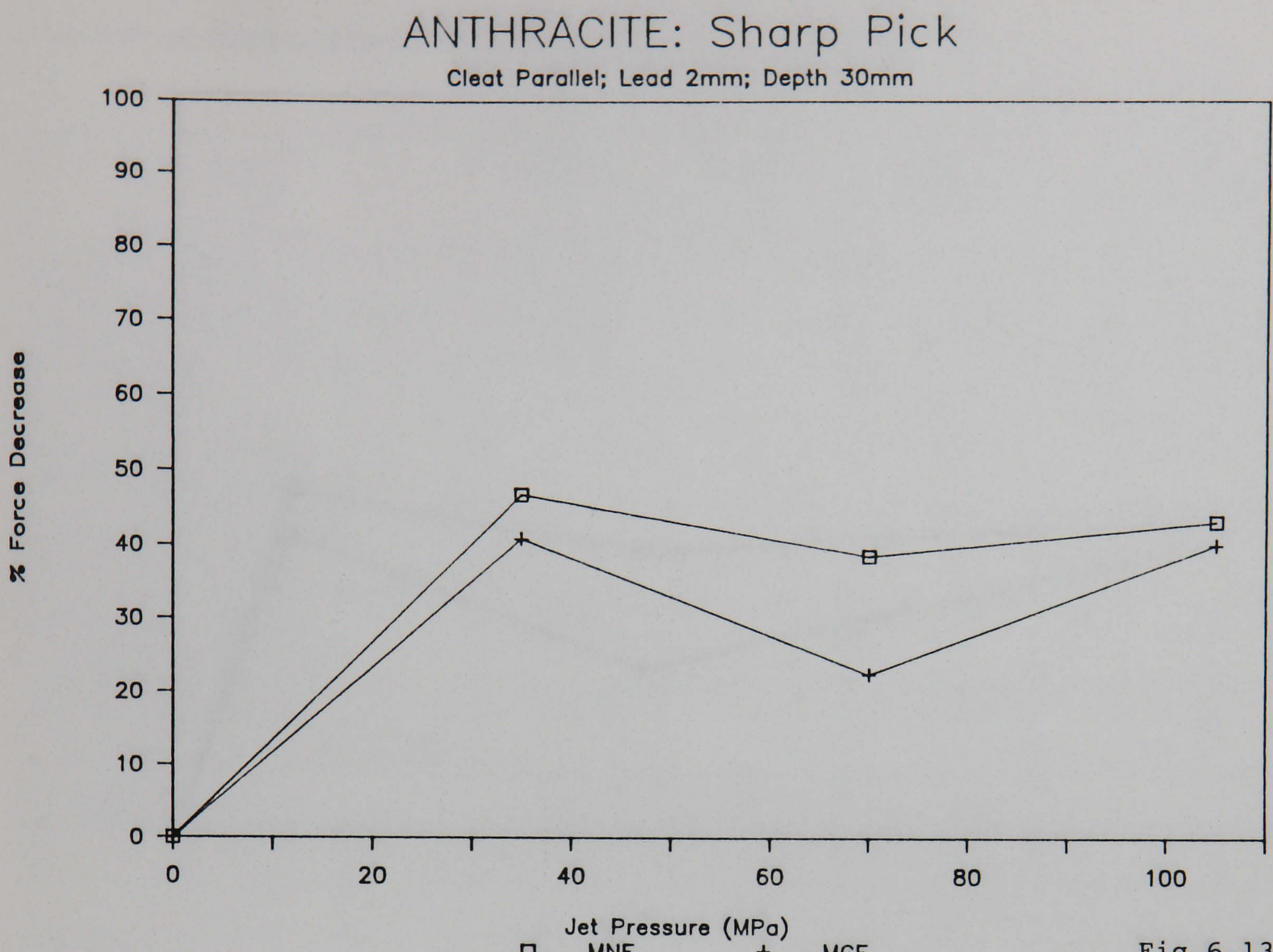


Fig.6.13

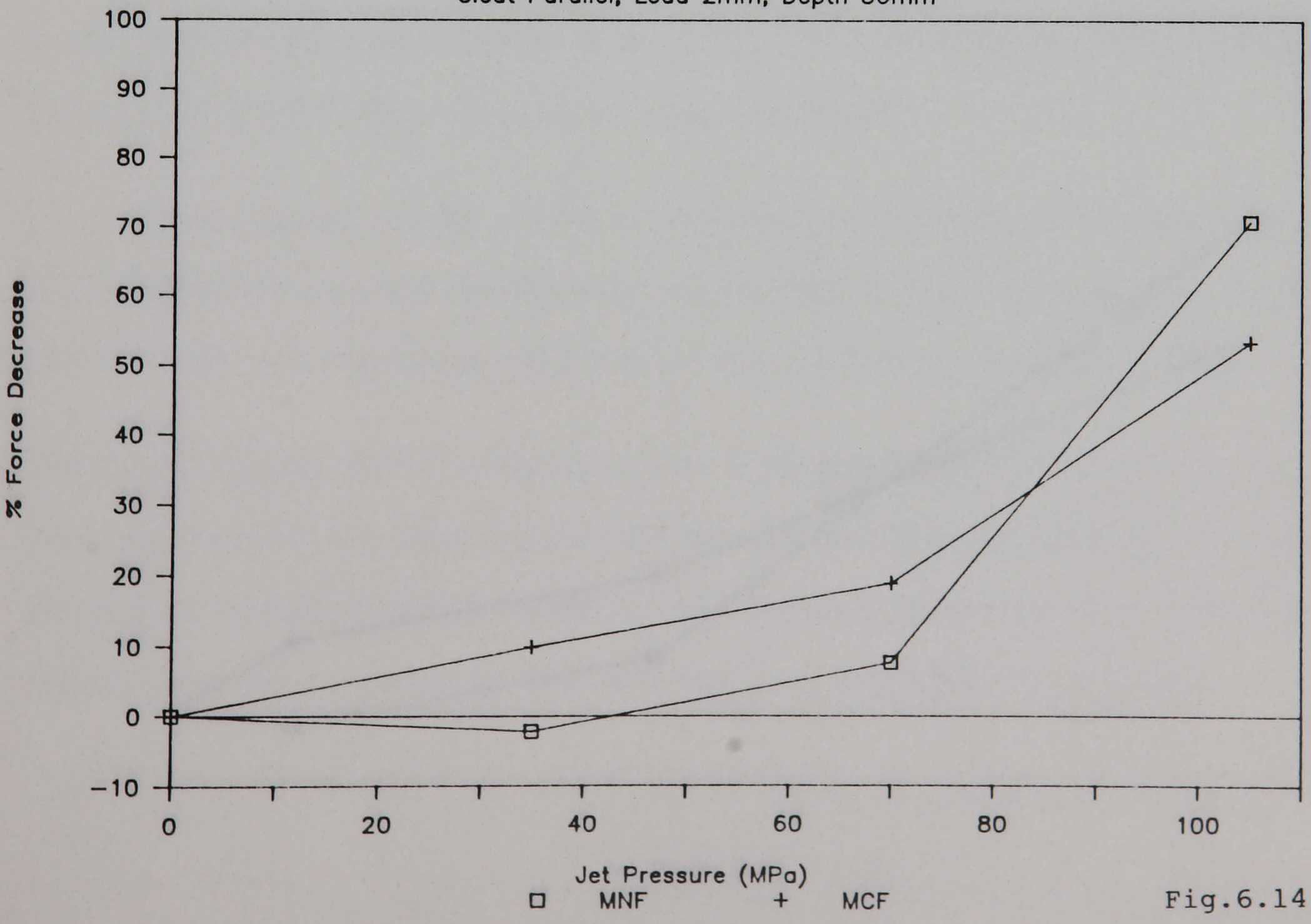


Fig.6.14

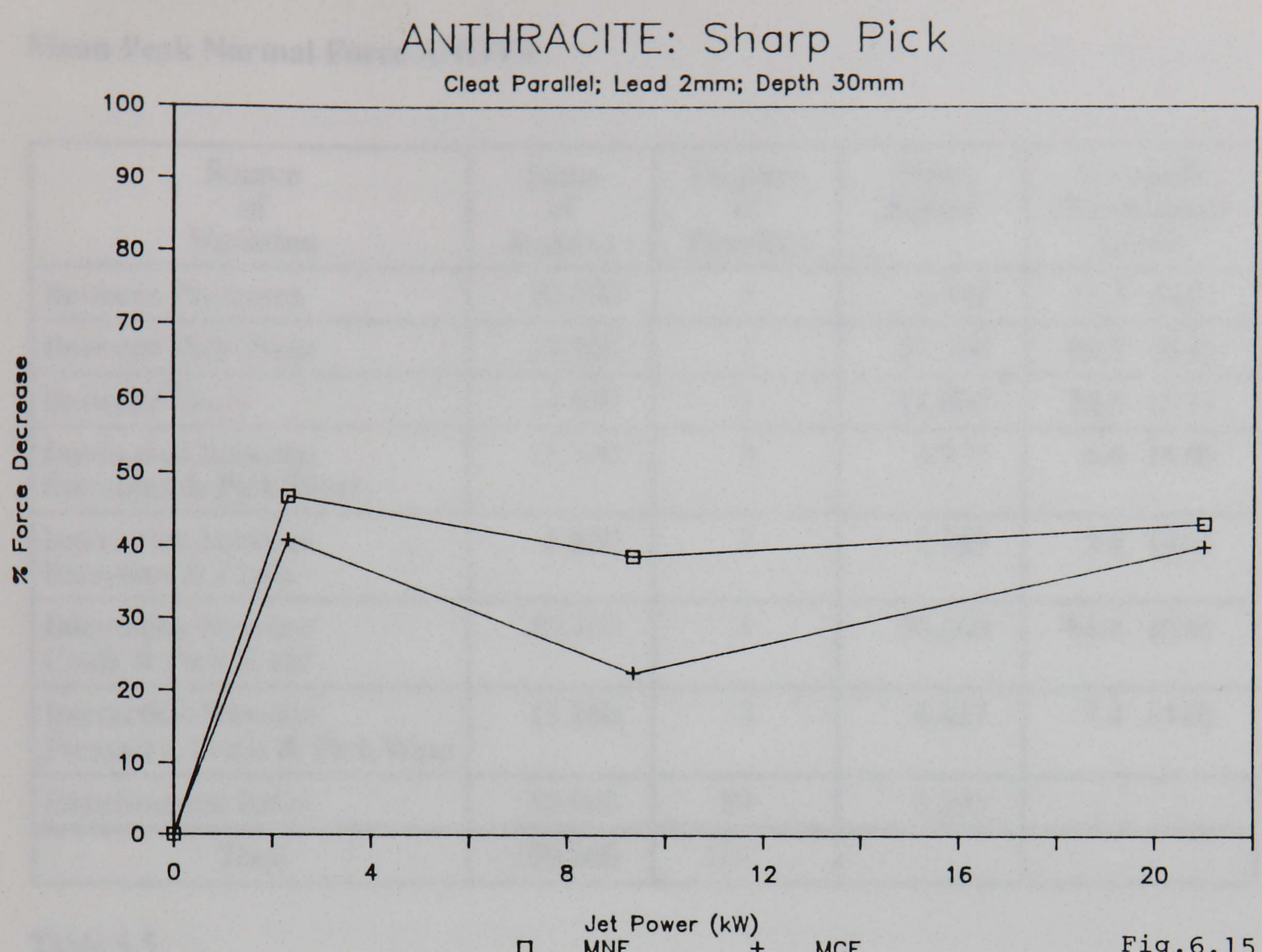


Fig.6.15

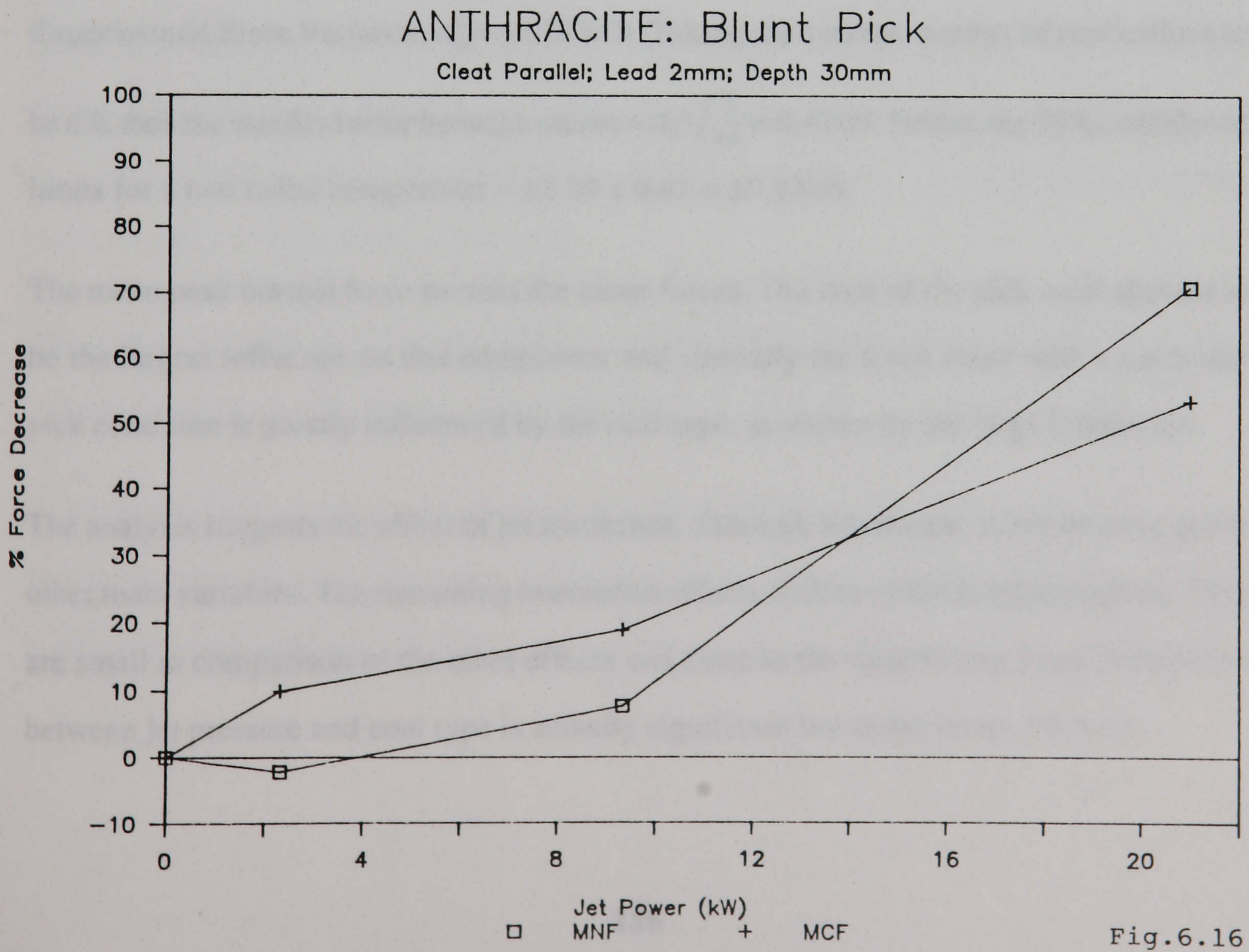


Fig.6.16

Mean Peak Normal Force ANOVA

Source of Variation	Sums of Squares	Degrees of Freedom	Mean Square	F-ratio & (Significance Level)
Between Pressures	20.500	3	6.833	11.5 (4.0)
Between Pick Wear	59.300	1	59.300	99.7 (6.9)
Between Coals	14.000	1	14.000	23.5 (6.9)
Interaction between Pressures & Pick Wear	11.800	3	3.933	6.6 (4.0)
Interaction between Pressures & Coals	6.800	3	2.267	3.8 (4.0)
Interaction between Coals & Pick Wear	50.360	1	50.360	84.6 (6.9)
Interaction between Pressures, Coals & Pick Wear	13.280	3	4.427	7.4 (4.0)
Experimental Error	52.960	89	0.595	
Total	229.000	104		

Table 6.5

Experimental Error Variance, $\sigma_0^2 = \pm 0.595$kN. Taking the average number of replications to be 6.6, then the standard error between means $= \sigma_0 \sqrt{\frac{2}{6.6}} = 0.42kN$. Hence, the 95% confidence limits for a two tailed comparison = ±2.20 x 0.42 = ±0.84kN.

The mean peak normal force mirrors the mean forces. The state of the pick wear appears to be the largest influence on this component and similarly the force value with a particular pick condition is greatly influenced by the coal type, as shown by the large interaction.

The analysis suggests the effect of jet assistance, although significant, is not as great as the other main variables. The remaining interaction effects shall be considered negligible. They are small in comparison to the other effects and close to the significance level. Interaction between jet pressure and coal type is actually significant but at the lower 5% level.

The mean peak forces are represented in Fig.6.17-32. A similar trend to that of the mean forces is indicated from the graphs. For the sharp pick in the Erin coal, Fig.6.17, only the 105MPa jet assisted cuts have been significantly reduced. In the blunt case, Fig.6.18, both the 35MPa and 105MPa treatments have produced a significant force reduction but the 70MPa pressure jet assisted tests did not. The blunt tool forces are 25% higher when unassisted and 20% higher when jet assisted, compared to the sharp tool results.

With the anthracite sharp pick cuts there are no significant differences in force value in the mean peak normal force, Fig.6.19. The sharp pick forces are uniformly lower than the corresponding ones in the Erin coal, but only the dry cut value is significantly lower. However, the 35MPa and 70MPa pressure jet cuts are borderline.

Fig.6.19-20 and Fig.6.23-24, show that the mean peak normal force has increased markedly with the blunt tool, illustrating the effect of the wear flat in the anthracite. The blunt pick, dry cut force is 3.7 times greater than the corresponding sharp pick force. The jet assisted forces have increased by 4.7, 4.1 and 1.4 times for the 35MPa, 70MPa and 105MPa pressure jet assisted cuts respectively. Although the force values with jet assistance at 35MPa and 70MPa, have increased more than the unassisted forces, their absolute values are close to the unassisted force values, indicating that for practical purposes, in terms of force reduction, these two jets are contributing very little.

Generally, the mean peak normal force experiences less force reduction compared to the mean normal force in both coals, Fig.6.25-32.

In the Erin coal the increased force reduction due to tool wear is small compared to that of the mean normal force. Mean peak normal force reductions with the blunt pick are only 6.5%, 1.9% and 8.8% greater than those for the sharp pick, for the three pressures used.

Reductions for the sharp pick in the anthracite are indicated in Fig.6.27,31, and are about half those of the mean normal force. With the blunt tool though a close match to the mean force is indicated.

Mean Peak Cutting Force ANOVA

Source of Variation	Sums of Squares	Degrees of Freedom	Mean Square	F-ratio & (Significance Level)
Between Pressures	85.400	3	28.467	27.0 (4.00)
Between Pick Wear	0.900	1	0.900	0.9 (6.93)
Between Coals	62.400	1	62.400	59.2 (6.93)
Interaction between Pressures & Pick Wear	3.700	3	1.233	1.2 (4.00)
Interaction between Pressures & Coals	9.080	3	3.027	2.9 (4.00)
Interaction between Coals & Pick Wear	3.330	1	3.330	3.2 (6.93)
Interaction between Pressures, Coals & Pick Wear	0.090	3	0.030	0.0 (4.00)
Experimental Error	93.800	89	1.054	
Total	258.700	104		

Table 6.6

Experimental Error Variance, $\sigma_0^2 = \pm 1.054$kN. The standard error between mean values = $\sigma_0\sqrt{\frac{2}{6.6}} = 0.57kN$. Thus, the 95% confidence limits for a two tailed significance test = ±2.20 x 0.57 = ±1.24kN.

Peak cutting force values are sensitive to changes in jet pressure and coal type. Differences due to pick wear condition are not significant within the same coal.

There is only one significant interaction term, that between jet pressure and coal type, and this is only significant (just) at the 5% level. Basically, all the interactions are very small and shall be ignored.

Mean peak cutting forces follow a similar pattern to the mean cutting force. Again tool wear has little effect on these forces in the Erin coal, Fig.6.17-18. The jet assisted cuts are all significantly reduced from the unassisted tests except in the case of the sharp pick at 70MPa jet pressure, but this is close to being significant.

Fig.6.19-20, illustrate the anthracite results. With the sharp pick, force reductions are achieved at all three jet pressures. A small increase in mean peak cutting force is experienced with the blunt tool over the sharp pick but this is not statistically significant. Hence, the blunt tool has had little effect on the mean peak cutting force - the largest single effect has been on the cuts taken with the 35MPa jet.

As with the mean cutting forces, the mean peaks in the Erin coal are generally higher than those in the anthracite. The unassisted dry cut forces in the Erin are significantly larger than those in the anthracite for both sharp and blunt picks. The jet assisted sharp pick force values in the Erin coal are also significantly higher than the corresponding anthracite cuts but this significance disappears and reduces with the blunt tools.

Fig.6.25-32, give the plots for the percentage force reductions. For both coals with both tool wear conditions the mean peak cutting force reductions are uniformly less than those gained for the mean cutting force. Between the two coals, the Erin coal has benefited more in terms of force reduction than the anthracite.

Greater mean peak cutting force reductions have been achieved with the blunt pick than with the sharp pick in the Erin and anthracite coals, except at the lowest pressure.

Mean Peak Sideway Force ANOVA

Source of Variation	Sums of Squares	Degrees of Freedom	Mean Square	F-ratio & (Significance Level)
Between Pressures	4.430	3	1.477	7.8 (4.0)
Between Pick Wear	0.170	1	0.170	0.9 (6.9)
Between Coals	19.720	1	19.720	102.2 (6.9)
Interaction between Pressures & Pick Wear	2.510	3	0.837	4.4 (4.0)
Interaction between Pressures & Coals	4.460	3	1.487	7.8 (4.0)
Interaction between Coals & Pick Wear	0.830	1	0.830	4.4 (6.9)
Interaction between Pressures, Coals & Pick Wear	1.210	3	0.403	2.1 (4.0)
Experimental Error	16.950	89	0.190	
Total	50.280	104		

Table 6.7

Experimental Error Variance, $\sigma_0^2 = \pm 0.190$kN. The standard error between the means = $\sigma_0\sqrt{\frac{2}{6.6}} = 0.190kN$. Therefore, the 95% confidence limits for a two tailed significance test = $\pm 2.20 \times 0.19 = \pm 0.17$kN.

The only relevant effect in this case is that due to the difference in coal properties. Other terms are significant but only by a small margin and consequently shall be regarded as negligible. The characteristics of the mean peak sideway forces are very similar to the mean forces. The forces are higher in the Erin coal and most gain may be obtained by the 35MPa, 2.33kW water jet, even with the blunt tool in the anthracite.

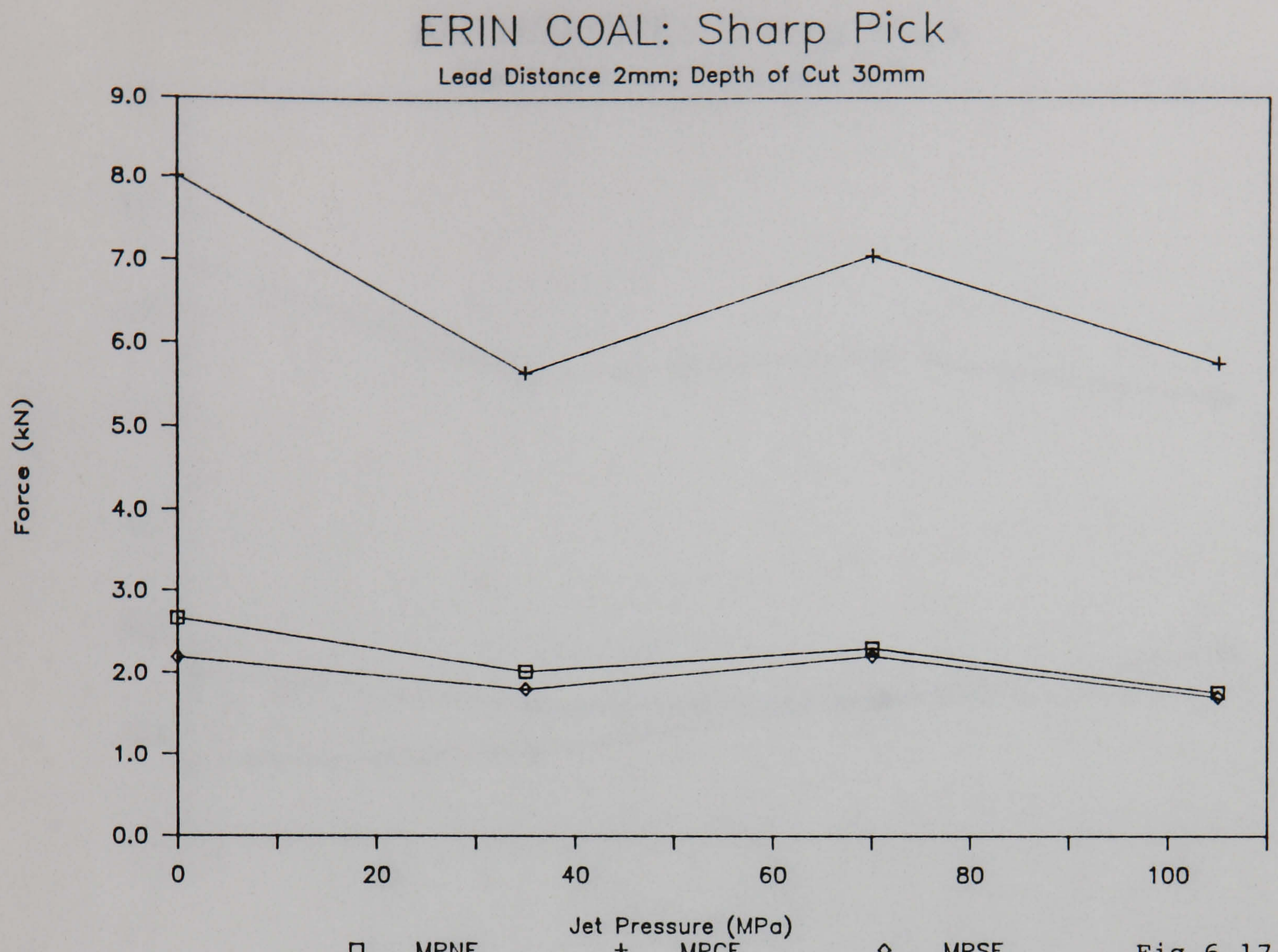


Fig.6.17

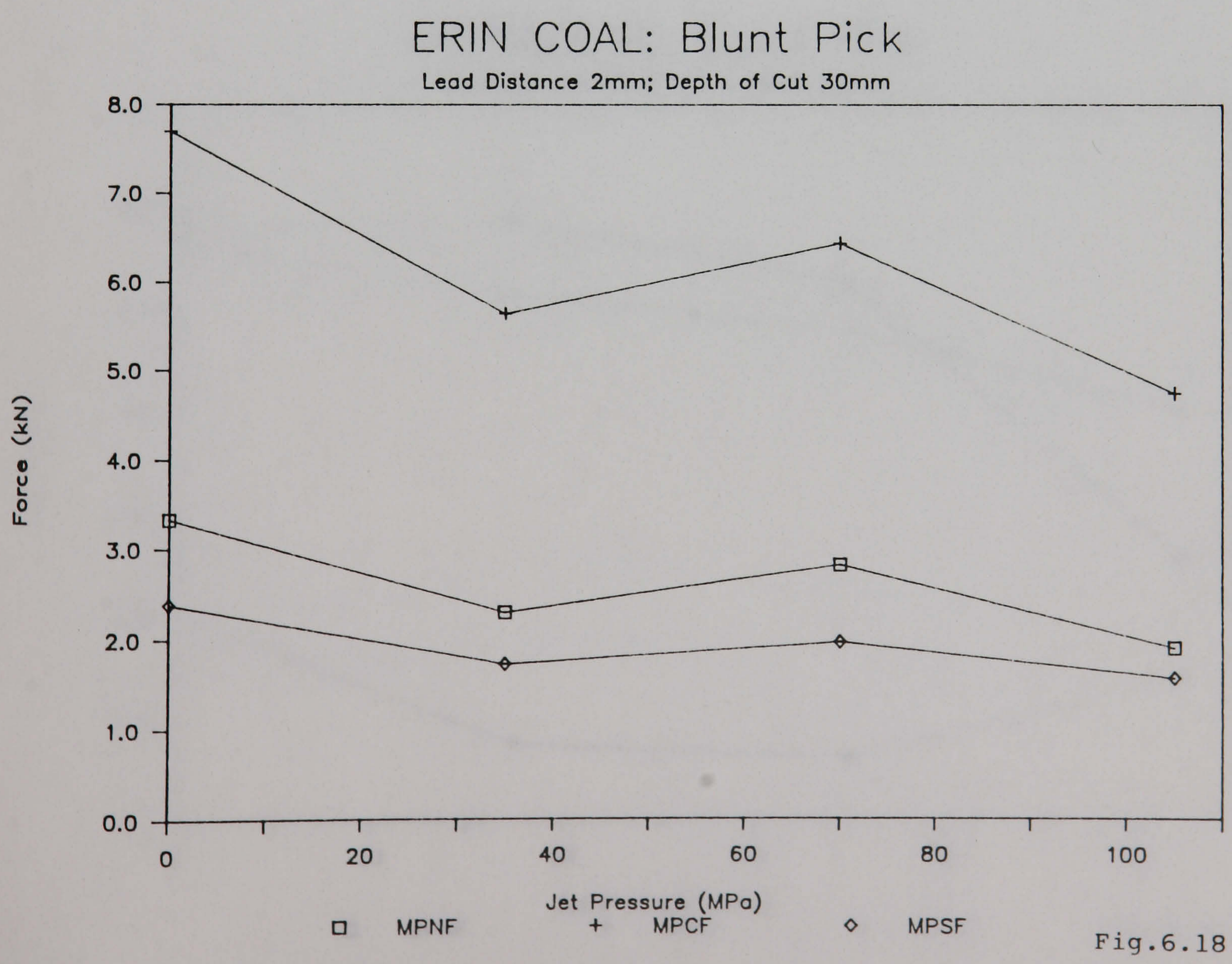


Fig.6.18

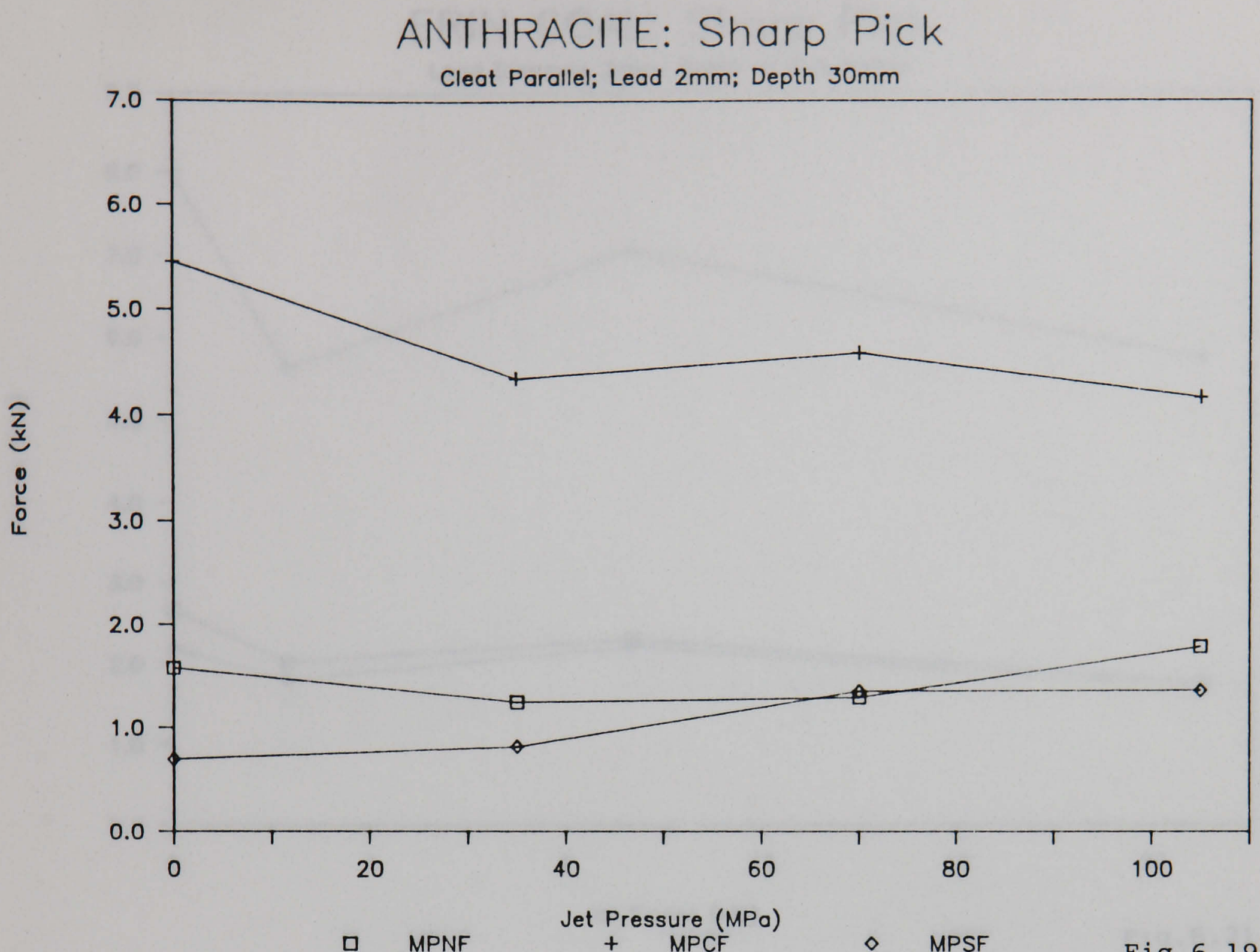


Fig.6.19

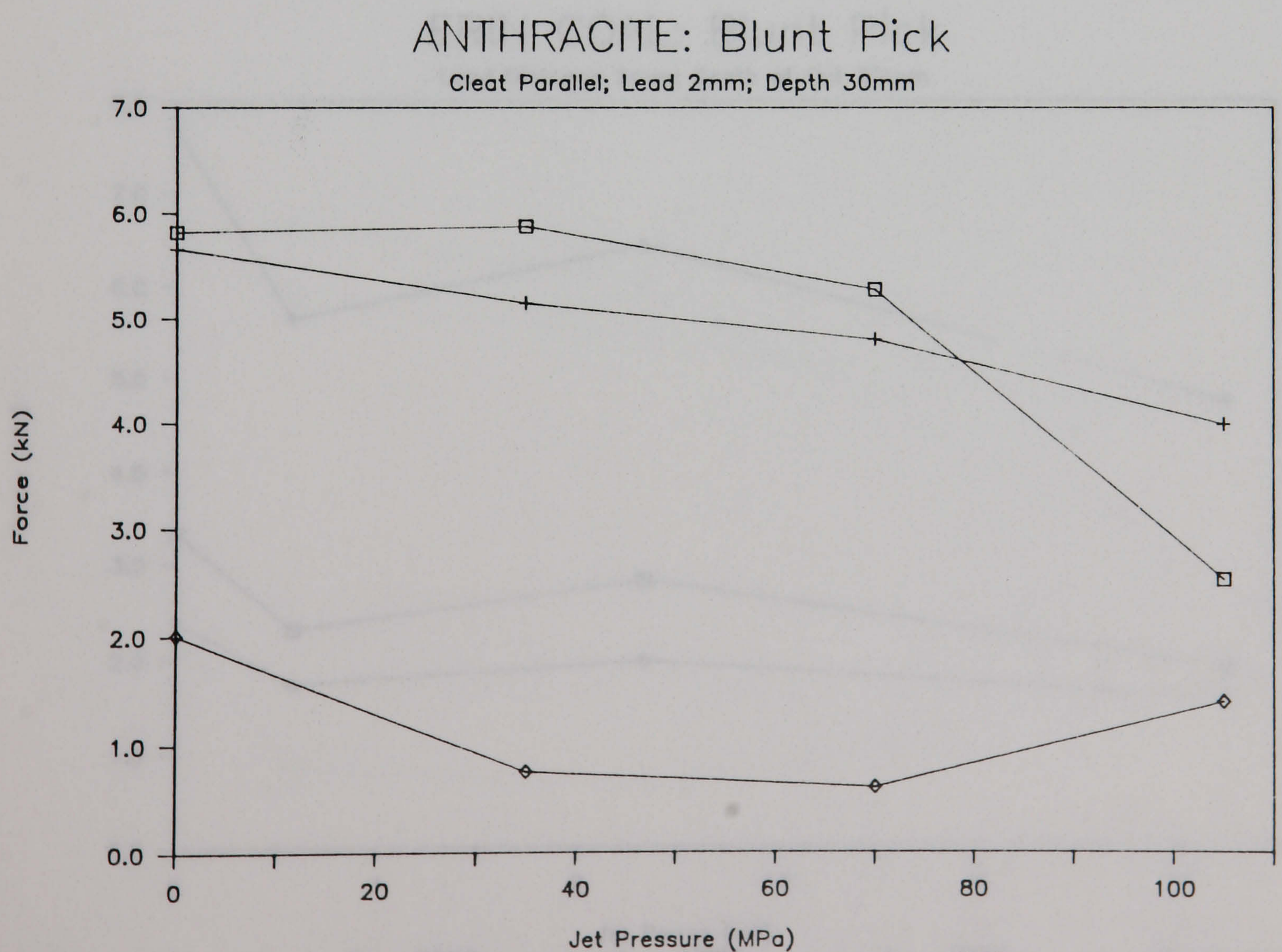


Fig.6.20

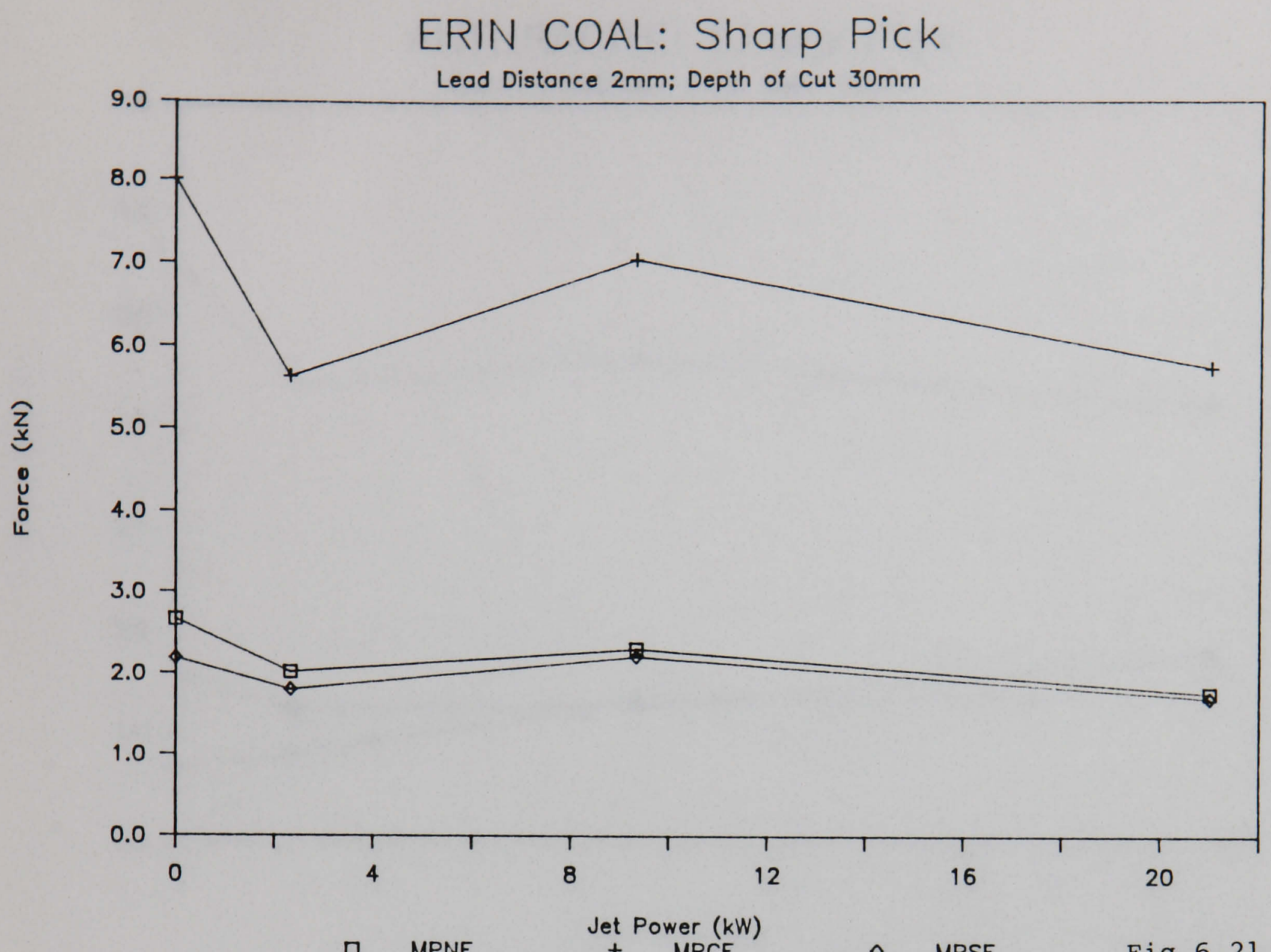


Fig.6.21

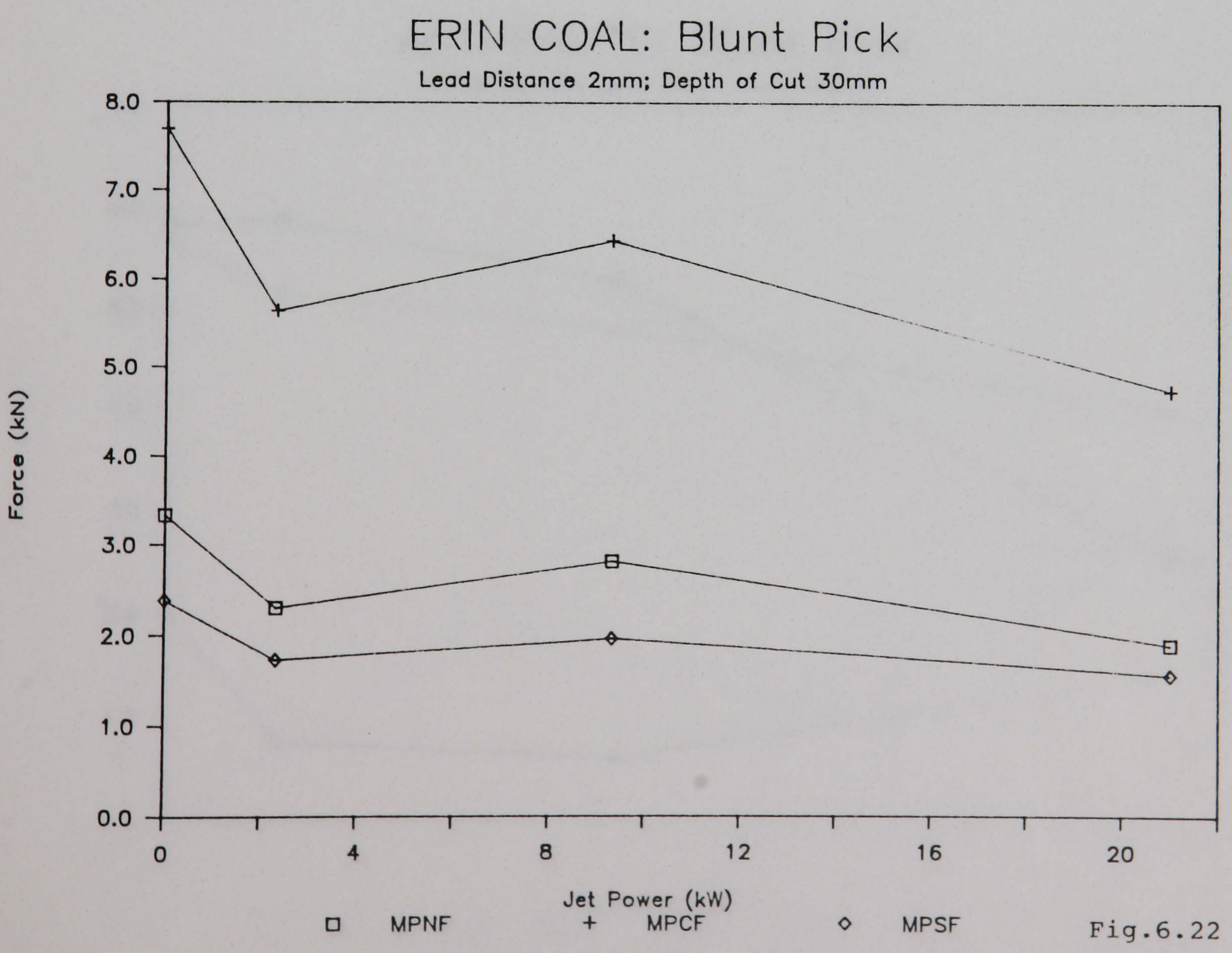


Fig.6.22

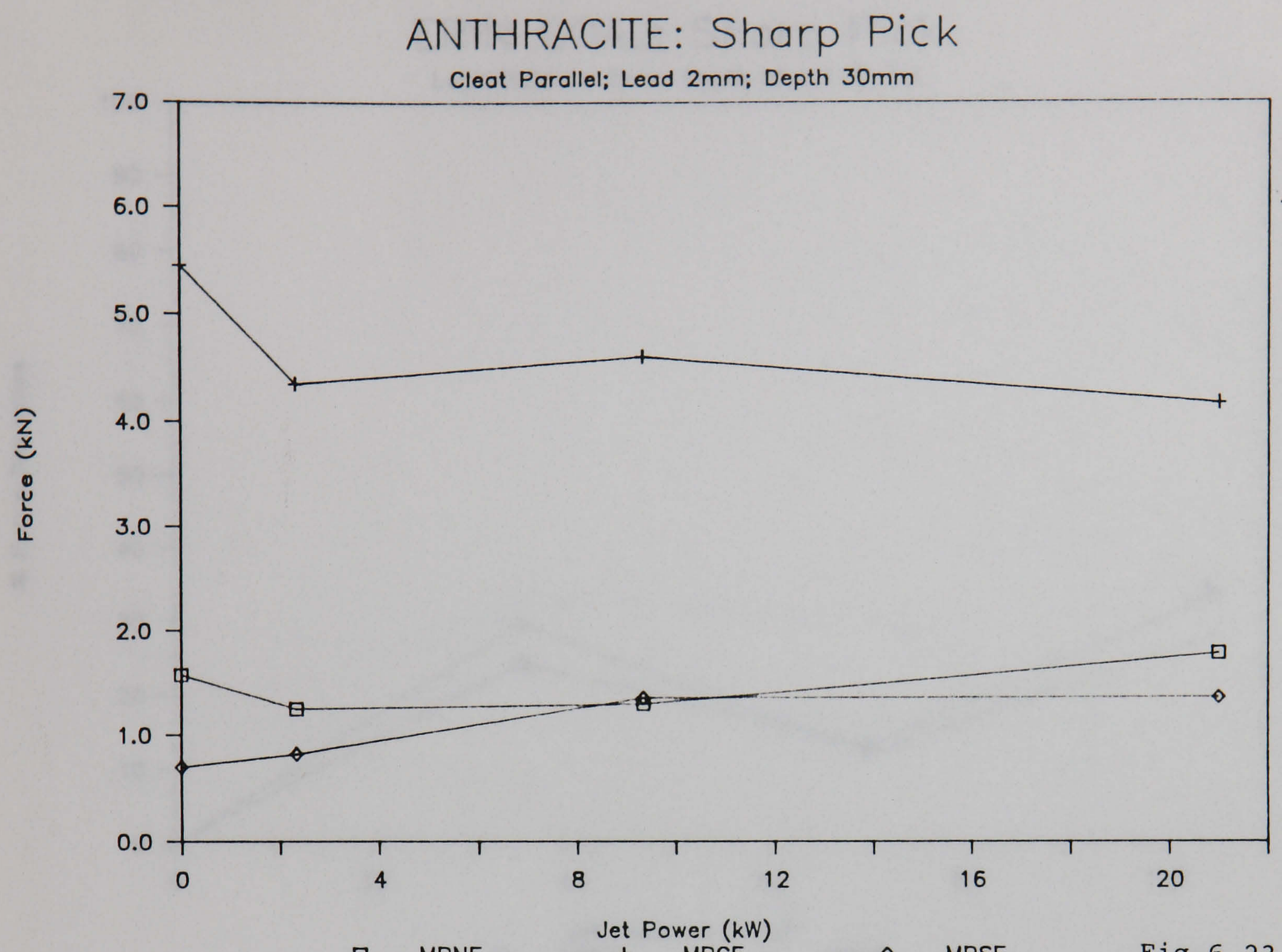


Fig.6.23

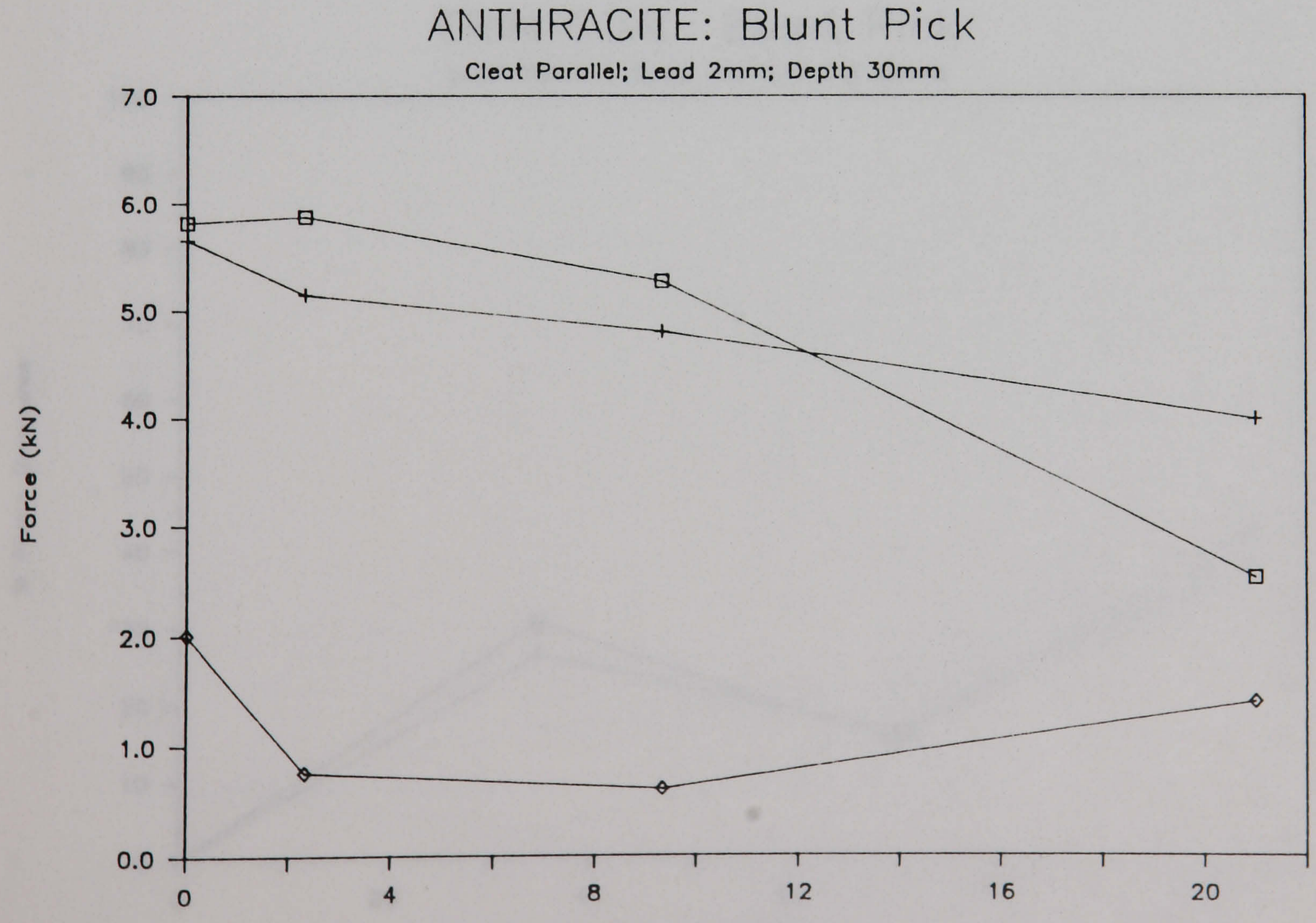


Fig.6.24

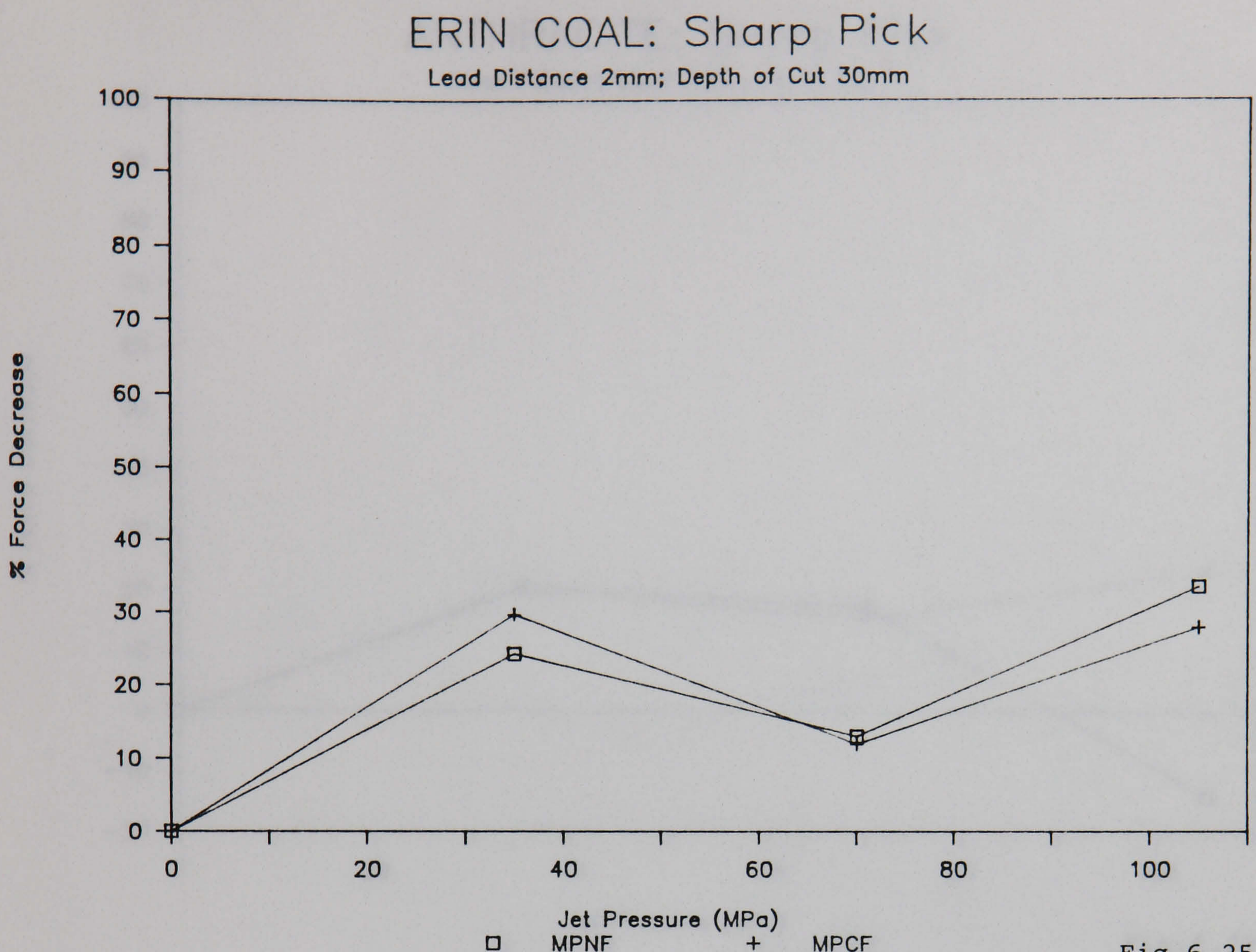


Fig.6.25

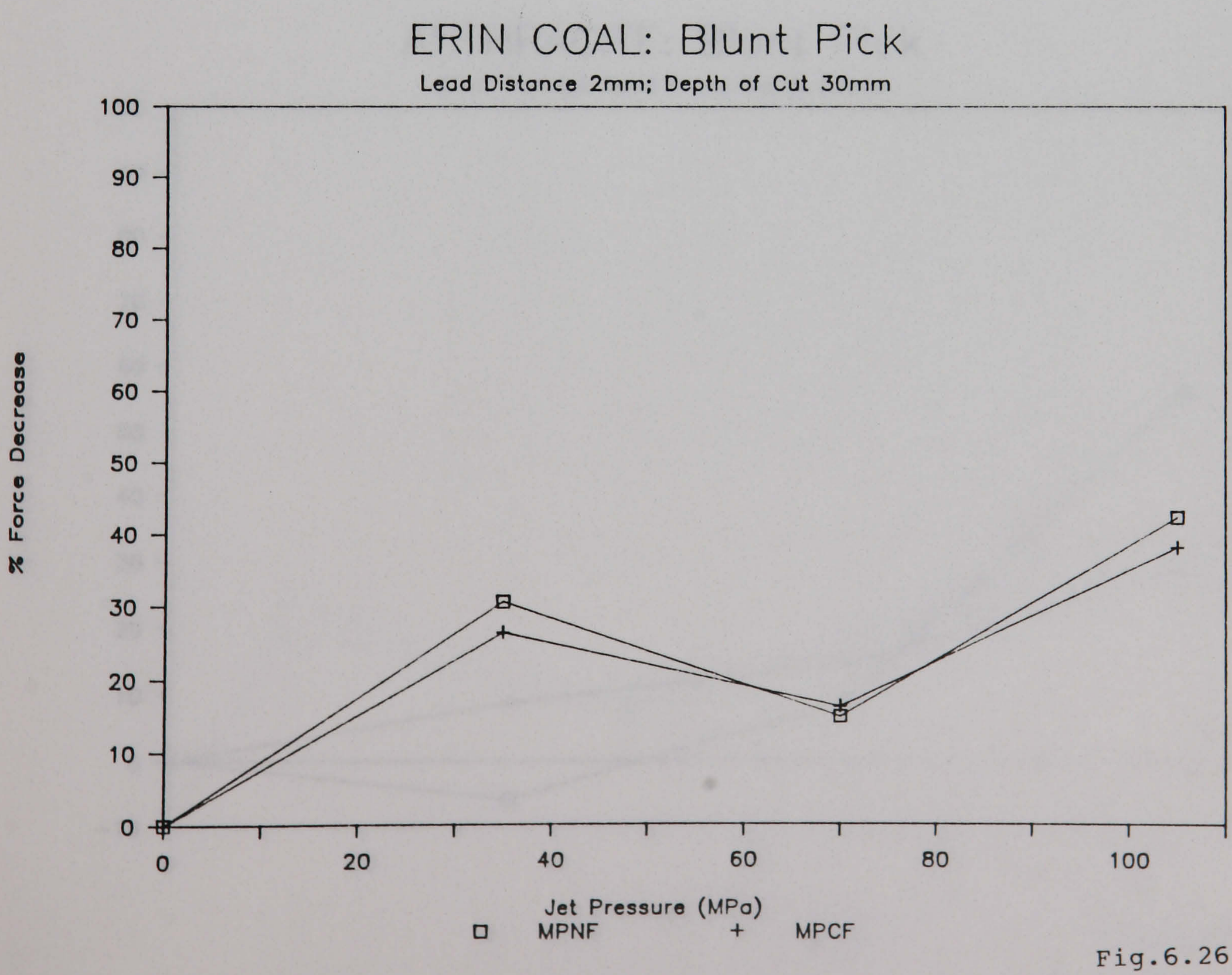


Fig.6.26

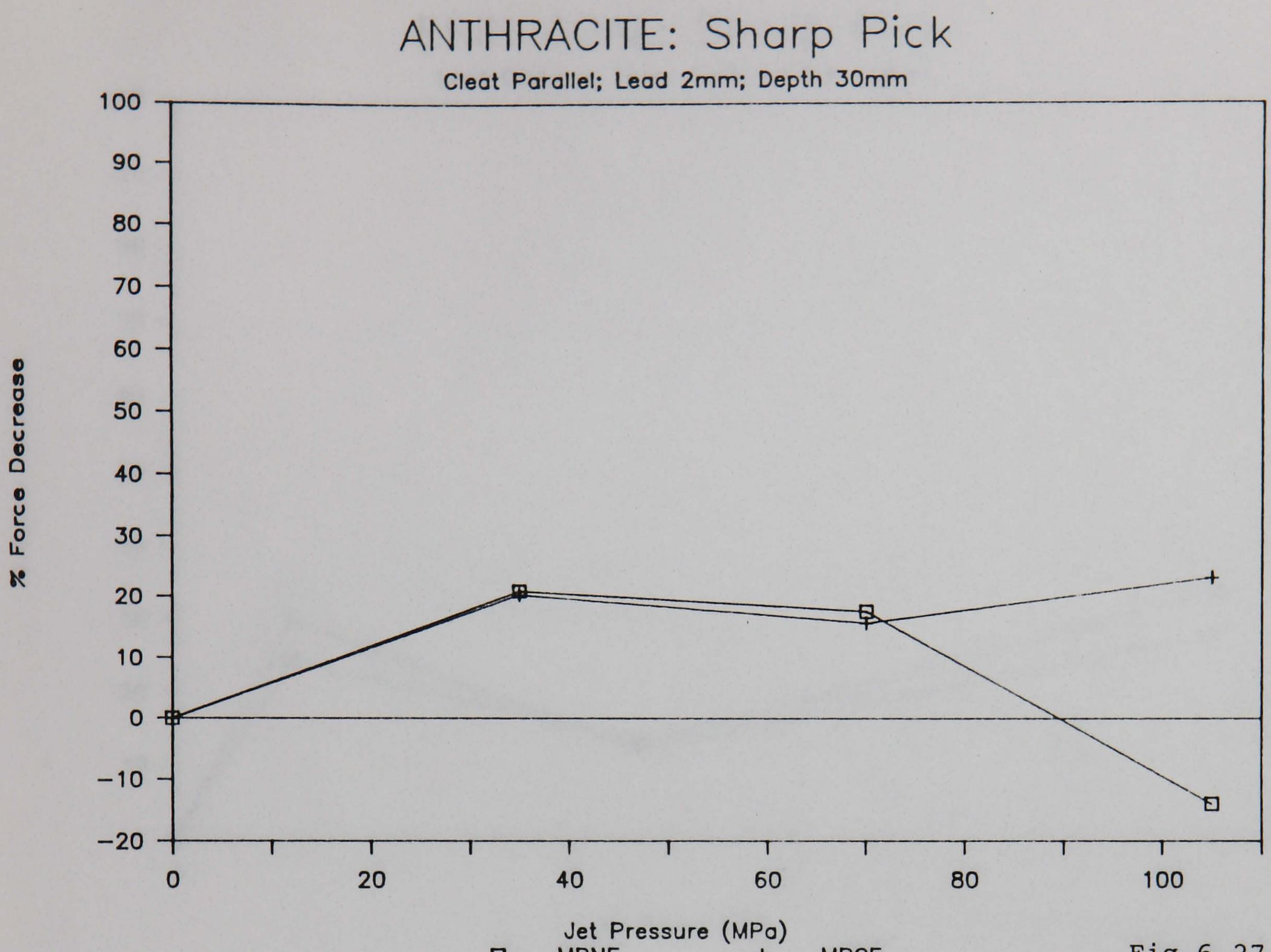


Fig.6.27

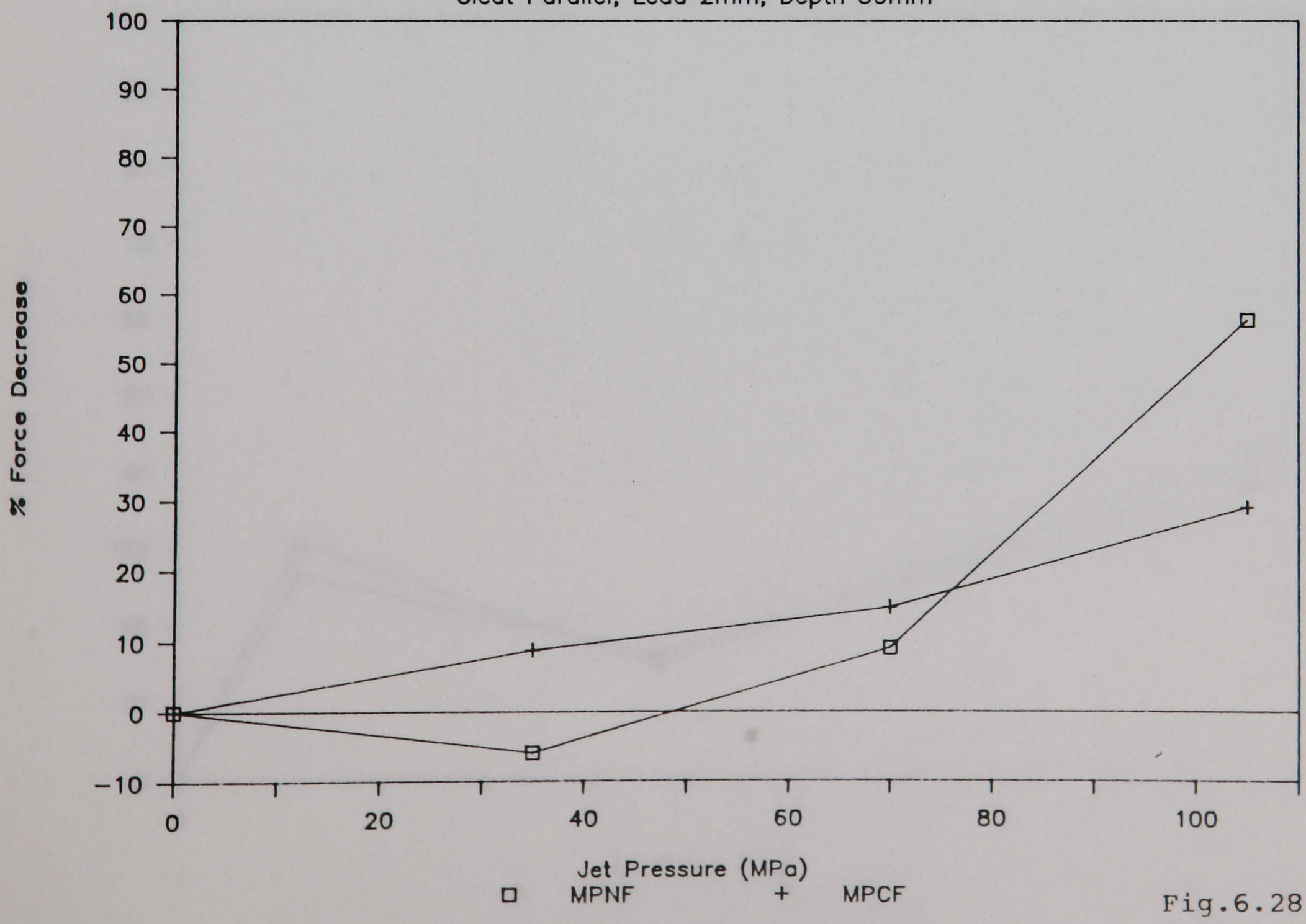


Fig.6.28

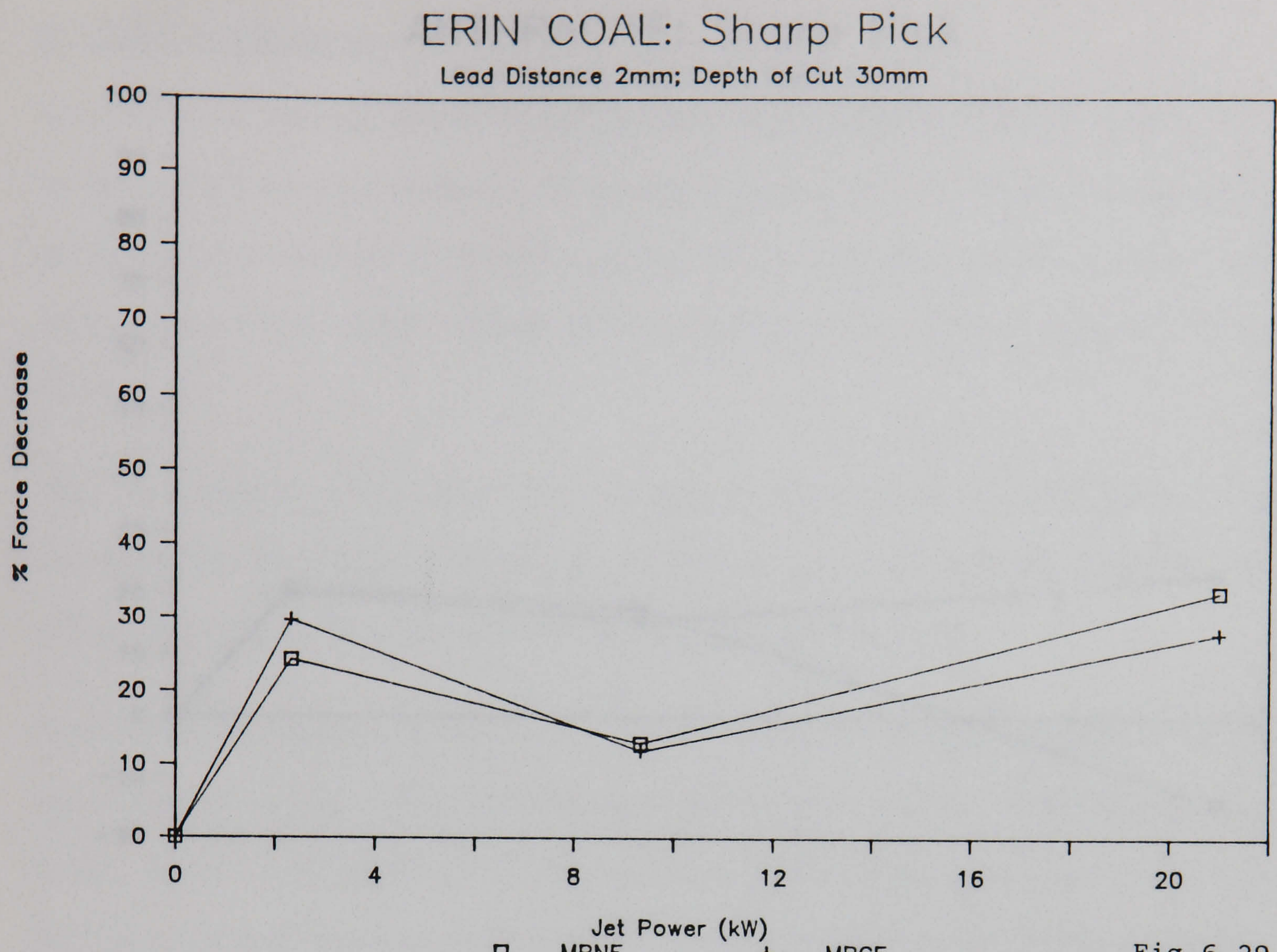


Fig.6.29

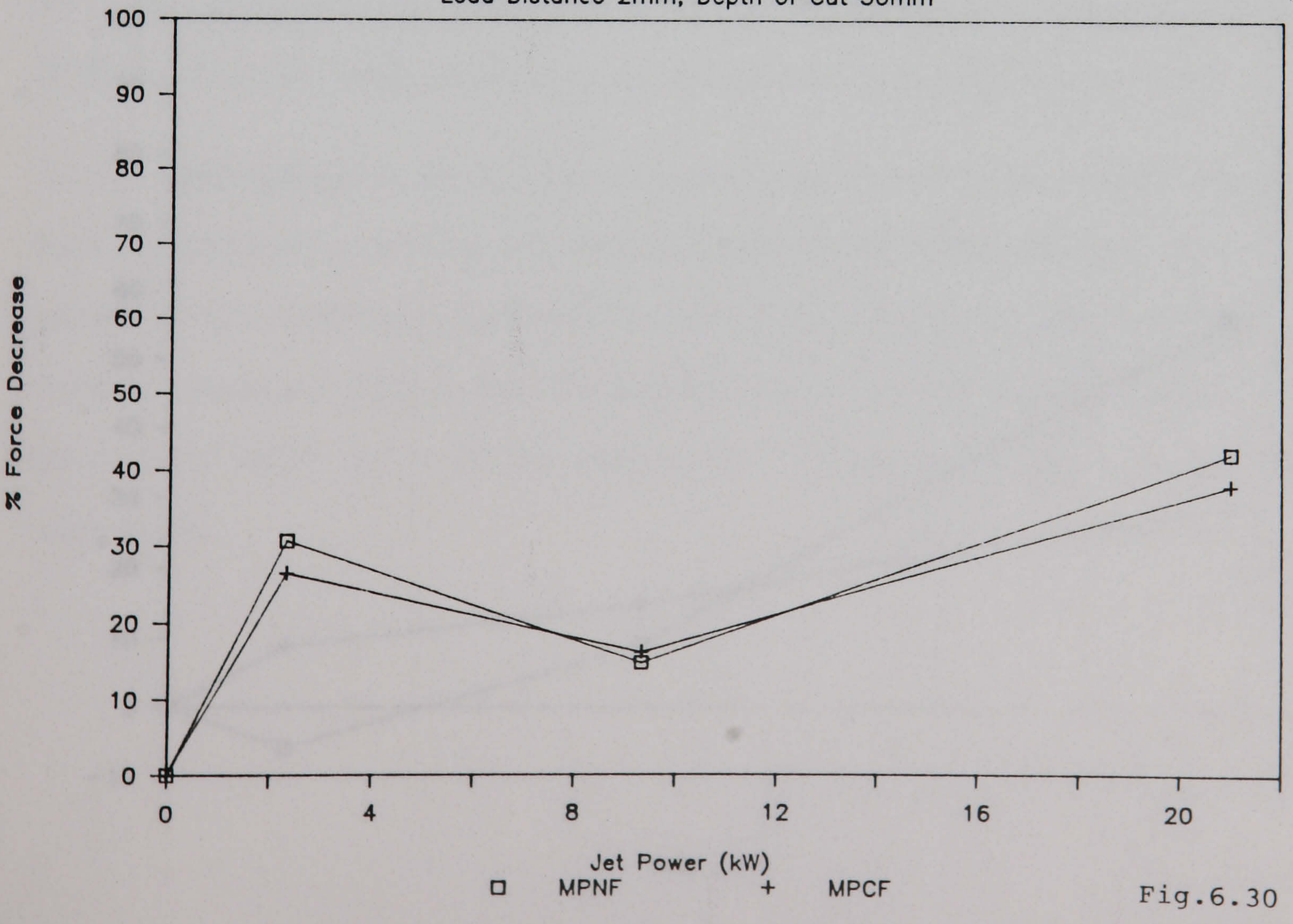


Fig.6.30

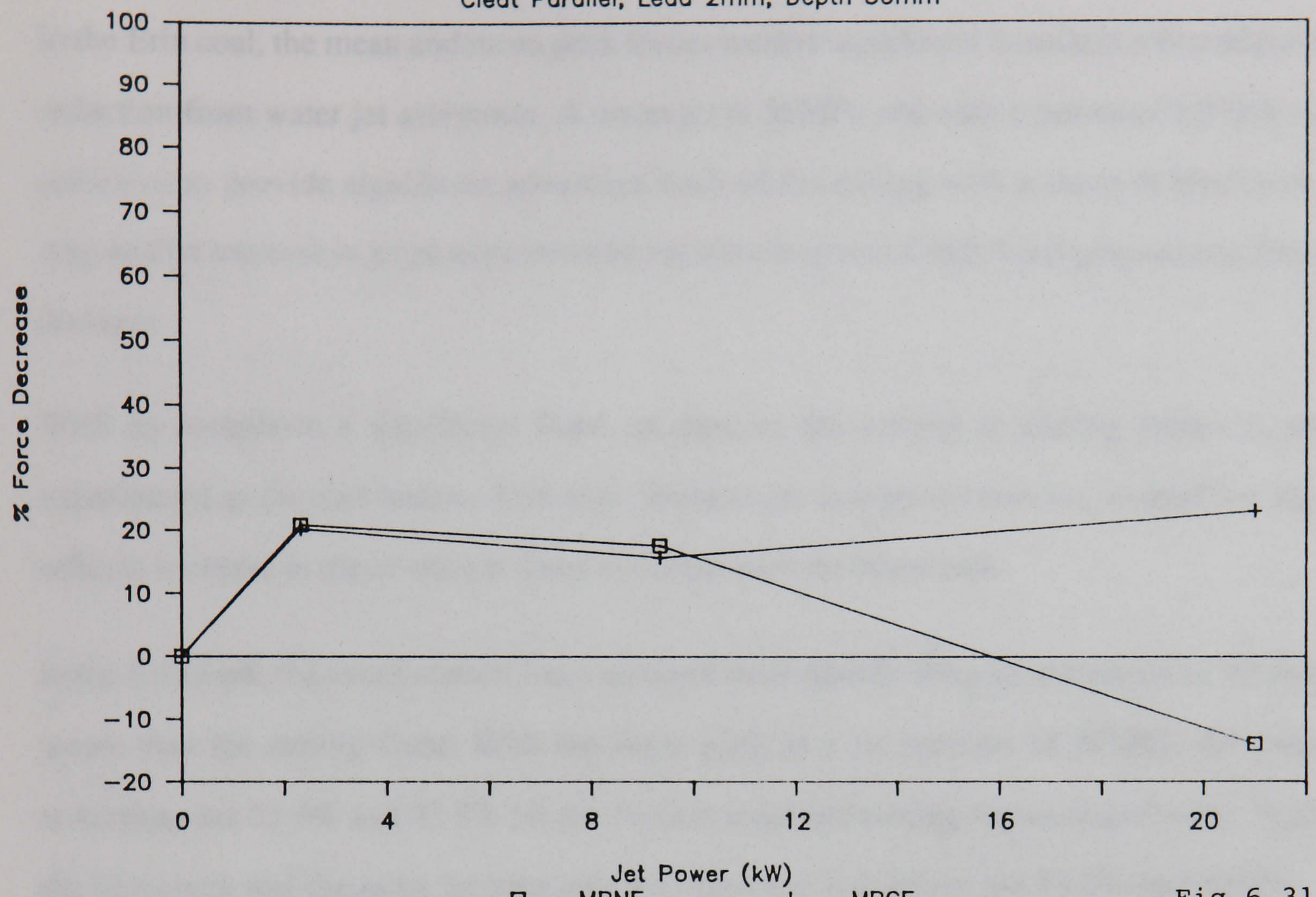


Fig.6.31

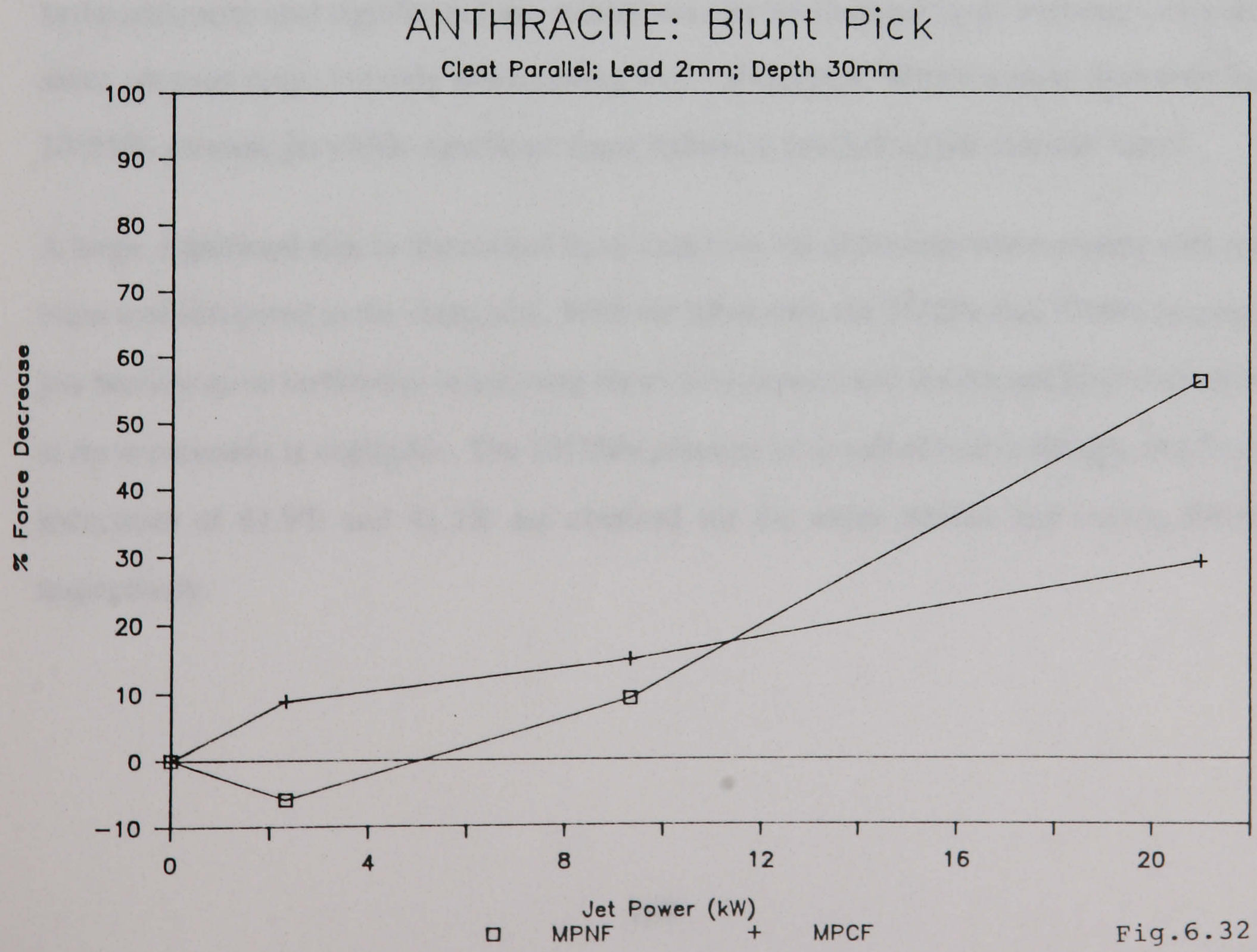


Fig.6.32

6.3.1.1 Conclusions

In the Erin coal, the mean and mean peak forces receive significant benefit in terms of force reduction from water jet assistance. A water jet at 35MPa and with a power of 2.33kW, is sufficient to provide significant advantage both whilst cutting with a sharp or blunt pick. Any further increase in jet power cannot be justified in terms of additional proportional force decrease.

With jet assistance a significant force increase in the normal or cutting forces is not experienced as the tool wears - Erin coal. Without jet assistance however, a small but significant increase in mean normal force occurred with the blunt tool.

In the Erin coal, the mean normal force receives more benefit from jet assistance as the tool wears than the cutting force. With the sharp pick, at a jet pressure of 35MPa, the force reductions are 25.4% and 33.3% for the mean normal and cutting forces respectively. With the blunt pick and the same jet pressure, the respective reductions are 54.6% and 33.9%.

In the anthracite coal significant force reductions may be procured by jet assistance over the entire pressure range but only when cutting with a sharp pick. With the blunt tool, only the 105MPa pressure jet yields significant force reduction (excluding the sideway force).

A large, significant rise in the normal force occurs in the anthracite when cutting with the blunt tool compared to the sharp pick. With the blunt tool, the 35MPa and 70MPa pressure jets become quite ineffective in assisting the cutting process and the normal force reduction at these pressures is negligible. The 105MPa pressure jet is still effective though, and force reductions of 61.9% and 41.3% are obtained for the mean normal and cutting forces respectively.

6.3.2 Cleat Orientation Trials

The purpose of these tests was to investigate the effect of high pressure water jet assistance on cutting performance with the cleat orientated in different positions relative to the cutting direction.

The factorial experiment is described in Table 6.1. Each cell contains the number of replications taken for that treatment. The mean and mean peak normal, cutting and sideway forces were recorded for each treatment. The coal debris was collected and sieved to find out the effect of cleat orientation on the size of the product.

	Cleat Parallel		Cleat Horizontal	
	Sharp Pick	Blunt Pick	Sharp Pick	Blunt Pick
0MPa	6X	4X	10X	8X
35MPa	4X	6X	8X	9X
70MPa	4X	4X	9X	10X
105MPa	7X	6X	9X	9X

Table 6.8

Mean Normal Force ANOVA

Source of Variation	Sums of Squares	Degrees of Freedom	Mean Square	F-ratio & (Significance Level)
Between Pressures	6.230	3	2.077	29.2 (4.0)
Between Pick Wear	17.590	1	17.590	247.0 (6.9)
Between Cleat	1.040	1	1.040	14.6 (6.9)
Interaction between Pressures & Pick Wear	3.782	3	1.261	17.8 (4.0)
Interaction between Pressures & Cleat	0.879	3	0.293	4.1 (4.0)
Interaction between Cleat & Pick Wear	0.511	1	0.511	7.2 (6.9)
Interaction between Pressures, Cleat & Pick Wear	0.640	3	0.213	3.0 (4.0)
Experimental Error	6.778	96	0.071	
Total	37.450	111		

Table 6.9

Experimental Error Variance, $\sigma_0^2 = \pm 0.071$kN. Using an average number of replications of 112/16 = 7.0, then the standard error between any two means is $\sigma_0\sqrt{\frac{2}{7.0}} = 0.14kN$. With twelve degrees of freedom the test statistic, t = 2.18, hence the 95% confidence limits for a two tailed significance test = ±2.18 x 0.14 = ±0.31kN.

Table 6.9, indicates that the greatest effect in the coal has been that due to tool wear and the other main effects are dwarfed by this effect. There also appears to be a sizeable interaction effect between jet pressure and tool wear. The other interactions, except the three-way one, are significant, but marginally so and hence are not as influential as the main effects.

The individual characteristics of the anthracite coal with the cleat orientated parallel to the direction of cut have already been detailed in the previous section and thus as far as possible shall not be repeated.

Considering the anthracite with the cleat horizontal to the direction of cut then, and applying the t-test to the mean normal force results, one can see from Fig.6.33, that with the sharp pick there has not been any significant effect over the whole pressure range. The 70MPa and 105MPa points have decreased but only by approximately 0.1kN. Also, the sharp pick mean normal force cuts in Fig.6.33, are not significantly lower than the corresponding results with the cleat parallel, over the pressure range and including the unassisted cuts.

Fig.6.34, illustrates the blunt tool results with the cleat horizontal. A force increase is observed with the 35MPa pressure jet but this is not statistically significant. Both the 70MPa and 105MPa pressure assisted treatments have produced a significantly reduced mean normal force. On the whole, the blunt pick mean normal forces have significantly increased over the sharp pick results. The increases are 3.2, 3.2, 2.7 and 1.9 times the sharp pick values at the jet pressures 0, 35MPa, 70MPa and 105MPa respectively. The corresponding increases with the cleat parallel, from Fig.6.3-4 are 2.9, 5.6, 4.4 and 1.5 times respectively.

The blunt pick, cleat horizontal results are significantly lower than the blunt pick, cleat parallel results (except the 105MPa treatment). This includes the dry cuts and so it seems that the mean normal force is less when cutting with the cleat horizontal to the cutting direction compared to the cleat parallel orientation. The reason why the sharp pick results did not prove significant in the same comparison then, is a matter of tool wear.

Fig.6.35-36, display the results with respect to jet power. With the blunt pick, only the 70MPa water jet has become effective in producing a significant mean normal force reduction when the cleat orientation has been changed from being parallel to horizontal.

Mean Cutting Force ANOVA

Source of Variation	Sums of Squares	Degrees of Freedom	Mean Square	F-ratio & (Significance Level)
Between Pressures	3.300	3	1.100	15.5 (4.0)
Between Pick Wear	1.120	1	1.120	15.8 (6.9)
Between Cleat	0.880	1	0.880	12.4 (6.9)
Interaction between Pressures & Pick Wear	1.020	3	0.340	4.8 (4.0)
Interaction between Pressures & Cleat	2.885	3	0.962	13.5 (4.0)
Interaction between Cleat & Pick Wear	0.234	1	0.234	3.3 (6.9)
Interaction between Pressures, Cleat & Pick Wear	0.437	3	0.146	2.1 (4.0)
Experimental Error	6.594	93	0.071	
Total	16.470	108		

Table 6.10

Experimental Error Variance, $\sigma_0^2 = \pm 0.071$kN. The standard error between mean values = $\sigma_0\sqrt{\frac{2}{6.8}} = 0.14kN$. Therefore, the 95% confidence limits for a two tailed significance test = $\pm 2.20 \times 0.14 = \pm 0.31$kN.

In this case all the main effects are highly significant but not greatly so. Also, the interaction between jet pressure and cleat is highly significant, suggesting that the mean cutting force varies not only due to jet pressure but how the pressure is combined with the cleat orientation.

Table 6.10, indicates that the force variation due to a change in jet pressure is significant. However, Fig.6.33-36 and the t-test reveal that this effect is not significant when the cleat is orientated horizontally, but only when it is parallel to the cutting direction. This point is true for both sharp and blunt picks.

This is also true for the significant effect due to pick wear. With the cleat horizontal, the t-test discloses no significant increase in the mean cutting force between the sharp and blunt picks over the whole pressure range, Fig.6.33-36. The significance derives from the results with the cleat parallel.

Cleat orientation does prove significant though and in both the sharp and blunt pick cutting tests. With the sharp pick, the cleat parallel forces are significantly higher in the dry cuts and with the treatment at 70MPa jet pressure. All the treatments with the blunt tool give significantly greater force values with the cleat parallel than those with the cleat horizontal. However, the jet assisted results are only marginally significant.

Thus the mean cutting force is lower with the cleat orientated horizontally to the cutting direction compared to the parallel orientation and especially when the pick is blunt.

Fig.6.37-40, show the percentage force reduction plots. The 35MPa pressure jet treatment causes a force increase with both sharp and blunt picks. The mean cutting force is affected more in terms of force reduction than the mean normal force by a change from a sharp to a blunt pick. The normal force experiences more benefit from jet assistance as the tool wears, as it were, and the cutting force generally less. This almost contrasts with the cleat parallel results, Fig.6.14,16. At the lower pressures the mean normal force reductions are drastically lowered when the blunt tool is used. The mean cutting forces are reduced also but not as much.

Mean Sideway Force ANOVA

Source of Variation	Sums of Squares	Degrees of Freedom	Mean Square	F-ratio & (Significance Level)
Between Pressures	0.117	3	0.039	3.2 (4.0)
Between Pick Wear	0.135	1	0.135	11.2 (6.9)
Between Cleat	0.018	1	0.018	1.5 (6.9)
Interaction between Pressures & Pick Wear	0.180	3	0.060	5.0 (4.0)
Interaction between Pressures & Cleat	0.475	3	0.158	13.2 (4.0)
Interaction between Cleat & Pick Wear	0.007	1	0.007	0.6 (6.9)
Interaction between Pressures, Cleat & Pick Wear	0.288	3	0.096	8.0 (4.0)
Experimental Error	1.121	93	0.012	
Total	2.341	108		

Table 6.11

Experimental Error Variance, $\sigma_0^2 = \pm 0.012$kN. The standard error between mean values = $\sigma_0\sqrt{\frac{2}{6.8}} = 0.06kN$. Therefore, the 95% confidence limits for a two tailed significance test = $\pm 2.20 \times 0.06 = \pm 0.13$kN.

The significant items in the mean sideway force are not greatly significant from the results in Table 6.11. The largest effect is that of the interaction between jet pressure and cleat orientation. Pick wear is also significant.

From Fig.6.3-4 and Fig.6.33-34, one can see that the cause of the significances in Table 6.11, can be attributed entirely to the large blunt pick sideway forces in Fig.6.4, when the cleat is parallel. There is an increase in sideway force between the sharp and blunt picks with the cleat horizontal, but this is not statistically significant, Fig.6.33-34.

ANTHRACITE: Sharp Pick

Cleat Horizontal; Lead 2mm; Depth 30mm

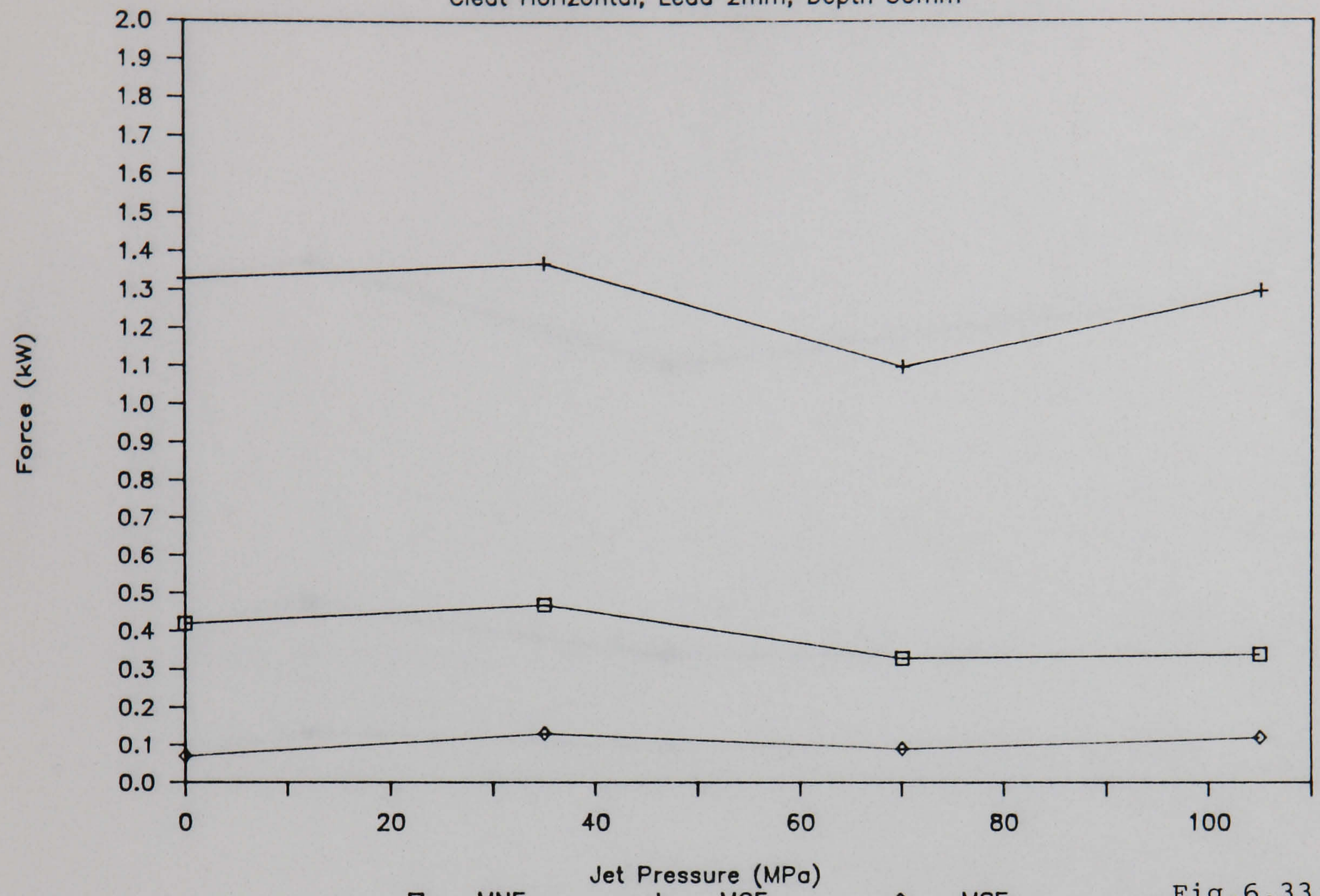


Fig.6.33

ANTHRACITE: Blunt Pick

Cleat Horizontal; Lead 2mm; Depth 30mm

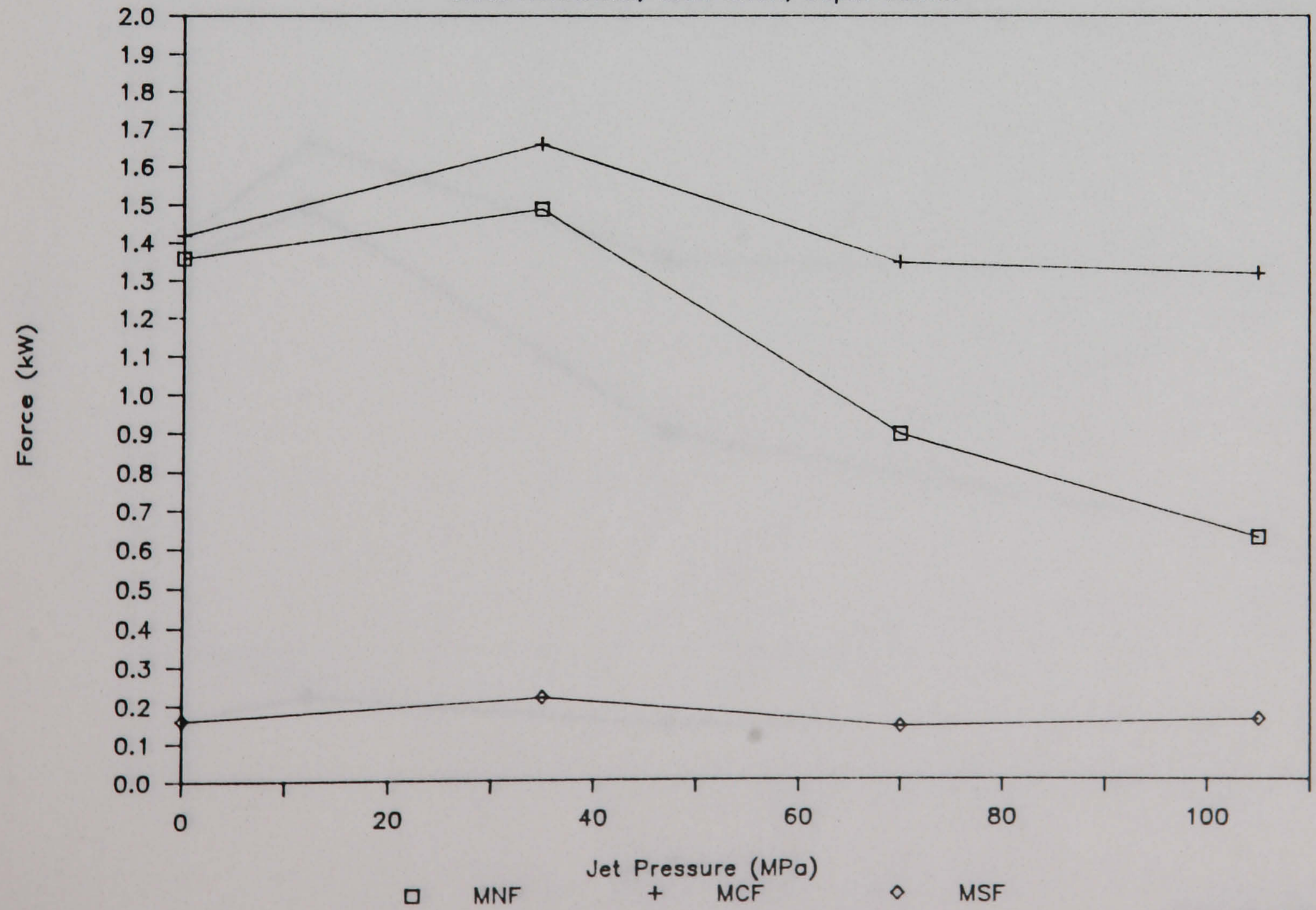


Fig.6.34

ANTHRACITE: Sharp Pick

Cleat Horizontal; Lead 2mm; Depth 30mm

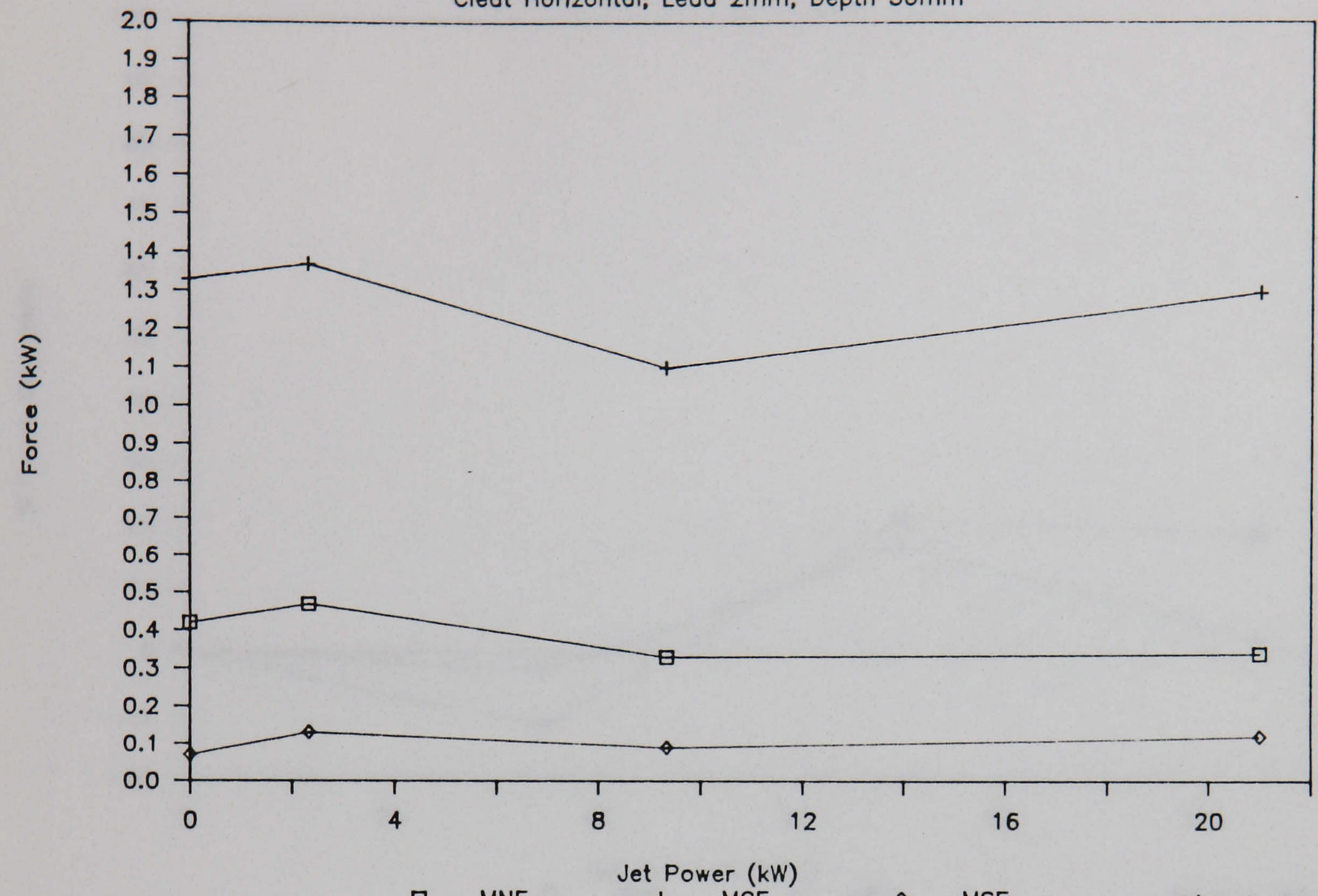


Fig.6.35

ANTHRACITE: Blunt Pick

Cleat Horizontal; Lead 2mm; Depth 30mm

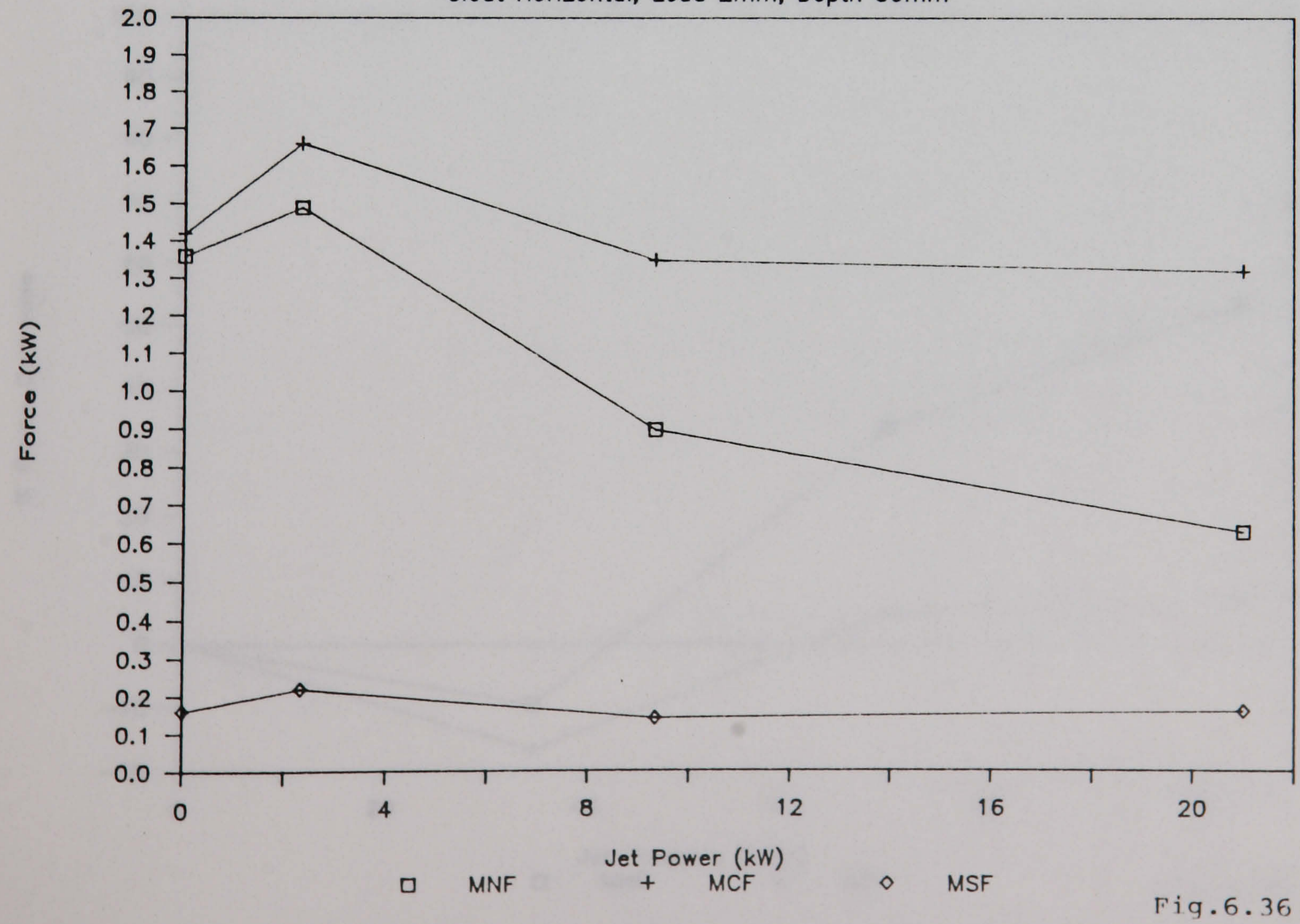


Fig.6.36

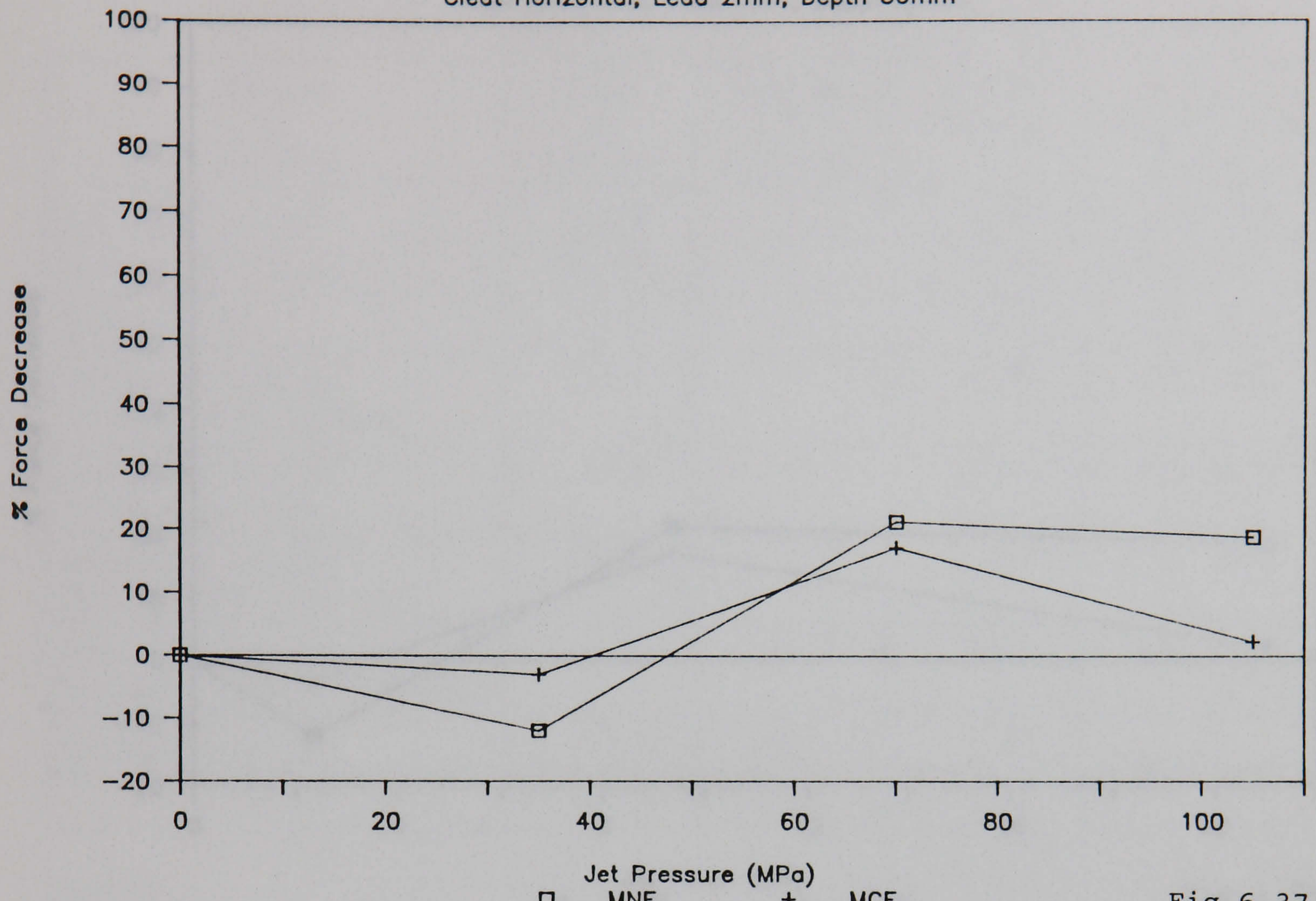


Fig.6.37

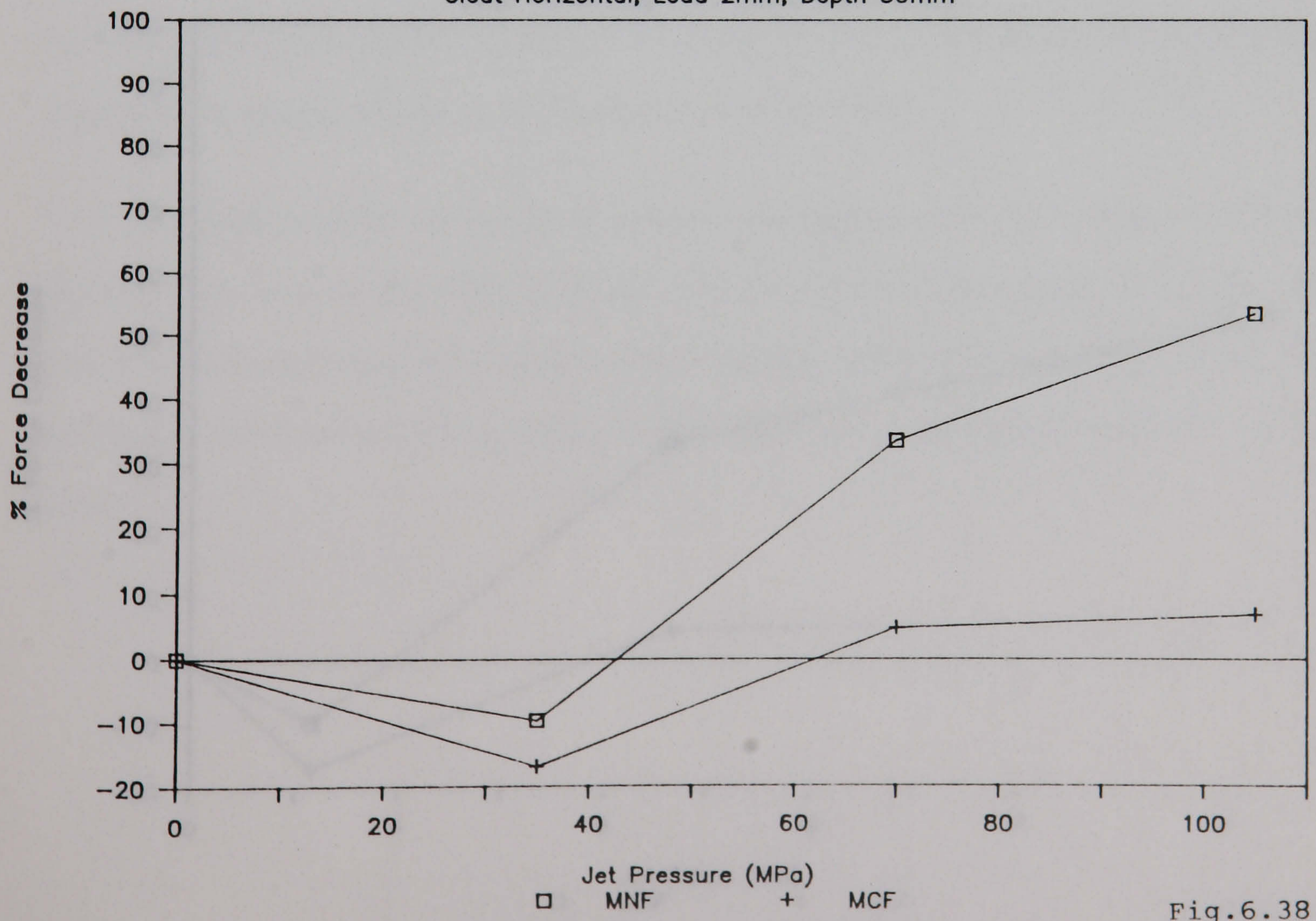


Fig.6.38

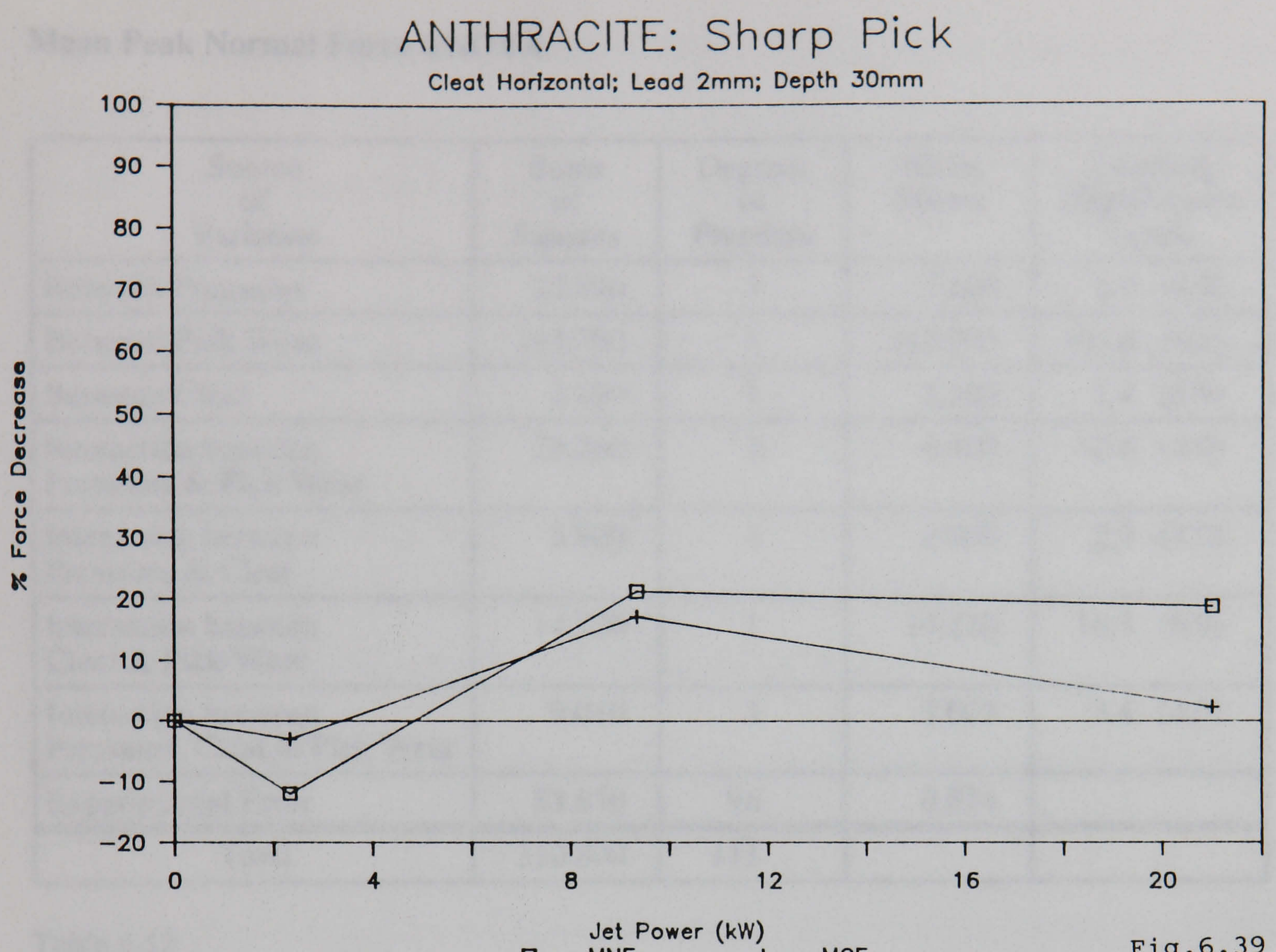


Fig.6.39

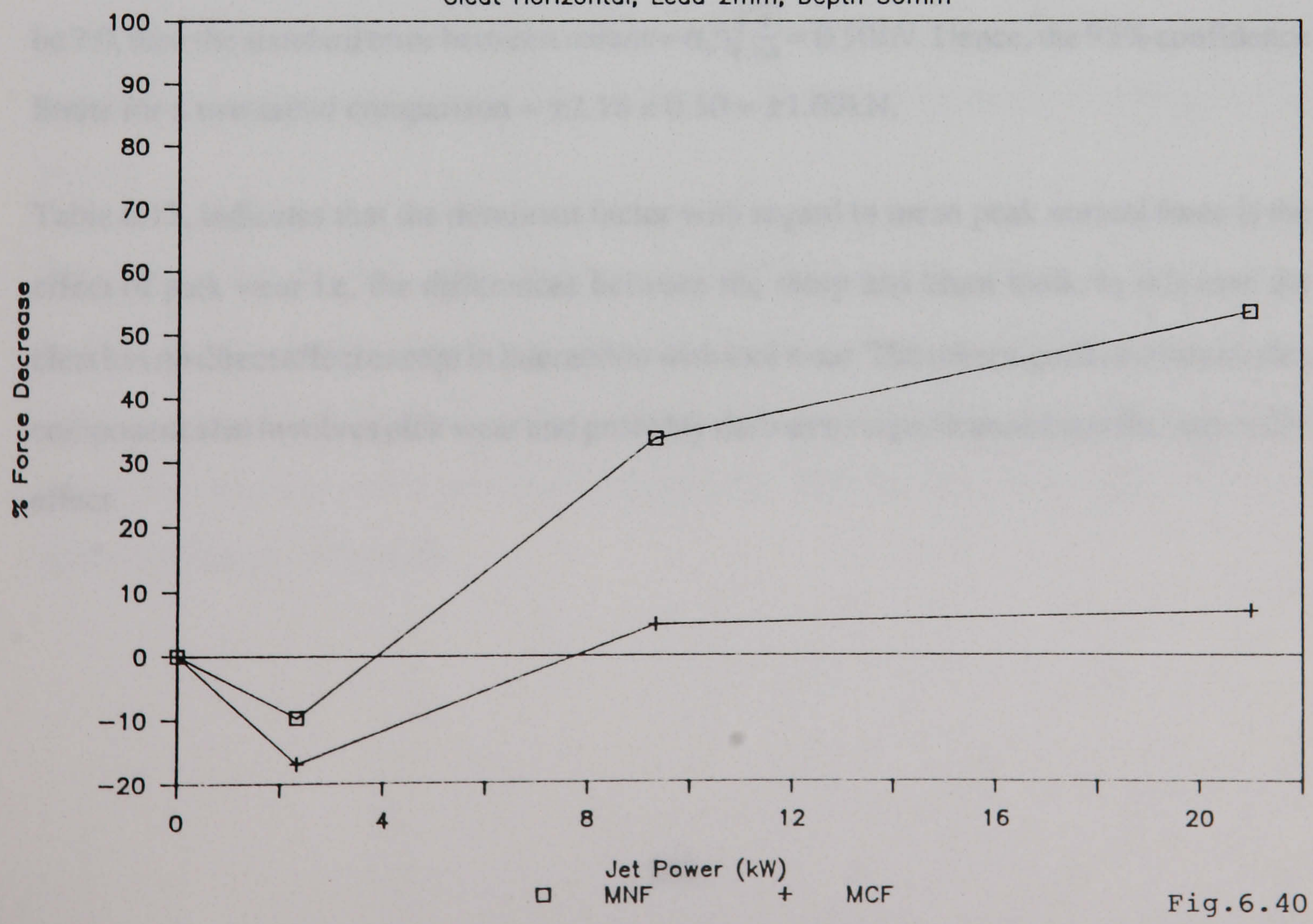


Fig.6.40

Mean Peak Normal Force ANOVA

Source of Variation	Sums of Squares	Degrees of Freedom	Mean Square	F-ratio & (Significance Level)
Between Pressures	22.800	3	7.600	8.7 (4.0)
Between Pick Wear	144.700	1	144.700	165.6 (6.9)
Between Cleat	2.100	1	2.100	2.4 (6.9)
Interaction between Pressures & Pick Wear	28.200	3	9.400	10.8 (4.0)
Interaction between Pressures & Cleat	5.900	3	2.000	2.3 (4.0)
Interaction between Cleat & Pick Wear	14.220	1	14.220	16.3 (6.9)
Interaction between Pressures, Cleat & Pick Wear	9.010	3	3.003	3.4 (4.0)
Experimental Error	83.870	96	0.874	
Total	310.800	111		

Table 6.12

Experimental Error Variance, $\sigma_0^2 = \pm 0.874$kN. Taking the average number of replications to be 7.0, then the standard error between means $= \sigma_0 \sqrt{\frac{2}{7.0}} = 0.50kN$. Hence, the 95% confidence limits for a two tailed comparison = ±2.18 x 0.50 = ±1.09kN.

Table 6.12, indicates that the dominant factor with regard to mean peak normal force is the effect of pick wear i.e. the differences between the sharp and blunt tools. In this case the cleat has no direct effect except in interaction with tool wear. The other significant interaction component also involves pick wear and probably derives its significance from the large main effect.

Fig.6.41-48, represent the mean peak forces with the cleat horizontal. Employing the t-test, from Fig.6.41, it is evident that there are no significant force changes with the sharp pick over the pressure range. The mean peak forces merely oscillate randomly about a mean of 2kN.

Compared to the cleat parallel tests, the sharp pick forces are not significantly different. This also holds for the blunt picks, hence the insignificant main effect in Table 6.12.

Compared with the sharp pick, cleat horizontal tests, the mean peak normal force blunt pick values have all significantly increased, Fig.6.41-42. The increases are 2.5, 1.8, 1.9 and 1.4 times at 0, 35MPa, 70MPa and 105MPa jet pressures respectively.

From Fig.6.42, the blunt pick forces have steadily decreased as the jet pressure has increased. All the jet assisted results are significantly lower than the dry cuts.

Fig.6.20 and Fig.6.42, indicate that the cleat horizontal results are lower than the cleat parallel ones except for the test treatment at 105MPa jet pressure. The dry cuts have not been significantly reduced but the treatments carried out at 35MPa and 70MPa jet pressure have been. Changing the cleat orientation has rendered the jet assistance effective at the lower pressures as well as at the 105MPa pressure. Fig.6.43-44, illustrate the results against jet power.

The plots of percentage force decrease in Fig.6.45-46, show that the mean normal force receives benefit at all pressures with the blunt pick and the advantage gradually increases with jet pressure. This contrasts with the cleat parallel results in Fig.6.28, where appreciable gain is not obtained until a greater jet pressure than 70MPa. The same results against jet power are shown in Fig.6.48.

Mean Peak Cutting Force ANOVA

Source of Variation	Sums of Squares	Degrees of Freedom	Mean Square	F-ratio & (Significance Level)
Between Pressures	11.710	3	3.900	7.8 (4.0)
Between Pick Wear	1.470	1	1.470	2.9 (6.9)
Between Cleat	1.120	1	1.120	2.2 (6.9)
Interaction between Pressures & Pick Wear	1.970	3	0.657	1.3 (4.0)
Interaction between Pressures & Cleat	2.760	3	0.920	1.8 (4.0)
Interaction between Cleat & Pick Wear	0.010	1	0.010	0.0 (6.9)
Interaction between Pressures, Cleat & Pick Wear	0.760	3	0.253	0.5 (4.0)
Experimental Error	46.780	89	0.503	
Total	66.580	104		

Table 6.13

Experimental Error Variance, $\sigma_0^2 = \pm 0.503$kN. The standard error between mean values = $\sigma_0\sqrt{\frac{2}{6.8}} = 0.38kN$. Thus, the 95% confidence limits for a two tailed significance test = ± 2.20 x $0.38 = \pm 0.84$kN.

Only one significant item is indicated by the F-ratios in Table 6.13; that variability caused by the jet pressures.

From the t-test, the jet assisted cuts with the sharp pick and cleat horizontal, have all been significantly reduced, Fig.6.41. However, there is no significant variation within the jet assisted tests.

Compared to the sharp pick results in Fig.6.19, there are no significant differences between the two cleat orientations at any pressure. Effectively, the mean peak cutting forces are approximately the same with the sharp pick between the two cleat positions.

A comparison between the sharp and blunt picks with the cleat horizontal, Fig.6.41-42, also returns an insignificant result.

There are no significant changes in peak cutting force within the blunt pick tests but the forces appear to be gently reducing with jet pressure.

Again, no significant difference using the t-test is observed between the blunt pick results with the cleats at 90° to one another.

As indicated in Table 6.13, the only significant effects are those due to the jet assistance. The results plotted against jet power are given in Fig.6.43-44.

The graphs of Fig.6.45-48, show that with the sharp pick a force reduction of 16.1% for the mean peak cutting force is procured with the 35MPa pressure jet, no additional gains being made by increasing the jet pressure further. This agrees with Fig.6.27, when the cleat is parallel.

In the case of the blunt picks, similar trends are observed, Fig.6.32,46, but the slopes are different. With the cleat parallel, the mean peak cutting force will receive more assistance as the jet pressure is increased. When the cleat is horizontal, the mean peak cutting force loses its assistance at a greater rate than when the cleat is parallel as the tool wears. The cleat is obviously affecting the jet assistance especially when one considers that cleat makes no difference to jet penetration.

The mean peak cutting force percentage reductions are much smaller than those of the mean peak normal force, thus the mean peak normal force gains most from jet assistance when the cleat is horizontal.

Mean Peak Sideway Force ANOVA

Source of Variation	Sums of Squares	Degrees of Freedom	Mean Square	F-ratio & (Significance Level)
Between Pressures	0.680	3	0.227	2.4 (4.0)
Between Pick Wear	0.890	1	0.890	9.6 (6.9)
Between Cleat	7.420	1	7.420	79.8 (6.9)
Interaction between Pressures & Pick Wear	3.650	3	1.217	13.1 (4.0)
Interaction between Pressures & Cleat	4.526	3	1.509	16.2 (4.0)
Interaction between Cleat & Pick Wear	0.083	1	0.083	0.9 (6.9)
Interaction between Pressures, Cleat & Pick Wear	0.653	3	0.218	2.3 (4.0)
Experimental Error	8.638	93	0.093	
Total	26.540	108		

Table 6.14

Experimental Error Variance, σ_0^2 = ±0.093kN. The standard error between the means = $\sigma_0\sqrt{\frac{2}{6.8}} = 0.165kN$. Therefore, the 95% confidence limits for a two tailed significance test = ±2.20 x 0.16 = ±0.36kN.

The most significant influence on the mean peak sideway force is the cleat orientation, Table 6.14. Fig.6.19-20,41-42, suggest this is due to the cleat parallel cuts. In the sharp pick tests, jet assistance has increased the sideway force in both cleat orientations and the jet assisted cleat horizontal values are significantly higher than the corresponding cleat parallel forces.

The cleat horizontal blunt pick jet assisted tests exhibit no significant force deviation from the dry cut values.

The cleat parallel blunt pick jet assisted results, Fig.6.20, show a significant reduction from the unassisted tests. Also, the jet assisted cleat parallel test results are significantly lower than the cleat horizontal values for the blunt tool.

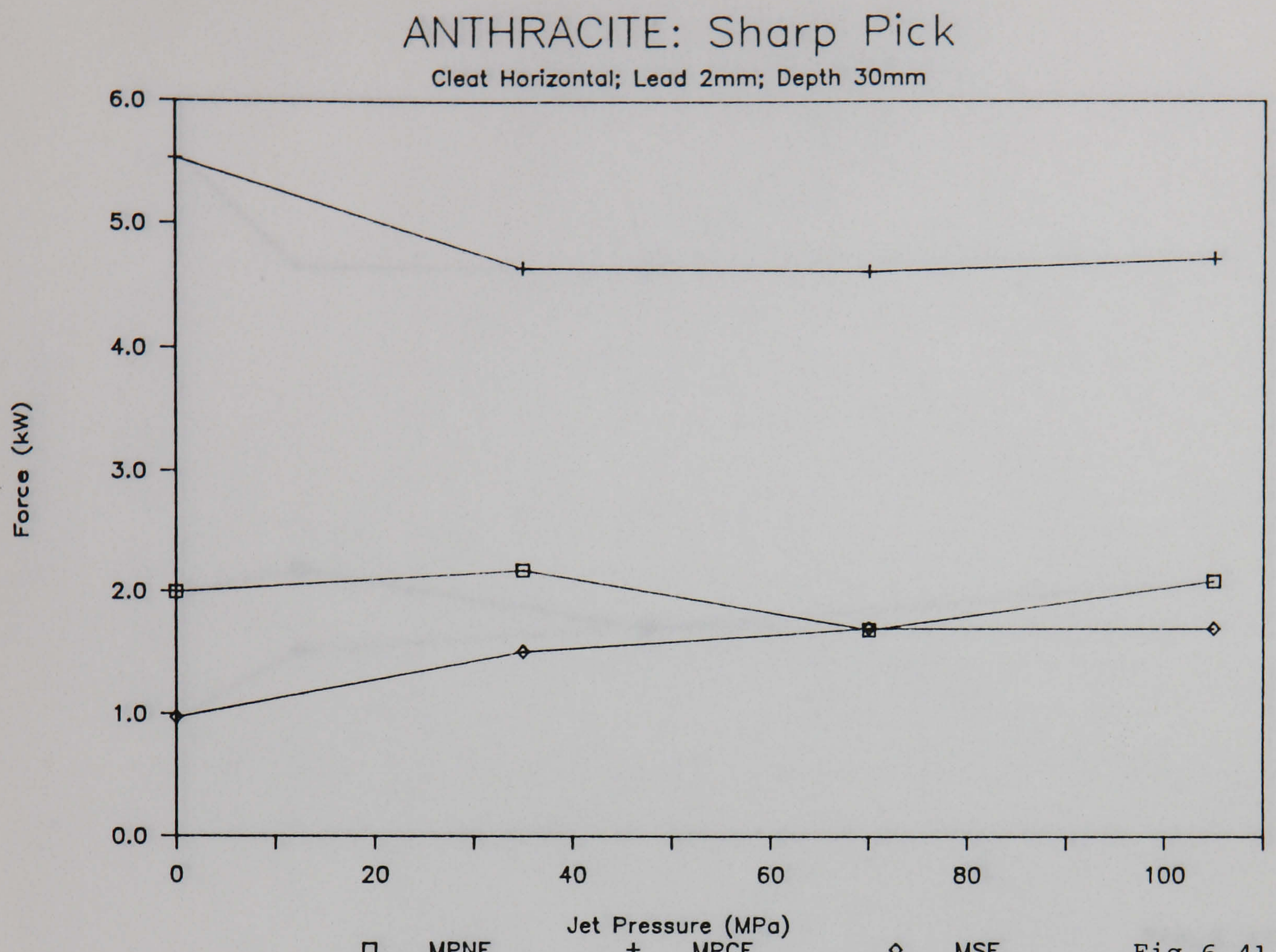


Fig.6.41

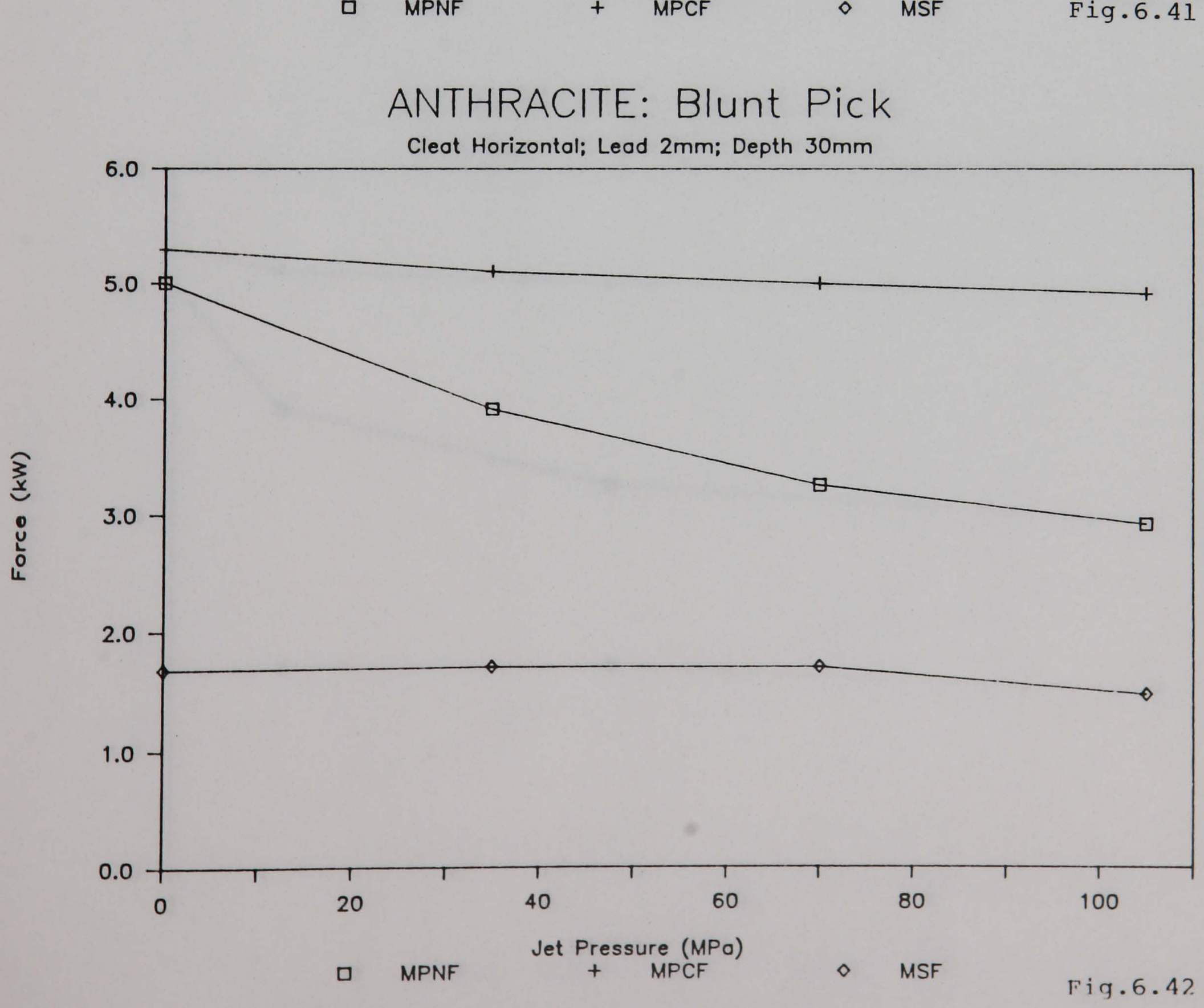


Fig.6.42

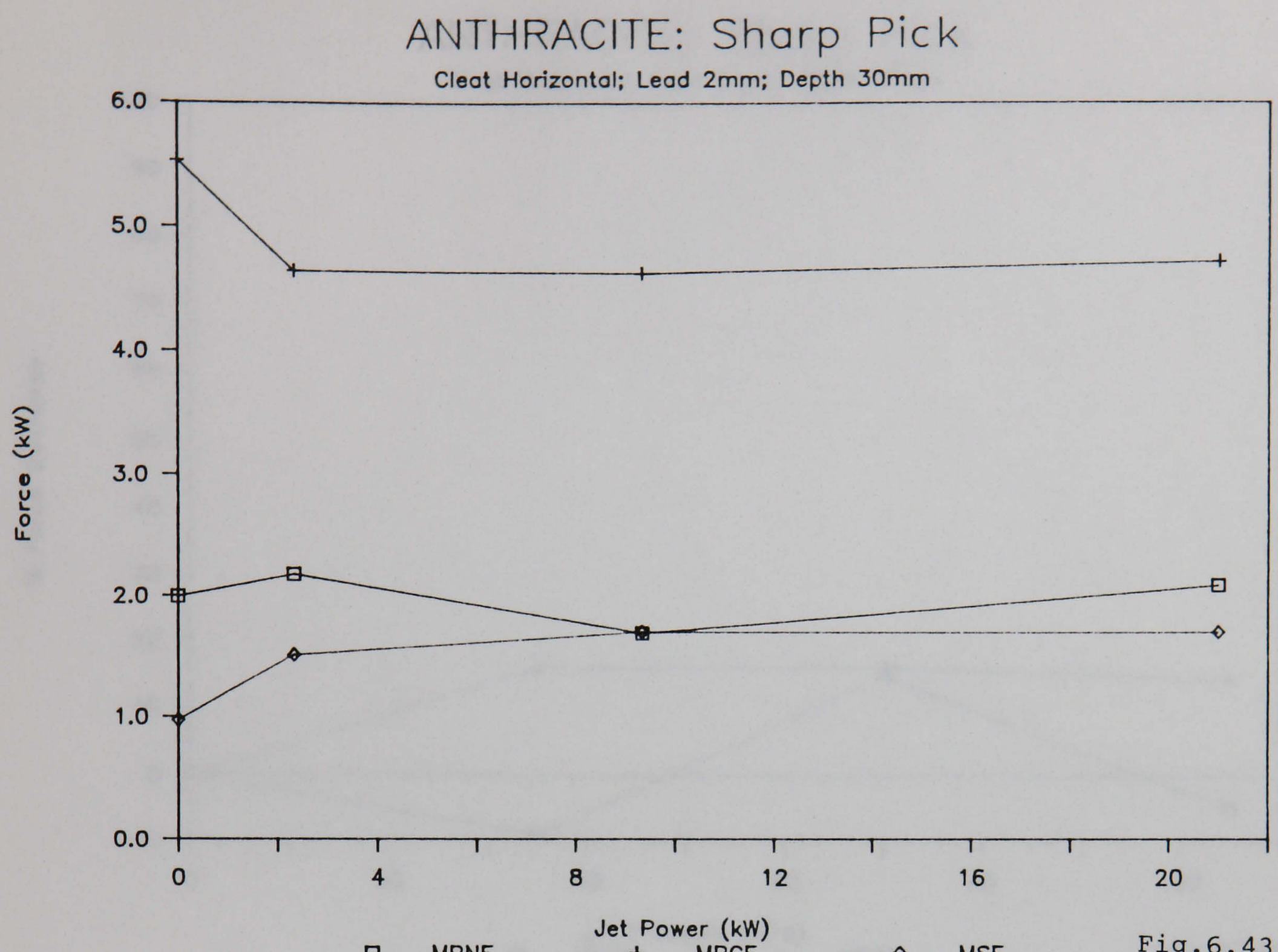


Fig.6.43

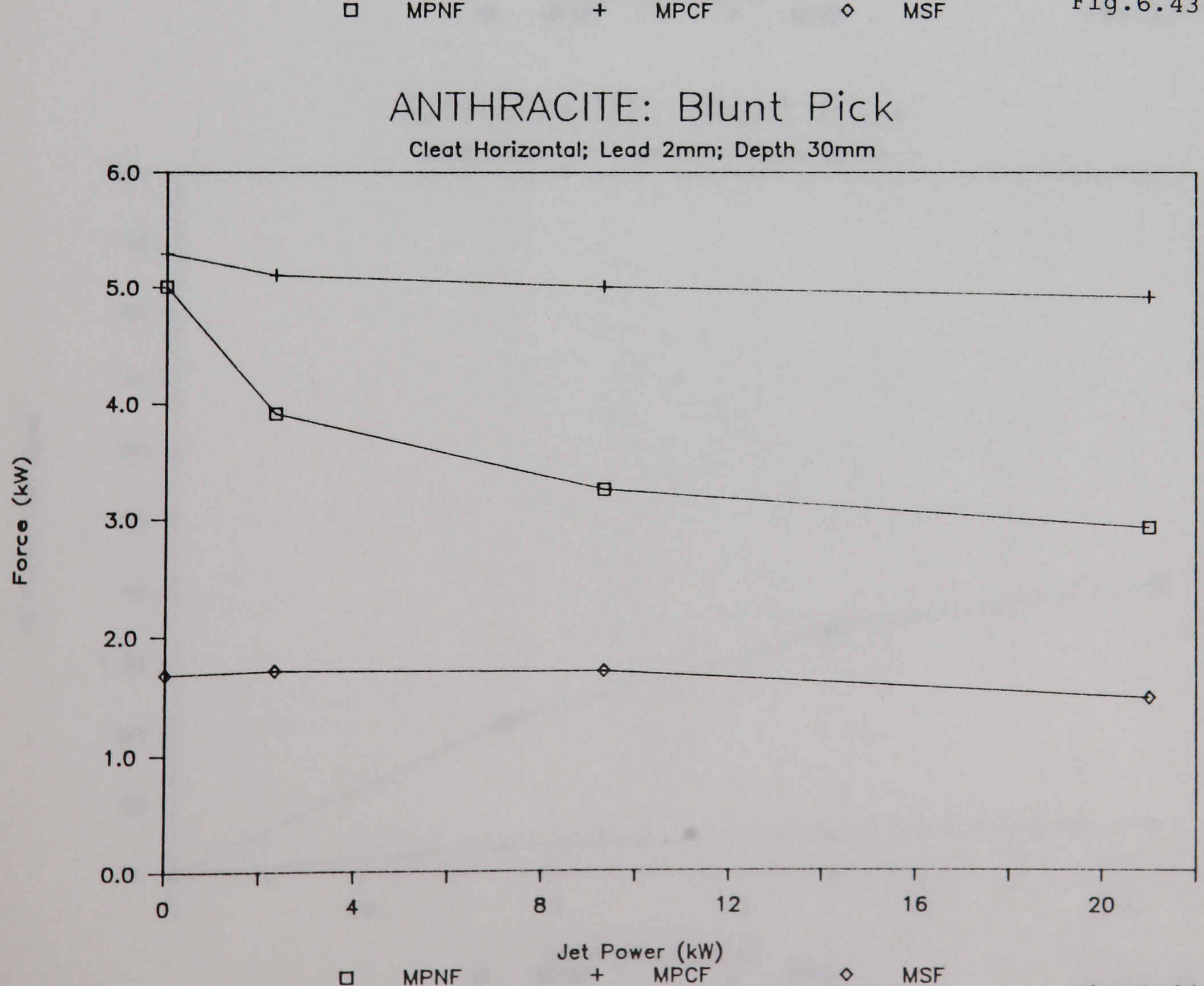


Fig.6.44

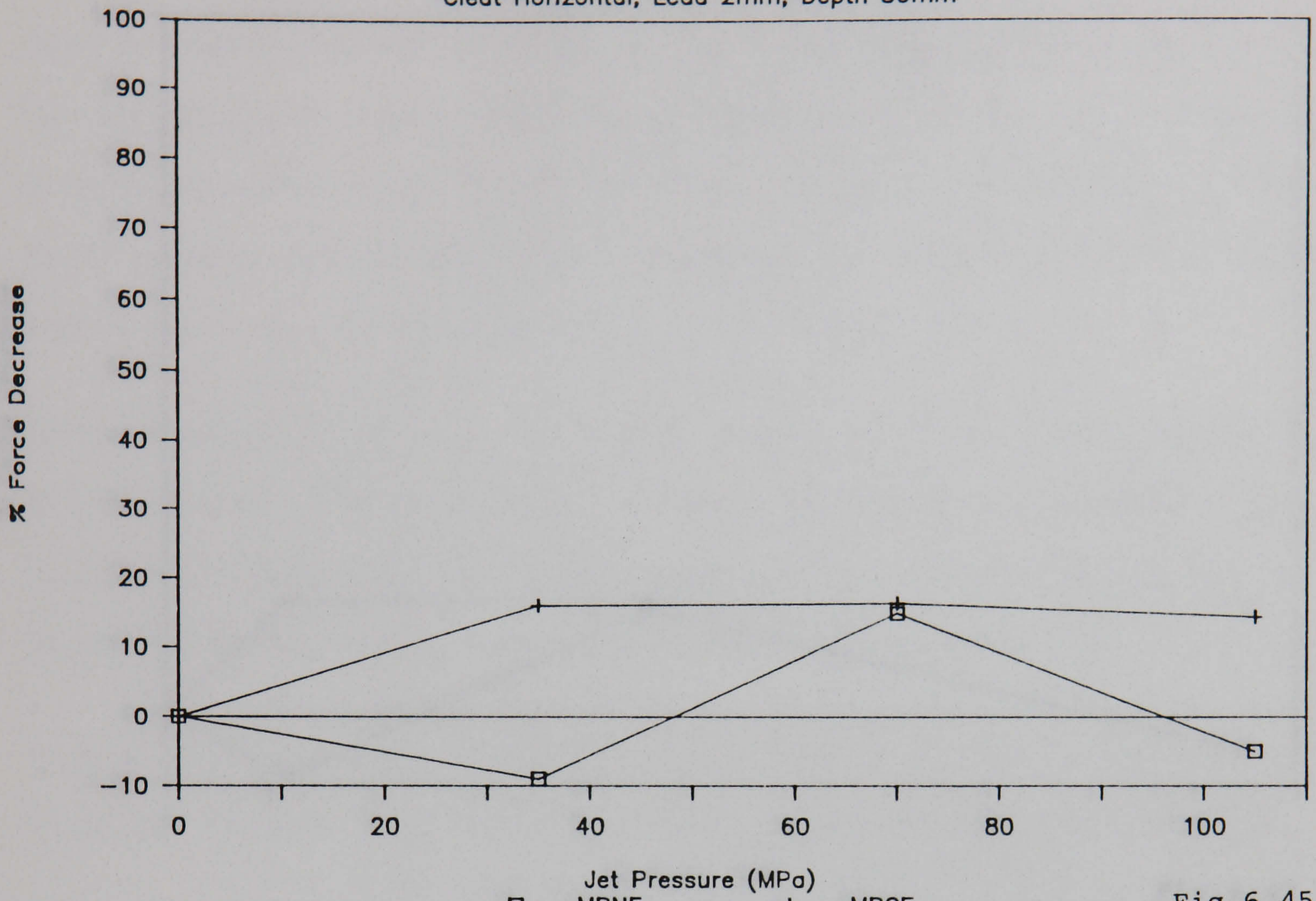


Fig.6.45

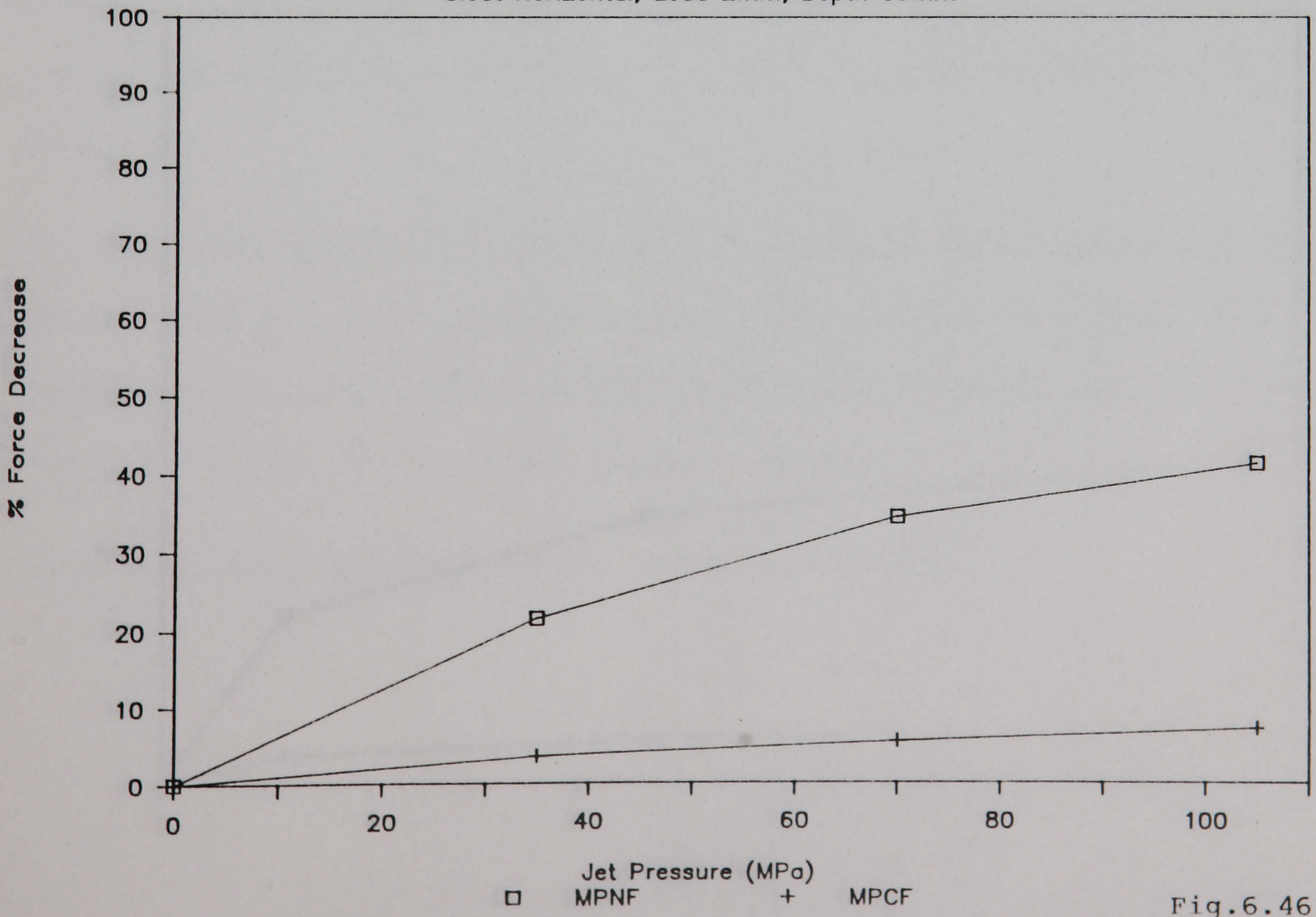


Fig.6.46

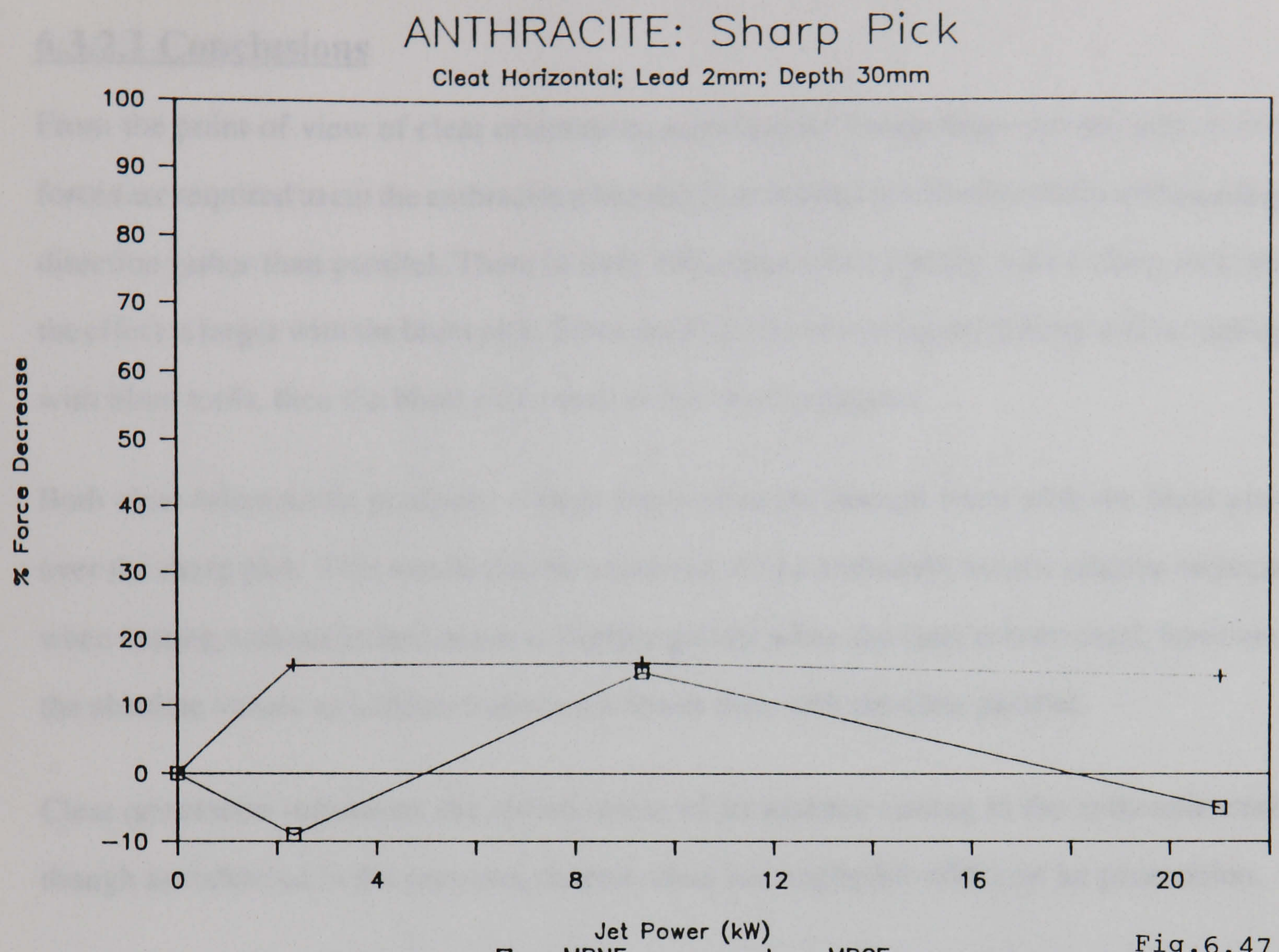


Fig.6.47

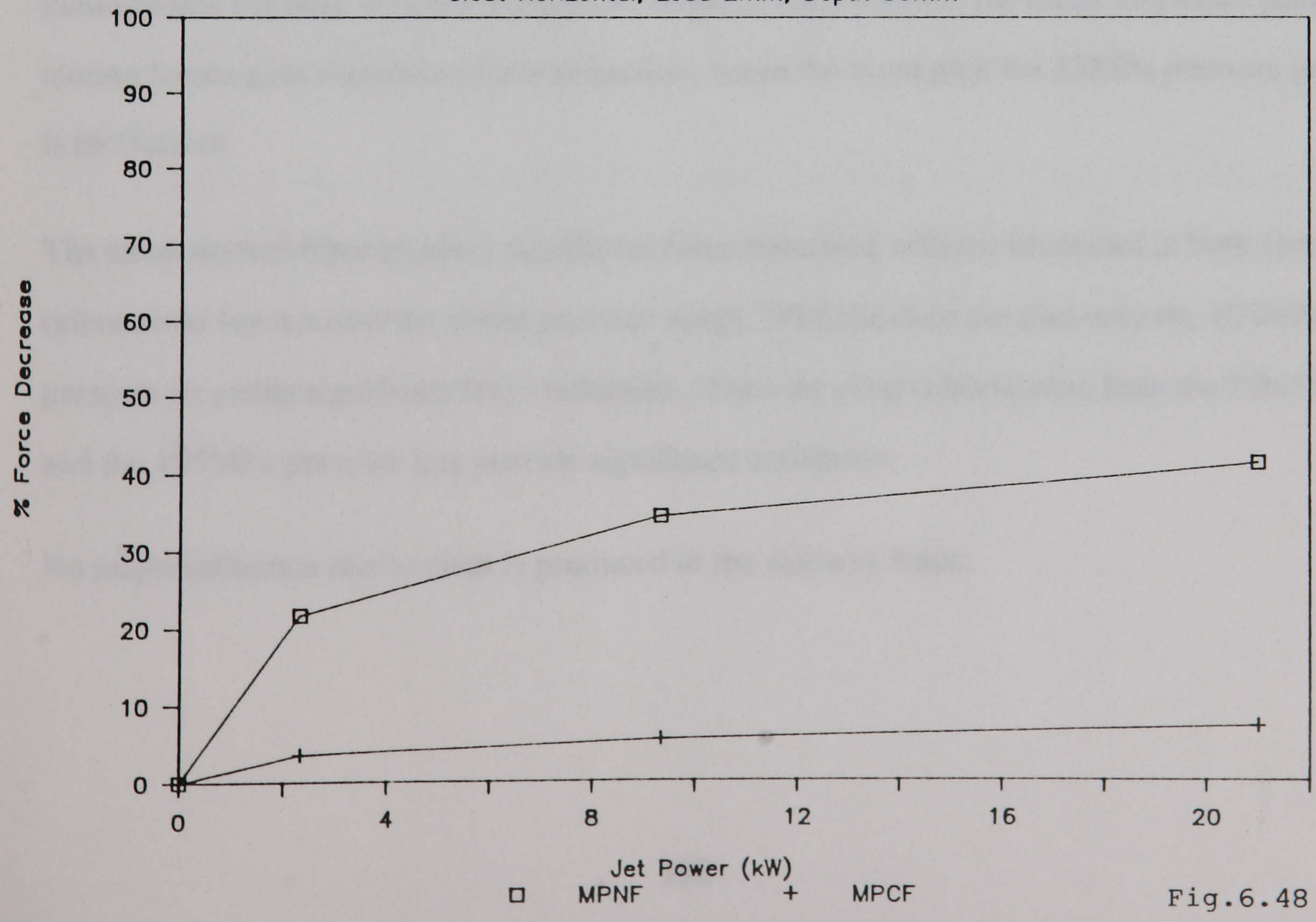


Fig.6.48

6.3.2.1 Conclusions

From the point of view of cleat orientation, significantly lower mean normal and cutting forces are required to cut the anthracite when the cleat is orientated horizontally to the cutting direction rather than parallel. There is little difference when cutting with a sharp pick but the effect is larger with the blunt pick. Since the majority of mining machinery will be cutting with blunt tools, then the blunt pick result is the most important.

Both cleat orientations produced a large increase in the normal force with the blunt pick over the sharp pick. This would also be a function of the anthracite but the relative increase when cutting without jet assistance is slightly greater when the cleat is horizontal; however, the absolute values as indicated above are lower than with the cleat parallel.

Cleat orientation influences the effectiveness of jet assisted cutting in the anthracite even though as indicated in the previous chapter, cleat has negligible effect on jet penetration.

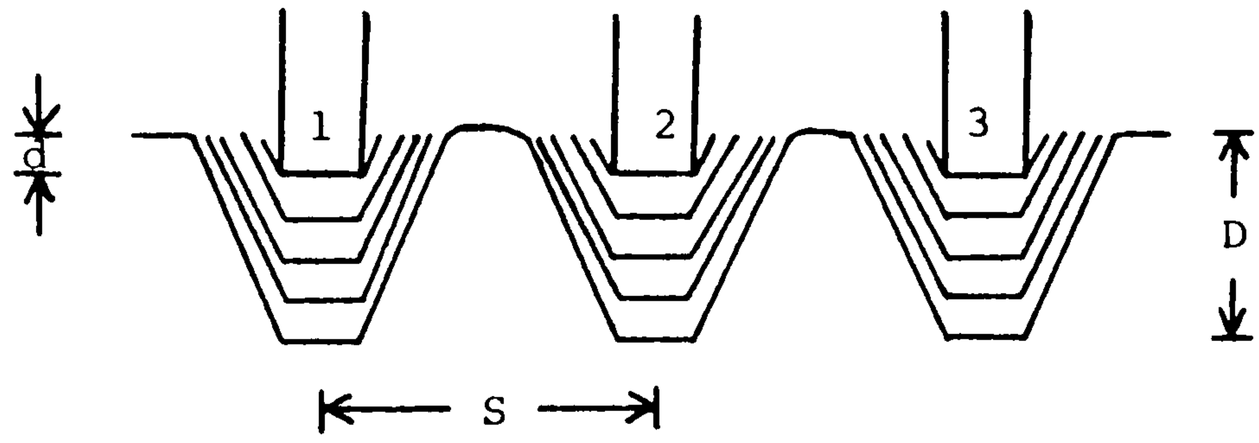
When the cleat is horizontal, no significant jet assistance is afforded the mean cutting force for both the sharp and blunt picks. However, some benefit is derived by the mean peak cutting force but only with the sharp pick. With the cleat parallel, the mean and mean peak cutting forces gain significant force reduction, but in the blunt pick the 35MPa pressure jet is ineffective.

The mean normal force receives significant force reduction with the blunt tool in both cleat orientations but not over the entire pressure range. With the cleat parallel only the 105MPa pressure jet yields significant force reduction. When the cleat is horizontal, both the 70MPa and the 105MPa pressure jets provide significant assistance.

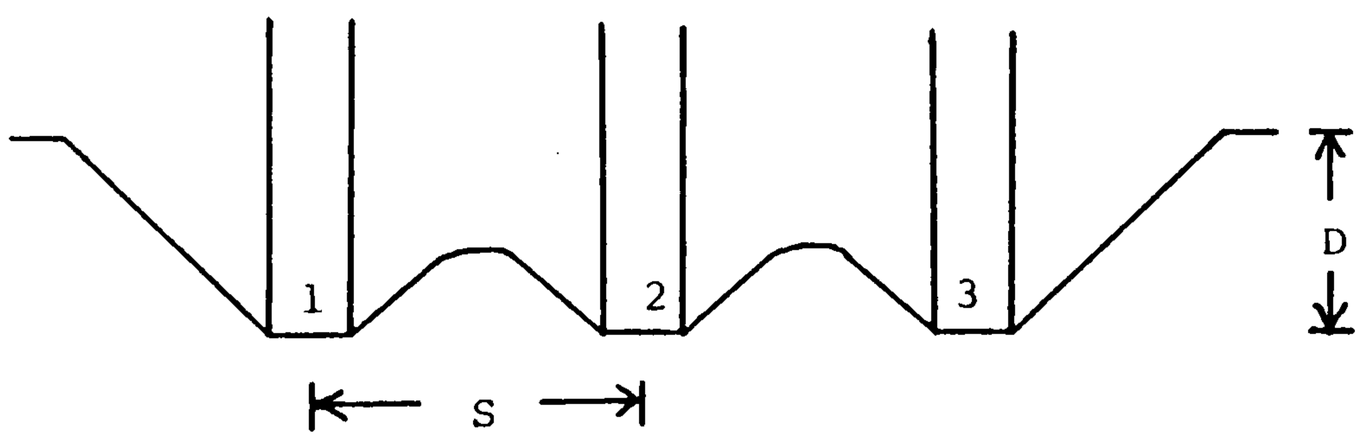
No major influence due to cleat is produced in the sideway force.

6.3.3 Breakout

The relative dimensions of depth of cut, line spacing and tool width basically determine whether a cutting system is efficient or not - in terms of cutting forces, specific energy, tool life and product size. (Pomeroy, 1963; Roxborough, 1973; Brooker, 1979).



a) Shallow cuts produce narrow channels and no interaction.



b) Deep cuts produce wide channels and interact.

Fig.6. 49 Effect of depth of cut on breakout.

The principle is illustrated in Fig.6.49. If a series of shallow cuts are taken as in Fig.6.49a, then little breakout occurs on either side of the tool; the product size will also be small. A continuation of this cutting regime will gradually lead to cores between the tools which will eventually completely disrupt the cutting process unless the tools are spaced closer.

Fig.6.49b, shows the way to avoid this: by taking deeper cuts but leaving the tools at the same spacing. This tends to produce less fines, reduce the specific energy and allows the majority of tools to experience relief from the preceding cut which reduces the cutting forces. For a coal cutting machine, the haulage rate may be increased leading to greater production.

Pomeroy, recommends a S/d ratio of 2.0 and Brooker, a minimum S/w ratio of 1.5, for efficient coal cutting. In this experiment the ratios were S/d = 2.33 and S/w = 2.80, and so theoretically the experiment represents an efficient cutting system.

An examination of the breakout was required to investigate the influence of the jet assistance on breakout.

6.3.3.1 Erin Coal - Cleat Parallel

Breakout in the Erin coal was characterised by high ridges between the grooves cut by the tool.

With the sharp pick cuts one could see the V-shape of the pick tip in the coal. The bottom of the grooves cut with the blunt tool were flat. This suggests that fracture was not occurring beneath the tip of the pick in both states of wear.

The dry cut blunt tool visibly created more breakout than the sharp pick and generally this was true with the jet assistance.

Plates 6.1-4, illustrate the breakout profiles of the sharp and blunt picks for the treatments at 35MPa and 105MPa water jet pressure. There is visibly more breakout at the higher pressure than the lower, despite the scale of each plate.



Plate 6.1 Breakout for Erin coal; sharp pick; 35MPa treatment.



Plate 6.2 Breakout for Erin coal; sharp pick; 35MPa treatment.



Plate 6.3 Breakout for Erin coal; sharp pick; 105MPa treatment.



Plate 6.4 Breakout for Erin coal; blunt pick; 105MPa treatment.

The heights of the ridges between the groves were measured though there was great variability and irregularity along the length of the cut. Generally the heights did not vary greatly between treatments. Averaged over the four treatments, the sharp pick heights were 20.7mm and the blunt pick 19.2mm. One can see the irregularities of the ridges, thus effectively there is little difference.

The factor that has influenced the breakout in the Erin coal then, is not so much the heights of the peaks but the amount of material taken from the sides of the ridges. This may be explained by looking at the cleat. The cleat is vertical and parallel to the cutting direction and the sides of the ridges are largely vertical, thus it seems that fracture is occurring along the cleat planes. In this situation the tool has majorly cut a groove through which to travel, extensive sidesplay not being made possible due to fracture along the cleat planes. Even with the 105MPa pressure jets in Plates 6.3-4, where most breakout has occurred, one cannot see a well defined V-shaped breakout pattern, one sees vertical lumps projecting up from the body of the coal.

Occasionally, almost horizontal or total breakout occurred between grooves, but this was not typical and was associated with areas of dull and dusty coal.

Fig.6.50, is a representation of the breakout found in a heavily cleated coal such as the Erin coal. The cutting sequence is the same as the one in the present study and illustrates the relieved cutting mode. Line one, would be the surface preparation cuts and line two, the actual cuts recorded in the tests.

The tool at 2B receives relief from the breakout at 2A and 1A. Coal may also breakout to the left and gain relief from 1B. The thick dark line is the breakout pattern which approximates the ones observed for dry cutting. With jet assistance more material would be loosened and broken away.

Idealized Breakout for Heavily Cleated Friable Coal

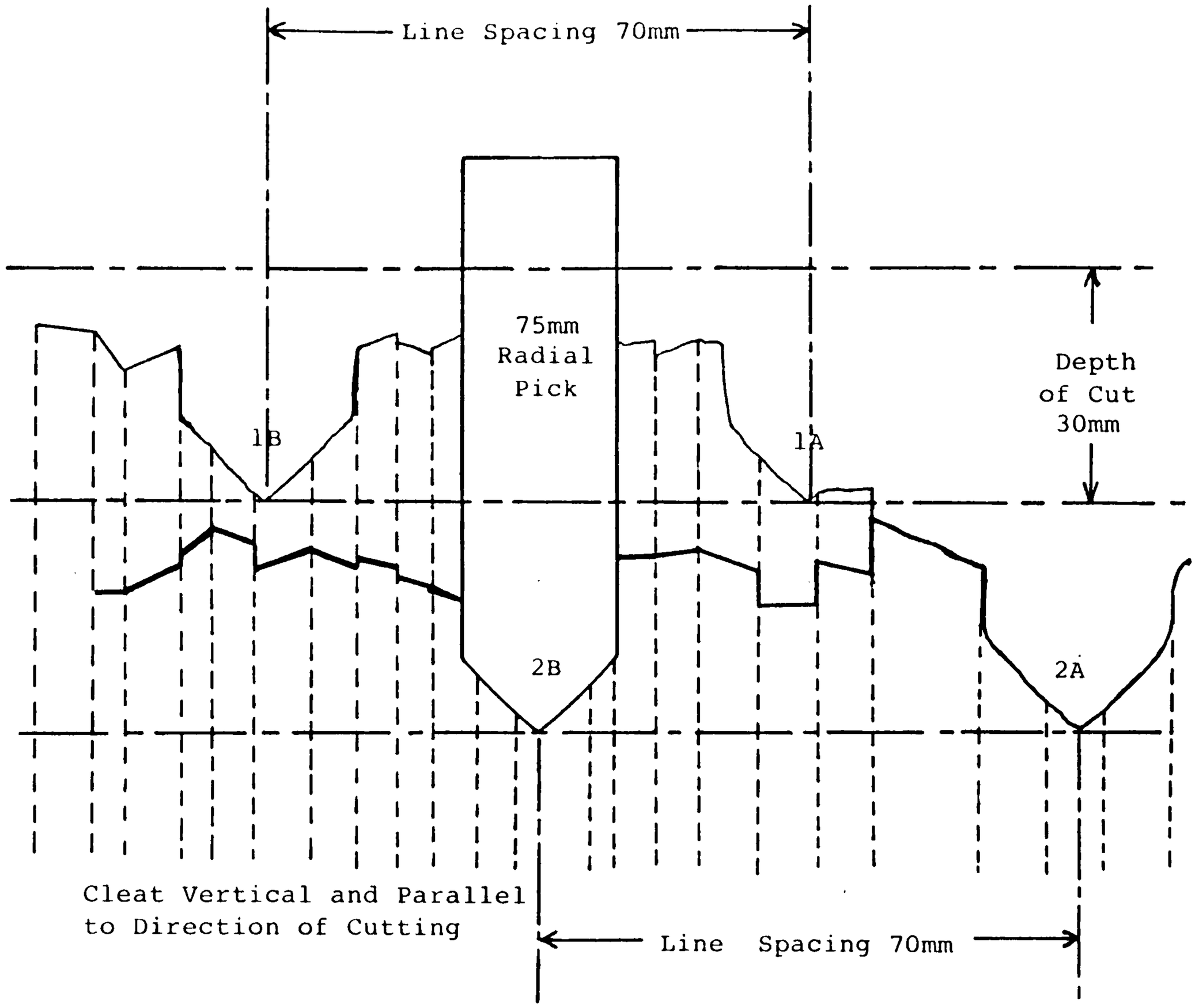


Fig.6.50

Graphs of coal yield against jet pressure and power are given in Fig.6.51-52. The graphs indicate that the blunt tool excavates slightly more coal than the sharp tool, except at 105MPa jet pressure. The averages over all treatments were 2.779kg/m and 2.820kg/m for the sharp and blunt tool respectively. The yield rises with jet pressure but only slightly.

6.3.3.2 Anthracite Coal - Cleat Parallel

Examples of the breakouts in the anthracite are given in Plates 6.5-8. One can immediately notice the difference in texture from the bituminous Erin coal. The high degree of shiny clarain and vitrain make the detail more difficult to discern. However, the coal in the ridges is not broken, heavily cleated and irregular but firmly bonded together, smoother and more regular.

In the dry cut tests, the breakout is less with the blunt tool than with the sharp pick, Plate 6.7. The V-shaped tip of the tool could be seen along the length of cut indicating that fracture did not extend beneath the tip. This occurred with the blunt pick also, and the bottom of the grooves were flat and 10mm wide, the width of the wear flat.

The breakout tended to increase as the jet pressure increased with both picks. Plates 6.5-6, illustrate the difference between the dry blunt pick and the blunt pick 35MPa and 70MPa pressure tests. With the 70MPa pressure treatment, the ridges between line spacings are much smaller and peak at about 10mm high. Larger undulations on the surface of the coal are visible with the unassisted blunt pick, Plate 6.5, but even so the same degree of grooving as in the Erin coal is not evident and more sidesplay is taking place. One can see this more clearly in Plate 6.7.

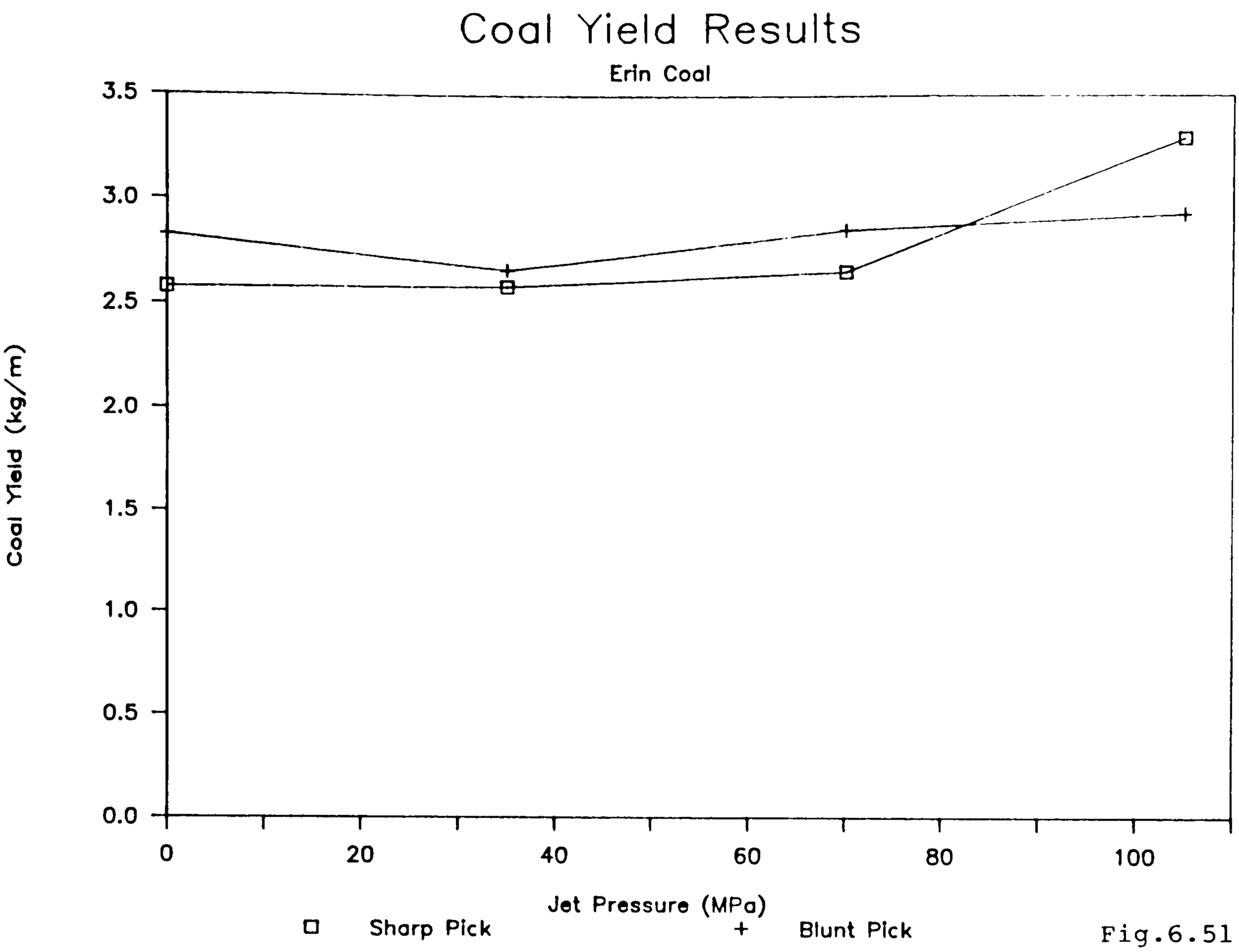


Fig.6.51

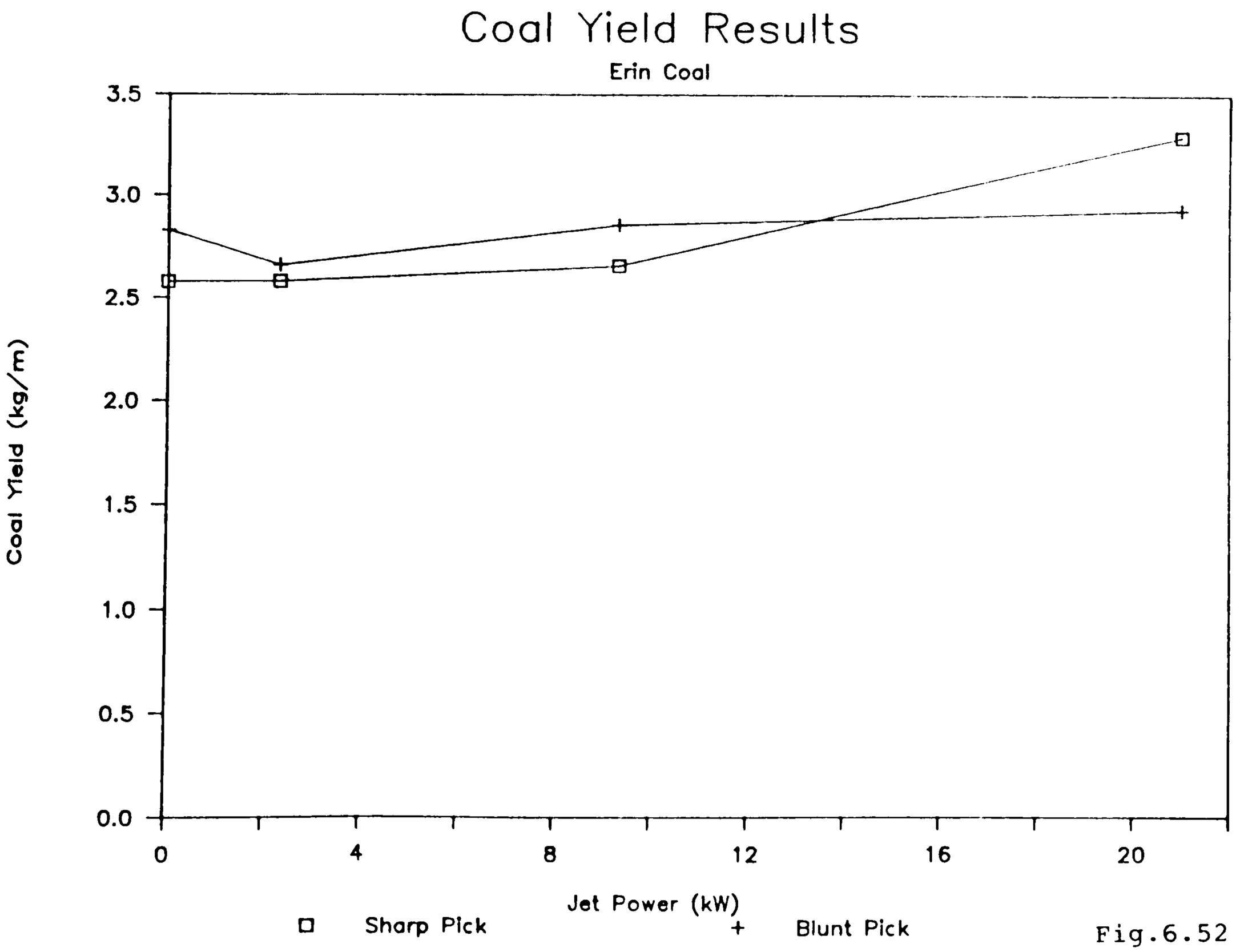


Fig.6.52



Plate 6.5 Breakout for the anthracite coal (cleat parallel); blunt pick; 35MPa treatment.



Plate 6.6 Breakout for the anthracite coal (cleat parallel); blunt pick; dry and 70MPa treatments.



Plate 6.7 Breakout for the anthracite coal (cleat parallel); sharp pick; dry treatment.

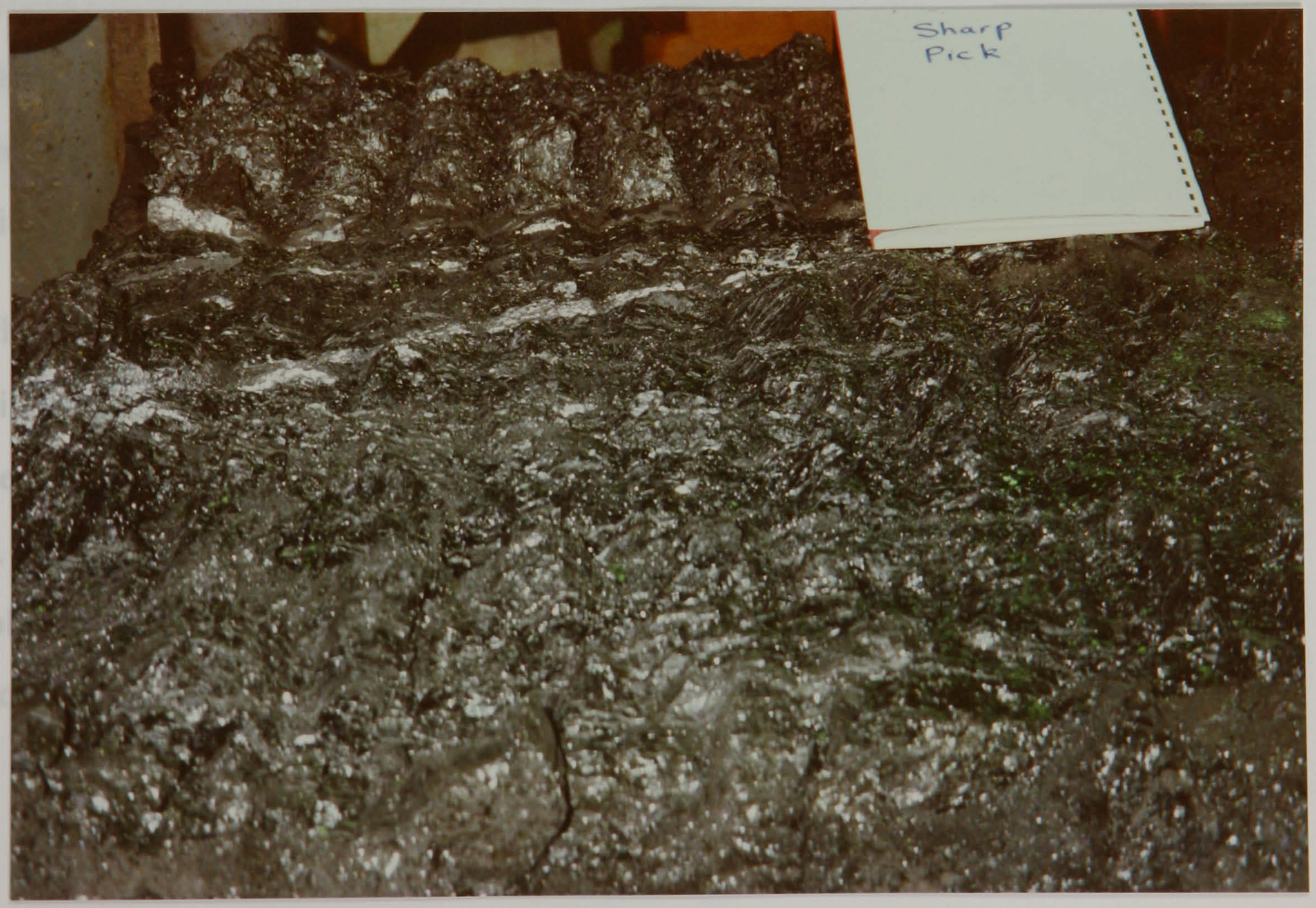


Plate 6.8 Breakout for the anthracite coal (cleat parallel); sharp pick; 70MPa treatment.

A diagrammatic representation of the breakout for unassisted cutting is given in Fig.6.53. The irregularity of the breakout makes it difficult to present a typical case. In some places the ridges were more pointed and with the dry blunt pick the sides of the ridges were higher and nearer to the vertical, breaking out along cleat planes. However, the difference in pattern to that of the Erin coal is evident.

The yields are plotted in Fig.6.54-55. Averaged over the pressure range the blunt tool gave a slightly greater yield: 3.110kg/m to 3.082kg/m. On average the anthracite released 0.296kg/m more coal than the Erin.

6.3.3.3 Anthracite Coal - Cleat Horizontal

The breakout patterns for the unassisted, dry tests with the sharp and blunt tool are illustrated in Plates 6.9-10 respectively. Some variability was observed between the two coal blocks that had been cast together to form the test specimen. In Plate 6.9, the coal nearest the bottom of the picture has the major cleat slightly inclined from the horizontal. The coal more to the top of the plate has not got such a well defined cleat structure, the cleat is more inclined and it contains a band of fused brittle coal across its width about 40mm wide.

From Plate 6.9, one can see the pointed groove made by the sharp pick and the breakout pattern inbetween. The ridges are up to 10-20mm high from the base of the groove. In Plate 6.10, the coal is viewed from a different position and the coal at the top of the picture is of interest. The grooves made by the tool may be seen and indicate the width of the wear flat for the blunt pick. The ridges inbetween are 9-15mm high and are fairly flat-topped following the direction of the cleat. The cleat is also inclined 9°-14° towards the reader.

Breakout for Cleat Parallel to Direction of Cut

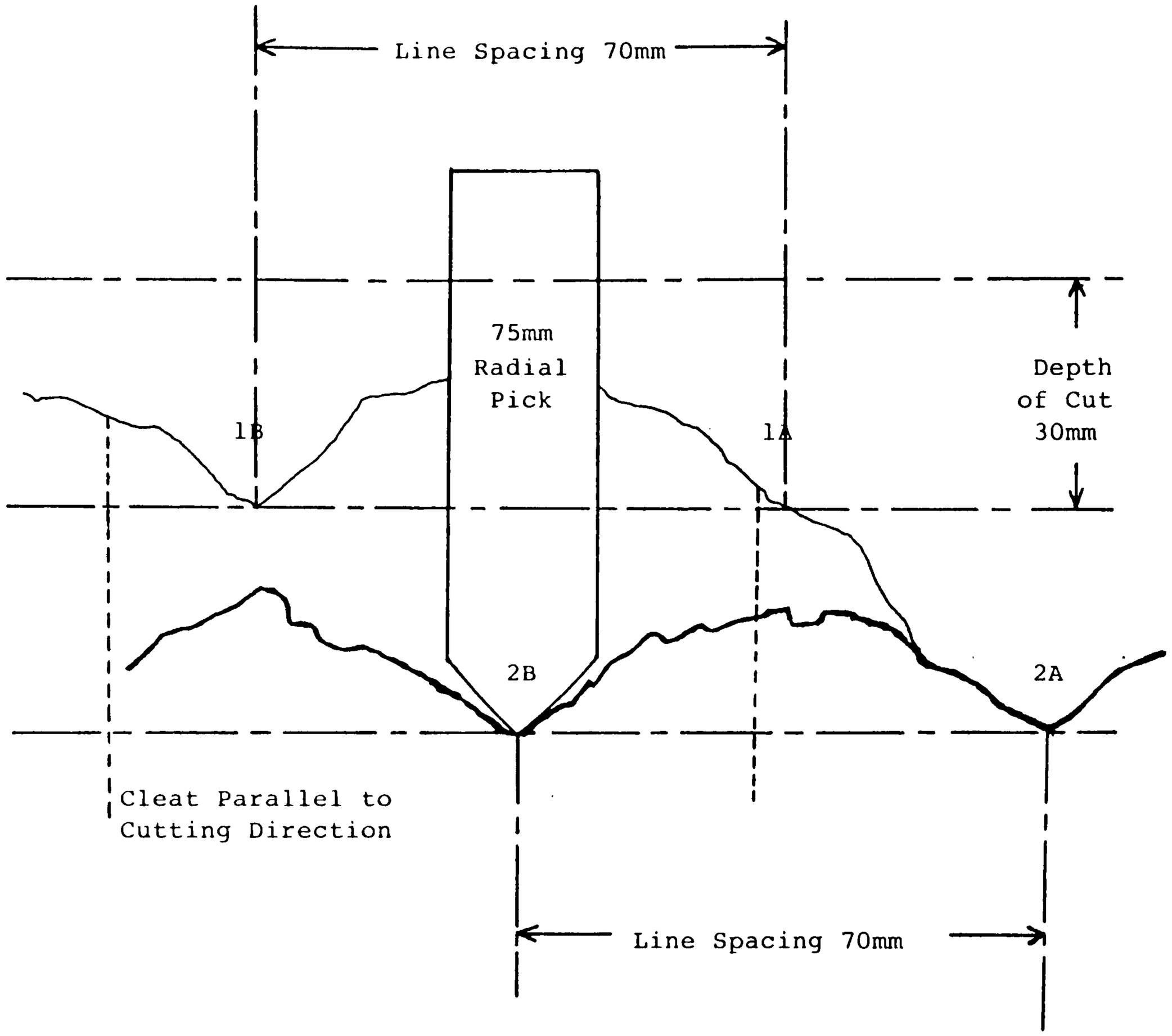


Fig.6.53

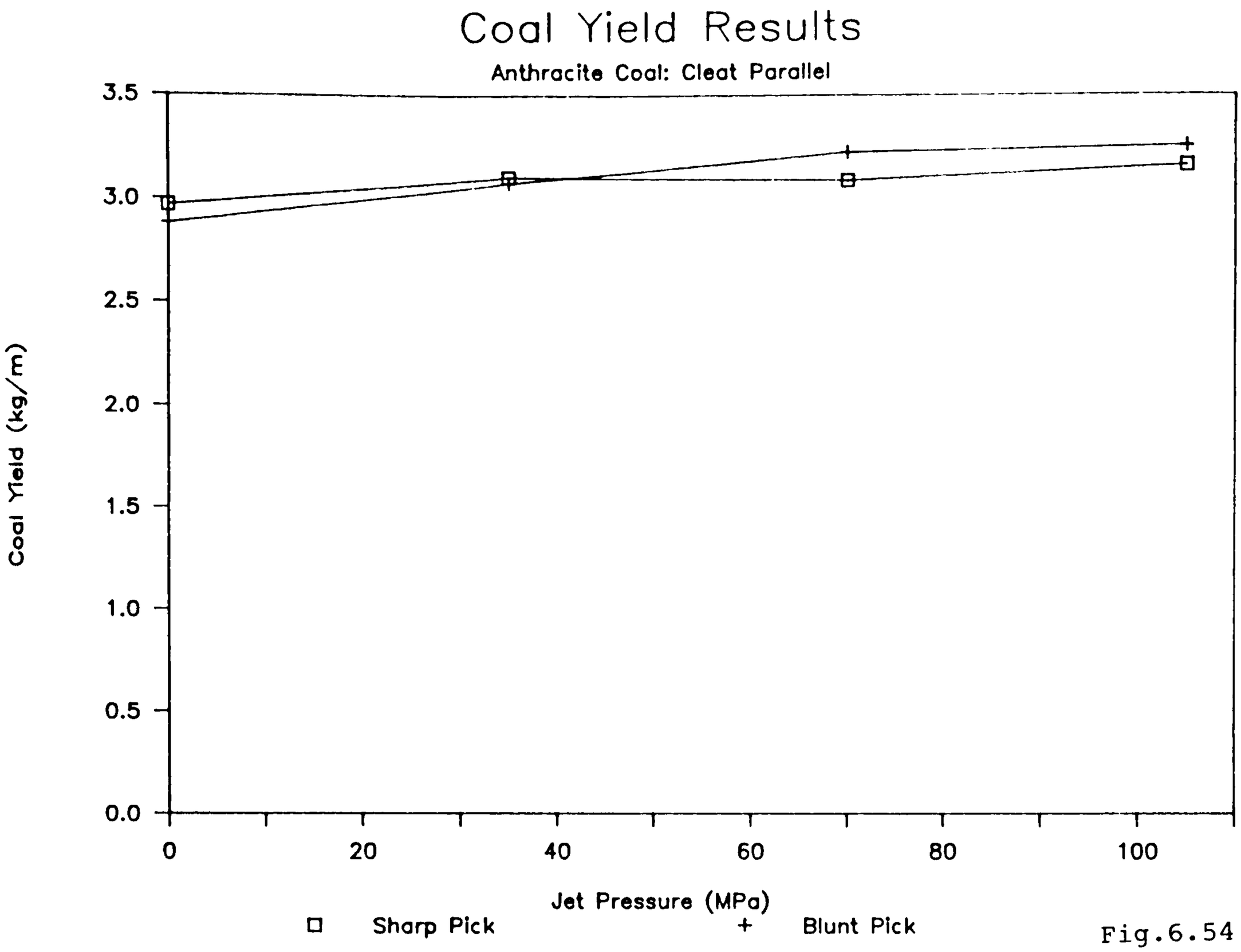


Fig.6.54

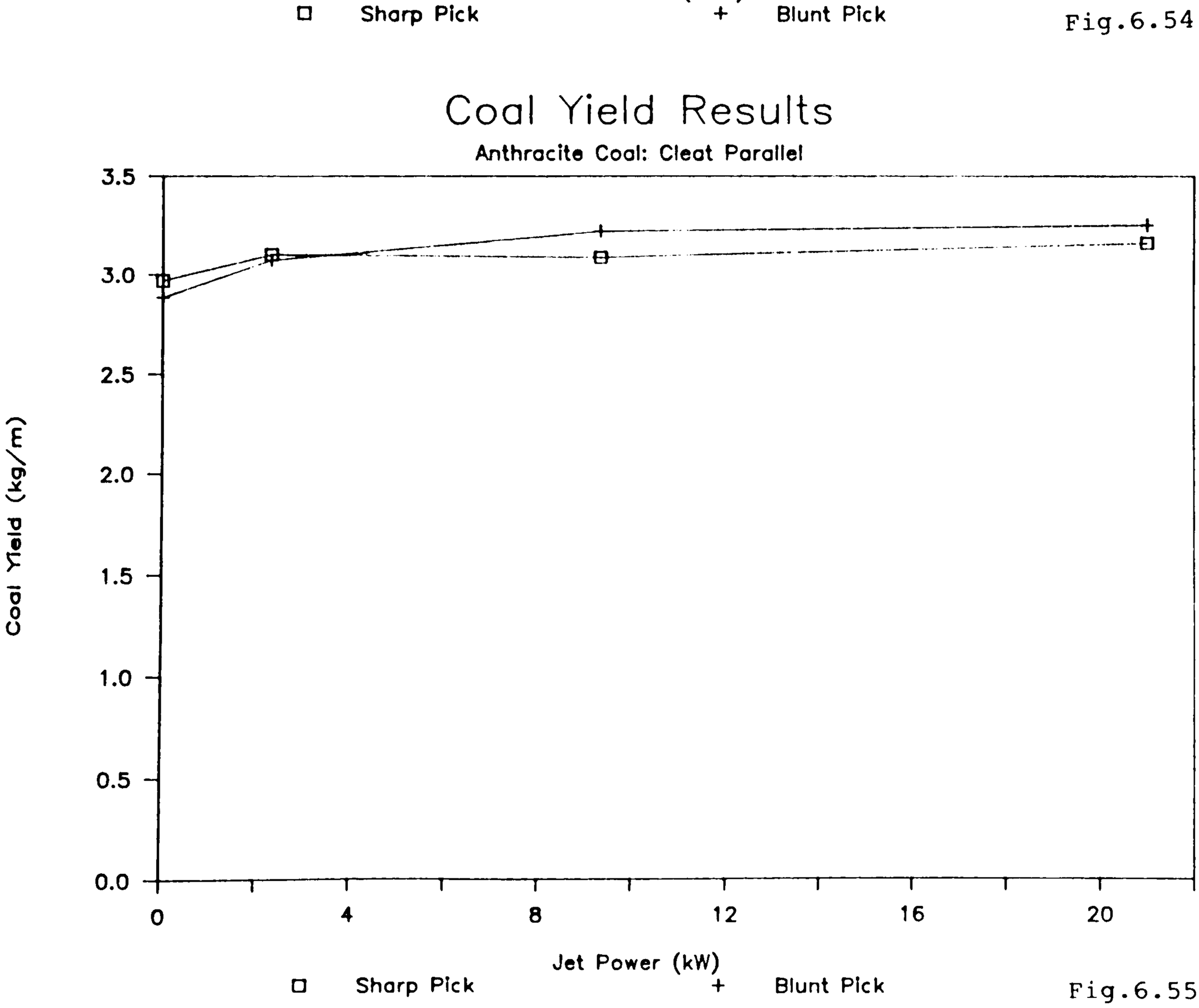


Fig.6.55

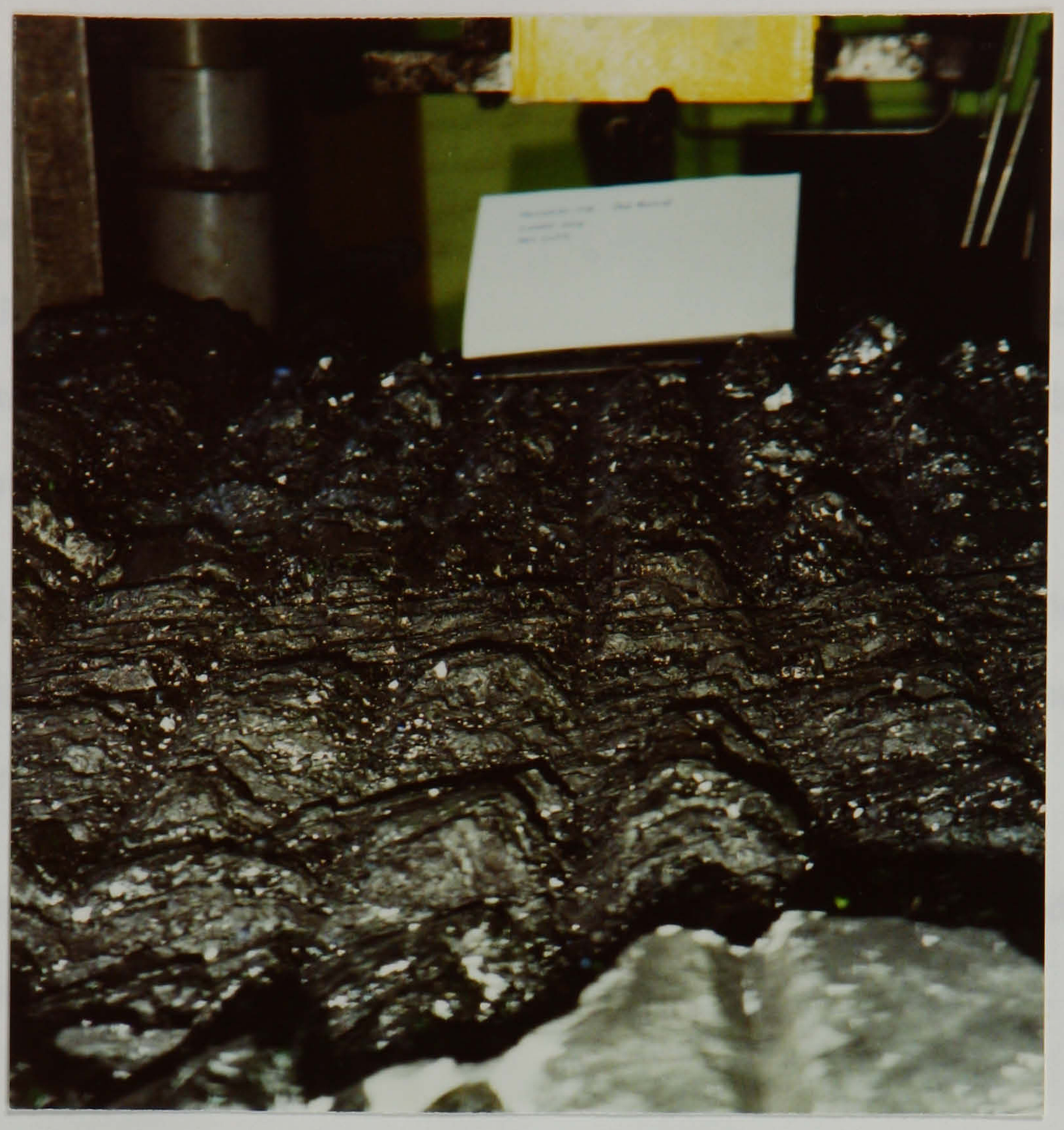


Plate 6.9 Breakout for the anthracite coal (cleat horizontal); sharp pick; dry treatment.



Plate 6.10 Breakout for the anthracite coal (cleat horizontal); blunt pick; dry treatment.

Plates 6.11-12, show the breakout pattern at 35MPa jet assistance for the sharp and blunt tools. In the centres of the illustrations one can see the levelled tops of the ridges inbetween the grooves left by the cutting tool. Average heights of the ridges from the bottom of the grooves are 13mm and 9mm respectively.

Fig.6.56, shows the typical breakout pattern observed when the cleat was horizontal. The breakout surfaces were flat and followed the inclination of the cleat. The thick dark line would be the breakout after cut 2B was taken.

On average the yield was less than with the cleat vertical: 3.096kg/m to 2.960kg/m. Yields are plotted in Fig.6.57-58, the blunt tool gave fractionally more yield than the sharp one.



Plate 6.11 Breakout for the anthracite coal (cleat horizontal); sharp pick; 35MPa treatment.



Plate 6.12 Breakout for the anthracite coal (cleat horizontal); blunt pick; 35MPa treatment.

Breakout for Cleat Horizontally Orientated

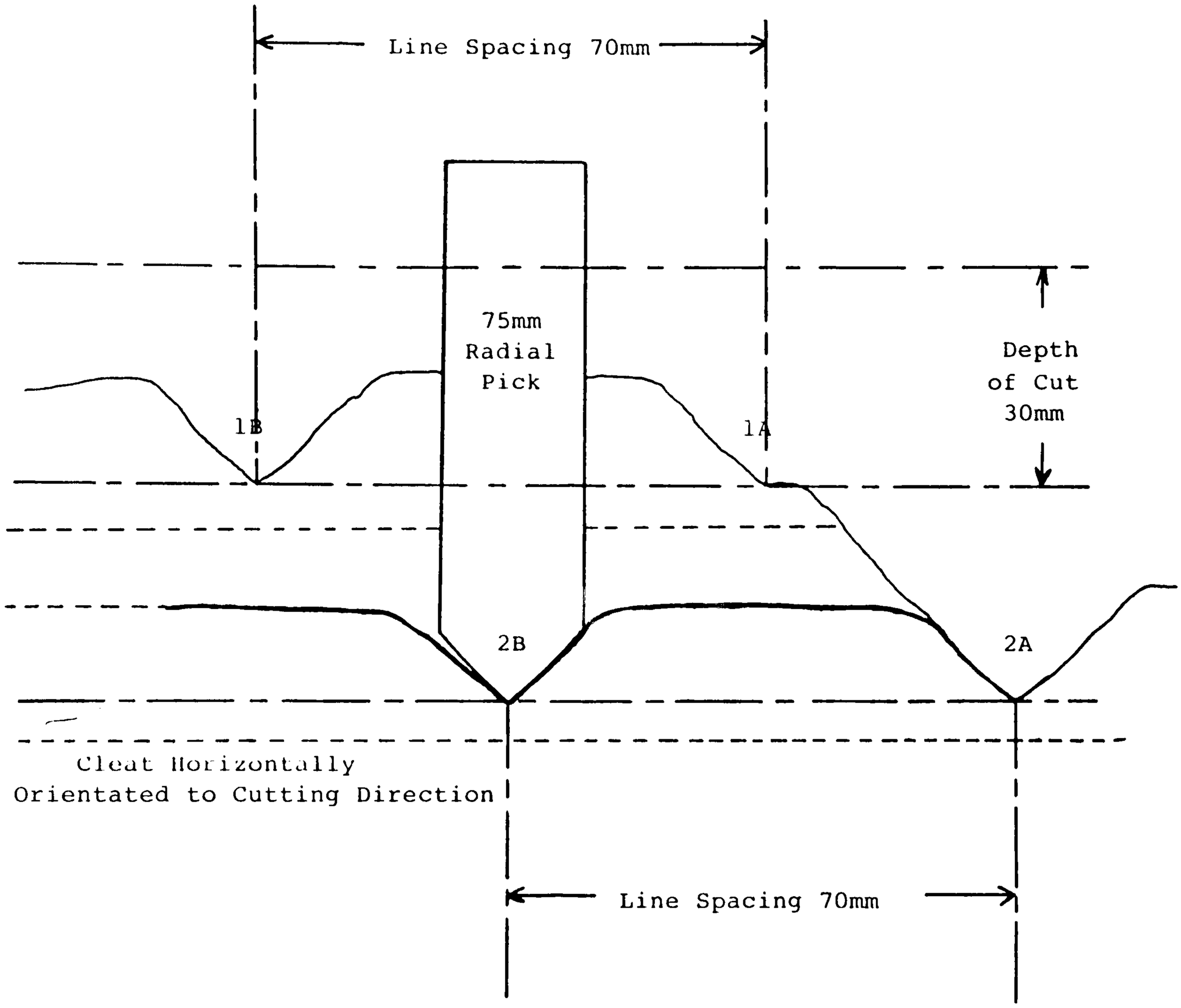


Fig.6.56

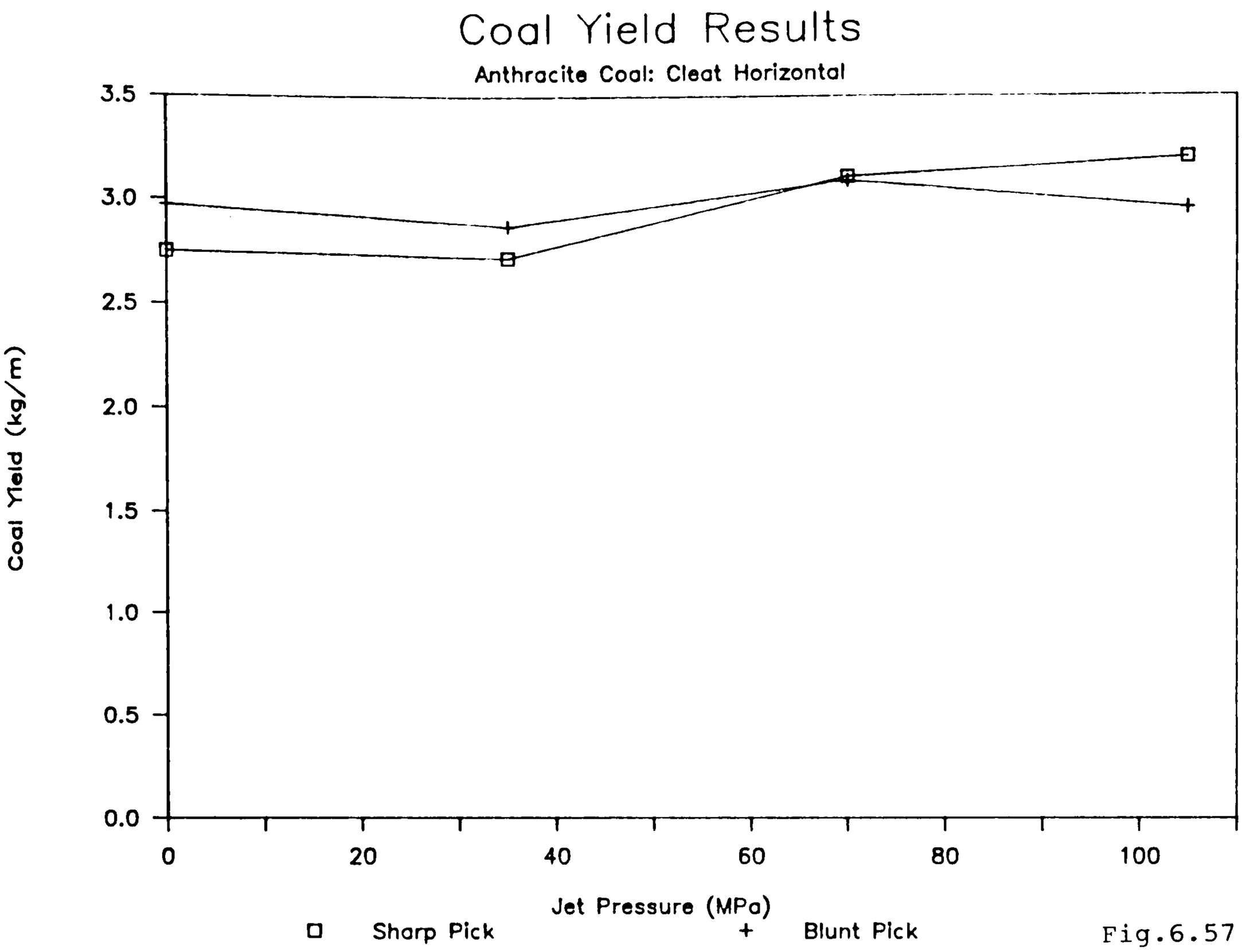


Fig.6.57

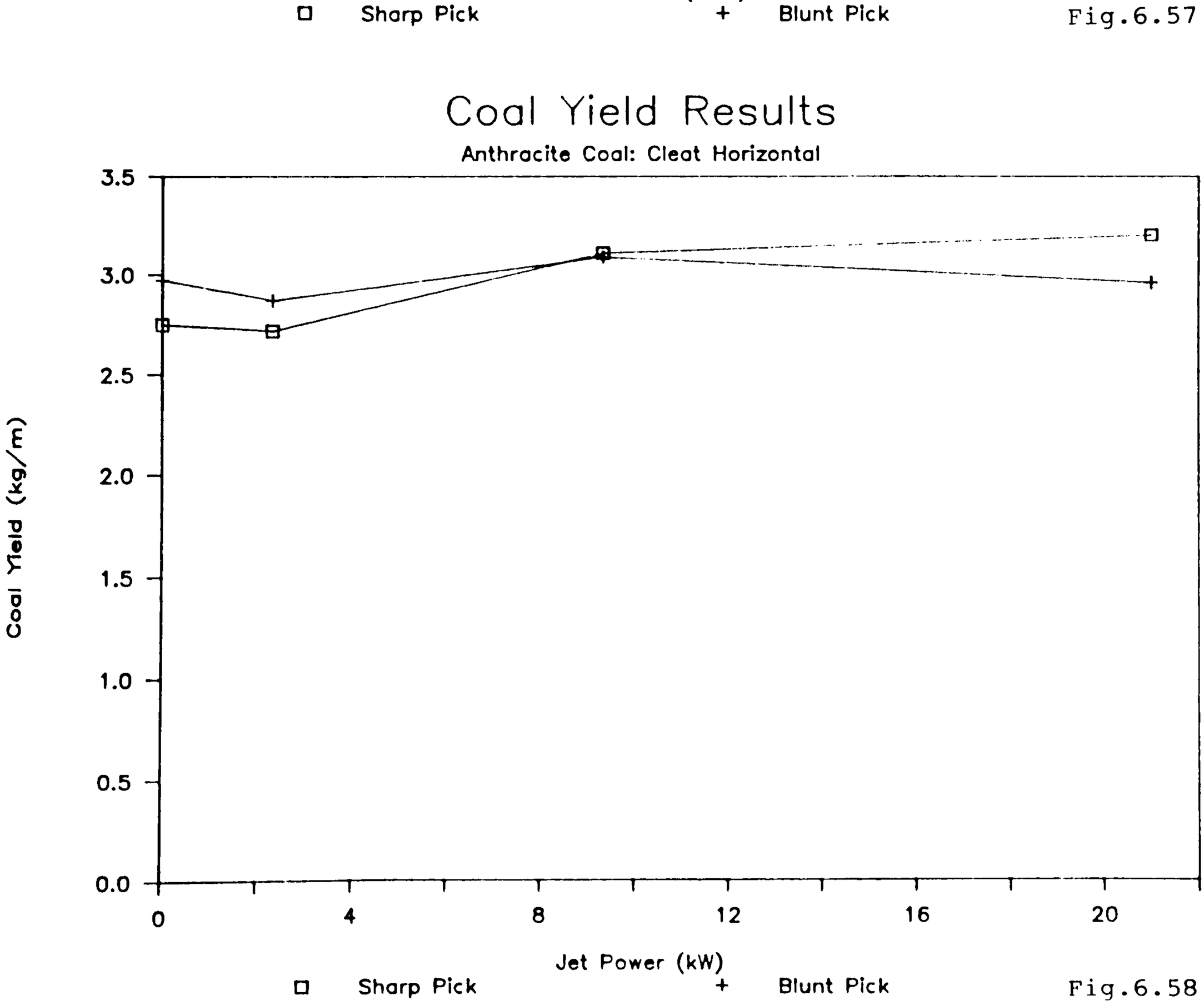


Fig.6.58

6.3.4 Specific Energy

Specific energy is a valuable index to determine the most efficient cutting system in terms of the energy required to excavate unit mass or volume of material. Specific energy for unassisted coal cutting is given by the equation below:

$$\text{Specific Energy, SE} = F_c \frac{\rho}{Y} \tag{6.1}$$

Where

F_c = Mean cutting force

ρ = Coal density

Y = Yield

The mean cutting force is used in the calculation since this is the average force acting in the direction work is being done. The normal force is perpendicular to this and hence cannot be used by the definition of work.

With jet assistance the jet does not act in the direction of travel of the pick but almost perpendicularly to it. If the jet energy is to be included in the calculation of the specific energy then only the component of the jet energy acting in the same direction as the cutting force should be included. However, the author thinks this is unreasonable since jets have been positioned behind the tool which theoretically increases the proportion of energy in the cutting direction, but this does not produce proportionally greater benefit with respect to force reduction than if the jet had been placed before the tool. Also, the jet is not being used primarily as a cutting agent, so in the present study the total jet energy has been included in the calculation of specific energy for the treatments with jet assistance.

The equation used for calculating the specific energy including jet energy is:

$$\text{Specific Energy, } SE_j = \left(F_{cj} + \frac{P_w}{v_t} \right) \frac{\rho}{Y_j} \tag{6.2}$$

Where

F_{cj} = Mean cutting force with jet assistance

ρ = Coal density

Y_j = Yield with jet assistance

P_w = Jet power

v_t = Cutting speed

The specific energies for the coals tested in the experiment are plotted in Fig.6.59-64. Actually, two sets of results are drawn: the plots with the specific energy increasing over the pressure and power ranges include the jet energy; the curves decreasing do not and are based merely on the reduced mean cutting force at that pressure or power.

Against jet pressure, specific energy increases exponentially over the range. Against jet power, the increase is linear. Without the jet energy included, the specific energy generally decreases with jet pressure. Curve fits to the graphs are in the appendices.

Taking the blunt tool results as the most important, there was little difference in specific energy between the Erin and anthracite with the cleat parallel for the unassisted tests; the Erin was fractionally greater. Between the cleat orientations in the anthracite though there was a 37% difference: cutting with the cleat horizontal is the most efficient, the values were, $0.715 MJ/m^3$ to $1.141 MJ/m^3$.

With jet assistance there is little difference in specific energies between cleat direction except at 105MPa jet pressure where the cleat parallel cutting becomes the most efficient. Also,

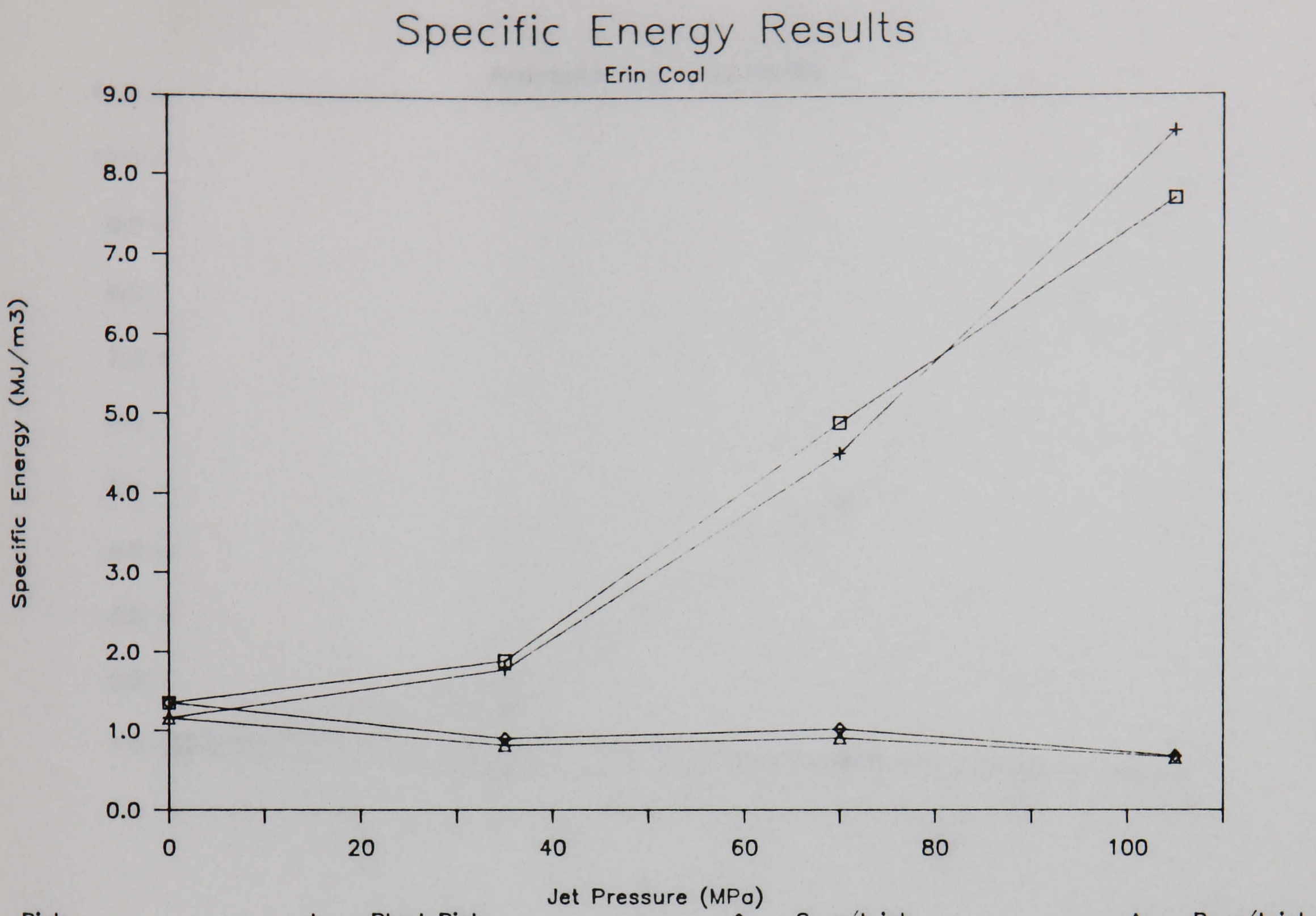


Fig.6.59

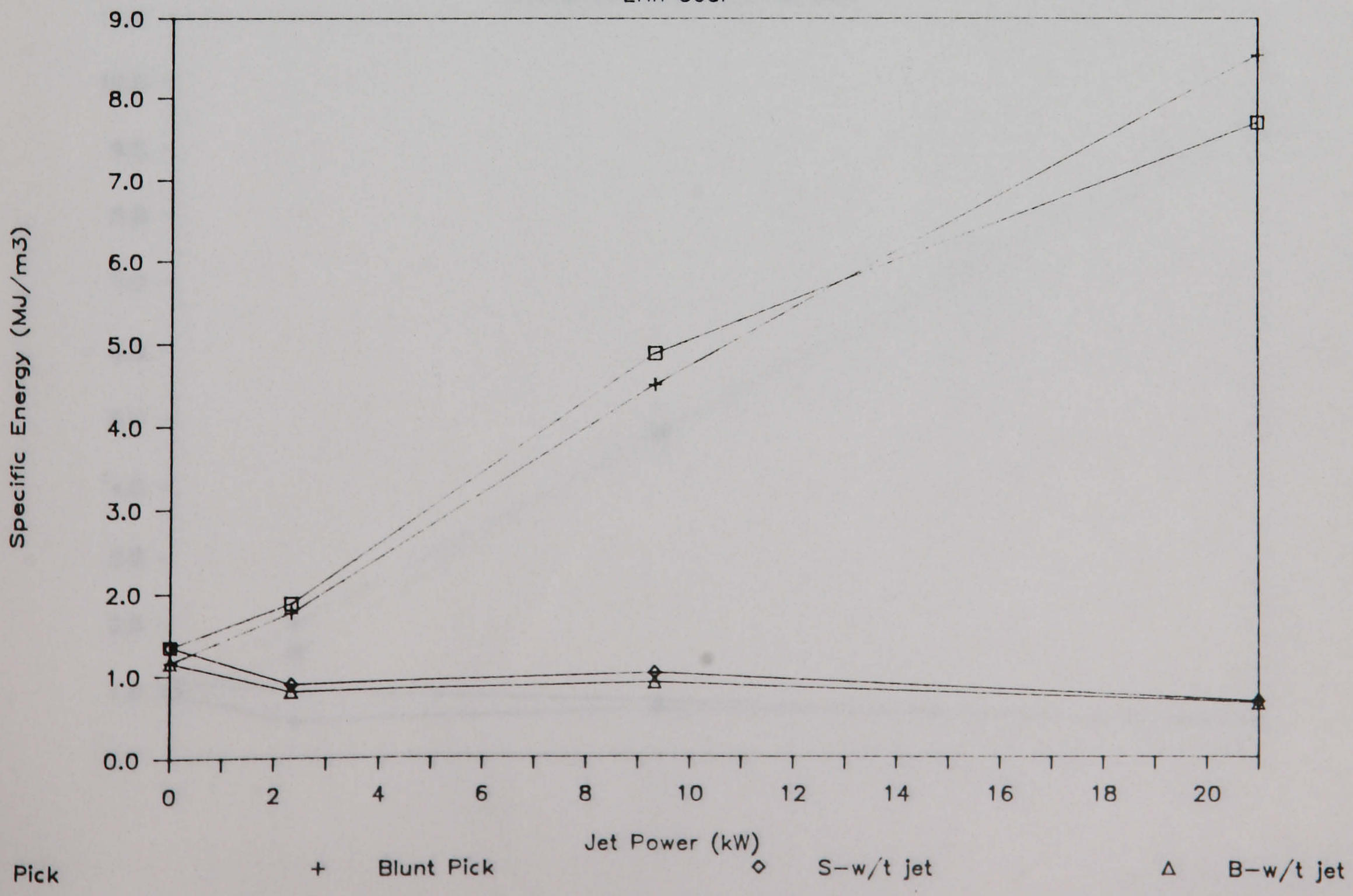


Fig.6.60

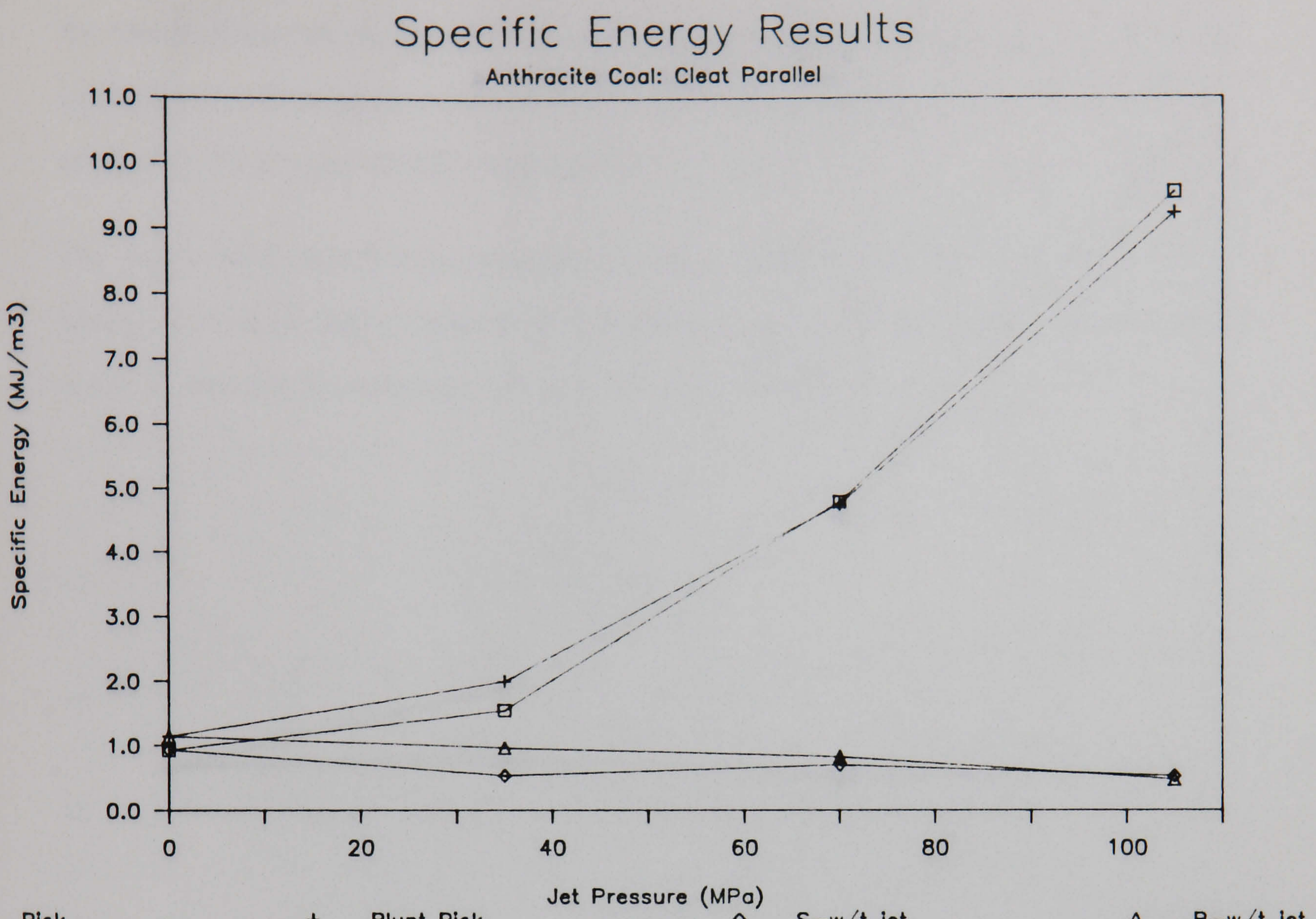


Fig.6.61

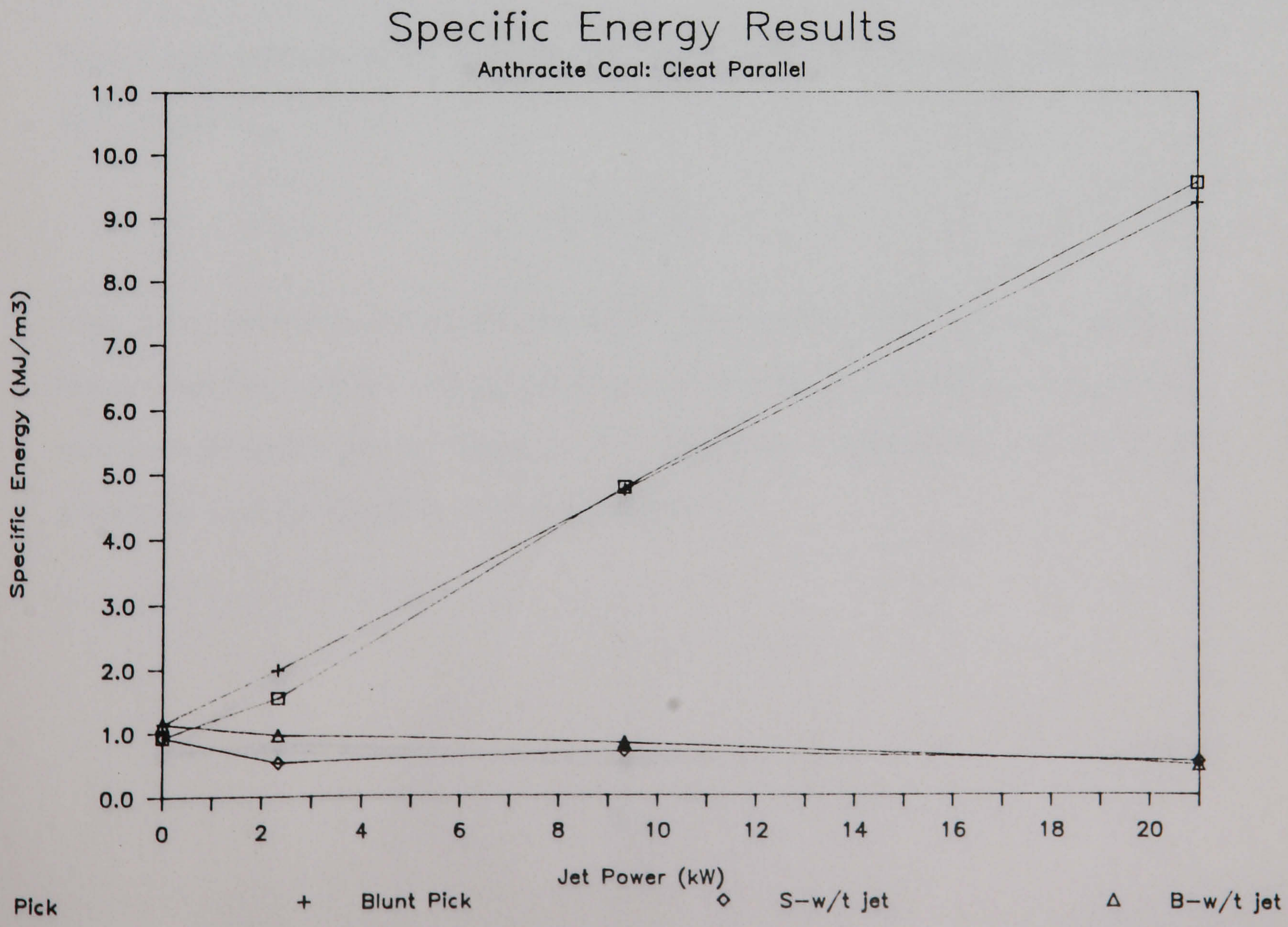


Fig.6.62

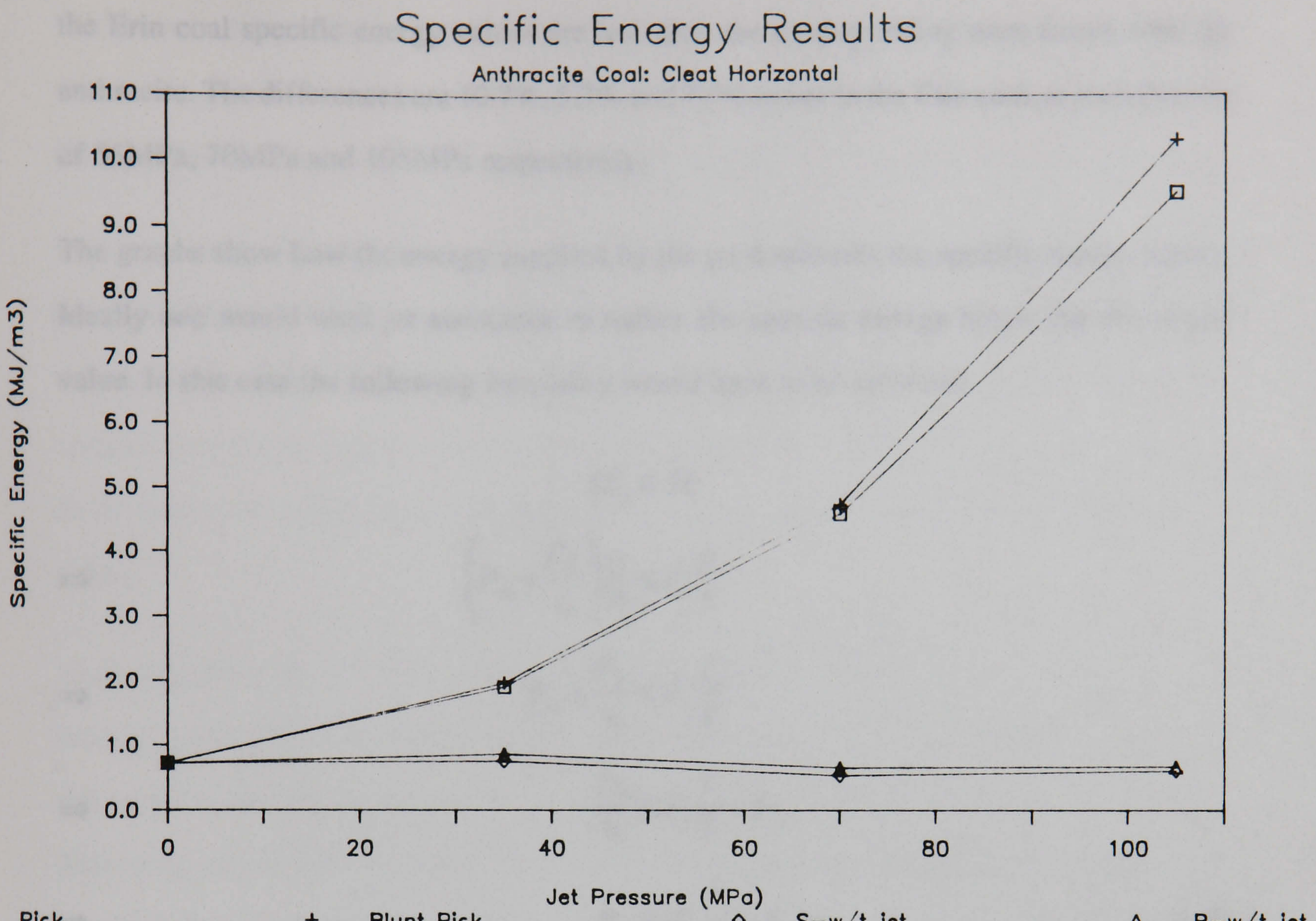


Fig.6.63

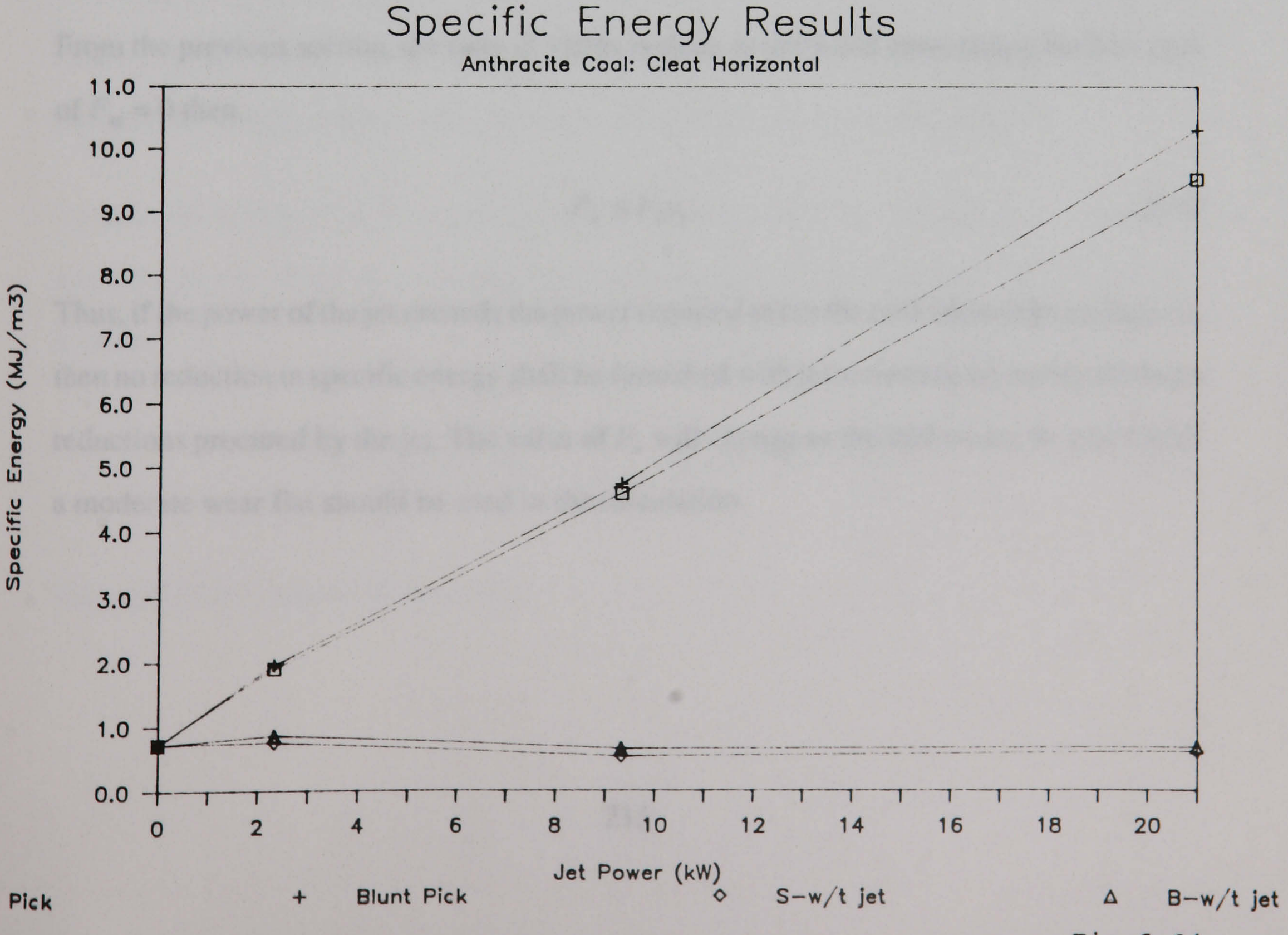


Fig.6.64

the Erin coal specific energy values are less than the corresponding ones found with the anthracite. The differences are 10.7%, 5.2% and 7.5% lower in the Erin coal, at jet pressures of 35MPa, 70MPa and 105MPa respectively.

The graphs show how the energy supplied by the jet dominates the specific energy values. Ideally one would want jet assistance to reduce the specific energy below the unassisted value. In this case the following inequality would have to be satisfied:

$$SE_j \le SE$$

$$\Rightarrow \quad \left(F_{cj} + \frac{P_w}{v_t}\right)\frac{\rho}{Y_j} \le F_c \frac{\rho}{Y}$$

$$\Rightarrow \quad F_{cj} + \frac{P_w}{v_t} \le F_c \frac{Y_j}{Y}$$

$$\Rightarrow \quad \frac{P_w}{v_t} \le F_c \frac{Y_j}{Y} - F_{cj}$$

$$\Rightarrow \quad P_w \le (F_c \frac{Y_j}{Y} - F_{cj})v_t \qquad (6.3)$$

From the previous section, the ratio of yields is close to unity and considering the best case of $F_{cj} = 0$ then,

$$P_w \le F_c v_t \qquad (6.4)$$

Thus, if the power of the jet exceeds the power required to cut the coal without jet assistance, then no reduction in specific energy shall be furnished with jet assistance no matter the force reductions procured by the jet. The value of F_c will change as the tool wears, so a tool with a moderate wear flat should be used in the calculation.

With respect to specific energy then, jet assistance has more potential or scope in situations where the specific energy to cut the mineral is already high i.e. in hard minerals and/or with fast cutting speeds, providing of course the jets can reduce the cutting forces sufficiently.

In the present study and for the above condition to be satisfied, the jet power should not exceed 2.98kW in the Erin coal; 2.18kW (cleat parallel) and 1.83kW (cleat horizontal) in the anthracite. From this one can see that the specific energy in the anthracite could not be reduced in this experiment. There was a possibility with the 35MPa pressure jet (2.33kW) in the Erin coal though, but the force reduction was not great enough, as will be explained below.

Assuming the cutting forces and yields remain constant with cutting speed and taking a cutting speed of 3.5m/s, typical of a coal winning machine, then if jet assistance is used in these coal types, the maximum jet powers that should be used are 9.50kW and 7.70kW. Assuming a maximum allowable flow rate of 4 l/min, then the maximum jet pressures that should be used are 142.5MPa and 115.5MPa, above these values and the specific energies will increase no matter what force reductions are achieved. These pressures are limits beyond which jet assistance will absolutely increase the specific energy, they do not guarantee that the specific energy will reduce if jets at pressures below these levels are used.

Equation (6.3) may be re-arranged to express what minimum force reduction is required at a certain jet power before a decrease in specific energy will be obtained. The relationship is below:

$$R \geq \frac{P_w}{F_c v_t} + 1 - \frac{Y_j}{Y} \qquad \text{where} \quad R = \frac{F_c - F_{cj}}{F_c} \tag{6.5}$$

Taking $Y_j/Y = 1$, then (6.5) becomes:

$$R \geq \frac{P_w}{F_c v_t} \tag{6.6}$$

As an example, consider the Erin coal tests at a jet pressure of 35MPa and power 2.33kW. Taking the blunt tool result, the unassisted cutting power was 2.98kW. Thus, the force reduction needed to reduce the specific energy at this pressure was:

$$R \geq \frac{2.33}{2.98} = 0.78$$

Therefore, at least a 78% mean cutting force reduction had to be gained from the 35MPa pressure jet before the specific energy would decrease; in actuality a 33% reduction was achieved.

Therefore, for the linear tests, two conditions have to be met before jet assisted cutting will reduce the specific energy:

- The total jet power must not exceed the power required to cut the mineral without jet assistance i.e. $F_c v_t$.

- The percentage force reduction must be greater than the ratio of gross jet power to the power needed to cut the mineral without jet assistance.

6.3.4.1 Specific Energy of Shearer Loaders

One may extend the idea to a shearer loader by calculating the specific energy from a consideration of the total energy used by the machine to cut the coal. Mort (1988), indicates that the machine power may be divided into four fundamental components: that to drive the drum; that to provide haulage thrust; that to energise the high pressure water pump; and if installed, that to run the water pump for the hollow shaft venturi or ventilator.

In the case of a shearer loader with a single drum it would be easier to calculate the yield in terms of drum diameter, d, web width, w_b, and haulage speed, S:

$$\text{Yield} = \mathrm{d} w_b \mathrm{S} \tag{6.7}$$

Thus, the following expressions may be obtained:

$$\text{Specific Energy without Jet Assistance} = \frac{wT + F_h S + P_{hsv}}{d w_b S} \tag{6.8}$$

$$\text{Specific Energy with Jet Assistance} = \frac{wT_j + F_{hj} S_j + P_{hsv} + nP_w}{d w_b S_j} \tag{6.9}$$

Where,

w = Drum angular velocity

F_{hj}, F_h = Haulage force with and without jet assistance

P_{hsv} = Hollow shaft venturi pump power

n = Number of water jets

d = Drum diameter

T_j, T = Drum torque with and without jet assistance

S_j, S = Haulage speed with and without jet assistance

P_w = Jet power

w_b = Web width

In this case for a reduction in specific energy the inequality would be:

$$\frac{wT_j + F_{hj}S_j + P_{hsrv} + nP_w}{dw_bS_j} \leq \frac{wT + F_hS + P_{hsrv}}{dw_bS} \tag{6.10}$$

$$\Rightarrow \qquad nP_w \leq w\left(T\frac{S_j}{S} - T_j\right) + (F_h - F_{hj})S_j + P_{hsrv}\left(\frac{S_j}{S} - 1\right) \tag{6.11}$$

Putting $R_t = \frac{T - T_j}{T}$ and $R_h = \frac{F_h - F_{hj}}{F_h}$, then equation (6.11) becomes:

$$nP_w \leq wT\left(\frac{S_j}{S} - 1 + R_t\right) + R_hF_hS_j + P_{hsrv}\left(\frac{S_j}{S} - 1\right) \tag{6.12}$$

Assuming the haulage speed would be maintained constant, $S_j/S = 1$, equation (6.12) reduces to:

$$nP_w \leq R_twT + R_hF_hS \tag{6.13}$$

Considering the best torque and haulage force reductions possible i.e. R_t and $R_h = 1$, then,

$$nP_w \leq wT + F_hS \tag{6.14}$$

i.e. Gross Jet Power ≤ Drum Power + Haulage Power

An average value of the torque and haulage force would have to be used to eliminate bias due to tool wear. Employing equation (6.14) as a guide-line, one can predict mathematically that for high volume coal production, if the total jet power utilized on the machine exceeds the cumulative unassisted drum and haulage power, then an automatic increase in specific energy will result despite any torque or haulage force reductions achieved.

Therefore, the two basic conditions that have to be met for a shearer loader before high pressure water jet assisted cutting will produce a reduction in the specific energy are:

- The total jet power must not exceed the unassisted cumulative drum and haulage power, and;

- The jet power used must be able to bring about torque and haulage force reductions, R_t and R_h, such that equation (6.13) is satisfied.

One can reduce the relationships further by dividing the drum torque and haulage force into their respective components. The drum torque comprises the torque required to rotate the drum whilst it is not cutting plus superimposed on this during excavation, the torque necessary to cut the mineral. Similarly the haulage force consists of the tractive force to traverse the machine along the a.f.c. plus a reaction force on the drum at the coal buttock i.e. the resultant of the normal forces acting on the picks. As a first approximation one shall ignore other forces that may be acting on the machine. Thus,

$$\mathrm{T} = I\alpha + F_c\frac{d}{2} \quad \text{and} \quad T_j = I\alpha + F_{cj}\frac{d}{2} \tag{6.15}$$

and,

$$F_h = \mu M g + F_n \quad \text{and} \quad F_{hj} = \mu M g + F_{nj} \tag{6.16}$$

Where

I = Moment of inertia of drum

α = Angular acceleration of drum

F_{cj}, F_c = Resultant mean cutting force with/without jet assistance

F_{nj}, F_n = Resultant mean normal force with/without jet assistance

μ = Coefficient of friction between shearer and a.f.c.

M = Mass of the shearer

d = Drum diameter

g = Acceleration due to gravity

Substituting expressions (6.15) and (6.16) into equation (6.10), then:

$$\frac{w\left(I\alpha + F_{cj}\frac{d}{2}\right) + (\mu M g + F_{nj})S_j + P_{hsv} + nP_w}{dw_b S_j} \leq \frac{w\left(I\alpha + F_c\frac{d}{2}\right) + (\mu M g + F_n)S + P_{hsv}}{dw_b S} \quad (6.17)$$

$$\Rightarrow \qquad nP_w \leq wI\alpha\left(\frac{S_j}{S} - 1\right) + w\frac{d}{2}\left(F_c\frac{S_j}{S} - F_{cj}\right) + (F_n - F_{nj})S_j + P_{hsv}\left(\frac{S_j}{S} - 1\right) \quad (6.18)$$

Putting $R_c = \dfrac{F_c - F_{cj}}{F_c}$ and $R_n = \dfrac{F_n - F_{nj}}{F_n}$, then equation (6.18) becomes:

$$nP_w \leq wI\alpha\left(\frac{S_j}{S} - 1\right) + w\frac{d}{2}F_c\left(\frac{S_j}{S} - 1 + R_c\right) + R_n F_n S_j + P_{hsv}\left(\frac{S_j}{S} - 1\right) \quad (6.19)$$

For one jet the equation is:

$$P_w \leq \frac{wI\alpha}{n}\left(\frac{S_j}{S} - 1\right) + w\frac{d}{2}\frac{F_c}{n}\left(\frac{S_j}{S} - 1 + R_c\right) + R_n\frac{F_n}{n}S_j + \frac{P_{hsv}}{n}\left(\frac{S_j}{S} - 1\right) \quad (6.20)$$

Taking $S_j/S = 1$, then (6.20) reduces to:

$$P_w \leq R_c w\frac{F_c}{n}\frac{d}{2} + R_n\frac{F_n}{n}S \quad (6.21)$$

The forces F_c and F_n represent the total resultant mean cutting and normal forces acting on the picks in the cut. These will comprise the vane and clearance kerf picks. Hence,

$$F_c = pF_{cv} + qF_{ck} \quad \text{and} \quad F_n = pF_{nv} + qF_{nk} \quad (6.22)$$

where, p and q are the number of vane and clearance kerf picks in the cut, F_{cv}, F_{ck}, F_{nv} and F_{nk} are the average vane and clearance kerf cutting and normal forces respectively, acting on a single respective pick. If each pick is jet assisted and a phasing system is employed, then n

= p + q. Assuming there are an equal number of vane and clearance kerf picks, then p = q = n/2. Also, the average clearance kerf pick forces will be r and s times greater than the average vane pick cutting and normal forces respectively. Thus (6.22) becomes:

$$F_c = \frac{n}{2}(F_{cv} + rF_{cv}) \qquad \text{and} \qquad F_n = \frac{n}{2}(F_{nv} + sF_{nv})$$

$$\Rightarrow \qquad F_c = F_{cv}\frac{n}{2}(1+r) \qquad \text{and} \qquad F_n = F_{nv}\frac{n}{2}(1+s)$$

$$\Rightarrow \qquad \frac{F_c}{n} = F_{cv}\frac{(1+r)}{2} \qquad \text{and} \qquad \frac{F_n}{n} = F_{nv}\frac{(1+s)}{2} \qquad (6.20)$$

Substituting (6.23) into (6.21):

$$P_w \le R_c w \frac{d}{2} F_{cv}\frac{(1+r)}{2} + R_n S F_{nv}\frac{(1+s)}{2} \qquad (6.24)$$

Since we are now dealing with average single pick vane tool forces which have been modelled in the laboratory, a tentative evaluation of the feasibility of high pressure water jet assisted cutting to shearers with respect to specific energy may be attempted from the laboratory results. One shall have to assume that the force reductions R_c and R_n are similar for the single vane pick results to those measured on the drum. Also, Brooker (1979), points out that the clearance kerf forces may be up to ten times greater than the vane pick levels, so values for r and s shall have to be assumed.

Taking the experimental results of the present study then, for the Erin coal we have: F_{cv} = 2.71kN; F_{nv} = 0.97kN; R_c = 0.33; and R_n = 0.25. For the shearer used at Golborne Colliery, Mort (1988) reports: d = 1.473m; w = 2 × π × 62/60 = 6.49 rads/sec; S = 0.076 m/s (4.56 m/min); then,

$$P_w \leq 0.33 \times 6.49 \times 2.71 \times 10^3 \times \frac{1.473}{2} \times \frac{(1+r)}{2} \quad + \quad 0.25 \times 0.97 \times 10^3 \times 0.076 \times \frac{(1+s)}{2}$$

$$P_w \leq 2137.3 \times (1 + r) \quad + \quad 9.2 \times (1 + s)$$

For a flow rate of 4 l/min say, the jet pressure, P, must not exceed:

$$P \leq 32.06 \times (1 + r) \quad + \quad 0.14 \times (1 + s)$$

For s = r, then: $P \leq 32.20 \times (1 + r)$

The Erin coal received the force reductions with a jet pressure of 35MPa. However, there is one crucial difference: the cutting speed was 1.1m/s, whereas in the case above it is 4.54m/s. One now has the problem of ascertaining if the same force reductions may be achieved at 4.54m/s with a jet pressure less than P.

Ip (1986), postulated that the criterion of force reduction for rocks with significant jet penetration, is jet penetration. Using this criterion, the jet at pressure P, must be able to penetrate the coal to the same depth as in the laboratory tests to furnish the same force reductions and lead to a decrease in the specific energy.

The measured kerf depth in the Erin coal that procured the above force reductions was 10.7mm (predicted 6.7mm). Predicting the penetration at 4.54m/s from Cooley's equation for coal, and for different values of r, we have:

For r = 1: $P \leq$ 64.4MPa: $h \leq$ 6.2mm

For r = 2: $P \leq$ 96.6MPa: $h \leq$ 9.5mm

For r = 3: $P \leq$128.8MPa: $h \leq$12.6mm

Therefore, if the clearance kerf tools receive the same force reductions and are about three times greater than the vane tool force levels, the specific energy will decrease if a jet pressure

of around 128.8MPa is used. However, this pressure is quite impracticable and if there were fifteen tools cutting at once, the necessary high pressure pump power would be at least 130kW.

6.3.4.2 Conclusions

Jet assistance did not reduce the specific energy in both coals: indeed an exponential increase was observed with jet pressure and a sharp linear one with jet power.

Despite the differences in the two coals, the specific energies for the unassisted blunt tool, cleat parallel, cuts were nearly identical. However, the influence of cleat is to reduce the specific energy when the cleat is horizontal.

With jet assistance in the anthracite, the cleat made little difference. Between the coals though, the Erin specific energies were lower.

Theoretical relationships may be derived to indicate whether one may obtain a reduction in specific energy from water jet assisted cutting. The theory may be applied to a shearer loader and results from the laboratory used to make a first appraisal of the feasibility of jet assistance in reducing the specific energy.

The theory and the experimental results indicate that the specific energy will increase if jet assistance over this pressure range is adopted to mine these coals. Supporting this is the fact that both Mort (1988) and Kovscek et al (1986) reported an increase in specific energy in their field trials. However, changing the operating parameters such as increasing a shearers haulage speed may make the proposition more tenable.

6.4 Particle Size Analysis

An important part of the experiment was to assess the influence of jet assisted cutting on the coal particle size distribution. Particular interest lay in whether the proportion of fine coal would be reduced by jet assistance and by how much. Fine coal is defined as the -0.5mm fraction: that size normally recovered from the run-of-mine by froth flotation.

Additionally, it has been estimated that 20%-25% of mine waste comprises fine coal, which is consequently lost. Also, the washing technique, froth flotation, costs approximately 21/2 times more than the processing methods of larger size fractions (HQTD Bulletin, 1987). Hence, a substantial benefit may be obtained if a cutting process is discovered that does not return such quantities of fines. Less coal would be wasted and the need for expensive froth flotation would be reduced. Therefore, what follows is an examination of the coal size distributions produced by the different treatments applied in this experiment.

6.4.1 Erin Coal - Cleat Parallel

The Erin coal results are presented in Fig.6.65-66. Each set of four columns represents the proportion of the total amount of coal remaining on that size of sieve.

The fines production is 10.4% and 9.8% for the sharp and blunt pick unassisted tests respectively. The 35MPa pressure treatment procures an 11.5% and 8.2% fines reduction with the sharp and blunt picks compared to the 'dry' cuts.

From an examination of Fig.6.65-66, the 35MPa water jet also gives the most reductions in the other small size fractions, 0.5mm, 3.15mm and 6.3mm, and the largest increases in the 12.5mm and 28mm fractions, for both pick conditions.

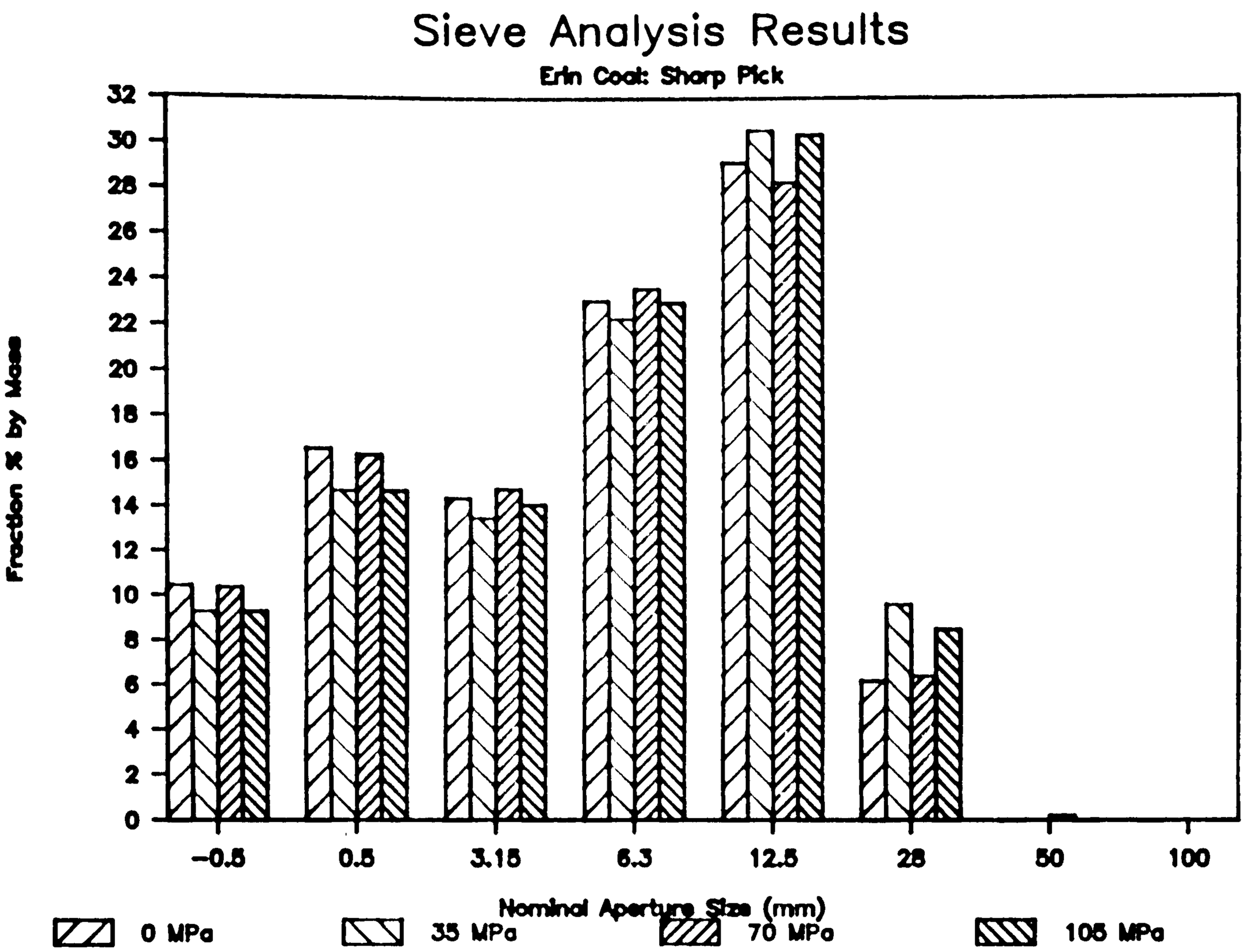


Fig.6.65

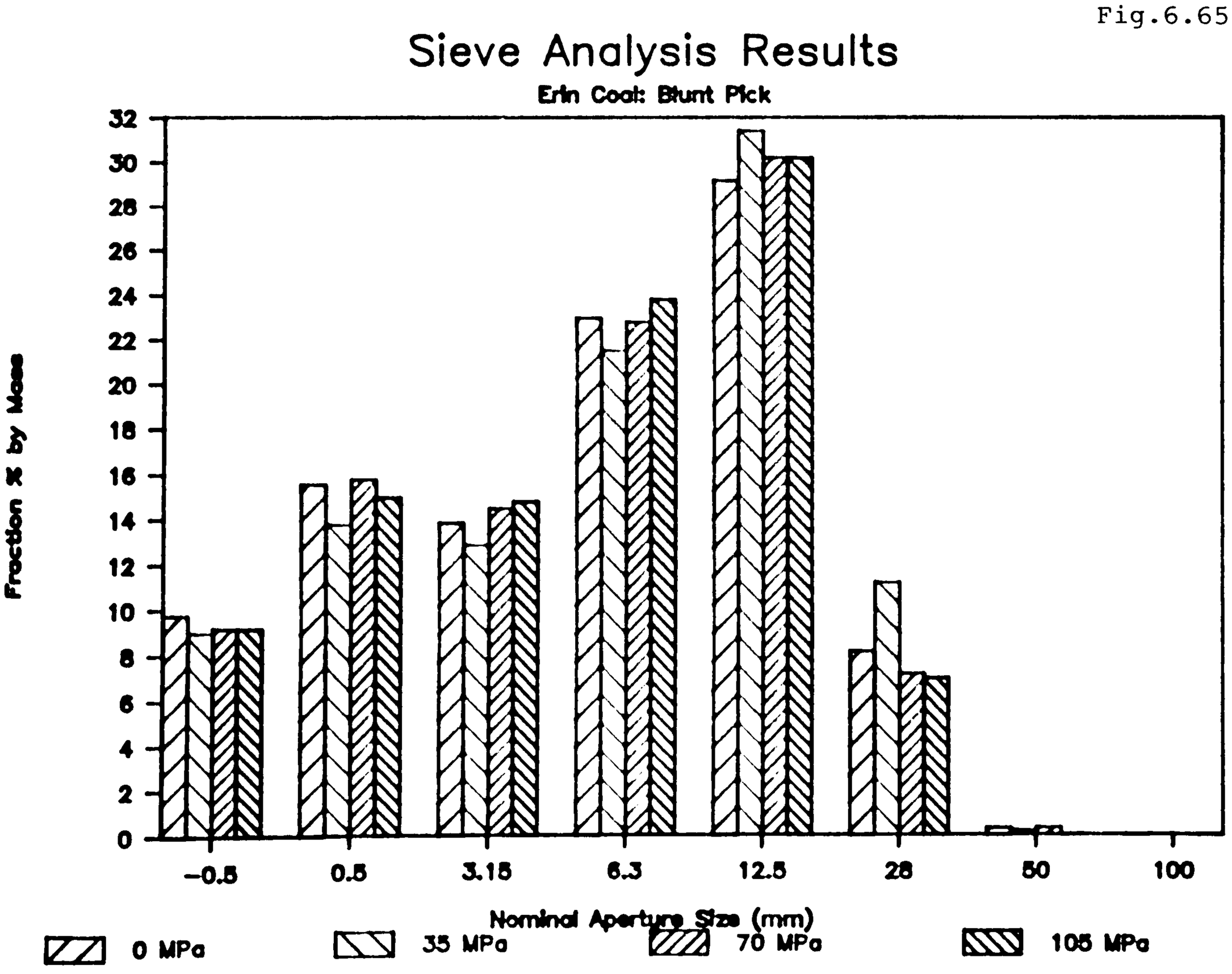


Fig.6.66

Fig.6.67-68, show the absolute percentage differences in the various size fractions compared to the unassisted cuts i.e. the zero line. Both graphs indicate that the 35MPa pressure treatment yields reductions of between 1%-2% in each fraction up to and including the 6.3mm size. Then, in the larger fractions there is an increase. Thus, larger size coal is being produced at the expense of the small coals. A similar pattern is observed for the sharp pick 105MPa pressure treatment. The 70MPa pressure jet affects no particular shift in particle size: the trace of the graph is merely oscillating about zero. The 105MPa treatment loses its salutary influence with the blunt tool.

Clearly then, the 35MPa jet pressure treatment provides the most benefit in the Erin coal with respect to size enhancement. The reductions made in the amounts of small coals produced are shown to result in more larger size coal.

Graphs of the cumulative percentage undersize are not given since the curves for the various treatments cannot easily be distinguished when plotted together. However, all the data fits remarkably well to the Rosin-Rammler relationship:

$$100 - P = 100e^{-b d^n} \qquad (6.25)$$

Where,

P = Cumulative percentage undersize

d = Nominal aperture size of the sieve

b and n, are constants for the particular size distribution

For the Erin coal, correlation coefficients to the above equation were typically 0.98. The actual equations for each treatment are included in the appendices.

The above equation may be rearranged to the form:

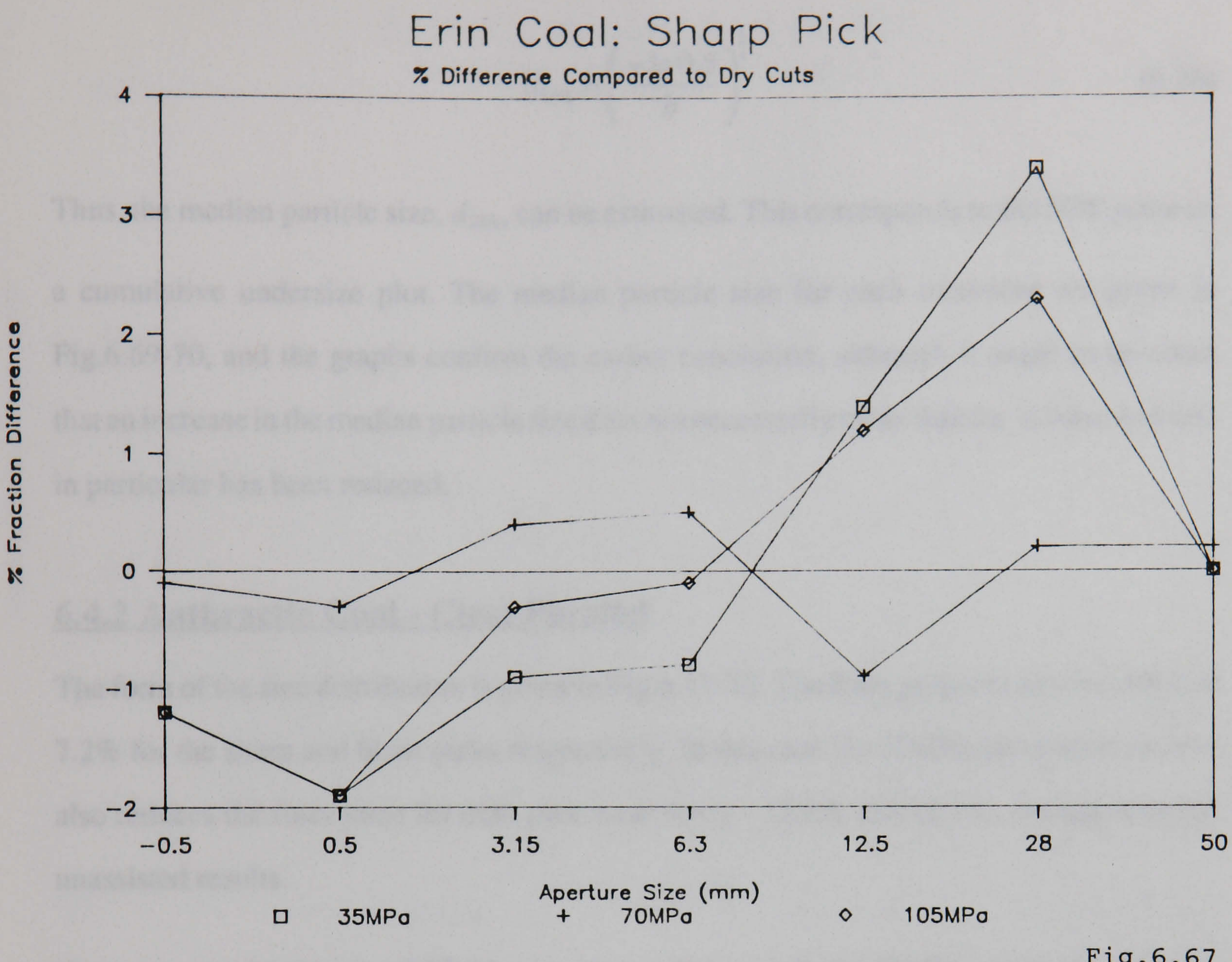


Fig.6.67

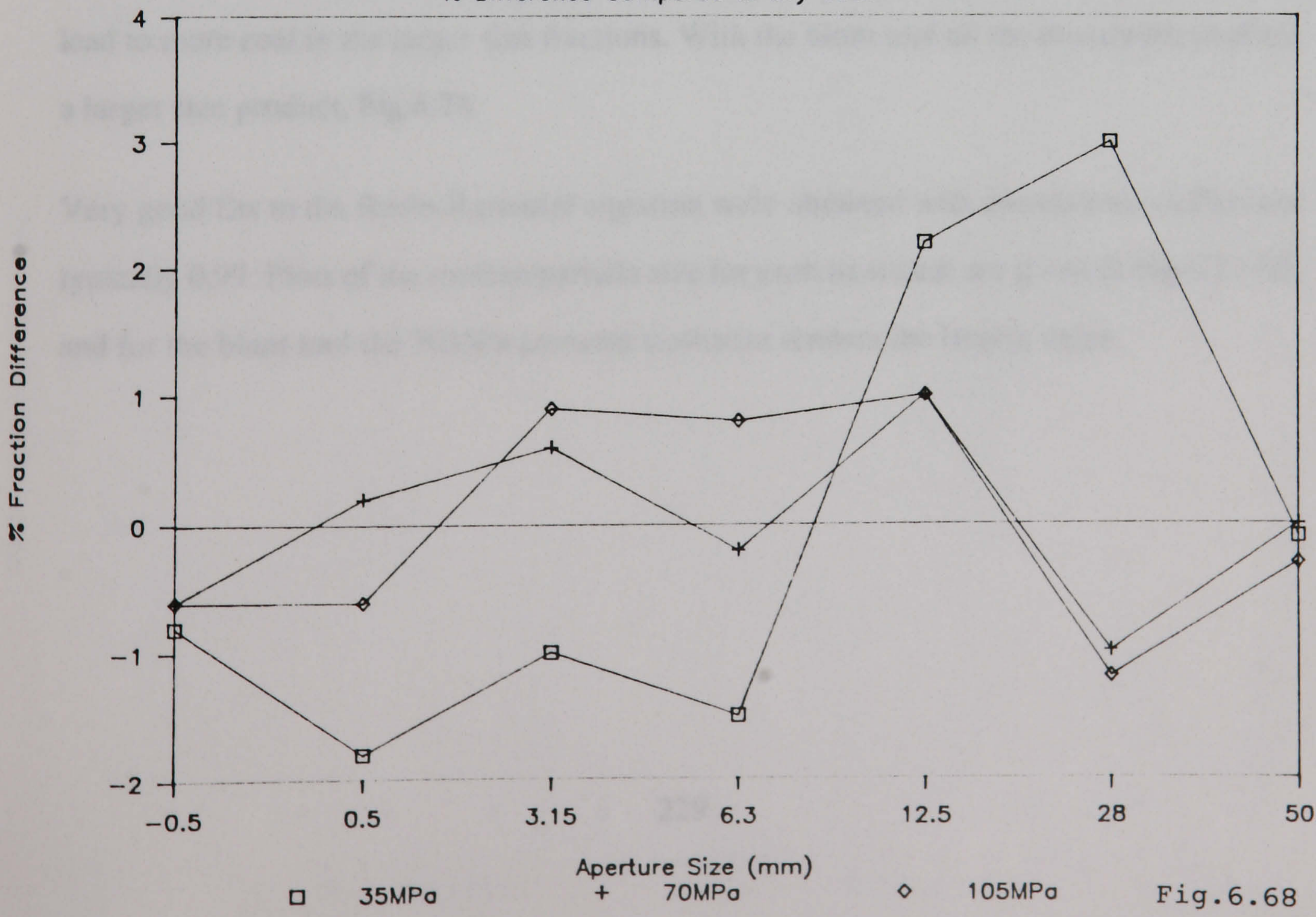


Fig.6.68

$$d_{50\%} = \left(\frac{-\ln 0.5}{b} \right)^{\frac{1}{n}} \tag{6.26}$$

Thus, the median particle size, $d_{50\%}$, can be estimated. This corresponds to the 50% point on a cumulative undersize plot. The median particle size for each treatment are given in Fig.6.69-70, and the graphs confirm the earlier conclusion, although it ought to be noted that an increase in the median particle size does not necessarily mean that the -0.5mm fraction in particular has been reduced.

6.4.2 Anthracite Coal - Cleat Parallel

The form of the size distribution is given in Fig.6.71-72. The fines proportions are 6.4% and 7.2% for the sharp and blunt picks respectively. In this case the 35MPa pressure treatment also reduces the fines most for both pick wear states - 12.5% and 18.1%, compared to the unassisted results.

However, considering Fig.6.73-74, one can see that overall, the 70MPa pressure jet has the best effect especially when the tool is blunt. Again, the reductions in the smaller size fractions lead to more coal in the larger size fractions. With the blunt tool all the treatments produce a larger size product, Fig.6.74.

Very good fits to the Rosin-Rammler equation were obtained with correlation coefficients typically 0.99. Plots of the median particle size for each treatment are given in Fig.6.75-76, and for the blunt tool the 70MPa pressure treatment renders the largest value.

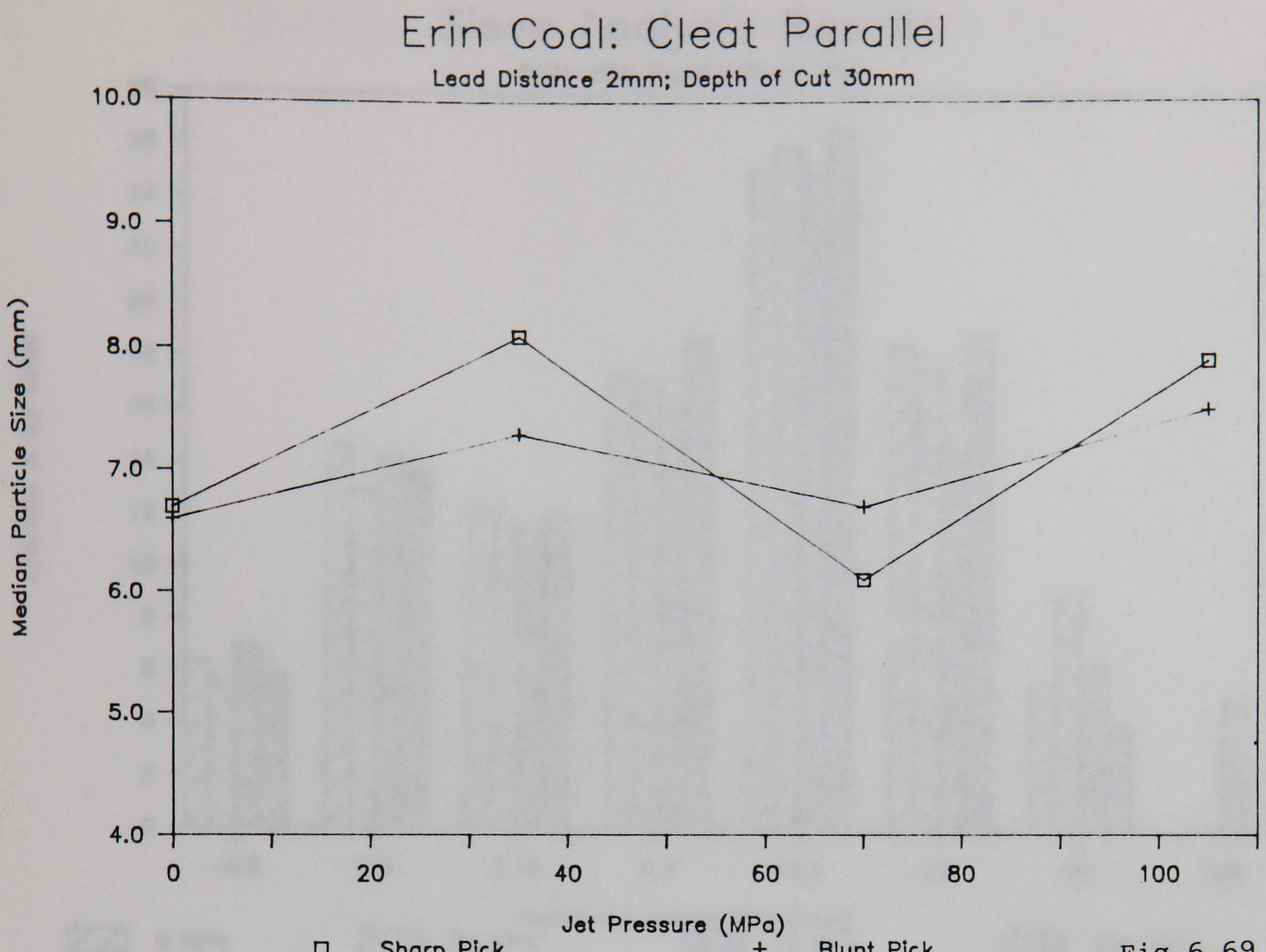


Fig.6.69

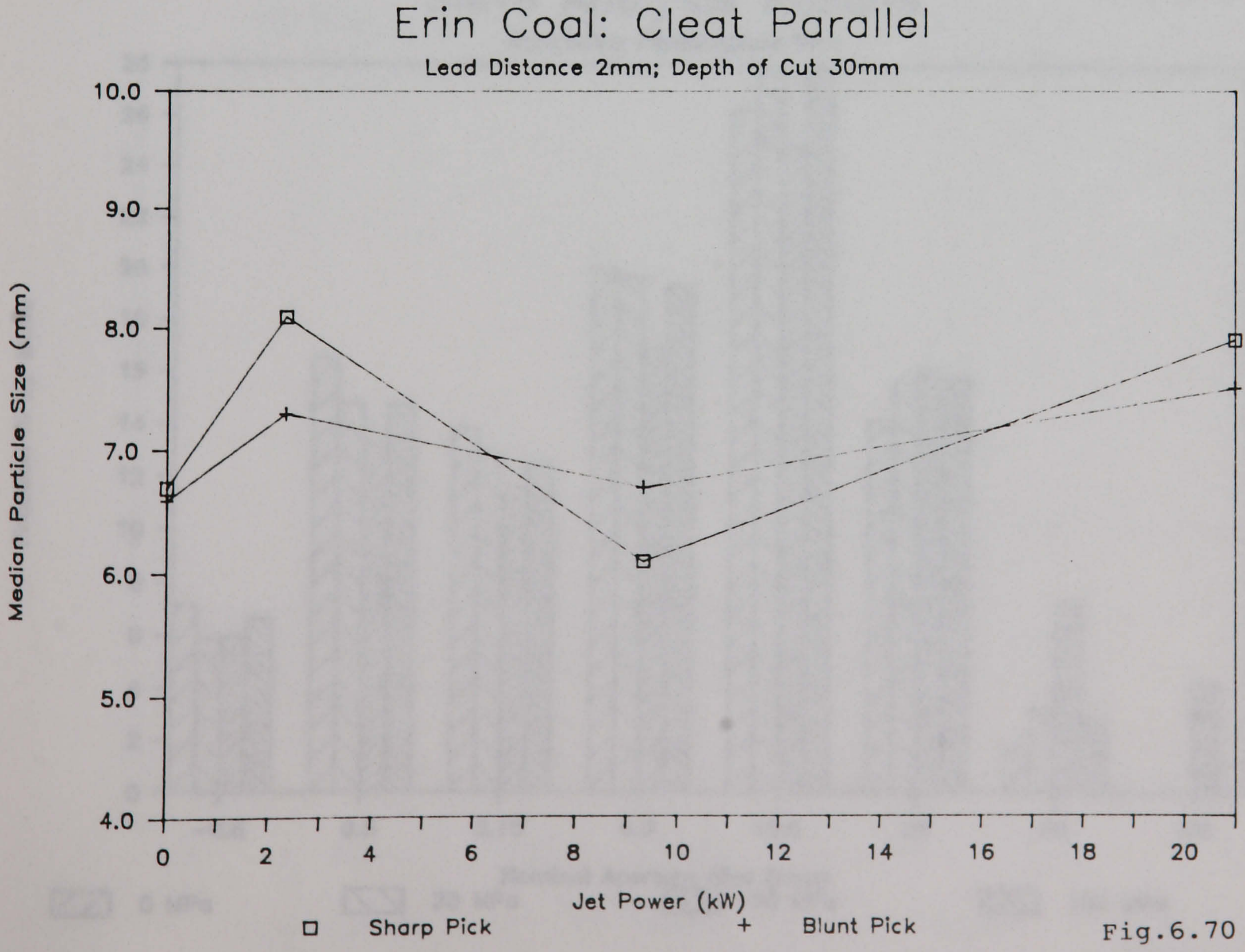


Fig.6.70

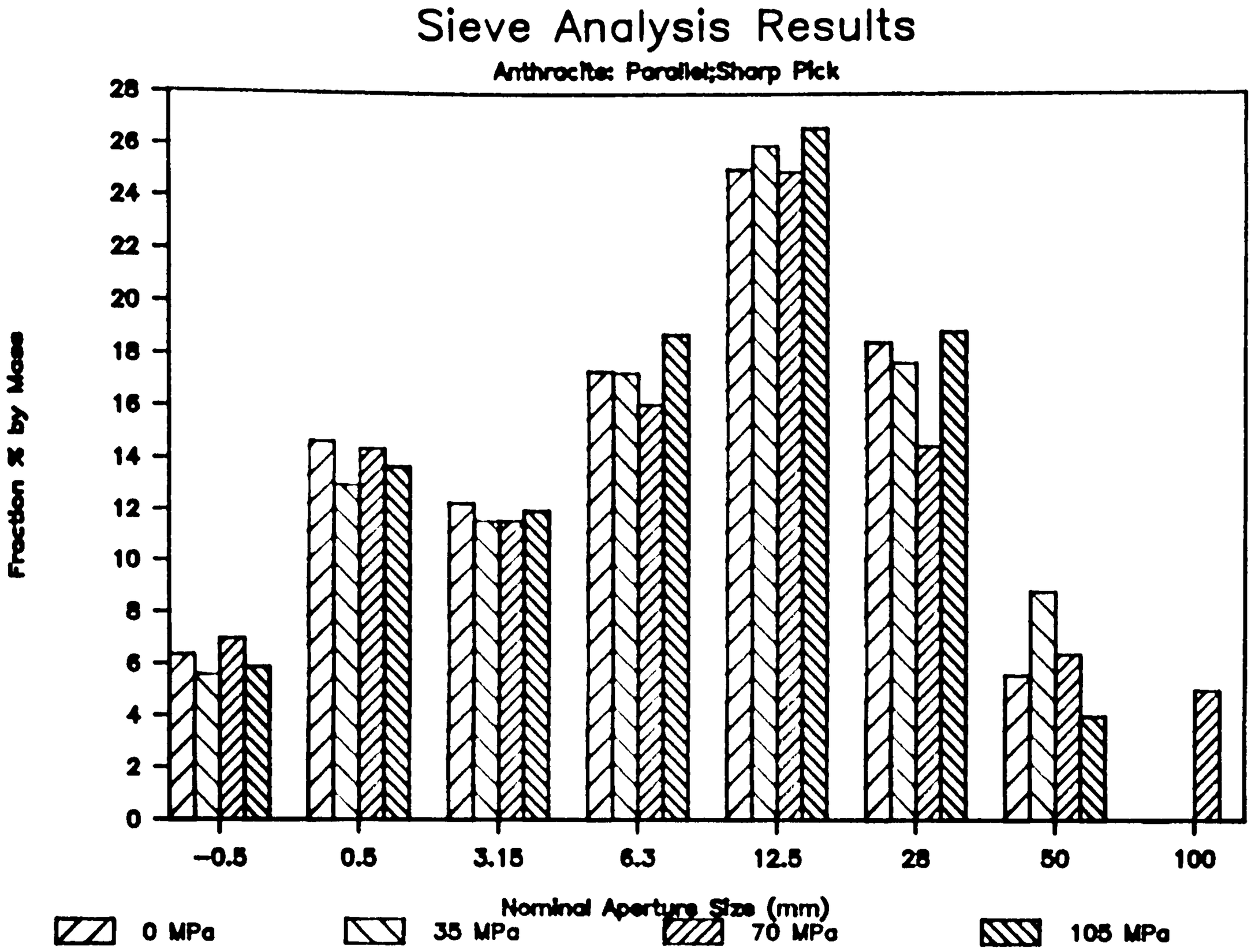


Fig.6.71

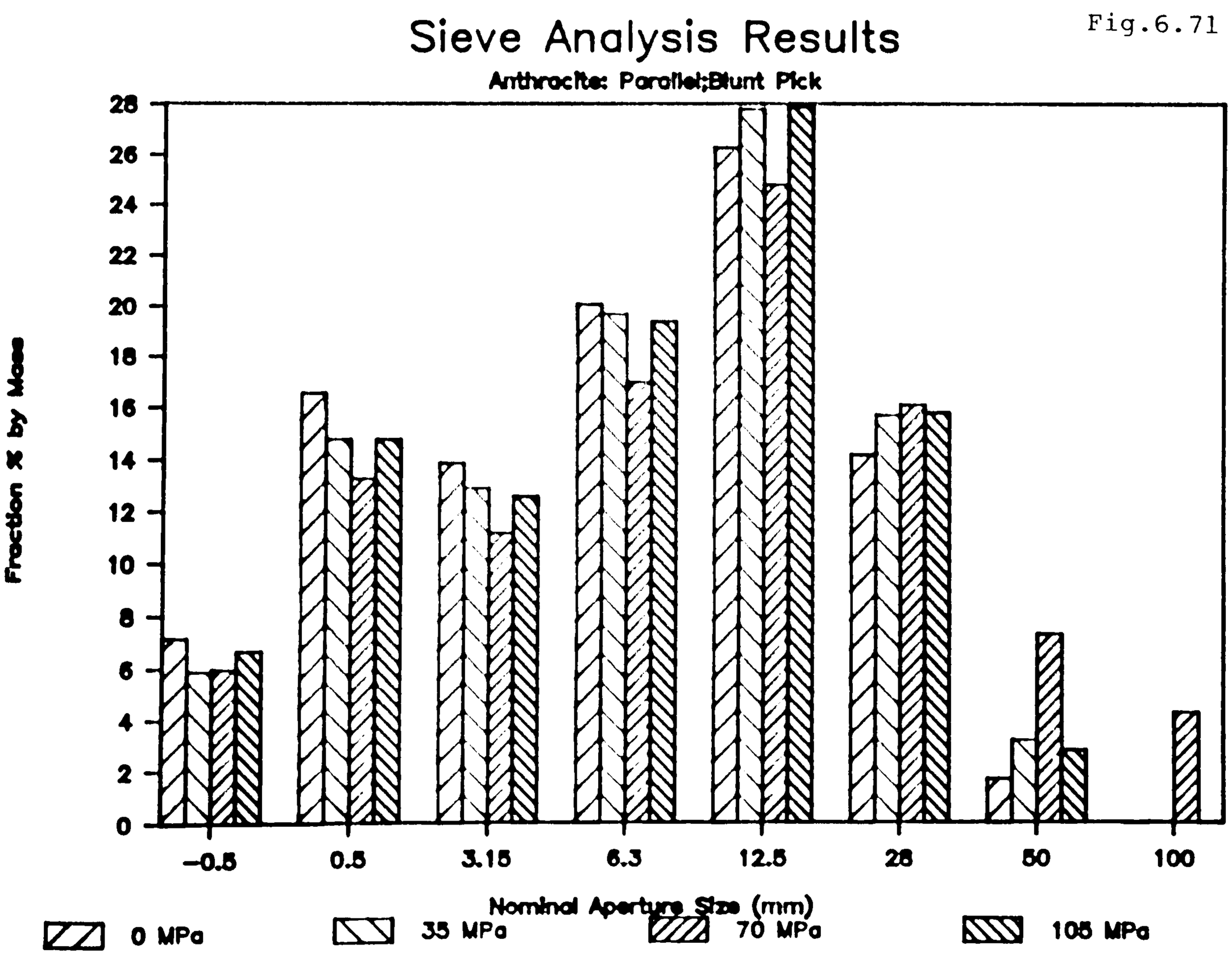


Fig.6.72

Anthracite: Cleat Parallel: Sharp Pick

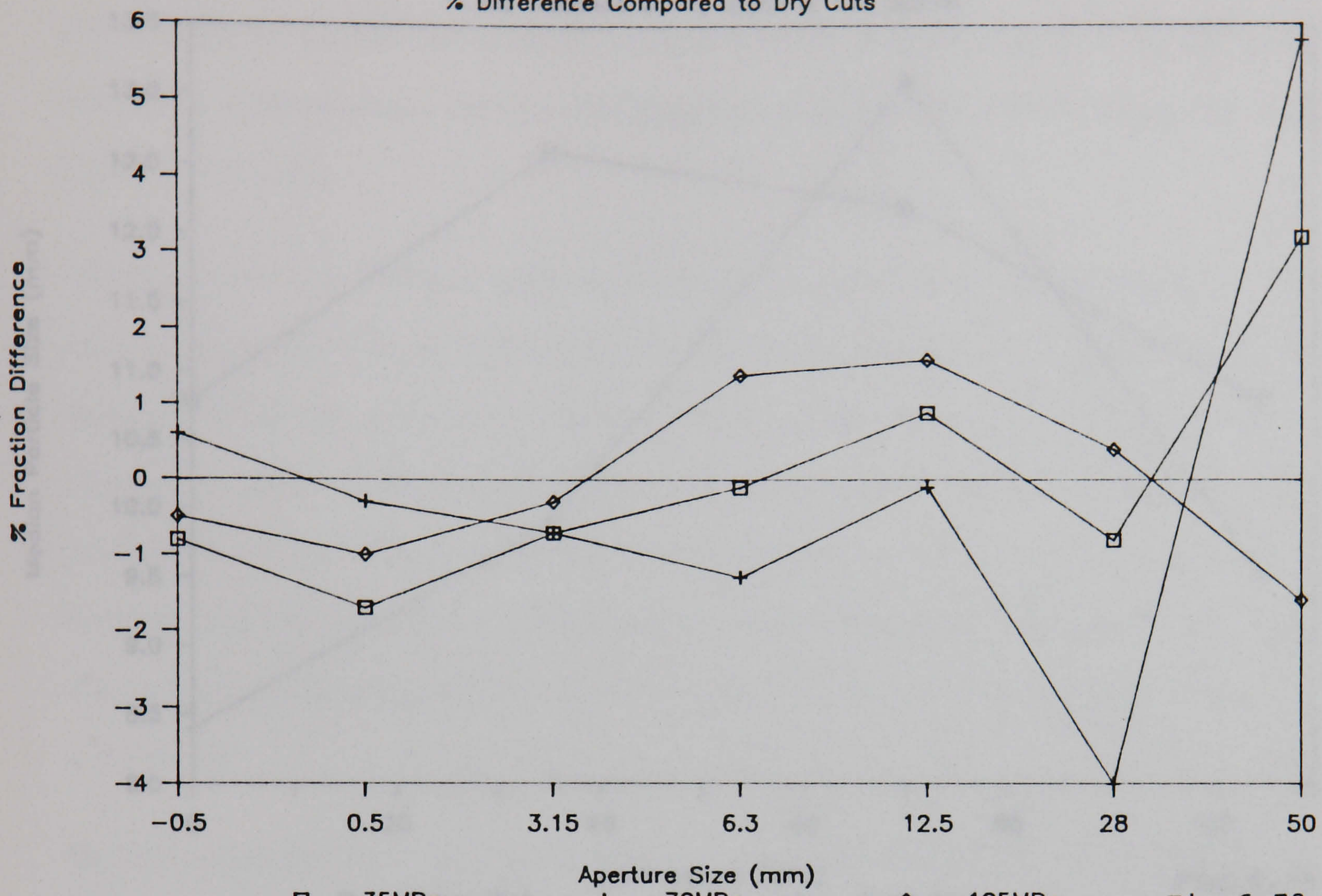


Fig.6.73

Anthracite: Cleat Parallel: Blunt Pick

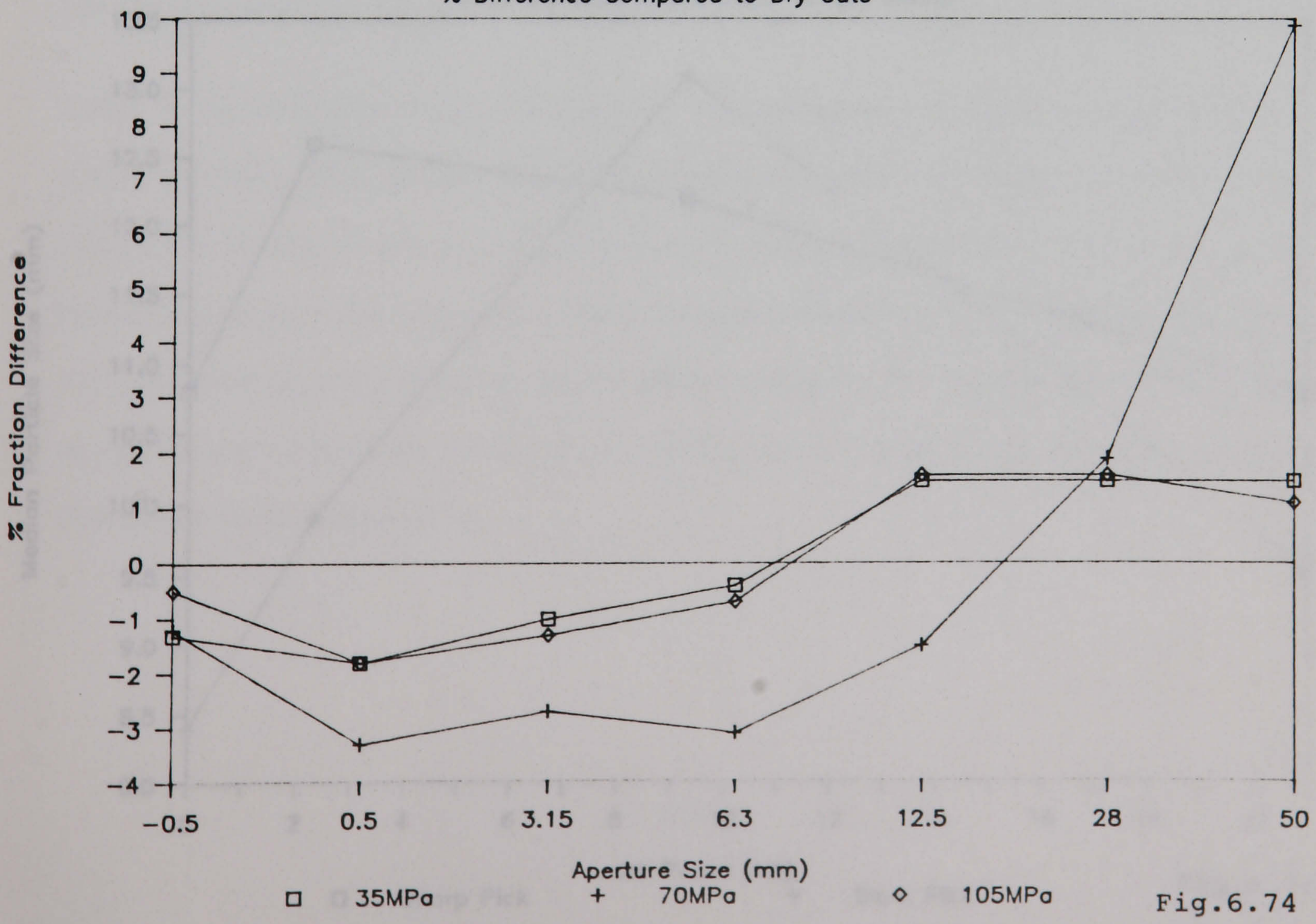


Fig.6.74

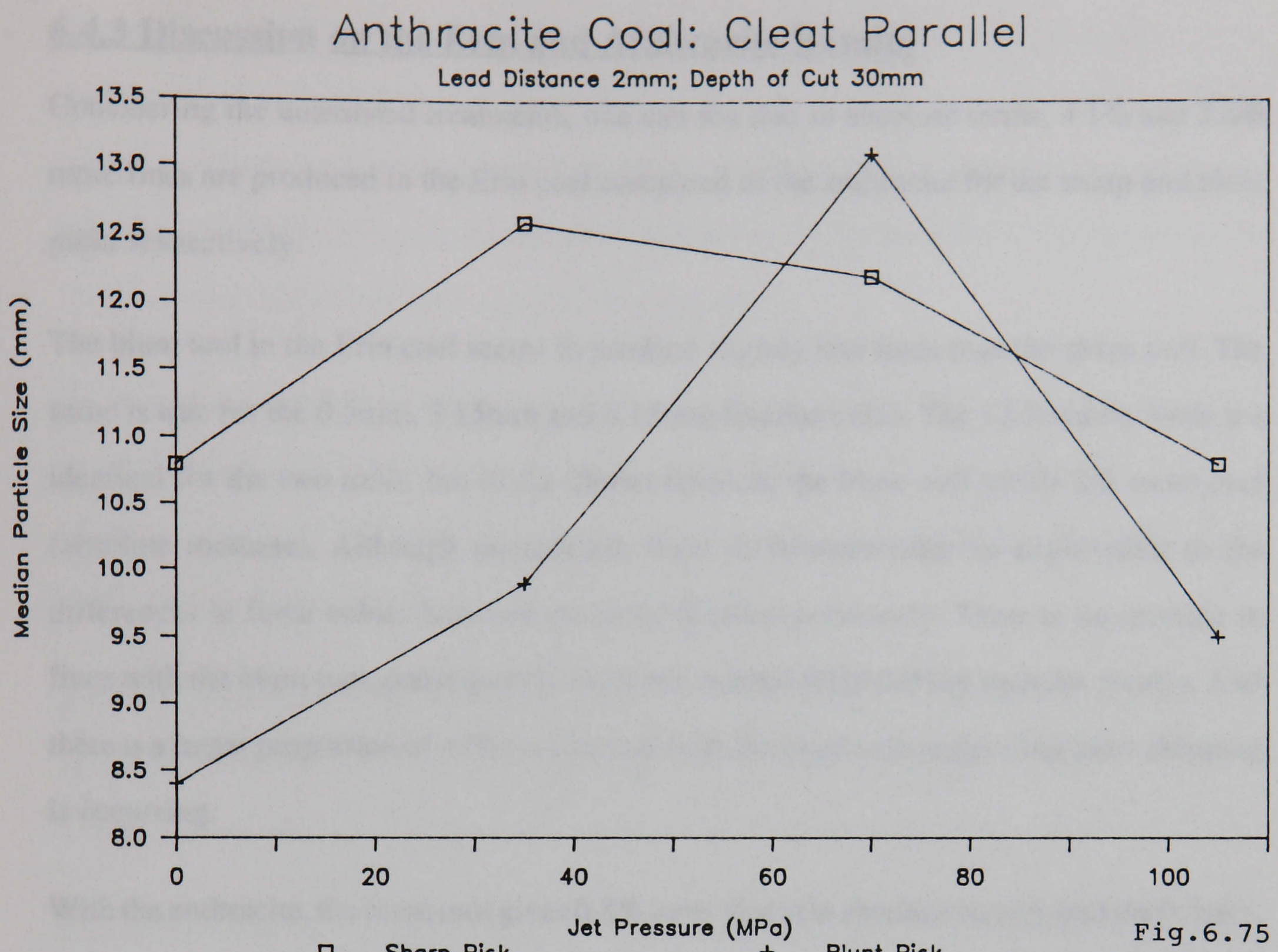


Fig.6.75

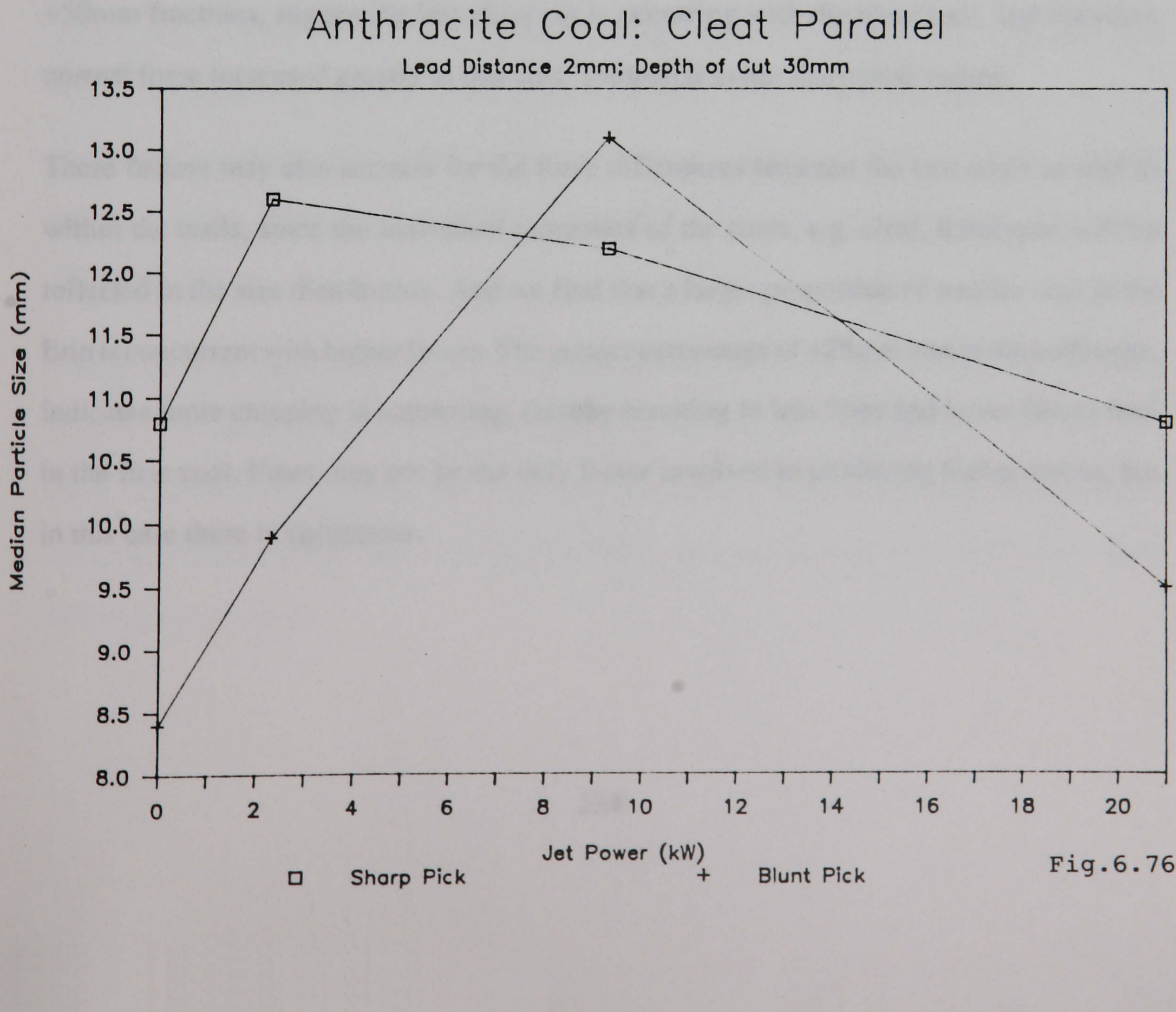


Fig.6.76

6.4.3 Discussion on the Erin and Anthracite Results

Considering the unassisted treatments, one can see that in absolute terms, 4.1% and 2.6% more fines are produced in the Erin coal compared to the anthracite for the sharp and blunt picks respectively.

The blunt tool in the Erin coal seems to produce slightly less fines than the sharp tool. The same is true for the 0.5mm, 3.15mm and 6.15mm fractions also. The 12.5mm fractions are identical for the two tools, but in the 28mm fraction, the blunt tool yields 2% more coal (absolute increase). Although unexpected, these differences offer an explanation to the differences in force values between the picks detailed previously. There is no increase in fines with the blunt tool, consequently the mean normal force did not increase greatly. And there is a larger proportion of +28mm size coal with the blunt tool, suggesting more chipping is occurring.

With the anthracite, the blunt tool gives 0.8% more fines (in absolute terms), and the 0.5mm, 3.15mm and 6.15mm size fractions increase also. There is a reduction in the 28mm and +50mm fractions, suggesting less chipping is occurring with the blunt tool, and the mean normal force increased greatly in this coal, compared to the sharp pick values.

These factors may also account for the force differences between the two coals as well as within the coals, since the individual properties of the coals, e.g. cleat, lithotypes, will be reflected in the size distribution. And we find that a larger proportion of smaller coal in the Erin is concurrent with higher forces. The greater percentage of +28mm size in the anthracite, indicates more chipping is happening, thereby resulting in less fines and lower forces than in the Erin coal. Fines may not be the only factor involved in producing higher forces, but in this case there is agreement.

If one takes a look at the general shape of all the size distributions one shall see that the 12.5mm fraction (i.e. 12.5mm - 28mm) is uniformly the largest. The 6.3mm one is usually the second largest and so on, despite the disparity in the coals. Obviously the sieve sizes affect the pattern, but the author suggests that it is also a function of the operating parameters viz. the depth of cut, line spacing and tool geometry.

For example, the nominal depth of cut in this experiment was 30mm. Therefore, it is not too surprising to discover that the largest size fraction is that one adjacent and less than the depth of cut i.e. 12.5mm - 28mm. If the depth of cut had been 15mm say, then one would expect the largest fraction to be the 6.3mm - 12.5mm one.

Similarly, the line spacing would influence the size of the largest particle that could be cut. At a 30mm depth of cut and a 20mm line spacing say, one would not expect to obtain such a large +28mm fraction, even in the anthracite: the breakout pattern would prevent it.

The influence of the tool geometry is more difficult to evaluate. However, the tool utilized in the present study had a pronounced ridge running down the centre of the carbide insert. This encourages the coal to break in tension to either side rather than in a vertical direction. Also, the curvature of the insert means that the bottom 9mm of the tip offers a negative rake angle to the coal which is more conducive to compressive crushing rather than tensile splitting. These factors strengthen the carbide tip but they may also be contributing to the fines production.

The quantity of coals making the size fractions greater than the depth of cut i.e. 28mm and +50mm, also indicates something of the coal's characteristics. More anthracite is found in these fractions than with the Erin coal and therefore it is not surprising that anthracite comprises more vitrinite and is not as heavily cleated, two factors that would allow brittle failure in large lumps.

With jet assistance the characteristic shape of the distribution is retained: merely the proportions within the individual fractions have altered. Thus the jet has not fundamentally changed the mode of fracture but modified it somewhat. For example, with the jet assisted treatments, the 3.15mm fraction does not suddenly appear the largest and the 12.5mm fraction the smallest. Only a variation of the same pattern occurs.

6.4.4 Anthracite Coal - Cleat Horizontal

The results are illustrated in Fig.6.77-78. The fines for the unassisted sharp and blunt pick treatments are 5.6% and 4.6% respectively (absolute percentages). With the sharp pick treatment, the 35MPa and 70MPa jets reduce the quantity of fines by 16.1% and 3.6% respectively, relative to the dry cuts.

Actually, all the blunt pick water jet assisted treatments increase the fines. This also occurs in the 0.5mm, 3.15mm and 6.3mm fractions, making jet assistance a definite hindrance in terms of size improvement.

Fig.6.79-80, shows the percentage differences in each fraction from the control of the unassisted tests. The graphs are not encouraging and enjoin one not to apply jet assistance when the cleat is horizontally orientated.

Plots of the median particle size, Fig.6.81-82, also indicate the detrimental influence of jet assistance.

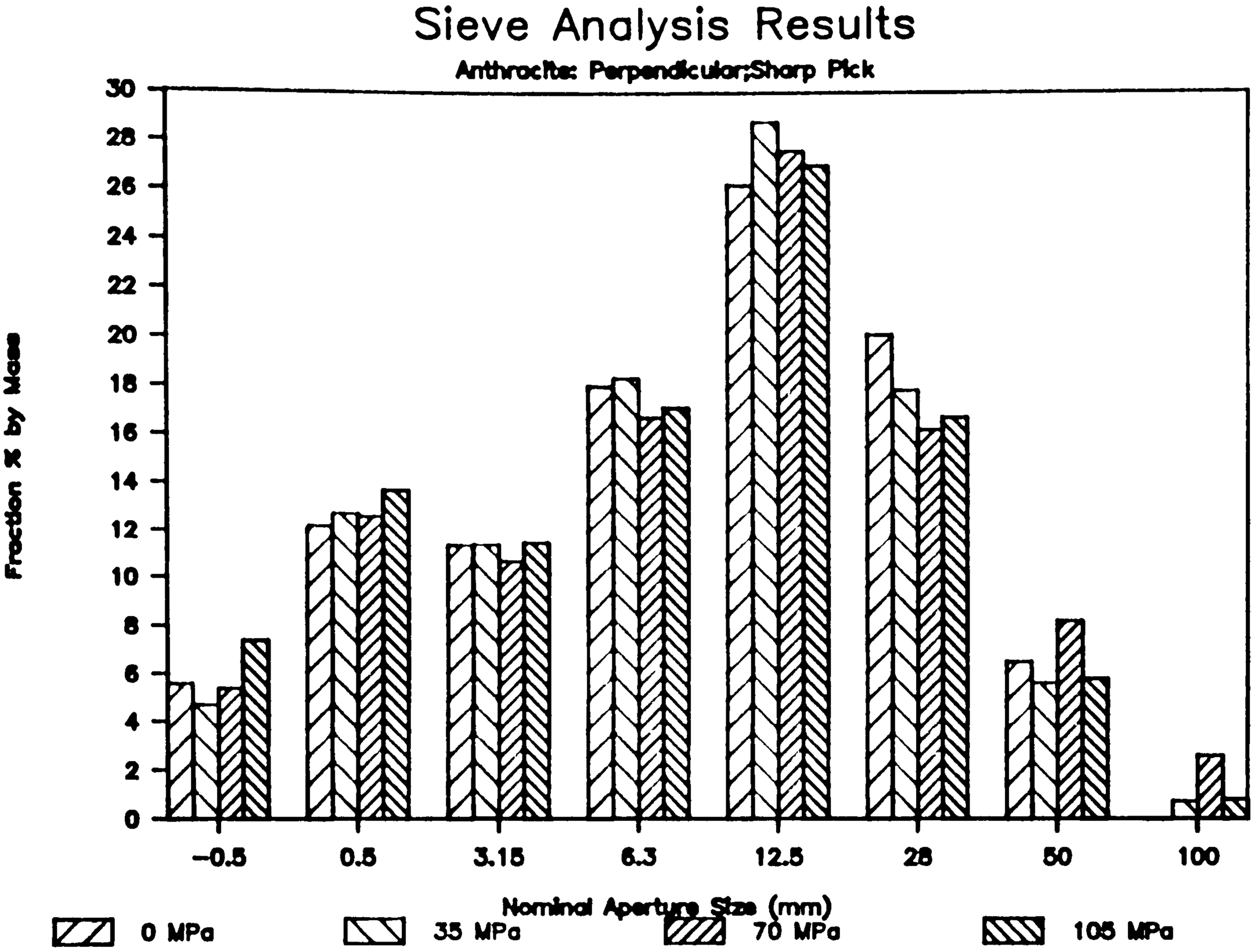


Fig.6.77

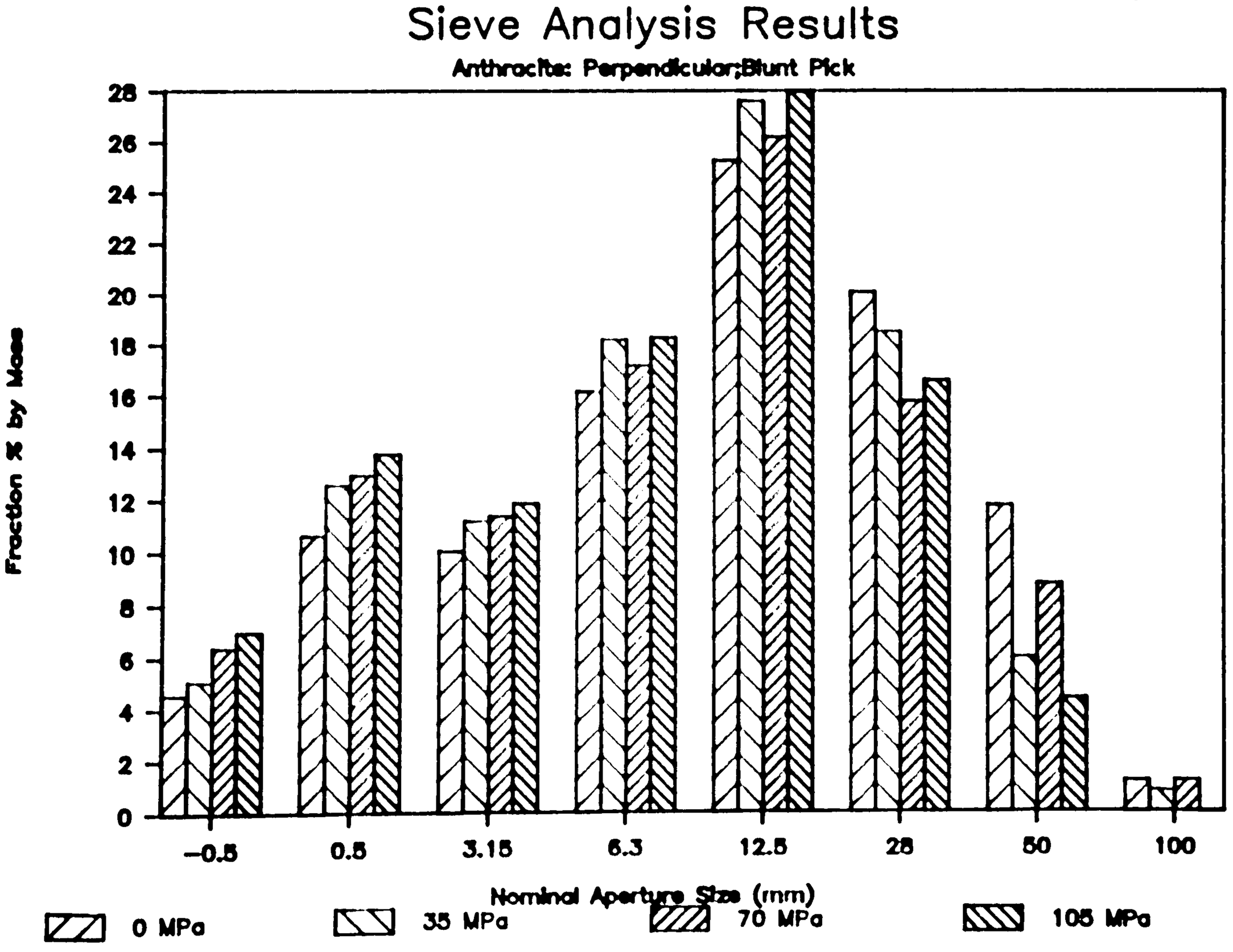


Fig.6.78

Anthracite:Cleat Horizontal: Sharp Pick

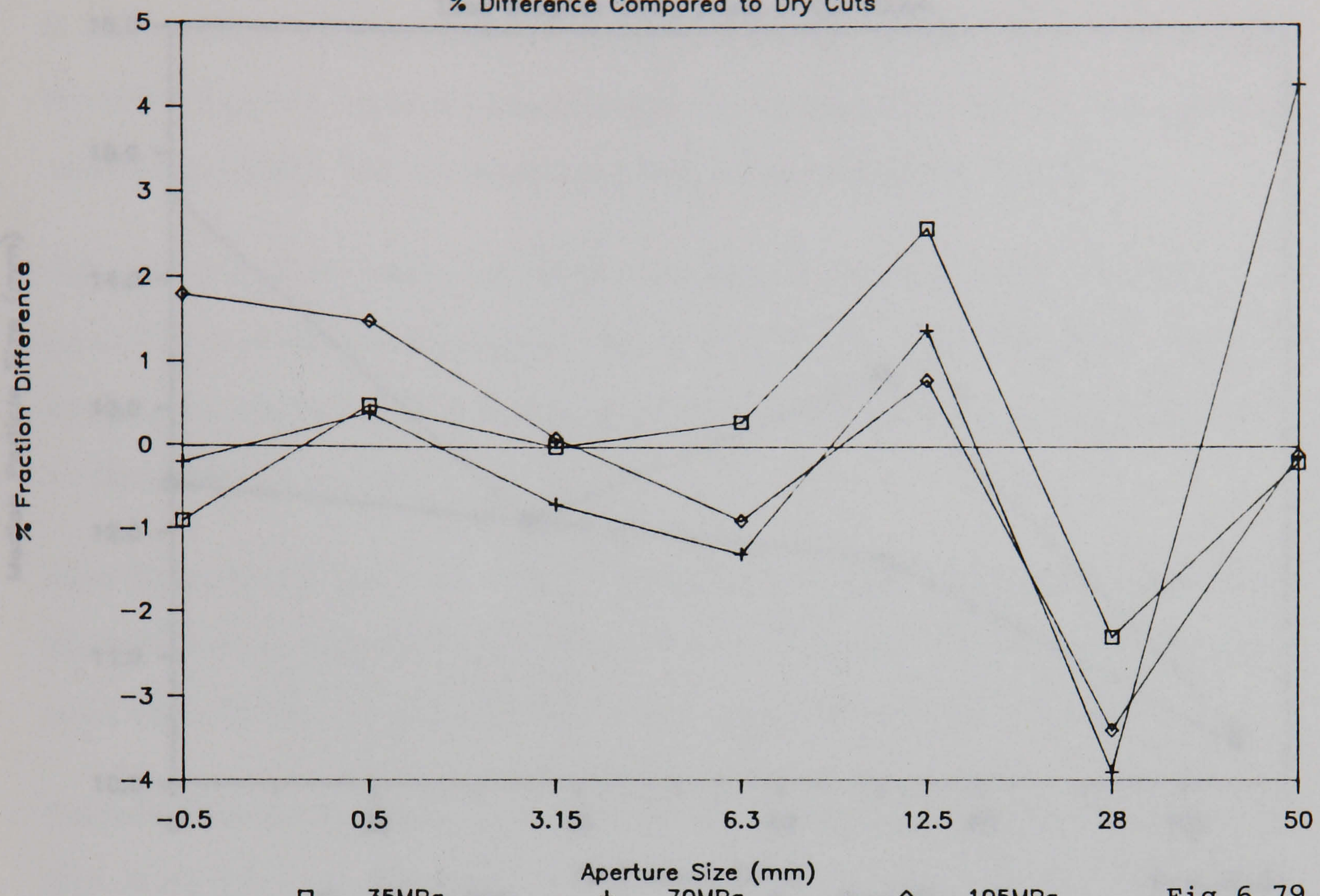


Fig.6.79

Anthracite:Cleat Horizontal: Blunt Pick

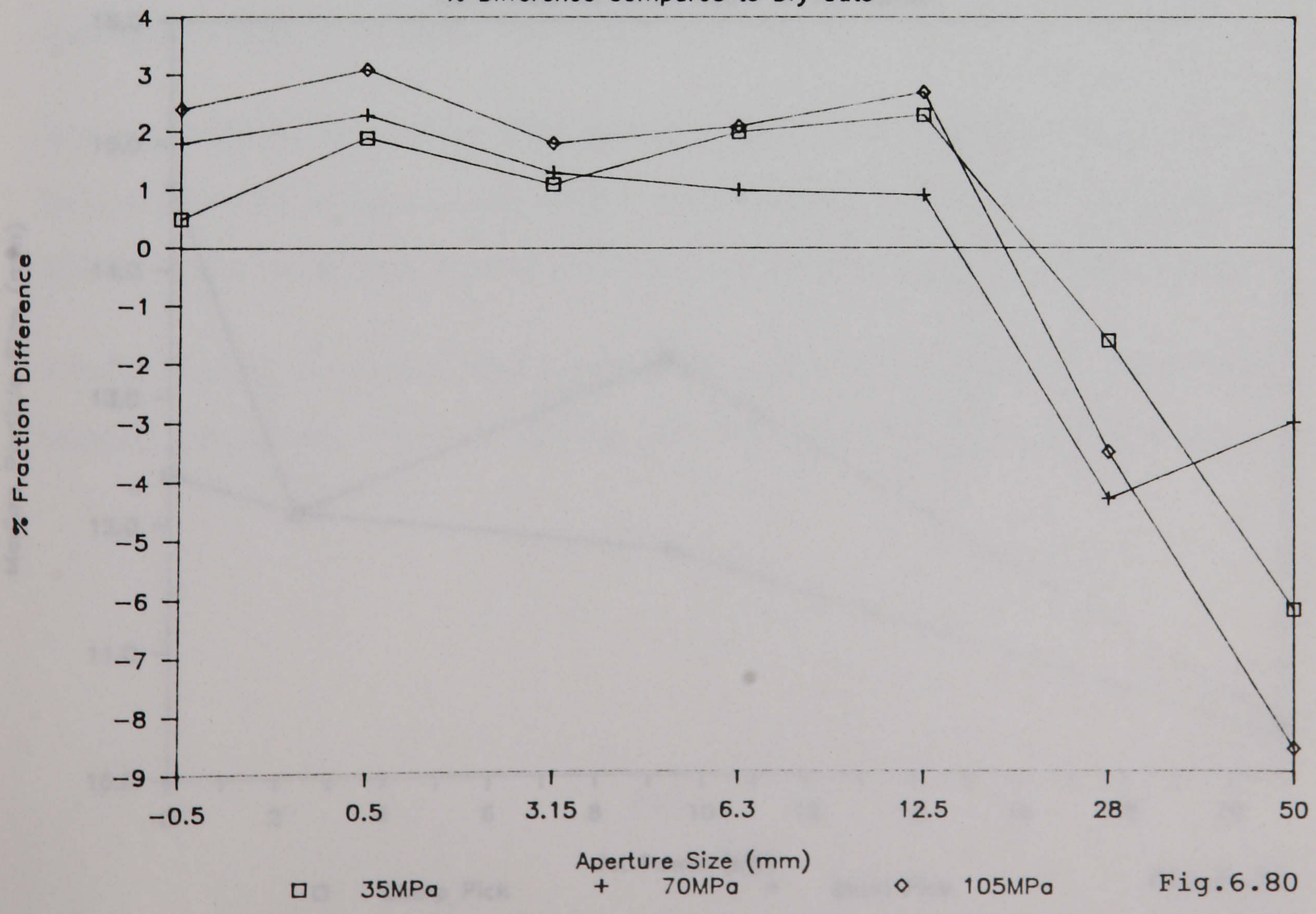


Fig.6.80

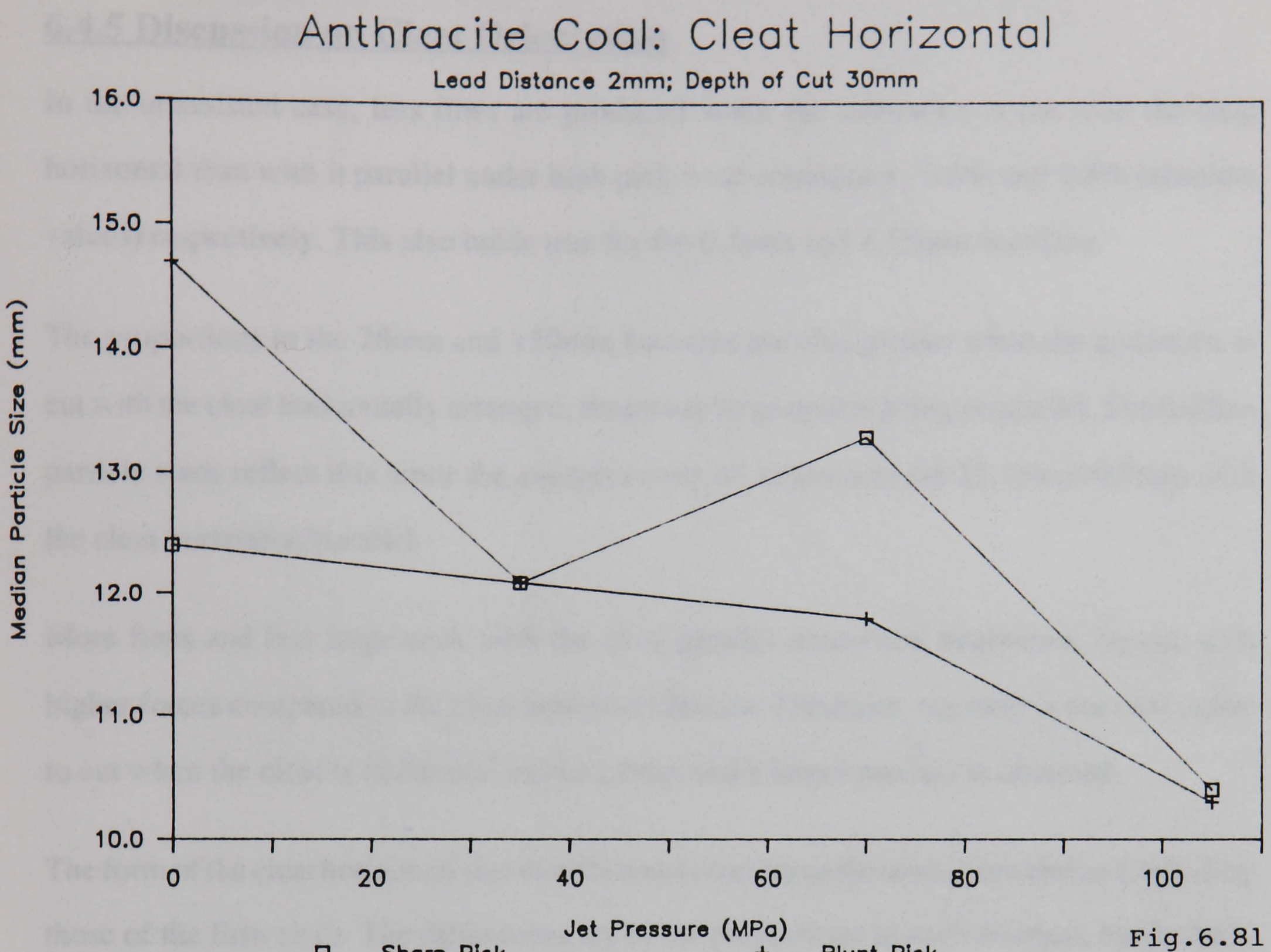


Fig.6.81

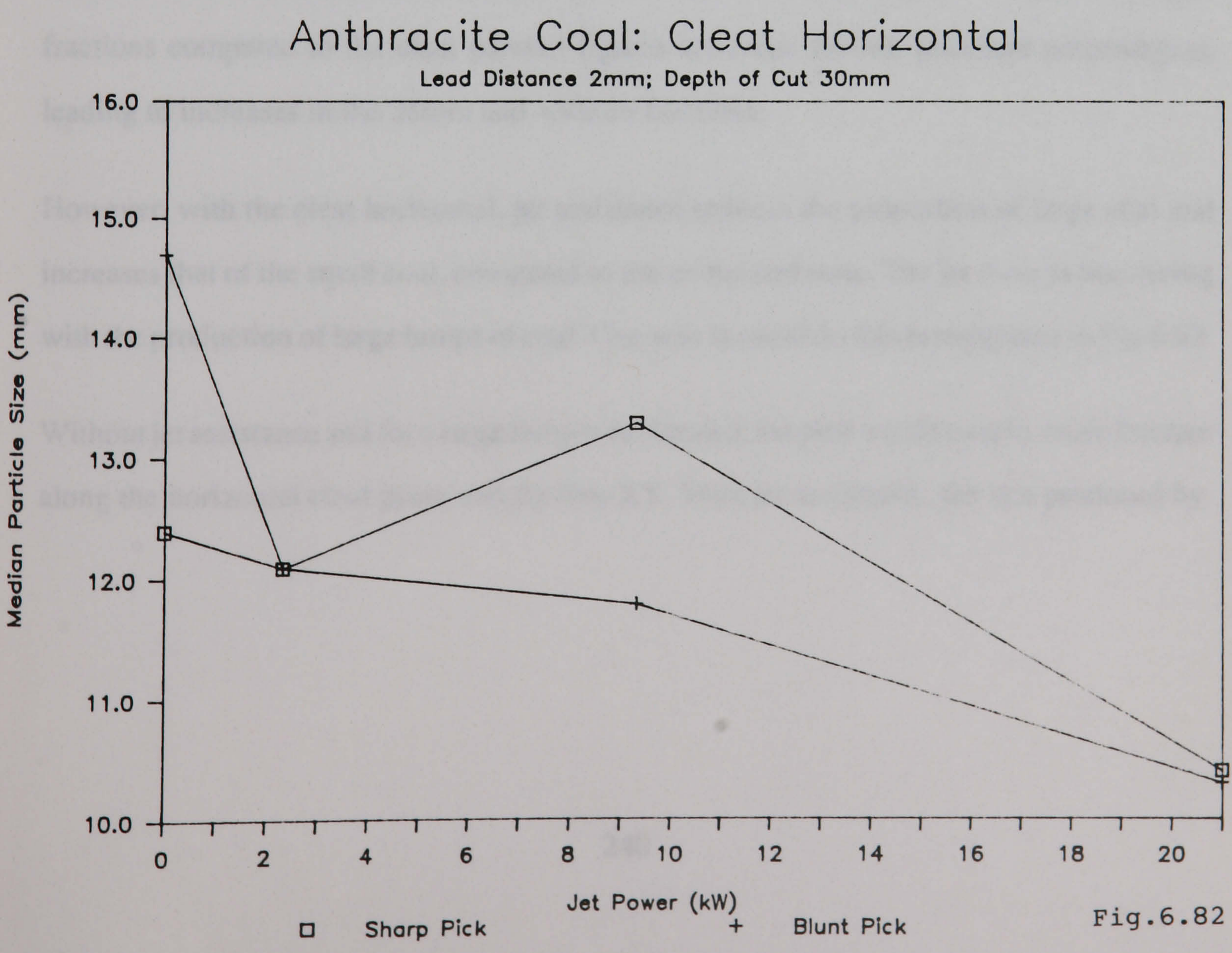


Fig.6.82

6.4.5 Discussion on Cleat Orientation

In the unassisted case, less fines are produced when the anthracite is cut with the cleat horizontal than with it parallel under both pick wear conditions - 0.8% and 2.8% (absolute values) respectively. This also holds true for the 0.5mm and 3.15mm fractions.

The proportions in the 28mm and +50mm fractions are also greater when the anthracite is cut with the cleat horizontally arranged: thus more large coal is being produced. The median particle sizes reflect this since the averages over all treatments are 12.1mm/10.9mm with the cleat horizontal/parallel.

More fines and less large coal, with the cleat parallel unassisted treatments, concur with higher forces compared to the cleat horizontal results. Therefore, not only is the coal easier to cut when the cleat is horizontal but less fines and a larger product is obtained.

The form of the cleat horizontal size distribution is similar to the ones given earlier (including those of the Erin coal). The differences lay in the proportions in each fraction. Particularly with the blunt unassisted tool, the decreases in the -0.5mm, 0.5mm, 3.15mm and 6.3mm fractions compared to the cleat parallel figures are from 3%-6% (absolute percentages), leading to increases in the 28mm and +50mm fractions.

However, with the cleat horizontal, jet assistance reduces the proportion of large coal and increases that of the small coal, compared to the unassisted tests. The jet then, is interfering with the production of large lumps of coal. One way it could do this is suggested in Fig.6.83.

Without jet assistance and for a large lump to be formed, the pick would tend to cause fracture along the horizontal cleat plane and the line XY. With jet assistance, the slot produced by

Suggested Breakout for Cleat Horizontally Orientated and with High Pressure Water Jet Assistance

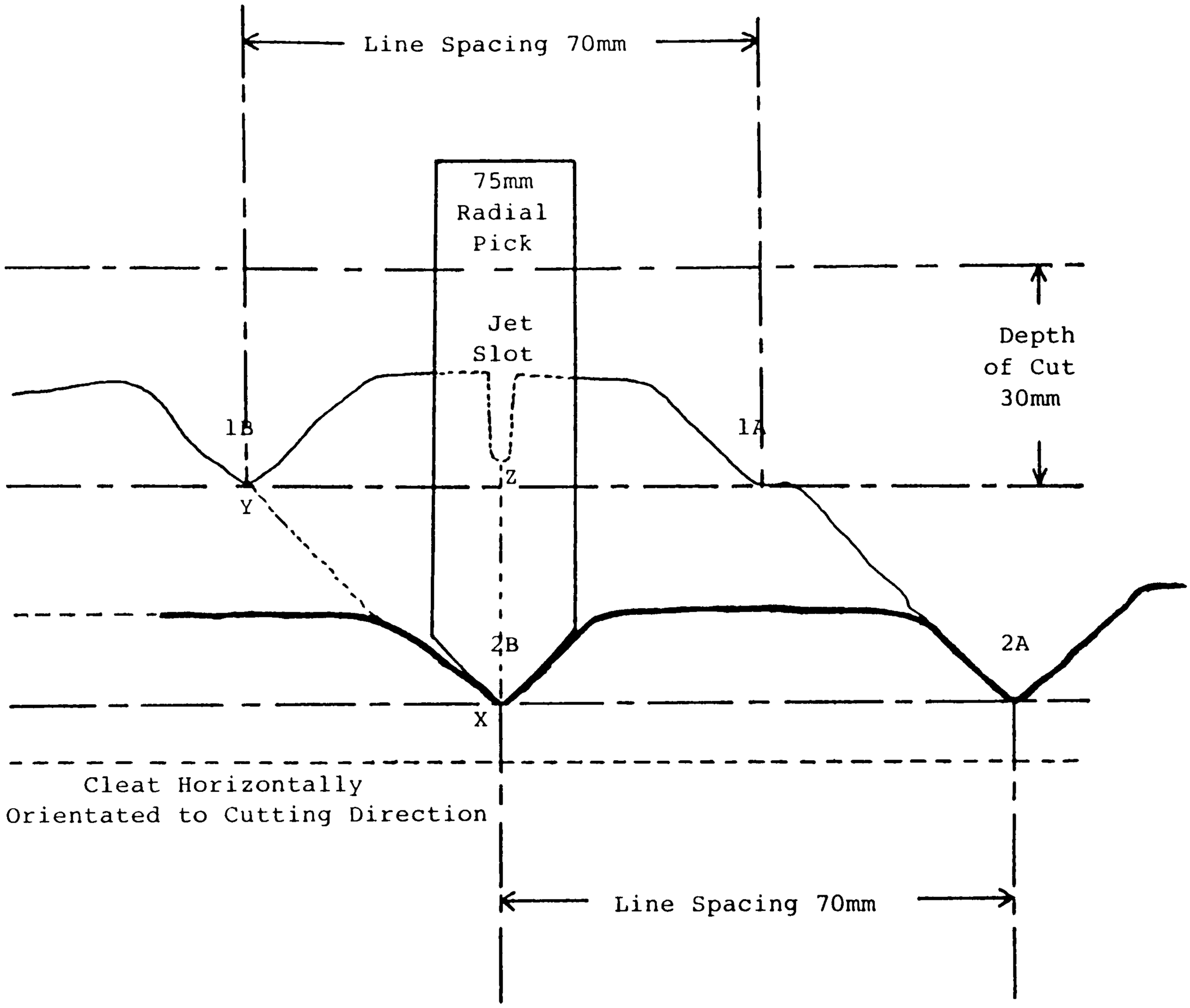


Fig.6.83

the jet would weaken the coal along the centre line of the pick. Thus a crack could propagate along ZX as well as XY and the cleat plane and thereby reduce the size of the lump formed. As the slot deepened with jet pressure the tendency for this to happen would be greater.

6.4.6 Conclusions

Jet assistance decreases the proportion of fine coal and increases the quantity of +28mm fraction coal in the Erin sample. The best result was obtained with the jet operating at 35MPa.

Fines reduction is also achieved in the anthracite when the cleat is orientated parallel to the direction of cut. The 35MPa pressure jet returns most fines reduction but considering the other size fractions as well, then the 70MPa pressure treatment yields the overall best size enhancement.

When the cleat is horizontal in the anthracite, jet assistance has a detrimental effect on coal size and actually increases the fines content.

The pick forces required to cut the coal when unassisted appear to be higher when the coal produces more fines and a lower proportion of large coal. With jet assistance this relation is not so simple since although the jet may be affording force reductions it may also be encouraging smaller coal to be formed, as in the case of the anthracite, cleat horizontal tests, Fig.6.82.

All the distributions fit very well to the Rosin-Rammler exponential equation and the median particle size is affected by coal type, cleat orientation and jet pressure. The average median particle sizes averaged over all the treatments for the coals are 7.1mm, 10.9mm and 12.1mm, for the Erin and anthracite (cleat parallel and horizontal) respectively.

Jet assistance does not drastically alter the form of the size distributions but modifies them to some extent. From this one infers that the essential cutting process is not fundamentally changed by the jet.

Apart from the cutting process, the coal size is influenced by the operating parameters i.e. depth of cut, line spacing and tool geometry. Deeper depths of cut and correspondingly wider line spacings increase the potential for producing larger size coal.

6.5 Summary

The more detailed conclusions are given throughout the text. Tests have revealed that both coals may receive force reductions with high pressure water jet assisted cutting. The minimum jet power at which major reductions are achieved depends upon the coal type - the heavily cleated, friable Erin coal requiring less power than the coherent, vitreous anthracite.

When the tool wears then more benefit is derived from jet assistance particularly in the normal force.

Cleat orientation influenced the effectiveness of jet assistance and the cutting forces without jet assistance. Benefit could be obtained at a lower jet pressure when the cleat was horizontal, but this was only significant in the normal force. Without jet assistance the anthracite was easier to cut when the cleat was horizontal compared to with it parallel.

The differences in the breakout can be seen to be influenced by the cleat and the coal lithotypes. Generally, jet assistance increased the breakout in both coals.

There was a tremendous increase in specific energy with jet power. Calculations were made which indicated that even with the 35MPa jet in the Erin coal where the specific energy was

not exorbitantly higher than in the unassisted case, over twice the actual force reductions gained in the cutting force would be needed to reduce the specific energy in the linear trials. An attempt to apply the laboratory results to predict if the specific energy of a shearer loader would be reduced gave a pessimistic conclusion. However, only one set of operating conditions were examined with the machine haulage speed being kept constant. In this respect there may be room for improvement.

Jet assistance reduced the fines and otherwise enhanced the coal size when the cleat was parallel in both coals. However, it proved to have a detrimental effect when the cleat was rotated 90°, in which case the fines were actually increased.

CHAPTER SEVEN

7 TEST SERIES ONE AND TWO RESULTS

7.1 Introduction

The experiments described in this section were performed at British Coal's Swadlincote Test Site, under the Rock Mechanics Branch, Headquarters Technical Department. Subsequently, all the force readings were abstracted and analysed in the Department of Mining Engineering, of the University of Newcastle upon Tyne, together with part of the sieve analysis.

7.2 Objectives and Research Programme

7.2.1 Objectives

The object of the experiment was to carry out an investigation into high pressure water jet assisted cutting of coal and from this assess what benefits may be expected in terms of enhanced cutting performance and size distribution of the cut product.

The criterion of increased cutting performance was the force reductions obtained in the three mutually perpendicular force components measured. Concerning the size distribution, particular interest lay in the influence of high pressure water jet assisted cutting on the fines production for the same reasons stated in the previous chapter. The operational factors such as offset and lead distances were examined to carry out a more detailed study and the tests were conducted in bituminous coal from the Erin Remainder, Opencast Site.

7.2.2 Test Programme

The research programme detailed here comprises two series as described below.

7.2.2.1 Test Series One

The main parameters influencing jet assisted cutting and the ones investigated in this series are indicated in the table below.

Factor	Level	Value
a) JET		
1. Jet Pressure	4	0, 35, 70, 105MPa
2. Jet Flow Rate	1	4 l/min
3. Nozzle Design	1	M.R.D.E.
4. Nozzle Material	1	Tungsten Carbide
5. Additive	0	None
6. Jet Type	1	Continuous
7. Jet Fluid	1	Water
b) OPERATIONAL		
8. Stand-off Distance	1	75mm
9. Lead Distance	1	2mm
10. Jet Position	1	Infront of Pick
11. Offset Distance	1	Zero
12. Cutting Mode	1	Relieved
13. Depth of Cut	1	30mm
14. Line Spacing	1	70mm
15. Cutting Speed	1	1.34m/s
16. Tool Type	1	75mm radial with HW tip
17. Tool Wear	2	Sharp/Blunt
18. Cutting w.r.t. Cleat	2	Parallel/Horizontal
19. Coal Type	1	Erin Coal (Bituminous)

Table 7.1

In these tests the flow rate was held constant at 4 l/min whilst the jet pressure was incremented in steps of 35MPa. 4 l/min per jet is considered the maximum allowable for the underground situation without causing excessive water to be released on to the coal face.

The stand-off distance is shown as 75mm, but this is the approximate distance from the nozzle exit to the tool tip rather than to the surface of the coal since with the relieved cutting mode the surface of the coal is irregular and depends upon the breakout pattern and might vary from treatment to treatment.

A relieved cutting regimen was adopted to model as closely as possible the actual cutting mode of underground coal cutting machinery. The 75mm heavy duty radial pick, which typically equips mining shearers, cut the coal. Both a sharp and artificially blunted tool were used and the tools were of the same specification as in the previous chapter.

The tests were carried out at the maximum cutting speed available to the linear rig (1.34m/s). The coal samples were arranged such that the cutting tool cut through the bedding planes for each cleat orientation.

The cutting forces (mean and mean peak) in three mutually perpendicular directions were recorded and used to assess the effectiveness of high pressure water jet assisted cutting over conventional cutting. All coal debris was collected and sized so the influence of jet assistance on fines production could be ascertained.

A series of additional tests to the above were performed with the sharp pick. These tests consisted of slotting the ridges in the breakout surfaces at different pressures and then cutting along the slots at a 30mm depth of cut but without further jet assistance. This was done for the three jet pressures indicated in Table 7.1.

All the treatments were replicated an average of ten times per treatment, hence in total 130 individually recorded cuts were made. The treatment order was randomized to comply with standard experimental procedure.

7.2.2.2 Test Series Two

Table 7.2 below describes the variables investigated in this test series.

Factor	Level	Value
a) JET		
1. Jet Pressure	1	70MPa
2. Jet Flow Rate	1	4 l/min
3. Nozzle Design	1	M.R.D.E.
4. Nozzle Material	1	Tungsten Carbide
5. Additive	0	None
6. Jet Type	1	Continuous
7. Jet Fluid	1	Water
b) OPERATIONAL		
8. Stand-off Distance	1	75mm
9. Lead Distance	4	2mm, 10mm, 50mm, 100mm
10. Jet Position	1	Infront of Pick
11. Offset Distance	3	0mm, 35mm, 50mm
12. Cutting Mode	1	Relieved
13. Depth of Cut	1	30mm
14. Line Spacing	1	70mm
15. Cutting Speed	1	1.34m/s
16. Tool Type	1	75mm radial with HW tip
17. Tool Wear	1	Sharp
18. Cutting w.r.t. Cleat	2	Parallel/Horizontal
19. Coal Type	1	Erin Coal (Bituminous)

Table 7.2

In these tests the effects of the lead and offset distances were examined at a constant jet pressure of 70MPa and flow rate of 4 l/min. The jet was positioned to the unrelieved side of the cutting tool as the offset distance was varied.

Again the cutting forces were recorded and the coal debris collected for a subsequent size analysis.

In total, 109 separate replicates were made, an average of nearly 11 per treatment and randomization was employed to nullify, as far as possible, systematic errors and variability within the coal.

7.3 Research Apparatus

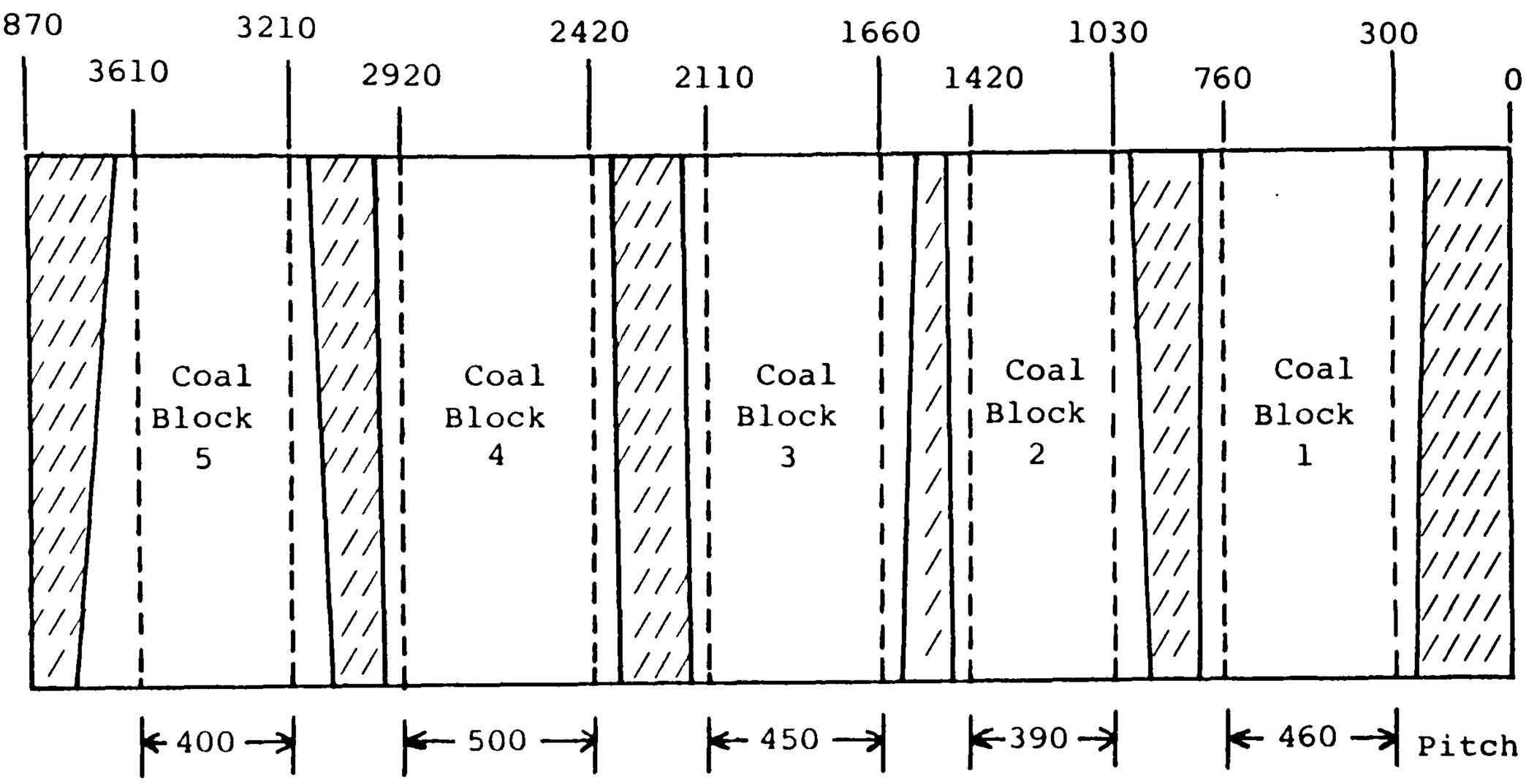
The research testing device has been used previously in hard rock cutting experiments (Morris and MacAndrew, 1986), to study the applicability of high pressure water jet assistance to tunnelling machines.

Basically, the apparatus is a modified linear planing machine with a stroke of 5.3m and a maximum cutting speed of 1.34m/s. The test specimen is mounted and secured on a traversing specimen table. A dynamometer capable of measuring forces up to 100kN (described in Chapter 2), is anchored on a substantial trestle with the water jet arrangement. The depth of cut, line spacing, lead distance, offset distance, and other parameters may be varied independently as required. High pressure water is supplied by a Presswell Hydraflow type HD70K pump.

Analogue signals from the dynamometer were recorded on a Racal 'Store 7DS' seven channel FM tape recorder. Force readings could also be obtained from a twelve channel UV recorder. The signal conditioning system was purpose built and designed by British Coal's instrumentation personnel.

Five coal blocks were cast in pitch on the specimen table. Their dimensions are illustrated in Fig.7.1. The shaded areas are regions of pitch between the coal specimens. Blocks 1, 3, 4 and 5 were orientated such that the cutting tool cut through the bedding planes and in a parallel direction to the vertical major cleat. Block 2, was inadvertently arranged such that

Plan View of Coal Blocks used in Test Series One and Two



Coal Blocks 1,3,4 & 5 - Cleat Parallel
Coal Block 2 - Cleat Horizontal

All dimensions in mm.

Fig.7.1

the major cleat was lying horizontally and thus at 90° to that in the other blocks. However, the forces in this block were isolated in the results analysis from the others and provided additional information on the effect of cleat orientation to jet assistance.

The cutting forces were calculated between the dashed lines in Fig.7.1, leaving a coal boarder of at least 50mm between the pitch so that the forces to cut the pitch would not be included in or affect the results. The analysis was conducted at Newcastle University in a similar manner to that described in Chapter 5. A force reading was taken for every 1.1mm length of cut.

7.4 Test Series One

7.4.1 Coal Cutting Results

The fundamental factorial design is described in Table 7.3 below. Each cell contains the number of replications for that treatment.

	Sharp Pick		Blunt Pick	
Jet Pressure	Cleat Parallel	Cleat Horizontal	Cleat Parallel	Cleat Horizontal
0MPa	13X	13X	12X	12X
35MPa	8X	8X	11X	11X
70MPa	12X	12X	12X	12X
105MPa	11X	11X	12X	12X

Table 7.3

Due to the variability between the forces in the coal blocks it was again necessary to take a severe statistical approach to the interpretation of the results. The forces for each coal block were used in the statistical analysis which was performed with the statistics software GLIM 3.12, available on Newcastle University's Mainframe computer. It was found during the

analysis that the forces in coal block 3 were the highest, sometimes as much as three times the values in block 1. This highlights the variability within coal: even though the blocks were abstracted from the same site, at the same time and probably in close proximity to one another.

Underground, the coal in a panel is subjected to various states of stress. Initially a particular section of the coal is confined and experiences the overburden pressure. As the coal face approaches this section of coal, the stresses rise and reach a peak, 1-3m behind the coal face, which is called the abutment pressure (Whittaker, 1974). This pressure may be up to two to three times the overburden stress (Farmer and Robertson, 1975). After this the stress suddenly drops to near zero along the face-line, hence, the coal along the face is usually relatively de-stressed. It is this phenomenon that makes extraction and roof support possible, otherwise the stresses would be too great to contend with.

Pomeroy (1963), conducted cutting trials with coal samples stressed up to 1000psi (6.89MPa) and observed the cutting forces to vary as the confining pressure increased. In some coals the forces reached a maximum at 500psi and then decreased to around the unstressed value as the pressure was raised further. Also, the confining pressure increased the cutting forces most in the heavily cleated coals; the joints being closed, thus making the coal harder to cut. From the experiment, Pomeroy, suggested that since the overburden pressure would be greater than the compressive strength of the coal at the face, it should supplement the forces required to cut the coal.

Also, Leonard (1979), reports that Protodyakanov, found the strength of coal to vary by as much as 30% within the same seam.

The variability within the test coal then, would probably be evident underground in the seam.

The abutment pressure makes it difficult to predict the cutting forces and from the previous

statements would appear to weaken the coal since it would be greater than its compressive strength. Therefore, the author thinks the un-stressed cutting trials should provide useful information that would be reproducible below ground.

The statistical analysis is given below. The figures in brackets are the values at which a treatment becomes significant at the 1% level i.e. highly significant.

Mean Normal Force ANOVA

Source of Variation	Sums of Squares	Degrees of Freedom	Mean Square	F-ratio & (Significance Level)
Between Pressures	7.0	3	2.3	0.9 (3.8)
Between Pick Wear	280.0	1	280.0	103.9 (6.7)
Between Cleat	44.0	1	44.0	16.3 (6.7)
Interaction between Pressures & Pick Wear	30.0	3	10.0	3.7 (3.8)
Interaction between Pressures & Cleat	9.0	3	3.0	1.1 (3.8)
Interaction between Cleat & Pick Wear	2.1	1	2.1	0.8 (6.7)
Interaction between Pressures, Cleat & Pick Wear	0.4	3	0.1	0.0 (3.8)
Experimental Error	994.5	369	2.7	
Total	1377.0	384		

Table 7.4

Since four coal blocks were used to calculate the forces for the cleat parallel tests and one for the cleat horizontal, the standard errors have to be weighted depending upon the statistical comparisons being made. Hence, the standard error within the cleat parallel treatments is

±0.37kN; within the cleat horizontal treatments it is ±0.73kN; and between the cleat orientations it is ±0.58kN. Thus the 95% confidence limits for a two-tailed test are ±0.73kN, ±1.53kN and ±1.18kN respectively.

Table 7.4 indicates that only the effects of cleat and pick wear are significant in the mean normal force, and the effect of tool wear is by far the greatest factor on this force component.

The results are plotted in Fig.7.2-7, and indicate there are no significant force decreases caused by jet assistance in the normal force. The trends with the sharp pick show some benefit but this is not realised with the blunt tool. The graphs show that the forces are lower with the cleat horizontal than with it parallel to the cutting direction and this is particularly so with the blunt tool. Also, the force increases due to cutting with the blunt tool are greater when the cleat is parallel than when it is horizontal and this is obtained over the whole pressure range.

Fig.7.6-7, show the results for the cleat parallel tests against jet power. Essentially, the form of the graphs are the same as those against jet pressure and so further graphs of jet power shall not be given. The curves are the same because the jet flow rate was maintained constant at 4 l/min. The jet powers at 35MPa, 70MPa and 105MPa pressures were 2.33kW, 4.67kW and 7.00kW respectively. Thus the power has increased in the ratio 1:2:3.

Fig.7.8-11, illustrate the percentage force differences compared to the unassisted cuts. In both cases of cleat orientations, the sharp tool receives benefit from jet assistance which is subsequently lost with the blunt tool. However, some assistance is afforded the blunt tool, as shown in Fig.7.11, at a jet pressure of 35MPa.

Mean Cutting Force ANOVA

Source of Variation	Sums of Squares	Degrees of Freedom	Mean Square	F-ratio & (Significance Level)
Between Pressures	3.0	3	1.0	0.4 (3.8)
Between Pick Wear	5.0	1	5.0	1.8 (6.7)
Between Cleat	141.0	1	141.0	51.8 (6.7)
Interaction between Pressures & Pick Wear	95.0	3	31.7	11.6 (3.8)
Interaction between Pressures & Cleat	13.0	3	4.3	1.6 (3.8)
Interaction between Cleat & Pick Wear	3.0	1	3.0	1.1 (6.7)
Interaction between Pressures, Cleat & Pick Wear	1.0	3	0.3	0.1 (3.8)
Experimental Error	1005.0	369	2.7	
Total	1266.0	384		

Table 7.5

The standard errors and 95% confidence limits are the same as those for the mean normal force in this case.

The cleat orientation has the most significant influence on the mean cutting force. The cleat horizontal mean cutting forces are all significantly lower than the corresponding cleat parallel ones for both sharp and blunt picks.

There is a significant interaction term between jet pressure and pick wear. For the sharp pick, cleat parallel tests, there are significant force decreases with the treatments at jet pressures of 70MPa and 105MPa. With the cleat horizontal, the 35MPa and 105MPa treatments have significantly decreased the mean cutting force also.

The blunt tool results are quite unexpected. There has been no significant change amongst the jet assisted values compared to the sharp pick results. However, the dry or unassisted force levels are significantly lower than those of the sharp pick, in both cleat orientations. The jet pressure effect then, has not shown up significant due to the blunt tool results.

The percentage force differences follow the same pattern as the mean normal force. With the blunt tool though the cutting force is increased more than the normal force, Fig.7.9,11.

Mean Sideway Force ANOVA

Source of Variation	Sums of Squares	Degrees of Freedom	Mean Square	F-ratio & (Significance Level)
Between Pressures	3.3	3	1.1	2.1 (3.8)
Between Pick Wear	0.2	1	0.2	0.4 (6.7)
Between Cleat	18.0	1	18.0	35.2 (6.7)
Interaction between Pressures & Pick Wear	5.9	3	2.0	3.8 (3.8)
Interaction between Pressures & Cleat	1.6	3	0.5	1.0 (3.8)
Interaction between Cleat & Pick Wear	0.2	1	0.2	0.4 (6.7)
Interaction between Pressures, Cleat & Pick Wear	1.6	3	0.5	1.0 (3.8)
Experimental Error	188.9	369	0.5	
Total	219.7	384		

Table 7.6

The 95% confidence limits for the two-tailed t-tests are ±0.32kN for the cleat parallel results; ±0.67kN for the cleat horizontal tests; and ±0.51kN when making comparisons between the two cleat orientations.

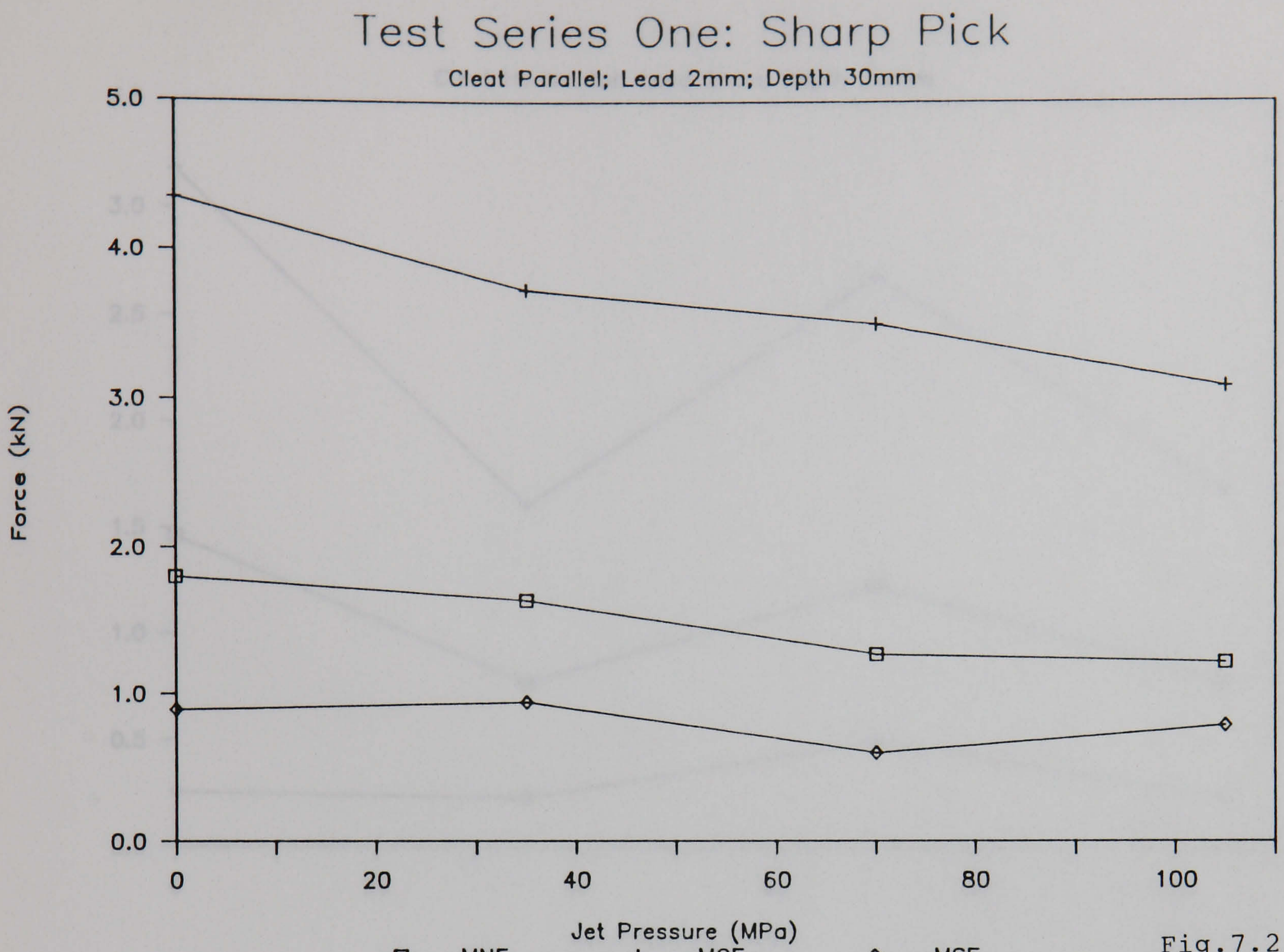

Test Series One: Sharp Pick
Cleat Parallel; Lead 2mm; Depth 30mm
5.0
4.0
3.0
2.0
1.0
0.0
Force (kN)
0
20
40
60
80
100
Jet Pressure (MPa)
MNF
MCF
MSF

Fig.7.2

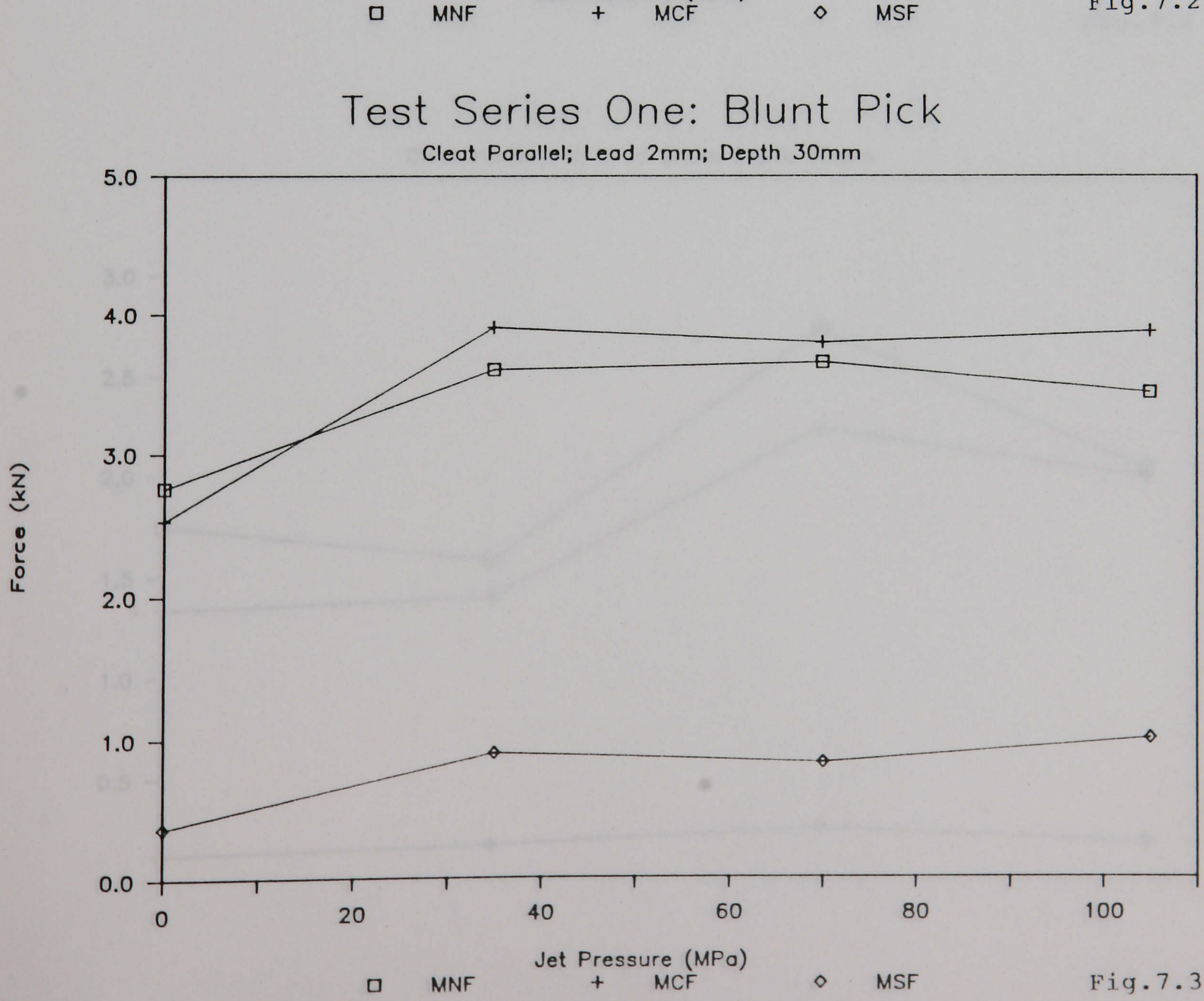

Test Series One: Blunt Pick
Cleat Parallel; Lead 2mm; Depth 30mm
5.0
4.0
3.0
2.0
1.0
0.0
Force (kN)
0
20
40
60
80
100
Jet Pressure (MPa)
MNF
MCF
MSF

Fig.7.3

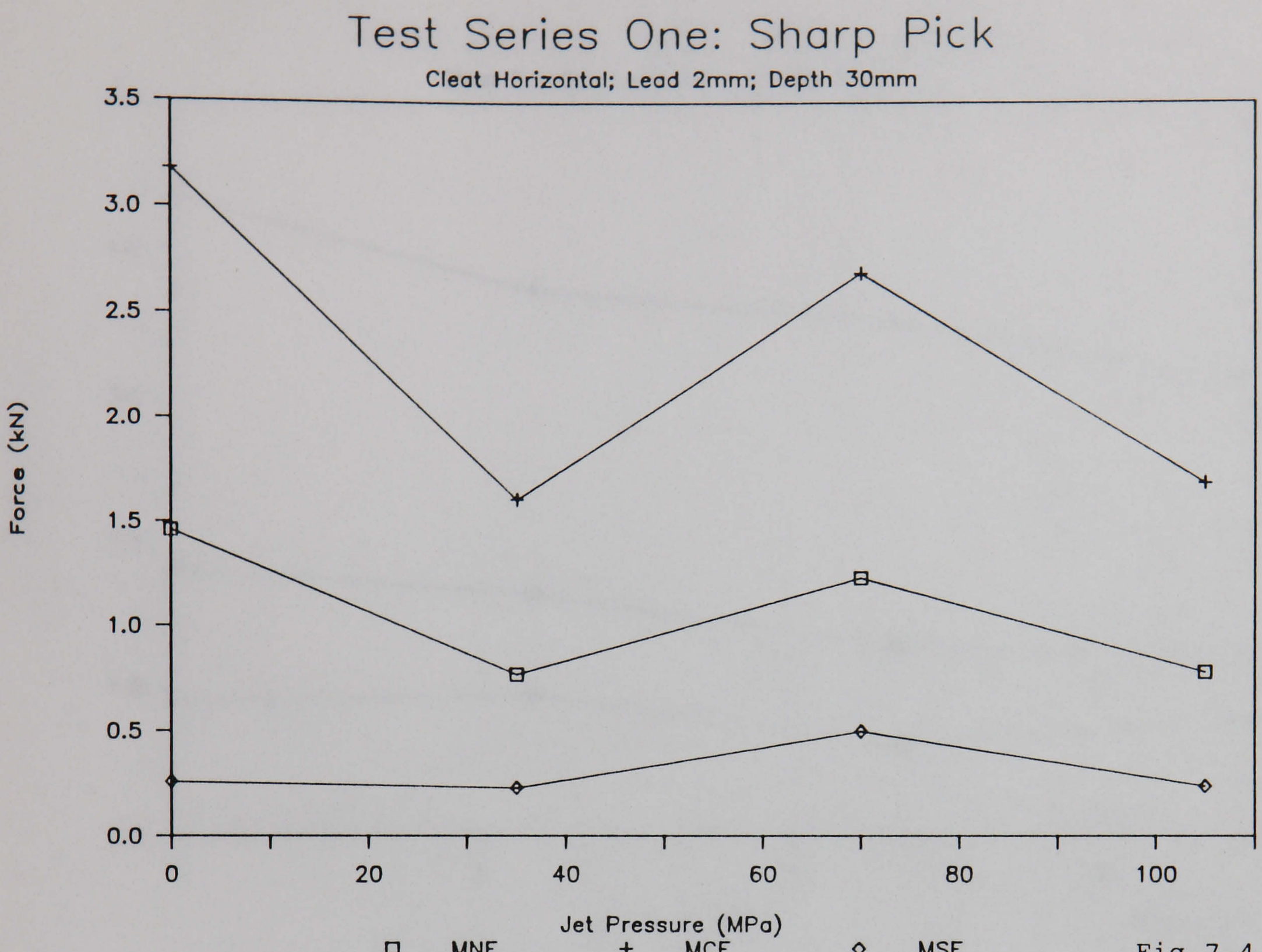

Test Series One: Sharp Pick
Cleat Horizontal; Lead 2mm; Depth 30mm
Force (kN)
3.5
3.0
2.5
2.0
1.5
1.0
0.5
0.0
0
20
40
60
80
100
Jet Pressure (MPa)
MNF
MCF
MSF

Fig.7.4

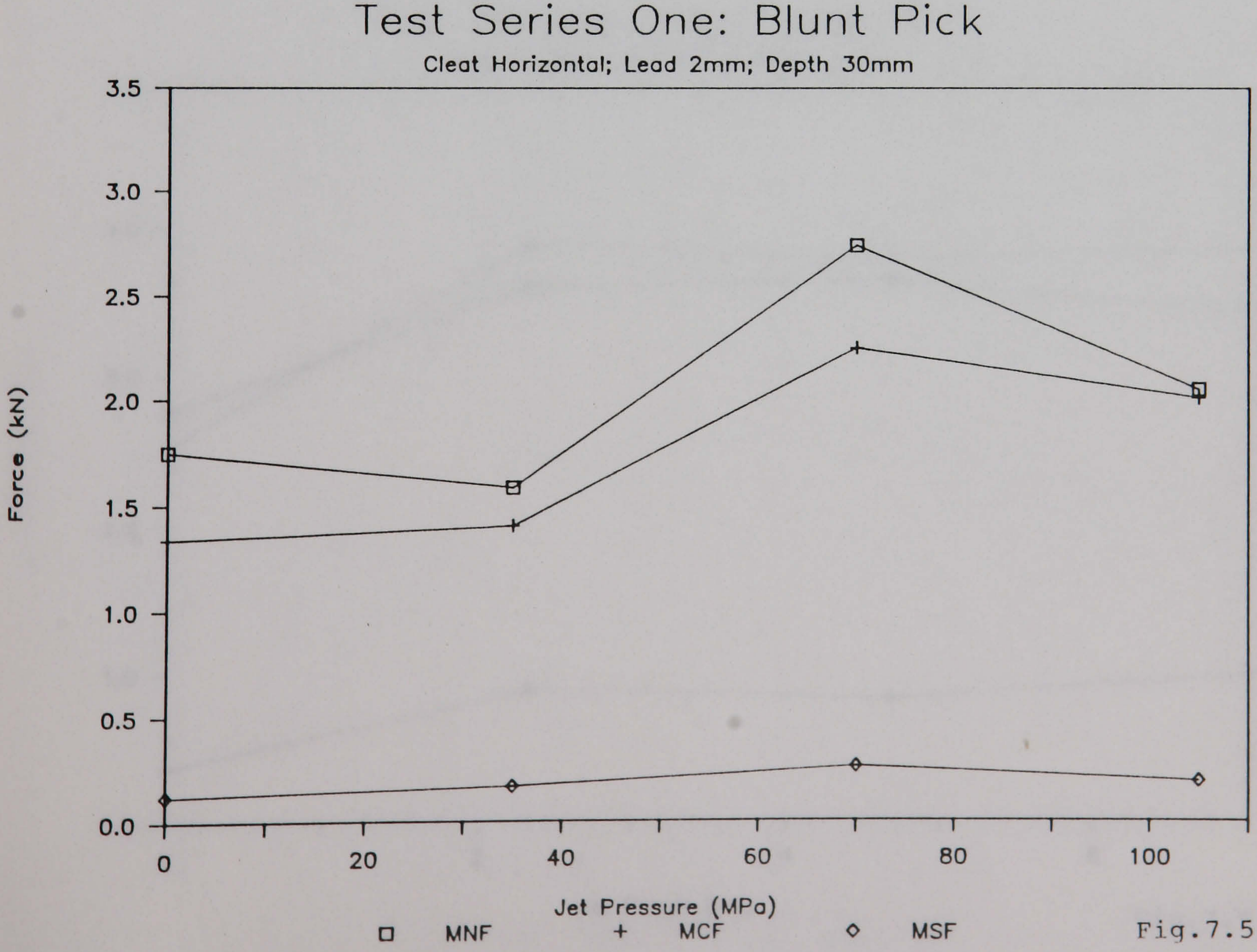

Test Series One: Blunt Pick
Cleat Horizontal; Lead 2mm; Depth 30mm
Force (kN)
3.5
3.0
2.5
2.0
1.5
1.0
0.5
0.0
0
20
40
60
80
100
Jet Pressure (MPa)
MNF
MCF
MSF

Fig.7.5

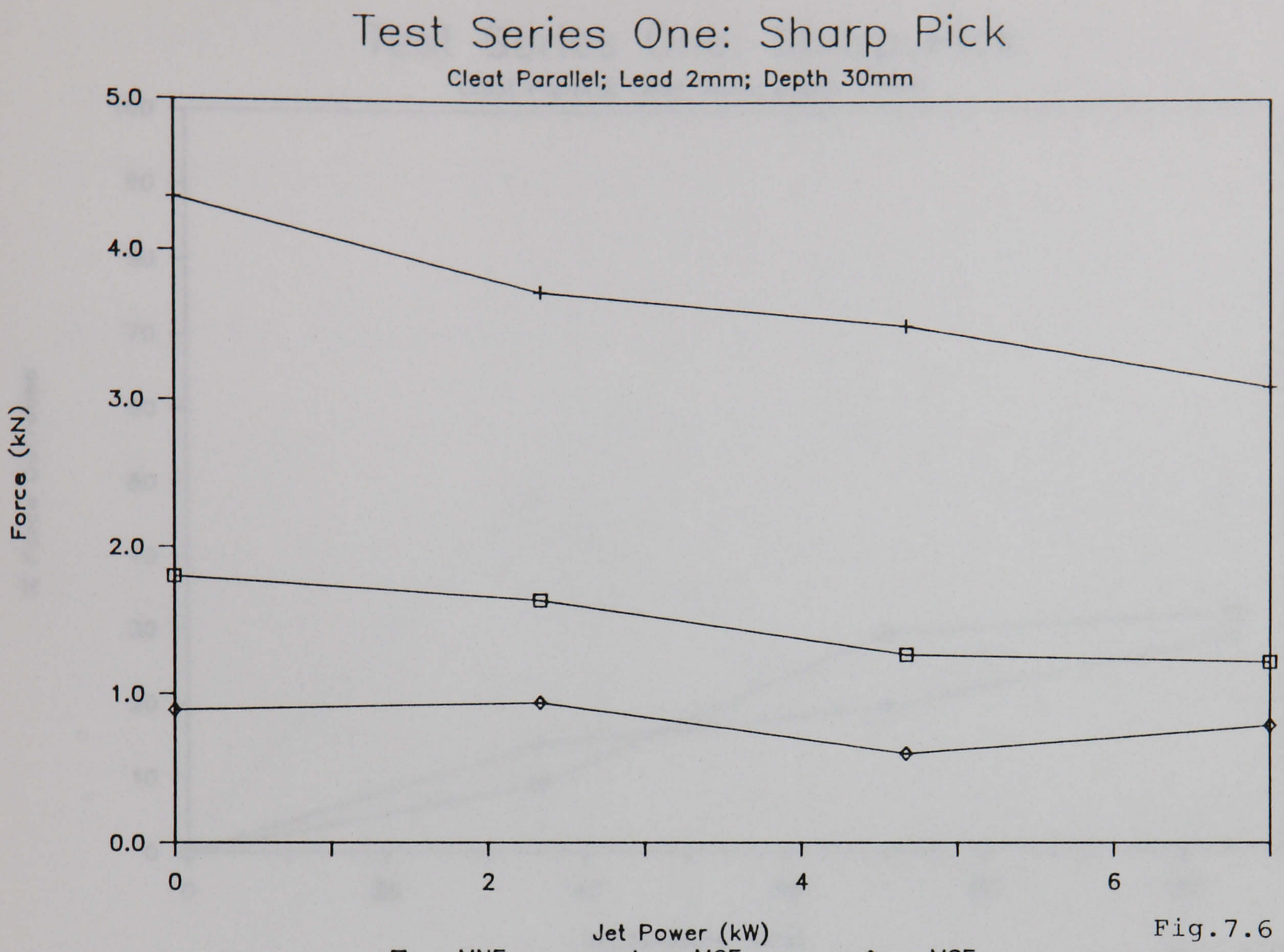

Test Series One: Sharp Pick
Cleat Parallel; Lead 2mm; Depth 30mm
5.0
4.0
3.0
2.0
1.0
0.0
Force (kN)
0
2
4
6
Jet Power (kW)
MNF
MCF
MSF

Fig.7.6

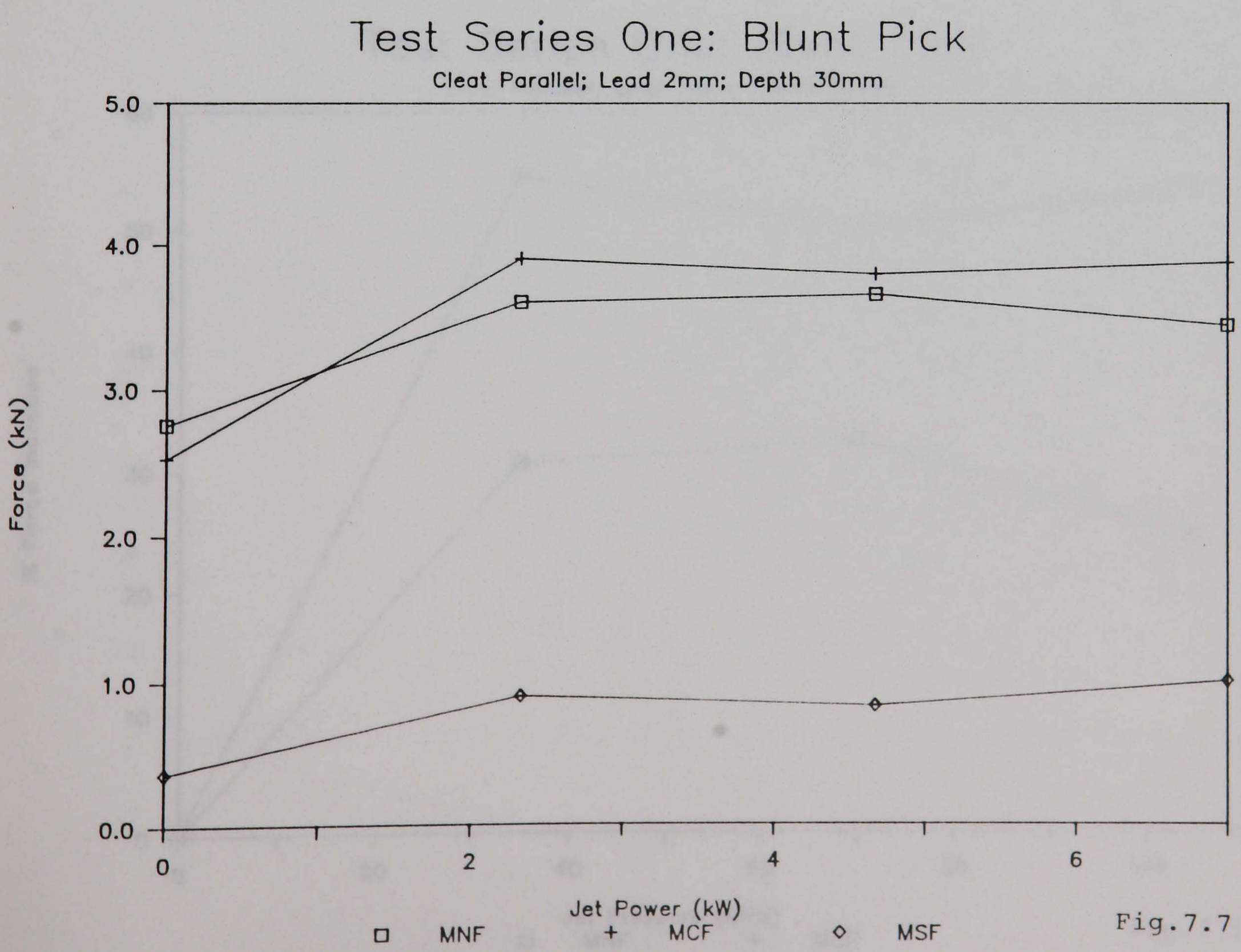

Test Series One: Blunt Pick
Cleat Parallel; Lead 2mm; Depth 30mm
5.0
4.0
3.0
2.0
1.0
0.0
Force (kN)
0
2
4
6
Jet Power (kW)
MNF
MCF
MSF

Fig.7.7

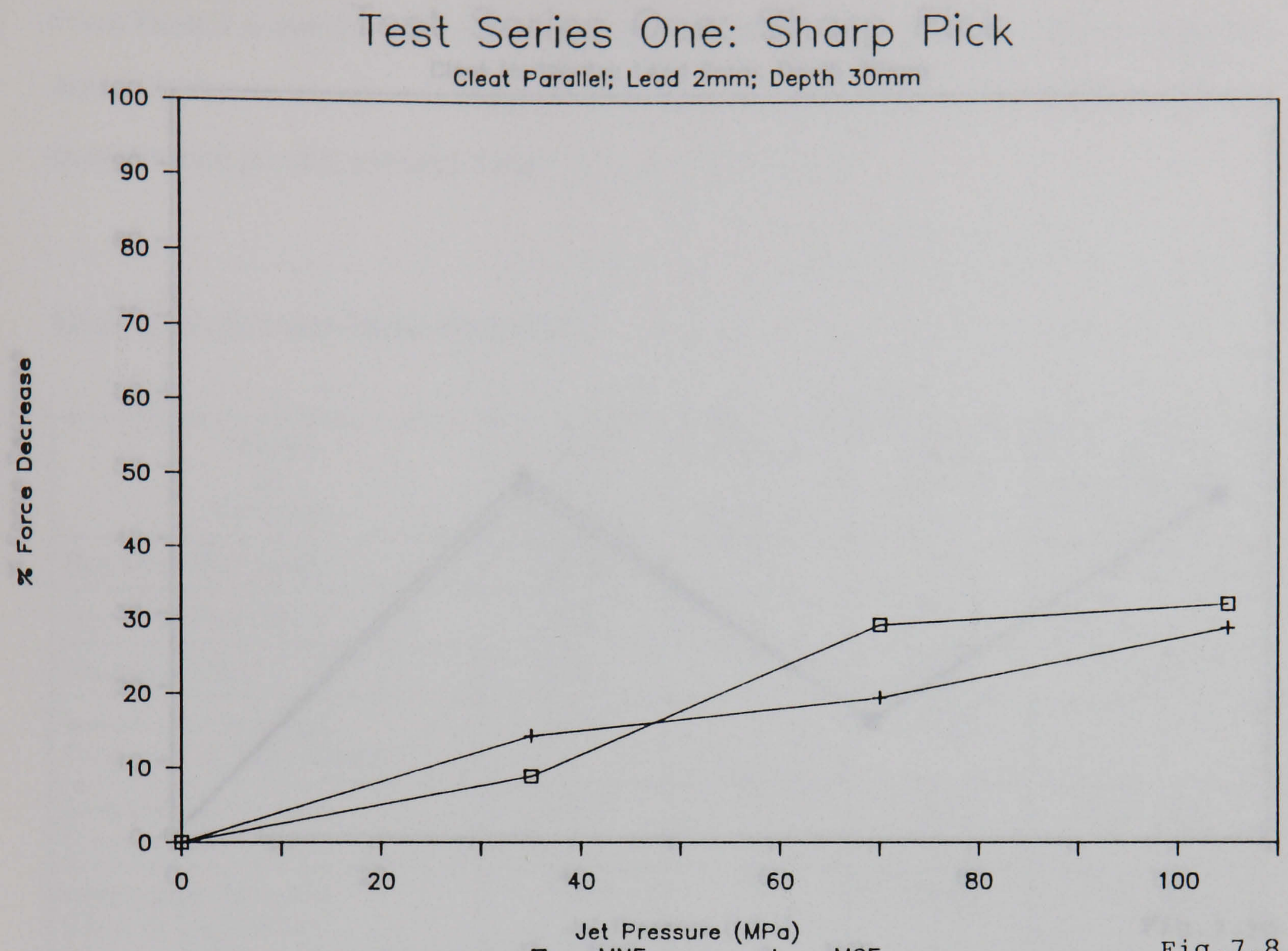

Test Series One: Sharp Pick
Cleat Parallel; Lead 2mm; Depth 30mm
% Force Decrease
100
90
80
70
60
50
40
30
20
10
0
0
20
40
60
80
100
Jet Pressure (MPa)
□ MNF + MCF

Fig.7.8

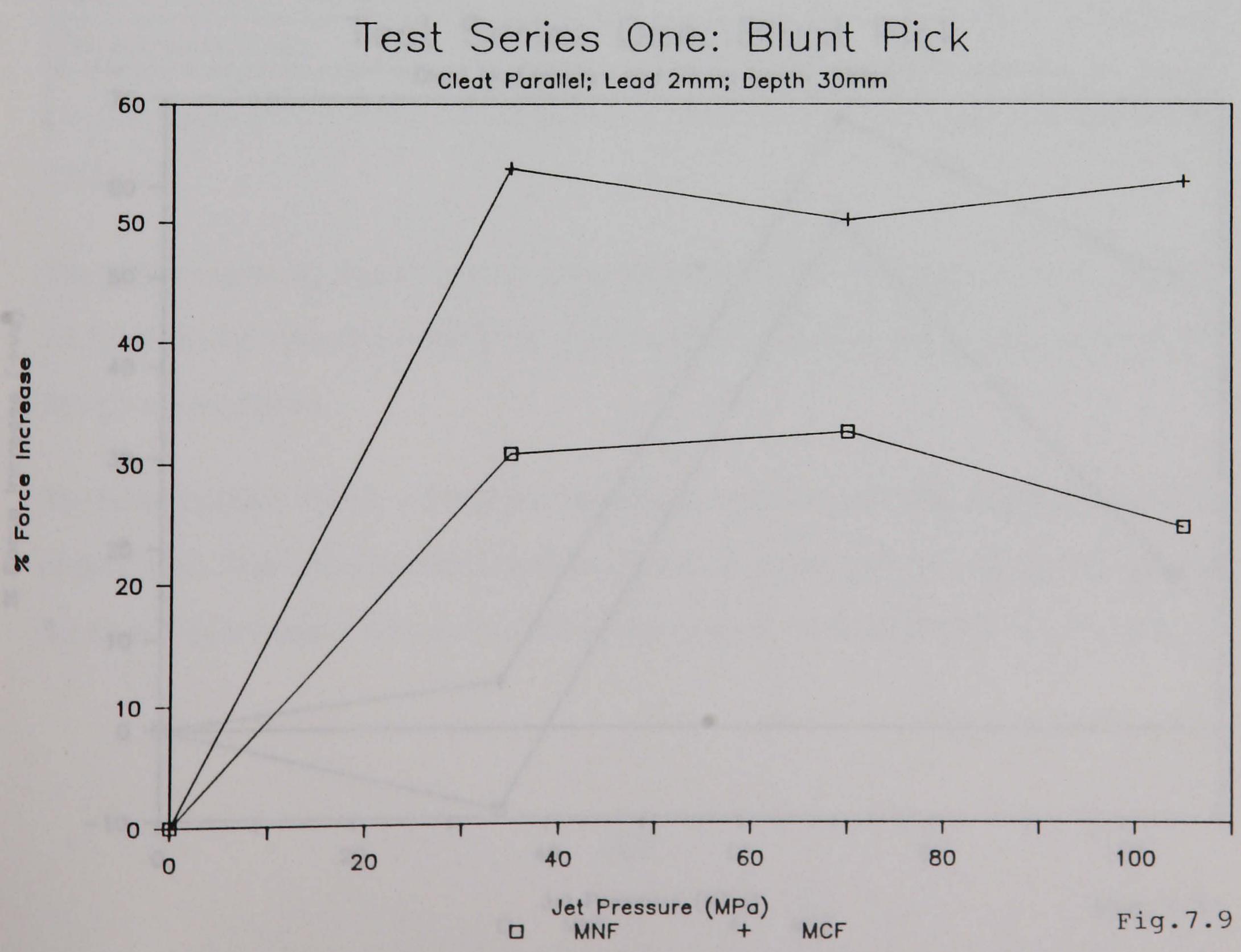

Test Series One: Blunt Pick
Cleat Parallel; Lead 2mm; Depth 30mm
% Force Increase
60
50
40
30
20
10
0
0
20
40
60
80
100
Jet Pressure (MPa)
□ MNF + MCF

Fig.7.9

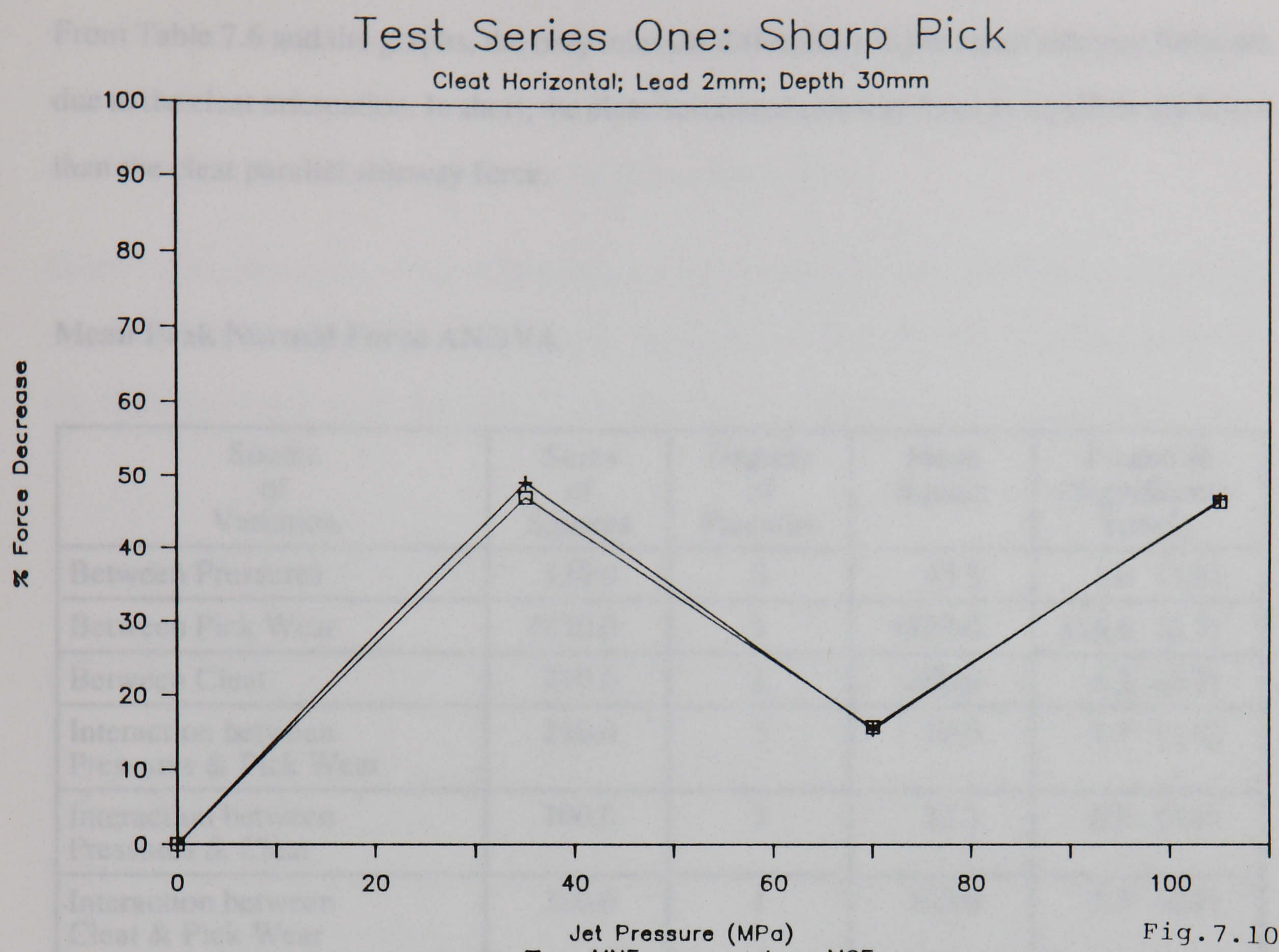


Fig.7.10

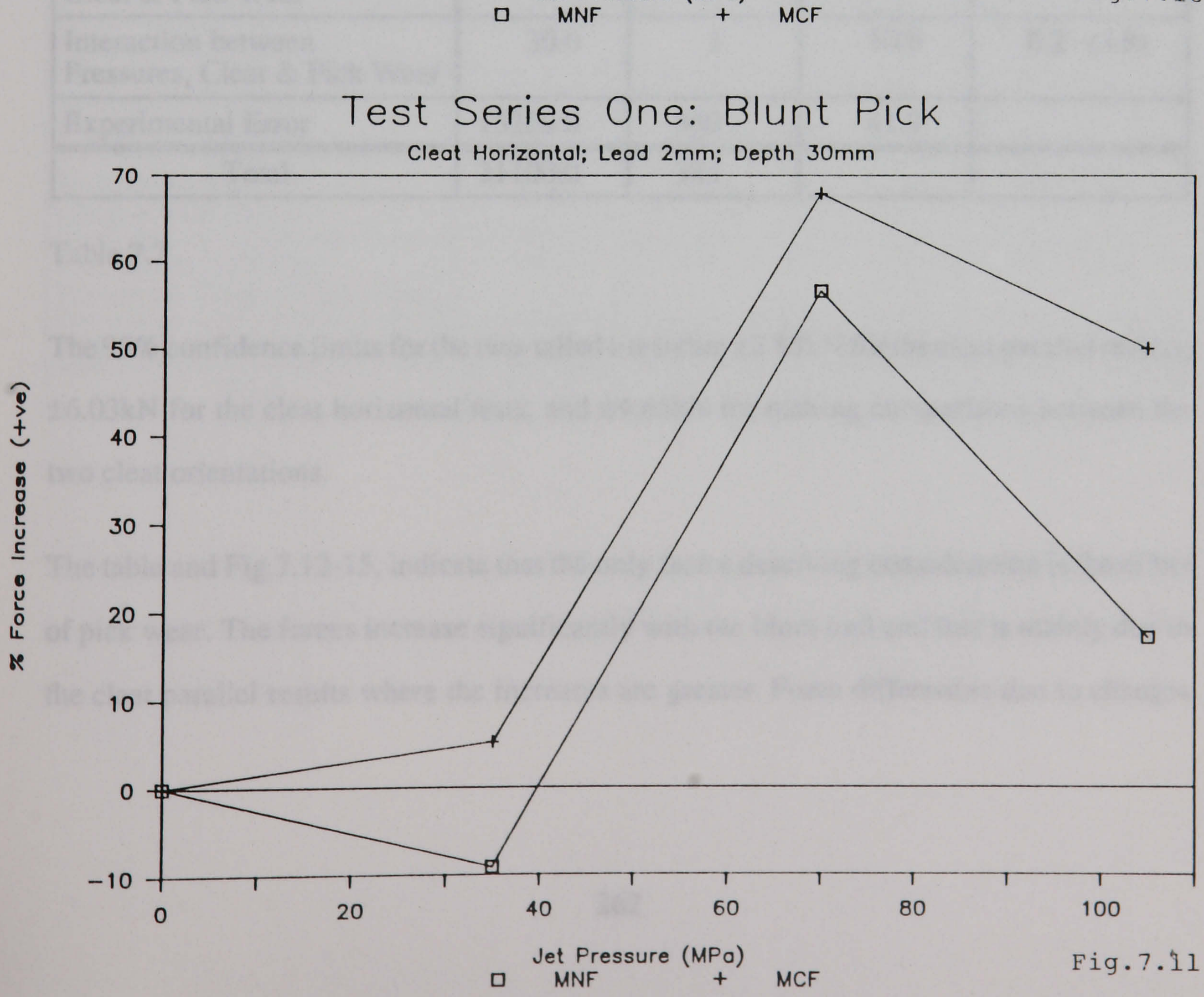


Fig.7.11

From Table 7.6 and the graphs, the only relevant differences in the mean sideway force are due to the cleat orientation. In short, the cleat horizontal sideway force is significantly lower than the cleat parallel sideway force.

Mean Peak Normal Force ANOVA

Source of Variation	Sums of Squares	Degrees of Freedom	Mean Square	F-ratio & (Significance Level)
Between Pressures	130.0	3	43.3	1.0 (3.8)
Between Pick Wear	4820.0	1	4820.0	116.6 (6.7)
Between Cleat	260.0	1	260.0	6.3 (6.7)
Interaction between Pressures & Pick Wear	210.0	3	70.0	1.7 (3.8)
Interaction between Pressures & Cleat	100.0	3	33.3	0.8 (3.8)
Interaction between Cleat & Pick Wear	300.0	1	300.0	7.3 (6.7)
Interaction between Pressures, Cleat & Pick Wear	30.0	3	10.0	0.2 (3.8)
Experimental Error	15250.0	369	41.3	
Total	21100.0	384		

Table 7.7

The 95% confidence limits for the two-tailed t-tests are ±2.85kN for the cleat parallel results; ±6.03kN for the cleat horizontal tests; and ±4.65kN for making comparisons between the two cleat orientations.

The table and Fig.7.12-15, indicate that the only factor deserving consideration is the effect of pick wear. The forces increase significantly with the blunt tool and this is mainly due to the cleat parallel results where the increases are greater. Force differences due to changes

in jet pressure have no statistical significance. The effect of cleat is actually significant but at the 5% level and is evident between the blunt tool results. It is also highly significant from the interaction term between cleat orientation and pick wear.

Graphs of the percentage force differences are given in Fig.7.16-19. Similar features to the mean forces are exhibited. Benefit from jet assistance is achieved in the sharp tool with only the 35MPa pressure treatment in Fig.7.19, showing any force reduction in the blunt tool.

Mean Peak Cutting Force ANOVA

Source of Variation	Sums of Squares	Degrees of Freedom	Mean Square	F-ratio & (Significance Level)
Between Pressures	300.0	3	100.0	4.1 (3.8)
Between Pick Wear	180.0	1	180.0	7.3 (6.7)
Between Cleat	356.0	1	356.0	14.4 (6.7)
Interaction between Pressures & Pick Wear	617.0	3	205.7	8.3 (3.8)
Interaction between Pressures & Cleat	135.0	3	45.0	1.8 (3.8)
Interaction between Cleat & Pick Wear	30.0	1	30.0	1.2 (6.7)
Interaction between Pressures, Cleat & Pick Wear	11.0	3	3.7	0.2 (3.8)
Experimental Error	9091.0	369	24.6	
Total	10720.0	384		

Table 7.8

The 95% confidence limits for the two-tailed t-tests are ±2.20kN for the cleat parallel results; ±4.66kN for the cleat horizontal tests; and ±3.58kN when making comparisons between the two cleat orientations.

All the main effects appear significant in Table 7.8. The largest effect is caused by the differences due to the cleat orientation such that the mean peak cutting forces are lower when the cleat is horizontal rather than parallel.

As with the mean cutting force, the unassisted or dry, blunt tool results are significantly lower than the sharp tool ones, in both cleat directions.

It is only with the sharp tool that significant force reductions are achieved through jet assistance and this occurs at jet pressures of 35MPa and 105MPa and for both cleat orientations.

From Fig.7.18-19, one can say that the 35MPa pressure treatment yields the best result when the cleat is horizontal.

Mean Peak Sideway Force ANOVA

Source of Variation	Sums of Squares	Degrees of Freedom	Mean Square	F-ratio & (Significance Level)
Between Pressures	15.0	3	5.0	1.2 (3.8)
Between Pick Wear	50.0	1	50.0	11.6 (6.7)
Between Cleat	85.0	1	85.0	19.7 (6.7)
Interaction between Pressures & Pick Wear	74.0	3	2.5	0.6 (3.8)
Interaction between Pressures & Cleat	24.0	3	8.0	1.8 (3.8)
Interaction between Cleat & Pick Wear	1.0	1	1.0	0.2 (6.7)
Interaction between Pressures, Cleat & Pick Wear	6.0	3	2.0	0.5 (3.8)
Experimental Error	1596.0	369	4.3	
Total	1851.0	384		

Table 7.9

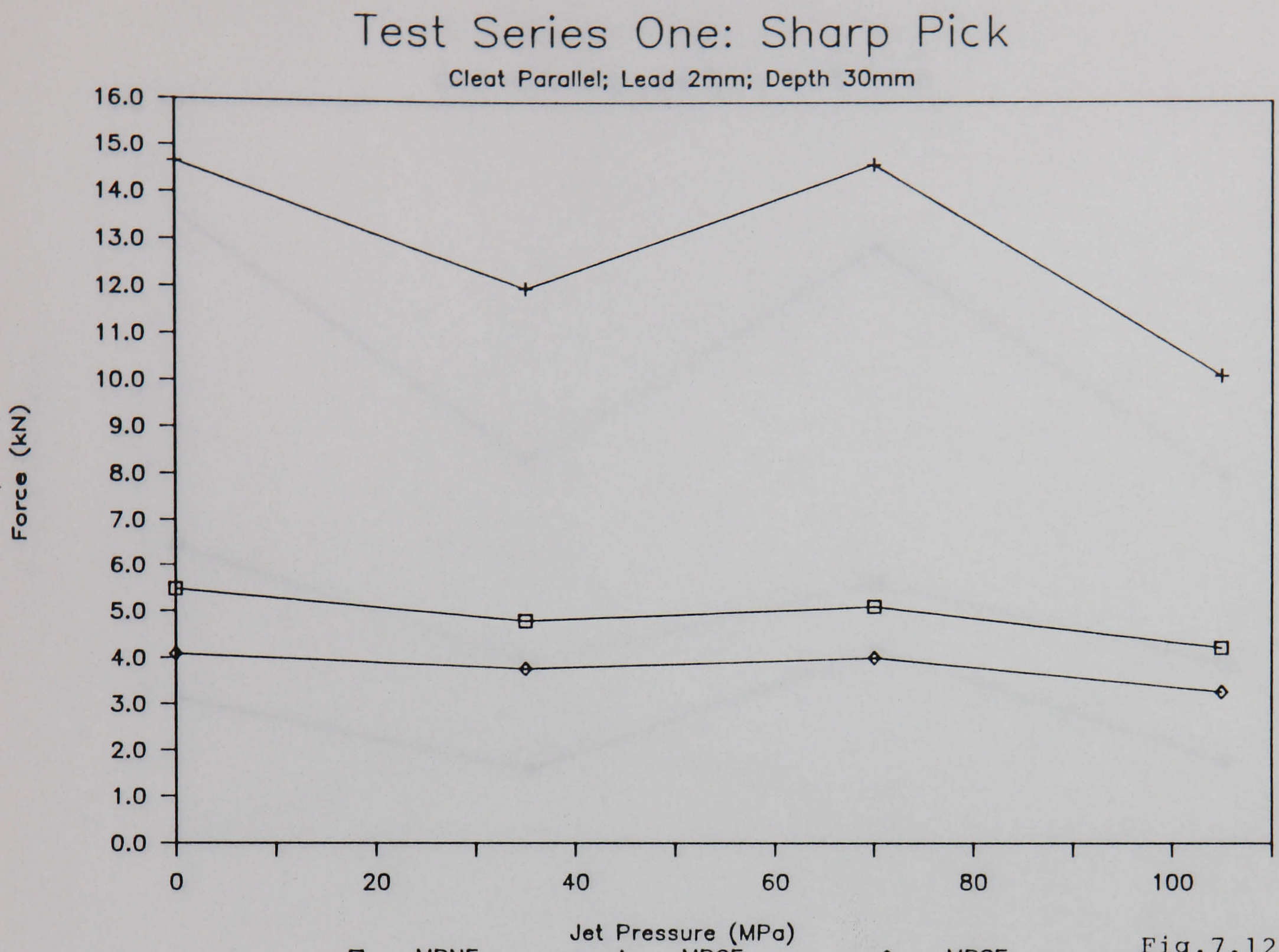


Fig.7.12

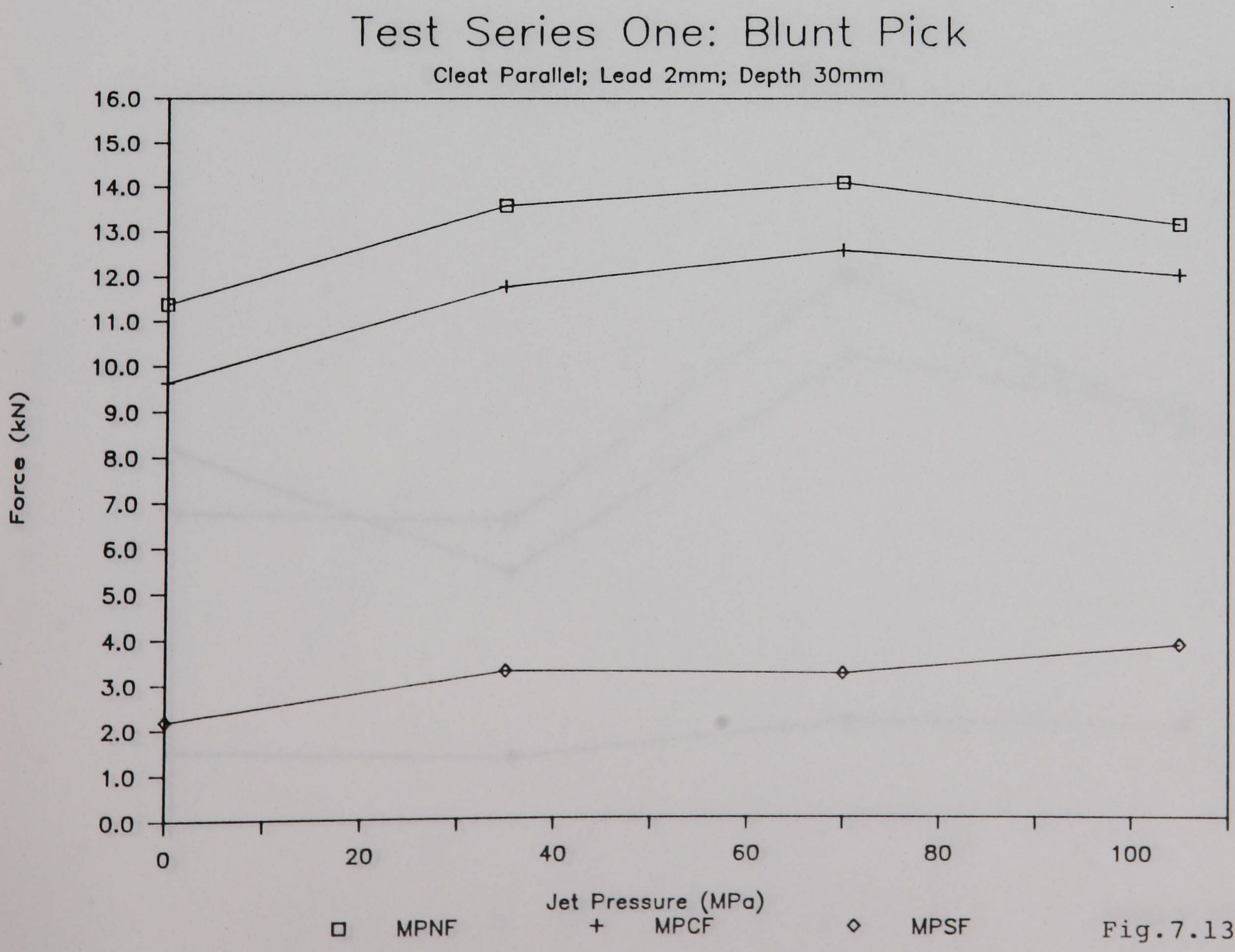


Fig.7.13

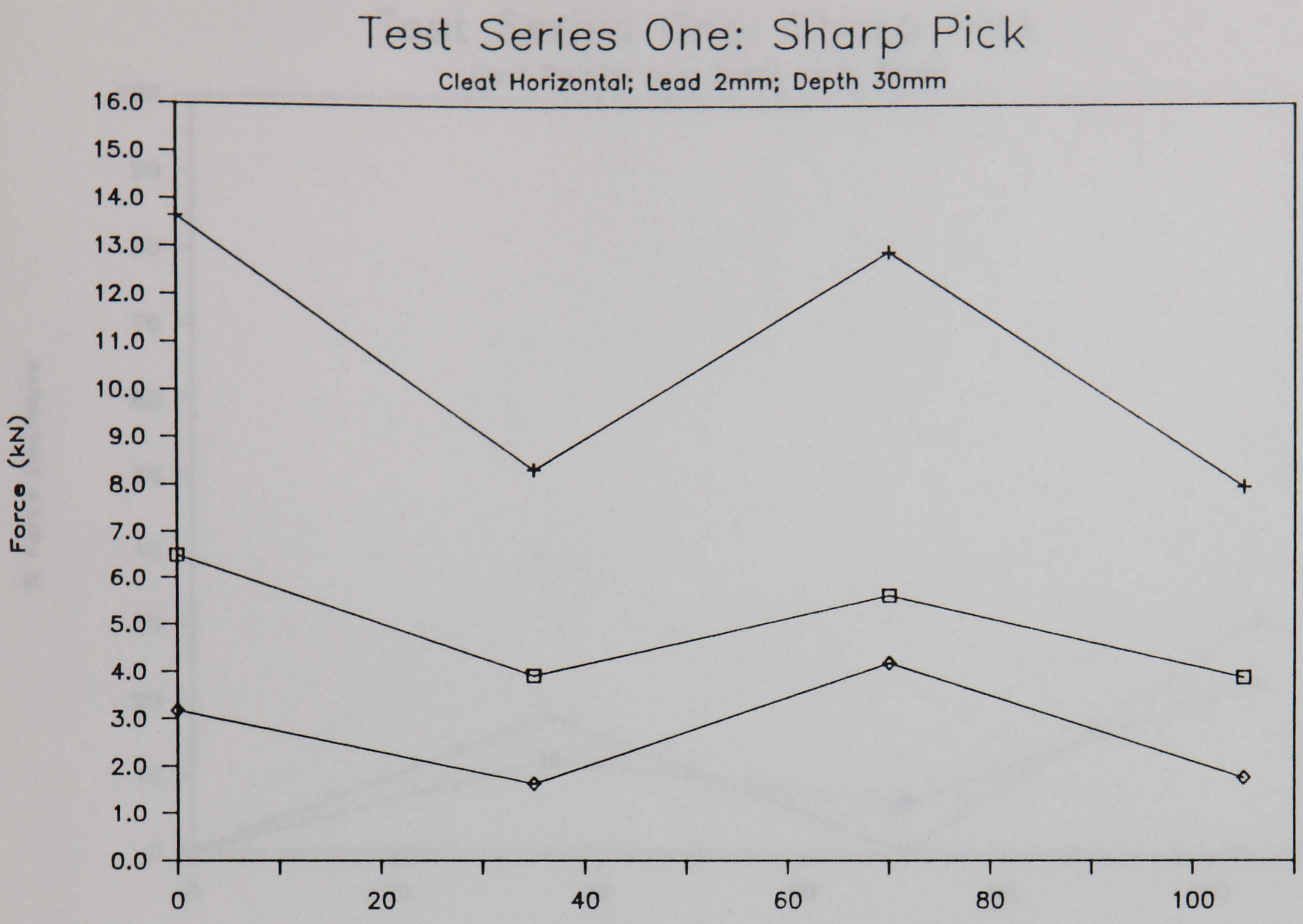


Fig.7.14

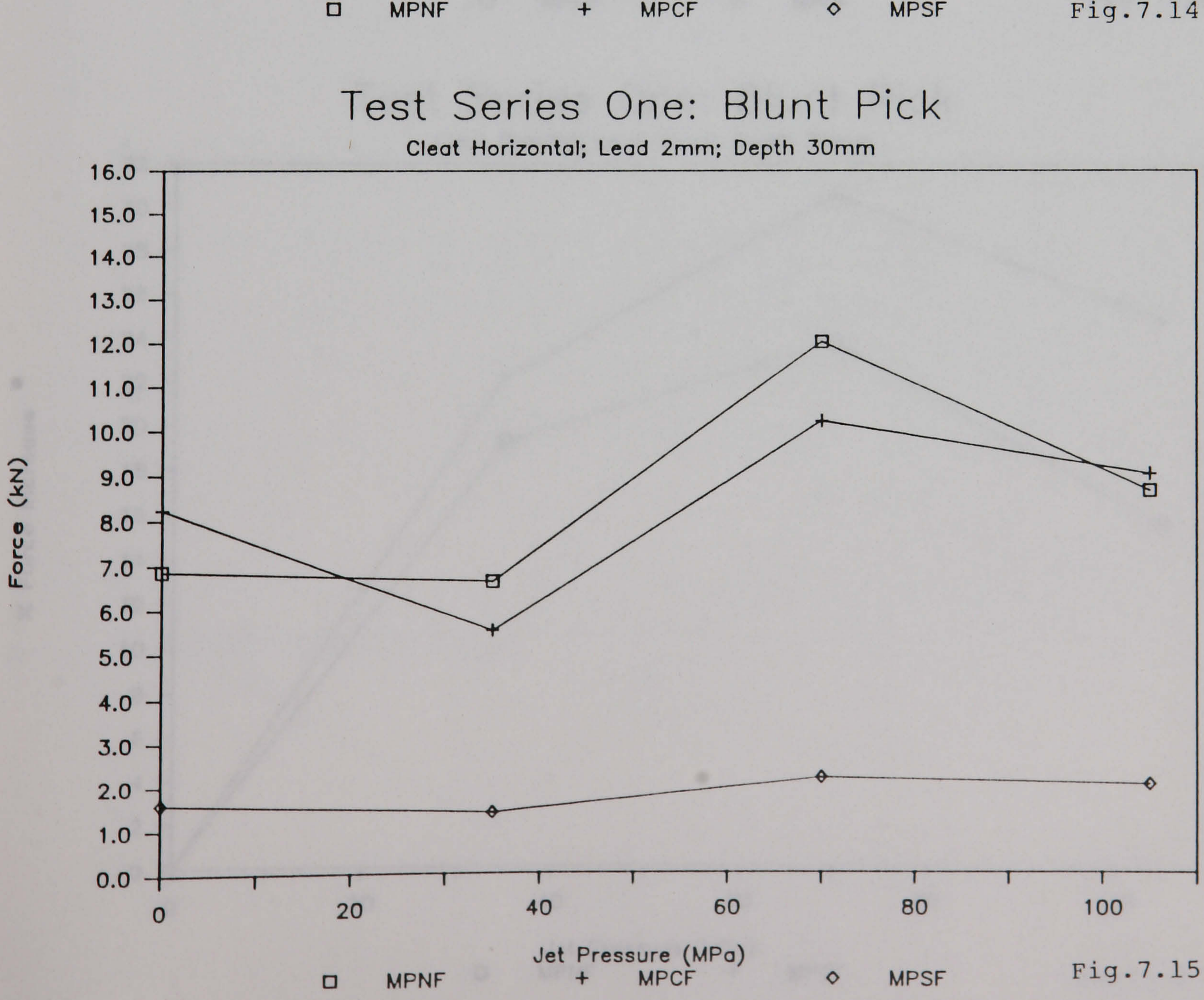


Fig.7.15

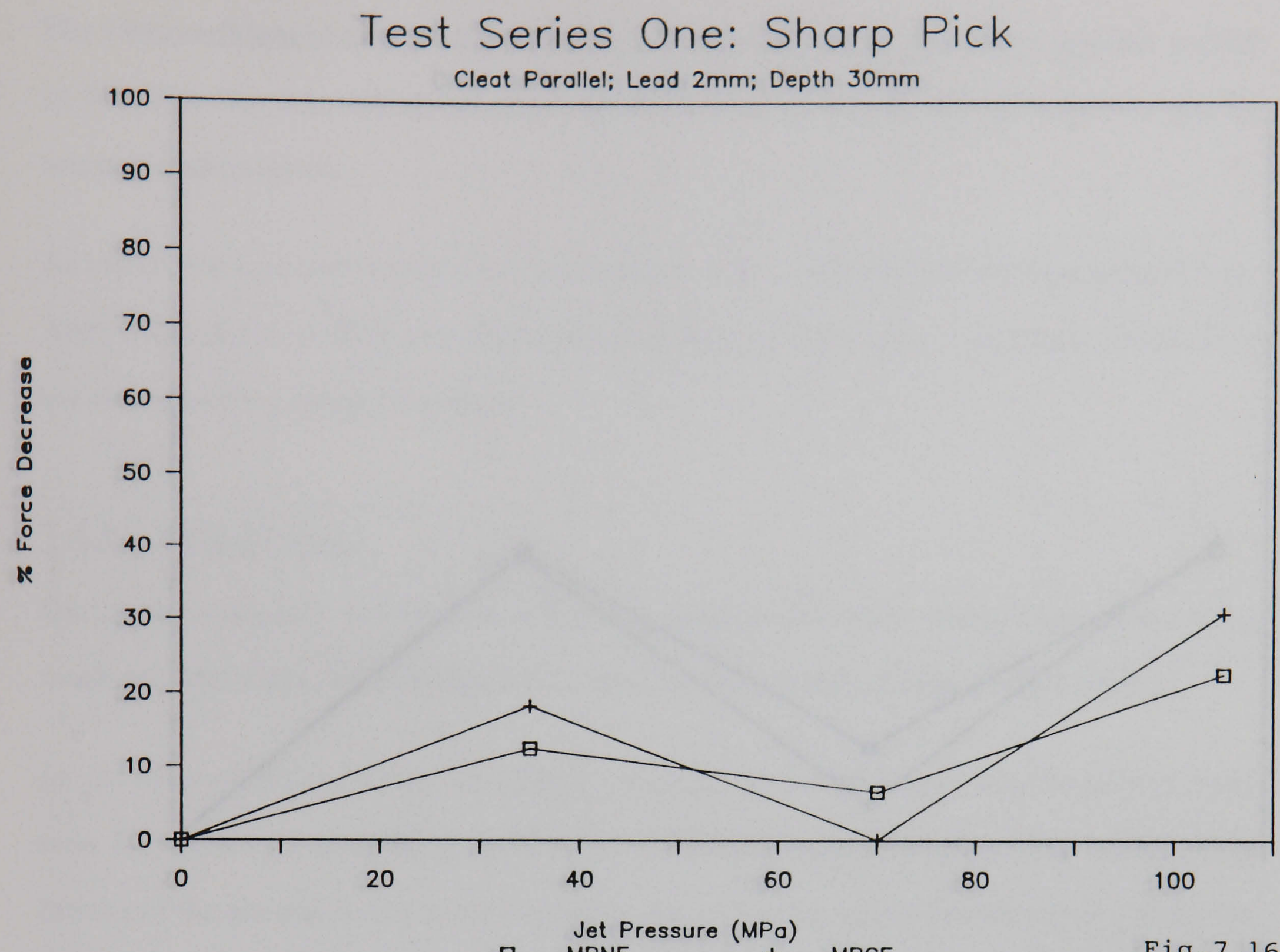


Fig.7.16

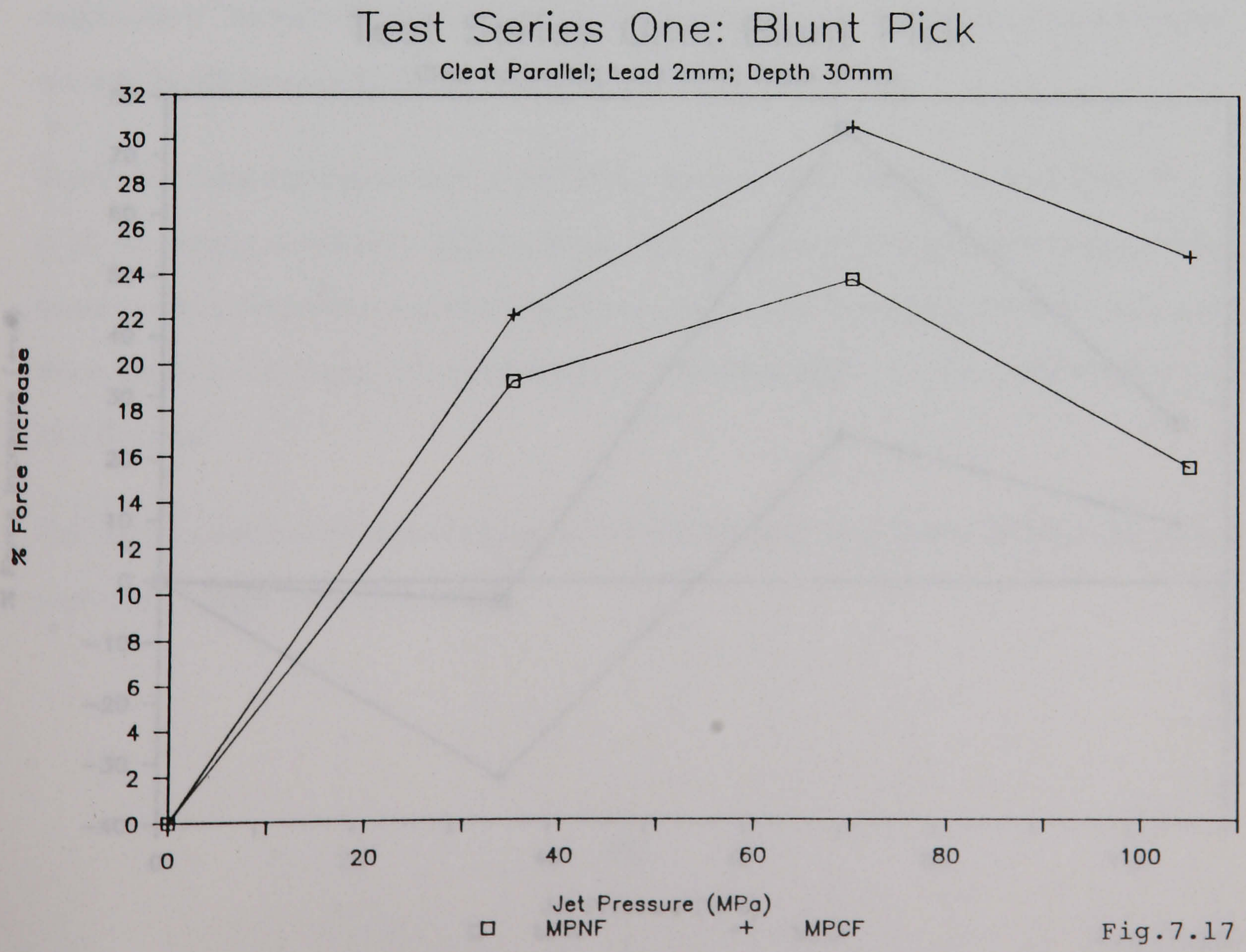


Fig.7.17

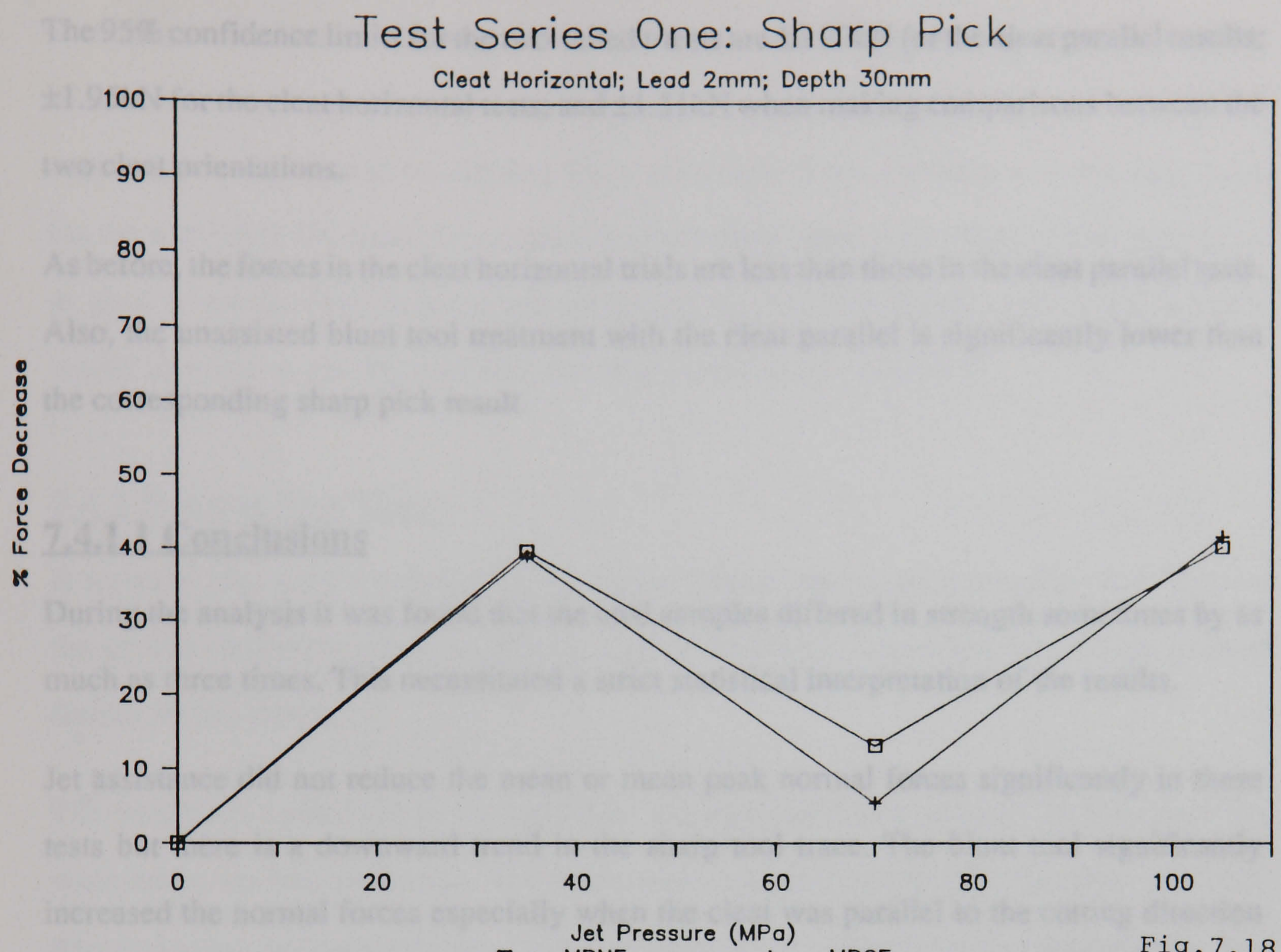


Fig.7.18

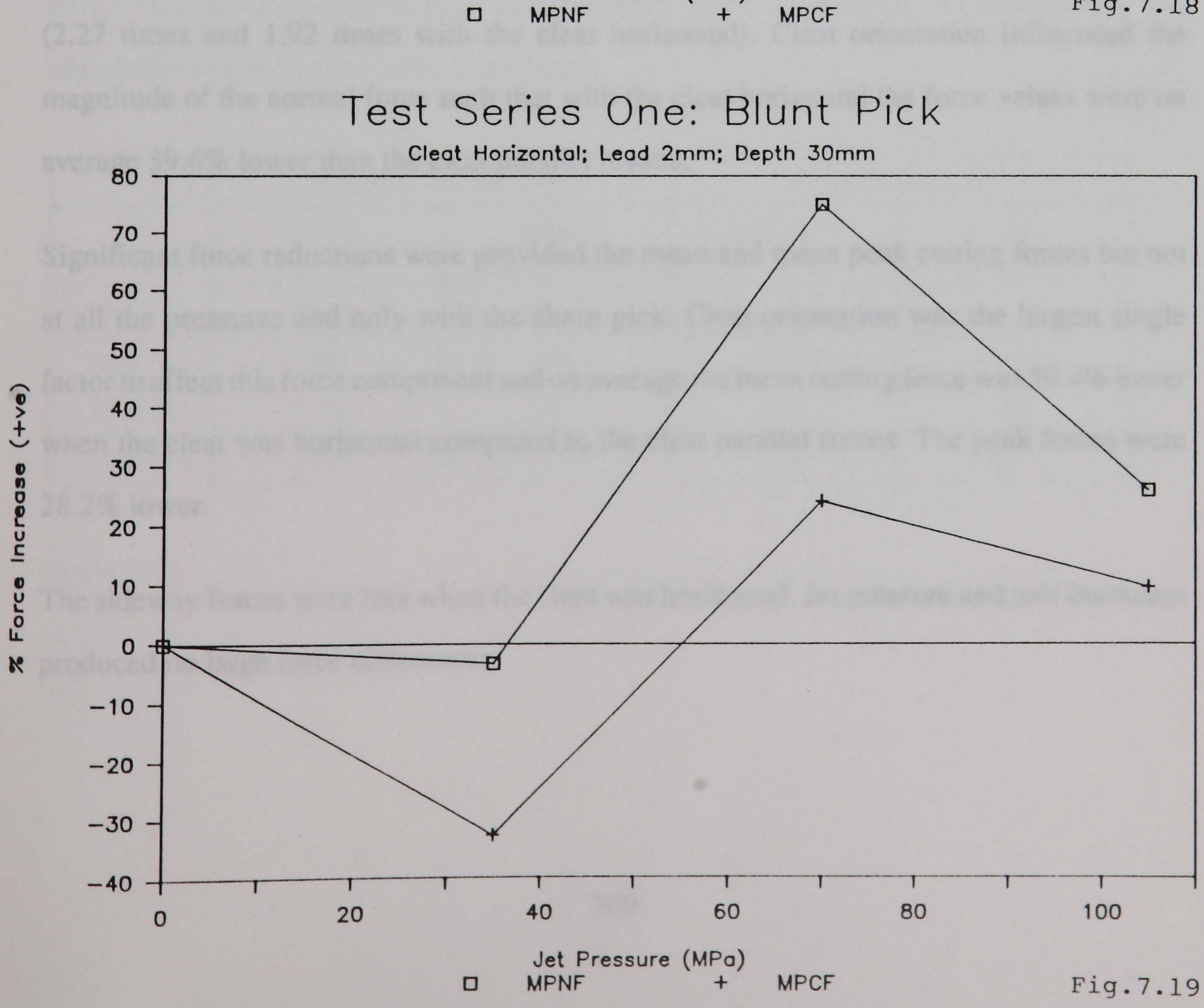


Fig.7.19

The 95% confidence limits for the two-tailed t-tests are ±0.92kN for the cleat parallel results; ±1.95kN for the cleat horizontal tests; and ±1.51kN when making comparisons between the two cleat orientations.

As before, the forces in the cleat horizontal trials are less than those in the cleat parallel tests. Also, the unassisted blunt tool treatment with the cleat parallel is significantly lower than the corresponding sharp pick result.

7.4.1.1 Conclusions

During the analysis it was found that the coal samples differed in strength sometimes by as much as three times. This necessitated a strict statistical interpretation of the results.

Jet assistance did not reduce the mean or mean peak normal forces significantly in these tests but there is a downward trend in the sharp tool trace. The blunt tool significantly increased the normal forces especially when the cleat was parallel to the cutting direction (2.27 times and 1.92 times with the cleat horizontal). Cleat orientation influenced the magnitude of the normal force such that with the cleat horizontal the force values were on average 39.6% lower than the cleat parallel results.

Significant force reductions were provided the mean and mean peak cutting forces but not at all the pressures and only with the sharp pick. Cleat orientation was the largest single factor to affect this force component and on average the mean cutting force was 50.4% lower when the cleat was horizontal compared to the cleat parallel forces. The peak forces were 28.2% lower.

The sideway forces were less when the cleat was horizontal. Jet pressure and tool bluntness produced no large force differences.

One cannot conclude from these tests that jet assistance promises extensive returns in terms of increased cutting performance and it appears that with the blunt tool there is no point in applying jet assistance if considering force reductions alone. Lower forces are required to cut the coal when the cleat is orientated in a horizontal plane. The effect of tool wear is not as great when the cleat is horizontal compared to when it is parallel and on the whole it would be better to cut this coal with the cleat horizontally orientated.

7.4.2 Pre-cut Slot Tests

A series of tests with the sharp tool were performed at the same jet pressures but this time the jet was used to cut a slot along the length of cut before the tool cut the coal but without further jet assistance.

The tests were carried out in the same coal samples and thus a comparison between cleat orientations has been made also. The results were analysed with those of the sharp pick from the previous section to assess the effect of pre-slotting as compared with hybrid cutting. The table below describes the basic experiment.

	Without Pre-cut Slot		With Pre-cut Slot	
Jet Pressure	Cleat Parallel	Cleat Horizontal	Cleat Parallel	Cleat Horizontal
0MPa	13X	13X		
35MPa	8X	8X	13X	13X
70MPa	12X	12X	6X	6X
105MPa	11X	11X	6X	6X

Table 7.10

Mean Normal Force ANOVA

Source of Variation	Sums of Squares	Degrees of Freedom	Mean Square	F-ratio & (Significance Level)
Between Pressures	10.6	3	3.5	2.9 (3.8)
Between Slot	0.2	1	0.2	0.2 (6.7)
Between Cleat	6.2	1	6.2	5.0 (6.7)
Interaction between Pressures & Slot	11.1	2	5.6	4.5 (4.7)
Interaction between Pressures & Cleat	3.0	3	1.0	0.8 (3.8)
Interaction between Cleat & Slot	0.3	1	0.3	0.2 (6.7)
Interaction between Pressures, Cleat & Slot	0.7	2	0.4	0.3 (4.7)
Experimental Error	345.7	281	1.2	
Total	377.8	294		

Table 7.11

The 95% confidence limits for the two-tailed t-tests are ±0.49kN for the cleat parallel results; ±1.04kN for the cleat horizontal tests; and ±0.80kN when making comparisons between the two cleat orientations.

Table 7.11, does not indicate a significant effect at the 1% level, however, the effects of jet pressure, cleat and the interaction term between jet pressure and 'slot' are significant at the 5% level though not shown.

Consequently, the t-tests do reveal significant force reductions in the mean normal force at the 5% level. In these comparisons only the sharp pick is being considered and thus the normal force in Fig.7.2, has been significantly reduced by the 70MPa and 105MPa pressure treatments.

The results for the pre-slotted tests are illustrated in Fig.7.20-23. The only significant mean normal force reduction is that caused by the slot made at 35MPa jet pressure with the cleat parallel, Fig.7.20.

The differences in mean normal forces between normal jet assistance with a lead distance of 2mm and pre-slotting are not significant for both cleat orientations. Thus, the forces are similar in both cases.

Pre-slotting exhibits the same trend as earlier with regard to cleat orientation in that the normal force with the cleat horizontal is lower than with it parallel: on average, 23.2% lower.

Mean Cutting Force ANOVA

Source of Variation	Sums of Squares	Degrees of Freedom	Mean Square	F-ratio & (Significance Level)
Between Pressures	68.3	3	22.8	7.5 (3.8)
Between Slot	9.2	1	9.2	3.0 (6.7)
Between Cleat	69.7	1	69.7	22.9 (6.7)
Interaction between Pressures & Slot	8.7	2	4.4	1.4 (4.7)
Interaction between Pressures & Cleat	4.8	3	1.6	0.5 (3.8)
Interaction between Cleat & Slot	1.3	1	1.3	0.4 (6.7)
Interaction between Pressures, Cleat & Slot	0.9	2	0.4	0.1 (4.7)
Experimental Error	855.1	281	3.0	
Total	1018.0	294		

Table 7.12

The 95% confidence limits for the two-tailed t-tests are ±0.77kN for the cleat parallel results; ±1.64kN for the cleat horizontal tests; and ±1.26kN when making comparisons between the two cleat orientations.

Cleat is the major factor with the mean cutting force. This was also apparent in the previous section. With the jet assisted treatments all the cleat horizontal results are significantly lower (or borderline and close) than the cleat parallel forces, Fig.7.2,4. And the same applies to the pre-slotted test results, Fig.7.20-21. This is despite the quite large confidence interval and would be reinforced by a one-tailed t-test.

For the jet assisted treatments, the same significant force reductions are obtained as in the previous section. With the pre-slotted cuts, all the slotted trials yielded a significantly lower cutting force with the cleat parallel. With the cleat horizontal, only the pre-slotting by the 35MPa jet procured a significant reduction.

As with the mean normal force, the pre-slotted tests did not significantly differ from those of the jet assisted test results. The existence of the slot seems to be enough to cause not dissimilar force reductions to those of the jet assisted cutting.

Test Series One: Sharp Pick

Cleat Parallel; Pre-Cut Slot;Depth 30mm

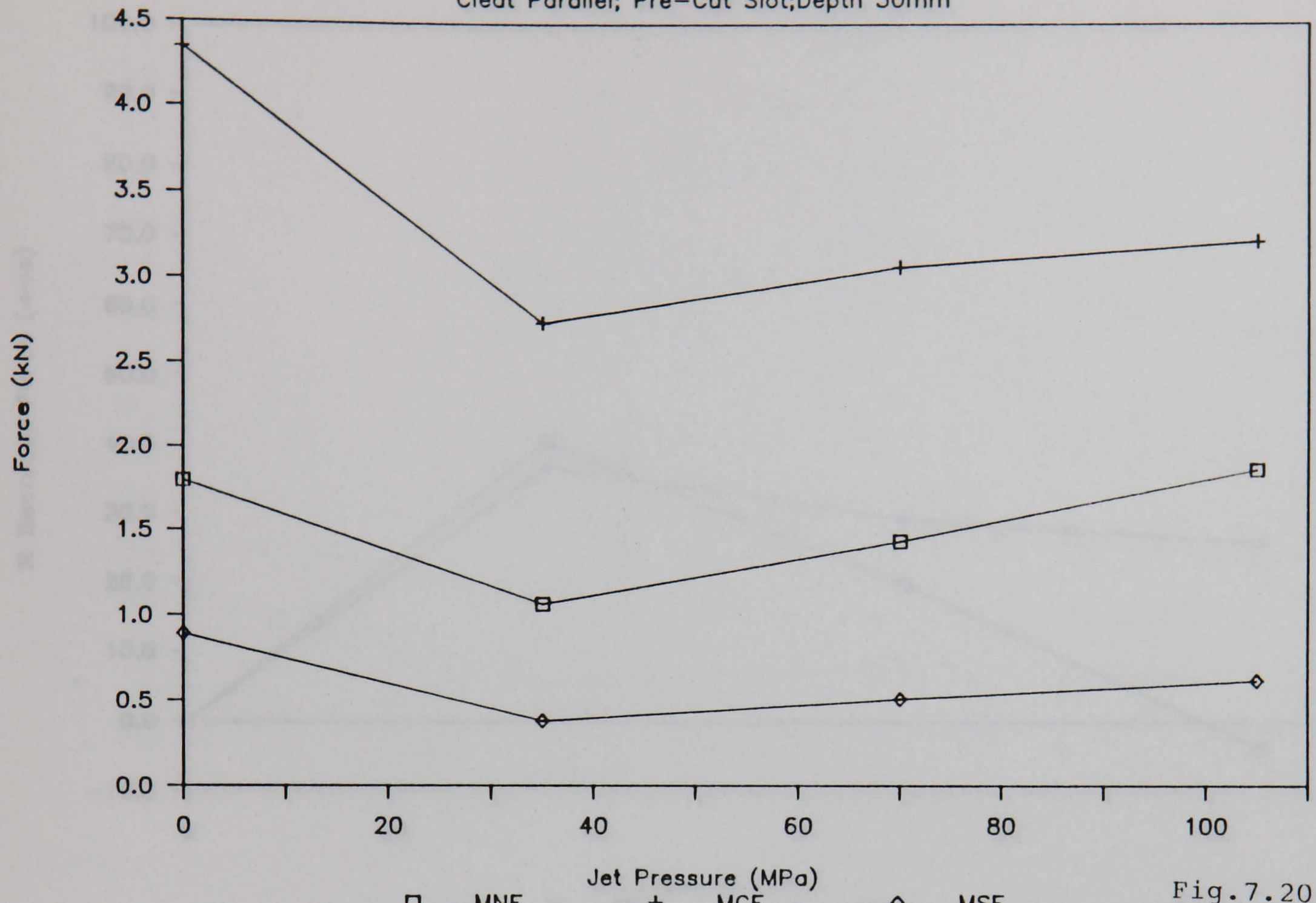


Fig.7.20

Test Series One: Sharp Pick

Cleat Horizontal;Pre-Cut Slot;Depth30mm

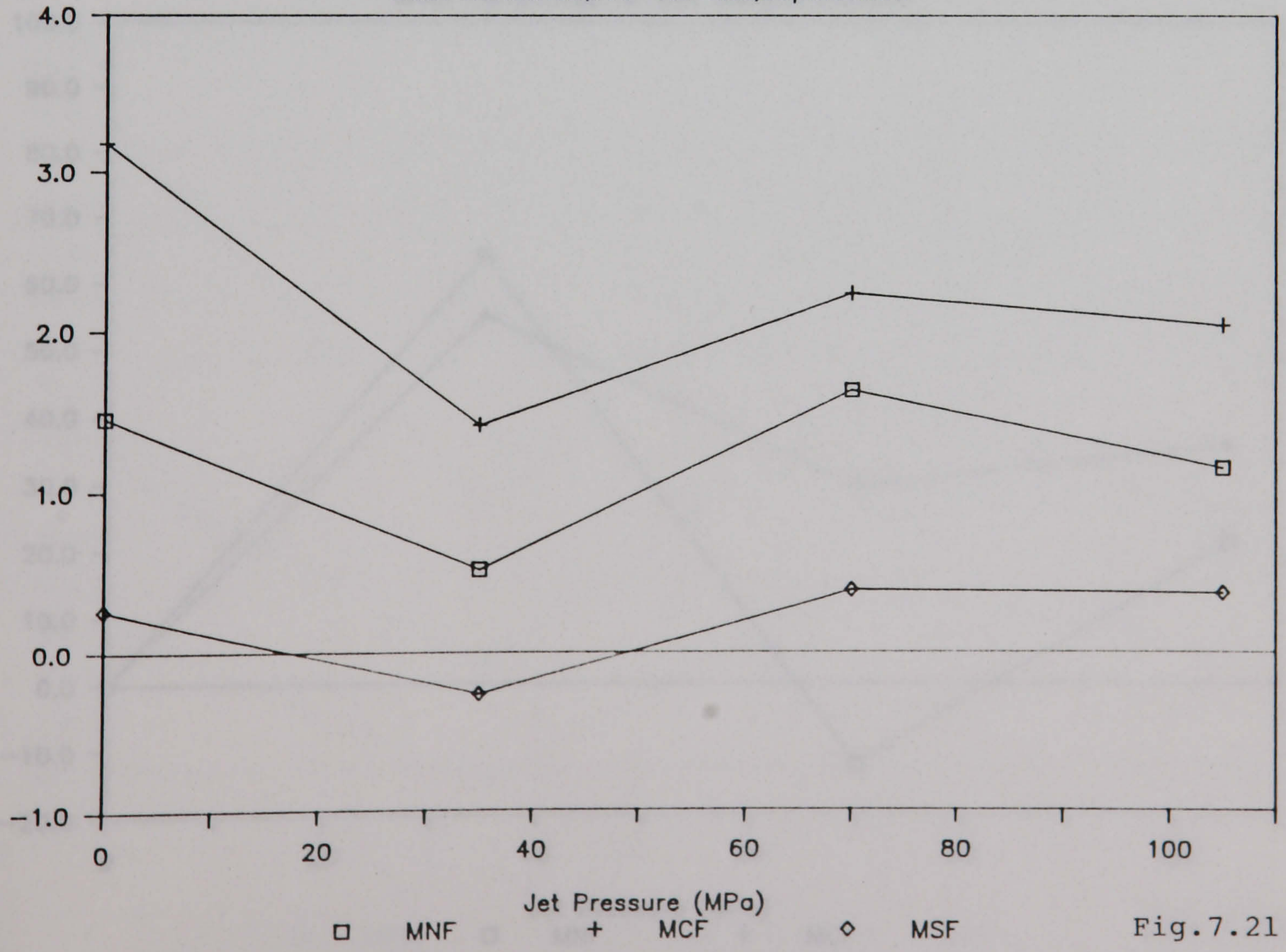


Fig.7.21

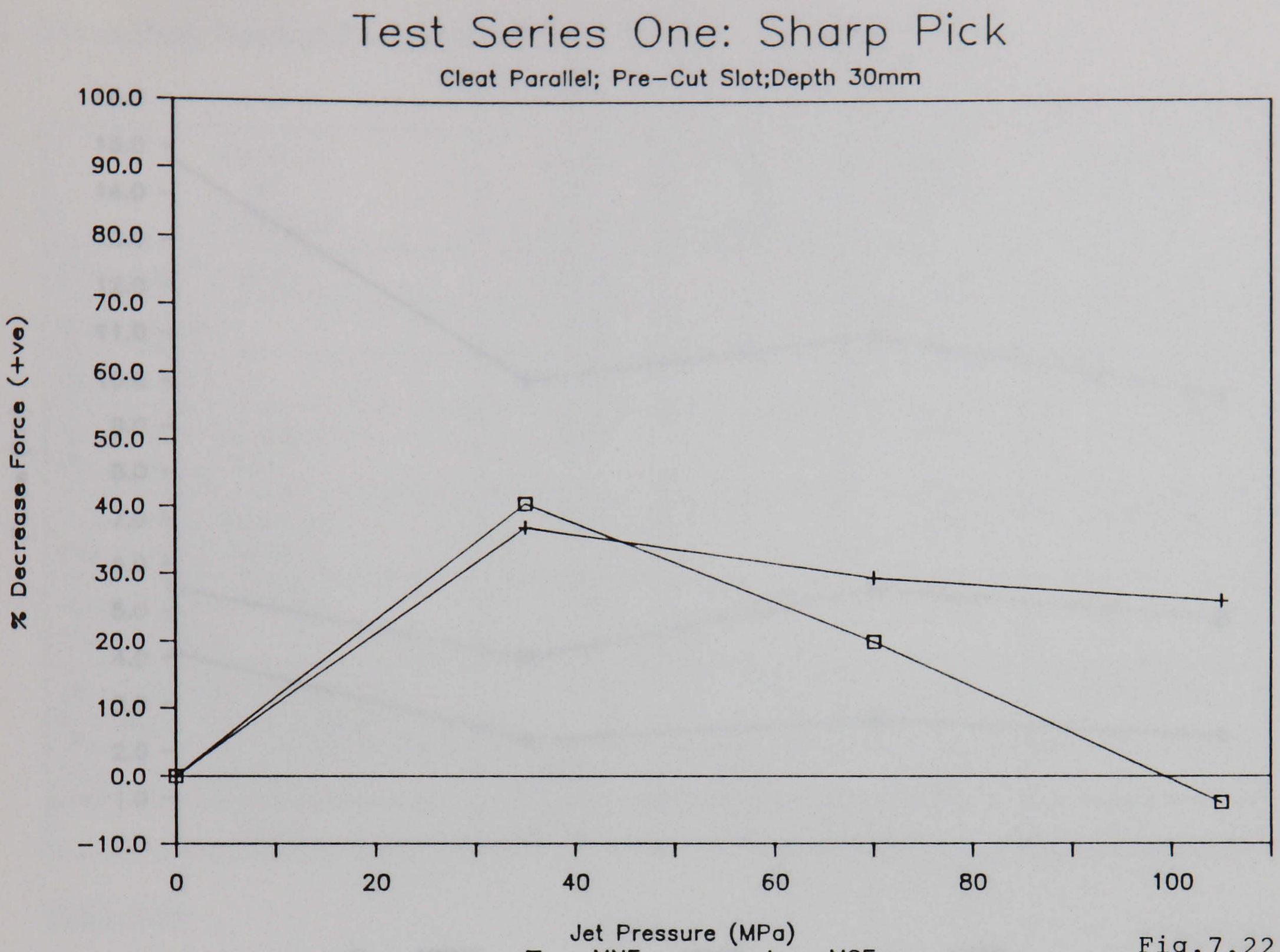


Fig.7.22

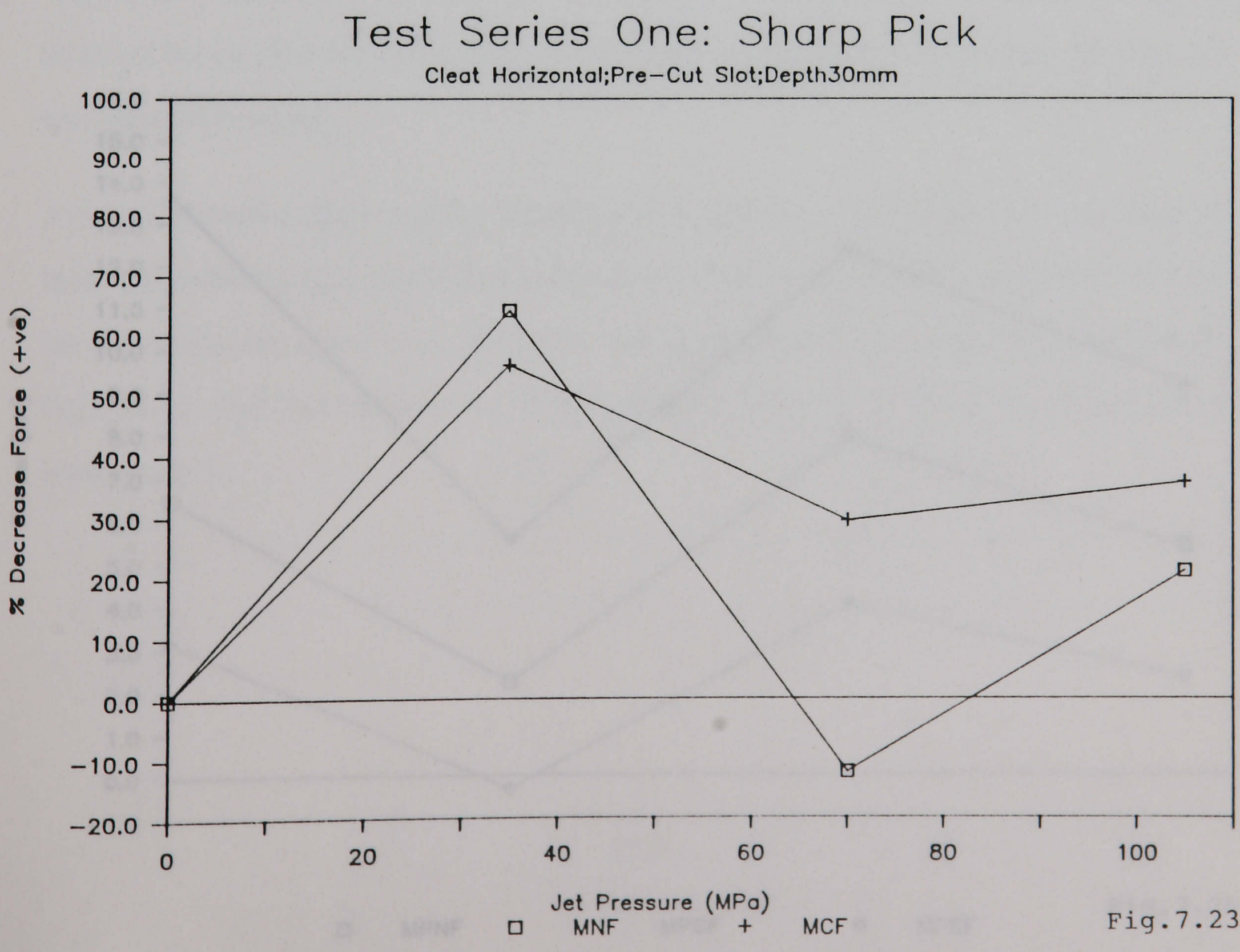


Fig.7.23

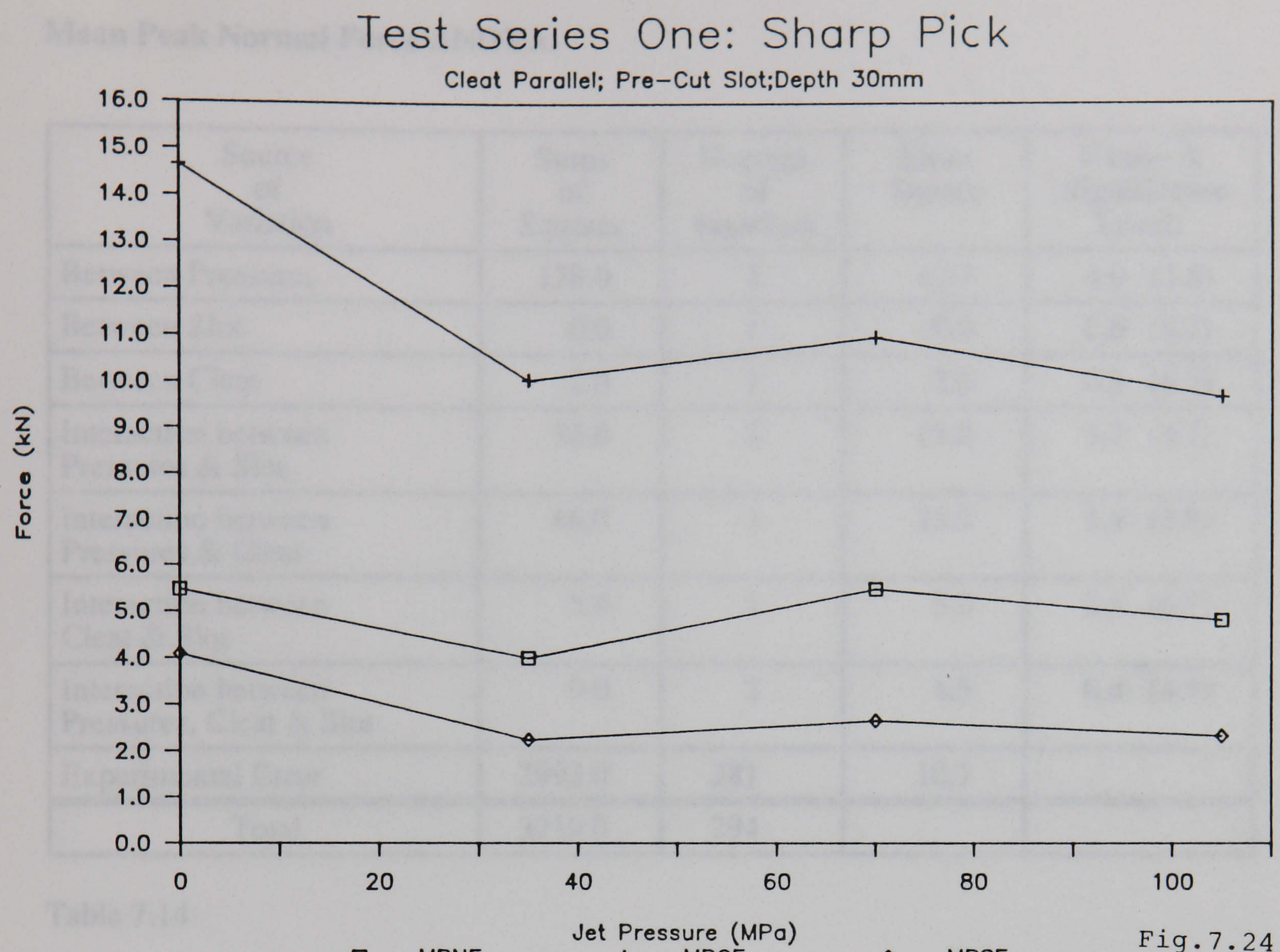


Fig.7.24

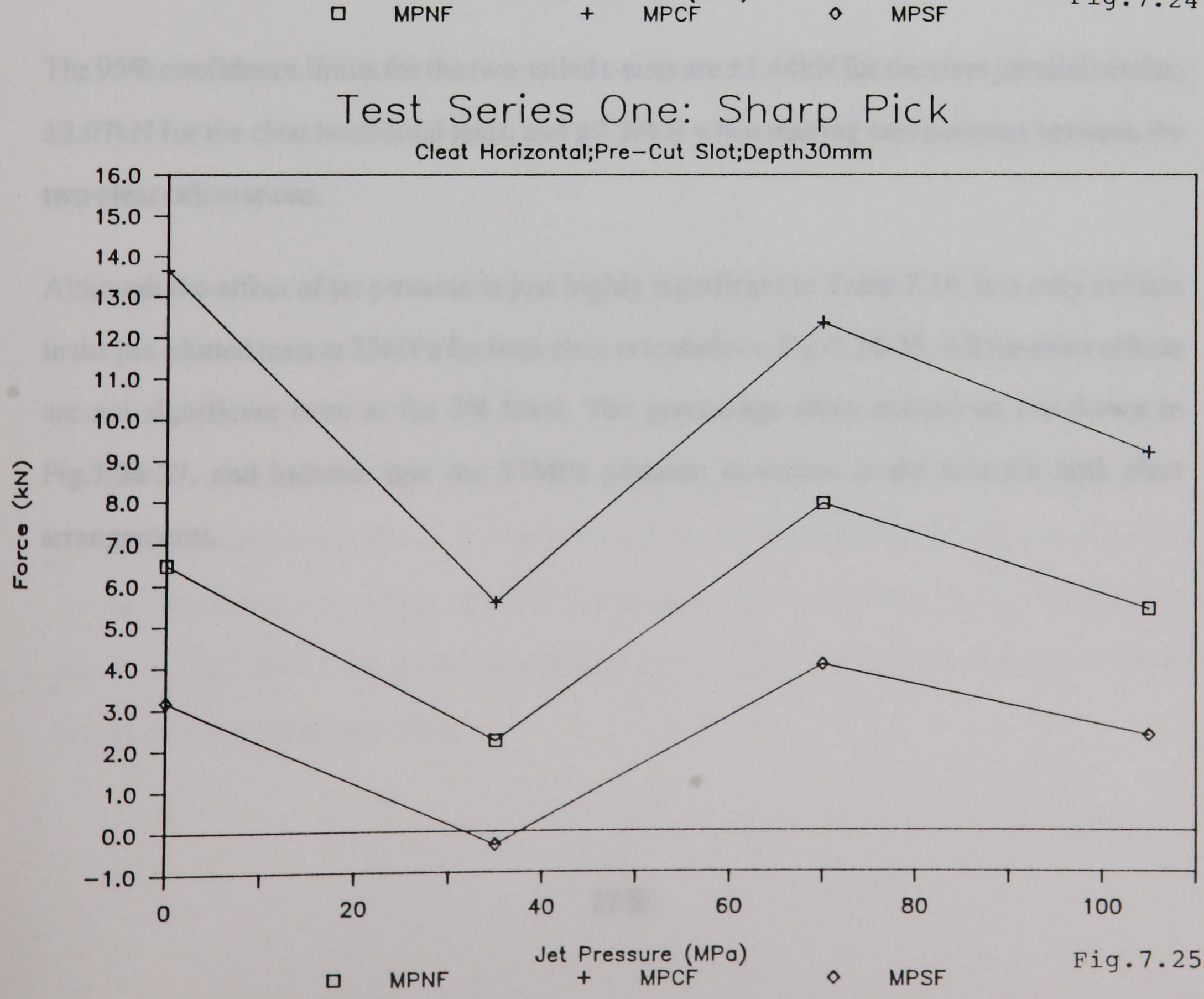


Fig.7.25

Mean Peak Normal Force ANOVA

Source of Variation	Sums of Squares	Degrees of Freedom	Mean Square	F-ratio & (Significance Level)
Between Pressures	128.0	3	42.7	4.0 (3.8)
Between Slot	0.0	1	0.0	0.0 (6.7)
Between Cleat	2.0	1	2.0	0.2 (6.7)
Interaction between Pressures & Slot	36.0	2	18.0	1.7 (4.7)
Interaction between Pressures & Cleat	46.0	3	15.3	1.4 (3.8)
Interaction between Cleat & Slot	5.0	1	5.0	0.5 (6.7)
Interaction between Pressures, Cleat & Slot	9.0	2	4.5	0.4 (4.7)
Experimental Error	2993.0	281	10.7	
Total	3219.0	294		

Table 7.14

The 95% confidence limits for the two-tailed t-tests are ±1.44kN for the cleat parallel results; ±3.07kN for the cleat horizontal tests; and ±2.36kN when making comparisons between the two cleat orientations.

Although the effect of jet pressure is just highly significant in Table 7.14, it is only evident in the pre-slotted tests at 35MPa for both cleat orientations, Fig.7.24-25. All the other effects are not significant even at the 5% level. The percentage force reductions are shown in Fig.7.26-27, and indicate that the 35MPa pressure treatment is the best for both cleat arrangements.

Mean Peak Cutting Force ANOVA

Source of Variation	Sums of Squares	Degrees of Freedom	Mean Square	F-ratio & (Significance Level)
Between Pressures	50.0	3	16.7	0.6 (3.8)
Between Slot	133.0	1	133.0	5.0 (6.7)
Between Cleat	144.0	1	144.0	5.5 (6.7)
Interaction between Pressures & Slot	46.0	2	23.0	0.9 (4.7)
Interaction between Pressures & Cleat	131.0	3	43.7	1.7 (3.8)
Interaction between Cleat & Slot	6.0	1	6.0	0.2 (6.7)
Interaction between Pressures, Cleat & Slot	16.0	2	8.0	0.3 (4.7)
Experimental Error	7421.0	281	26.4	
Total	8947.0	294		

Table 7.15

The 95% confidence limits for the two-tailed t-tests are ±2.28kN for the cleat parallel results; ±4.83kN for the cleat horizontal tests; and ±3.72kN when making comparisons between the two cleat orientations.

The slot and cleat effects are not highly significant (i.e. at the 1% level) but significant at the 5% level. The unassisted or dry cuts bear no significant differences between one another, the significance appears between the jet assisted and pre-slotted treatments and the pre-slotted cuts show lower forces in both cleat orientations. Similarly to the mean cutting force, the cleat horizontal mean peak cutting forces are generally lower than the cleat parallel ones but the significance is between the 35MPa treatments. The percentage force differences are shown in Fig.7.26-27, for the pre-slotted tests, and suggest the 35MPa treatment to be the best in terms of force reduction.

Mean Peak Sideway Force ANOVA

Source of Variation	Sums of Squares	Degrees of Freedom	Mean Square	F-ratio & (Significance Level)
Between Pressures	119.0	3	39.7	5.8 (3.8)
Between Slot	78.0	1	78.0	11.4 (6.7)
Between Cleat	48.0	1	48.0	7.0 (6.7)
Interaction between Pressures & Slot	9.0	2	4.5	0.7 (4.7)
Interaction between Pressures & Cleat	58.0	3	19.3	2.8 (3.8)
Interaction between Cleat & Slot	5.0	1	5.0	0.7 (6.7)
Interaction between Pressures, Cleat & Slot	7.0	2	3.5	0.5 (4.7)
Experimental Error	1923.0	281	6.8	
Total	2247.0	294		

Table 7.16

The 95% confidence limits for the two-tailed t-tests are ±1.16kN for the cleat parallel results; ±2.46kN for the cleat horizontal tests; and ±1.89kN when making comparisons between the two cleat orientations.

All the main effects are highly significant. There appears to be more variation in the cleat horizontal results than with the cleat parallel ones. This suggests that when the cleat is horizontal the tool is less constrained by the coal. When the cleat is vertical and parallel to the direction of cut the tool is quite steady in the cut and the curves in Fig.7.12,24 are more regular or even.

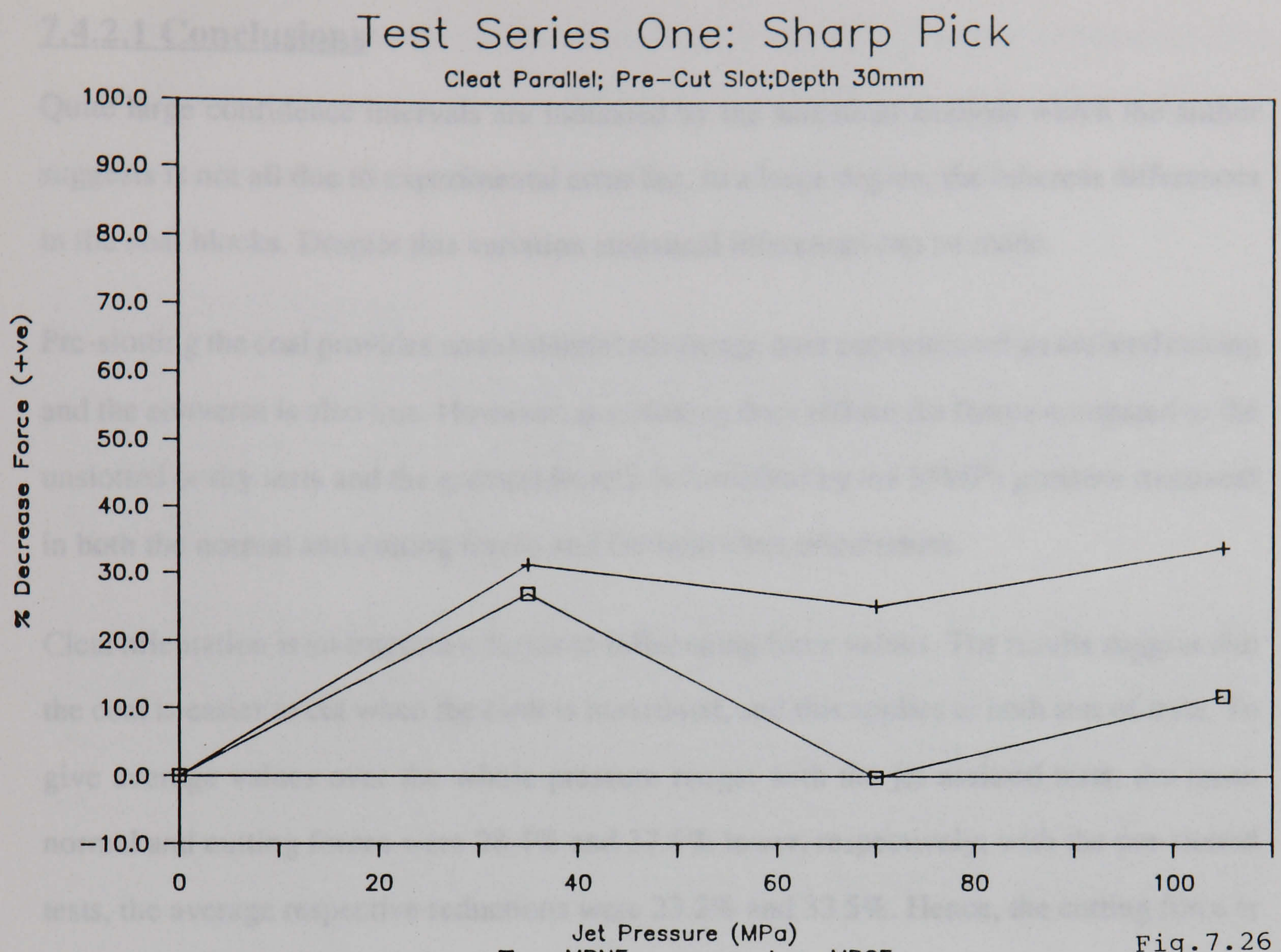


Fig.7.26

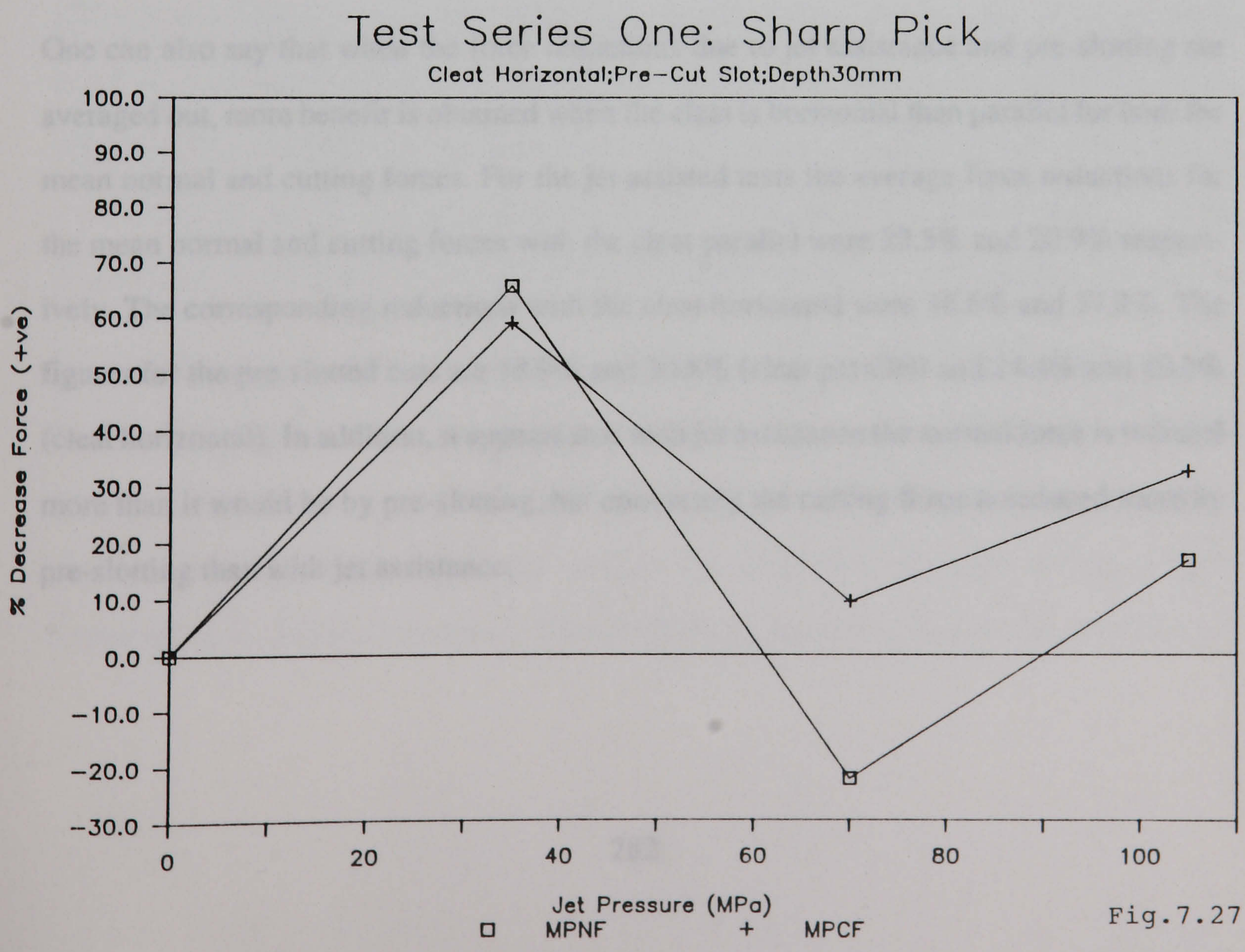


Fig.7.27

7.4.2.1 Conclusions

Quite large confidence intervals are indicated by the statistical analysis which the author suggests is not all due to experimental error but, to a large degree, the inherent differences in the coal blocks. Despite this variation statistical inferences can be made.

Pre-slotting the coal provides no substantial advantage over conventional jet assisted cutting and the converse is also true. However, pre-slotting does reduce the forces compared to the unslotted or dry tests and the greatest benefit is furnished by the 35MPa pressure treatment in both the normal and cutting forces and for both cleat orientations.

Cleat orientation is an important factor in influencing force values. The results suggest that the coal is easier to cut when the cleat is horizontal, and this applies to both sets of tests. To give average values over the whole pressure range: with the jet assisted tests, the mean normal and cutting forces were 28.4% and 37.6% lower, respectively; with the pre-slotted tests, the average respective reductions were 23.2% and 33.5%. Hence, the cutting force is reduced most, by about 10% more than the mean normal force.

One can also say that when the force reductions due to jet assistance and pre-slotting are averaged out, more benefit is obtained when the cleat is horizontal than parallel for both the mean normal and cutting forces. For the jet assisted tests the average force reductions for the mean normal and cutting forces with the cleat parallel were 23.5% and 20.9% respectively. The corresponding reductions with the cleat horizontal were 36.6% and 37.2%. The figures for the pre-slotted cuts are 18.9% and 30.8% (cleat parallel) and 24.4% and 40.2% (cleat horizontal). In addition, it appears that with jet assistance the normal force is reduced more than it would be by pre-slotting, but conversely the cutting force is reduced more by pre-slotting than with jet assistance.

The sideway force seems more stable when cutting with the cleat vertical and parallel to the cutting direction. However, it is also greater in value than when cutting with the cleat in a horizontal plane, so it cannot be considered as an important advantage.

7.4.3 Specific Energy

Fig.7.28-29, show the specific energy plots for the sharp and blunt tool tests. In this case it was not possible to separate the effects of cleat orientation and so the yield from coal block 2 is included in the calculations.

Two sets of results are plotted. The curves increasing over the jet pressure and power ranges include the energy supplied by the jet. The curves practically constant over the ranges do not include the jet energy but merely the tool cutting force at that jet pressure or power. Since the jet flow rate was held constant at 4 l/min, and the cutting speed is greater at 1.34m/s, the specific energy at 105MPa pressure is not as high as in the previous chapter compared to the unassisted cuts.

There is some disparity with the unassisted or dry cut values, between the sharp and blunt tools, and the linearity of the curves suffers, nevertheless, correlation coefficients of the order of 0.97 are obtained for the curves with the jet energy included. Neither curve displays a reduction in specific energy and therefore the force reductions and increase in yields obtained from jet assistance are not sufficient to offset the extra energy delivered by the jet.

The specific energies for the pre-slotted tests are given in Fig.7.30-31. In this case the specific energy of the 35MPa treatment is just less than the unslotted treatment value. This is for the sharp pick though which is not considered as important as the blunt pick result. If the blunt pick result would follow closely the trend of the sharp pick, the result would be quite encouraging. A similar occurrence is found with the jet assisted 35MPa sharp pick treatment

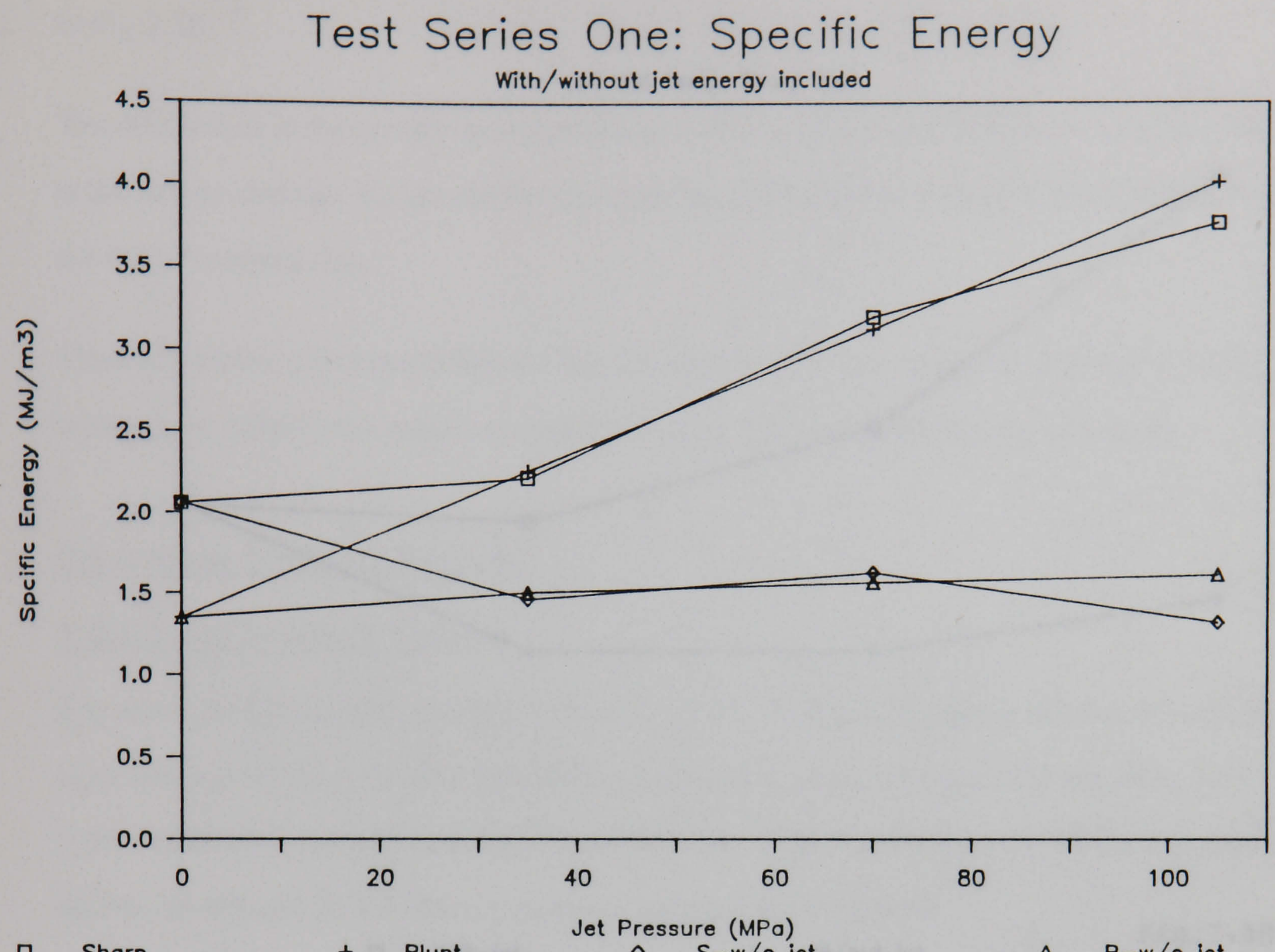


Fig.7.28

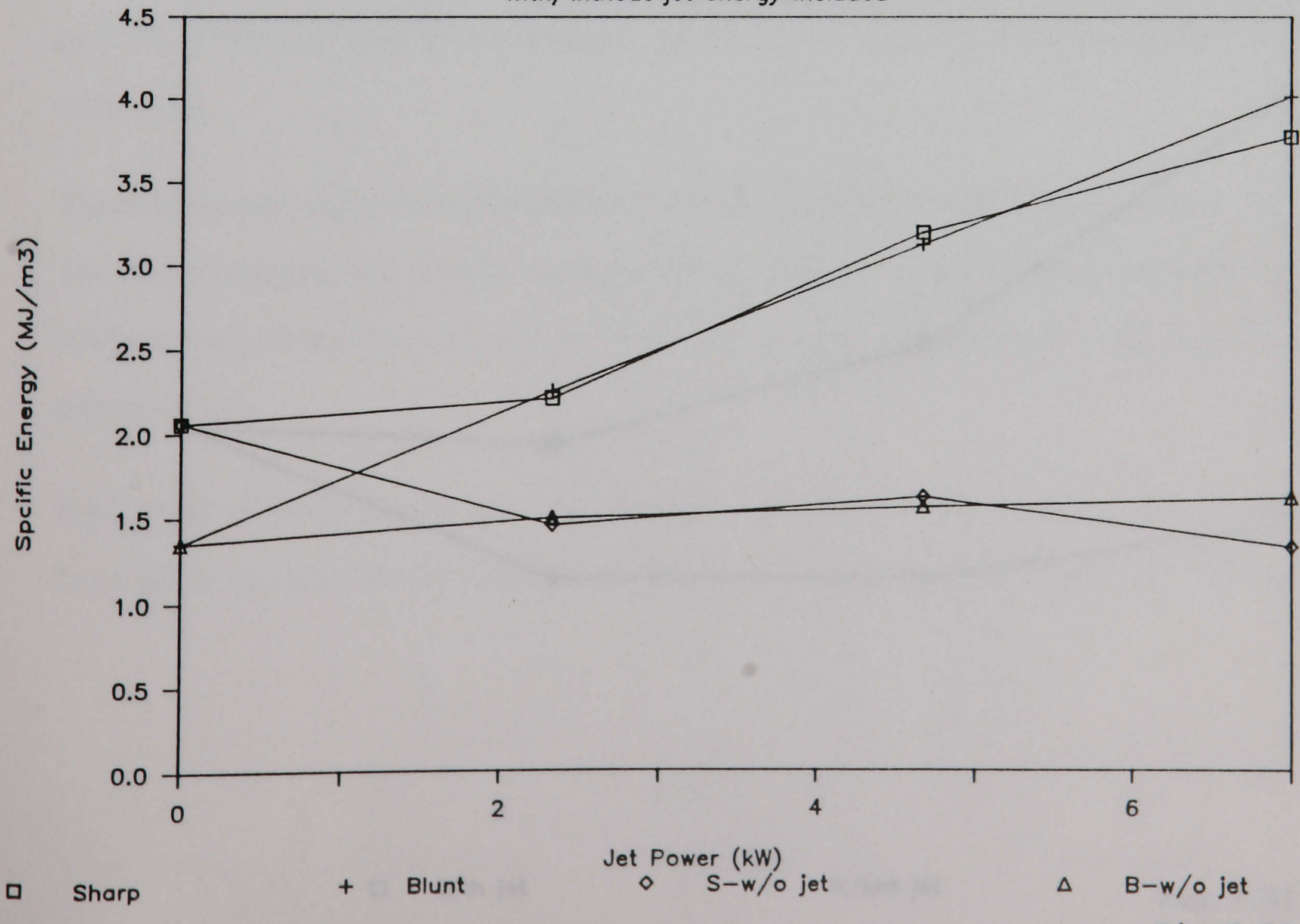


Fig.7.29

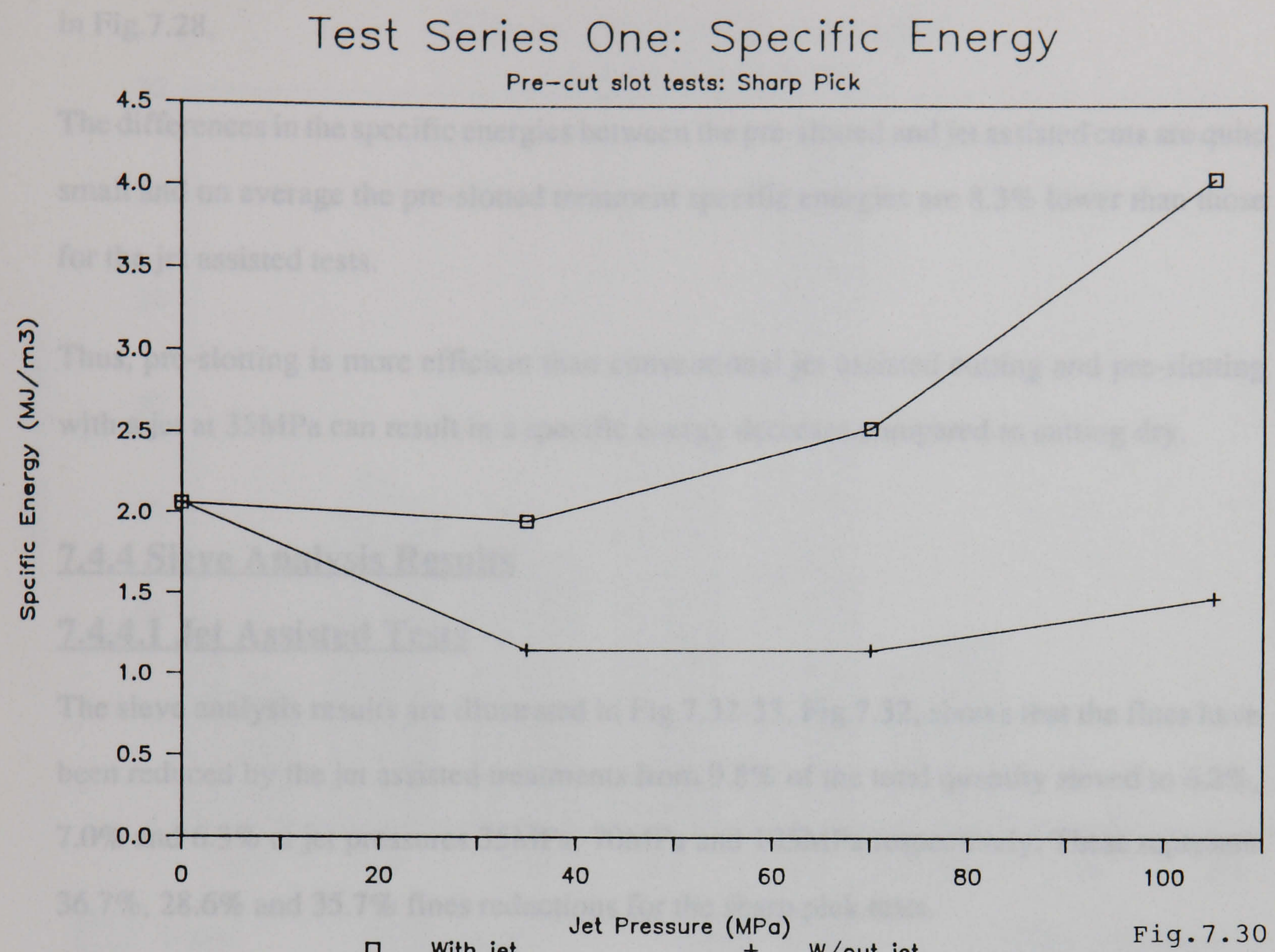


Fig.7.30

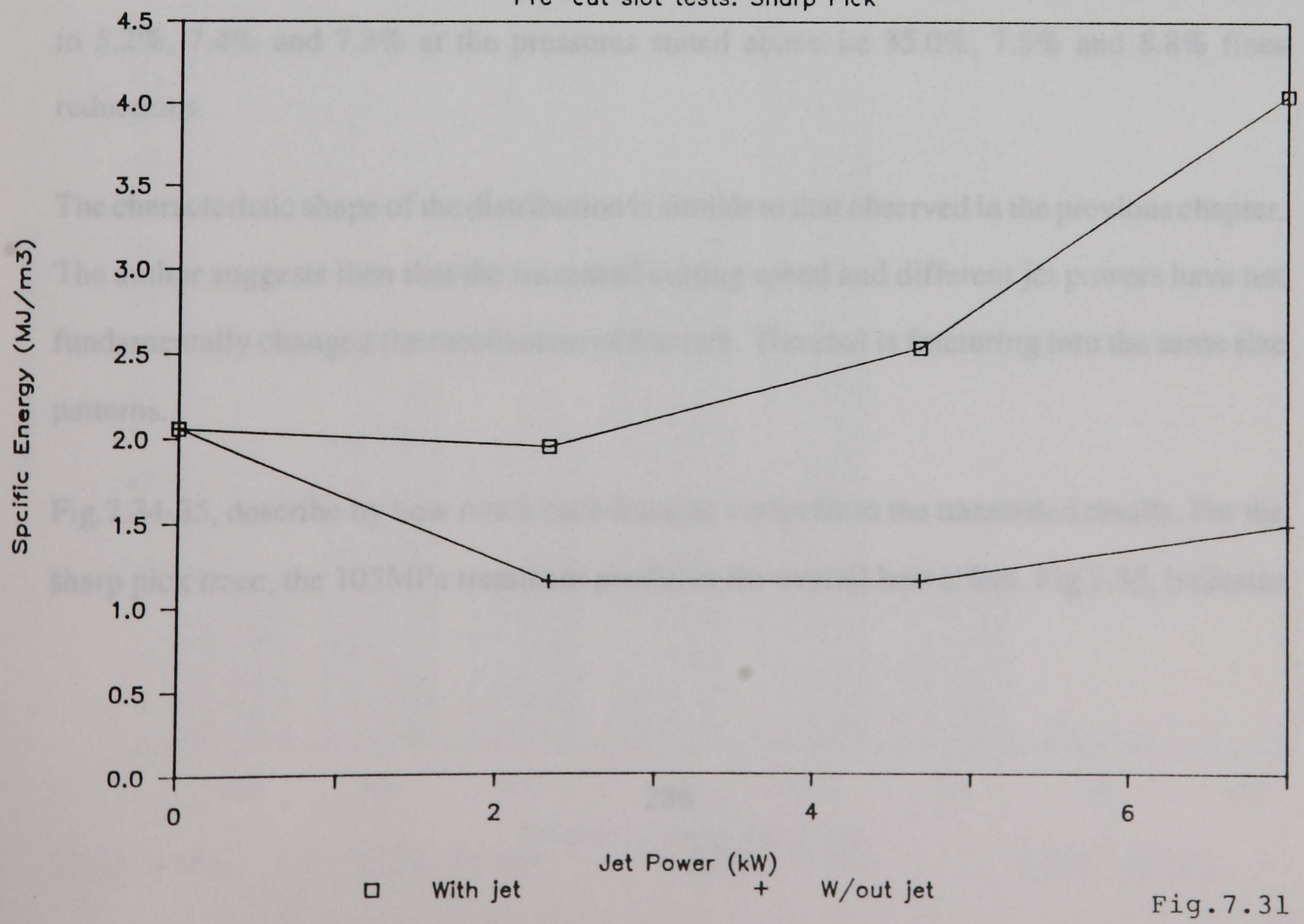


Fig.7.31

in Fig.7.28.

The differences in the specific energies between the pre-slotted and jet assisted cuts are quite small and on average the pre-slotted treatment specific energies are 8.3% lower than those for the jet assisted tests.

Thus, pre-slotting is more efficient than conventional jet assisted cutting and pre-slotting with a jet at 35MPa can result in a specific energy decrease compared to cutting dry.

7.4.4 Sieve Analysis Results

7.4.4.1 Jet Assisted Tests

The sieve analysis results are illustrated in Fig.7.32-33. Fig.7.32, shows that the fines have been reduced by the jet assisted treatments from 9.8% of the total quantity sieved to 6.2%, 7.0% and 6.3% at jet pressures 35MPa, 70MPa and 105MPa respectively. These represent 36.7%, 28.6% and 35.7% fines reductions for the sharp pick tests.

Fig.7.33, gives the blunt tool results. Despite the apparent force increases with the blunt tool, the fines production has been reduced by jet assistance from 8.0% of the total debris to 5.2%, 7.4% and 7.3% at the pressures stated above i.e 35.0%, 7.5% and 8.8% fines reductions.

The characteristic shape of the distribution is similar to that observed in the previous chapter. The author suggests then that the increased cutting speed and different jet powers have not fundamentally changed the mechanism of fracture. The coal is fracturing into the same size patterns.

Fig.7.34-35, describe by how much each fraction varies from the unassisted results. For the sharp pick trace, the 105MPa treatment produces the overall best effect. Fig.7.35, indicates

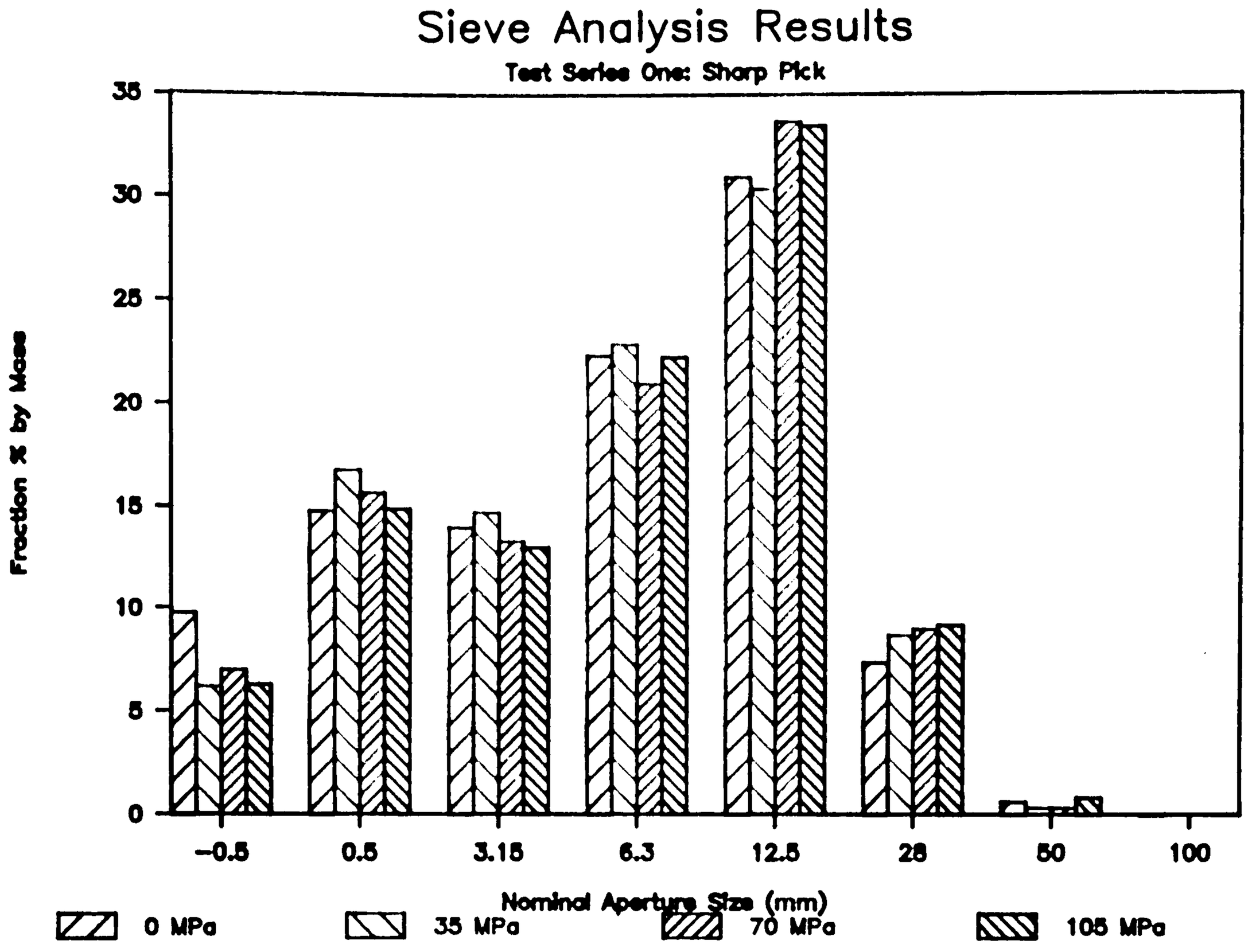


Fig.7.32

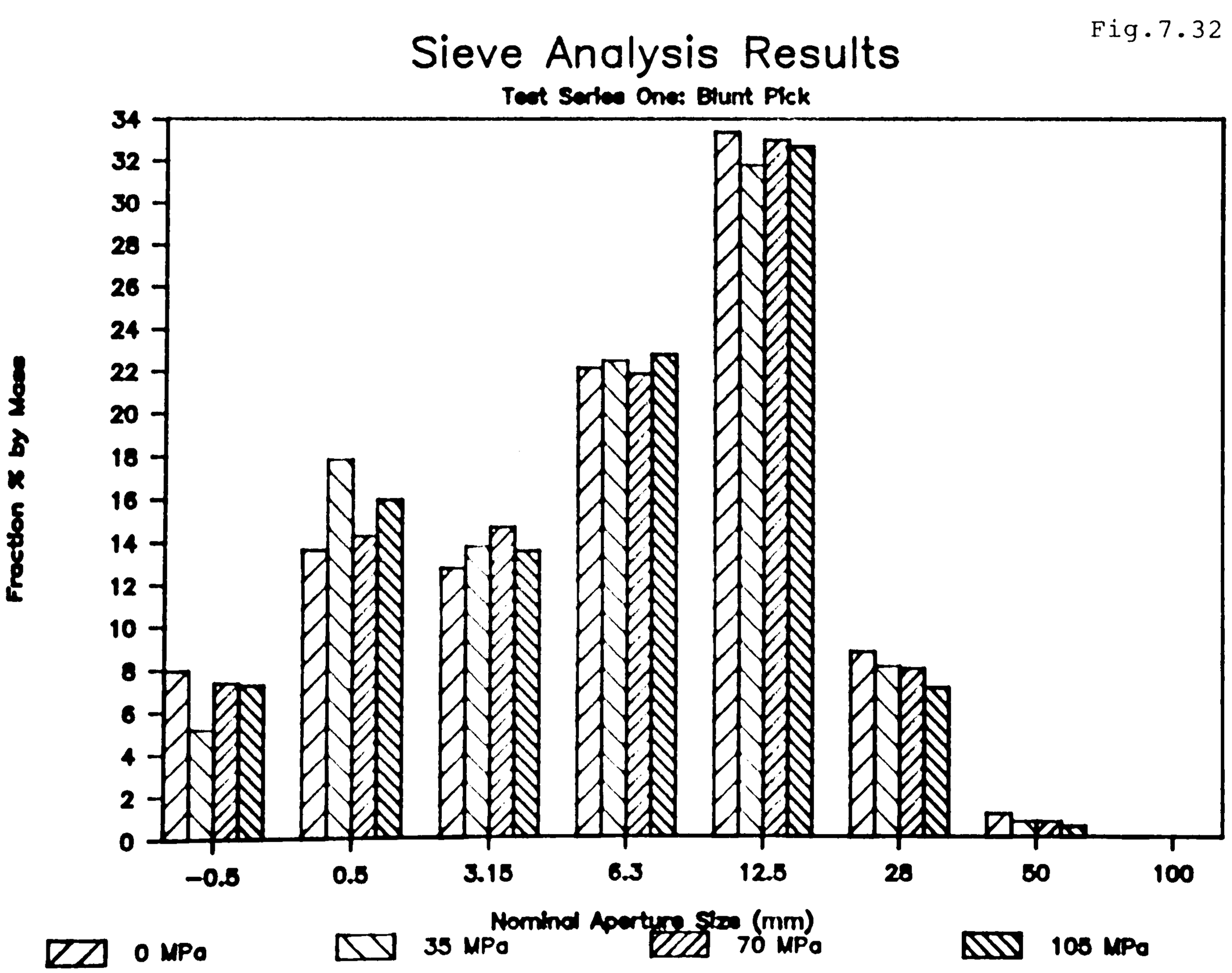


Fig.7.33

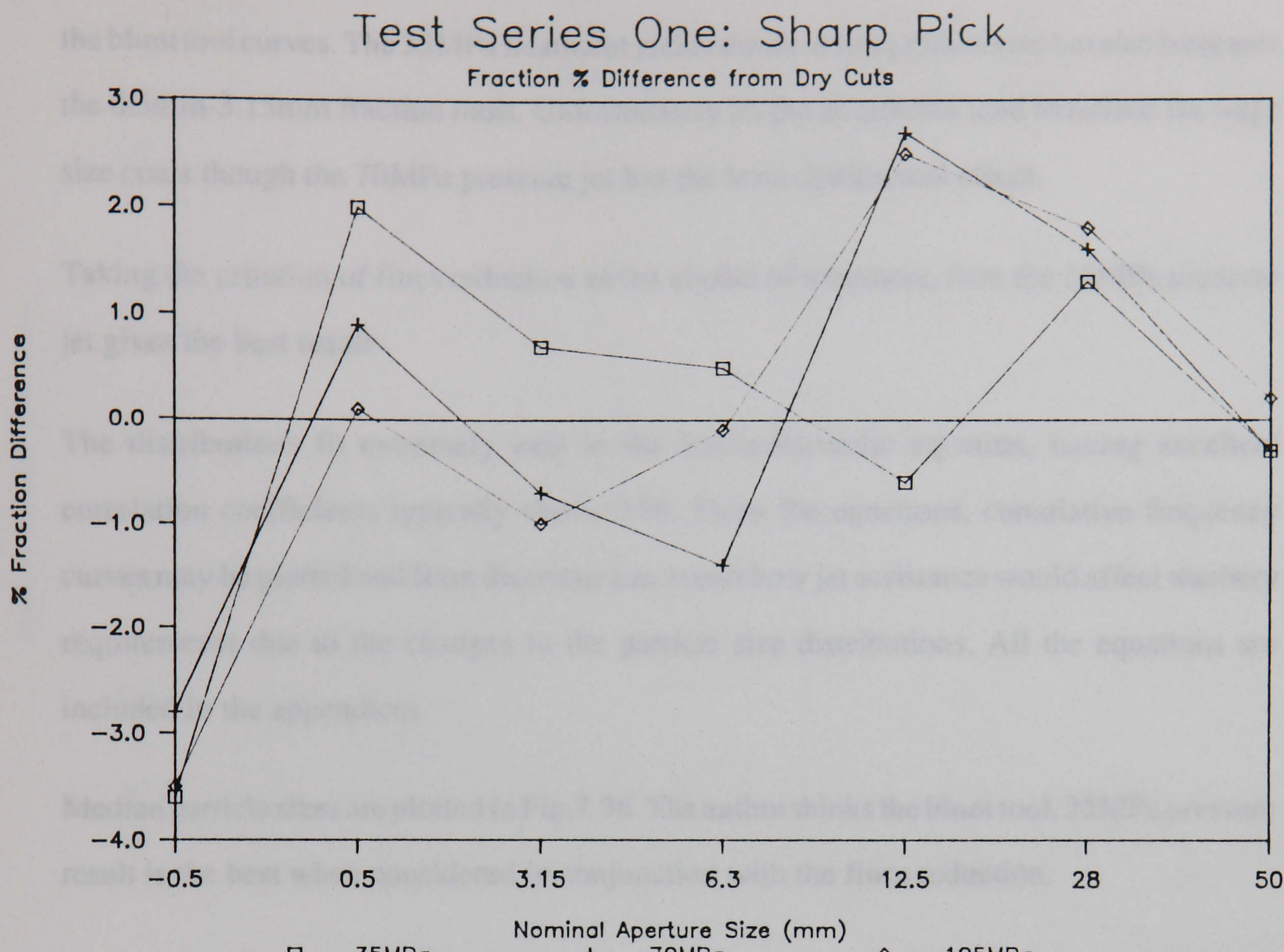


Fig.7.34

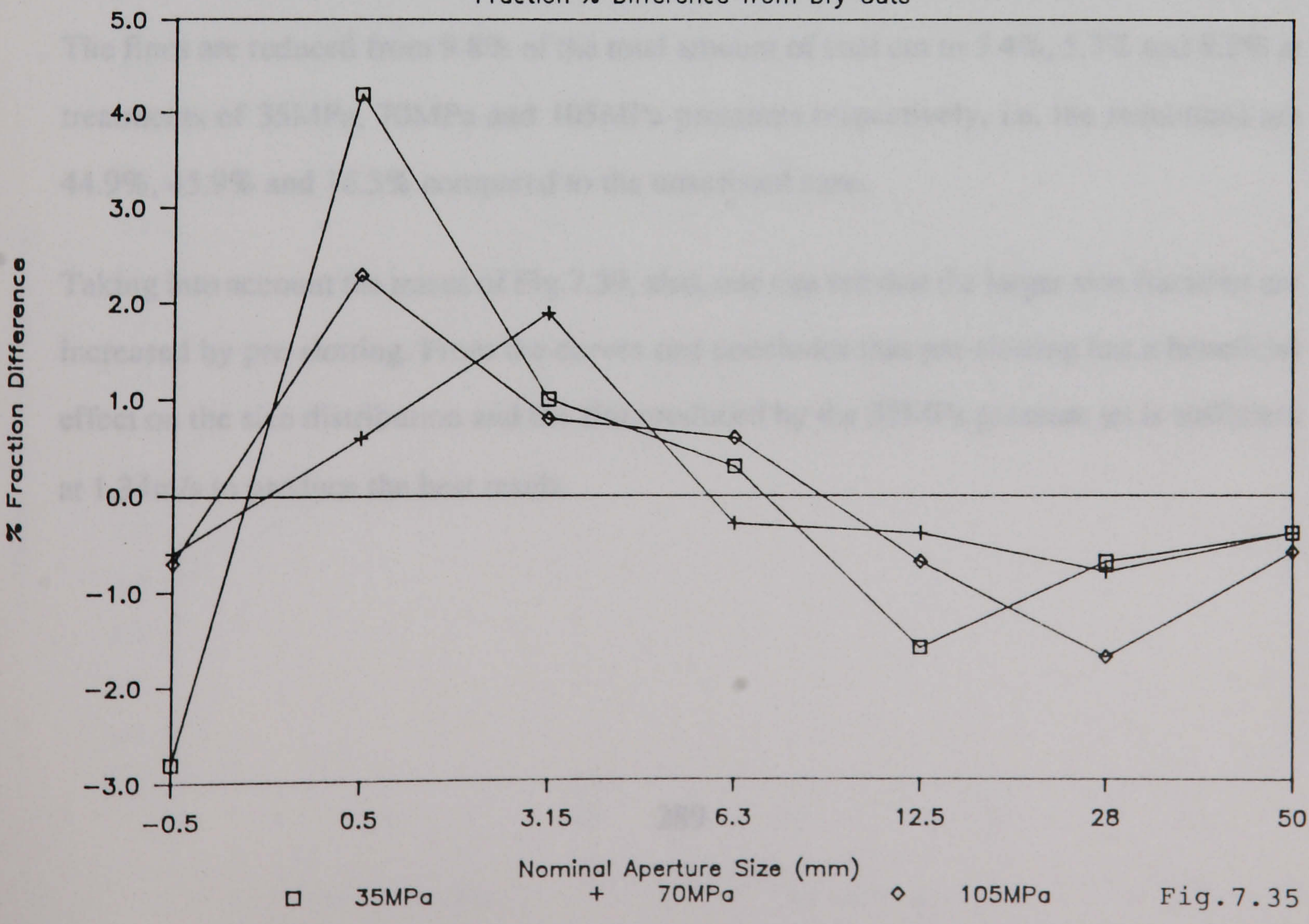


Fig.7.35

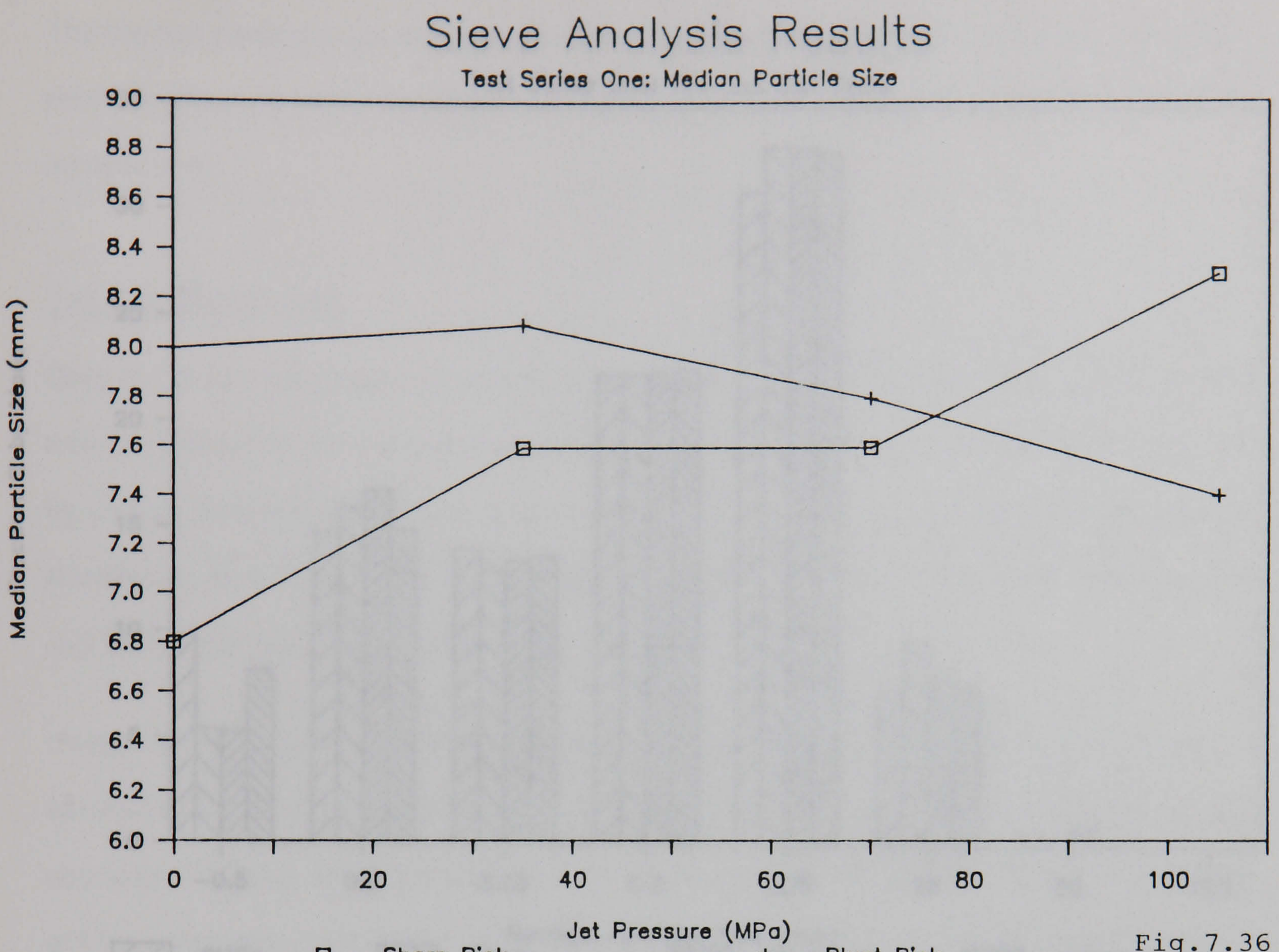


Fig.7.36

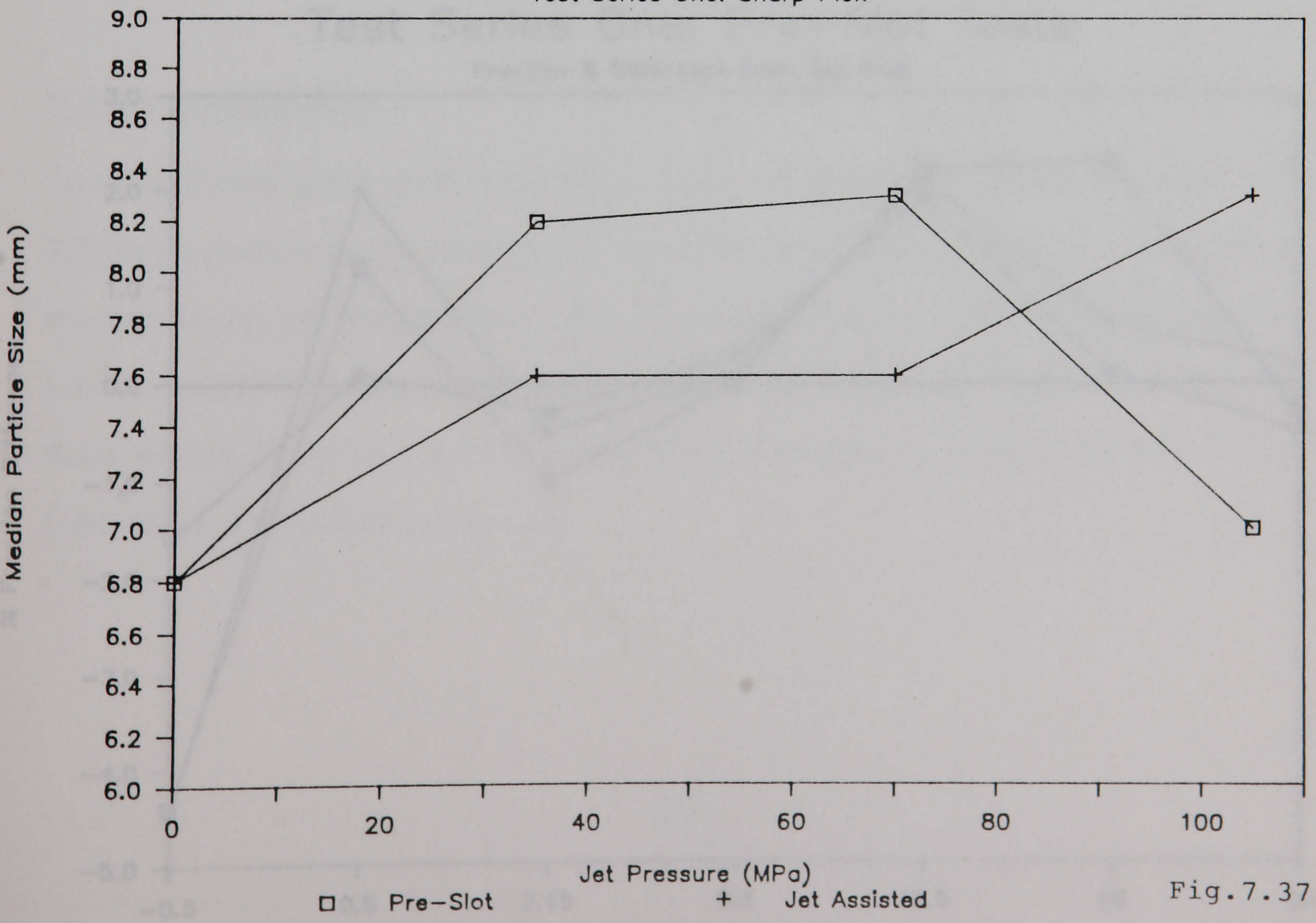


Fig.7.37

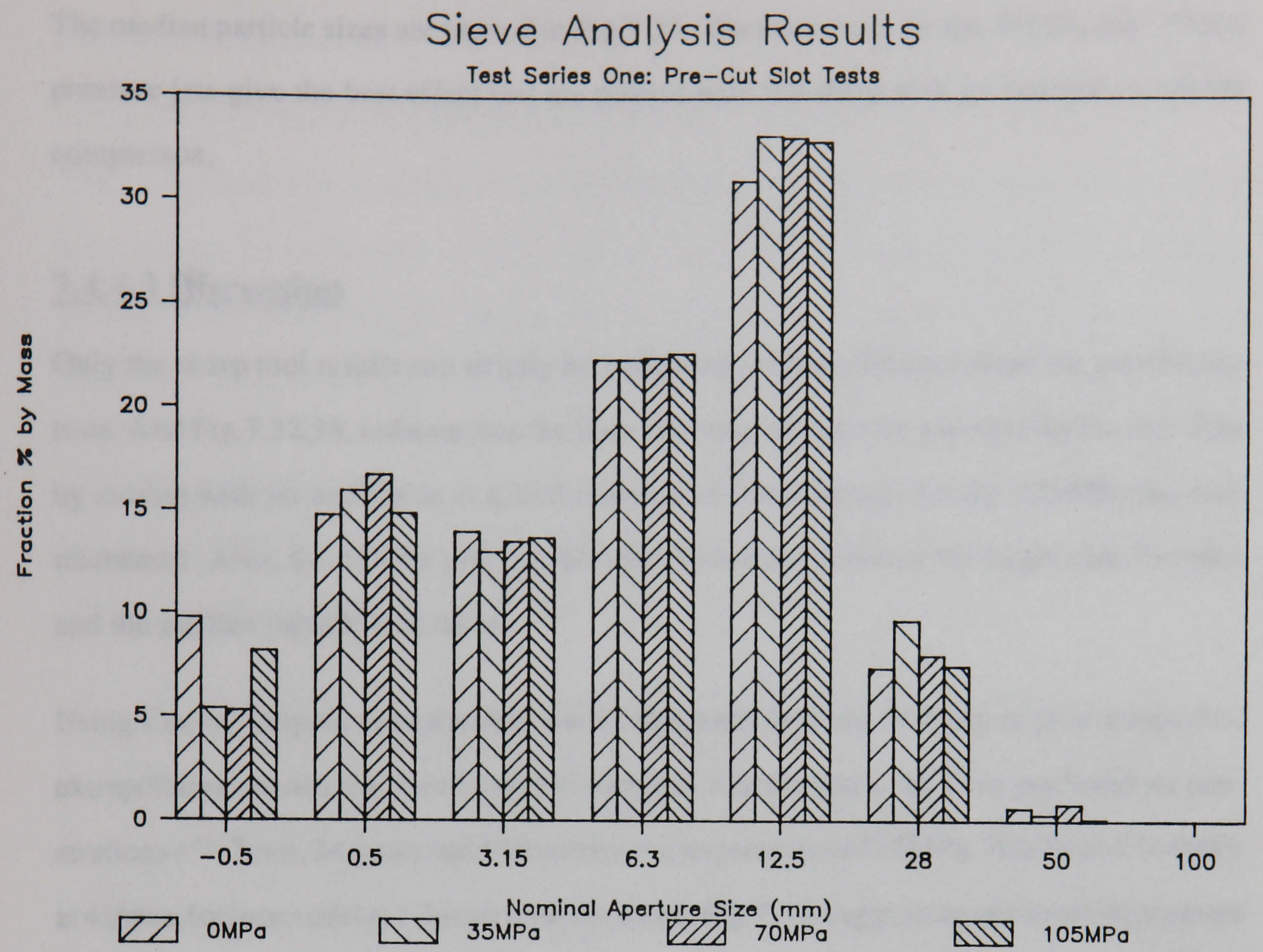


Fig.7.38

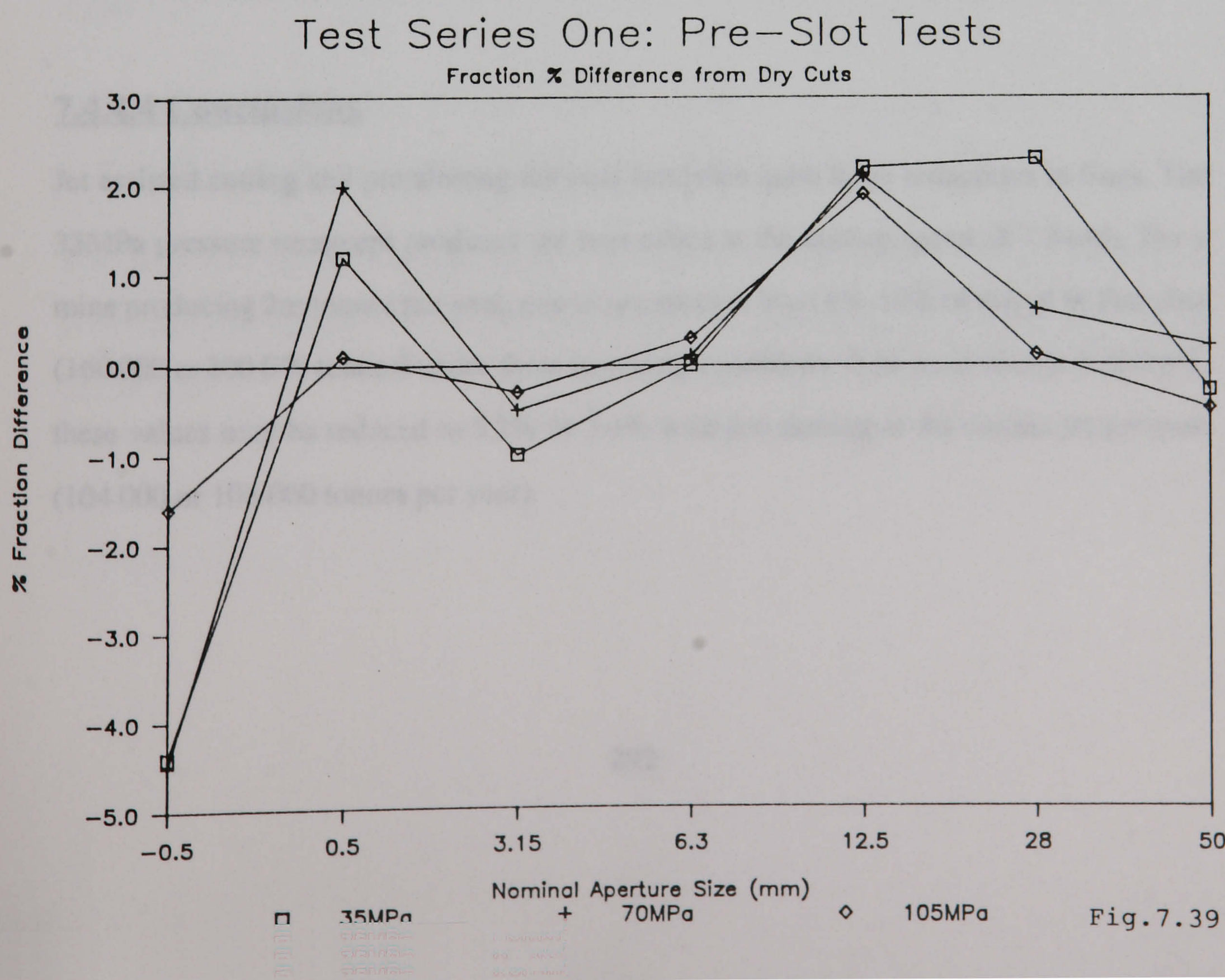


Fig.7.39

The median particle sizes are plotted in Fig.7.37. The slots made by the 35MPa and 70MPa pressure jets give the best effect and are plotted with the sharp pick jet assisted values for comparison.

7.4.4.3 Discussion

Only the sharp tool results can strictly be compared to those obtained from the pre-slotting tests. And Fig.7.32,38, indicate that the fines are reduced more by pre-slotting the coal than by cutting with jet assistance at a lead distance of 2mm (except for the 105MPa pressure treatment). Also, the 35MPa pressure pre-slot treatment increases the larger size fractions and the median particle size more.

Using Cooley's equation to translate the jet pressures in terms of depth of penetration (but extrapolating outside the speed range covered in chapter four), we have predicted jet penetrations of 9.7mm, 24.2mm and 40.6mm for the jet pressures of 35MPa, 70MPa and 105MPa at 4 l/min, for intact coal at 1.34m/s traverse speed. Fig.7.37, suggests an optimum jet pressure hence slot depth for pre-slotting that will produce a maximum median particle size. This would be between 35MPa and 70MPa pressure or 9.7mm and 24.2mm penetration.

7.4.4.4 Conclusions

Jet assisted cutting and pre-slotting the coal furnishes quite large reductions in fines. The 35MPa pressure treatment produces the best effect at the cutting speed of 1.34m/s. For a mine producing 2m tonnes per year, one may expect at least 8%-10% of this to be fine coal (160 000 to 200 000 tonnes) under these operating conditions. If jet assistance is employed, these values may be reduced to 5.2% or 5.4% with pre-slotting at the correct jet pressure (104 000 or 108 000 tonnes per year).

7.5 Test Series Two

7.5.1 Lead and Offset Distance Analysis

This test series investigated the effects of offset distance and lead distance with jet assistance at a constant jet pressure of 70MPa, a flow rate of 4 l/min, a cutting speed of 1.34m/s and cutting with a sharp pick. The programme was conducted in the same coal specimens as in Test Series One, and the pick force analysis was carried out in the same fashion.

The table below describes the basic factorial experiment. During the analysis it was found that one of the treatments had not been recorded on the tape and this is left blank in the table. Unfortunately, the size distribution for the treatment was not available either.

	Lead Distance			
Offset Distance	2mm	10mm	50mm	100mm
0mm	12X	11X	11X	11X
35mm	10X	10X	9X	11X
50mm	12X	12X	12X	

Table 7.17

The number of replications for each treatment are shown in the table and in total 121 cuts were made giving an average of 11 replications per treatment.

The forces for the two cleat orientations were isolated and treated as a further comparison in the statistical analysis. The analysis was carried out as before using the statistics package GLIM 3.12.

Mean Normal Force ANOVA

Source of Variation	Sums of Squares	Degrees of Freedom	Mean Square	F-ratio & (Significance Level)
Between Lead	3.3	3	1.1	2.1 (3.8)
Between Offset	27.8	2	13.9	26.6 (4.6)
Between Cleat	7.2	1	7.2	13.8 (6.7)
Interaction between Lead & Offset	15.9	5	3.2	6.1 (3.1)
Interaction between Lead & Cleat	1.3	3	0.4	0.8 (3.8)
Interaction between Cleat & Offset	0.1	2	0.1	0.1 (4.6)
Interaction between Lead, Cleat & Offset	0.8	5	0.2	0.3 (3.1)
Experimental Error	260.2	498	0.5	
Total	316.6	519		

Table 7.18

The 95% confidence limits for the two-tailed t-tests are ±0.32kN for the cleat parallel results; ±0.68kN for the cleat horizontal tests; and ±0.52kN when making comparisons between the two cleat orientations.

The results are presented in two different ways. In the first set of graphs, Fig.7.40-47, the forces are plotted against offset distance for the two cleat orientations, the ensuing graphs present the forces against lead distance.

With the mean normal force the offset distance and cleat orientation are highly significant factors on the force levels. There is also a significant interaction term between the lead and offset distances which means that the value of the normal force at any particular lead distance depends upon the offset distance it is combined with.

A striking effect is observed in Fig.7.40-41, where the offset distance of 35mm produces a very large force reduction. The force value at 50mm offset and 2mm lead distance is also significantly lower than the zero offset treatment.

Fig.7.42-47, do not show the same marked force decrease at the 35mm offset distance. With a lead distance of 10mm, the 35mm offset level still yields the lowest mean normal force in both cleat directions but the differences are not significant. Fig.7.44-45, show the normal force decreasing gradually as the offset distance is increased, the difference between the zero offset and 50mm offset is significant in the cleat parallel case. Fig.7.46-47, indicate a significant decrease with the cleat parallel at a 35mm offset. The trend then, is for the offset to reduce the normal force, and an optimum position for this cutting regime is suggested at 35mm.

Generally, all the cleat horizontal mean normal force values are lower than the corresponding cleat parallel ones and follow the same trends.

Fig.7.48-53, illustrate the same results against the lead distance. When the offset is zero, then the jet at a lead distance of 10mm gives the best mean normal force decrease with the cleat parallel. With the cleat horizontal the 100mm lead distance gives a slightly better force reduction than that at 10mm, Fig.7.48,49.

At offset distances of 35mm and 50mm the trend with lead distance is reversed. Fig.7.50-53, show a sudden increase in the forces as the lead distance is increased from 2mm to 10mm. Therefore, when the offset is not zero it appears that a lead distance of 2mm is better than 10mm or more.

The significance between the offset distances is due to the differences in the 2mm lead distance results. The force values at 10mm, 50mm and 100mm lead distances do not sig-

nificantly differ from one offset distance to the next and this is for both cleat orientations. This is indicated in Table 7.18, by the insignificant lead distance effect and the highly significant interaction of lead and offset distances.

Mean Cutting Force ANOVA

Source of Variation	Sums of Squares	Degrees of Freedom	Mean Square	F-ratio & (Significance Level)
Between Lead	47.0	3	15.7	7.6 (3.8)
Between Offset	161.0	2	80.5	39.3 (4.6)
Between Cleat	95.0	1	95.0	46.4 (6.7)
Interaction between Lead & Offset	109.0	5	21.8	10.6 (3.1)
Interaction between Lead & Cleat	7.0	3	2.3	1.1 (3.8)
Interaction between Cleat & Offset	3.0	2	1.5	0.7 (4.6)
Interaction between Lead, Cleat & Offset	2.0	5	0.4	0.2 (3.1)
Experimental Error	1071.0	523	2.0	
Total	1495.0	544		

Table 7.19

The 95% confidence limits for the two-tailed t-tests are ±0.63kN for the cleat parallel results; ±1.34kN for the cleat horizontal tests; and ±1.04kN when making comparisons between the two cleat orientations.

In the case of the mean cutting force all the main effects of lead distance, offset distance and cleat orientation are highly significant. The interaction between the lead and offset distance is also significant.

The curves follow the same trends as the mean normal force but the differences are greater.

All the graphs indicate that the coal is easier to cut when the cleat is horizontally orientated.

The best operating conditions are at a lead distance of 2mm and an offset distance of 35mm.

Mean Sideway Force ANOVA

Source of Variation	Sums of Squares	Degrees of Freedom	Mean Square	F-ratio & (Significance Level)
Between Lead	19.3	3	6.4	8.6 (3.8)
Between Offset	27.3	2	13.6	18.3 (4.6)
Between Cleat	8.2	1	8.2	11.0 (6.7)
Interaction between Lead & Offset	5.2	5	1.0	1.4 (3.1)
Interaction between Lead & Cleat	2.9	3	1.0	1.3 (3.8)
Interaction between Cleat & Offset	3.2	2	1.6	2.1 (4.6)
Interaction between Lead, Cleat & Offset	1.1	5	0.2	0.3 (3.1)
Experimental Error	382.3	513	0.7	
Total	449.5	534		

Table 7.20

The 95% confidence limits for the two-tailed t-tests are ±0.38kN for the cleat parallel results; ±0.81kN for the cleat horizontal tests; and ±0.62kN when making comparisons between the two cleat orientations.

All three main effects are significant. The offset distance is the major factor and an offset distance of 35mm generally produces the minimum mean sideway force which is significantly lower than that at an offset distance of zero when the cleat is parallel.

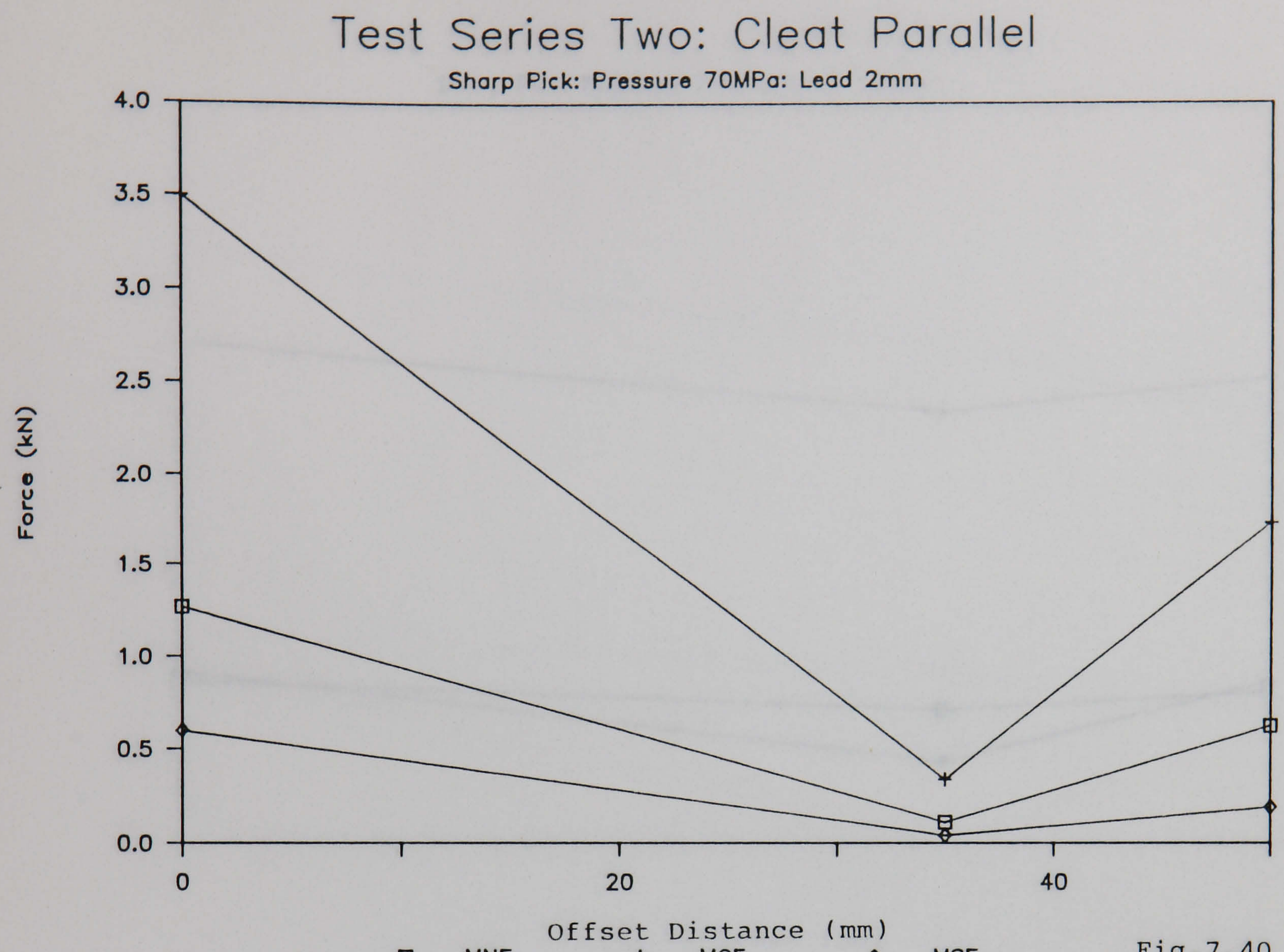


Fig.7.40

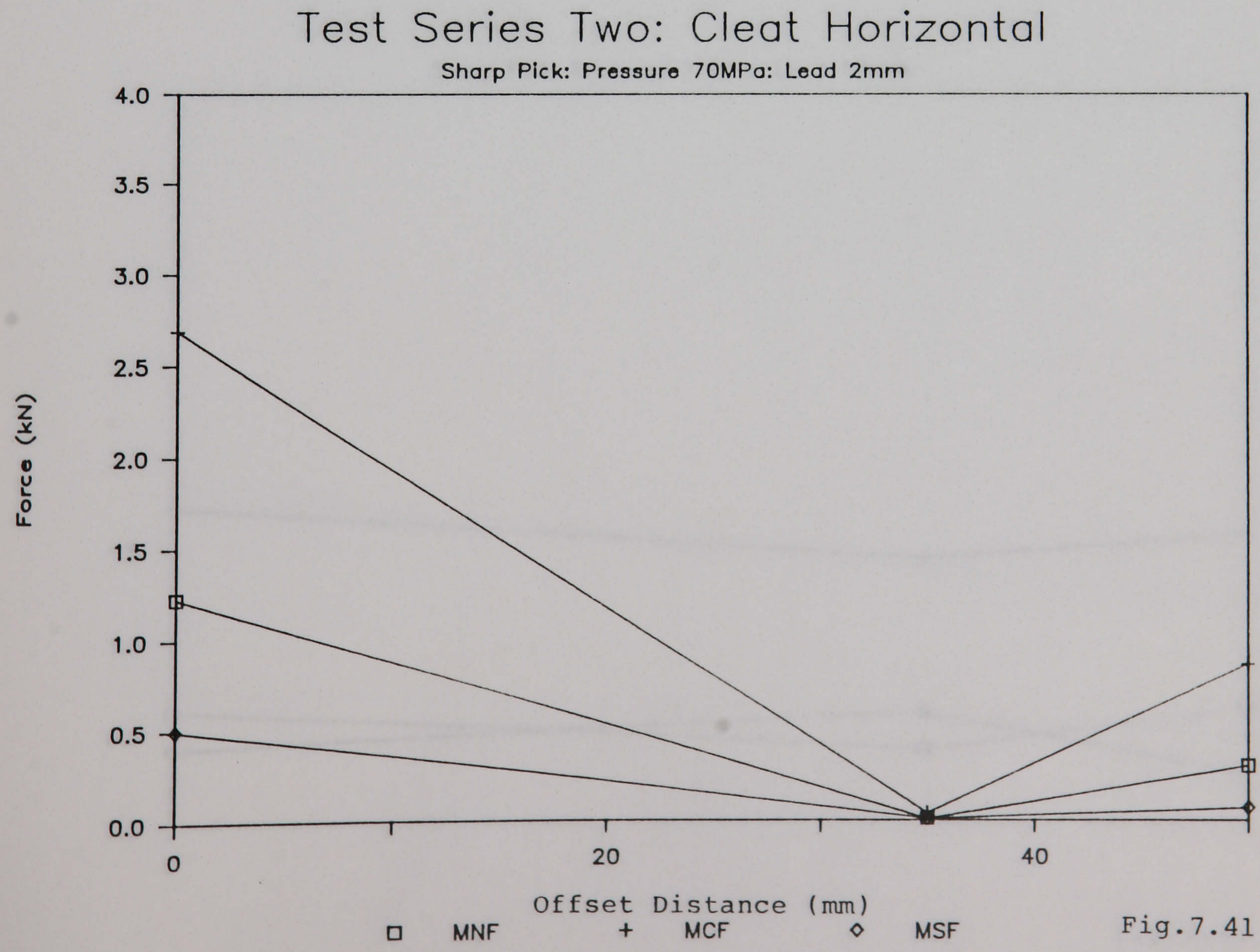


Fig.7.41

Test Series Two: Cleat Parallel

Sharp Pick: Pressure 70MPa: Lead 10mm

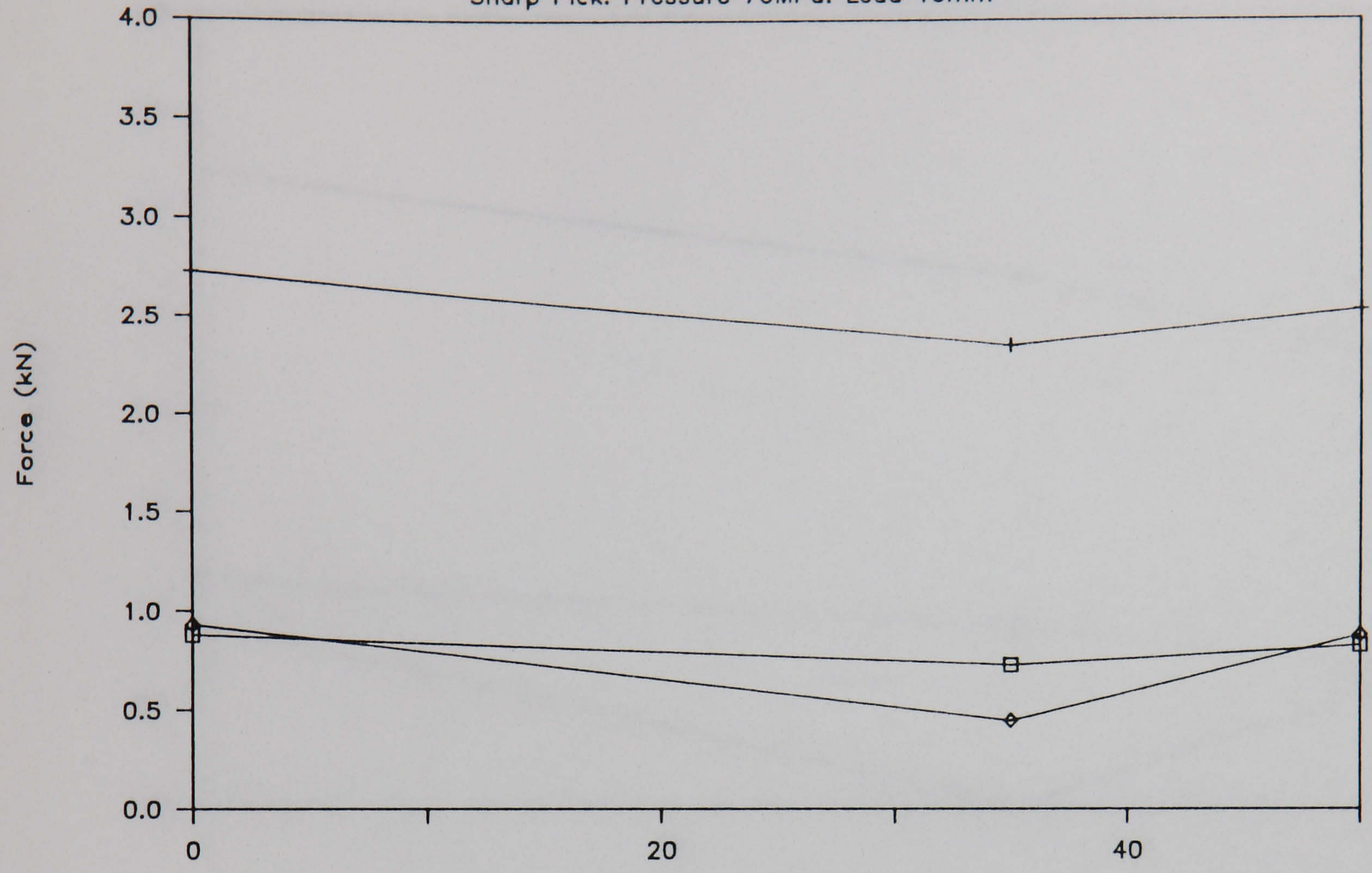


Fig.7.42

Test Series Two: Cleat Horizontal

Sharp Pick: Pressure 70MPa: Lead 10mm

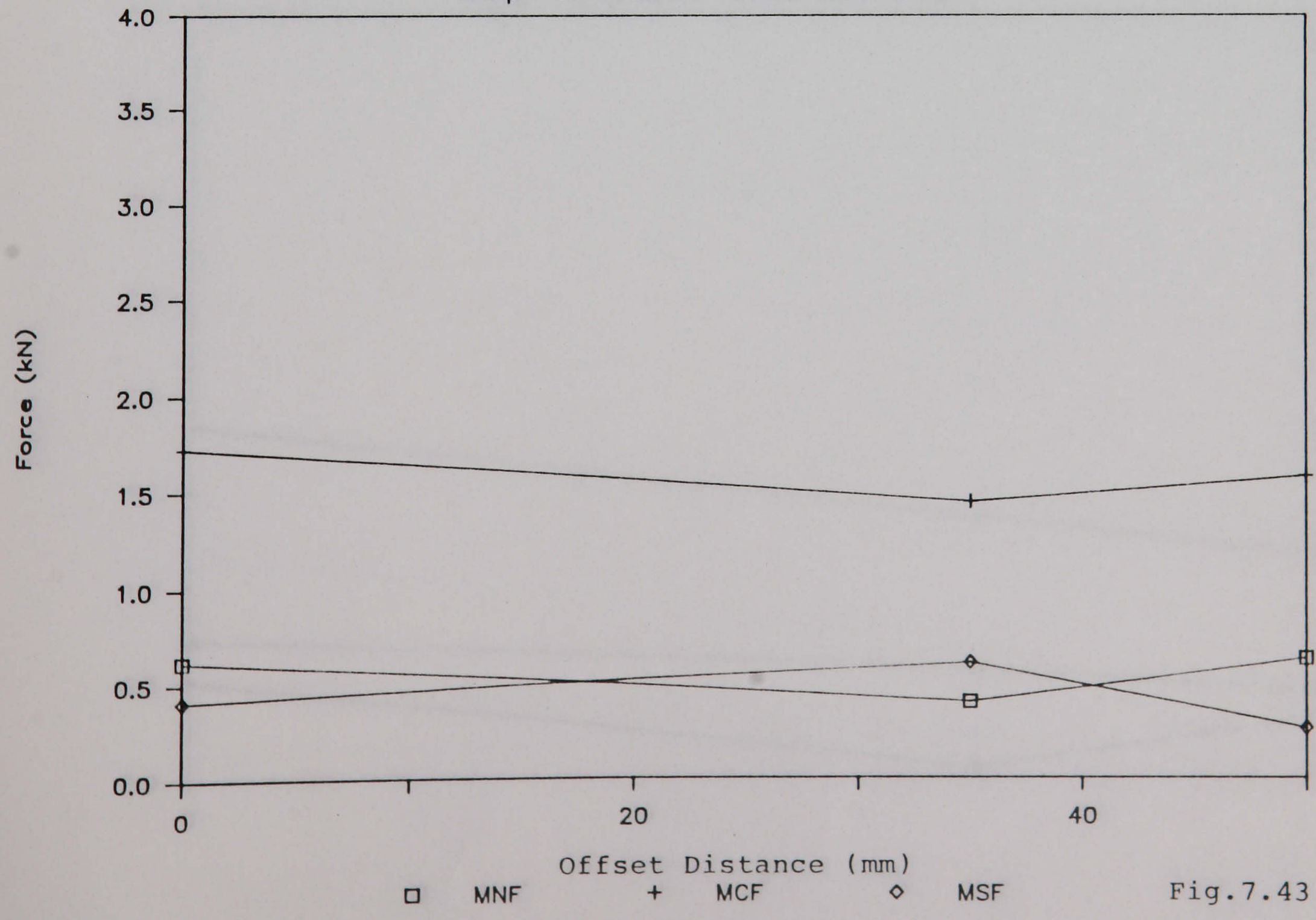


Fig.7.43

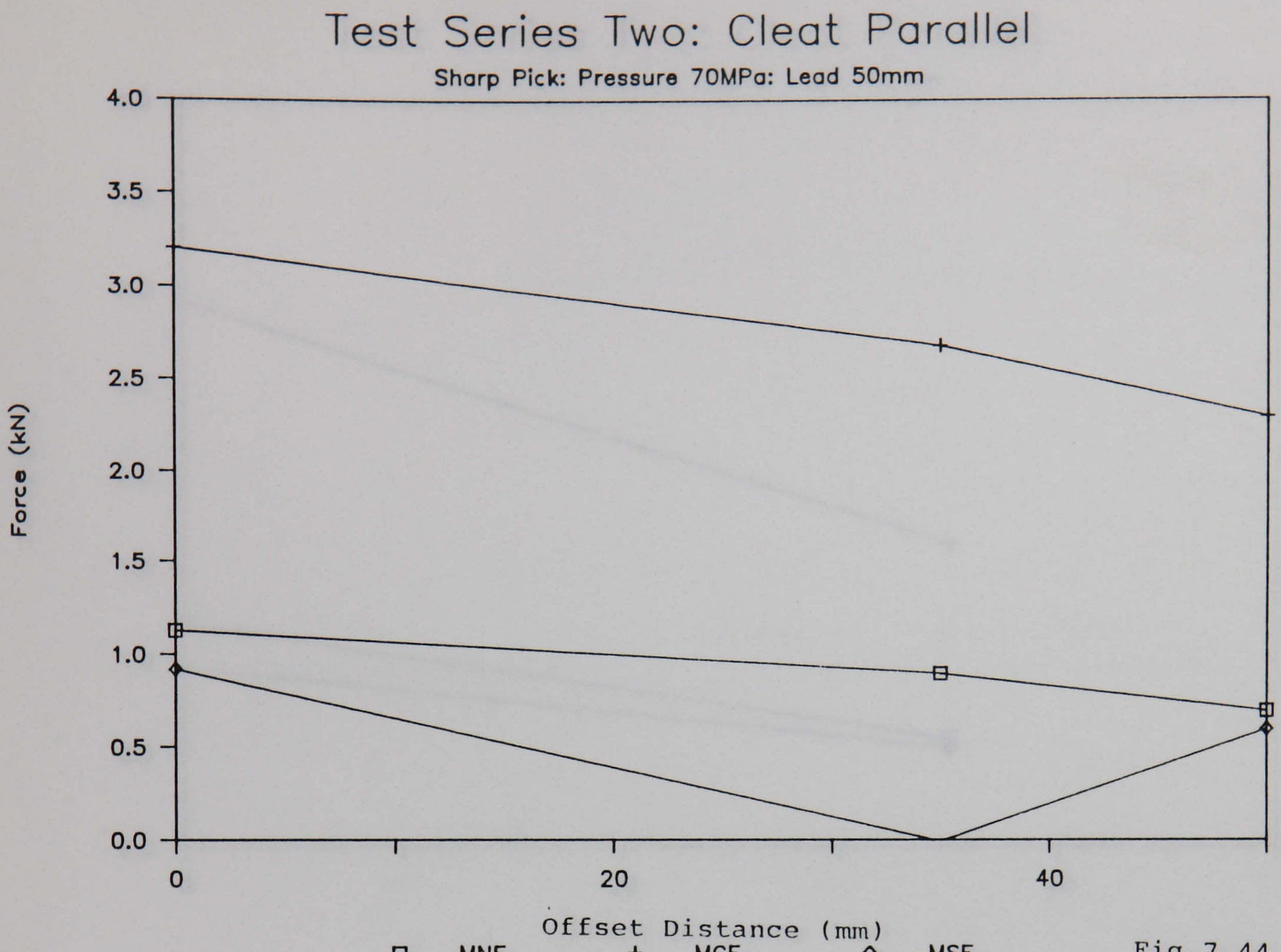


Fig.7.44

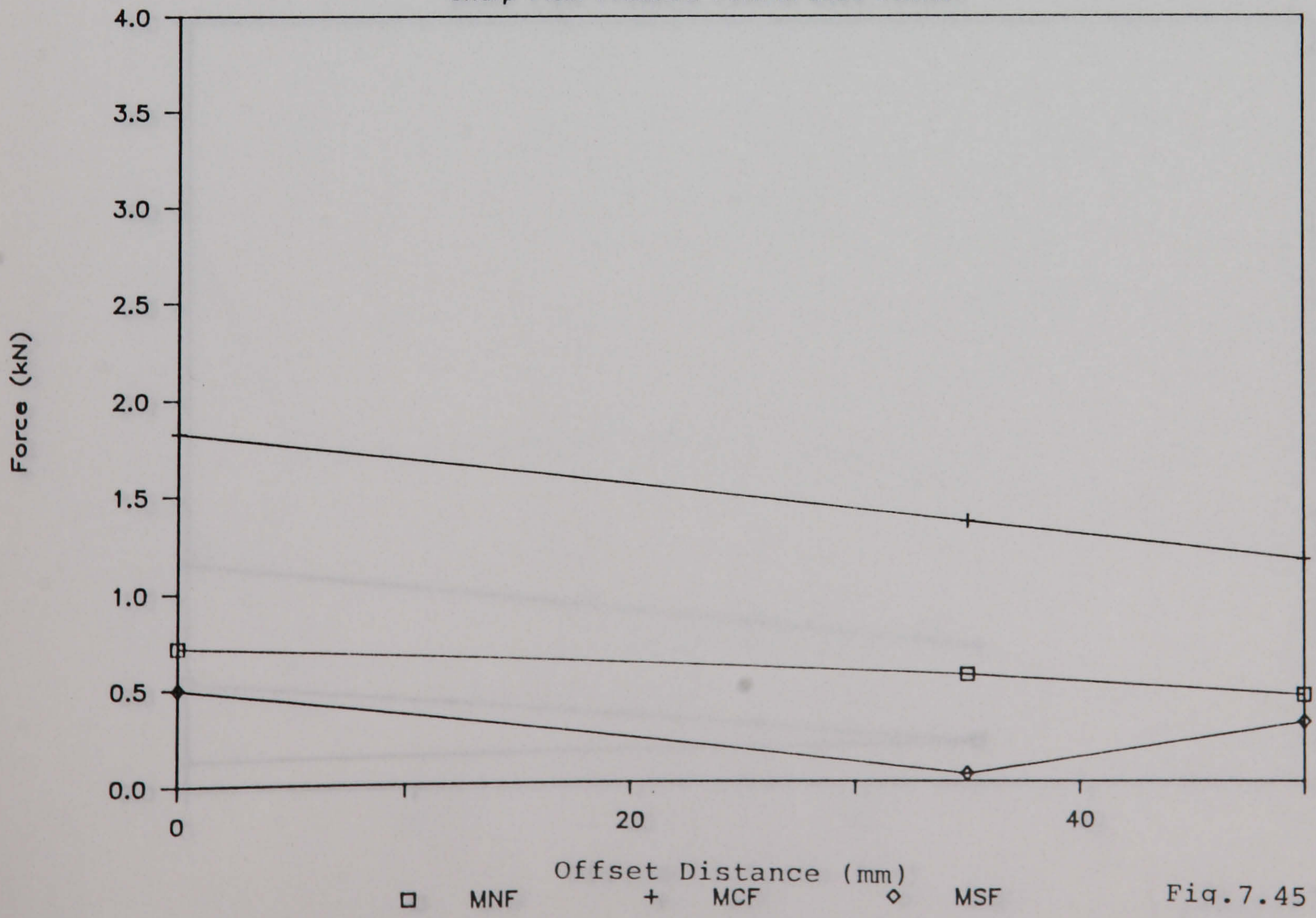


Fig.7.45

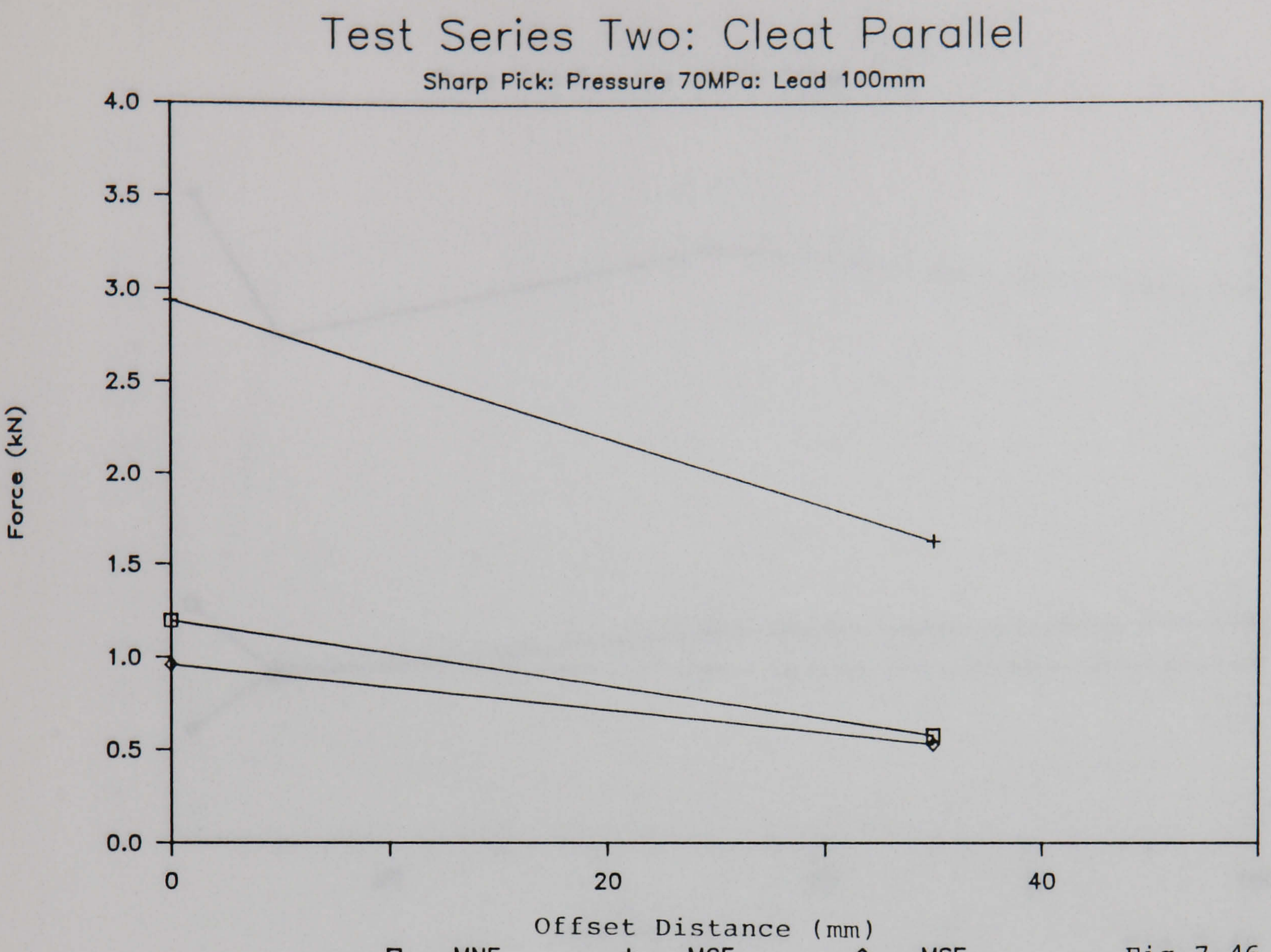


Fig.7.46

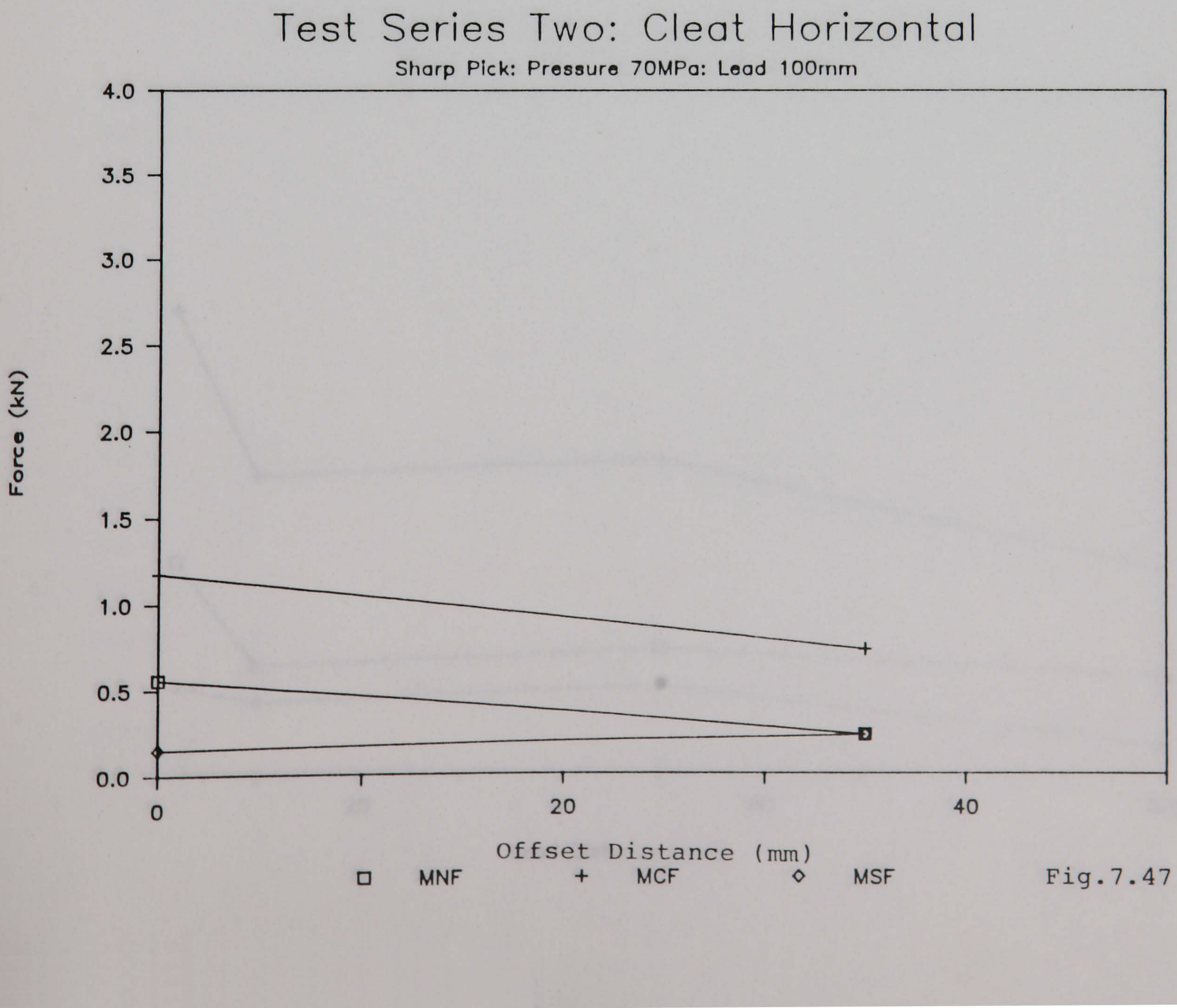


Fig.7.47

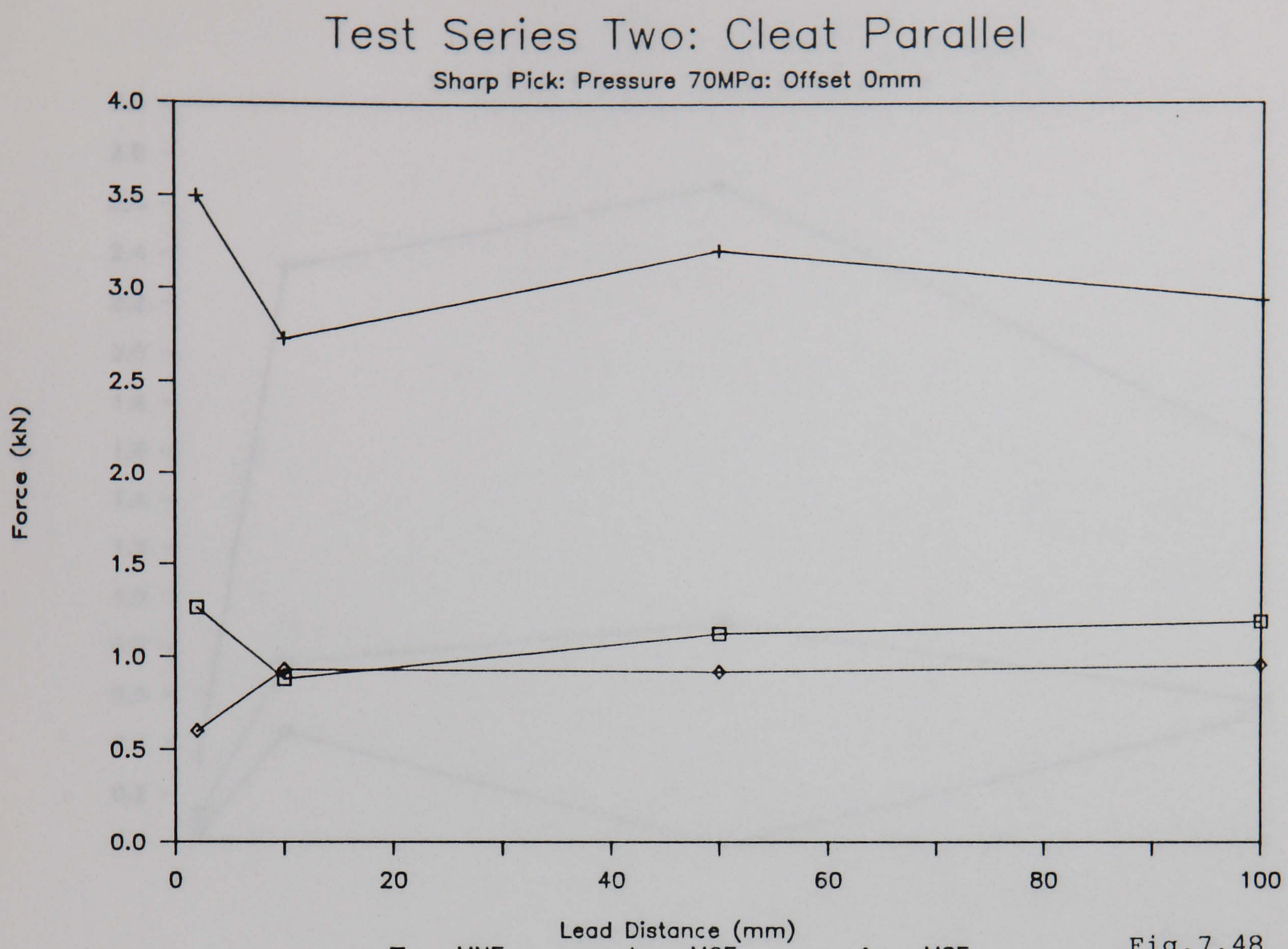


Fig.7.48

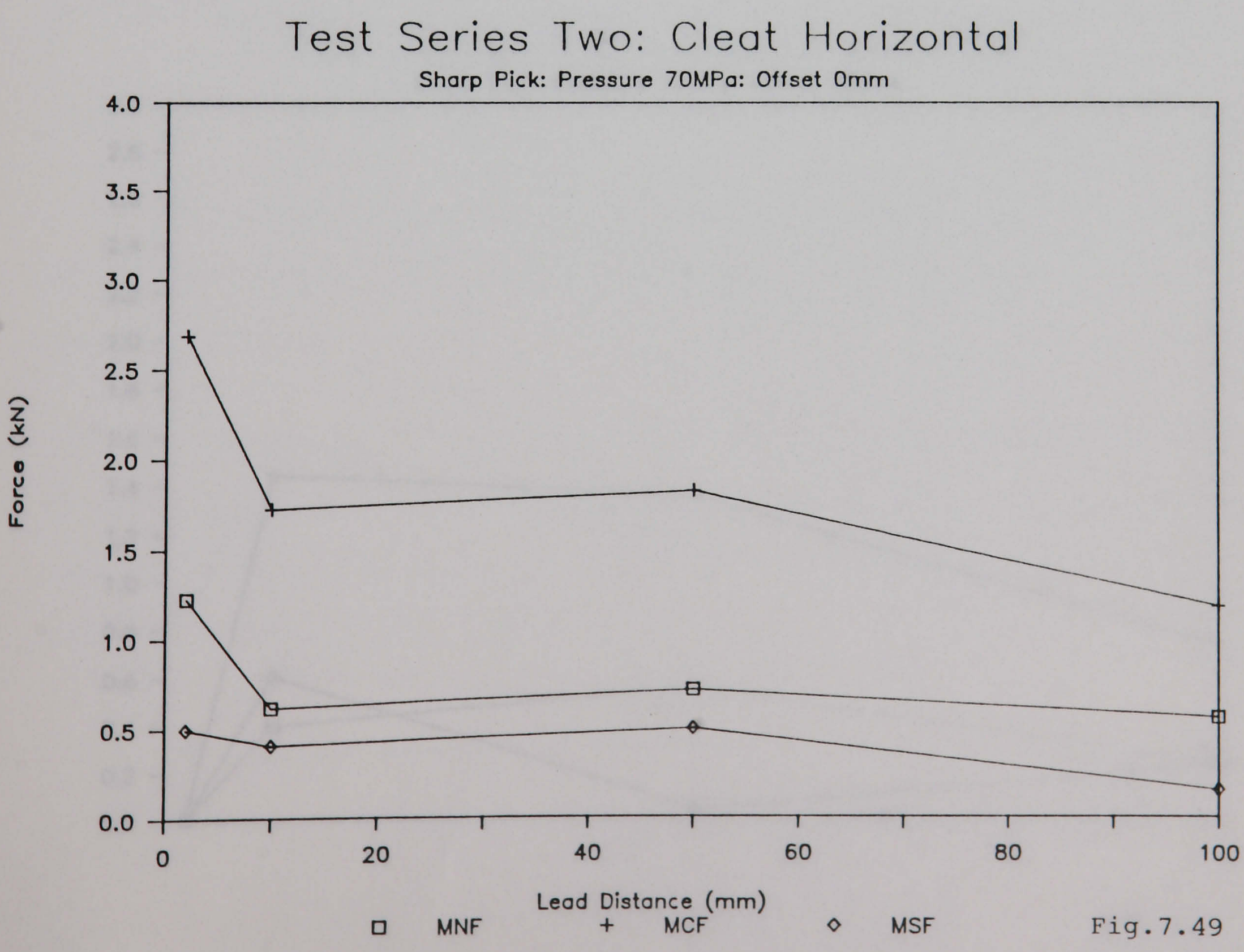


Fig.7.49

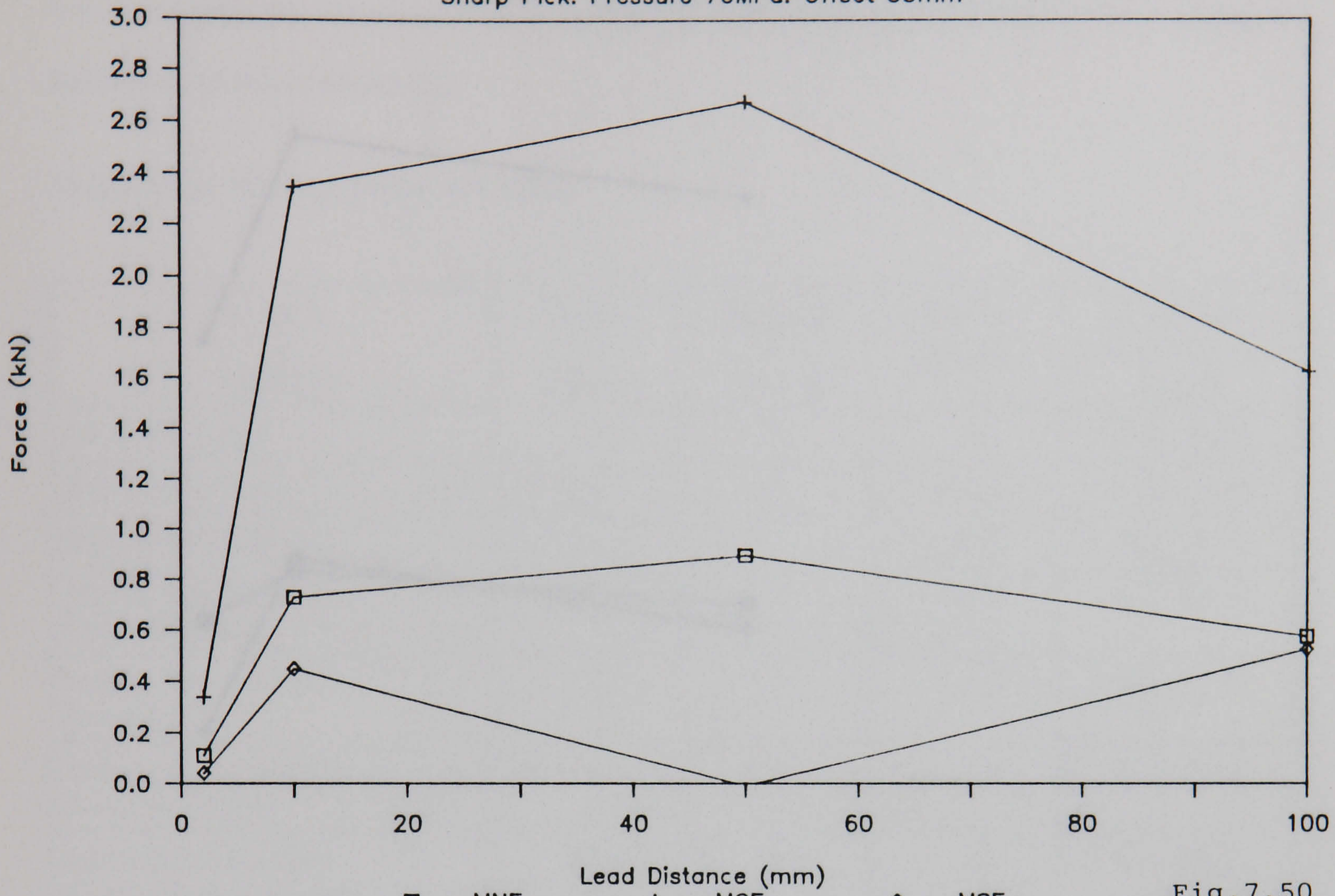


Fig.7.50

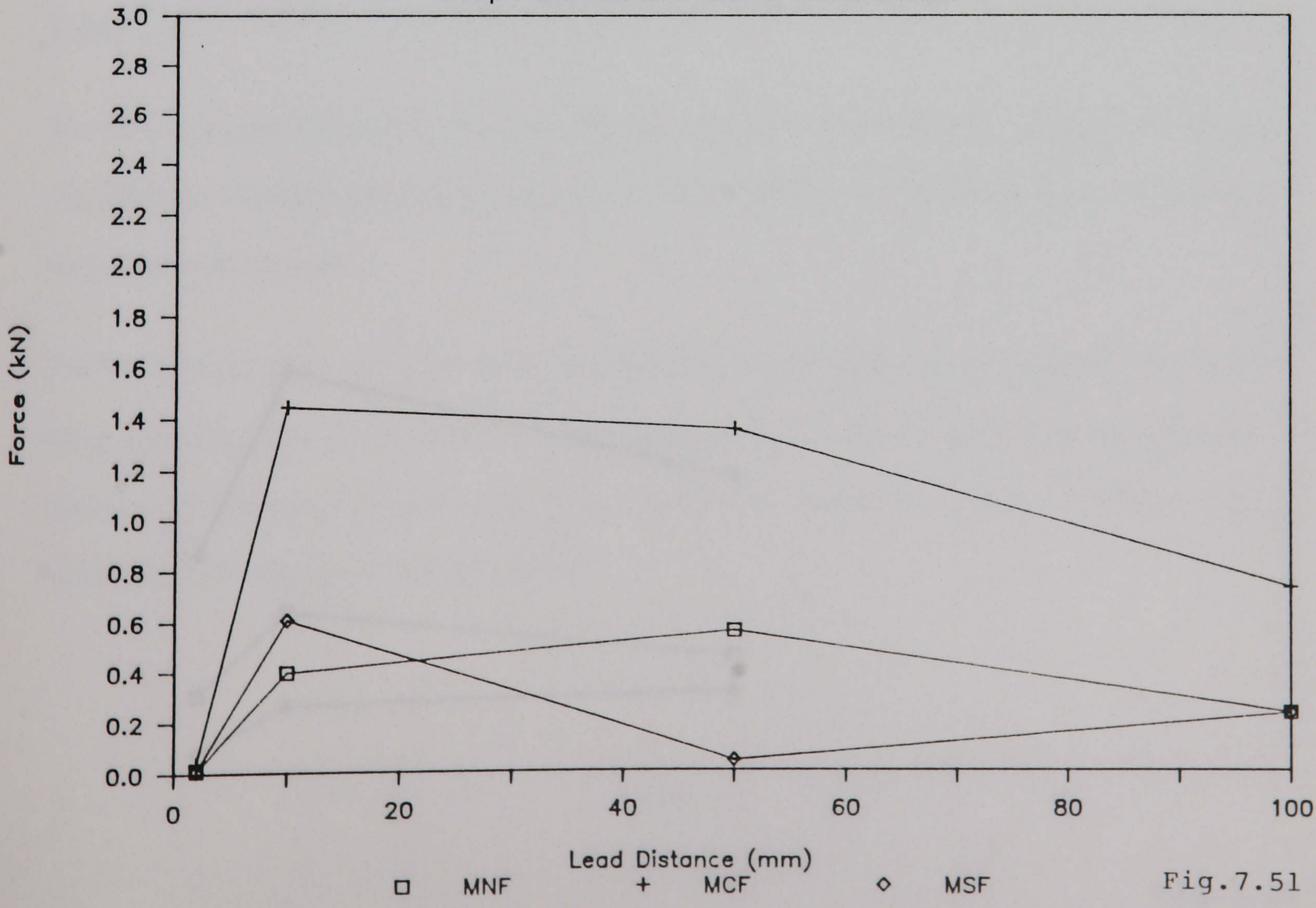


Fig.7.51

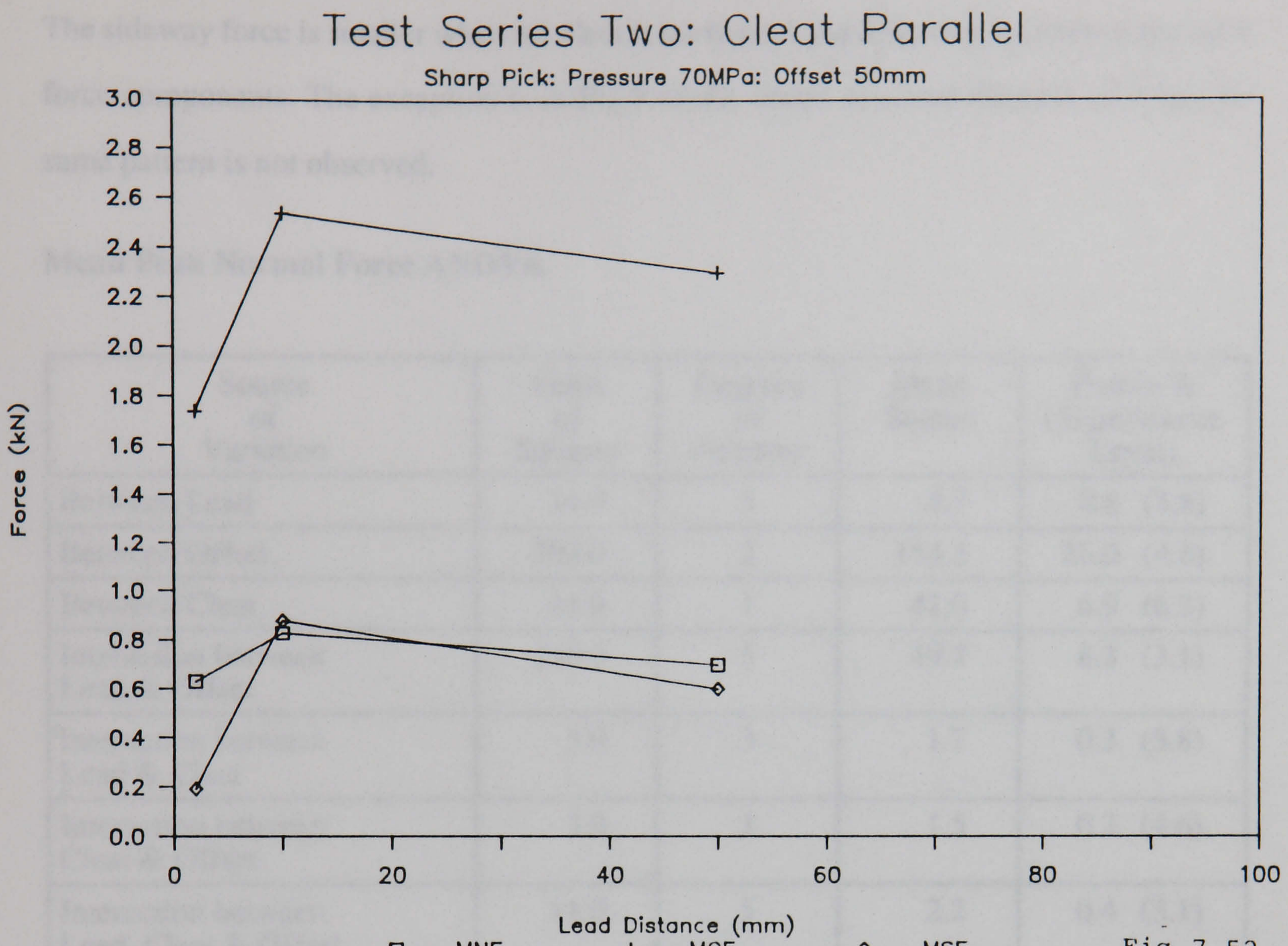


Fig.7.52

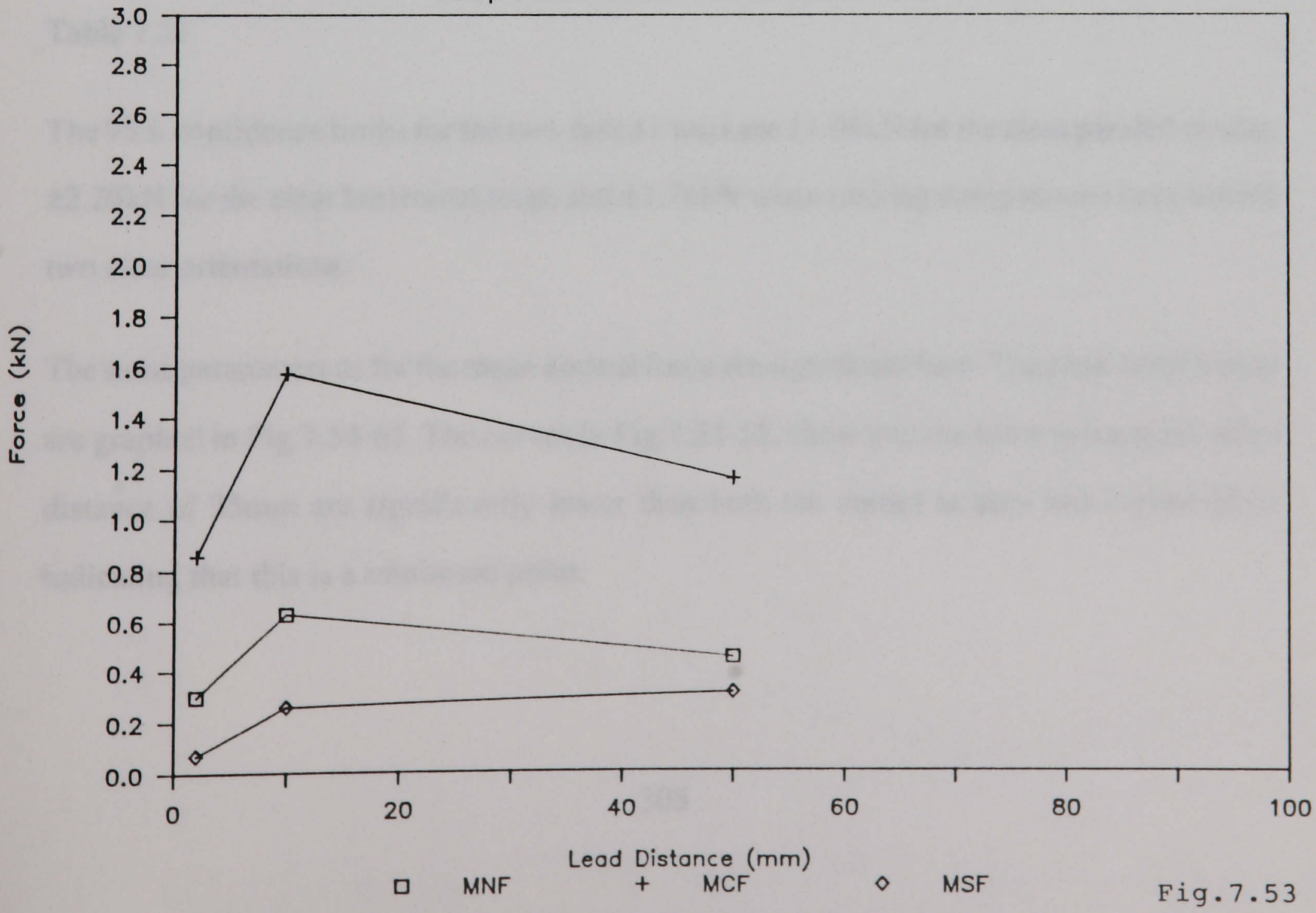


Fig.7.53

The sideway force is smaller when the cleat is horizontal and follows the trends of the other force components. The exception is in Fig.7.48,49, where at a lead distance of 2mm, the same pattern is not observed.

Mean Peak Normal Force ANOVA

Source of Variation	Sums of Squares	Degrees of Freedom	Mean Square	F-ratio & (Significance Level)
Between Lead	14.0	3	4.7	0.8 (3.8)
Between Offset	309.0	2	154.5	26.0 (4.6)
Between Cleat	41.0	1	41.0	6.9 (6.7)
Interaction between Lead & Offset	246.0	5	49.2	8.3 (3.1)
Interaction between Lead & Cleat	5.0	3	1.7	0.3 (3.8)
Interaction between Cleat & Offset	3.0	2	1.5	0.3 (4.6)
Interaction between Lead, Cleat & Offset	11.0	5	2.2	0.4 (3.1)
Experimental Error	2955.0	498	5.9	
Total	3584.0	519		

Table 7.21

The 95% confidence limits for the two-tailed t-tests are ±1.08kN for the cleat parallel results; ±2.29kN for the cleat horizontal tests; and ±1.76kN when making comparisons between the two cleat orientations.

The same parameters as for the mean normal force are significant here. The peak force results are graphed in Fig.7.54-67. The curves in Fig.7.54-55, show that the force value at an offset distance of 35mm are significantly lower than both the values at zero and 50mm offset indicating that this is a minimum point.

Test Series Two: Cleat Parallel

Sharp Pick: Pressure 70MPa: Lead 2mm

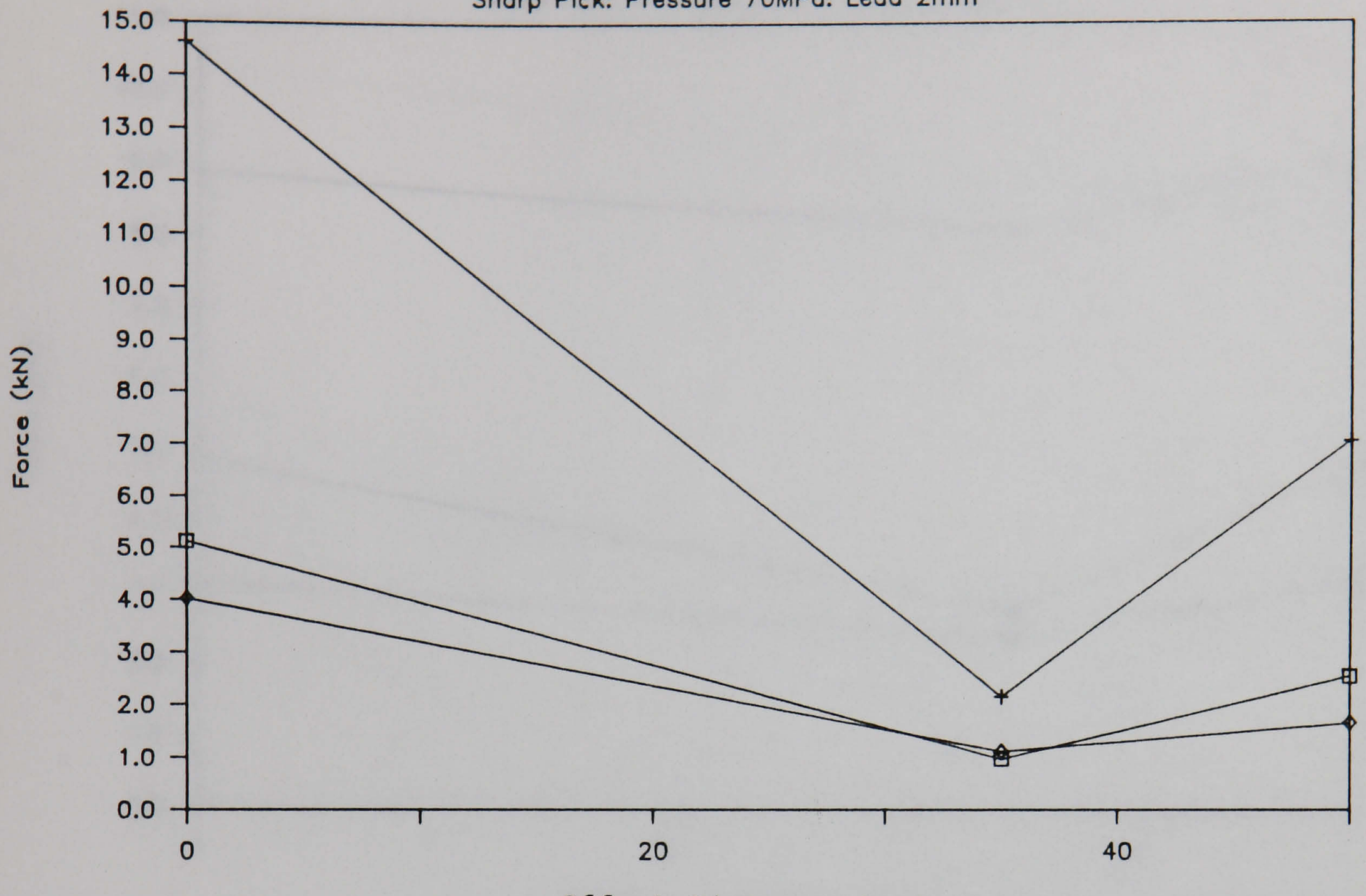


Fig.7.54

Test Series Two: Cleat Horizontal

Sharp Pick: Pressure 70MPa: Lead 2mm

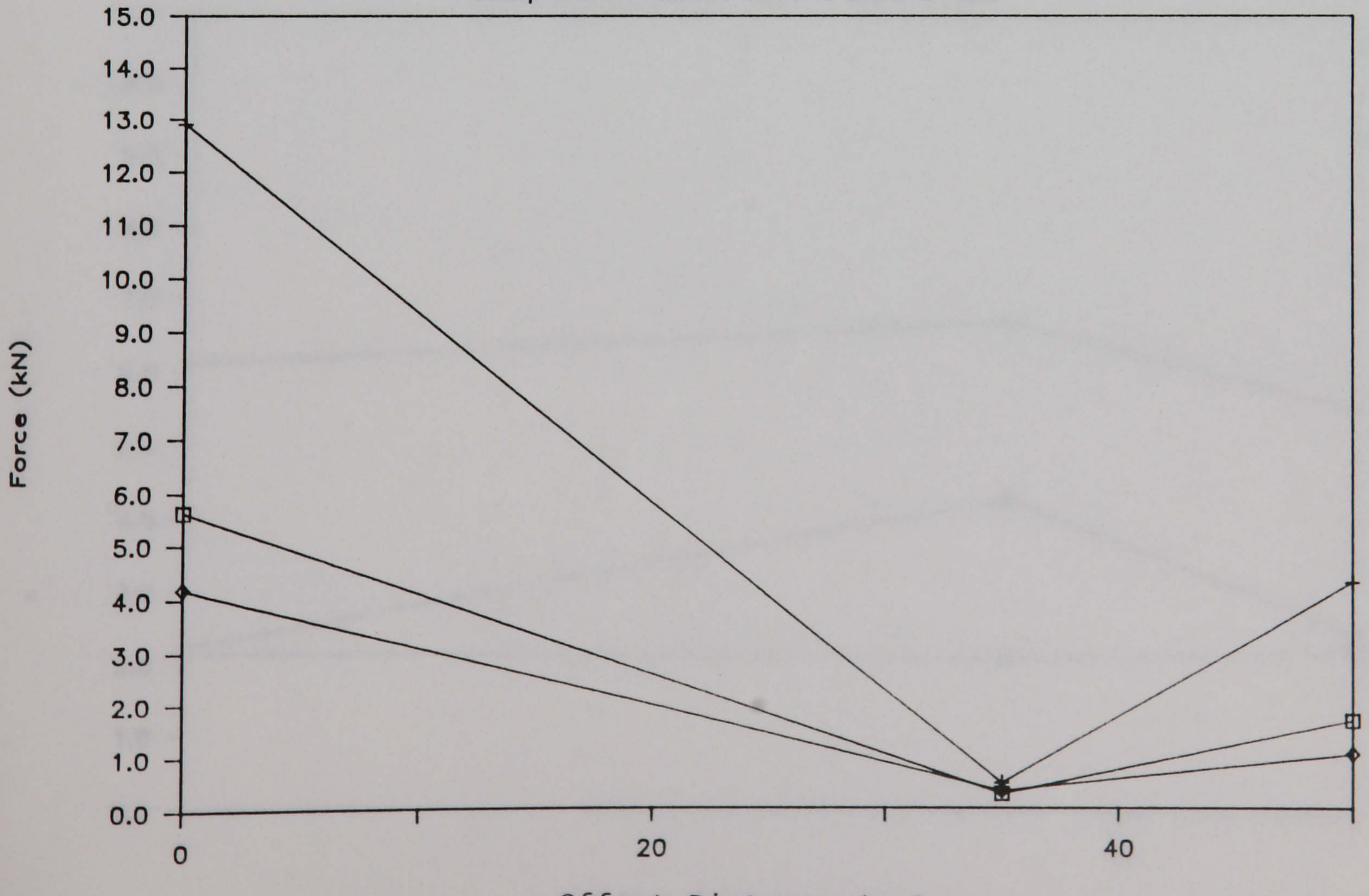


Fig.7.55

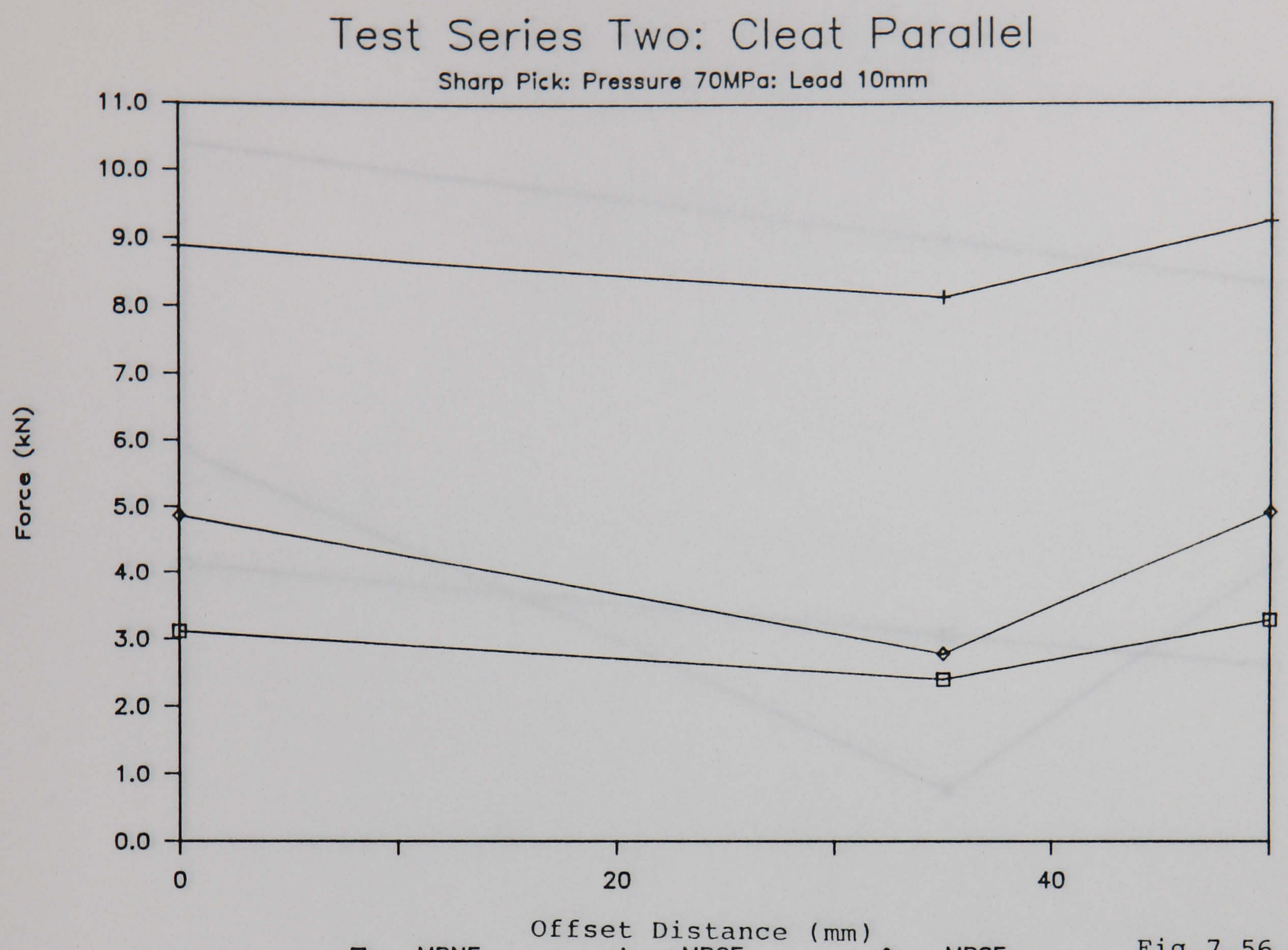


Fig.7.56

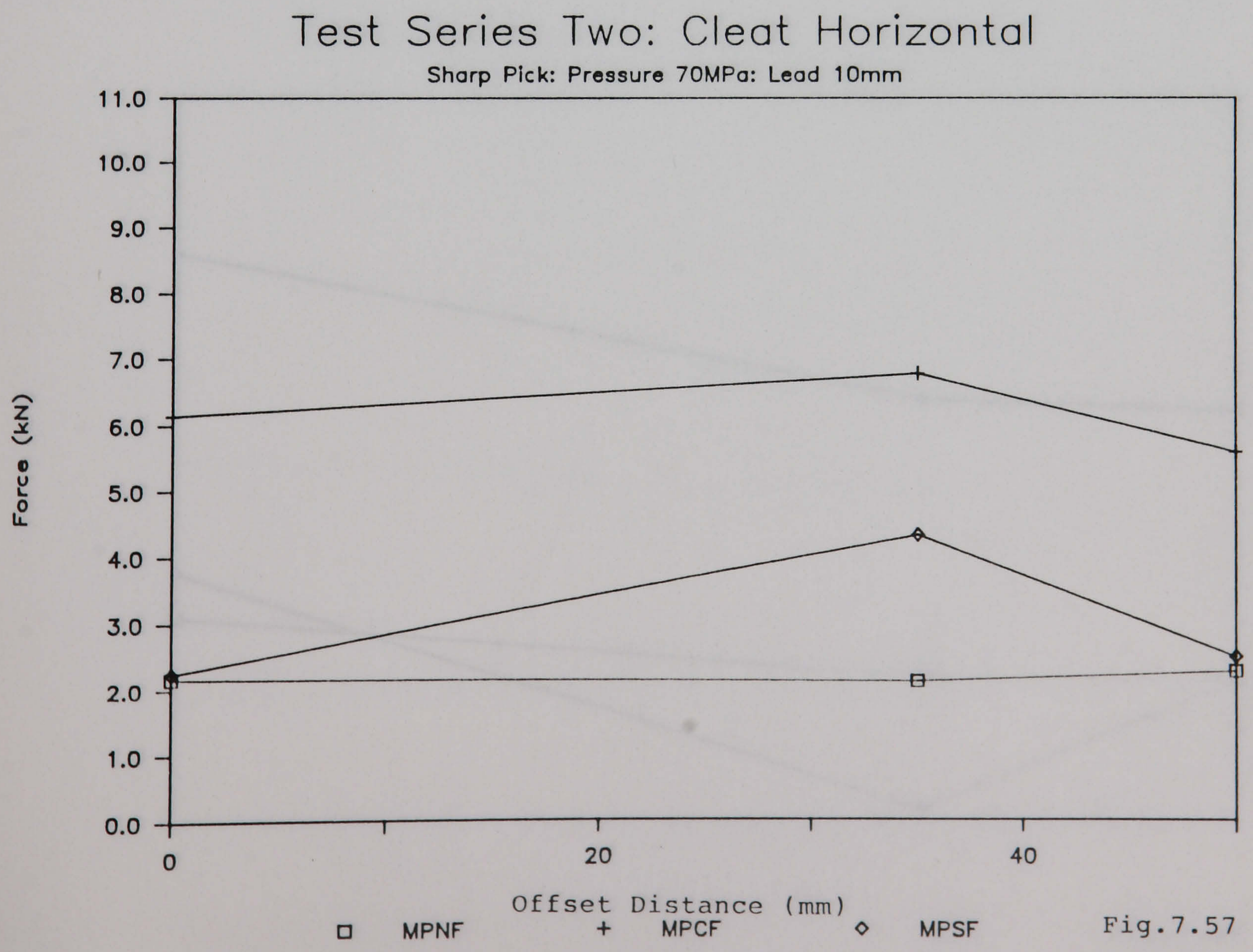


Fig.7.57

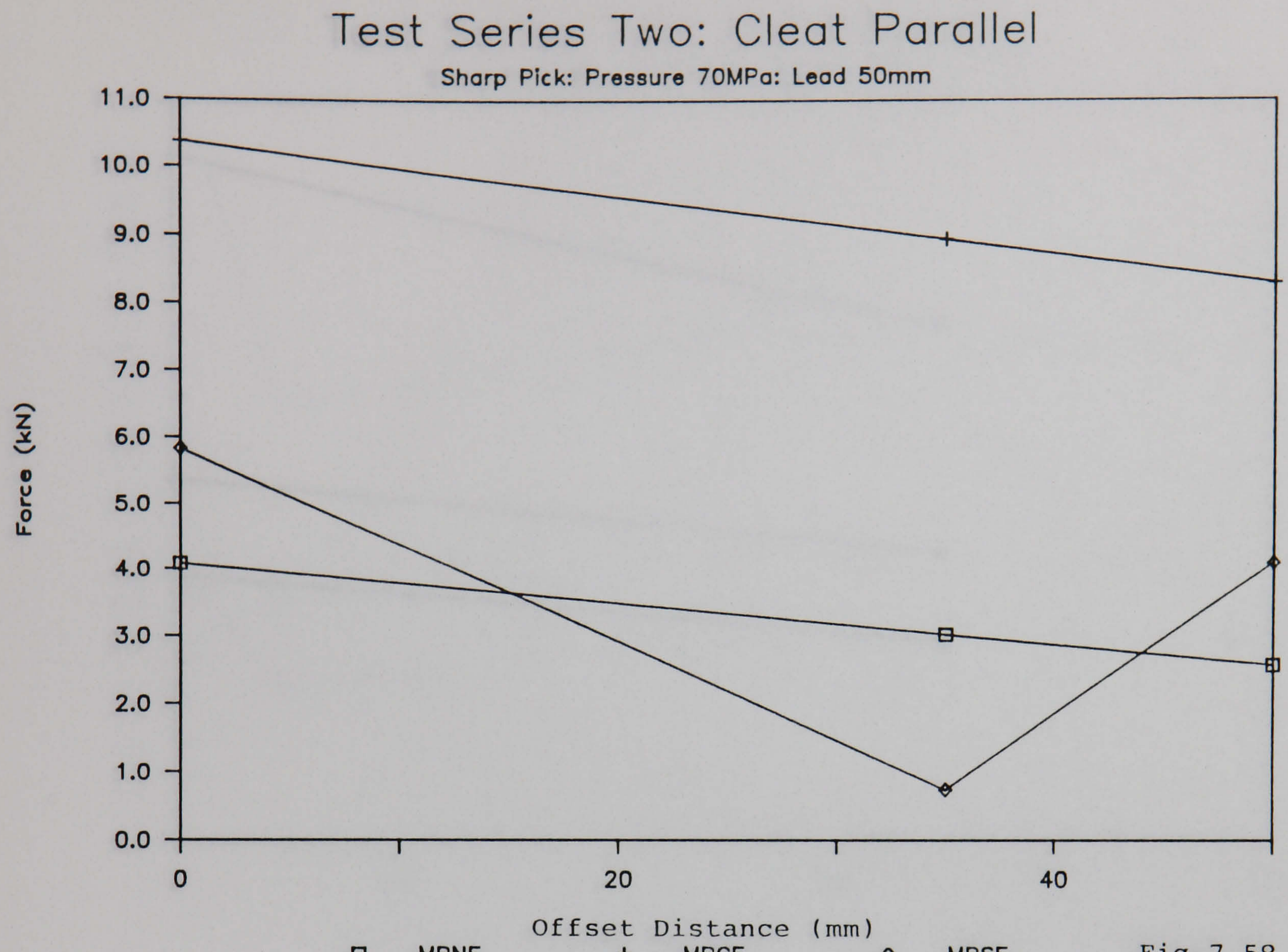


Fig.7.58

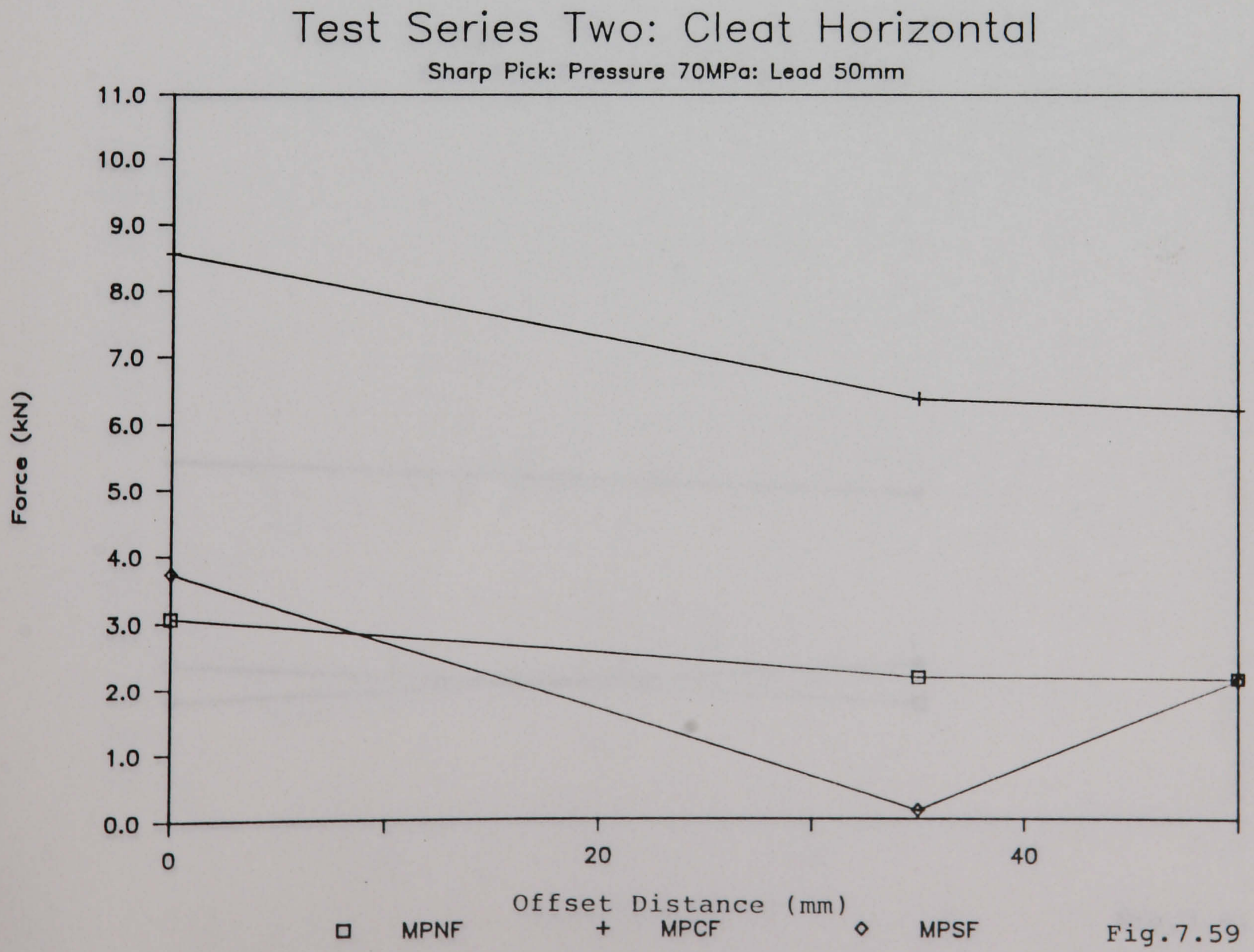


Fig.7.59

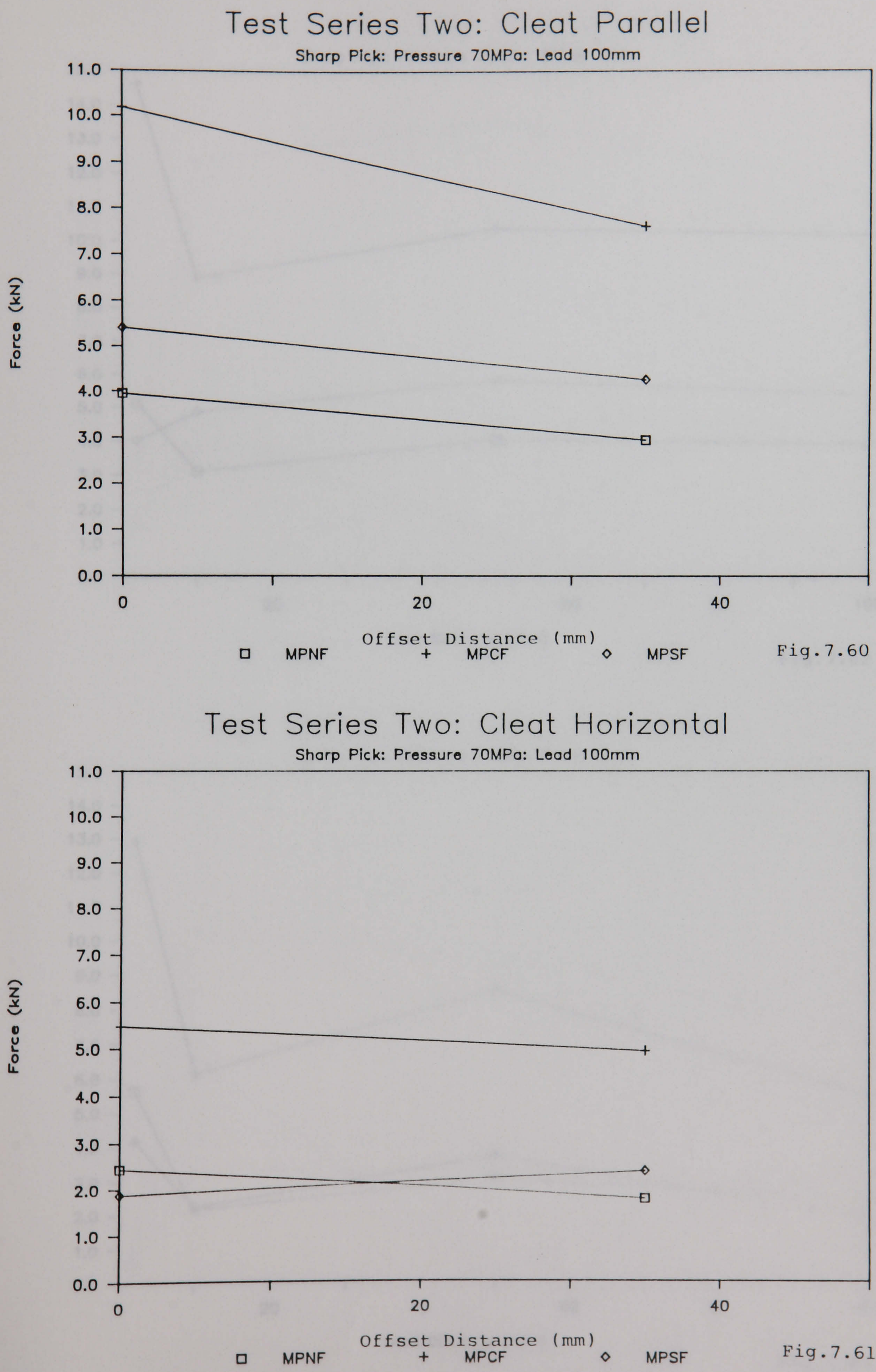


Fig.7.60

Fig.7.61

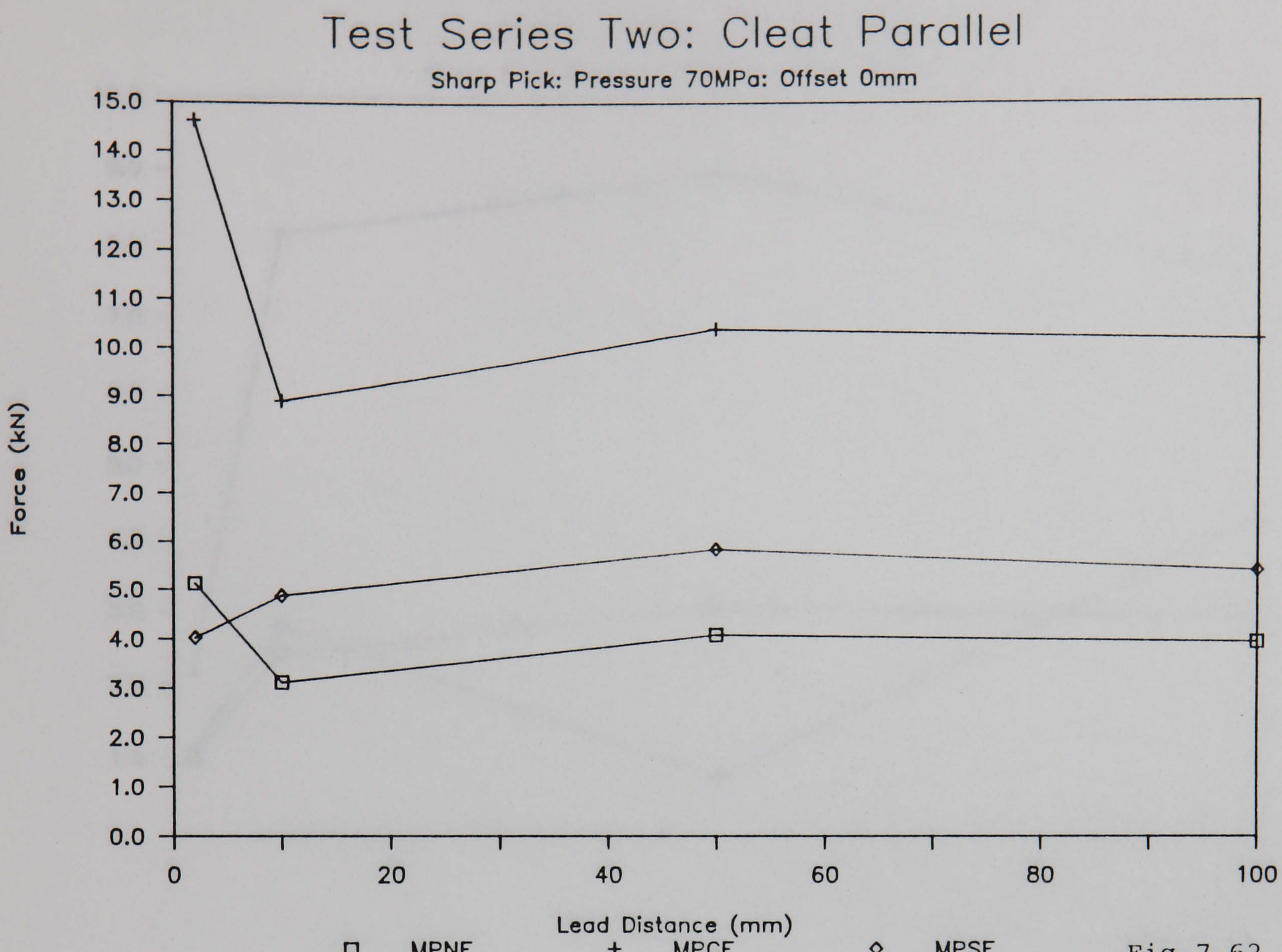


Fig.7.62

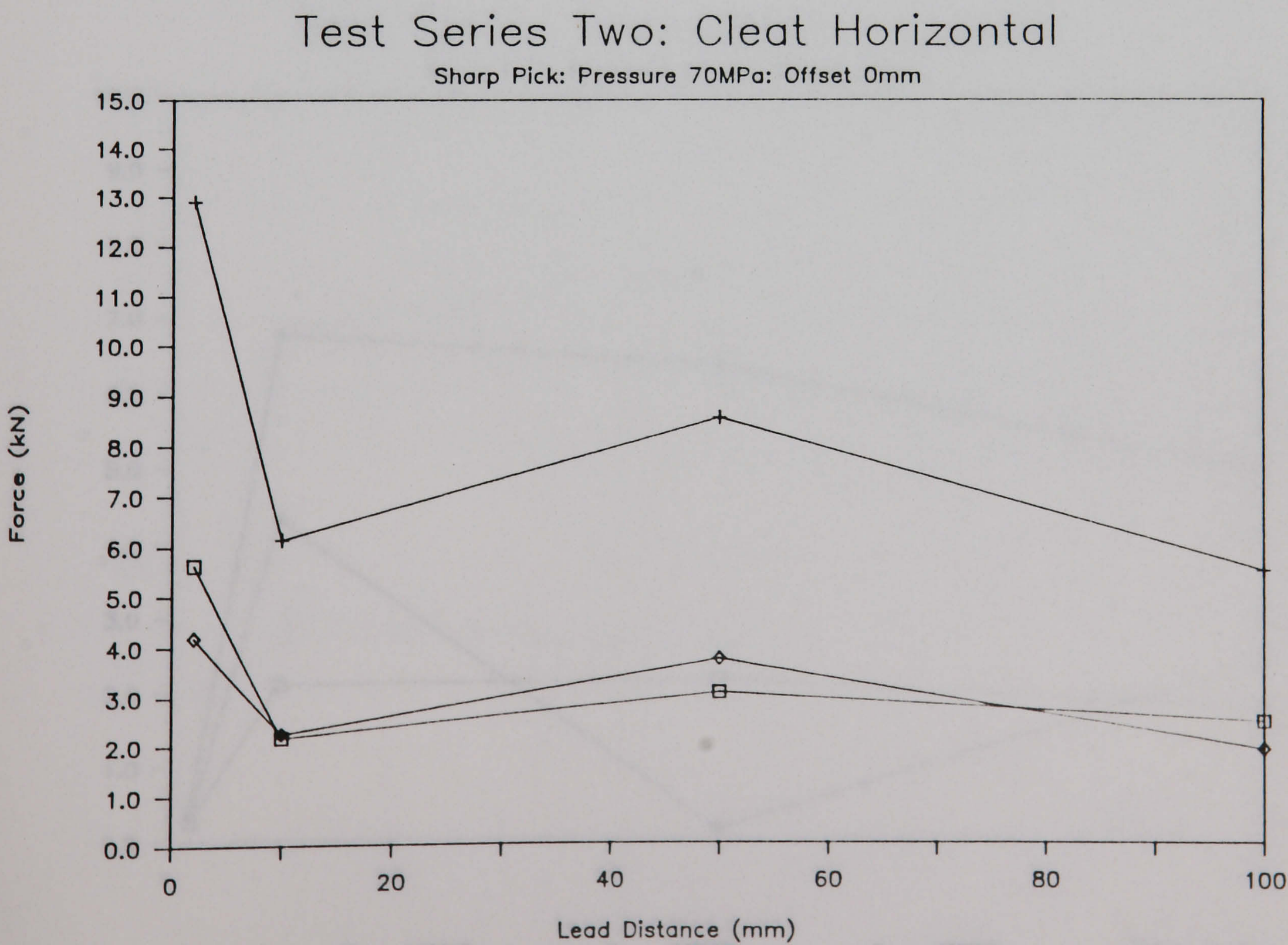


Fig.7.63

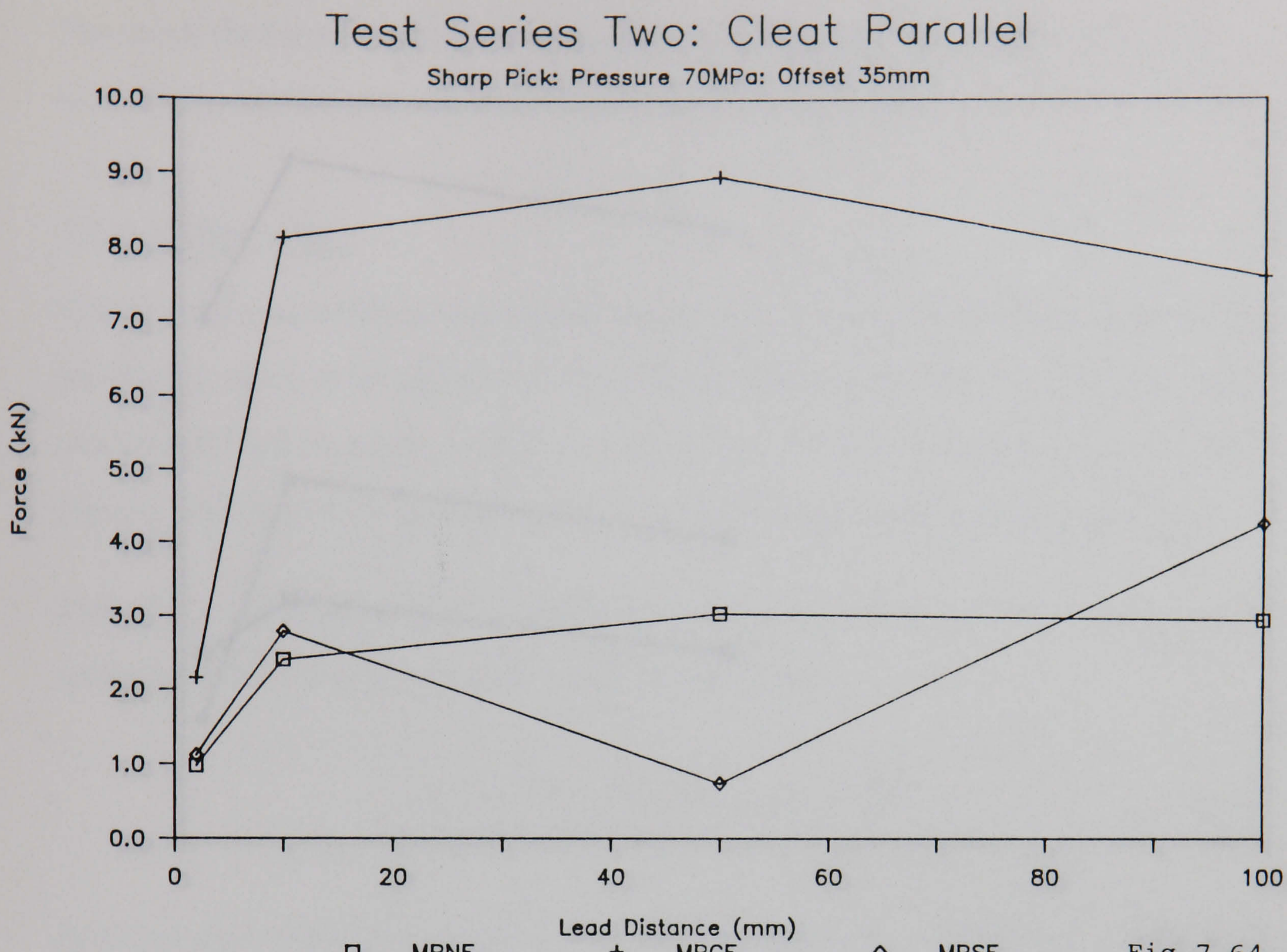


Fig.7.64

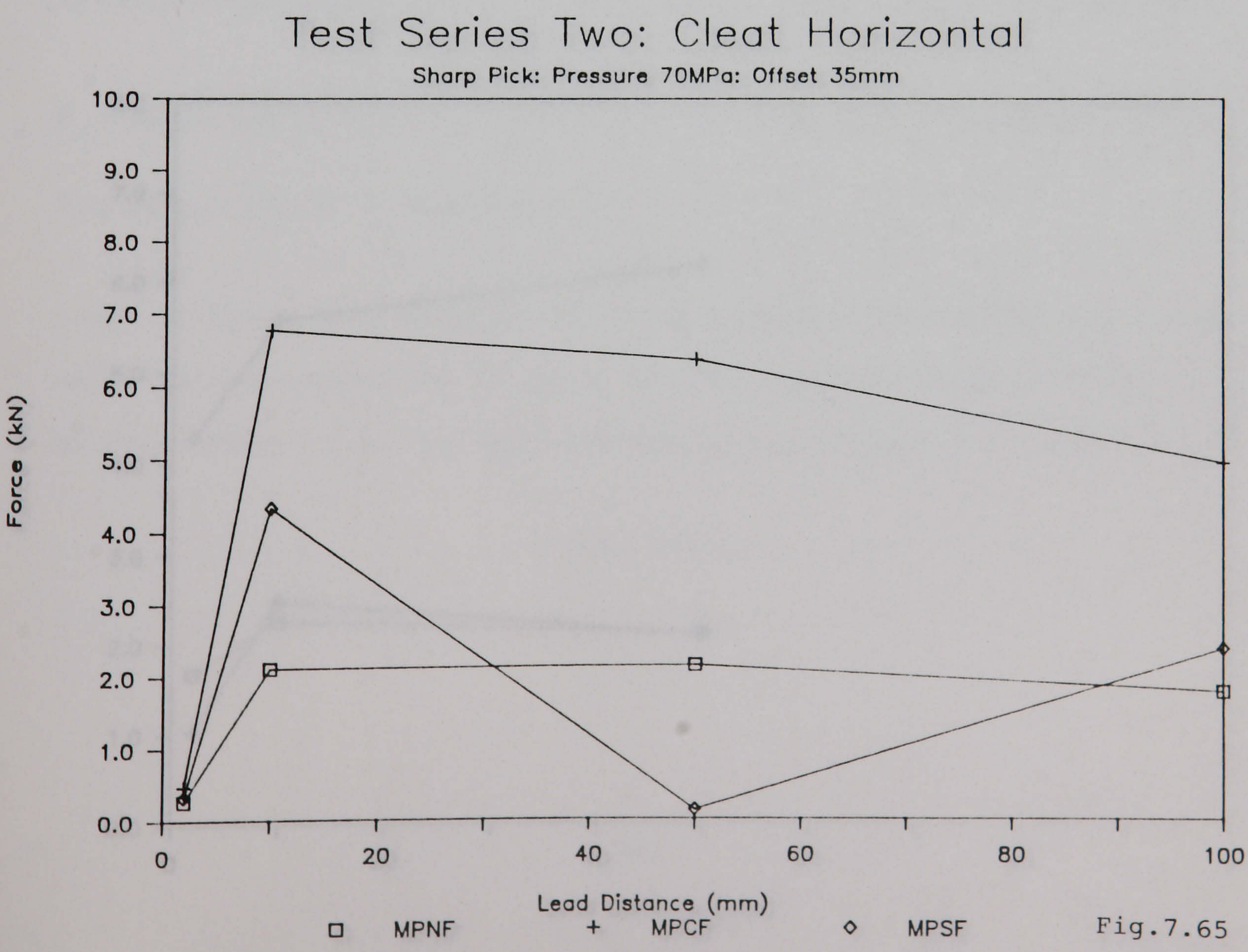


Fig.7.65

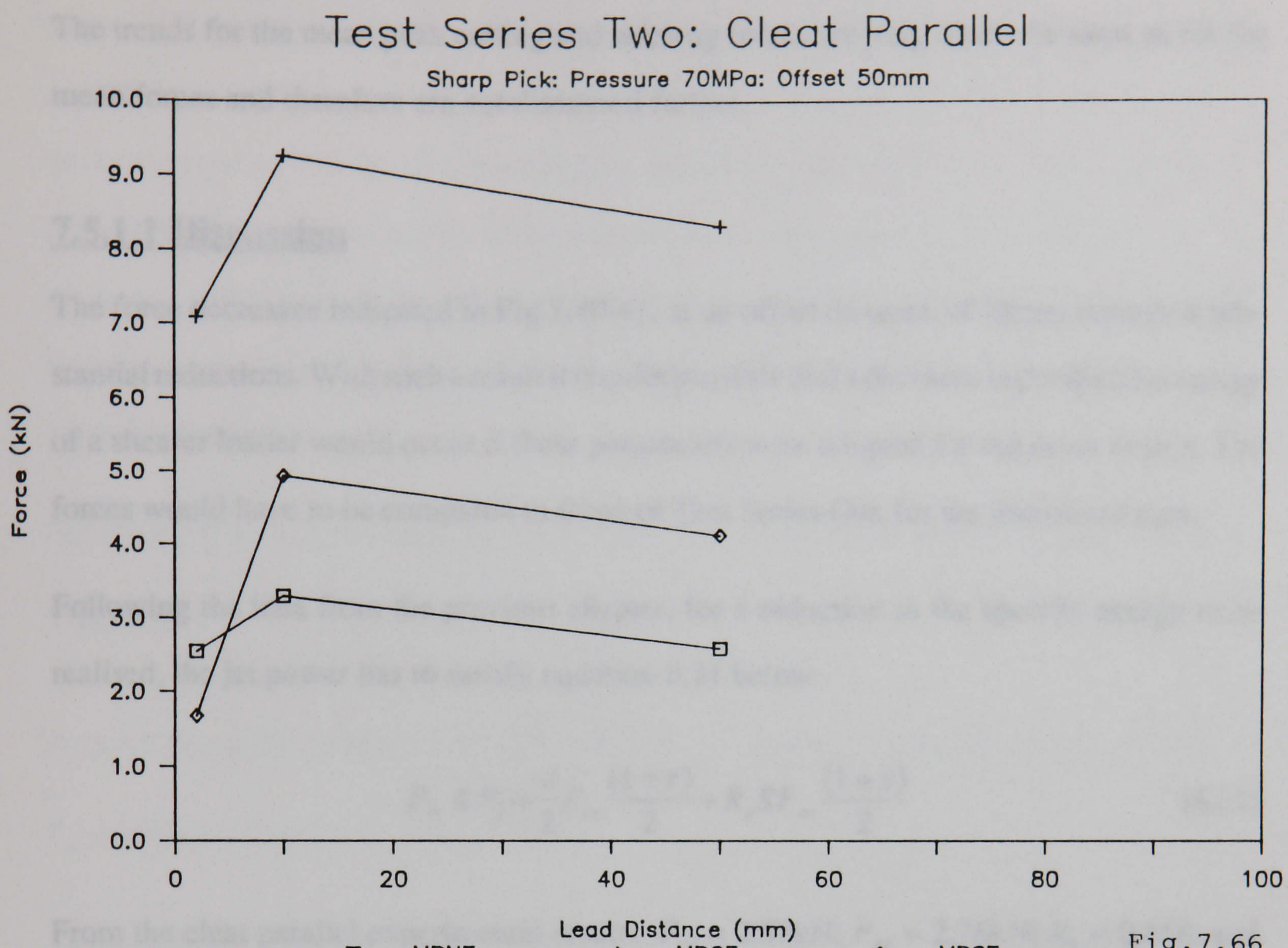


Fig.7.66

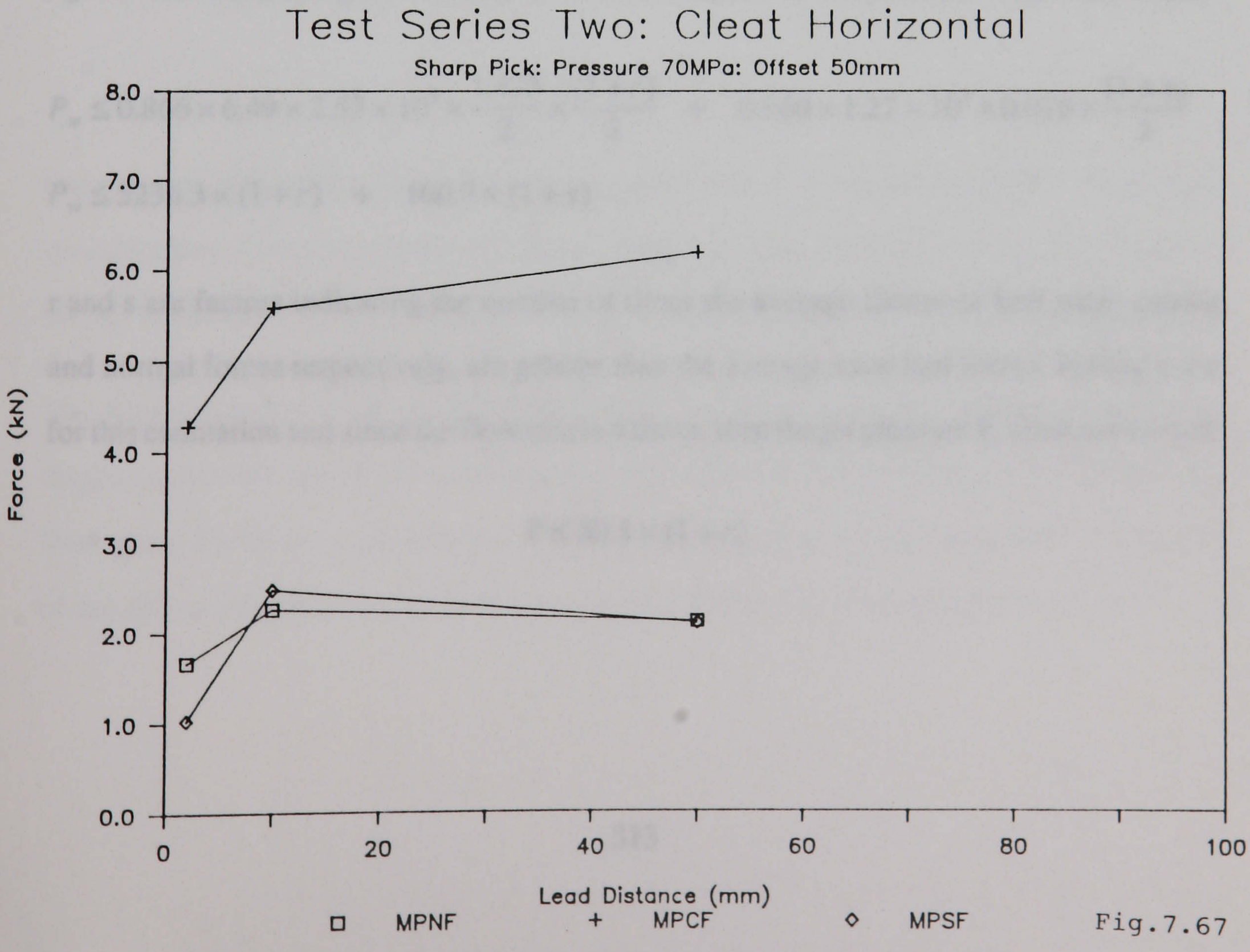


Fig.7.67

The trends for the mean peak cutting and sideway forces are very much the same as for the mean forces and therefore are not discussed further.

7.5.1.1 Discussion

The force decreases indicated in Fig.7.40-41, at an offset distance of 35mm represent substantial reductions. With such a result it is quite possible that a decrease in the specific energy of a shearer loader would occur if these parameters were adopted for the drum design. The forces would have to be compared to those of Test Series One for the unassisted cuts.

Following the idea from the previous chapter, for a reduction in the specific energy to be realised, the jet power has to satisfy equation 6.21 below:

$$P_w \leq R_c w \frac{d}{2} F_{cv} \frac{(1+r)}{2} + R_n S F_{nv} \frac{(1+s)}{2} \qquad (6.21)$$

From the cleat parallel experimental results: F_{cv} = 2.53kN; F_{nv} = 2.76kN; R_c = 0.866; and R_n = 0.960. Also, using d= 1.473m; w = 2 × π × 62/60 = 6.49rad/sec; S = 0.076m/s, then,

$$P_w \leq 0.866 \times 6.49 \times 2.53 \times 10^3 \times \frac{1.473}{2} \times \frac{(1+r)}{2} \quad + \quad 0.960 \times 1.27 \times 10^3 \times 0.076 \times \frac{(1+s)}{2}$$

$$P_w \leq 5236.3 \times (1+r) \quad + \quad 100.7 \times (1+s)$$

r and s are factors indicating the number of times the average clearance kerf mean cutting and normal forces respectively, are greater than the average vane tool forces. Putting s = r, for this estimation and since the flow rate is 4 l/min, then the jet pressure P, must not exceed:

$$P \leq 80.1 \times (1+r)$$

For r = 1, P≤160.2MPa, which at 4.54m/s would give a predicted jet penetration of 37.7mm. At 70MPa and 1.34m/s traverse speed the predicted penetration is 24.2mm, and this would be the penetration that would obtain the necessary force reductions. Thus, from a theoretical appraisal the specific energy could be reduced (since the required jet penetration could be achieved) with jet assistance and the jet operating at an offset distance of 35mm and 2mm lead distance. However, the practical consideration of generating the high pressure for the water jet remains.

For the cleat horizontal mode: F_{cv} = 2.69kN; F_{nv} = 1.23kN; R_c = 0.985; and R_n = 0.992.

Therefore,

$$P_w \leq 0.970 \times 6.49 \times 1.34 \times 10^3 \times \frac{1.473}{2} \times \frac{(1+r)}{2} \quad + \quad 0.994 \times 1.75 \times 10^3 \times 0.076 \times \frac{(1+s)}{2}$$

$$P_w \leq 3106.4 \times (1+r) \quad + \quad 66.1 \times (1+s)$$

Again putting s = r, and the flow rate is 4 l/min, thus the jet pressure must satisfy the conditions below:

$$P \leq 47.6 \times (1+r)$$

For r = 1, P≤191.4MPa. From Cooley's equation and at a cutting speed of 4.54m/s, one would expect the jet to penetrate 47.3mm. Therefore, with the cleat horizontal the specific energy is predicted to decrease with jet assistance at the correct operating configuration.

The breakout patterns are not available but to give an idea of what could be expected a diagrammatic illustration of the operating configuration for the test series is given in Fig.7.68. During cut 2B, the jet at an offset of 35mm would penetrate the coal at point X in the path of cut 1B, to a depth X' depending upon the jet pressure. Similarly, the previous cut 2A

Operational Parameters in Test Series Two

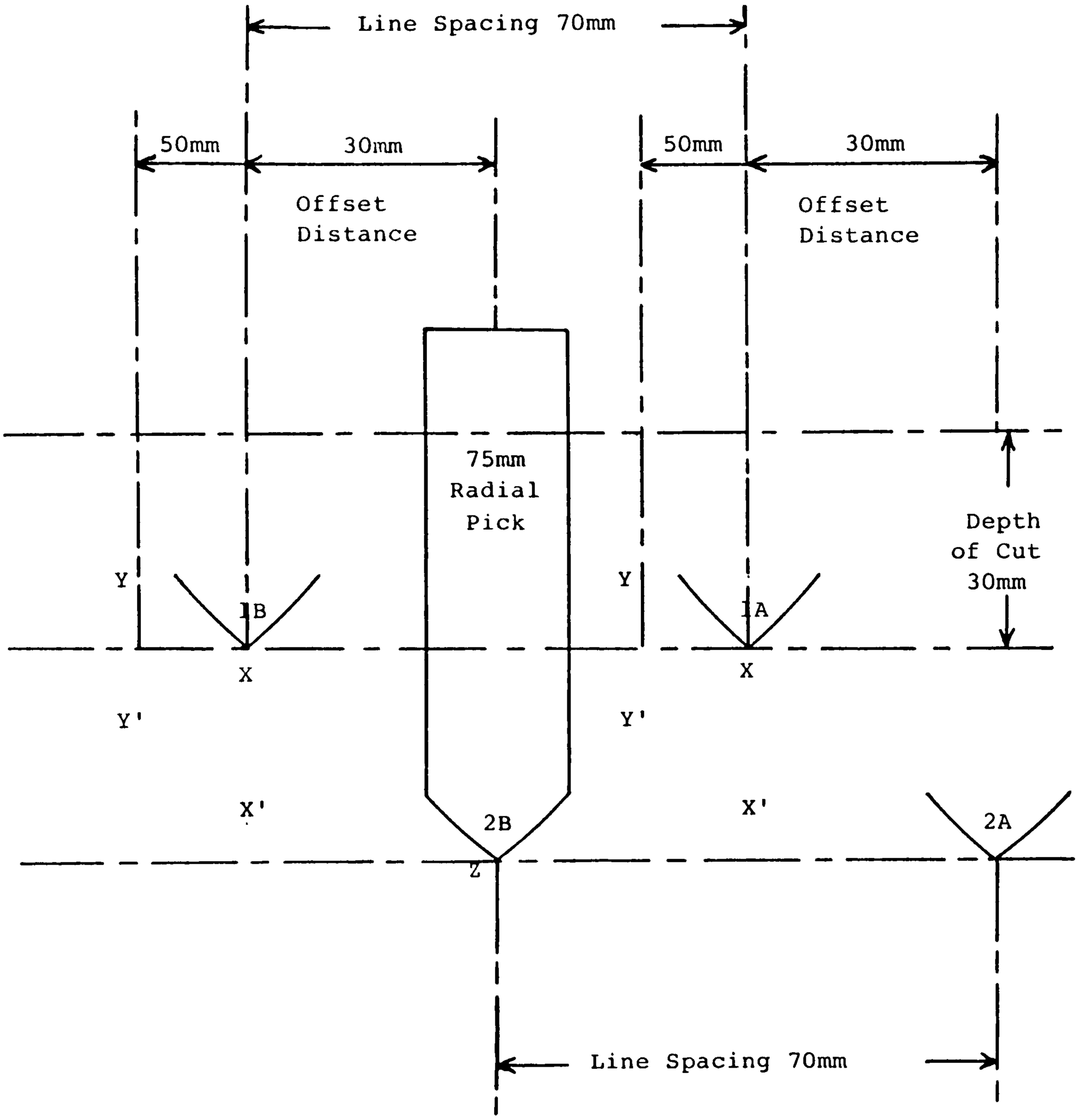


Fig.7.68

would have received assistance from the jet penetrating at 1A. In this case one would expect the breakout to be symmetrical about the tool at 2B say. Possibly the breakout would extend from Z to X', or from a point on either side of the tool to X'.

For the 50mm offset distance, the jet would penetrate the coal at some point Y. But one would expect Y to be above X, since there would be a ridge of coal inbetween the lines of cut. The jet, at the same pressure as before, would penetrate the same distance but to a depth Y' say. From the geometry of the situation one would expect the breakout to be asymetrical about the tool at 2B and extend from Z to Y', or from some point at the side of the tool to Y', giving a larger ridge of coal inbetween the lines of cut than previously with an offset distance of 35mm.

In both cases the cutting forces are reduced with the offset rather than running the jet in-line with the tool and from the diagram this may be due to the jet offering relief to the unrelieved side of the cut. The influence of the lead distance is not as clear.

7.5.1.2 Conclusions

The best operating conditions are at a 35mm offset distance and a lead distance of 2mm. Generally, for a line spacing of 70mm and depth of cut of 30mm, an offset distance of 35mm seems the best at the other lead distances also i.e. an offset distance midway between line spacings.

Using the optimum conditions it appears that the specific energy of a shearer loader could be reduced. The appraisal is very approximate but nevertheless it is quite auspicious and much more promising than that carried out in chapter six.

The effect of the lead distance depends upon how it is combined with the offset and this is shown by the significant interaction terms between lead and offset distances in the analysis of variance tables. At a zero offset it is better to have a 10mm lead distance. At the 35mm and 50mm offsets a 2mm lead distance is suggested.

Similar trends are observed in both the cleat orientations. The coal is easier to cut when the cleat is horizontal at any set of parameters investigated in this series and this is confirmed by the highly significant cleat terms in the analysis of variance tables.

7.5.2 Sieve Analysis Results

Fig.7.69-72, show the size distributions with the lead distance as the constant parameter and the offset distance varying. All four charts show that an offset distance of 35mm gives least fines, viz. 5.2%, 3.2%, 4.8% and 5.6% of the total at 2mm, 10mm, 50mm and 100mm lead distances respectively. The optimum treatment appears to be at an offset distance of 35mm and a lead distance of 10mm: the fines production is only 3.2%.

Fig.7.73-75, illustrate the same results but with the offset distance as the parameter and the lead distance variable. From the fines point of view, the best set of operating conditions are those at an offset distance of 35mm at all the lead distances - Fig.7.74 showing the least fines. Again, the 10mm lead distance yields the minimum fines content.

The distributions were fitted to the Rosin-Rammler equation and the median particle size calculated. Fig.7.76 depicts the median particle sizes against the offset distance. The curves suggest an optimum at the 35mm point which is consistent with the previous conclusions. The same results are plotted against lead distance in Fig.7.77. An optimum lead distance of 10mm is indicated by the graphs.

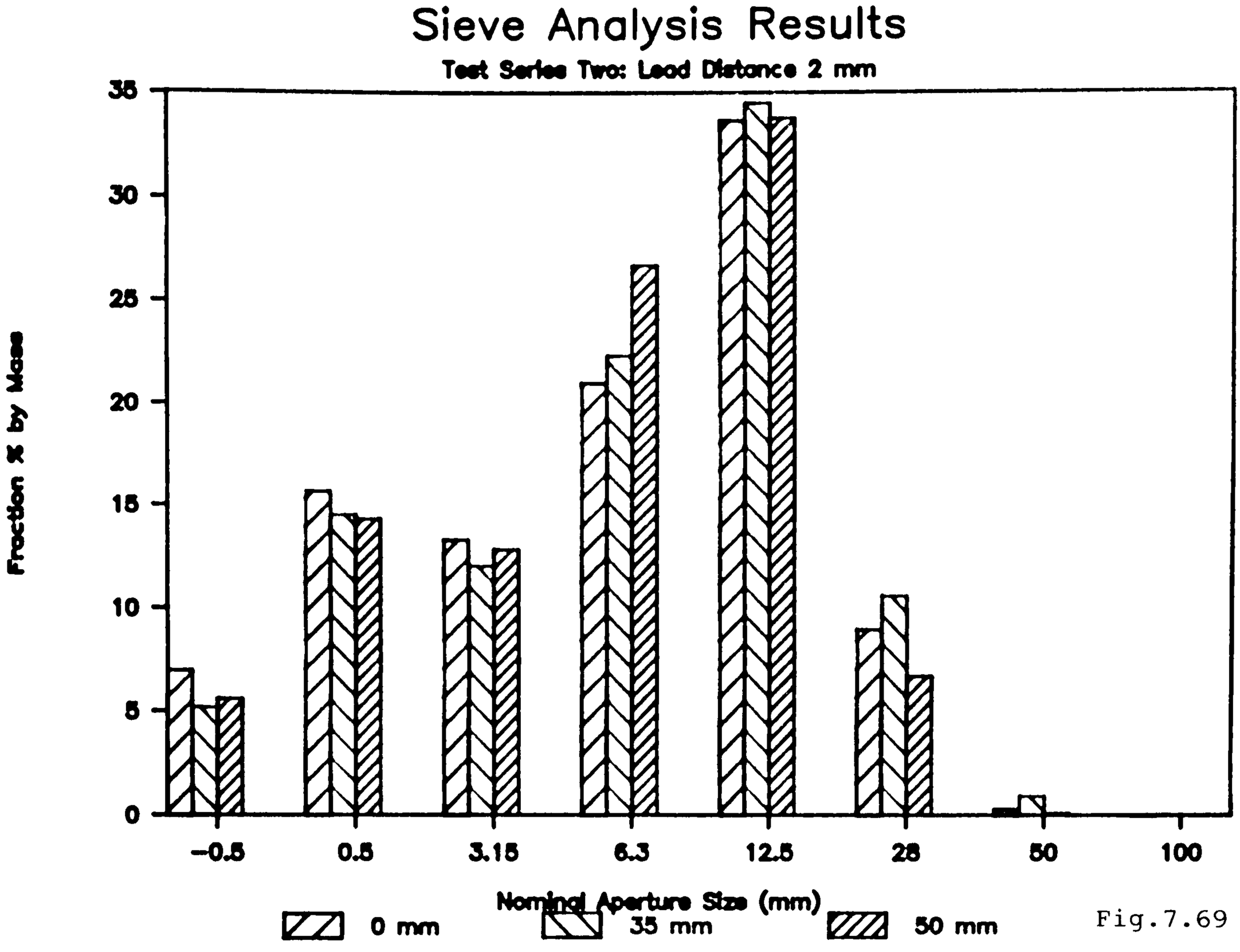


Fig.7.69

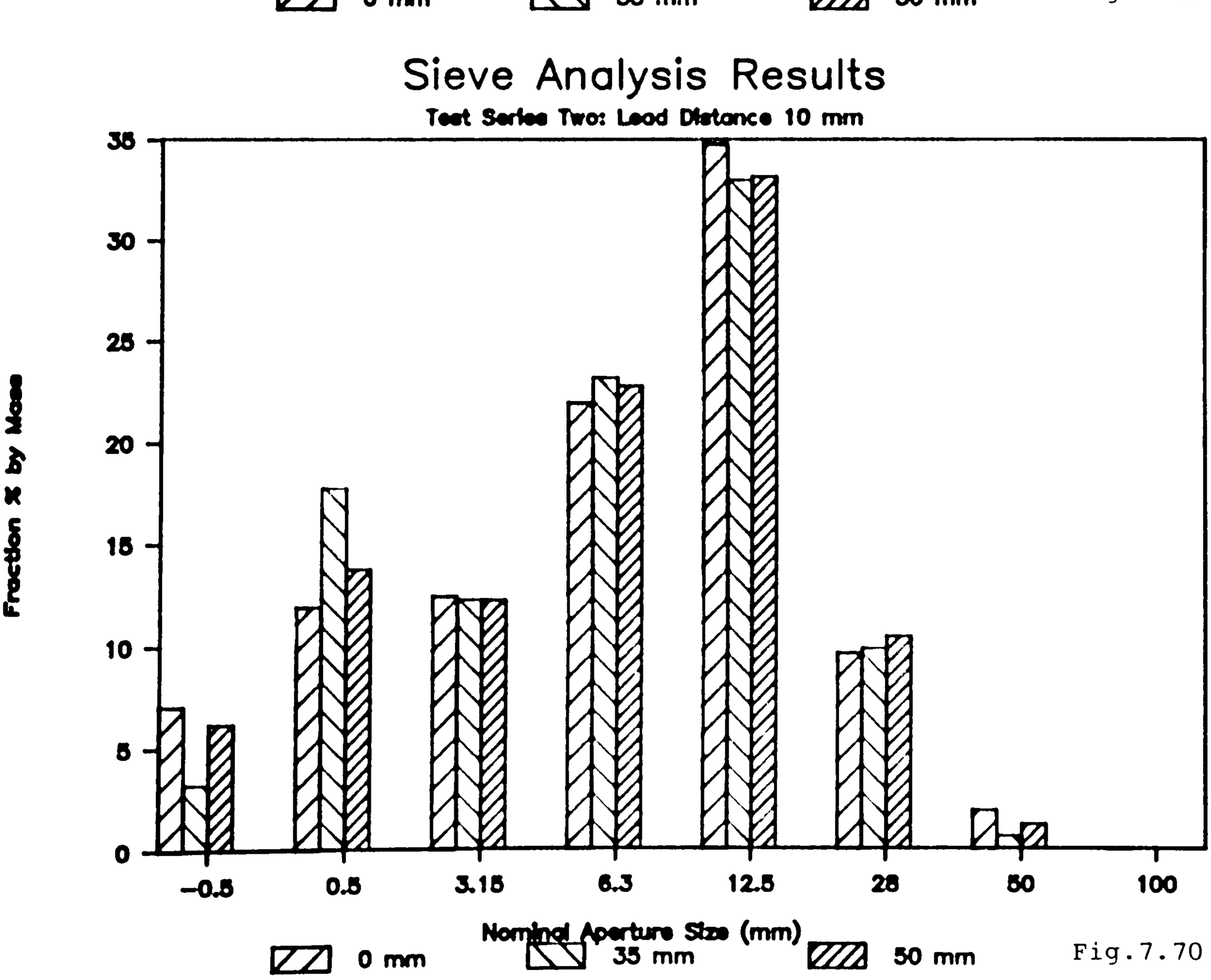


Fig.7.70

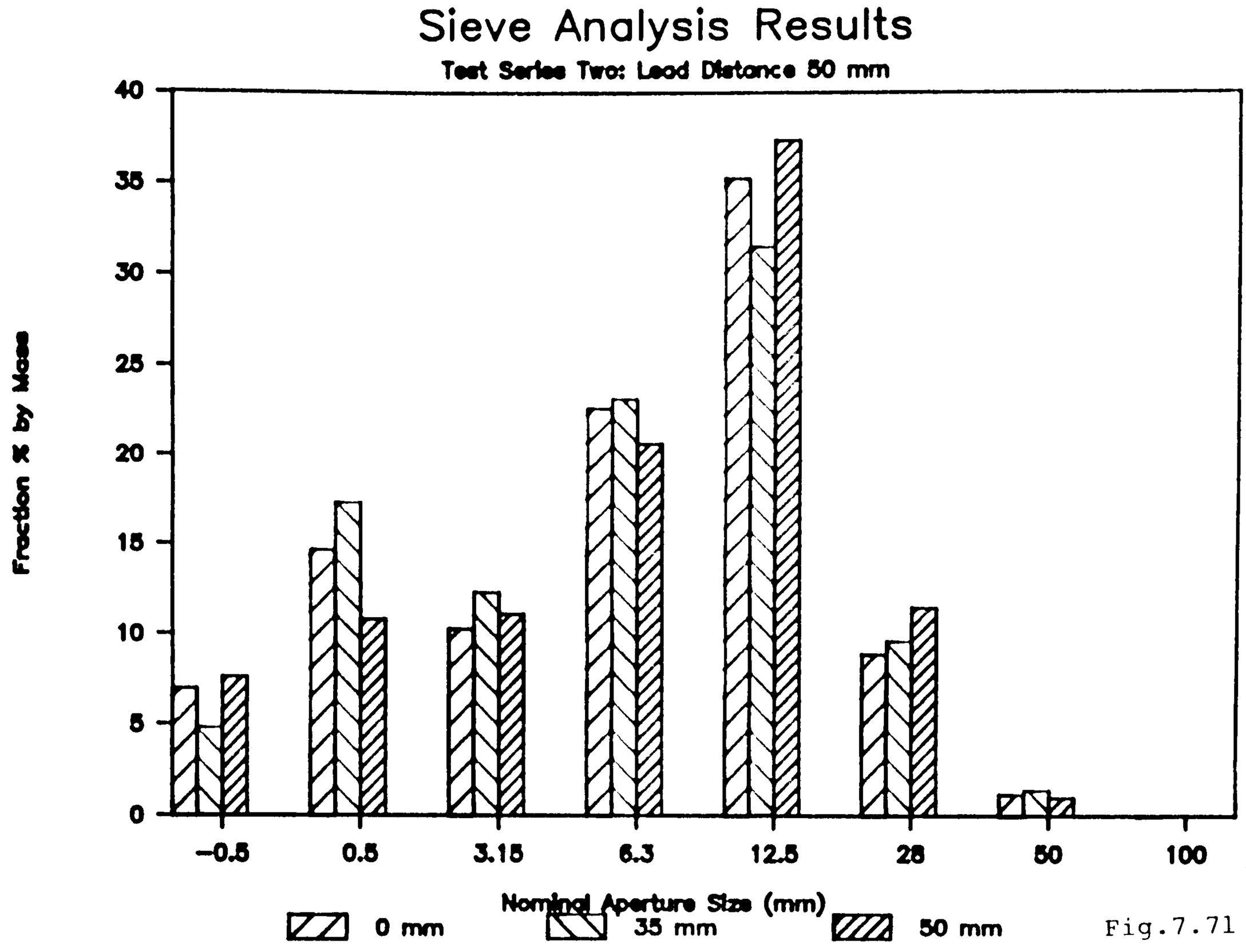


Fig.7.71

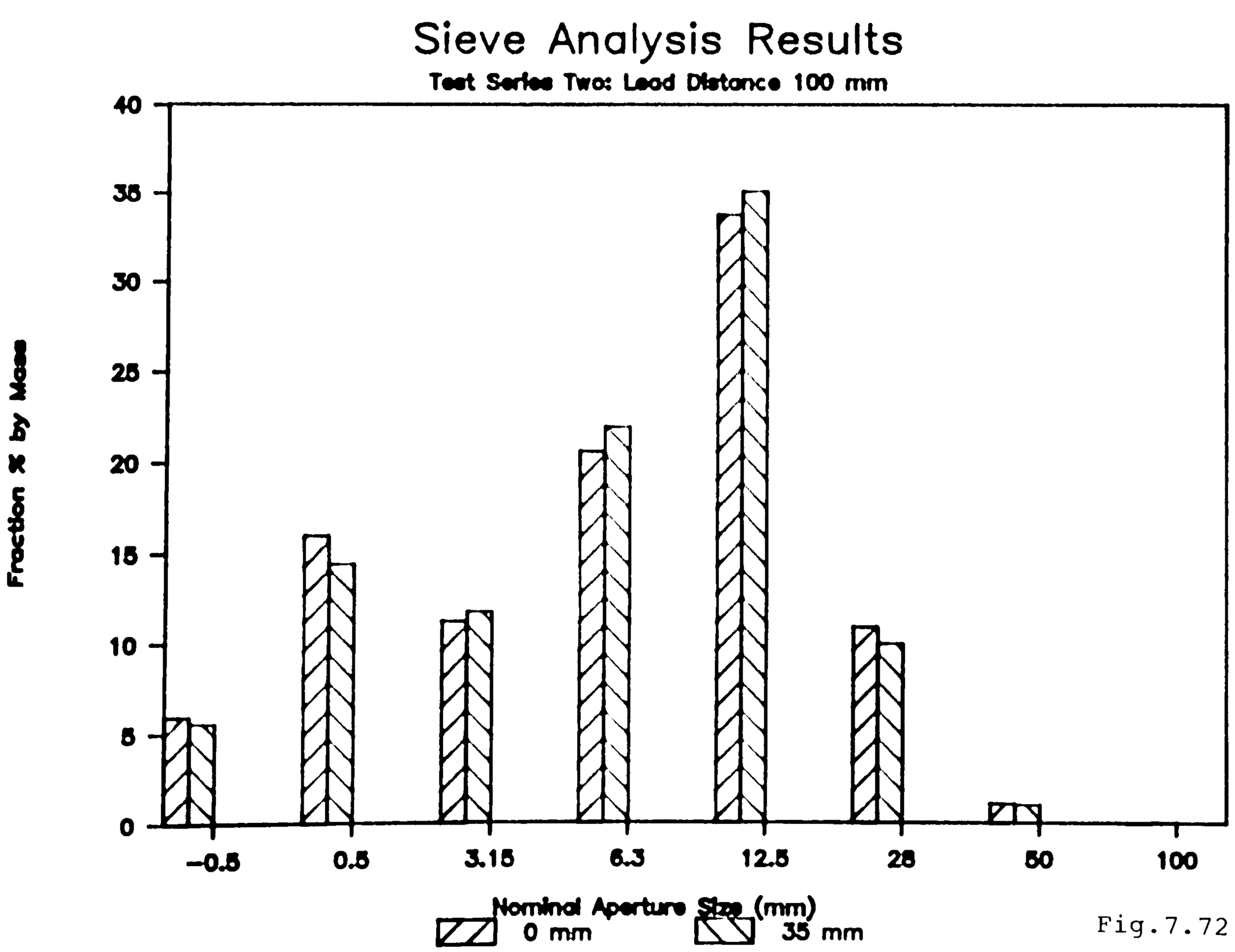


Fig.7.72

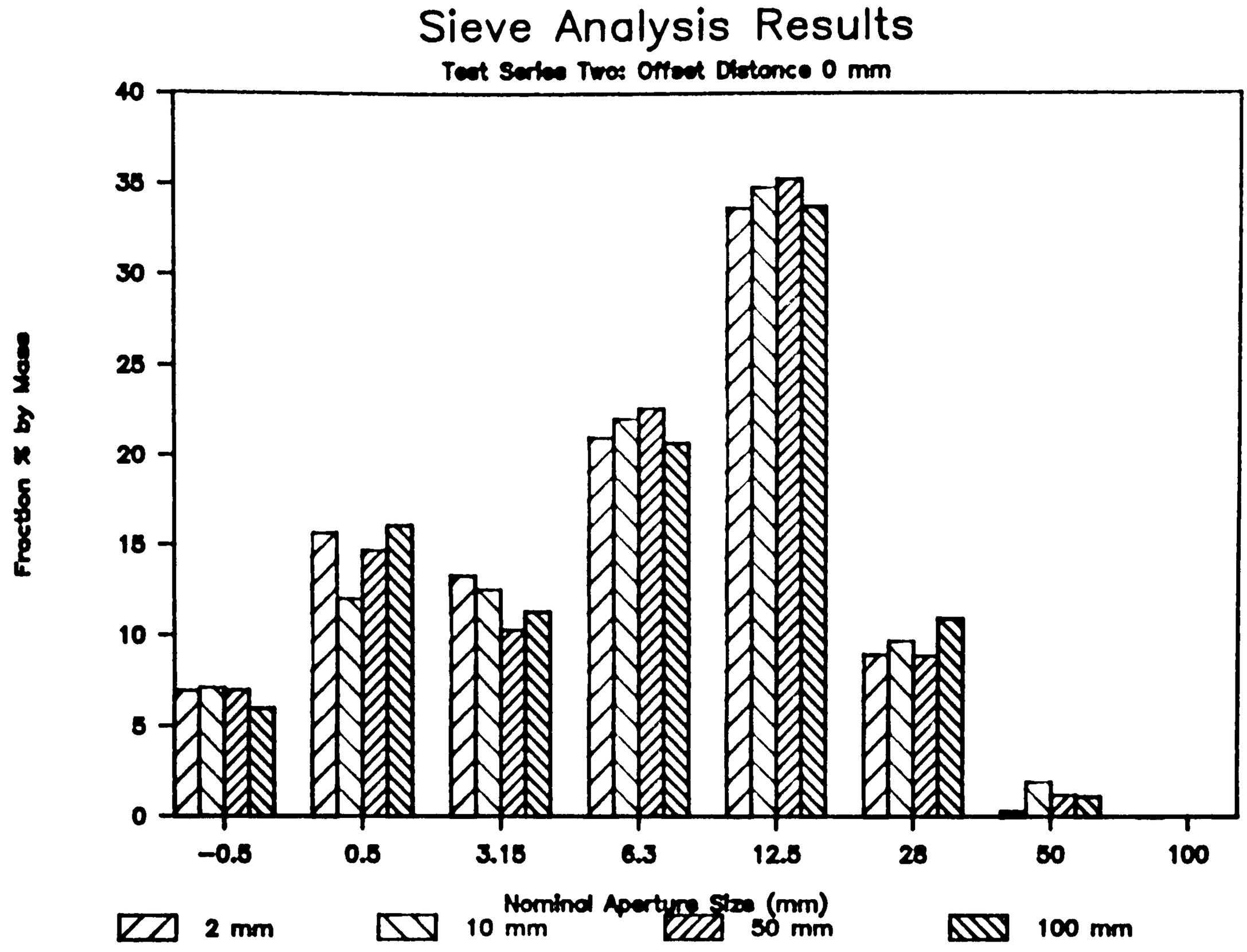


Fig.7.73

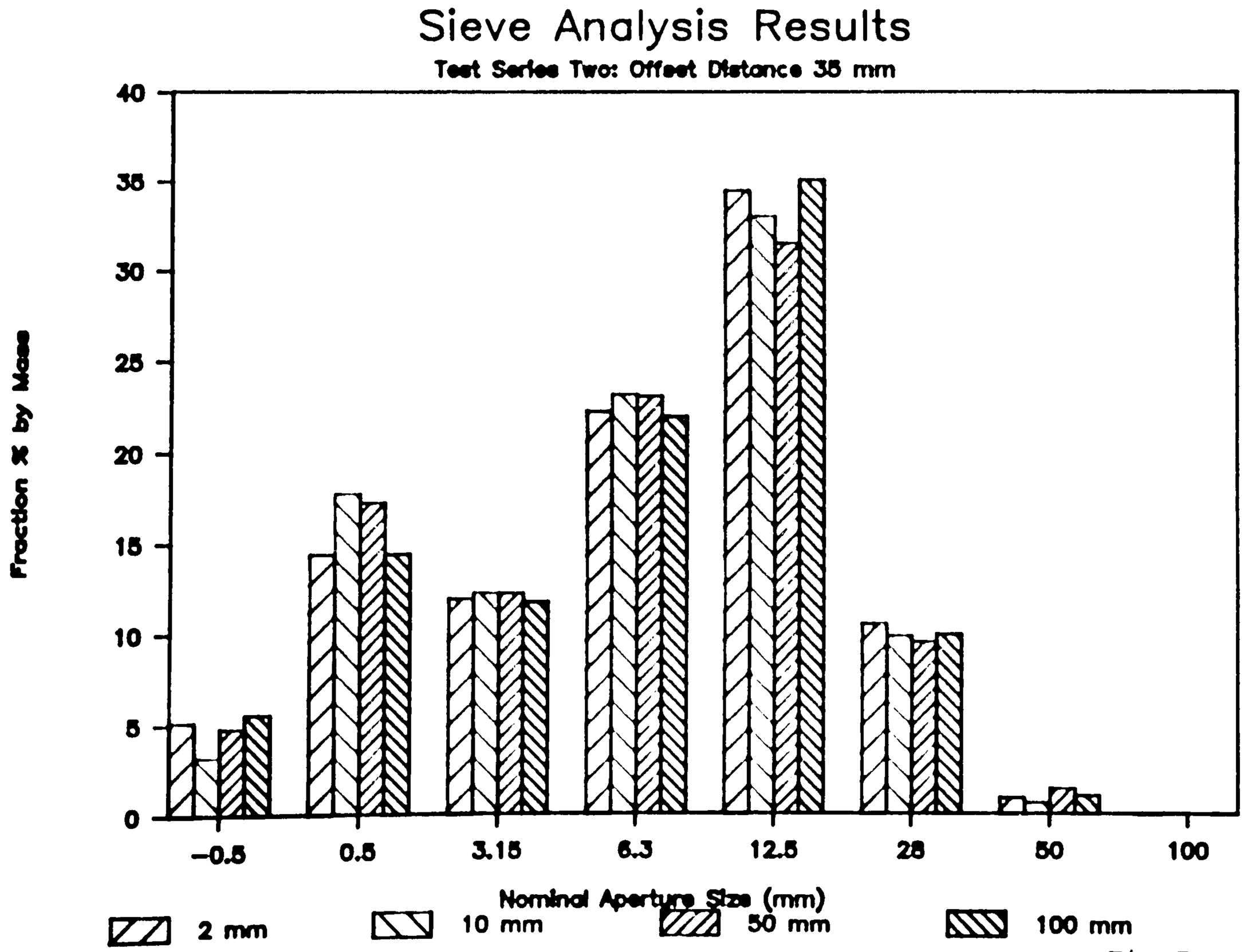


Fig.7.74

Sieve Analysis Results

Test Series Two: Offset Distance 50mm

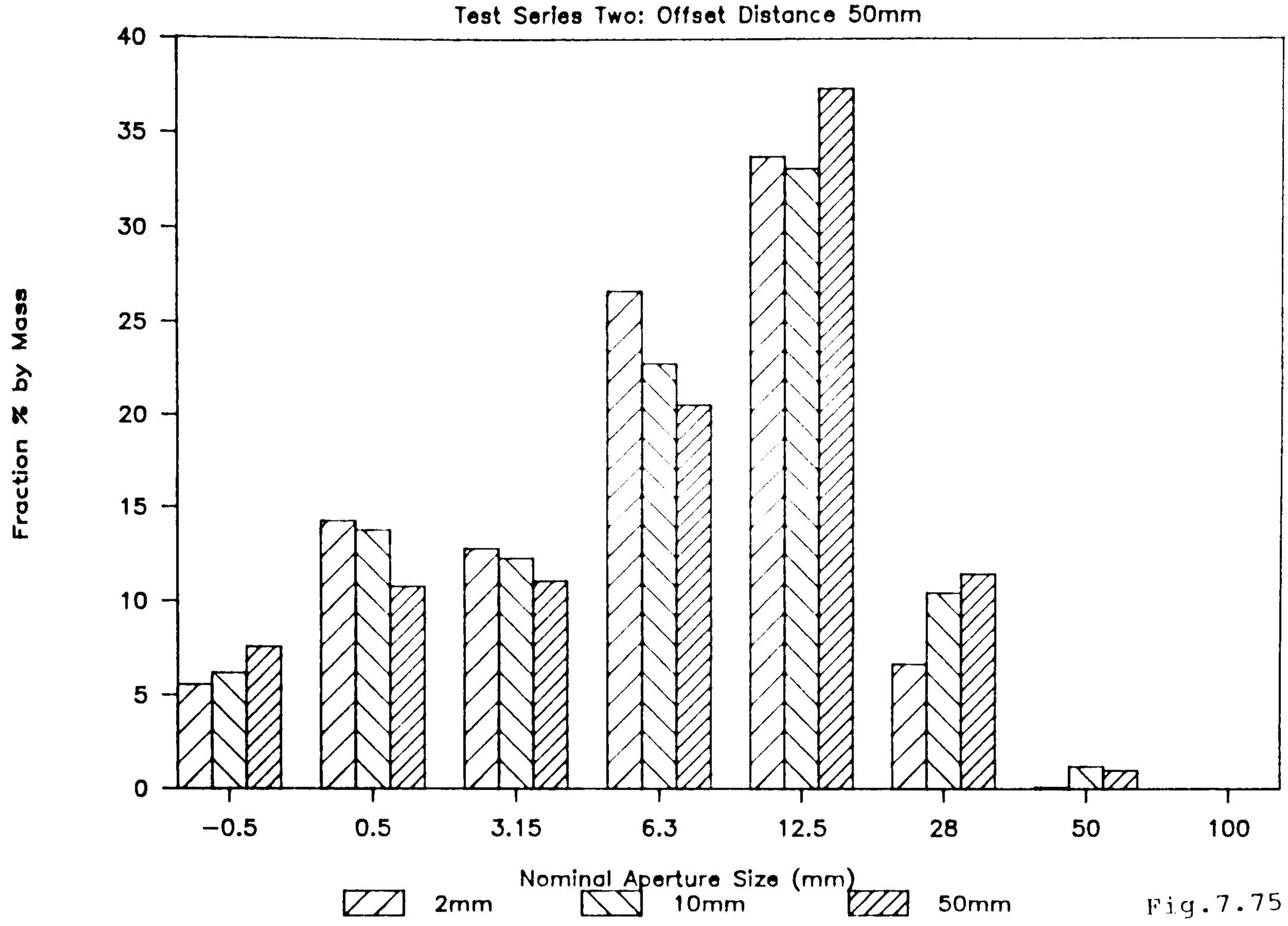


Fig.7.75

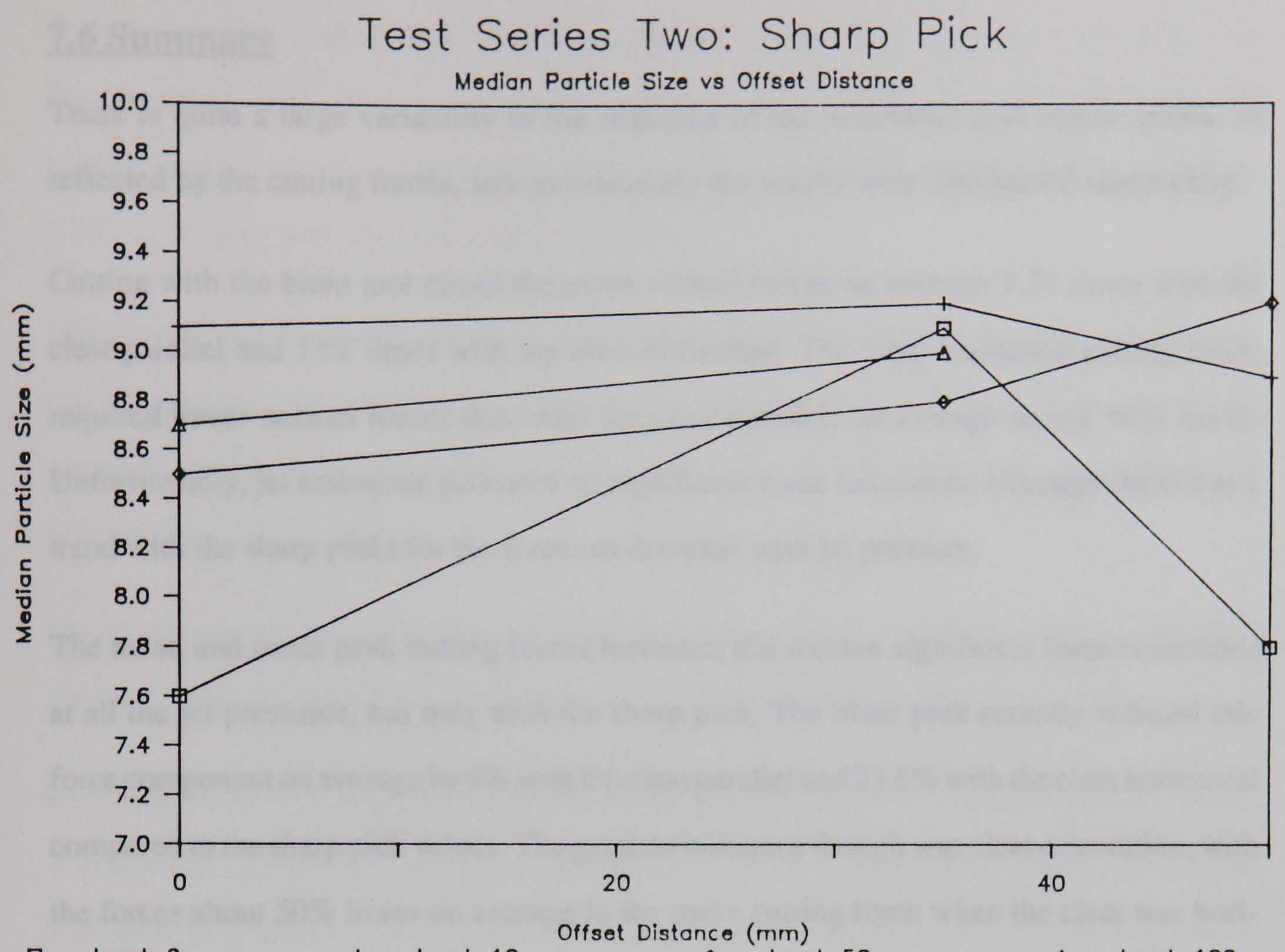


Fig.7.76

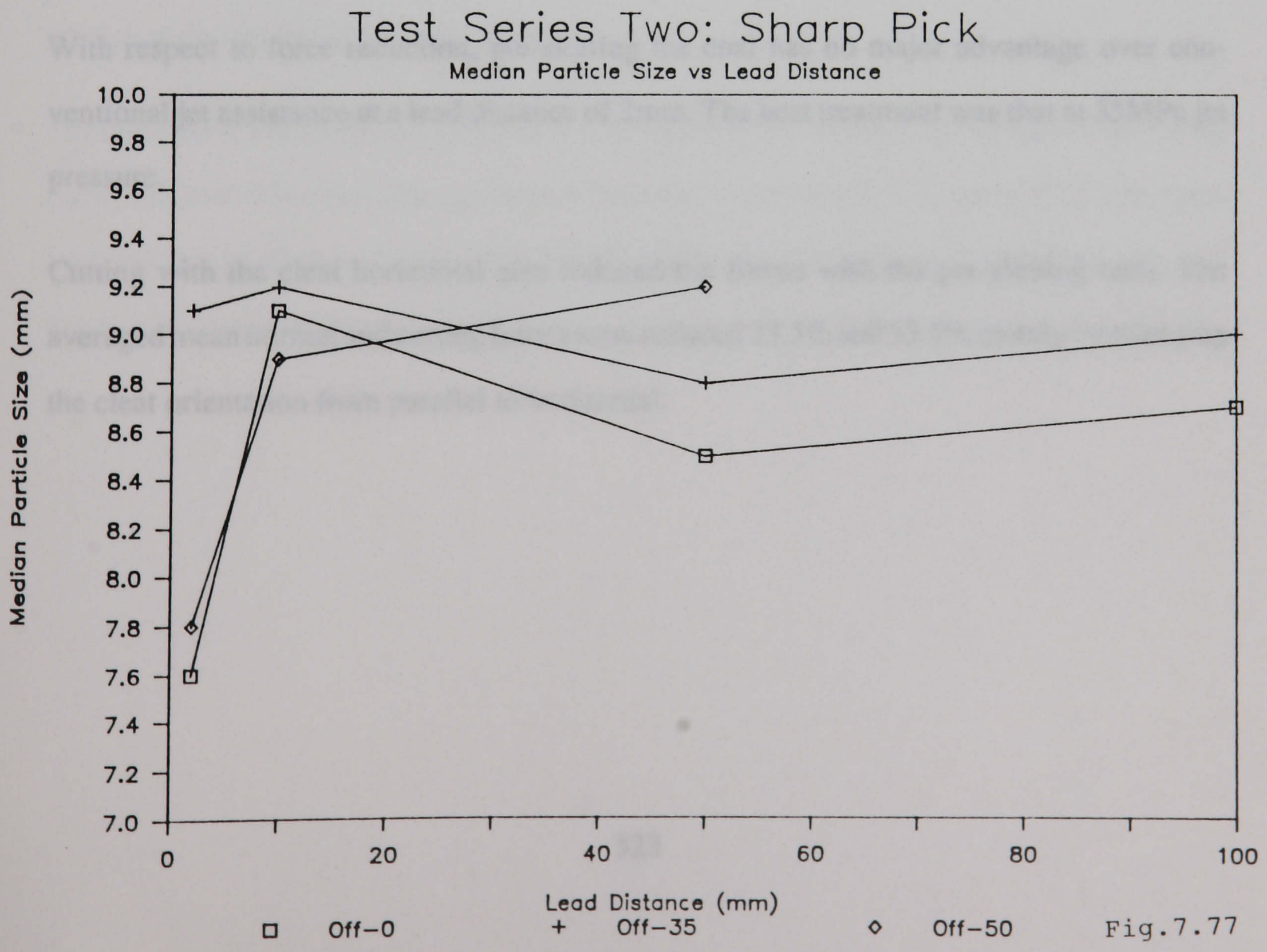


Fig.7.77

Specific energy increased linearly with jet assistance and did not indicate a reduction over the unassisted value. With pre-slotting, the 35MPa pressure treatment reduced the specific energy slightly with the sharp pick. Overall, the pre-slotting specific energies were around 8.3% lower than with conventional jet assistance.

Despite the poor force reductions and influence on specific energy, jet assistance did reduce the fines make at all pressures and including the blunt tool. The 35MPa pressure treatment appeared the best with fines reductions of 36.7% and 35.0% for the sharp and blunt tool respectively.

Pre-slotting the coal also decreased the fines and again with the 35MPa pressure jet yielding the best result at a 44.9% reduction and a small increase in the +28mm size coal.

Test Series Two revealed more promising effects as a consequence of applying jet assistance. The optimum position of the jet is at a lead distance of 2mm and an offset distance of 35mm. This gave the greatest force reductions such that even the specific energy of a shearer loader is anticipated to decrease compared to dry cutting. However, the pressures involved would present technical and safety problems.

The fines make was quite low. Least fines were obtained when the offset distance was 35mm for all the lead distances. The optimum treatment was at an offset distance of 35mm and a lead distance of 10mm, giving only 3.2% fines. The curves of the median particle size also suggest this configuration as the best.

CHAPTER EIGHT

8 DISCUSSION, CONCLUSIONS AND RECOMMENDATIONS

8.1 Discussion

A two dimensional side view of the blunt cutting tool is given in Fig.8.1, and a suggested cutting process is described. The forces exerted on the coal by the tool will not act at one point but over the areas of contact with the coal. The diagram considers the forces to act over four regions. Force A, acts on the part of the tool with a positive rake angle. Force N, acts at point P, where the rake angle is zero. Force B, acts on the negative rake angle part and C, on the wear flat. The friction forces F and G also exist and in the directions shown since one is considering the forces exerted on the coal by the pick not vice versa (they are shown on the inside of the tip for clarity).

The face of the HW tip is ridged and circular with a radius of 23.8mm (further details are given in the appendices) thus there will be some point on the arc, P, where the rake angle is zero to the coal. At this point no frictional force will act but a pure normal force. Hence a major principal force or stress will be exerted on the coal in the direction of travel. Therefore at 45° to this plane, a maximum shear stress, τ, will act on planes PR and PQ. The shear stress along PQ will increase and be enhanced by A, as the tool penetrates the coal. Consequently shear failure would occur along PQ which would be the secondary chip described by Tecen (1982).

The shear stress along PR and the force B, would tend to create a crushed zone in the region of PTS as the pick entered the coal. A normal stress, σ, will be acting at 90° to the plane PR which when large enough will be responsible for creating a large primary chip, say from T to U. This would be the Evans chip for a wedge shape tool. Cleat orientation and bedding planes would complicate the matter since fracture once started usually propagates along

Idealised Mechanism of Coal Fracture with a Radial Pick

Bedding planes are vertical and the cleat parallel or horizontal to the traverse direction.

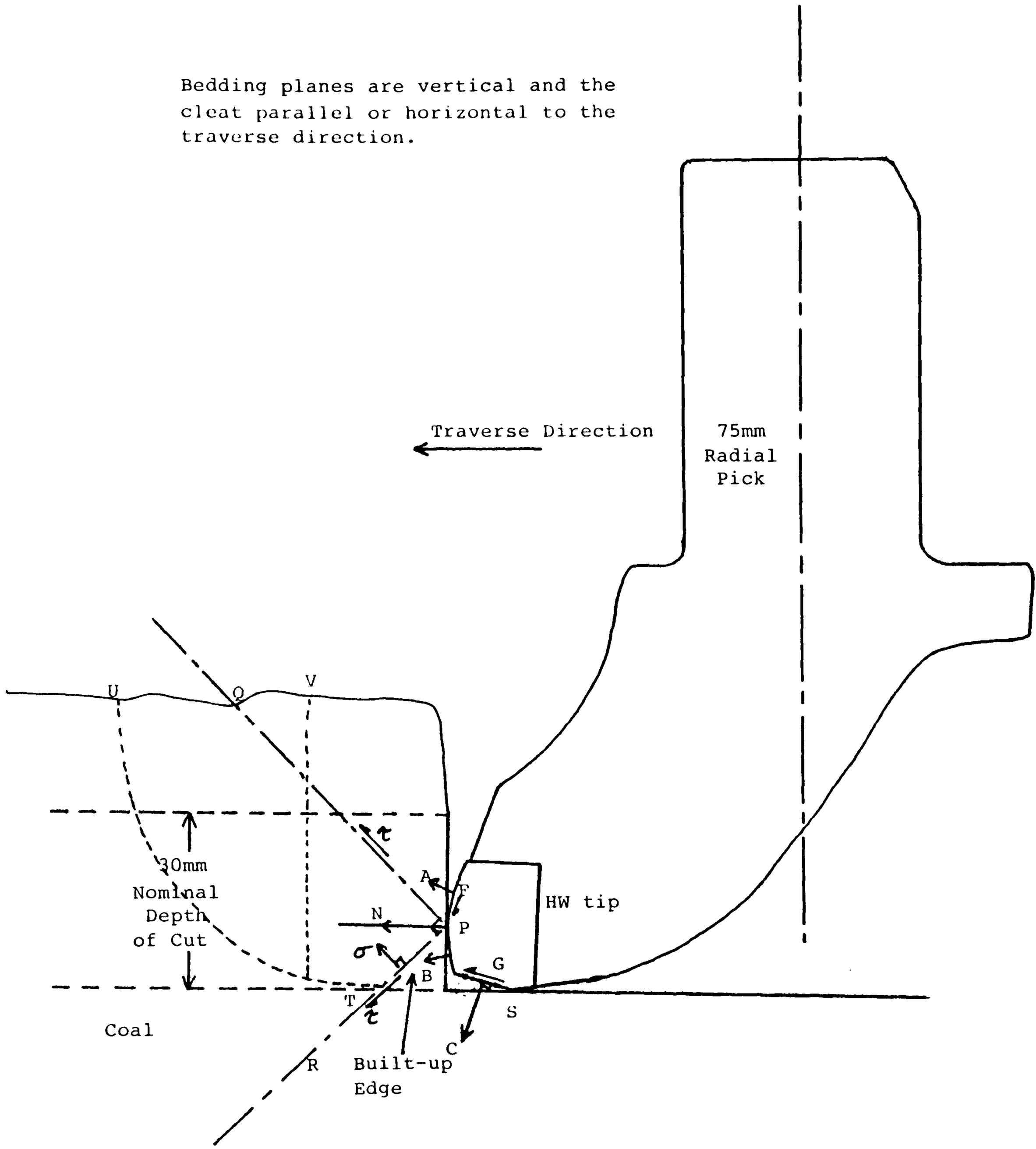


Fig.8.1

these planes and this has been shown to be the case by the breakout patterns discussed earlier and the work of Pomeroy (1963). Therefore, a weak bedding plane might intercept the crack and fracture continue from T to V instead.

The process is idealised, would occur in three dimensions and almost instantaneously since the speed of crack propagation in coal is around 500m/s (O'Dogherty and Burney, 1963); and it would be cyclic.

One can see from this representation how it would be easier to cut with the cleat horizontal and also how the depth of cut and tool geometry would affect the product size. The diagram illustrates that it would be impossible to get large coal with shallow depths of cut and in this respect the trend to use extra heavy duty 105mm reach radial picks on shearer drums is justified (Hurt and McStravick, 1988). If half the depth of cut was taken the crushed zone PTS, would comprise a larger proportion of the final product.

Although theoretical the idea does give credence to the formation of the built-up edge and that one should expect a built-up edge to form as soon as one introduces negative rake on the tool face. With positive rake, wedge shaped tools, neither Evans nor Pomeroy, reported observing this phenomenon. Theoretically, a built-up edge would not form on a wedge shaped tool unless a wear flat developed and the author suggests this is one reason why wedge shaped tools require much smaller forces to cut the coal - no energy is wasted in creating the crushed zone PTS. The size of the crushed zone illustrated is the theoretical maximum.

The author always observed the V-shaped impression of the sharp pick tip and the flat bottomed groove left by the blunt tool in all the treatments and the breakout in the anthracite nearly always propagated 5mm-10mm above the base of the pick suggesting that a built-up edge was forming.

The action of the jet is not very clear from the results. In hard rock, Tecen (1982) and especially Ip (1986), determined zones of penetration of the jet giving a very comprehensive account of the influence of the jet in each zone.

In the coal, the relieved cutting pattern meant that the depth of cut was actually greater than the nominal 30mm and the jet tended to penetrate further than expected during hybrid cutting. Therefore establishing an optimum penetration is quite difficult. However, Fig.8.2, indicates the same diagram but the line JJ depicts the path the jet would travel at a lead distance of 2mm.

During the hybrid tests the 35MPa pressure jet was never observed to have penetrated beneath the pick tip. Also, its measured penetration in intact Erin and anthracite coals at 1.1m/s were 10.7mm and 6.5mm respectively. It seems then that even in broken or loosened coal this jet would not approach the pick tip or the crushed zone and in the Erin coal this treatment gave very good force reductions. Its action then is postulated to be one of debris clearance and weakening the coal for the tool and built-up edge to fracture. In the anthracite it had a similar effect but gave little relief to the blunt tool normal force.

The 70MPa pressure jet gave measured penetrations of 28.2mm in the Erin and 21.3mm (cleat parallel) and 15.8mm (cleat horizontal) in the anthracite during the jet penetration tests. In this case it is quite possible that the built-up edge could be disturbed. Indeed in the Erin, sharp tool treatment and the anthracite (cleat horizontal) blunt tool tests a few places were observed where the jet had penetrated beneath the pick tip. Thus the jet at 70MPa pressure was penetrating in the area of the crushed zone and pick tip. Therefore its effect would be to flush the broken coal away from the pick but also disturb the built-up edge and inhibit cutting somewhat, but still offer relief to the base of the pick and thereby reduce the

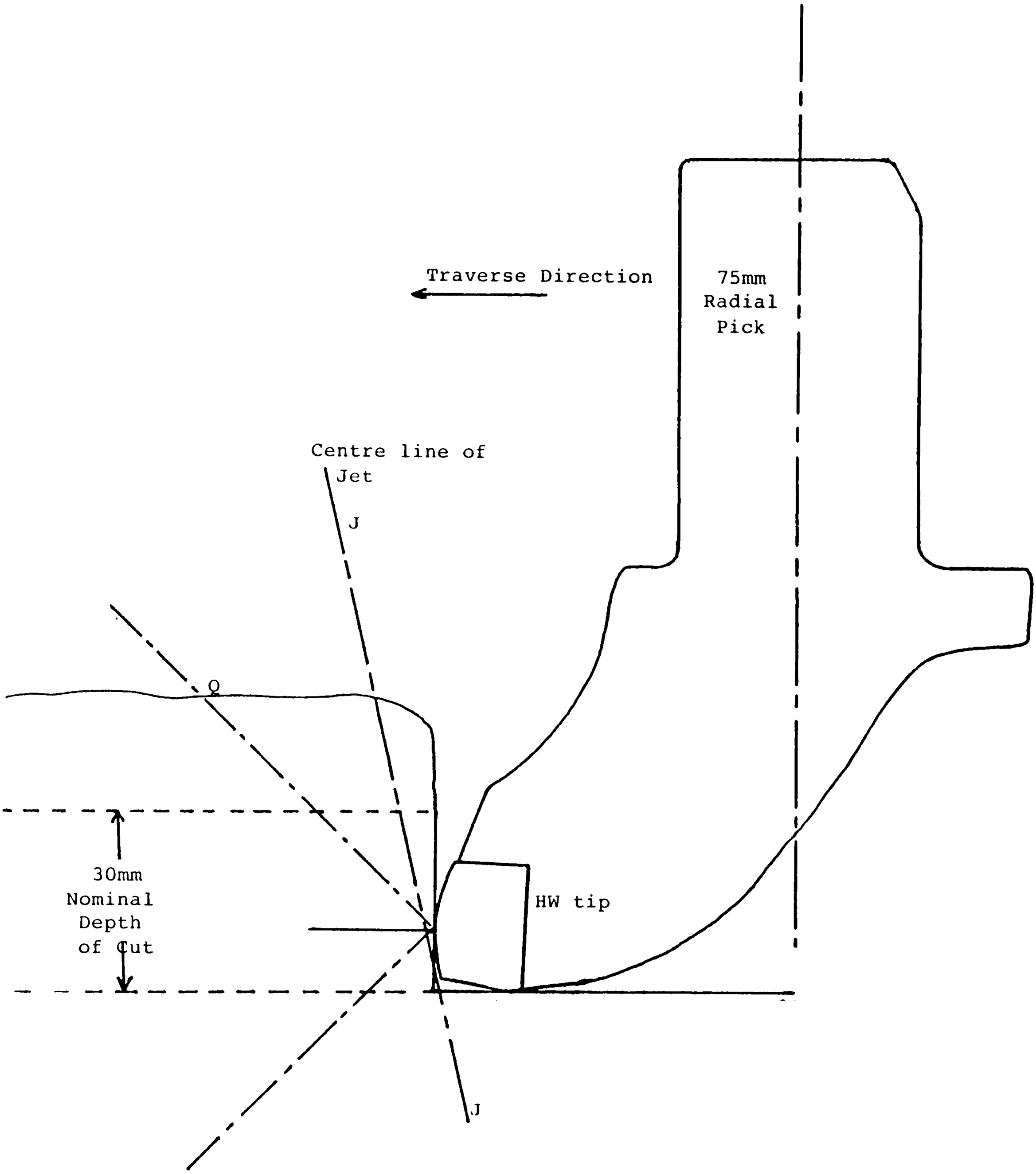

Traverse Direction
75mm
Radial
Pick
Centre line of
Jet
J
Q
30mm
Nominal
Depth
of Cut
HW tip
J

Fig.8.2

forces. Some evidence for this is suggested from the cleat parallel tests where especially with the sharp pick there is a small rise in the forces, particularly the cutting force, compared to the 35MPa pressure jet results.

Measured penetrations for the 105MPa pressure (21kW) jet are 26.4mm for the Erin and 22.1mm (cleat parallel) and 27.5mm (cleat horizontal) for the anthracite. During the cutting trials the jet penetrated beneath the tool tip in all the treatments. Consequently, although the built-up edge would be continuously eroded, nevertheless force reduction would be obtained due to extensive relief beneath the pick tip. This is particularly evident with the blunt tool in the anthracite.

For the results of Test Series One and Two, the coal although Erin, was stronger than the coal tested at Newcastle as indicated by the forces involved. In addition the cutting speed was faster at 1.34m/s compared to 1.1m/s and the jet powers were lower for the 70MPa and 105MPa pressure jets. Therefore one would expect the jet penetrations to differ from those given above.

The sharp pick received force reduction but the blunt pick seems to have derived no relief whatsoever, which was unexpected. The blunt pick in the anthracite obtained benefit and hence one is surprised that even the 105MPa pressure jet in Test Series One had no impact on the blunt tool forces.

The pre-cut slot test results are quite interesting. In this case the influence of the slot produced by the jet is examined without the dynamic effect of the water, however, the slot is essentially infinitely long which is not strictly the case in hybrid cutting.

From the percentage force decrease graphs of Fig.7.22-23, one can suggest that an optimum jet penetration exists over this pressure range and this would be that made by the 35MPa pressure (2.33kW) jet. Remembering that the cuts were relieved, pre-slotting (not found

particularly beneficial in other rocks) is sufficient to offer relief perhaps due to cracks propagating to the slot. The author thinks that blunt tool tests ought to be done to confirm this result.

The lead and offset distance tests in Test Series Two, produced a striking result. At an offset distance midway between the pick line spacing i.e. 35mm, and at a lead distance of 2mm, extensive force reductions were obtained which made the possibility of decreasing the specific energy of a shearer loader (under a certain set of operating conditions) quite likely. Considering the already high cost of equipping a modern heavy duty longwall coal face, this is a positive result since it offers the potential to reduce unit costs at the same time as producing less fines.

The force levels at the other lead distances and 35mm offset also were less than with the offset at zero. One can foresee practical difficulties in positioning the jet on a vane to achieve these operating parameters but the effort would appear to be worthwhile.

Jet assistance usually brings about a reduction in fines regardless of whether force reduction is obtained. The exception is with the blunt tool in the anthracite where the cleat was horizontal. On way it could do this is through debris clearance.

Without jet assistance the debris is cleared away from the tool by the force imparted to the coal by the tool and any subsequent impacts between adjacent coal particles. A certain degree of secondary crushing may be involved in this process. The water jet, under pressure, can enter and propagate cracks formed by the pick and propel the coal away from the cutting area preventing further degradation. Indeed in the Erin and anthracite cleat parallel test fines reduction was commonly accompanied with +28mm size coal increase.

One might say that the mass of coal eroded in the slot accounts for the fines reduction, but one would have to assume that all this coal would escape collection and if it did not it would actually contribute to the fines make since the jet does not strictly cut but erode, producing very small particles. Also, one would not get the increased median particle size commonly observed with jet assistance.

8.2 Conclusions

A series of experiments have been carried out in two coals, one highly cleated and friable bituminous coal, the other, a shiny black, high rank, brittle anthracite. Jet penetration, cutting forces, breakout, specific energy and particle size distribution have been ascertained for the coals in the laboratory. In one suite of tests the lead and offset distances were examined also.

The laboratory differs from the underground environment, the important differences being that the cutting speed would be three to four times greater; the tool would travel an approximately circular path which means that the depth of cut would be varying continuously; and obviously the coal is in situ. Laboratory tests elsewhere suggest that cutting speed does not affect the forces per se but attendant factors such as increased tool temperature and wear do. In this respect the results are limited.

However, other factors have been closely modelled and these are: a realistic depth of cut; line spacing; a relieved cutting mode; and testing with an actual production tool in both sharp and blunt states. The test medium itself was from a coal seam and not simulated coal. The water jet pressures, flow rates and powers covered a range that could be employed below ground and exceeded it with the 105MPa pressure jet. The lead and offset distances were also controlled to cover a realistic spectrum.

A very important aspect has been sizing the product into the Rosin-Rammler sieve series for all the treatments. This gives direct information on washery modifications that may be required should a particular treatment be adopted.

8.2.1 Jet Penetration

The jet penetration experiment showed that jet pressure, traverse speed and coal type are major factors affecting kerf depth. The weaker Erin coal suffered deeper penetration than the harder anthracite. Cleat orientation was found to be a negligible (significant at the 10% level) factor on penetration.

The coal cutting tests revealed that the jet penetrated further during hybrid cutting than when merely slotting intact, solid coal. The 105MPa jet uniformly penetrated beneath the cutting tool in all the treatments which was to a greater depth than that measured in the slotting experiment. It appears that with hybrid cutting the coal is loosened by the pick allowing the jet to penetrate deeper and this effect was greater in the Erin coal than in the anthracite.

Regarding hydraulic specific energy the low power/high traverse rate jet proved to be the most efficient.

8.2.2 Cutting Performance

Cutting performance can be improved by jet assistance. With the Erin coal significant benefit was achieved with the 35MPa pressure (2.33kW) jet in both the sharp and blunt tools. Further increase in jet pressure and power was not justified in terms of the additional decrease in the cutting forces. The Erin coal tested in Test Series One, was harder requiring larger cutting forces. However, jet assistance did procure force reductions with the sharp pick. With the blunt tool only the 35MPa pressure jet yielded force reductions and only when the cleat was horizontal.

8.2.3 Breakout

Breakout between the two coals was different, not only in extent but in manner. This can be attributed to the difference in cleat frequency, friability and coal lithotypes. Breakout occurred along cleat planes and was greater in the anthracite with extensive sidesplay in both cleat orientations. The Erin coal left ridges 20mm high between line spacings, the grooves being approximately the width of the cutting tool depending upon the jet pressure.

The cutting system used would not cause coring in either coal and form this viewpoint is workable.

8.2.4 Specific Energy

On the whole specific energy increased with jet assistance. The basic relationship is a linear increase with jet power. From this aspect the 35MPa pressure or 2.33kW jet gave the best result in that the specific energy increase was not exorbitant.

Pre-slotting the coal gave an 8.3% decrease in specific energy compared to 'conventional' jet assistance and a slight decrease in specific energy was obtained with the 35MPa pressure treatment compared to cutting dry.

Theoretical criteria have been derived to predict if jet assistance may reduce the specific energy. The relationships for the shearer loader depend upon the same jet penetration at different cutting speeds yielding identical force reductions. The idea may easily be adapted to double ended shearers and other mining machines.

The laboratory results and the theoretical expressions imply that jet assistance with a lead distance of 2mm and an offset of zero would not reduce the specific energy, however, only

one set of operating parameters were investigated. The derived expressions allow one to experiment with the operating parameters and chose a set that would at least minimise the specific energy if not reduce it less than the unassisted case.

A very encouraging result in terms of potential specific energy decrease was that appraisal made with an offset distance of 35mm and a lead distance of 2mm. If a shearer drum could accommodate this arrangement then specific energy reduction appears quite possible.

8.2.5 Size Distribution

All the jet assisted treatments improved the size distribution except with the blunt tool, cleat horizontal trials in the anthracite. Generally fines reduction was best with the 35MPa pressure jet, including the pre-cut slot results, with usually an accompanying increase in the +28mm size coal.

Fines reductions were also achieved in Test Series Two. The best result was obtained at a lead distance of 10mm and an offset of 35mm, with only 3.2% of the whole product being fines. Generally, the treatments with an offset distance of 35mm produced the least fines.

All the size distributions gave very good correlations to the Rosin-Rammler equation and can be used to predict what washery requirements would be needed should a particular treatment be applied.

The form of the distributions did not change greatly with jet assistance, and the author therefore suggests that indeed the jet was assisting the mode of fracture by the tool and not fundamentally changing it to a different process.

8.3 Recommendations

A major problem with jet penetration is interpolating the slot depth that would be made by a jet at faster traverse speeds than one has tested. This obviously may lead to errors and is not satisfactory. Thus jet penetration tests need to be conducted at traverse speeds up to 5m/s to embrace the cutting speeds of shearer drums. The flow rate could be limited to 4 l/min or less and the pressure increased up to 105MPa, since it is highly improbable that extant underground machinery will be equipped to take pressures greater than this.

Also, to augment ones understanding of the relative importance of pressure and flow rate on jet penetration, tests may be done at a constant jet power but with varying combinations of pressure and flow rate to see if an optimum combination of jet pressure and flow rate exists that gives a maximum penetration. If this is repeated for a number of jet powers then a curve of maximum penetration against jet power (but for an optimum combination of pressure and flow rate) could be established. This would then minimise the jet power required to achieve a certain penetration and consequently the specific energy would be minimised.

More bituminous coals could be tested at different strengths and cleat frequency. This would indicate if jet assistance would be universally applicable and beneficial throughout the British Coalfields.

One particular area that requires further investigation is that of varying the lead and offset distances. Only one jet pressure (70MPa) was used in Test Series Two and the results were very encouraging, therefore similar tests over a wider pressure range ought to be done. In addition a blunt tool as well as a sharp one should be used.

Tool geometry influences the cutting forces and so tests with a sharp and blunt pencil point tool would reveal if the cutting forces may be reduced with a different tool design.

Since extra heavy duty radial picks are being introduced in to the field, tests to determine whether jet assistance has a beneficial effect with these tools should be done and at similar jet pressures.

A size analysis should be done in all subsequent cutting tests on coal. Different tool designs may produce less fines than the 75mm reach radial pick without the need to apply jet assistance and therefore it would be useful to know the size distribution the coal is breaking up into. The Rosin-Rammler sieve series is suitable for this and allows one to describe the distribution by means of a mathematical relationship.

REFERENCES

REFERENCES

Allington, A.V. 'The Machining of Rock Materials.'
Unpublished Ph.D. Thesis, University of Newcastle upon Tyne, 1969.

Barham, D.K. and Buchanan, D.J. 'A Review of Water Jet Assisted Cutting Techniques for Rock and Coal Cutting Machines.'
The Mining Engineer, pp. 6-14, July 1987.

Baumann, L., Boeing, R. and Hessling, M. 'Fundamental Investigations into the Improvement of Water-Jet Performance by the use of Abrasive Additives.'
Proceedings, 8th International Symposium on Jet Cutting Technology, Durham, England, 9-11 Sept. 1986. BHRA.

Baumann, L. and Henneke, J. 'Attempt of Technical-Economical Optimization of High-Pressure Jet Assistance for Tunnelling Machines.'
Proceedings, 5th International Symposium on Jet Cutting Technology, Hanover, FRG, 2-4 June 1980. BHRA.

Brook, N. and Page, C.H. 'Energy Requirements for Rock Cutting by High Speed Water Jets.'
Proceedings, 1st International Symposium on Jet Cutting Technology, Coventry, 5-7 April 1972.

Brooker, C.M. 'Theoretical and Practical Aspects of Cutting and Loading by Shearer Drums.'
Colliery Guardian, Coal International, Part 1, pp. 9-16, Jan. 1979, Part 2, pp. 41-50, Apr. 1979.

Clark, R.A. 'Success for Anderson Strathclyde High-Pressure Water Roadheader.'
Colliery Guardian, pp. 255-256, July/August 1984.

Conn, A.F. and Rudy, S.L. 'Conservation and Extraction of Energy with the Cavijet.'
Proceedings, 4th International Symposium on Jet Cutting Technology, Canterbury, England, 12-14 April, 1978. BHRA.

Cooley, W.G. 'Correlation of Data on Jet Cutting by Water Jets using Dimensionless Parameters.'
Proceedings 2nd Int. Symp. on Jet Cutting Technology, Cambridge, U.K. 2-4 Apr. 1980. BHRA.

Crow, S.C. 'A Theory of Hydraulic Rock Cutting.'
Int. J. Rock Mech. Min. Sci. & Geomech. Abstr. Vol.10, pp. 567-584, 1973.

Davies, O.L. 'Statistical Methods in Research and Production.'
ICI Ltd. Oliver and Boyd. 1961.

Du Plessis, M.P. and Hashish, M. 'Experimental and Theoretical Investigations of Hydraulic Cutting of a Western Canadian Coal.'
Proceedings 5th Int. Symp. on Jet Cutting Technology, Hanover, FRG, 2-4 June 1980. BHRA.

Enever, J.R. and Tooley, S.M. 'A Laboratory Assessment of the Hydraulic Cuttability of an Australian Black Coal.'
Proceedings of the Australasian Institute of Mining and Metallurgy, 290 (2), pp. 65-70, March 1985.

Evans, I. 'A Theory on the basic mechanics of Coal Ploughing.'
Proc. Int. Symp. on Mining Res. Vol. 2 London Pergamon P 761 et seg.

Evans, I. 'The force required to cut coal with blunt wedges.'
Int. J. Rock Mech. & Min. Sci. Vol. 2 pp.1-12, 1965.

Fairhurst, C.E. and Deliac, E.P. 'Water-Jet-Assisted Rock Cutting - The Effect of Pick Traverse Speed.'
Proceedings 8th Int. Symp. on Jet Cutting Technology, Durham, 9-11 Sept. 1986. BHRA.

Farmer, I.W. and Robertson, J.T. 'The Effect of Pack Construction on Roadway Stability behind Working Faces.'
The Mining Engineer, Vol. 134, pp. 599-606, 1975.

Fauvel, O.R. 'Implications of Laboratory Rock Cutting for the Design of a Tunnel Boring Machine Cutter Head.'
Unpublished Ph.D. Thesis, University of Newcastle upon Tyne, 1981.

Fowell, R.J. and Johnson, S.T. 'The Applicability of Hybrid, High Pressure Water Jet Assisted Cutting for the Excavation of Coal.'
A Preliminary Report to the National Coal Board, University of Newcastle upon Tyne, March 1984.

Fowell, R.J., Ip. C.K. and Johnson, S.T. 'Water Jet Assisted Drag Tool Cutting: Parameters for Success.'
Proceedings 8th Int. Symp. on Jet Cutting Technology, Durham, 9-11 Sept. 1986. BHRA.

Fowell, R.J., Johnson, S.T. and Ip, C.K. 'Further Studies in Water Jet Assisted Drag Tool Cutting in Rock.'
Proceedings, 3rd US Water Jet Symposium, Pittsburgh, 1985.

Harris, H.D. and Mellor, M. 'Cutting Rock with Water Jets.'
Int. J. Rock. Mech. Min. Sci. & Geomech. Abstr., Vol. 11, pp. 343-358, 1974.

Hashish, M. and Du Plessis, M.P. 'The Application of a Generalized Jet Cutting Equation.'
Proceedings, 4th International Symposium on Jet Cutting Technology, Canterbury, England, 12-14 April, 1978. BHRA.

Henkel, E.H. 'Aims for a High Pressure Water Jet Assisted Coal Winning System.'
Proceedings, 5th International Symposium on Jet Cutting Technology, Hanover, FRG, 2-4 June, 1980. BHRA.

Henkel, E.H. 'Development Work for Coal Winning Technology.'
Water-Jet-Assisted Cutting. Proceedings: Bureau of Mines Open Industry Meeting, Pittsburg, PA, USA, 21 June 1984.

Henkel, E.H. and Kraemer, T. 'Development and Testing New Actuated Winning Techniques.'
Glueckauf; 117 (15); 919-925, (in German). Glueckauf + Translation; 117 (15); 412-414, 6 Aug. 1981, (in English).

Hood, M. 'Cutting Strong Rock with a Drag Bit Assisted by High-Pressure Water Jets.'
Journal of the South African Institute of Mining and Metallurgy, 77 (4), pp. 79-90, 1976.

Hood, M., Knight, G.C. and Thimons, E.D. 'A Review of Water-Jet-Assisted Rock Cutting.'
Information Circular 9273. US Bureau of Mines, Pittsburgh, PA, USA. 1990.

Hurt, K.G. and Evans, I. 'Point Attack Tools: An Evaluation of Function and Use for Rock Cutting.'
The Mining Engineer, pp. 673-675, March 1981.

Hurt, K.G. and McStravick, F.G. 'High Performance Shearer Drum Design.'
Colliery Guardian, 236 (12), pp. 428-429, Dec. 1988.

Ip, C.K. 'Laboratory Water Jet Assisted Drag Tool Rock Cutting Studies at High Traverse Speeds.'
Unpublished Ph.D. Thesis, University of Newcastle upon Tyne, 1986.

Ip, C.K. and Fowell, R.J. 'Mechanisms of Water Jet Assisted Drag Tool Cutting of Rock.'
Proceedings, 60th Int. Congress on Rock Mechanics. Int. Soc. for Rock. Mech., Rotterdam, pp. 667-674, 1987.

Kenny, P. and Johnson, S.N. 'The Effect of Wear on the Performance of Mineral-Cutting Tools.'
Colliery Guardian, 224 (6), pp. 246-252, June 1976.

Kenny, P. and Johnson, S.N. 'Non-blunting Tool for Cutting Coal and Rock.'
Colliery Guardian, 225, pp. 760-763, Oct. 1977.

Kogelmann, W.J. 'Computer-Controlled Water-Jet Assisted Roadheaders and Shearers.'
Glueckauf, 122 (8), 556-563, 1986, (in German). Glueckauf + Translation, 122 (8), 162-165, 1986, (in English).

Kogelmann, W.J. and Thimons, E.D. 'Development and Testing of a Water Jet Assisted Longwall Shearer.'
US Bureau of Mines, Pittsburgh, PA, USA. Pittsburgh Research Centre. Longwall USA Conference, 17-19 June, 1986.

Kouzmich, I.A. and Tolchenkin, Yu.A. 'Hydromechanical Cutters for Shearer Loaders and Heading Machines.'
Ugol Ukrainy (Ukrainian SSR), 4, pp.19-21, April 1985.

Kovscek, P.D., Evans, R.J., and Taylor, C.D. 'Cutting Trials with a Water Jet Assisted Longwall Coal Shearer.'
Proceedings, 3rd US Water Jet Conference, University of Pittsburgh, 1985.

Kovscek, P.D., Taylor, C.D. and Thimons, E.D. 'Linear Cutting Apparatus for Evaluating Mining Applications of Water-Jet-Assisted Cutting.'
Proceedings, 5th American Water Jet Conference, Toronto, Canada, pp. 39-47, 29-31 Aug. 1989.

Kuzmich, I.A. 'Some Relationships in the Coal Penetration by High Pressure Thin Water Jets.'
Proceedings, 1st International Symposium on Jet Cutting Technology, Coventry, England, 1972. BHRA.

Kuzmich, I.A., Goldin, J.A., Ruthberg, M.I., and Frolov, V.S. 'A Combined Method of Rock Breakage.'
Proceedings, 6th International Symposium on Jet Cutting Technology, Guildford, England, 6-8 April, 1982. BHRA.

Leach, S.J. and Walker, G.L. 'The Application of High Speed Jets to Cutting.'
Proceedings, Roy. Soc. Vol. 260A pp. 295-315, London, 1966.

Leonard, J.W. 'Coal Preparation.'
The American Institute of Mining, Metallurgical, and Petroleum Engineers, Inc. Port City Press, Inc.

MacAndrew, K.M., Morris, C.J. and Hurt, K.G. 'A Study of the Cutting of Hard Rocks with High Pressure Water Jet Assistance.'
Underground Mining Methods and Technology, pp. 271-280, 1987.

Matsuki, K., Okumura, K. and Nakadate, H. 'Some aspects of Slot Cutting of Rocks with High Speed Water Jets both in Air and Water.'
Proceedings, 9th International Symposium on Jet Cutting Technology, Sendai, Japan, 4-6 Oct. 1988.

Mazurkiewwicz, M. and Summers, D.A. 'The Structural Properties of Coal and their Effect on Coal Excavation by High Pressure Water Jet Impact.'
Symposium on Ground Movement and Control Related to Coal Mining, The AusIMM, pp. 51-56, Aug. 1986.

Morris, C.J. 'The Design of Shearer Drums with the aid of a Computer.'
The Mining Engineer, pp. 289-295, Nov. 1980.

Morris, C.J. and MacAndrew, K.M. 'A Laboratory Study of High Pressure Water Jet Assisted Cutting.'
Proceedings 8th Int. Symp. on Jet Cutting Technology, Durham, 9-11 Sept. 1986. BHRA.

Morris, C.J. and Tomlin, M.G. 'Experience with Boom-type Roadheaders Equipped with High Pressure Water Jet Systems for Roadway Drivage in British Coal Mines.'
Water-Jet-Assisted Cutting. Proceedings: Bureau of Mines Open Industry Meeting, Pittsburg, PA, USA, 21 June 1984.

Mort, D. 'The Application of High Pressure Water Jets to Longwall Mining.'
The Mining Engineer, pp. 344-350, Jan. 1988

Nakaya, M., Kitagawa, T. and Satake, S. 'Concrete Cutting with Abrasive Water-Jet.'
Proceedings, 7th International Symposium on Jet Cutting Technology, Ottawa, Ontario, Canada, 26-28 June 1984.

Nienhaus, K., Weigelt, H., and Thimons, E.D. 'The Development of a Water Jet Assisted Shearer Loader.'
Proceedings, 8th International Symposium on Jet Cutting Technology, Durham, England, 9-11 Sept. 1986. BHRA.

Nikonov, G.P. 'Research into the Cutting of Coal by Small Diameter, High Pressure Water Jets.'
Dynamic Rock Mechanics. Society of Mining Engineers, Chapter 34, New York, 1971.

Nikonov, G.P. and Goldin, Y.A. 'Coal and Rock Penetration by Small Diameter, High Pressure Water Jets.'
Proceedings 1st Int. Sump. on Jet Cutting Technology, Coventry, England, 1972. BHRA.

Nishimatsu, Y. 'The Mechanics of Rock Cutting.'
Int. J. Rock Mech. Min. Sci., Vol. 9, 1972.

O'Dogherty, M.J. and Burney, A.C. 'A Laboratory Study of the Effect of Cutting Speed on the Performance of two Coal Cutter Picks.'
Colliery Engineering, pp. 51-54, Feb. 1963 and pp. 111-114, Mar. 1963.

Pomeroy, C.D. 'The Breakage of Coal by Wedge Action.'
Colliery Guardian, pp. 642-677, 21 Nov. 1963.

Pomeroy, C.D. 'Mining Applications of the Deep Cut Principle.'
The Mining Engineer, pp. 506-515, June 1968.

Pomeroy, C.D. and Brown, J.H. 'Laboratory Investigations of Cutting Processes Applied to Coal-Winning Machines.'
Journal of Strain Analysis, Vol. 3, No. 3, 1968.

Pugh, W.L. 'The Use of High Pressure Water Jets in the Western Area.'
The Mining Engineer, 145 (297), pp. 541-548, June 1986.

Rehbinder, G. 'Slot Cutting in Rock with a High Speed Water Jet.'
Int. J. Rock. Mech. Min. Sci. & Geomech. Abstr., Vol. 14, pp. 229-234, 1977.

Reichman, J.M. 'Optimization of Water-Jet Systems for Mining Applications.'
Water-Jet-Assisted Cutting. Proceedings: Bureau of Mines Open Industry Meeting, Pittsburgh, PA, USA, 21 June 1984.

Roxborough, F.F. 'Cutting Rock with Picks."
The Mining Engineer, pp.445-455, June 1973.

Saunders, D.A. and Blackwell, A. 'Water Jet Cutting of Coal.'
BHRA Project RP 11892. Report PR 1712. BHRA, Cranfield, Bedford, England, June 1981.

Shavlovsky, D.S. 'Hydrodynamics of High Pressure Fine Continuous Jets.'
Proceedings, 1st International Symposium on Jet Cutting Technology, Coventry, England, 1972. BHRA.

Singhal, R.K., Stewart, D.B. and Bacharach, J.P.L. 'Frictional Ignition Control.'
Colliery Guardian, 235 (5), pp. 176-182, May 1987.

Souder, W.E. and Evans, R.J. 'Water-Jet Coal Cutting: the Resurgence of an old Technology.'
Proceedings of the 1983 Rapid Excavation and Tunnelling Conference. Chicago, IL, USA, 12-16 June 1983. New York, USA, American Institute of Mining, Metallurgical and Petroleum Engineers, Vol. 2, pp. 719-739, 1983.

Summers, D.A. 'The Application of High Pressure Water Jet Technology.'
Notes for the Water Jet Short Course. University of Missouri-Rolla, Rock Mechanics & Explosives Research Centre. May 1983.

Summers, D.A. 'The Water Jet Plough.'
Water-Jet-Assisted Cutting. Proceedings: Bureau of Mines Open Industry Meeting, Pittsburg, PA, USA, 21 June 1984.

Summers, D.A. and Barker, C.R. 'Surface Trials of the Hydrominer.'
Proceedings, 4th International Symposium on Jet Cutting Technology, Canterbury, England, 12-14 April 1878. BHRA.

Summers, W.A. and Summers, D.A. 'The Application of High Pressure Water Jets to Longwall Mining.'
The Mining Engineer, pp. 915-924, June 1980.

Taylor, C.D., Thimons, E.D. and Kovscek, P.D. 'Evaluation of Water-Jet-Assisted Cutting Capability on Longwall Shearers.'
Report of Investigations 9270. US Bureau of Mines, Pittsburgh, PA, USA. 1989

Trueman, R. 'A Literature Review of the Ignition of Methane-Air Mixtures by Coal-Cutting Picks.'
Journal of the South African Institute of Mining and Metallurgy, pp. 209-215, July 1985.

Tecen, O. 'High Pressure Water Jet Assisted Drag Tool Cutting of Rock Materials.'
Unpublished Ph.d. Thesis, University of Newcastle upon Tyne, 1982.

Vallve, F.X., Mohaupt, U.H., Kalbfleisch, J.G. and Burns, D.J. 'Relationships between Jet Penetration in Concrete and Design Parameters of a Pulsed Water-Jet Machine.'
Proceedings, 5th International Symposium on Jet Cutting Technology, Hanover, FRG, 2-4 June 1980. BHRA.

Wang, F.D. and Wolgamott, J. 'Application of Water-Jet Assisted Pick Cutter for Rock Fragmentation.'
Proceedings, 4th International Symposium on Jet Cutting Technology, Canterbury, England, 1978.

Whittaker, B.N. 'An Appraisal of Strata Control Practice.'
The Mining Engineer, Vol. 134, pp. 9-23, Oct. 1974.

Wood, P.A. 'Water Jet/Jet Assisted Cutting and Drilling.
IEA Coal Research, London, Report ICTIS/TR37, March 1987.

Yanaida, K. and Ohashi, A. 'Flow Characteristics of Water Jets in Air.'
Proceedings 5th Int. Symp. on Jet Cutting Technology, Hanover, FRG, 2-4 June 1980. BHRA.

BIBLIOGRAPHY

Cochran, W.G. and Cox, G.M. 'Experimental Designs.'
John Willey & Sons, 1957.

Evans, I. and Pomeroy, C.D. 'The Strength, Fracture and Workability of Coal.'
Pergamon Press, 1966.

Jaeger, J.C. and Cook, N.G. 'Fundamentals of Rock Mechanics.'
Chapman and Hall, London, 1979.

Massey, B.S. 'Mechanics of Fluids.'
Van Nostrand Reinhold (UK), 1987.

Monro, D.M. 'Fortran 77.'
Arnold, 1987.

Wills, B.A. 'Mineral Processing Technology: An Introduction to the Practical Aspects of Ore Treatment and Mineral Recovery.'
Pergamon Press, 1982.

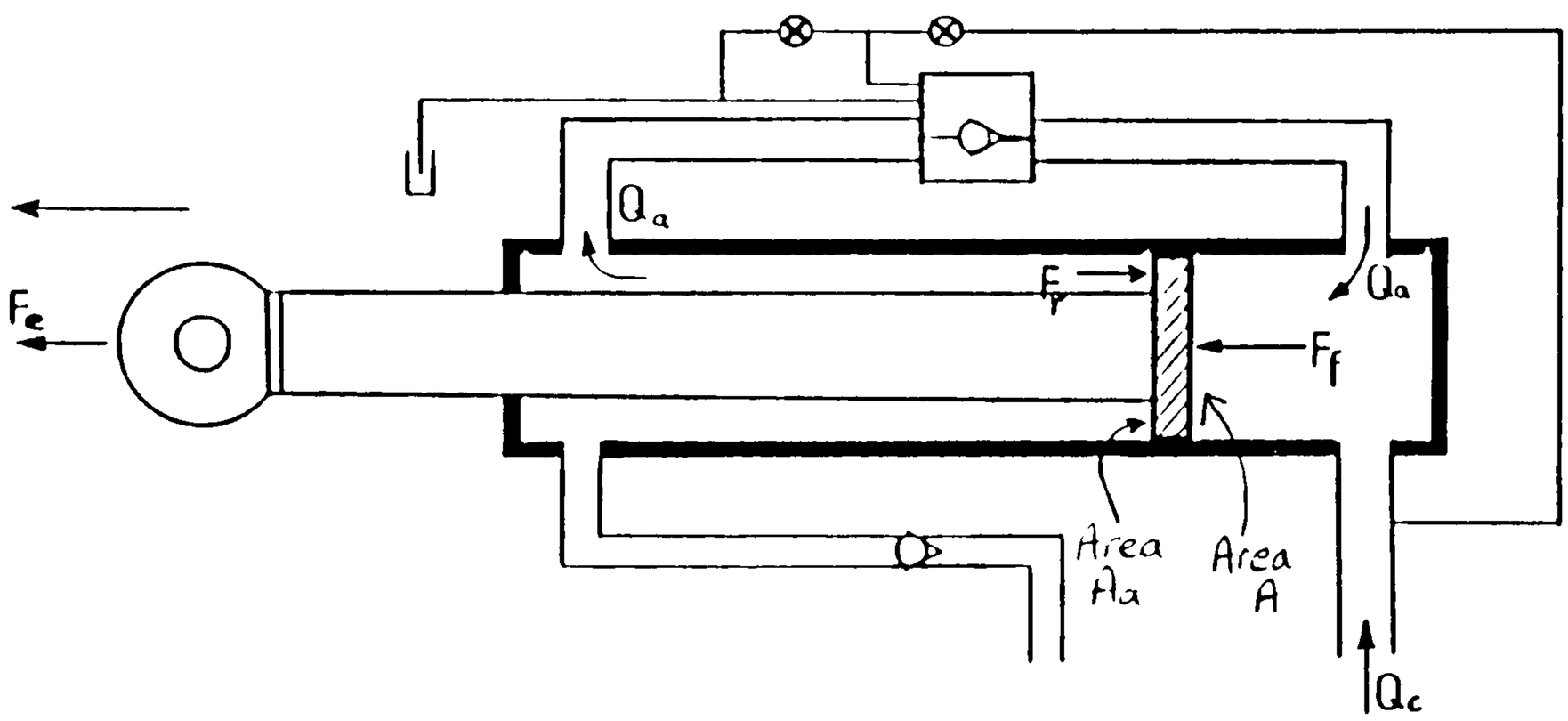
APPENDICES

APPENDICES

1 HIGH SPEED HYDRAULIC CYLINDER DETAILS

Specifications: Stroke = 2083mm (82in)
Bore = 102mm (4in)
Diameter = 81mm (3 3/16in)

The ram is a double acting hydraulic cylinder designed to operate at a pressure up to 20.67MPa (3000psi). A diagram is given below illustrating the immediate circuitry associated with it.



Area of the ram bore, A = $\pi/4.(0.102)2 = 8.171\times10^{-3}$m2.
Area of the annulus, $A_a = \pi/4.(0.1022 - 0.0812) = 3.018\times10^{-3}$m2.

Volume of the cylinder when the ram is fully extended, V = $2.083 \times A = 0.017$m2 = 17 litres

Volume of the annulus side when the ram is fully withdrawn, V_a = $2.083 \times A_a = 6.286\times10^{-3}$m2 = 6.29 litres

1.1 Considering the Forces Acting on the Ram

a. Forward Direction: Consider the ram extending under its maximum designed pressure, 20.67MPa (3000psi). Assume that no counteracting force F_r, acts on the annulus and neglecting frictional resistance. This will produce the maximum possible force F_e, that the ram can develop.

$$F_e = F_f \quad = \text{Pressure} \times \text{Area}$$
$$= 20.67\times10^{-6} \times 8.171\times10^{-3}$$
$$= 169\text{kN}$$

b. Reverse Direction: Consider the ram retrieving under an oil pressure of 20.67MPa and with no force F_f acting to oppose this motion.

$$-F_e = F_r \quad = 20.67\times10^{-6} \times 3.018\times10^{-3}$$
$$= 62.4\text{kN}$$

Thus these are the maximum forces that the ram can exert in either direction. With this arrangement, as the ram extends hydraulic oil is circulated through a pilot operated check valve to the opposite side of the ram cylinder. This is done to provide an adequate oil flow rate such that a ram velocity of 1.1m/s can be maintained over the entire length of cut.

Since the oil is circulated from the annulus, the oil pressure on both sides of the ram must be equal, i.e. 20.67MPa. Hence, the ram extends due to pressure acting over the differential area.

Therefore, the maximum effective force F_e, that can be exerted is $F_f - F_r$.

$F_e = 169 - 62.4 = 106.6,\ 107\text{kN}$

This is more than adequate for the coal cutting experiment and indeed the limiting force factor is the design capacity of the dynamometer.

1.2 Considering the necessary Flow Rates

The ram is required to traverse at 1.1m/s over the length of cut in the coal, but let us say over its whole stroke. From the Continuity Equation, Q = A.v for a fluid of constant density.

Where Q = Flow Rate
A = Cross-sectional area (8.171×10^{-3}m2)
v = Fluid Velocity (1.1m/s)

Thus $Q = 8.171\times10^{-3} \times 1.1 = 9$ litres/sec

Therefore a total flow rate Q_t, of 9 l/s at 20.67MPa is needed to extend the ram at 1.1m/s. Q_t is made up of oil circulating from the annulus and from the accumulators.

Flow rate from the annulus, $Q_a = A_a.v$
$= 3.018\times10^{-3} \times 1.1 = 3.32$ l/s

Thus the flow rate required from the accumulators,

$Q_c = Q_t - Q_a$
$= 9 - 3.32$
$= 5.68$ l/s at 20.67MPa

One may now proceed to calculate what pressure the accumulators have to be charged to, to guarantee the necessary flow rate.

1.3 Accumulators and gas back-up bottle

Volume of gas back-up bottle = 90.1 litres
Effective volume of each accumulator = 49.2 litres
Total nitrogen volume = $90.1 + 2 \times 49.2$
= 188.5 litres
The accumulators are presently pre-charged at 13.79MPa (2000psi)

a. To determine the volume of oil needed to be pumped into the accumulators to raise the nitrogen pressure up to 20.67MPa (3000psi).

Assuming adiabatic compression during pumping, then
P.V = constant Where P = pressure; V = volume
Before pumping, P1 = 13.79MPa and V1 = 188.5 l. After pumping, P2 = 20.67MPa and V2 = ?

$$P1.V1 = P2.V2 \quad \Rightarrow \quad V2 = V1\frac{P1}{P2} \quad \Rightarrow \quad V2 = 188.5 \times \frac{13.79}{20.68}$$

$$V2 = 125.7\text{litres}$$

Therefore the volume of oil pumped into the accumulators to raise the pressure to 20.67MPa,
= 188.5 - 125.7 = 62.8litres

b. To calculate the additional oil needed to be pumped into the accumulators to ensure a flow rate of 5.68 l/s at 20.67MPa (3000psi).

To maintain the required speed the oil pressure should be 20.67MPa at the end of the ram's stroke. Also, the total volume of oil needed to fully extend the ram is,
= V - V_a = 17 - 6.29 = 10.71 litres
Thus at least this extra volume of oil must be entered into the accumulators. Hence taking P1 = 20.67MPa, V1 = 125.7 l, P2 = ?, and V2 = 115 l (125.7 - 10.71), then

$$P2 = P1\frac{V1}{V2} = 20.67 \times \frac{125.7}{115} = 22.6MPa$$

This is the final charging pressure of the accumulators in their present state to ensure the cutting speed of 1.1m/s.

1.4 Low Pressure Pump

The low pressure gear pump is rated at 182 l/min at 2.76MPa (40gpm at 400psi).

1.4.1 Force Calculations

Considering the forces developed by the ram activated by the low pressure pump in a similar manner as previously.

Force on the ram in the forward direction	$= 2.76\times10^{6} \times 8.171\times10^{-3} = 22.6\text{kN}$
Force on the ram in the	$= 2.76\times10^{6} \times 3.018\times10^{-3} = 8.3\text{kN}$
Resultant thrust	$= 22.6 - 8.3 = 14.4\text{kN}$

When cutting a sample employing the low pressure circuit, the ram should stall if a reaction greater than 14.3kN is experienced.

1.4.2 Speed Calculations

The total flow rate into the hydraulic cylinder Q_t, will consist of that from the annulus Q_a, and that from the low pressure pump, Q_p.

$$Q_t = Q_a + Q_p$$

$$\text{but} Q_t = \text{A.v}$$

$$Q_a = A_a.v$$

$$\text{and} Q_p = 3.03 \times 10^{-3} m^3/s \quad (182\ l/\text{min})$$

$$\text{A.v} = A_a.v + Q_p$$

$$\text{v} = \frac{Q_p}{A - A_a} = \frac{3.03 \times 10^{-3}}{(8.171 - 3.018) \times 10^{-3}} = 0.59 m/s$$

This theoretical value compares favourable with the actually measured velocity of 0.56m/s.

MODEL NUMBERS

AC | 54 | 0 | 7A - 00 - 20 | 1

ACCUMULATOR BLADDER TYPE

NOMINAL VOLUME-LITRES

BLADDER MATERIAL
0 = Nitrile Standard
1 = Butyl
2 = Low Temperature Nitrile
See form no. AC100-031-88 for complete details.

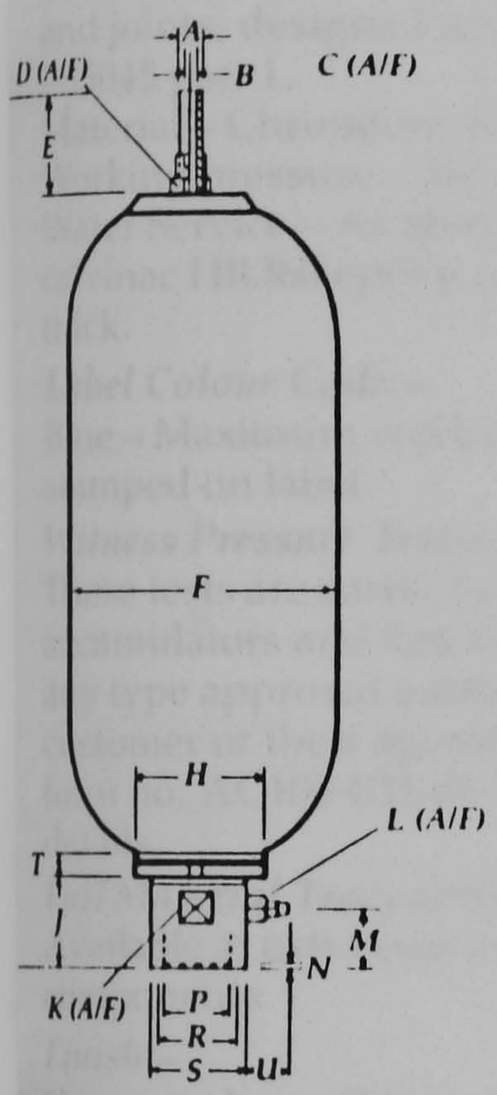
SPARE BLADDERS
Quote full Part No. as follows AC5407A-**-201. This Part No. also includes transfer tube, locknut and gas valve stem 'O' ring seal.

BLADDER STEM
1A = For back-up bottle connection (20 to 54L) terminating in 19mm OD stand pipe.
3A = As 1A but terminating in 7/8" x 14 NF2 male thread.
7A = For back-up bottle connection (54L) terminating in 38mm OD stand pipe.
8A = For back-up bottle connection (20 to 54L) terminating in 7/8" x 14" NF2 male thread.
SB = For back-up bottle connection (4 and 10L) terminating in ½" BSP female.

SPECIAL ACCUMULATORS
00 = Standard.
02 = Water service, EN57 corrosion protected fluid port, shell interior epoxy resin.
13 = Fluid Port NPT thread mineral oil service.
14 = Fluid Port NPT thread water service.
NOTE:
Many more alternatives are available for non-standard bladder stems and fluid ports. Please advise us of your requirement.

MAXIMUM WORKING PRESSURE
20 = 207 bar 34 = 345 bar

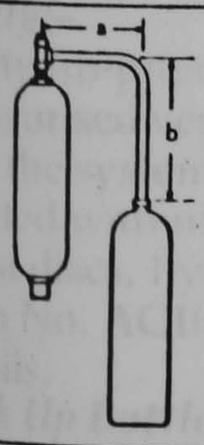
TEST CERTIFICATION
1 = Lloyds – Standard.
See Form No. AC100-031-88 for complete details.



DIMENSIONS

Nominal Capacity Litres	Effective Gas Volume Litres	Working Pressure Bars	Max. Av. Flow Rate L Min Lt/Min	Weight Kilos	A Inches	B	D mm	E mm	F mm	G mm	H mm	J mm	K mm	L mm	M mm	N mm	P Inches	R mm	S mm	T mm	U mm
100		207	477	12 5	3/8x14 NF 2	1" BSP	34	92 0	165	484 0	81	88 5	56 0	21	40	1 6	1¼ BSP	53 0	60 0	13	36
100		345	477	15 20	3/8x14 NF 2	1" BSP	34	92 0	170	484 0	81	88 5	56 0	21	40	1 6	1¼ BSP	53 0	60 0	13	36
100		207	365	37 90	3/8x14 NF 2	19 05	34	92 0	220	581 0	100	90 0	70 0	21	40	1 6	2 BSP	73 4	76 2	20	36
100		345	365	40 50	3/8x14 NF 2	19 05	34	92 0	230	581 0	100	90 0	70 0	21	40	1 6	2 BSP	73 4	76 2	20	36
100		207	365	40 50	3/8x14 NF 2	19 05	34	75 5	220	870 0	100	90 0	70 0	21	40	1 6	2 BSP	73 4	76 2	20	36
100		345	365	63 20	3/8x14 NF 2	19 05	34	75 5	230	870 0	100	90 0	70 0	21	40	1 6	2 BSP	73 4	76 2	20	36
100		207	365	52 30	3/8x14 NF 2	19 05	34	75 5	220	1143 0	100	90 0	70 0	21	40	1 6	2 BSP	73 4	76 2	20	36
100		345	365	76 80	3/8x14 NF 2	19 05	34	75 5	230	1143 0	100	90 0	70 0	21	40	1 6	2 BSP	73 4	76 2	20	36
100		207	365	65 50	3/8x14 NF 2	19 05	34	75 5	220	1393 0	100	90 0	70 0	21	40	1 6	2 BSP	73 4	76 2	20	36
100		345	365	103 00	3/8x14 NF 2	19 05	34	75 5	230	1393 0	100	90 0	70 0	21	40	1 6	2 BSP	73 4	76 2	20	36
100		207	365	87 50	M50x1 5	19 05	70	93 5	220	1936 5	100	90 0	70 0	21	40	1 6	2 BSP	73 4	76 2	20	36
100		345	365	142 00	M50x1 5	19 05	70	93 5	230	1936 5	100	90 0	70 0	21	40	1 6	2 BSP	73 4	76 2	20	36
100		207	749	87 50	M50x1 5	38 10	70	110	220	1953 0	100	90 0	70 0	21	40	1 6	2 BSP	73 4	76 2	20	36
100		345	749	142 00	M50x1 5	38 10	70	110	230	1953 0	100	90 0	70 0	21	40	1 6	2 BSP	73 4	76 2	20	36

ristie interconnecting pipework kit to connect accumulator to back-up bottle.



Part Description AC10010/A or B	/A SIZE /B	
	37-54 litre Models	54 litre Model only
1 – Equal tee – Branch having air valve assembly fitted	19mm O.D.	38 mm O.D.
1 – Length of high-pressure steel tube	19mm O.D.	38mm O.D.
1 – BSP Adaptor	19mm-1" BSP	38mm-1" BSP
1 – Dowty Seal	1"	1"
Dimension 'a'	381mm	381mm
Dimension 'b'	686mm	1245mm

ett Christie Hydraulics Limited have a policy of nuous product development. The company es the right to change specification contained in ublication without prior notice.

An Expamet International Company

nd and Produced by Leighton Advertising Ltd. Printed in England

FAWCETT ■ CHRISTIE
HYDRAULICS LTD
Sandycroft Industrial Estate,
Chester Road, Sandycroft,
Deeside, Clwyd CH5 2QP
Telephone: Hawarden (0244) 535515
Telex: 617026
Facsimile: (0244) 533002

FCH

In Hydraulics

FCH

TRANSFER BARRIER ACCUMULATORS 207 and 345 bar

FOR USE WITH BACK UP BOTTLES

SPECIFICATION

Shell:–
Oil service – seamless shell free from welds and joints, designed and manufactured to BS5045 part 1.
Material – Chromium-molybdenum steel.
Working pressure – 207 and 345 bar.
Water Service – As above with interior calvinac HR360 epoxy resin lined 0.18-0.25 thick.

Label Colour Code:–
Blue – Maximum working pressure, stamped on label.

Witness Pressure Tests:–
These tests are carried out on complete accumulators and can be undertaken for any type approval authority or any customer or their agents at extra cost. See form no. AC100-031-88 for complete details.

Full Material Traceability:–
Available at extra cost on all major components.

Finish:–
One coat short oil based alkyd paint standard.

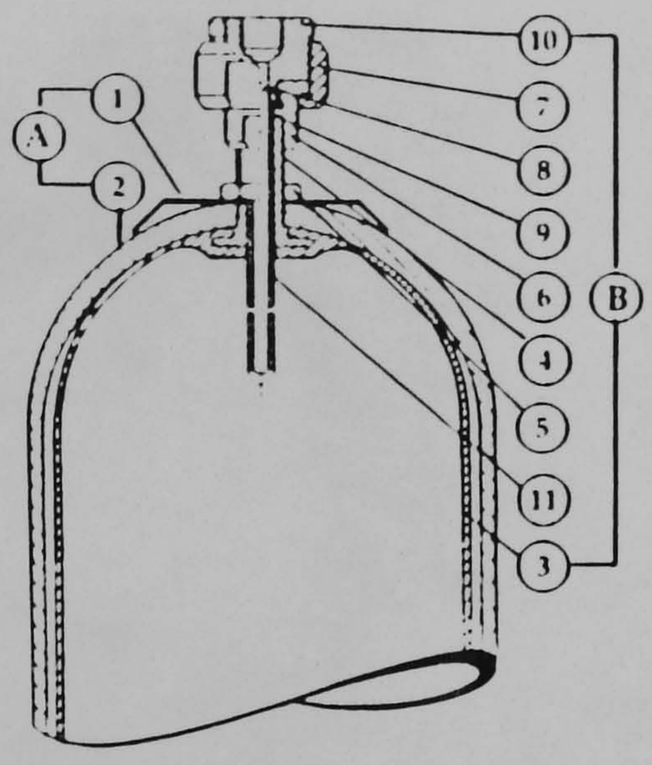
Gas Connection:–
Transfer Barrier Accumulators are fitted with standpipe adaptors see adjacent and over for details.

Bladder:–
An extensive range of bladder materials is offered to suit most applications see form no. AC100-031-88 for complete details.

Fluid Port Assembly:–
Black phosphated, integral high flow fluid port and poppet valve assembly, complete with elastomeric filler to prevent bladder rupture on precharge and air bleed valve.

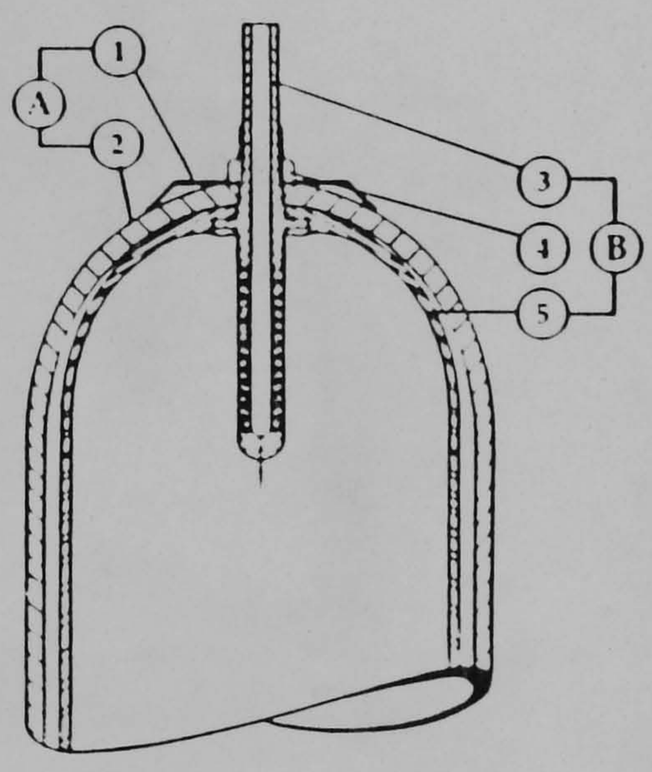
Safety:–
All hydro-pneumatic accumulators are gas pressurised vessels and it is recommended that the system in which they are installed is fitted with maximum safety devices, eg. Burst discs, hydraulic relief valve. See form No. AC100-072-88 for installation details.

Back Up Bottles:– Part No. AC27800.
50 litre capacity – 207 bar standard.
For higher pressures contact Head Office.
Gas connection 1" BSP.
See over for pipework details.
Fluid port arrangement is the same as standard bladder accumulator see form no. AC100-051-88.



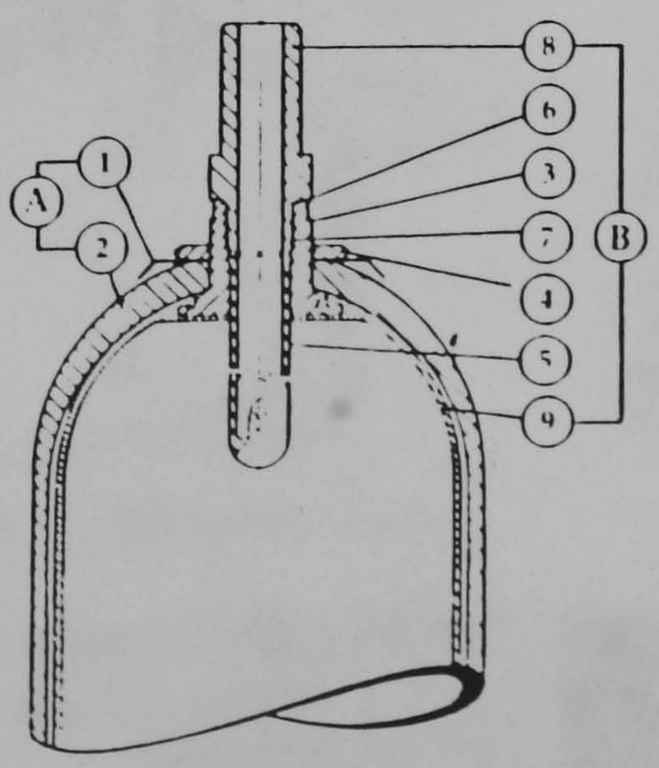
TYPE SB
4 litre models.

KEY	ITEM
A	Shell Assembly comprising
1	Nameplate
2	Shell
B	Bladder Assembly comprising
3	Bladder
4	Stem
5	Locknut
6	Union Nut Adaptor
7	Union Nut
8	Bonded seal
9	Rubber seal
10	Transfer Stem Connector
11	Transfer Port Tube



TYPE 01
10 to 37 litre models.

KEY	ITEM
A	Shell Assembly comprising
1	Nameplate
2	Shell
B	Bladder Assembly comprising
3	Transfer Stem
4	Locknut
5	Bladder



TYPE 7A
54 litre models only.

KEY	ITEM
A	Shell Assembly comprising
1	Nameplate
2	Shell
B	Bladder Assembly comprising
3	Transfer Stem
4	Locknut
5	Transfer Tube
6	'O' Ring
7	Rubber Washer
8	Adaptor
9	Bladder

NSTALLATION and SERVICING of RANSFER BARRIER ACCUMULATORS

pection of Accumulator

pect accumulator and pipework for sible damage during transit.
Check bladder stem locknut and fluid port locking ring for tightness.
Inspect pipework and fittings.
Check that the working pressure stamped on the accumulator shell is equal to, or greater than, the maximum pressure of the system.

vicing:

change a bladder the following cedure should be adopted.
Isolate accumulator from system fluid line and release accumulator fluid pressure by opening bleed valve.
Remove gas valve sealing cap and fit a suitable charging set (Part No. AC10500). Open gas valve by turning handwheel clockwise and vent gas by cracking bleed screw on side of charging set. When gauge reads zero screw up handwheel and remove charging set.
Disconnect pipework and tee piece from accumulator and remove accumulator from system.
Position accumulator, ensuring easy accessibility and clamp securely.
Remove bleed valve and bleed adaptor from fluid port body.
With suitable 'C' spanner remove locking ring and flanged washer from fluid port body.

nsfer Barrier:

Push fluid port body into accumulator, remove 'O' ring and fold anti extrusion ring until sufficiently collapsed to allow removal from shell.
The fluid port body can then be removed from inside the accumulator shell.

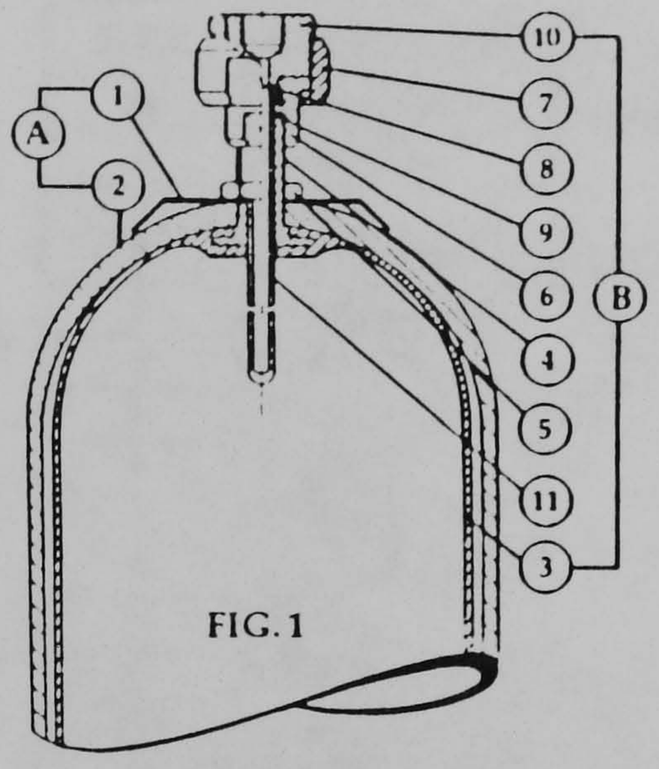


FIG. 1

TYPE SB 4 litre models.

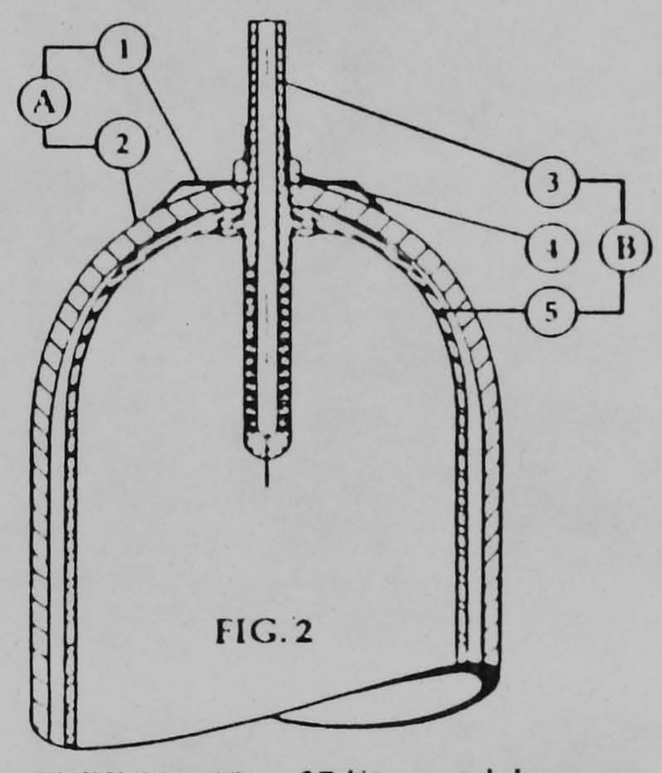


FIG. 2

TYPE 01 10 to 37 litre models.

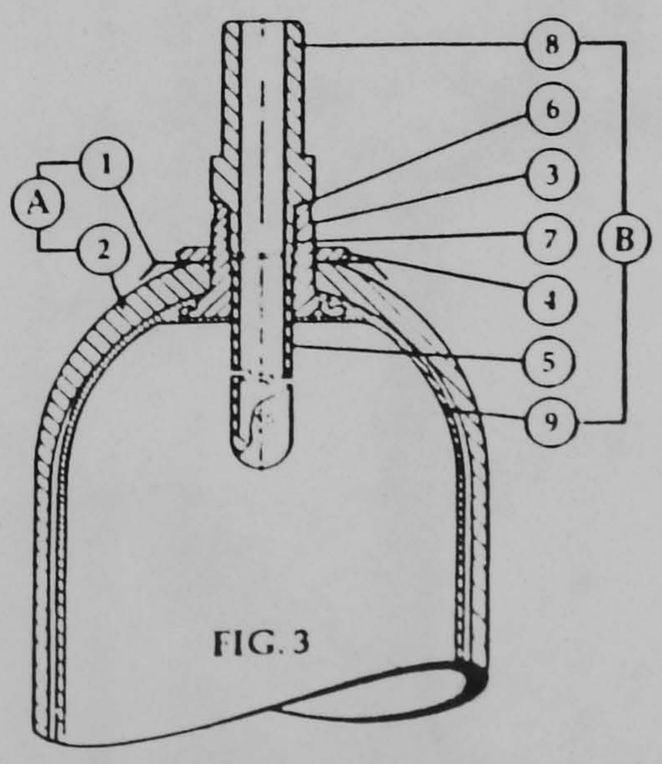


FIG. 3

TYPE 7A 54 litre models only.

j. Removal of transfer tube assembly.
   i. 4 litre models (Fig. 1). Unscrew union nut (7) and remove union nut adaptor (6). Remove transfer stem connector (10) and withdraw transfer tube. Remove locknut (5) and label (1) and withdraw bladder through fluid port end of shell.
   ii. 10 to 37 litre models (Fig. 2). Remove locknut (4) and label (1). Withdraw bladder through fluid port end of shell.
   iii. 54 litre model (Fig. 3). Remove adaptor (8), 'O' ring seal (7) flat washer (6) and transfer tube (5). Remove locknut (4) and label (1) and withdraw bladder through fluid port end of shell.
k. Clean inside shell and all components.
l. To fit a new bladder, roll up bladder longitudinally, edges towards the centre, to expel air and lightly cover with system fluid.
m. Enter stem of bladder through fluid port end of accumulator and push bladder completely into shell until stem emerges through hole at opposite end. Fit label and locknut.
n. Replace transfer tube assembly, reversing the procedure j.
p. Pour into shell approximately 10% of accumulator volume, of system fluid to act as cushion fluid and lubrication.
q. To complete assembly reverse procedure followed in steps c to h, ensuring that the shear ring is in position in the gas valve housing on (AC54*7A) models only.
r. Precharge accumulator adopting procedure on form no. AC100-071-88.

* refers to bladder material.

Note:
Spare bladder should be stored in the following manner to give maximum shell life:–
Inflate bladder to natural size with nitrogen gas and store in the sealed black plastic bag provided away from sunlight and electrical equipment.

ell Christie Hydraulics Limited have a policy of nuous product development. The company es the right to change specification contained in ublication without prior notice.

An Expamet International Company

d and Produced by Leighton Advertising Ltd. Printed in England

FAWCETT CHRISTIE
HYDRAULICS LTD
Sandycroft Industrial Estate,
Chester Road, Sandycroft,
Deeside, Clwyd CH5 2QP
Telephone: Hawarden (0244) 535515
Telex: 617026
Facsimile: (0244) 533002

FCH

INSTALLATION and SERVICING of STANDARD ACCUMULATORS

Inspection of Accumulator

Fawcett Christie Accumulators are thoroughly inspected at the factory, prior to despatch, and are ready for installation following precharging.
After unpacking, inspect accumulator for possible damage caused in transit.

a. Check locknut (6) and locking ring (14) for tightness.
b. Inspect Bleed Plug (17) if provided for visual signs of damage ensuring that it is fully tightened.
c. Check that the working pressure stamped on the accumulator shell is equal to, or greater than, the maximum pressure of the system.

Installation Recommendations:

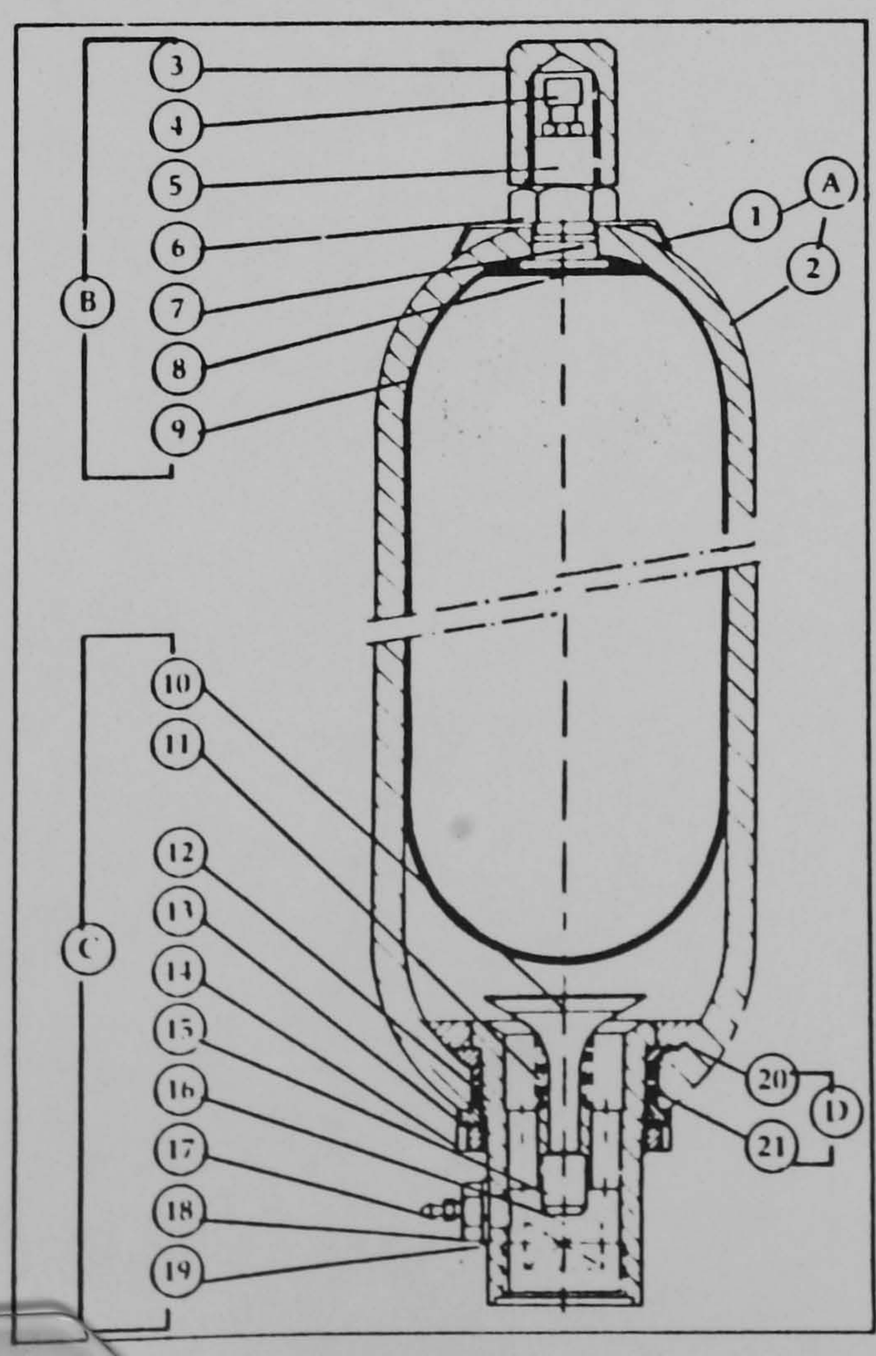
a. All accumulators are supplied unprecharged unless precharge pressure is specified when ordering. Prior to installation all accumulators must be precharged with nitrogen – for precharging procedure see form no. AC100-071-88.
b. For ease of servicing/checks, a safety block (form no. AC100-061-88) should normally be fitted between the accumulator and the fluid pressure line. In addition, on storage applications, a check valve fitted between pump and accumulator will ensure non-reversal of pump.
c. For fluid port connection thread see form no. AC100-051-88.
If it is necessary to adapt to another size Fluid Port Adaptors are available see form no. AC100-066-88.
d. For maximum efficiency and life, accumulators should be mounted vertically where possible, fluid port down. For other attitudes contact Head Office.
e. A range of clamps and brackets are available to assist in installation see form no. AC100-064-88 for details.

Servicing: Fig. 1.
To change a bladder the following procedure should be adopted.

a. Isolate accumulator from system fluid pressure line and release accumulator fluid pressure by opening bleed valve (17).
b. Remove accumulator from system, on larger units the use of lifting caps available from Fawcett Christie are recommended.
c. Position accumulator, ensuring easy accessibility and clamp securely.

KEY	ITEM
A	Shell Assembly comprising:
1	Nameplate
2	Shell
B	Bladder Assembly comprising:
3	Protective Cap
4	Sealing Cap
5	Gas Valve Assembly
6	Locknut
7	'O' Ring
8	Gas Valve Stem
9	Bladder
C	Fluid Port Assy. comprising:
10	Poppet Valve
11	Poppet Spring
12	Fluid Port
13	Flanged Washer
14	Locking Ring
15	Piston
16	Collets
17	Bleed Valve
18	Bleed Adaptor
19	Bonded Seal
D	Supplementary Parts
20	Anti-Extrusion Ring
21	Fluid Port 'O' Ring Seal

NOTE: *On models of 3 litres and below the gas valve assembly is integral with gas valve stem.*



d. Remove protective cap (3) and sealing cap (4) from the gas valve and fit a suitable charging set (Part No. AC10500) to the accumulator gas valve. Open gas valve by turning handwheel clockwise and vent gas by cracking bleed screw on side of charging set. When gauge reads zero screw up handwheel and remove charging set.
e. For accumulators of 4 litres capacity and above remove gas valve assembly (5). For accumulators under 4 litres capacity remove valve core using tool provided with each replacement bladder.
f. Remove bleed valve (17) and bleed adaptor (18) from fluid port body.
g. With suitable 'C' spanner remove locking ring (14) and flanged washer (13) from fluid port body.
h. Push fluid port body into accumulator, remove 'O' ring (21) and fold anti extrusion ring (20) until sufficiently collapsed to allow removal from shell.
j. The fluid port can then be removed from inside the accumulator shell.
k. Remove bladder locking nut (6) and label and withdraw bladder (9) through fluid port end of shell.
l. Clean inside of shell and all components.
m. To fit a new bladder, first remove gas valve assembly and locknut, then roll up bladder longitudinally, edges towards the centre, to expel air and lightly cover with system fluid.
n. Enter gas valve stem of the bladder through fluid port end of accumulator and push bladder completely into shell until gas valve stem emerges through hole at opposite end. Fit label and locknut and replace gas valve assembly.
p. Pour into shell approximately 10% of accumulator volume, of system fluid to act as cushion fluid and lubrication.
q. To complete the assembly reverse the procedure followed in steps d to k.
r. Precharge accumulator adopting procedure on form no. AC100-071-88.

Note:
Spare bladder should be stored in the following manner to give maximum shelf life:–
Inflate bladder to natural size with nitrogen gas and store in the sealed black plastic bag provided, away from sunlight and electrical equipment.

2 CUTTING FORCE RESULTS SUMMARY

2.1 Chapter Six Results

Erin Coal (Cleat Parallel):

S - Sharp B - Blunt	MNF (kN)	MCF (kN)	MSF (kN)	MPNF (kN)	MPCF (kN)	MPSF (kN)
0MPa-S	0.71	2.88	0.37	2.67	8.02	2.19
35MPa-S	0.35	1.92	0.25	2.02	5.64	1.80
70MPa-S	0.56	2.25	0.36	2.32	7.06	2.22
105MPa-S	0.44	1.84	0.28	1.77	5.77	1.71
0MPa-B	0.97	2.71	0.48	3.34	7.70	2.38
35MPa-B	0.44	1.79	0.22	2.31	5.65	1.74
70MPa-B	0.66	2.15	0.33	2.84	6.44	1.98
105MPa-B	0.37	1.59	0.25	1.92	4.75	1.58

Table A1

Anthracite Coal (Cleat Parallel):

S - Sharp B - Blunt	MNF (kN)	MCF (kN)	MSF (kN)	MPNF (kN)	MPCF (kN)	MPSF (kN)
0MPa-S	0.62	1.86	0.12	1.58	5.46	0.70
35MPa-S	0.33	1.10	0.10	1.25	4.35	0.82
70MPa-S	0.38	1.44	0.19	1.30	4.60	1.36
105MPa-S	0.35	1.11	0.11	1.80	4.19	1.37
0MPa-B	1.80	2.20	0.64	5.82	5.66	2.01
35MPa-B	1.84	1.98	0.03	5.88	5.15	0.76
70MPa-B	1.66	1.78	0.15	5.28	4.81	0.61
105MPa-B	0.52	1.02	0.14	2.54	4.00	1.41

Table A2

Anthracite Coal (Cleat Horizontal):

S - Sharp B - Blunt	MNF (kN)	MCF (kN)	MSF (kN)	MPNF (kN)	MPCF (kN)	MPSF (kN)
0MPa-S	0.42	1.33	0.07	2.00	5.53	0.97
35MPa-S	0.47	1.37	0.13	2.18	4.64	1.51
70MPa-S	0.33	1.10	0.09	1.70	4.62	1.71
105MPa-S	0.34	1.30	0.12	2.10	4.73	1.71
0MPa-B	1.36	1.42	0.16	5.01	5.30	1.68
35MPa-B	1.49	1.66	0.22	3.92	5.11	1.72
70MPa-B	0.90	1.35	0.14	3.27	5.01	1.72
105MPa-B	0.63	1.32	0.16	2.93	4.92	1.49

Table A3

2.2 Chapter Seven Results

2.2.1 Test Series One

Erin Coal (Cleat Parallel):

S - Sharp B - Blunt	MNF (kN)	MCF (kN)	MSF (kN)	MPNF (kN)	MPCF (kN)	MPSF (kN)
0MPa-S	1.80	4.35	0.89	5.49	14.66	4.09
35MPa-S	1.64	3.73	0.94	4.81	11.99	3.77
70MPa-S	1.27	3.50	0.60	5.13	14.64	4.02
105MPa-S	1.22	3.09	0.79	4.25	10.13	3.28
0MPa-B	2.76	2.53	0.36	11.39	9.64	2.18
35MPa-B	3.61	3.91	0.90	13.59	11.78	3.28
70MPa-B	3.66	3.80	0.83	14.10	12.59	3.21
105MPa-B	3.44	3.88	1.00	13.16	12.03	3.84

Table A4

Erin Coal (Cleat Horizontal):

S - Sharp B - Blunt	MNF (kN)	MCF (kN)	MSF (kN)	MPNF (kN)	MPCF (kN)	MPSF (kN)
0MPa-S	1.46	3.18	0.26	6.50	13.65	3.17
35MPa-S	0.77	1.61	0.23	3.92	8.32	1.64
70MPa-S	1.23	2.69	0.50	5.64	12.91	4.19
105MPa-S	0.78	1.69	0.24	3.89	7.96	1.77
0MPa-B	1.75	1.34	0.12	6.88	8.24	1.60
35MPa-B	1.59	1.41	0.17	6.65	5.54	1.39
70MPa-B	2.74	2.25	0.26	12.04	10.23	2.18
105MPa-B	2.05	2.01	0.19	8.66	9.03	2.02

Table A5

Pre-cut Slot Results (Cleat Parallel):

Sharp Pick	MNF (kN)	MCF (kN)	MSF (kN)	MPNF (kN)	MPCF (kN)	MPSF (kN)
0MPa	1.80	4.35	0.89	5.49	14.66	4.09
35MPa	1.07	2.74	0.38	4.00	10.05	2.25
70MPa	1.44	3.07	0.51	5.50	10.97	2.66
105MPa	1.87	3.22	0.62	4.84	9.69	2.34

Table A6

Pre-cut Slot Results (Cleat Horizontal):

Sharp Pick	MNF (kN)	MCF (kN)	MSF (kN)	MPNF (kN)	MPCF (kN)	MPSF (kN)
0MPa	1.46	3.18	0.26	6.50	13.65	3.17
35MPa	0.52	1.42	-0.27	2.22	5.57	-0.33
70MPa	1.64	2.24	0.39	7.96	12.36	4.04
105MPa	1.15	2.04	0.37	5.40	9.18	2.32

Table A7

2.2.2 Test Series Two

Erin Coal (Cleat Parallel):

Offset Distance	Force (kN)	Lead Distance			
		2mm	10mm	50mm	100mm
0mm	MNF	1.27	0.88	1.13	1.20
	MCF	3.50	2.73	3.21	2.94
	MSF	0.60	0.93	0.92	0.96
	MPNF	5.13	3.12	4.09	3.96
	MPCF	14.64	8.89	10.39	10.19
	MPSF	4.02	4.87	5.83	5.41
35mm	MNF	0.11	0.73	0.90	0.58
	MCF	0.34	2.35	2.68	1.68
	MSF	0.04	0.45	-0.01	0.53
	MPNF	0.98	2.41	3.04	2.96
	MPCF	2.16	8.14	8.95	7.62
	MPSF	1.12	2.79	0.74	4.27
50mm	MNF	0.63	0.83	0.70	
	MCF	1.74	2.54	2.30	
	MSF	0.19	0.88	0.60	
	MPNF	2.55	3.30	2.59	
	MPCF	7.09	9.26	8.32	
	MPSF	1.67	4.93	4.12	

Table A8

Erin Coal (Cleat Horizontal):

Offset Distance	Force (kN)	Lead Distance			
		2mm	10mm	50mm	100mm
0mm	MNF	1.23	0.62	0.72	0.56
	MCF	2.69	1.73	1.83	1.18
	MSF	0.50	0.41	0.50	0.15
	MPNF	5.64	2.17	3.07	2.45
	MPCF	12.91	6.15	8.57	5.49
	MPSF	4.19	2.25	3.74	1.88
35mm	MNF	0.01	0.40	0.56	0.23
	MCF	0.04	1.45	1.36	0.73
	MSF	0.01	0.61	0.04	0.23
	MPNF	0.27	2.12	2.16	1.78
	MPCF	0.48	6.78	6.38	4.95
	MPSF	0.33	4.34	0.13	2.39
50mm	MNF	0.30	0.63	0.45	
	MCF	0.86	1.58	1.16	
	MSF	0.07	0.26	0.31	
	MPNF	1.67	2.27	2.13	
	MPCF	4.29	5.59	6.20	
	MPSF	1.03	2.49	2.11	

Table A9

3 SPECIFIC ENERGY CURVE FITS

3.1 Chapter Six Results

All the equations apply to the curves with the jet energy included.

Erin Coal (Cleat Parallel):

Sharp Pick	SE = 0.6547 + 0.0630.MPa	r = 0.9680
	SE = 1.2435 exp(0.0176.MPa)	r = 0.9834
	SE = 1.4382 + 0.3089.kW	r = 0.9911
	SE = 1.6064 exp(0.0819.kW)	r = 0.9542
Blunt Pick	SE = 0.2669 + 0.0711.MPa	r = 0.9556
	SE = 1.0582 exp(0.0198.MPa)	r = 0.9912
	SE = 1.0901 + 0.3562.kW	r = 0.9995
	SE = 1.4024 exp(0.0926.kW)	r = 0.9692

Anthracite Coal (Cleat Parallel):

Sharp Pick	SE =-0.1541 + 0.0831.MPa	r = 0.9525
	SE = 0.8478 exp(0.0231.MPa)	r = 0.9902
	SE = 0.7988 + 0.4179.kW	r = 0.9991
	SE = 1.1845 exp(0.1078.kW)	r = 0.9631
Blunt Pick	SE = 0.2241 + 0.0773.MPa	r = 0.9579
	SE = 1.0828 exp(0.0204.MPa)	r = 0.9968
	SE = 1.1259 + 0.3868.kW	r = 1.0000
	SE = 1.4601 exp(0.0947.kW)	r = 0.9646

Anthracite Coal (Cleat Horizontal):

Sharp Pick	SE =-0.1697 + 0.0831.MPa	r = 0.9612
	SE = 0.7684 exp(0.0246.MPa)	r = 0.9979
	SE = 0.8124 + 0.4142.kW	r = 0.9996
	SE = 1.1314 exp(0.1107.kW)	r = 0.9378
Blunt Pick	SE =-0.2991 + 0.0903.MPa	r = 0.9560
	SE = 0.7599 exp(0.0254.MPa)	r = 0.9982
	SE = 0.7486 + 0.4521.kW	r = 0.9993
	SE = 1.1319 exp(0.1145.kW)	r = 0.9393

3.2 Chapter Seven Results

The equations are for the Test Series One results and only apply to the curves with the jet energy included.

Erin Coal:

Sharp Pick	SE = 1.8960 + 0.0174.MPa	r = 0.9691
	SE = 1.9656 exp(0.0062.MPa)	r = 0.9706
	$SE = 1.9502(1 + MPa)^{0.1069}$	r = 0.7874
Blunt Pick	SE = 1.3585 + 0.0253.MPa	r = 1.0000
	SE = 1.4505 exp(0.0103.MPa)	r = 0.9860
	$SE = 1.2895(1 + MPa)^{0.2101}$	r = 0.9514

Pre-cut Slot Results:

SE = 1.6700 + 0.0187.MPa	r = 0.8748
SE = 1.8013 exp(0.0065.MPa)	r = 0.8906
$SE = 1.9058(1 + MPa)^{0.0916}$	r = 0.5895

4 ROSIN-RAMMLER CURVE FITS

4.1 Chapter Six Results

The constants in the tables below are for the Rosin-Rammler equation:

$$100 - P = 100e^{-b.d^n}$$

for the size distributions obtained in chapter six.

S - Sharp B - Blunt	Erin Coal (Cleat Parallel)		Anthracite Coal (Cleat Parallel)		Anthracite Coal (Cleat Horizontal)	
Jet Pressure	b	n	b	n	b	n
0MPa-S	0.1566	0.7797	0.1019	0.8053	0.0863	0.8282
35MPa-S	0.1378	0.7722	0.0894	0.8090	0.0755	0.8902
70MPa-S	0.1446	0.8686	0.1123	0.9982	0.0855	0.8089
105MPa-S	0.1370	0.7853	0.0923	0.9932	0.1073	0.7958
0MPa-B	0.1358	0.8639	0.1138	0.8508	0.0695	0.8561
35MPa-B	0.1196	0.8828	0.0950	0.8656	0.0797	0.9964
70MPa-B	0.1301	0.8828	0.0966	0.7649	0.0961	0.8005
105MPa-B	0.1372	0.8064	0.1035	0.8432	0.1051	0.8086

Table A10

4.2 Chapter Seven Results

4.2.1 Test Series One

S - Sharp B - Blunt	Erin Coal		Pre-cut Slot	
Jet Pressure	b	n	b	n
0MPa-S	0.1351	0.8499		
35MPa-S	0.0990	0.9618	0.0865	0.9882
70MPa-S	0.1037	0.9337	0.0892	0.9702
105MPa-S	0.0961	0.9317	0.1133	0.9341
0MPa-B	0.1125	0.8722		
35MPa-B	0.0903	0.9754		
70MPa-B	0.1080	0.9075		
105MPa-B	0.1095	0.9207		

Table A11

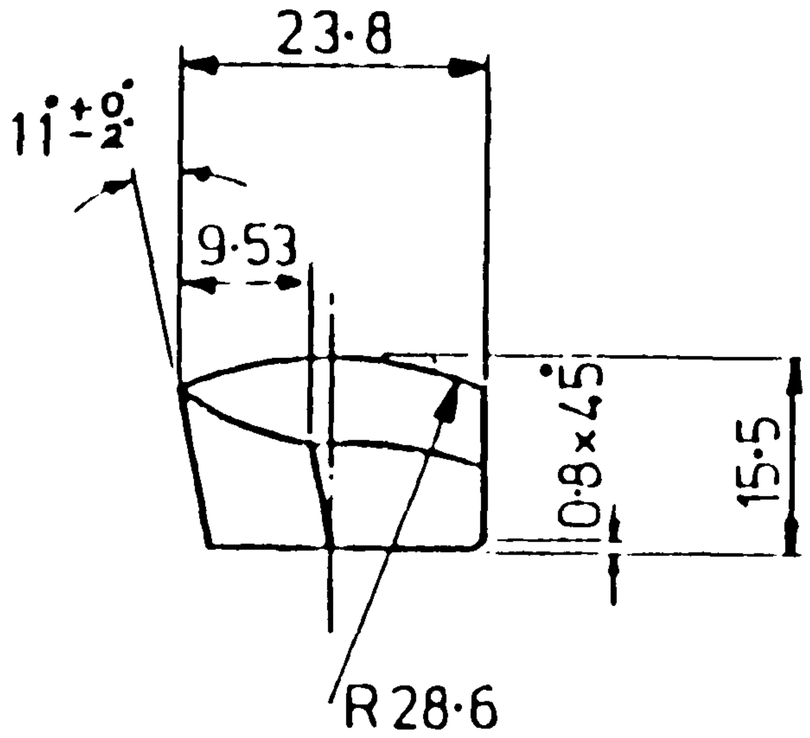
4.2.2 Test Series Two

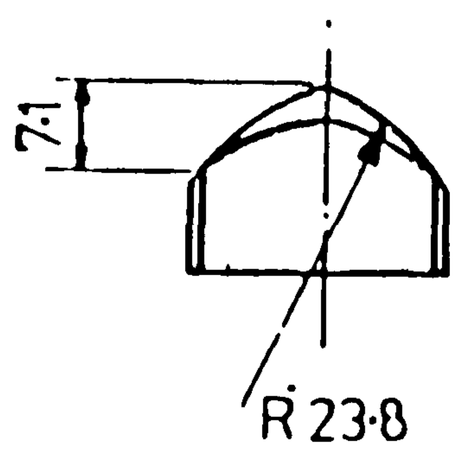
Jet Pressure 70MPa	Offset Distance 0mm		Offset Distance 35mm		Offset Distance 50mm	
Lead Distance	b	n	b	n	b	n
2mm			0.0823	0.9650	0.0838	1.0285
10mm	0.0994	0.8791	0.0640	1.0755	0.0929	0.9196
50mm	0.1019	0.8950	0.0848	0.9637	0.0981	0.8824
100mm	0.0946	0.9188	0.0867	0.9472	0.0955	0.9196

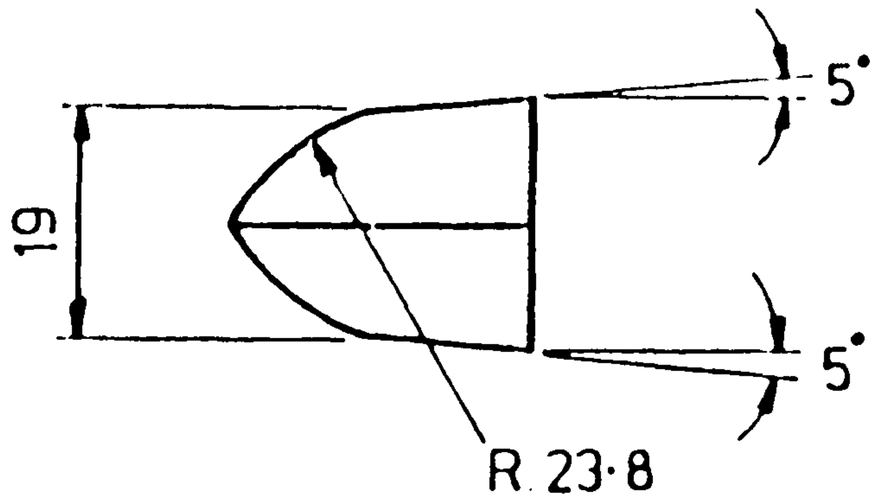
Table A12

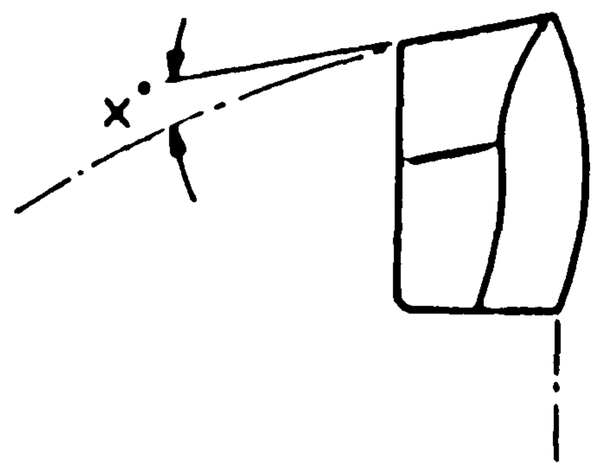
5 HW TIP DESIGN

Carbide	Grade CXT
Cobalt Content	9.5%
Hardness	1210 HV30
Grain Size	3.5 micron.
Braze Strength	15.0 tons/sq.in minimum









Size in mm

```
1           PROGRAM SORT3F
2     C
3     C Program to read data from 3 datafiles, convert the
4     C raw data into forces (kN), and write the results in
5     C a new datafile, NORM, CUTT, SIDE, represent the raw
6     C data for the normal, cutting and sideway forces.
7     C
8           DIMENSION NORM(4100), CUTT(4100), SIDE(4100), ZLIM(2),
9        +        LIMIT(4), TAR(3), FORCE(4100,3)
10          INTEGER   NDATA, I, NORM, CUTT, SIDE, DAY, MONTH,
11       +        ZLIM, ZCOUNT, A, R, Z1, J, LIMIT, TAR,
12       +        BLOCK, SUM1, SUM2, DISTS, DIFF, TOTAL,
13       +        ZNUM, FCOUNT
14          REAL     ZN, ZC, ZS, ZNF, ZCF, ZSF, POS1, POS2,
15       +        SPEED, CONVT, NCALN, CCALC, SCALS, FORCE
16    C
17          PARAMETER (NCALN  =  -0.01180)
18    C
19          PARAMETER (CCALC  =  -0.01000)
20    C
21          PARAMETER (SCALS  =  0.00820)
22    C
23          PRINT *, 'Enter the date this cut was taken:
24          READ (*,'(BN,12)') DAY
25          READ (*,'(BN,12)') MONTH
26          PRINT*
27    C
28    C     PRINT *, 'Enter the position of the cut on the tape:'
29    C     READ (*,' (BN,F5.1)') POS1
30    C     READ (*,' (BN,F5.1)') POS2
31          PRINT*
32          PRINT*
33          PRINT*, 'READing data'
34    C
35          NDATA =  0
36    C
37          DO 10 I = 1, 4100
38           READ (10,'(BN,14)',END=10) NORM(I)
39           READ (11, (BN,14)',END=10) CUTT(I)
40           READ (12,'(BN,14)',END=10) SIDE(I)
41           NDATA = NDATA + 1
42       10 CONTINUE
43          PRINT*, 'Data READ successfully:'
44          PRINT*, 'Rows of data READ = ', NDATA
45    C
46    C
47    C To calculate the zero datum for each cut.
48    C
49          PRINT*, 'Enter zero value:'
50          READ (*,'(BN,13)') Z1
51    C
52          ZCOUNT = 0
53          ZLIM(1) = 4
54          ZLIM(2) = 3 + Z1
55          DATA ZN /0.0/, ZC /0.0/, ZS /0.0/
56    C
57          DO 210 R = ZLIM(1), ZLIM(2)
58            ZN = ZN + NORM(R)
```

```
59              ZC = ZC + CUTT(R)
60              ZS = ZS + SIDE(R)
61              ZCOUNT = ZCOUNT + 1
62       210  CONTINUE
63    C
64          IF (ZCOUNT .NE. Z1) THEN
65            PRINT*, 'Zero Error : ZCOUNT = ',ZCOUNT,' <> ',Z1
66            STOP
67          END IF
68    C
69          ZNF = ZN / ZCOUNT
70          ZCF = ZC / ZCOUNT
71          ZSF = ZS / ZCOUNT
72          PRINT*,'ZNF = ',ZNF
73          PRINT*,'ZCF = ',ZCF
74          PRINT*, ZSF = ',ZSF
75    C
76    C
77    C To calculate how much of the cut to ignore.
78    C Speed in m/s, all distances in mm.
79    C
80              SPEED = 1.10
81              PRINT*,'Enter total length of cut (mm):'
82              READ(*,'(BN,14)') LENGTH
83              PRINT*,'Enter TAR(1) (mm):'
84              READ(*,'(BN,13)') TAR(1)
85              PRINT*,'Enter 1st length of cut (mm):'
86              READ(*,'(BN,13)' BLOCK(1)
87              PRINT*,'Enter TAR(2) (mm):'
88              READ(*,'(BN,13)') TAR(2)
89              PRINT*,'Enter 2nd length of cut (mm):'
90              READ(*,'(BN,13)') BLOCK(2)
91              PRINT*,'Enter TAR(3) (mm):'
92              READ(*,'(BN,13)') TAR(3)
93              BLOCK(3) = 0
94    C
95    C  To convert LENGTH into sample units.
96    C
97                  TOTAL = NINT (2.331 * LENGTH)
98    C
99    C  Convert distances into sample units.
100   C
101             CONVT = REAL(TOTAL) / REAL(LENGTH)
102   C
103             SUM1 = 0
104             SUM2 = 0
105             DO 230 I = 1, 3
106               TAR(I) = NINT(CONVT * TAR(I))
107               BLOCK(I) = NINT(CONVT * BLOCK(I))
108               SUM1 = SUM1 + TAR(I)
109               SUM2 = SUM2 + BLOCK(I)
110   230       CONTINUE
111             DISTS = SUM1 + SUM2
112             DIFF = DISTS - TOTAL
113             PRINT*, 'DIFF = ', DIFF
114   C
115             J = ABS(DIFF)
116             IF (J .EQ. 0) THEN
```

```
117             GOTO 240
118           ELSE IF (J. GT. 5) THEN
119             PRINT*, 'Please check the parameters in DIST.'
120             PRINT*, 'Are the values correct?'
121             STOP
122           ELSE
123             J1 = INT(DIFF/2.0) * (-1)
124             J2 = NINT(DIFF/2.0) * (-1)
125             BLOCK(1) = BLOCK(1) + J1
126             BLOCK(2) = BLOCK(2) + J2
127           END IF
128   C
129    240    CONTINUE
130   C
131           PRINT*,'BLOCK(1) = ',BLOCK(1)
132           PRINT*,'BLOCK(2) = ',BLOCK(2)
133   C
134           LIMIT(1) = TAR(1) + 3 + Z1 + 1
135           LIMIT(2) = LIMIT(1) + BLOCK(1) - 1
136           LIMIT(3) = LIMIT(2) + TAR(2) + 1
137           LIMIT(4) = LIMIT(3) + BLOCK(2) - 1
138   C
139           PRINT*, 'LIMIT(1) = ', LIMIT(1)
140           PRINT*, 'LIMIT(2) = ', LIMIT(2)
141           PRINT*, 'LIMIT(3) = ', LIMIT(3)
142           PRINT*, 'LIMIT(4) = ', LIMIT(4)
143   C
144   C
145   C Data and position of cut on tape is written
146   C into the data file (year is changed by editting
147   C the program).
148   C
149               WRITE (20,'(4X,A,2(I2,A),12)')'Date cut was taken = ',
150        +        DAY, '-', MONTH, '-90'
151               WRITE (20,'(/ 4X,A,F5.1,A,F5.1/)')'Position of cut on tape = ',
152        +        0.0, ' - ',0.0
153   C
154   C Write data in 3 column array file with a title
155   C at the head of each colum.
156   C
157               WRITE (20,'(4X,A)')'NOTE: The forces are from two coal blocks.'
158               WRITE (20,'(4X,A,A/)')'The number of data from each block is',
159        +          ' shown below.'
160               WRITE (20,'(4X,A,I4)')'Rows of data for BLOCK(1) = ',BLOCK(1)
161               WRITE (20,'(4X,A,14)')'Rows of data for BLOCK(2) = ',BLOCK(2)
162               WRITE (20,'(/4X,A,3X,A,2A,A)')'Normal', 'Cutting',
163        +          'Sideways'
164               WRITE (20,'(4X,A3X,A,2XA/)')'======', '======',
165        +       '======'
166   C
167   C
168   C Convert raw data into froce values and write these in a
169   C new datafile assigned to unit 20.
170   C
171             FCOUNT = 0
172             DO 250 A = 1, 3, 2
173               DO 260 R = LIMIT(A), LIMIT(A+1)
174                 RN = NORM(R) - ZNF
```

```
175                 RC = CUTT(R) - ZCF
176                 RS = SIDE(R) - ZSF
177                 FORCE(R,1) = NCALN * RN + 0.0298
178                 FORCE(R,2) = CCALC * RC + 0.1404
179                 FORCE(R,3) = SCALS * RS + 0.0440
180                 WRITE(20,'(3(3X,F7.2))') FORCE(R,1), FORCE(R,2), FORCE(R,3)
181                 FCOUNT = FCOUNT + 1
182   260       CONTINUE
183   250     CONTINUE
184   C
185           PRINT*,'Data converted into Force values and transfered.'
186           PRINT*,'Rows of data in Force-file = ', FCOUNT
187   C
188           STOP
189           END
```

```
1           PROGRAM CUT
2     C
3     C To calculate the mean and mean peak forces.
4     C
5           CHARACTER*720 INFO1(10), INFO2(10), INFOB1(1)*28,
6        +      INFOB2(1)*28
7           DIMENSION RMNF(3), RMCF(3), RMSF(3), RAMNF(3), RAMCF(3),
8        +      RAMSF(3), RMPNF(2), RMPCF(2), RMPST(2), RMMNF(2),
9        +      RMMCF(2), RMMSF(2), BLOCK(2)
10          COMMON   /CUTD/ DFORCE(4100,3)
11          COMMON   /LIN/ LIMIT(4), COUNT(3)
12          INTEGER  I, R, C, LIMIT, BLOCK, COUNT, LENGTH, FN
13          REAL     RMNF, RMCF, RMSF, RAMNF, RAMCF, RAMSF, RMPNF,
14       +      RMPCF, RMPSF, AVPNF, AVPCF, AVPSF, RMMNF, RMMCF,
15       +      RMMSF, AVMNF, AVMCF, FIVE, DFORCE
16          PARAMETER (FIVE = 0.05)
17    C
18    C Read information at beginning of datafile.
19    C
20          READ (10,'(4X,A)') (INFO1(I), I = 7)
21          READ (10,'(4X,A,I4)') INFOB1, BLOCK(1)
22          READ (10,'(4X,A,I4)') INFOB2, BLOCK(2)
23          READ (10,'(4X,A)') (INFO2(I), I = 1, 4)
24    C
25    C READ the data.
26    C
27          READ (10,15,ERR=25,END=20) ((DFORCE(R,C),C=1,3),R=1,4100)
28     15   FORMAT(3(3X,F7.2))
29     20   CONTINUE
30    C
31    C Set limnits for calculation of forces for each coal block.
32    C
33          LIMIT(1) = 1
34          LIMIT(2) = BLOCK(1)
35          LIMIT(3) = BLOCK(1) + 1
36          IF (BLOCK(2)  .EQ. 0) THEN
37             LIMIT(4) = LIMIT(3) + 1
38             COUNT(2) = 1
39          ELSE
40             LIMIT(4) = LIMIT(3) + BLOCK(2) - 1
41             COUNT(2) = NINT(FIVE * BLOCK(2))
42          END IF
43    C
44          LENGTH = BLOCK(1) + BLOCK(2)
45          COUNT(1) = NINT(FIVE * BLOCK(1))
46          COUNT(3) = NINT(FIVE * LENGTH)
47    C
48          PRINT*,'LIMIT(1) = ', LIMIT(1)
49          PRINT*,'LIMIT(2) = ', LIMIT(2)
50          PRINT*,'LIMIT(3) = ', LIMIT(3)
51          PRINT*,'LIMIT(4) = ', LIMIT(4)
52          PRINT*,'COUNT(1) = ', COUNT(1)
53          PRINT*,'COUNT(2) = ', COUNT(2)
54          PRINT*,'COUNT(3) = ', COUNT(3)
55    C
56          PRINT*,'Analysing data now.'
57    C
58          CALL MEAN (RMNF, RMCF, RMSF, RAMNF, RAMF, RAMSF)
```

```
C
      CALL PEAK (RMPNF, RMPCF, RMPSF)
C
      CALL AVPMAX (AVPNF, AVPCF, AVPSF)
C
      CALL PEAKM (RMMNF, RMMCF, RMMSF)
C
      CALL AVPMIN (AVMNF, AVMCF, AVMSF)
C
C WRITE results in a table at the end of the data file and
C onto the terminal screen.
C
      DO 30 FN = 6, 10, 4
      WRITE (FN,*)
      WRITE (FN,100) '*******************************',
     +       '*******************************',
      WRITE (FN,100) '*          *   TOTAL   *',
     +       '  BLOCK1   *   BLOCK2  *',
      WRITE (FN,100) '*******************************',
     +       '*******************************',
      WRITE (FN,110) '* MNF       = ',RMNF(3),'    =',
     +       ' ',RMNF(1),'     = ',RMNF(2),'    *'
      WRITE (FN,110) '* MNF (ABS)  = ',RAMNF(3),'    -',
     +       ' ',RAMNF(1),'     = ',RAMNF(2),'    *'
      WRITE (FN,110) '* MPNF       = ',AVPNF,'    =',
     +       ' ',RMPNF(1),'     = ',RMPNF(2),'    *'
      WRITE (FN,110) '* MPNF (MIN)  = ',AVMNF,'    =',
     +       ' ',RMMNF(1),'     = ',RMMNF(2),'    *'
      WRITE (FN,100) '*==============================',
     +       '==============================*'
      WRITE (FN,110) '* MCF       = ',RMCF(3),'    =',
     +       ' ',RMCF(1),'     = ',RMCF(2),'    *'
      WRITE (FN,110) '* MCF (ABS)  = ',RAMCF(3),'    =',
     +       ' ',RAMCF(1),'     = ',RAMCF(2),'    *'
      WRITE (FN,110) '* MPCF       = ',AVPCF,'    =',
     +       ' ',RMPCF(1),'     = ',RMPCF(2),'    *'
      WRITE (FN,110) '* MPCF (MIN)  = ',AVMCF,'    =',
     +       ' ',RMMCF(1),'     = ',RMMCF(2),'    *'
      WRITE (FN,100) '*==============================',
     +       '==============================*'
      WRITE (FN,110) '* MSF       = ',RMSF(3),'    =',
     +       ' ',RMSF(1),'     = ',RMSF(2),'    *'
      WRITE (FN,110) '* MSF (ABS)  = ',RAMSF(3),'    =',
     +       ' ',RAMSF(1),'     = ',RAMSF(2),'    *'
      WRITE (FN,110) '* MPSF       = ',AVPSF,'    =',
     +       ' ',RMPSF(1),'     = ',RMPSF(2),'    *'
      WRITE (FN,110) '* MPSF (MIN)  = ',AVMSF,'    =',
     +       ' ',RMMSF(1),'     = ',RMMSF(2),'    *'
      WRITE (FN,100) '*******************************',
     +       '*******************************'
   30 CONTINUE
C
  100 FORMAT (4X,A,A)
  110 FORMAT (4X,A,F6.2,A,A,F6.2,A,F6.2,A)
      STOP
   25 PRINT*,'Error in READing data.'
      STOP
      END
```

```
C
C=============================================================
C
      SUBROUTINE DATA
C
C To supply uncorrupted data to each subroutine.
C
      COMMON /CUTD/ DFORD(4100,3)
      COMMON /VALUES/ FORCE(4100,30
      INTEGER R, C
      REAL FORCE, DFORCE
C
      DO 700 C = 1, 3
        DO 710 R = 1, 4100
          FORCE(R,C) = DFORCE(R,C)
 710    CONTINUE
 700  CONTINUE
C
      RETURN
      END
C
C=============================================================
C
      SUBROUTINE MEAN (RMNF, RMCF, RMSF, RAMNF, RAMCF,
RAMSF)
C
C To calc. the mean forces.
C
      DIMENSION ADD(3,3), A(3), B(3), DENOM(3), RMNF(3), RMCF(3),
     +    RMSF(3), ABL(3,3), RAMNF(3), RAMCF(3), RAMSF(3)
      COMMON /LIM/ LIMIT(4), COUNT(3)
      COMMON /VALUES/ FORCE(4100,3)
      INTEGER A, B, M, R, LIMIT, COUNT
      REAL ADD, ABL, FORCE, RMNF, RMCF, RMSF, DENOM, RAMNF,
     +    RAMCF, RAMSF
C
      CALL DATA
      DATA ADD /9*0.0/, DENOM /3*0.0/, ABL /9*0.0/
      DATA A /1,3,1/, b /2,4,4/
C
      DO 210 M = 1, 3
        DO 200 R = LIMIT(A(M)), LIMIT(B(M))
          ADD(M,1) = ADD(M,1) + FORCE(R,1)
          ADD(M,2) = ADD(M,2) + FORCE(R,2)
          ADD(M,3) = ADD(M,3) + FORCE(R,3)
          ABL(M,1) = ABL(M,1) + ABS(FORCE(R,1))
          ABL(M,2) = ABL(M,2) + ABS(FORCE(R,2))
          ABL(M,3) = ABL(M,3) + ABS(FORCE(R,3))
          DENOM(M) = DENOM(M) + 1
 200    CONTINUE
        RMNF(M) = ADD(M,1) / DENOM(M)
        RMCF(M) = ADD(M,2) / DENOM(M)
        RMSF(M) = ADD(M,3) / DENOM(M)
        RAMNF(M) = ABL(M,1) / DENOM(M)
        RAMCF(M) = ABL(M,2) / DENOM(M)
        RAMSF(M) = ABL(M,3) / DENOM(M)
 210    CONTINUE
C
```

```
174           RETURN
175           END
176   C
177   C=======================================================
178   C
179           SUBROUTINE PEAK (RMPNF, RMPCF, RMPFSF)
180   C
181   C To calc. the mean peak forces using the highest 5% of the
182   C values (95 percentiles).
183   C
184           DIMENSION MAX(2,3), CENT(2,3), A(2), B(2), RMPNF(2),
185        +            RMPCF(2), RMPSF(2)
186           COMMON /LIM/ LIMIT(4), COUNT(3)
187           COMMON /VALUES/ FORCE(4100,3)
188           INTEGER LIMIT, R, C, M, A, B, COUNT, TURNS, X
189           REAL FORCE, MAX, CENT, RMPNF, RMPCF, RMPSF
190   C
191           CALL DATA
192           DATA A/1,3/, B/2,4/, CENT/6*0.0/
193   C
194           DO 320 C = 1, 3
195            DO 310 M = 1, 2
196            X = 0
197          DO 330 TURNS = 1, COUNT(M)
198           MAX (M,C) = -50.0
199              DO 300 R = LIMIT(A(M)), LIMIT(B(M))
200                IF (FORCE(R,C) .GE. MAX(M,C)) THEN
201                  MAX(M,C) = FORCE(R,C)
202                  X = R
203                END IF
204    300       CONTINUE
205              CENT(M,C) = CENT(M,C) + MAX(M,C)
206              FORCE(X,C) = -51.0
207    330     CONTINUE
208    310    CONTINUE
209    320     CONTINUE
210   C
211           DO 340 M = 1, 2
212             RMPNF(M) = CENT(M,1) / COUNT(M)
213             RMPCF(M) = CENT(M,2) / COUNT(M)
214             RMPSF(M) = CENT(M,3) / COUNT(M)
215    340    CONTINUE
216   C
217           RETURN
218           END
219   C
220   C
221   C=======================================================
222   C
223               SUBROUTINE AVPMAX (AVPNF, AVPCF, AVPSF)
224   C
225   C To calc. the mean peak forces using the highest 5% of the
226   C values (95 percentiles).
227   C
228               DIMENSION CENT(3), MAX(3)
229               COMMON /LIM/ LIMIT(4), COUNT(3)
230               COMMON /VALUES/ FORCE(4100,3)
231               INTEGER LIMIT, R, C, M, COUNT, TURNS, X
```

```
232           REAL FORCE, MAX, CENT, AVPNF, AVPCF, AVPSF
233   C
234           CALL DATA
235           DATA CENT/3*0.0/
236   C
237           DO 420 C = 1, 3
238            X = 0
239            DO 430 TURNS = 1, COUNT(3)
240              MAX (C) = -50.0
241              DO 400 R = LIMIT(1), LIMIT(4)
242                IF (FORCE(R,C0 .GE. MAX(C)) THEN
243                  MAX(C) = FORCE(R,C)
244                  X = R
245                END IF
246    400         CONTINUE
247                CENT(C) = CENT(C) + MAX(C)
248                FORCE(X,C) = -51.0
249    430       CONTINUE
250    420     CONTINUE
251   C
252             AVPNF = CENT(1) / COUNT(3)
253             AVPCF = CENT(2) / COUNT(3)
254             AVPSF = CENT(3) / COUNT(3)
255   C
256           RETURN
257           END
258   C
259   C=============================================================
260   C
261           SUBROUTINE PEAKM (RMMNF, RMMCF, RMMSF)
262   C
263   C To calc. the mean peak forces using the highest 5% of the
264   C values (95 percentiles).
265   C
266           DIMENSION MIN(2,3), A(2), B(2), RMMNF(2),
267       +       RMMCF(2), RMMSF(2)
268           COMMON /LIM/ LIMIT(4), COUNT(3)
269           COMMON /VALUES/ FORCE(4100,3)
270           INTEGER LIMIT, R, C, M, A, B, COUNT, TURNS, X
271           REAL FORCE, MIN, CENT, RMMNF, RMMCF, RMMSF
272   C
273           CALL DATA
274           DATA A/1,3/, B/2,4/, CENT/6*0.0/
275   C
276           DO 520 C = 1, 3
277            DO 510 M = 1, 2
278           X = 0
279            DO 530 TURNS = 1, COUNT(M)
280             MIN (M,C) = 50.0
281             DO 500 R = LIMIT(A(M)), LIMIT(B(M))
282               IF (FORCE(R,C) .LE. MIN(M,C)) THEN
283                 MIN(M,C) = FORCE(R,C)
284                 X = R
285               END IF
286    500       CONTINUE
287              CENT(M,C) = CENT(M,C) + MIN(M,C)
288              FORCE(X,C) = 51.0
289    530     CONTINUE
```

```
510   CONTINUE
520  CONTINUE
C
      DO 540 M = 1, 2
        RMMNF(M) = CENT(M,1) / COUNT(M)
        RMMCF(M) = CENT(M,2) / COUNT(M)
        RMMSF(M) = CENT(M,3) / COUNT(M)
540   CONTINUE
C
      RETURN
      END
C
C=====================================================
C
          SUBROUTINE AVPMIN (AVMNF, AVMCF, AVMSF)
C
C To calc. the mean peak forces using the highest 5% of the
C values (95 percentiles).
C
      DIMENSION CENT(3), MIN(3)
      COMMON /LIM/ LIMIT(4), COUNT(3)
      COMMON /VALUES/ FORCE(4100,3)
      INTEGER LIMIT, R, C, M, COUNT, TURNS, X
      REAL FORCE, MIN, CENT, AVMNF, AVMCF, AVMSF
C
      CALL DATA
      DATA CENT/3*0.0/
C
      DO 620 C = 1, 3
      X = 0
       DO 630 TURNS = 1, COUNT(3)
        MIN (C) = 50.0
        DO 600 R = LIMIT(1), LIMIT(4)
          IF (FORCE(R,C) .LE. MIN(C)) THEN
            MIN(C) = FORCE(4,C)
            X = R
          END IF
600     CONTINUE
        CENT(C) = CENT(C) + MIN(C)
        FORCE(X,C) = 51.0
630    CONTINUE
620   CONTINUE
C
      AVMNF = CENT(1) / COUNT(3)
      AVMCF = CENT(2) / COUNT(3)
      AVMSF = CENT(3) / COUNT(3)
C
      RETURN
      END
```